ICE PROTECTION INVESTIGATION FOR ADVANCED ROTARY-WING AIRCRAFT

LOCKHEED-CALIFORNIA CO.

PREPARED FOR
ARMY AIR MOBILITY RESEARCH AND DEVELOPMENT LABORATORY

AUGUST 1973

AD-771182

UNCLASSIFIED

Security Classification

DOCUMENT CONTROL DATA - R & D

(Security classification of title, body of abstract and indexing annotation must be entered when the overall report is classified)

1. ORIGINATING ACTIVITY (Corporate author)	2a. REPORT SECURITY CLASSIFICATION
Lockheed-California Company Burbank, California	Unclassified
	2b. GROUP

3. REPORT TITLE

ICE PROTECTION INVESTIGATION FOR ADVANCED ROTARY-WING AIRCRAFT

4. DESCRIPTIVE NOTES *(Type of report and inclusive dates)*

5. AUTHOR(S) *(First name, middle initial, last name)*

. B. Werner

6. REPORT DATE	7a. TOTAL NO. OF PAGES	7b. NO. OF REFS
;ust 1973	~~388~~ 392	93
8a. CONTRACT OR GRANT NO.)02-72-C-0054 9a. PROJECT NO. 2205AA54	9a. ORIGINATOR'S REPORT NUMBER(S) USAAMRDL Technical Report 73-38	
c.	9b. OTHER REPORT NO(S) *(Any other numbers that may be assigned this report)* LR 25327-10	

10. DISTRIBUTION STATEMENT

proved for public release; distribution unlimited.

11. SUPPLEMENTARY NOTES	12. SPONSORING MILITARY ACTIVITY
	Eustis Directorate U.S. Army Air Mobility R&D Laboratory Fort Eustis, Virginia

13. ABSTRACT

. study program was conducted for the U.S. Army AMRDL to define ice protection requirements for advanced rotary-wing aircraft. The study included investigation into: (1) the hazards of flying through ice, (2) probability of icing, (3) vehicle ice accretion rates, (4) current ice protection system designs, (5) operational limitations of current helicopters, and (6) advanced deicing concepts.

Information for the flight hazards of icing was obtained from flight test results of a number of aircraft, including National Research Council of Canada, Ottawa spray-rig tests where available. Icing probability data were obtained from a compilation of worldwide weather survey data. Data are presented on icing frequency of occurrence and severity and are used to establish meteorological design conditions. Component ice accretion rates and ice shapes were generated analytically using digital computer techniques, and were used to establish anti-/deicing system design criteria. A survey of current ice protection system designs includes thermal, mechanical, and chemical systems. The systems are evaluated in terms of weight, reliability, and vehicle performance penalties for each system. The appropriateness and applicability of the various concepts to the affected components of rotary-wing aircraft are discussed, along with the sensitivity of the performance to meteorological conditions. The need for in-flight measurement of icing severity is also discussed. Knowledge obtained from the survey contributed to the determination of the limitations of these systems and the aircraft upon which they are installed. Investigation was conducted to determine advanced concepts which show promise for future research and development, and the greatest potential for advancement of the state of the art of deicing systems.

DD FORM 1 NOV 68 1473 REPLACES DD FORM 1473, 1 JAN 64, WHICH IS OBSOLETE FOR ARMY USE.

UNCLASSIFIED

Security Classification

14. KEY WORDS	LINK A		LINK B		LINK C	
	ROLE	WT	ROLE	WT	ROLE	WT
Ice Protection Advanced Rotary-Wing Aircraft Deicing Concepts						

DEPARTMENT OF THE ARMY
U. S. ARMY AIR MOBILITY RESEARCH & DEVELOPMENT LABORATORY
EUSTIS DIRECTORATE
FORT EUSTIS, VIRGINIA 23604

This report was prepared by the Lockheed-California Company under the terms of Contract DAAJ02-72-C-0054. The report contains information pertaining to rotary-wing aircraft ice protection systems which can be used in establishing requirements for future R&D programs and for the design and test of ice protection systems for existing helicopters. This report presents an analysis of the problems associated with rotary-wing aircraft ice protection, the capability of existing technology to support future requirements, and the R&D necessary to satisfy future objectives; however, the conclusions and recommendations made herein are based on the following assumptions:

1. Icing conditions considered are those created by flight in supercooled clouds only.

2. Army aircraft will not be required to fly in icing severity levels greater than moderate.

3. Existing helicopters are representative of future Army helicopters.

The project engineer for this effort was Mr. Meyer B. Salomonsky, Military Operations Technology Division.

it

Project 1F162205AA54
Contract DAAJ02-72-C-0054
USAAMRDL Technical Report 73-38
August 1973

ICE PROTECTION INVESTIGATION FOR ADVANCED ROTARY-WING AIRCRAFT

Final Report

Lockheed-California Company Report LR 25327-10

by

J. B. Werner

Prepared by

Lockheed-California Company
Burbank, California

for

EUSTIS DIRECTORATE
U. S. ARMY AIR MOBILITY RESEARCH AND DEVELOPMENT LABORATORY
FORT EUSTIS, VIRGINIA

ABSTRACT

A study program was conducted for the U. S. Army AMRDL to define ice protection requirements for advanced rotary-wing aircraft. The study included investigations into: (1) the hazards of flying through ice, (2) probability of icing, (3) vehicle ice accretion rates, (4) current ice protection system designs, (5) operational limitations of current helicopters, and (6) advanced deicing concepts.

Information for the flight hazards of icing was obtained from flight test results of a number of aircraft, including National Research Council of Canada, Ottawa spray-rig tests where available. Icing probability data were obtained from a compilation of worldwide weather survey data. Data are presented on icing frequency of occurrence and severity and are used to establish meteorological design conditions. Component ice accretion rates and ice shapes were generated analytically using digital computer techniques, and were used to establish anti-/deicing system design criteria. A survey of current ice protection system designs includes thermal, mechanical, and chemical systems. The systems are evaluated in terms of weight, reliability, and vehicle performance penalties for each system. The appropriateness and applicability of the various concepts to the affected components of rotary-wing aircraft are discussed, along with the sensitivity of the performance to meteorological conditions. The need for in-flight measurement of icing severity is also discussed. Knowledge obtained from the survey contributed to the determination of the limitations of these systems and the aircraft upon which they are installed. Investigation was conducted to determine advanced concepts which show promise for future research and development, and the greatest potential for advancement of the state of the art of deicing systems.

FOREWORD

This report presents the results of a study program on ice protection requirements for advanced rotary-wing aircraft. This program was conducted by the Lockheed-California Company under Contract DAAJ02-72-C-0054 (Project 1F162205AA54) to the Eustis Directorate, U. S. Army Air Mobility Research and Development Laboratory (USAAMRDL), Fort Eustis, Virginia.

The program was performed during the period from April 1972 through March 1973. Technical monitoring of the project for USAAMRDL was by M. B. Salomonsky.

The Lockheed program was under the technical direction of J. B. Werner, Senior Research and Development Engineer. Additional Lockheed personnel contributing to the program included E. V. Ashburn, G. F. Bollinger, M. J. Cronin, S. N. Miller, H. C. Moe, A. M. Petach, K. K. Schmidt, and S. T. Tuan.

TABLE OF CONTENTS

LIST OF ILLUSTRATIONS

LIST OF TABLES

LIST OF SYMBOLS

A - area, ft^2

a - radius of water droplet, ft

ADP - aerodynamic discontinuity principle

AUW - All Up Weight, lb

B - barometric ambient pressure, psia

BHP - brake horsepower

C - airfoil chord length or body characteristic length, ft

C_d - drag coefficient, dimensionless

C_i - specific heat of ice, Btu/lb-°F

C_L - lift coefficient, dimensionless

C_P - specific heat, Btu/lb-°F

C_P - surface pressure coefficient = $\frac{p_{local} - p_{amb}}{p_{amb}}$, dimensionless

CPS - cycles per second

C_w - specific heat of water, Btu/lb-°F

D - drag force, lb

d - maximum thickness of airfoil, ft

E - bleed penalty per heating capability, $\frac{hp}{kw}$

EAPS - engine air particle separator

E_m - water collection efficiency, dimensionless

EOT - Energy On Time, sec

fps - feet per second

G - percentage of freezing point depressant in final mixture

g - gravitational acceleration constant, 32.17 ft/sec^2

LIST OF SYMBOLS (Continued)

g/m^3 - grams per cubic meter

h - heat transfer coefficient, $Btu/hr\text{-}ft^2\text{-}°F$

hp - horsepower

in. H_g - inches of mercury

in. H_2O - inches of water

J - Joules constant, 778 ft-lb/Btu

K - water droplet inertia parameter, $2a^2 UY_d/9 C\mu_a g$

K - relative bleed air availability - Btu/hr-shp

K_o - modified inertia parameter $(\lambda/\lambda_s) K$

K^1 - corrected bleed air availability - Btu/hr-shp

k - conductivity, $Btu/hr\text{-}ft^2\text{-}°F$

km - kilometers

kt - knots

L_e - latent heat of evaporation of water, Btu/lb

L_f - latent heat of fusion of water, 144 Btu/lb

L_s - latent heat of sublimation of ice, Btu/lb

LWC - Liquid Water Content, g/m^3

MMH/CA 90% CL - corrective maintenance man-hours that are within 90% of total

MTBF - mean time between failures = $\frac{\text{(flight hours) (quantity)}}{\text{total primary failures}}$

MTBM - mean time between unscheduled replacements = $\frac{\text{total flight hours}}{\text{total unscheduled replacements}}$

MTMA - mean time between maintenance action = $\frac{\text{total flight hours}}{\text{total maintenance action}}$

m - meters

mb - millibars

LIST OF SYMBOLS (Continued)

msl - mean sea level

NRP - normal rated power, percent

n - freezing fraction

P - probability of exceedance

p - partial pressure of water vapor (at t_{se} or t_{∞})

Pr - Prandtl Number = $\frac{kC_p}{\mu}$, dimensionless

psi - pounds per square inch

q - heat rate, Btu/hr

RAS - Real Air Speed

R - free-stream Reynolds number of water droplet, dimensionless

R_w - water catch rate, lb/hr-ft^2 or lb/hr-ft span, as noted in text

R'_w - water runback rate, lb/hr-ft^2

r - recovery factor (0.85 for laminar flow and 0.9 for turbulent flow)

r_i - distance between body point i and flow field point (ξ,η), nondimensionalized by chord length

rpm - revolutions per minute

S/C - fraction of chord length, measured along surface, dimensionless

SHP - shaft horsepower

S_l - lower surface droplet impingement limit

S_u - upper surface droplet impingement limit

$S_{y_{o,l}}/C$ - ordinate value of lower impingement limit, non-dimensionalized

$S_{y_{o,u}}/C$ - ordinate value of upper impingement limit, non-dimensionalized

t - time, sec

LIST OF SYMBOLS (Continued)

TAS	-	true airspeed
T_r	-	recovery temperature, °F
T_{ok}	-	datum temperature (wet air boundary layer temperature), °F
T_{se}	-	skin equilibrium temperature, °F
T_∞	-	ambient air temperature, °F
U	-	free-stream air velocity, ft/sec or kt, as noted in text
U_x	-	x-component of water droplet velocity, ft/sec
V	-	free-stream air velocity, knots TAS or ft/sec as noted in text
V_x	-	x-component of local air velocity, ft/sec
$\bar{v}$	-	local vector difference between velocity of the droplet and velocity of air, ft/sec
w	-	watts
W_a	-	total engine gas generator flow rate
W_{bl}	-	compressor air bleed flow rate
W_f	-	required weight of freezing depressant mixture, by weight
W_m	-	water catch rate, lb/hr-ft span
X	-	percent, by weight, of freezing point depressant in the fluid mixture
X/C	-	fraction of chord length, measured along chord, dimensionless
x_i	-	x-ordinate of body point i, nondimensionalized by chord length
y_i	-	y-ordinate of body point i, nondimensionalized by chord length
α	-	angle of attack, degrees
β	-	local impingement efficiency, dimensionless
ΔP	-	pressure drop
γ_a	-	density of air, lb/ft^3

LIST OF SYMBOLS (Continued)

γ_d - density of water droplet, lb/ft^3

λ/λ_s - ratio of true travel distance of a water droplet in still air to its travel distance in still air obeying Stokes' law.

μ - microns (droplet diameter)

μ_a - viscosity of air, $lb\text{-}sec/ft^2$ or slugs/ft-sec

ρ_a - density of air, $slugs/ft^3$

ρ_w - density of water droplet, $slugs/ft^3$

σ - standard deviation, dimensionless; also ratio of air density at a given condition to air density to standard sea-level conditions

ϕ - impingement parameter = R_u^2/K

ψ - scale modulus = R_u/K

ξ - x distance to a point in the flow field,

η - y distance to a point in the flow field

SECTION 1 INTRODUCTION

In recent years, rotary-wing aircraft have been found increasingly useful in a large number of military activities. These applications include search and rescue of crew members from downed aircraft, transportation of troops outside of combat zones, and airmobile operations. The latter includes the direct participation in action by transportation of troops to and from combat zones, lending fire support, logistics support and cover for ground forces, observation of ground activities, and medical evacuation of wounded personnel. Other services performed by rotary-wing aircraft include mail delivery to remote field stations, utility inspection and repair, and traffic control functions. The widespread use of Army rotary-wing aircraft and the increased emphasis now being placed on all-weather, round-the-clock operation of such craft has made reliable operation in adverse weather conditions an urgent safety-of-flight requirement for all instrument-certified rotary-wing aircraft.

All-weather aircraft must be designed to ensure safe flight in icing conditions and yet not burden overall aircraft performance with unnecessary penalties due to the ice protection system. Thus the effects of ice accretion on aircraft performance and handling qualities must be assessed and balanced against the cost of providing and maintaining a system capable of ice removal or prevention. In assessing the effects of ice accretion on aircraft performance (i.e., drag, stability, vibration level, etc.), one must consider the available engine power margin and percentage of flight hours for which ice protection is necessary. The cost of providing an ice protection system, then, is measured in terms of added aircraft weight, the availability of thermal energy, and the power loss or increased fuel consumption due to use of that energy. Therefore, the icing problem can be examined in terms of (1) flight envelope requirements and (2) aerodynamic performance, handling qualities, and vibration levels as influenced by ice formations on the affected areas.

Rotary-wing aircraft are limited by lower L/D's than fixed-wing aircraft and thus constrained by shorter range capabilities and lower operational ceilings. They are far more sensitive than fixed-wing aircraft to potential self-deployment constraints such as enroute navigation facilities, wind and icing conditions at the intermediate altitudes, cloud cover, and alternate landing/refueling locations. The flight regime of rotary-wing aircraft in clouds with supercooled water droplets or in icing fog is highly conducive to ice accretion.

During rotary-wing operational service in Europe, and particularly in West Germany, the U. S. Army came face-to-face with an urgent need for all-weather capability to increase mission capability and yet not compromise vehicle safety. The topography of some regions of West Germany, for instance, is characterized by substantial changes in terrain elevation and

by rapidly changing local weather conditions that are difficult to forecast. The combination of low ceiling, icing conditions in the clouds, and terrain features obscured by clouds presents difficult flying problems, as a result, there can be expected to be no flying for as many as 55 days during winter months (depending upon the minimum allowable flight ceiling) if no ice protection is provided.

Whereas the engine and engine inlet ice-protection requirements and design practices for rotary-wing aircraft are not appreciably different from those of fixed-wing aircraft, blade icing does introduce special problems. The blade icing occurs despite centrifugal forces, rapidly degrading the aerodynamic efficiency of the blade and creating a serious condition of unbalance and vibration due to unsymmetrical ice shedding. It follows that for most, if not all, helicopters, flight in icing conditions of moderate intensity is not feasible without ice protection to ensure blade balance and aerodynamic efficiency.

It is the purpose of this report to address itself to the icing problems of rotary-wing aircraft and the techniques required to solve these problems. Particular attention is given to the hazards of flying in icing conditions and to an in-depth investigation of meteorological conditions associated with low-altitude flight. Other aspects presented in this report include calculation of ice accretion rates, determination of the adequacy of existing ice protection techniques and optimum application of these techniques (based on weight, performance penalties and reliability considerations), determination of capabilities and limitations of adverse weather protection installations on rotary-wing aircraft, and exploration of airborne icing instrumentation methods. Finally, the direction for appropriate research and development efforts to overcome identified deficiencies and problems is delineated.

SECTION 2 HAZARDS OF FLYING THROUGH ICE

This section reviews operational data and flight test experience with various helicopters under natural and simulated icing conditions. It is shown that flight safety can be compromised to an unacceptable degree without provisions for adverse weather protection on the vehicle. Available accident statistics are reviewed, and finally, components are discussed that require ice protection as revealed by flight test experience.

2.1 FLIGHT EXPERIENCE

2.1.1 Review of Operational Data

Experience of the U. S. Army in Europe

Among the significant factors that contributed toward launching this investigation for advanced rotary-wing aircraft is the severe operational restriction experienced by the U. S. Army in the European theater with helicopters that lack all-weather capability. The problems and consequences resulting from this lack of all-weather capability are brought to light in an Army letter.*

1. "U. S. Army helicopters do not possess a deicing or anti-icing capability. This is a significant deterrent to helicopter operations in the European theater.

2. "Weather phenomena in Germany are said to be more unpredictable than in most other parts of the world. This is primarily due to the combination of latitude and longitude and the west to east Alps range relative to the predominate maritime winds. This situation causes rapidly changing weather conditions. Isolated local weather phenomena are difficult to forecast and aviators are often caught in these local conditions.

3. "Assuming that helicopters are prohibited from flying when ceilings are less than 1500 feet, (due to icing conditions), a total of 55 days during October-March can be expected to be non-flying. If helicopters were equipped with a deicing system capable of handling at least light ice, it is probable that weather conditions on 30 of these 55 days could be considered acceptable for flying. These data, of course, are not conclusive because they are based on assuming an altitude ceiling that may be conservatively high when compared to rigorously derived future requirements; however, they do provide limited justification for requiring helicopters to have a deicing capability.

*Letter AEUTAVG-6 from 15th Aviation Group (Combat) APO 09025 to Commander in Chief USAREUR and Seventh Army (Attn: Aviation Safety Officer), Subject: "Helicopter Deicing System," dated 12 May 1970.

4. "The topography of West Germany is characterized by severe changes in terrain elevation. The combination of low ceiling, icing conditions in the clouds and terrain features obscured by clouds, presents difficult flying conditions. In many cases, the aviator is forced to abort the mission and land or return to home station. In most cases, an aviator piloting an aircraft equipped with deicing equipment could continue the mission by climbing into the clouds. Currently the only action a helicopter pilot can take against icing is to avoid the region characterized by this adverse combination of weather and terrain features.

5. "Increased mission capability, plus safety considerations clearly establish the need for helicopter deicing capability. Once a system is developed, priority should be given to modifying helicopters in Europe, if practical, or assigning new helicopters with this capability to Europe."

The rotary-wing operational problems in icing conditions are aggravated, no doubt, by local weather changes in West Germany but are by no means unique to Europe. However, it is the U. S. Army in Europe that focused attention on this problem to promote awareness of the magnitude of operational limitations imposed by the lack of true all-weather capability on rotary-wing aircraft and to initiate plans for corrective action.

Pertinent Information From Other Sources

At the International Helicopter Ice Protection Conference (Ottawa, May 24-26 1972), an audience discussion regarding the necessity of ice protection for helicopters yielded the following pertinent information:

1. New York Airways is shut down an average of one day/month in the winter due to forecast icing, and they have been shut down as long as three consecutive days.

2. The Canadian Navy finds its operations restricted 25 percent of the time off the coast of Nova Scotia in the winter.

3. Approximately 7 percent of the helicopter training flights in the United Kingdom are curtailed due to forecast icing.

4. Many Russian rotorcraft are provided with ice-protection equipment. Therefore, considerations related to maintaining parity would dictate all-weather capability for U. S. Army airmobile operations.

5. The Canadian Armed Forces are equipping 37 S-61 Sea Kings with rotor ice-protection at a cost of 3 million dollars.

6. Snow ingestion is turning out to be an unexpectedly serious problem as a cause for engine flameouts.

7. Light helicopters are quite power limited, and thus are sensitive to drag changes on the rotor system due to ice buildup.

8. Larger helicopters are not as sensitive to drag changes but are more sensitive to vibration and damage due to uncontrolled ice shedding.

The preceding summary of rotary-wing aircraft experience under adverse weather conditions infers the potential operational benefits inherent from equipping such vehicles with all-weather capability.

2.1.2 Flight Profile Considerations

Ice accretion on aircraft surfaces is associated with flight at speeds slower than Mach 0.9 through subfreezing clouds of supercooled water droplets (which usually occur from sea level to 20,000 feet). Since the rotary-wing aircraft's flight regime is well within the constraints of this icing envelope, flight profile details must be examined to assess the impact of all-weather capability on operational considerations. Flight in icing conditions implies flight in clouds with visibility restricted to 100 to 200 feet (even for moderate to light icing). Therefore, it is unlikely that the direct combat segment of the mission will be carried out under icing conditions. For a ferry flight, it is also likely that it will be possible to select a cruise altitude where icing can be avoided. Mission aspects of rotary-wing flight which would be most concerned with the needs for adverse weather capability include:

1. Takeoff and landing, including autorotation

2. Climb and descent

3. Low-altitude flight from base to target

4. Deliberate evasive flight (or hiding) in clouds

For those phases of flight where it is unlikely that icing can be avoided, the question then arises:

Will the time that must be spent in an icing condition cause a flight safety problem? The answer to this question is related to the consideration of three factors:

1. The total time spent in icing during the sensitive flight modes

2. The horizontal and vertical extent of the icing condition (the probable time spent in icing relative to the mission time)

3. The sensitivity of the rotorcraft (and its components) to the total accumulation of ice which is likely to occur.

Representative mission times for the critical flight periods for several types of missions are shown in Table I. Based on the data in Table I it appears that the maximum duration of rotorcraft icing encountered during airmobile operation may last up to one hour under "idealized" severe icing conditions. Considering the nonuniformity of natural icing clouds and the rapid variation in liquid water content (LWC), a maximum equivalent icing duration between one-half and one hour under maximum continuous icing conditions is probably more realistic.

TABLE I. TYPICAL ROTORCRAFT LOW ALTITUDE FLIGHT CONDITIONS

Mission	Time (min)	Distance (mi)
Reconnaissance		
Takeoff and Landing	3	0
Climb and Descent*	2	3/4
Low-Altitude Flight	24	60
Antimechanized		
Takeoff and Landing	3	0
Climb and Descent	2	3/4
Low-Altitude Flight	27	85
Attack Mission 1		
Takeoff and Landing (Main Base)	3	0
Climb and Descent	2	3/4
Low-Altitude Flight**	16	20
Takeoff and Landing (Forward Base)	3	0
Climb and Descent	2	3/4
Low-Altitude Flight**	16	20
Attack Mission 2		
Takeoff and Landing (Main Base)	3	0
Climb and Descent	2	3/4
Low-Altitude Flight**	17	17
Takeoff and Landing (Forward Base)	3	0
Climb and Descent	2	3/4
Low-Altitude Flight**	15	16
Takeoff and Landing (Forward Base)	3	0
Climb and Descent	2	3/4
Low-Altitude Flight**	26	20

* Rate of Climb = 1200 - 1500 fps
Rate of Descent = 2600 fps

** Includes hover while sighting and firing on targets

2.1.3 Rotor Unbalance and Vibration Due to Icing-Analytical Results

Before reviewing the flight test experience associated with flight of rotary-wing aircraft in icing, a theoretical analysis was conducted in an effort to yield a better understanding of the problems and consequences resulting from ice accretions on an unprotected rotor. The analysis was conducted in

three steps to determine (1) the degree of helicopter rotor unbalance due to ice shedding, (2) the criteria for self-shedding of ice accretions from rotor blades, and (3) the vibration levels induced by unsymmetrical ice shedding.

Rotor Unbalance Due to Self-Shedding

Potential unbalanced forces for a four-blade rotor system due to natural (noninduced) shedding of ice from the main and tail rotors have been calculated. These are plotted in Figure 1, showing the force developed as a function of the spanwise length of blade ice which is shed after varying times in the clouds without icing protection. Based on these forces, the vibration response of the structure was determined on a high-speed computer. The vibration response at the crew stations for the following assumed configurations is shown in Figure 2.

1. Ice sheds from the outer 2 feet of one main rotor blade after 10 minutes in the icing cloud.

2. Ice sheds from the entire length of one main rotor blade (from root to tip) after 10 minutes in the clouds.

3. Ice sheds from the entire length of one tail rotor blade after 3 minutes in the cloud (higher centrifugal forces cause shedding in less time than for the main rotor).

The results show that the vibration level produced by the tail rotor blade, shedding ice completely (3), is the most severe. Levels as high as 1.59 g at 20.7 cps are indicated. The main rotor causes 0.15 to 0.25 g at 4.1 cps when one blade is cleared over its entire length. If only the outer 2 feet of a main blade is cleared, the response at the crew station is only 0.04 g at 4.1 cps.

The effect of these vibration levels on the crew performance is also shown in Figure 2, which was obtained from the Shock and Vibration Handbook (Reference 1). These data show that intolerable levels would be generated at the crew stations if the extreme assumption is made that either rotor would shed a full span of ice accretion from one blade. It is recognized that for the random shedding pattern occurring under actual flight conditions, instantaneous shedding of a full span of ice from a blade is extremely remote. Therefore, for this case the results may be viewed as a theoretical extreme rather than being representative of actual flight in icing.

Rotor Ice-Shedding Criteria

An analysis has been conducted on rotor shed characteristics and allowable ice thickness versus "g" level. Reference 2 contains information on adhesive properties of ice as a function of bond temperature. Excerpts from

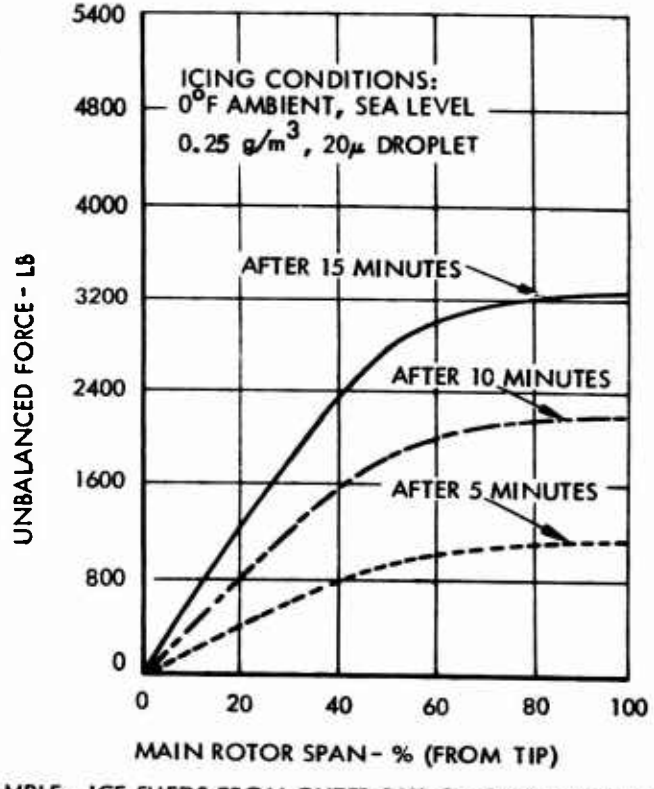

EXAMPLE: ICE SHEDS FROM OUTER 20% OF ONE MAIN ROTOR BLADE AFTER 10 MINUTES IN ICING CLOUD AND RESULTS IN 800 POUNDS OF UNBALANCED FORCE

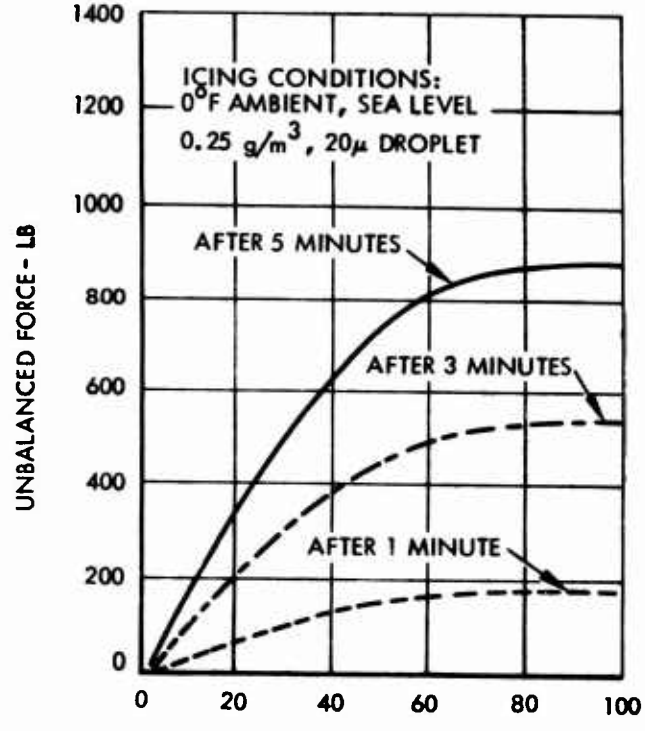

EXAMPLE: ICE SHEDS FROM OUTER 20% OF ONE TAIL ROTOR BLADE AFTER 3 MINUTES IN ICING CLOUD AND RESULTS IN 208 POUNDS OF UNBALANCED FORCE

Figure 1. Rotor Unbalanced Due to Self-Shedding.

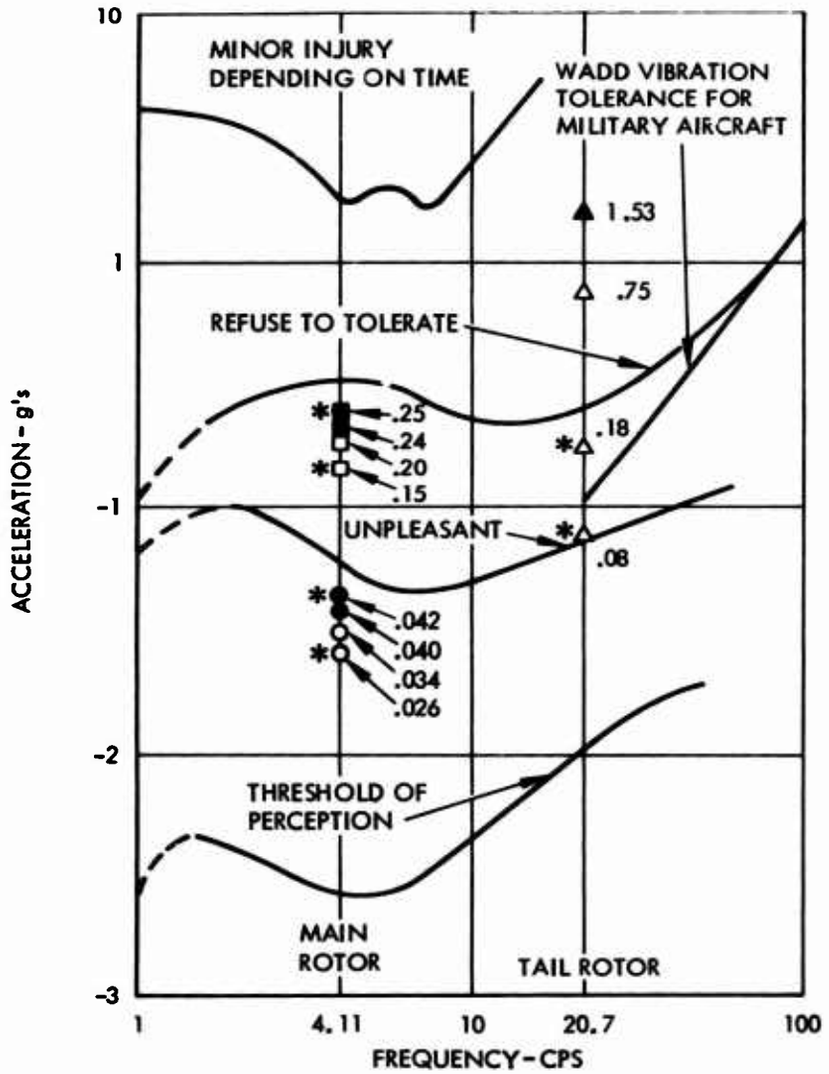

ASSUMED NATURAL ICE-SHEDDING CONFIGURATIONS:

- O OUTER 2 FT OF ONE MAIN ROTOR BLADE AFTER 10 MINUTES.
- □ ONE MAIN ROTOR BLADE FROM HINGE TO TIP AFTER 10 MINUTES.
- △ ONE TAIL ROTOR BLADE FROM SHANK TO TIP AFTER 3 MINUTES.
- * 90° OUT OF PHASE
  OPEN - PILOT
  SOLID - GUNNER

SOURCE OF HUMAN TOLERANCE DATA:
SHOCK & VIBRATION HANDBOOK, VOL 3 BY HARRIS & CREDE, 1961
McGRAW HILL

Figure 2. Human Vibration Tolerance Data.

this information have been replotted as Figure 3. As expected, the shear force required for its removal increases with decreasing temperature. Also shown on this figure is the standard deviation of removal force (versus temperature). Sixty-three percent of the sheds would occur within ±1 standard deviation (σ), and 95 percent would occur within $\pm 2\sigma$. Based upon the mean shear strength, an analysis was performed to determine the "critical" ice buildup for self-shedding when the centrifugal force equals the shear force. The results of this are shown in Figure 4 for a main rotor, and in Figure 5 for an antitorque rotor. Figure 4 was prepared for a rotor rpm of 250 (a tip speed of approximately 660 fps at 50 feet diameter), and Figure 5 was prepared for a tail rotor speed of 1240 rpm. Comparing the two figures, the "critical" ice thickness for the tail rotor is one-fifth that for the main rotor at equivalent rotor stations (root-to-root, tip-to-tip, etc.) and the same temperatures.

Typically, ice will shed more frequently from the tip areas due to the higher centrifugal force and higher equilibrium temperature. It is also apparent that, even considering the scatter in the shear strength, it is unlikely that a whole blade would shed at once.

The ice thicknesses determined above can be compared with an "acceptable" thickness based upon a rotor imbalance criteria of 0.1 g, which would be a barely tolerable vibration level value for short time exposure.

Vibration Levels

First order estimates have been made of vibration levels associated with asymmetric ice shedding, and the results are shown in Figures 6 through 8. Figure 6 shows the vibration level for a four-blade main rotor, assuming that various amounts of ice are shed from the outer half of one blade.

The vibration level is a function of the unbalanced weight, rotor assembly weight, location of the rotor with respect to the center of gravity (cg) of the aircraft, the moment of inertia of the aircraft, the damping characteristics of the structure, and the rotor speed. To simplify the analysis, the cg of the aircraft was assumed to be stationary and the fuselage was assumed as a rigid body. The maximum vibration level, in terms of g's, occurs at the rotor assembly and linearly reduces to zero at the cg. At any other location, the vibration level is proportional to the maximum level by the ratio of the distance from the location to the cg to that from the rotor to the cg.

The most critical unbalance case will be for the ice shed completely on one blade of the rotor while the other blades remain unshed. However, as observed earlier, this condition is considered to be highly unlikely and has not been observed during any flight tests. Therefore, the case analyzed for the main rotor has ice shed only on the outer half of one blade. As for the tail rotor, the effects of ice shed from both the outer half and one whole blade were calculated.

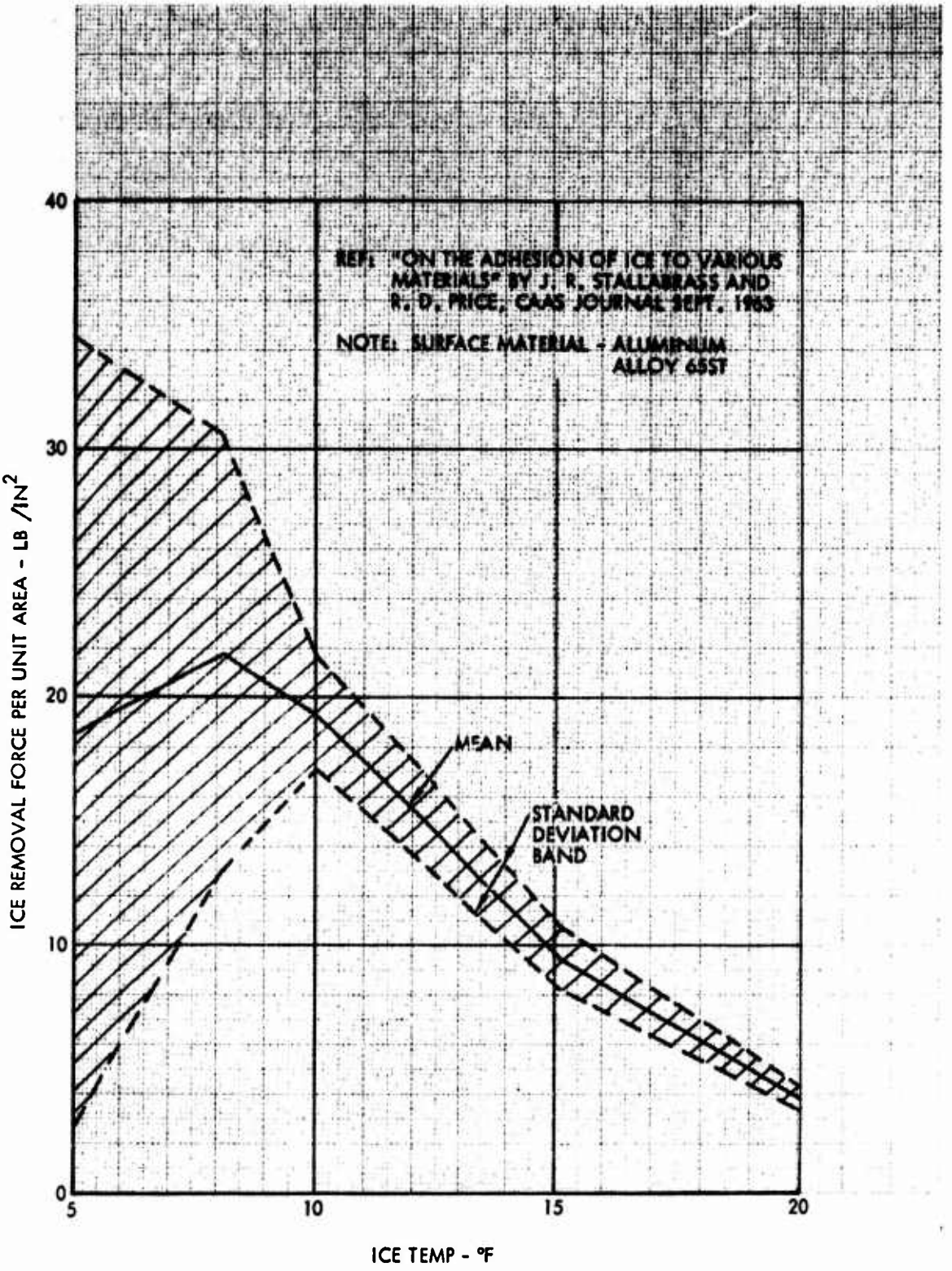

Figure 3. Shear Strength of Ice.

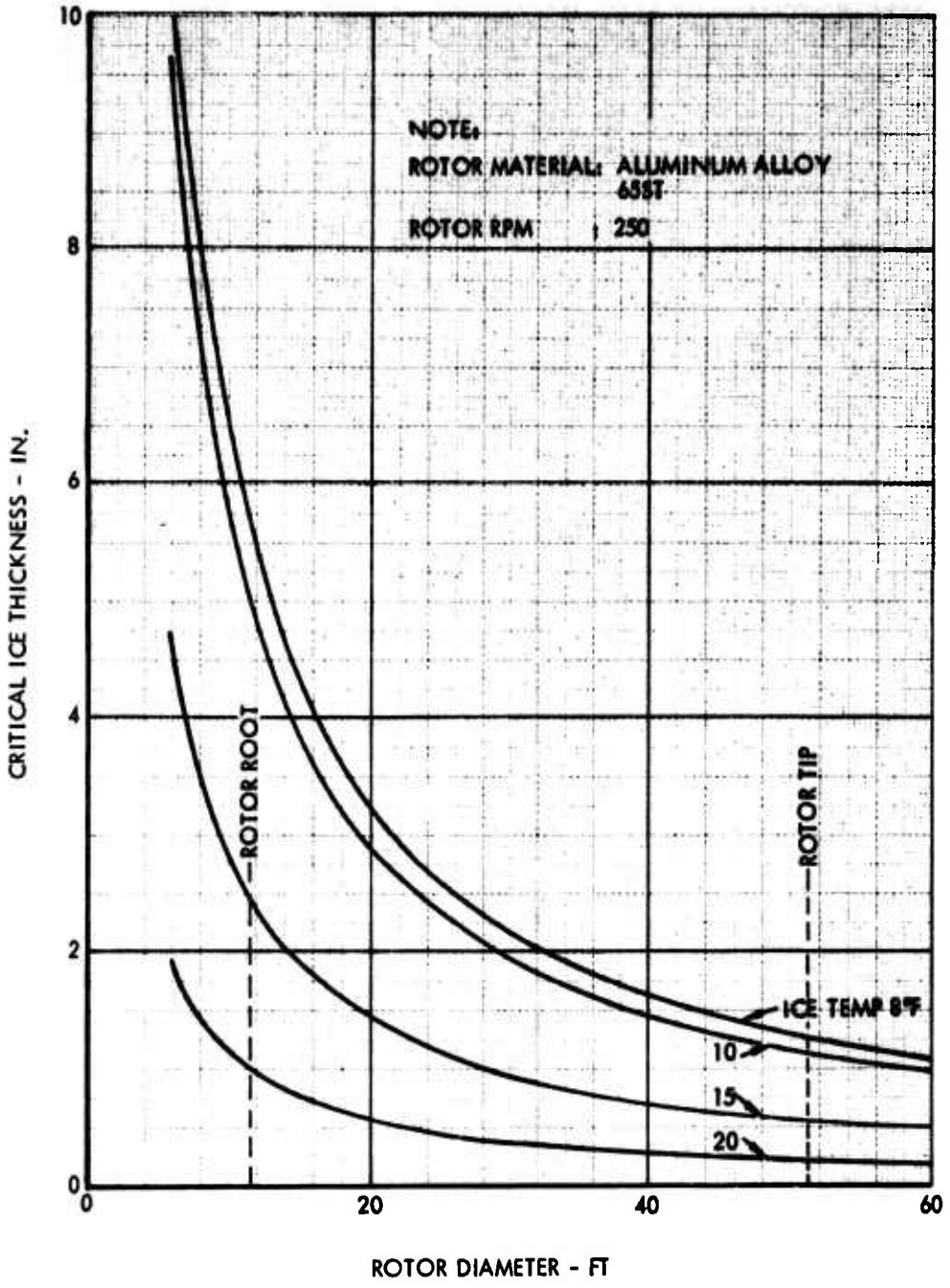

Figure 4. Self-Shedding Critical Ice Thickness, Main Rotor.

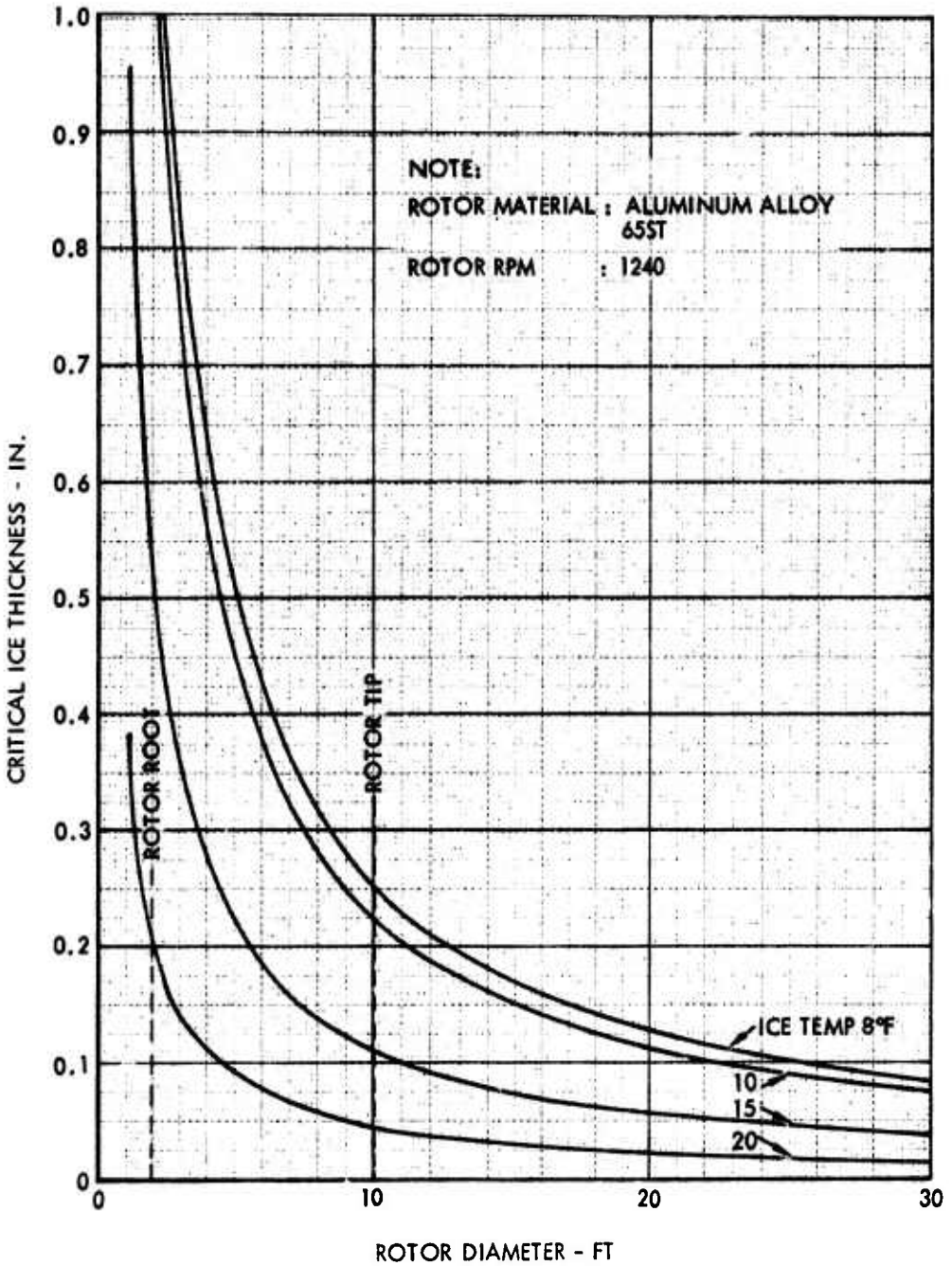

Figure 5. Self-Shedding Critical Ice Thickness, Tail Rotor.

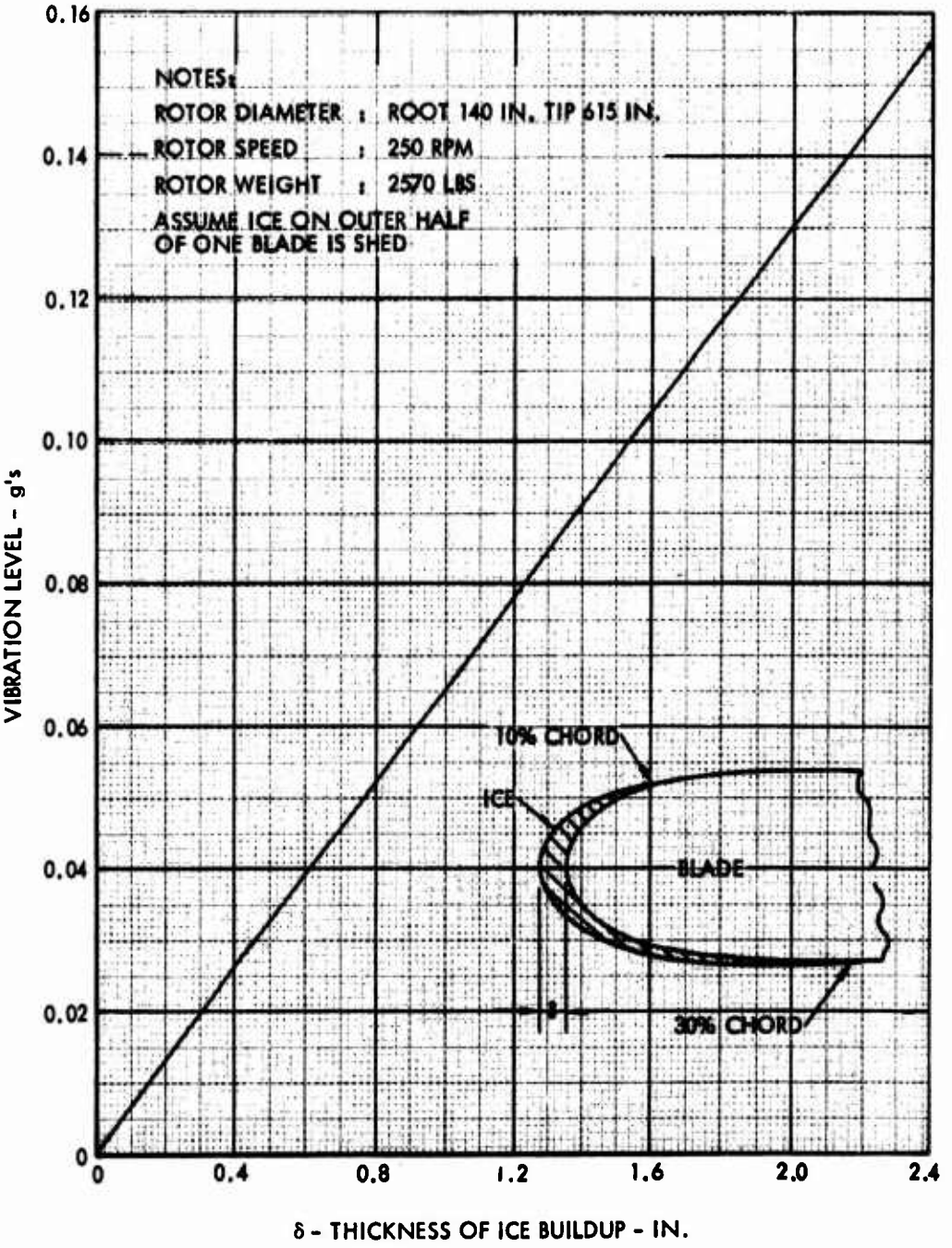

Figure 6. Vibration Level Due to Ice Shed, Four-Blade Main Rotor.

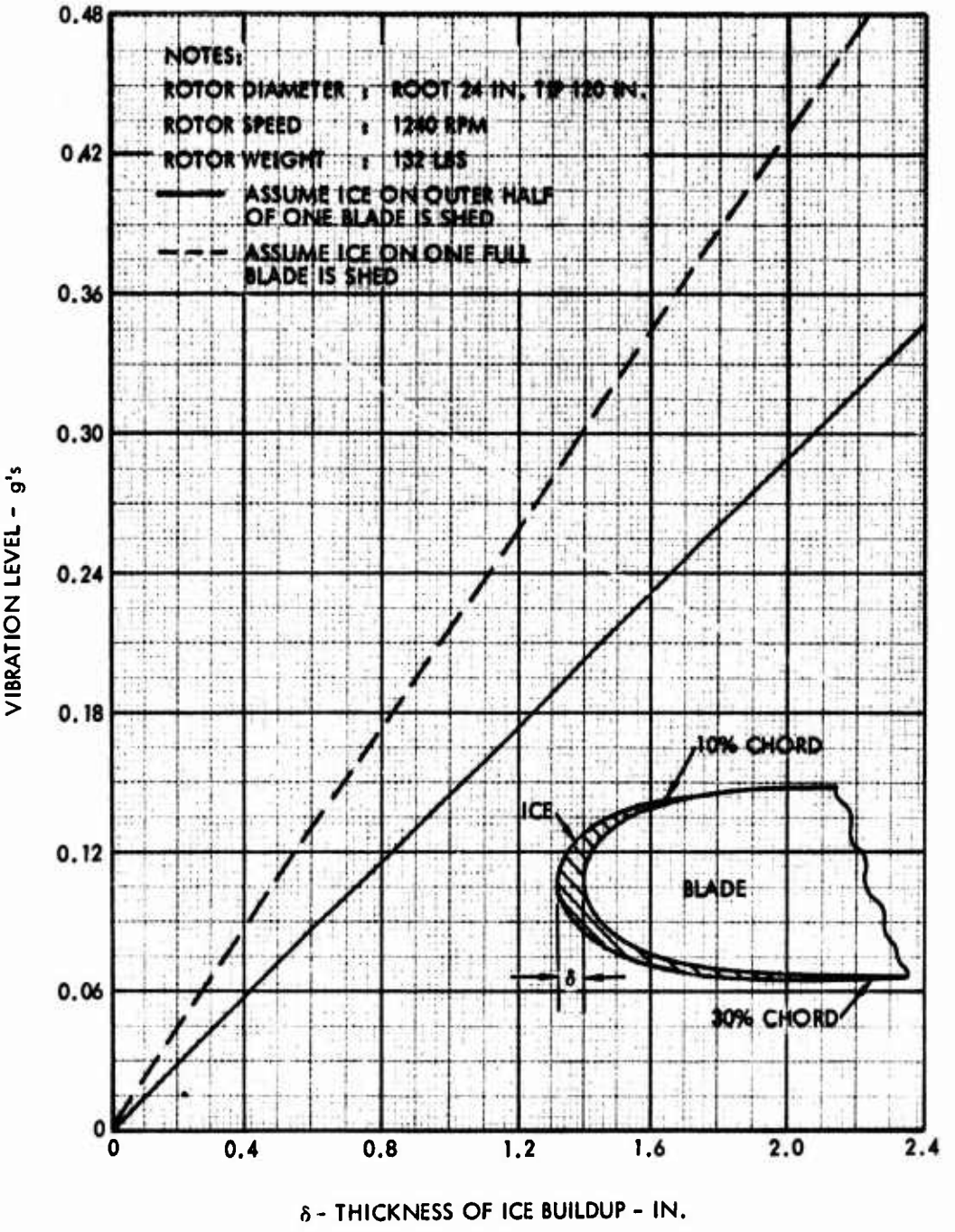

Figure 7. Vibration Level Due to Ice Shed, Four-Blade Tail Rotor.

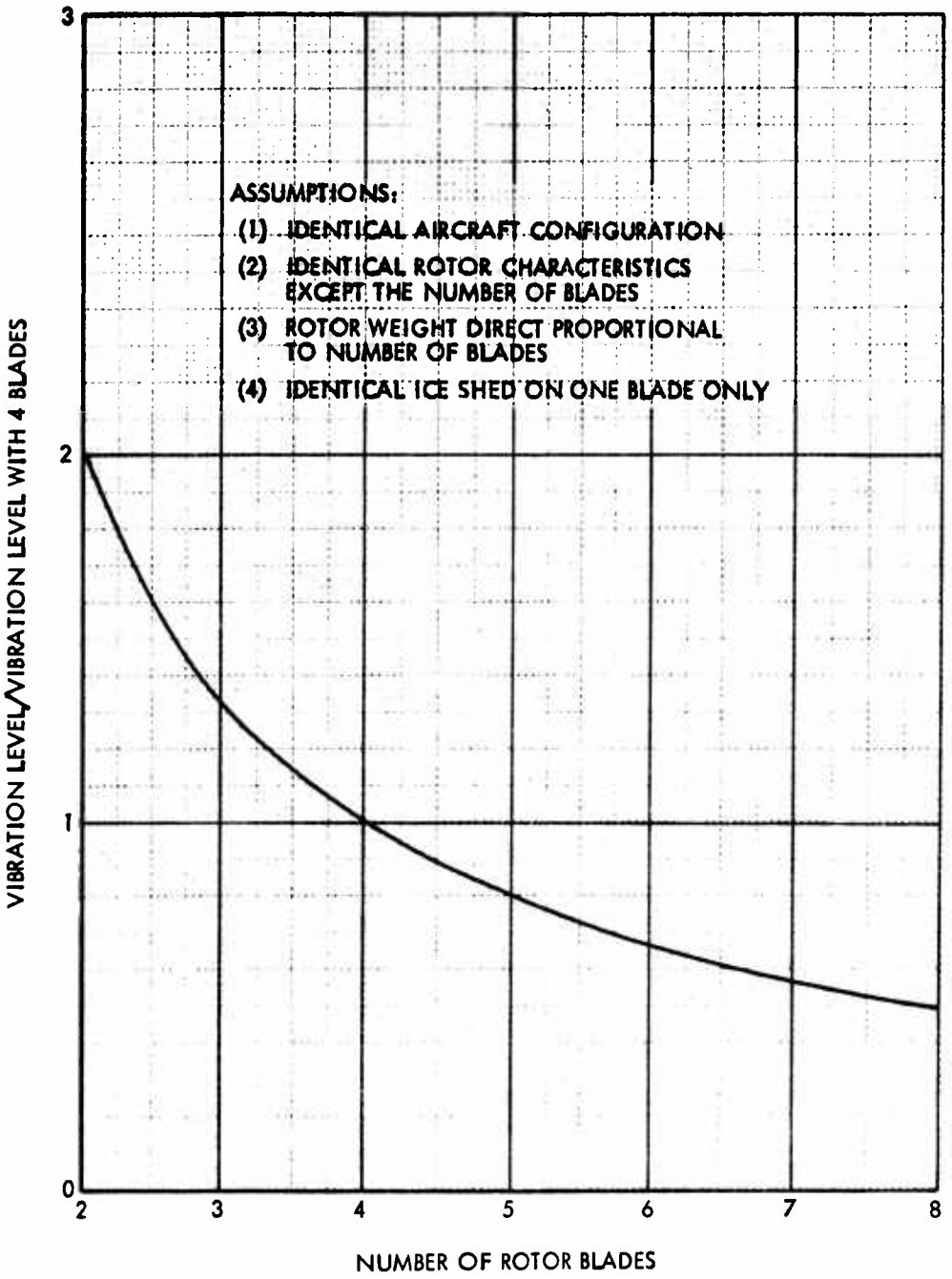

Figure 8. Effect of Blade Number on Vibration Level.

The vibration levels, shown in Figures 6 and 7, are the maximum values occurring at the rotor assembly. The level which can be felt in the cockpit depends upon the relative location of the cockpit with respect to the center of gravity of the aircraft. For example, on one aircraft, the vibration produced by the tail rotor is attenuated approximately 46 percent at the copilot's station and only 30 percent at the pilot's station.

Vibration levels are influenced by the number of blades, as shown in Figure 8. As expected, the vibration level decreases with an increasing number of blades (for a constant rotor mass) since the unbalance represents a smaller percentage of the mass. It is difficult to compare the absolute effects among rotors with different numbers of blades since the rotors are designed for different aircraft configurations. In order to have a meaningful comparison, the calculation is assumed for the same aircraft fitted with different rotor assemblies which differ only in the number of blades with a proportional change in rotor weight. The results are shown in Figure 8.

Figure 9 shows tolerable vibration levels based upon the human factors criteria of Reference 3. Unbalance allowables from a fatigue standpoint are approximately .035 g, and the short term structural allowables are approximately 0.1 g. Thus, the crews are more limiting than the structure for vibration and represent a fortunate operational safety factor.

While the self-shedding configurations assumed in the analysis may not be precisely representative of the actual random ice-shedding pattern occurring under flight test conditions, the analytical results are very useful as a guide to the designer in assessing the magnitude of the problem and deciding whether ice protection provisions are required for the rotor blades. Based on the results presented herein, it has been concluded that for cases wherein ice shedding is induced solely by centrifugal forces, an ice protection system is required to control the shedding pattern, and thus ensure that blading balance is maximized. In this manner vibration can be held to levels that can be tolerated by the crew.

2.1.4 Results of Flight Tests in Icing Conditions

The Icing Helicopter Spray Rig of the National Research Council of Canada (NRC) at Ottawa offers the most suitable ground test facility to experimentally evaluate the sensitivity of rotary-wing aircraft to ice accretions. The facility can accommodate helicopters to a 55-foot blade diameter. Although the cloud width at the spray nozzles is 75 feet, the cloud contracts at the helicopter hover location to approximately 40 feet. Therefore, for vehicles with a blade diameter larger than 40 feet, judicious interpretation of test results is required. The icing tests are conducted at the prevailing local ambient temperature, and the droplet size can be varied within the 30 to 60 micron range at a liquid water content (LWC) of up to 0.9 gram/cubic meter.

More expensive and/or time-consuming alternatives to hover icing tests at the Ottawa spray rig are helicopter flight tests in simulated icing condi-

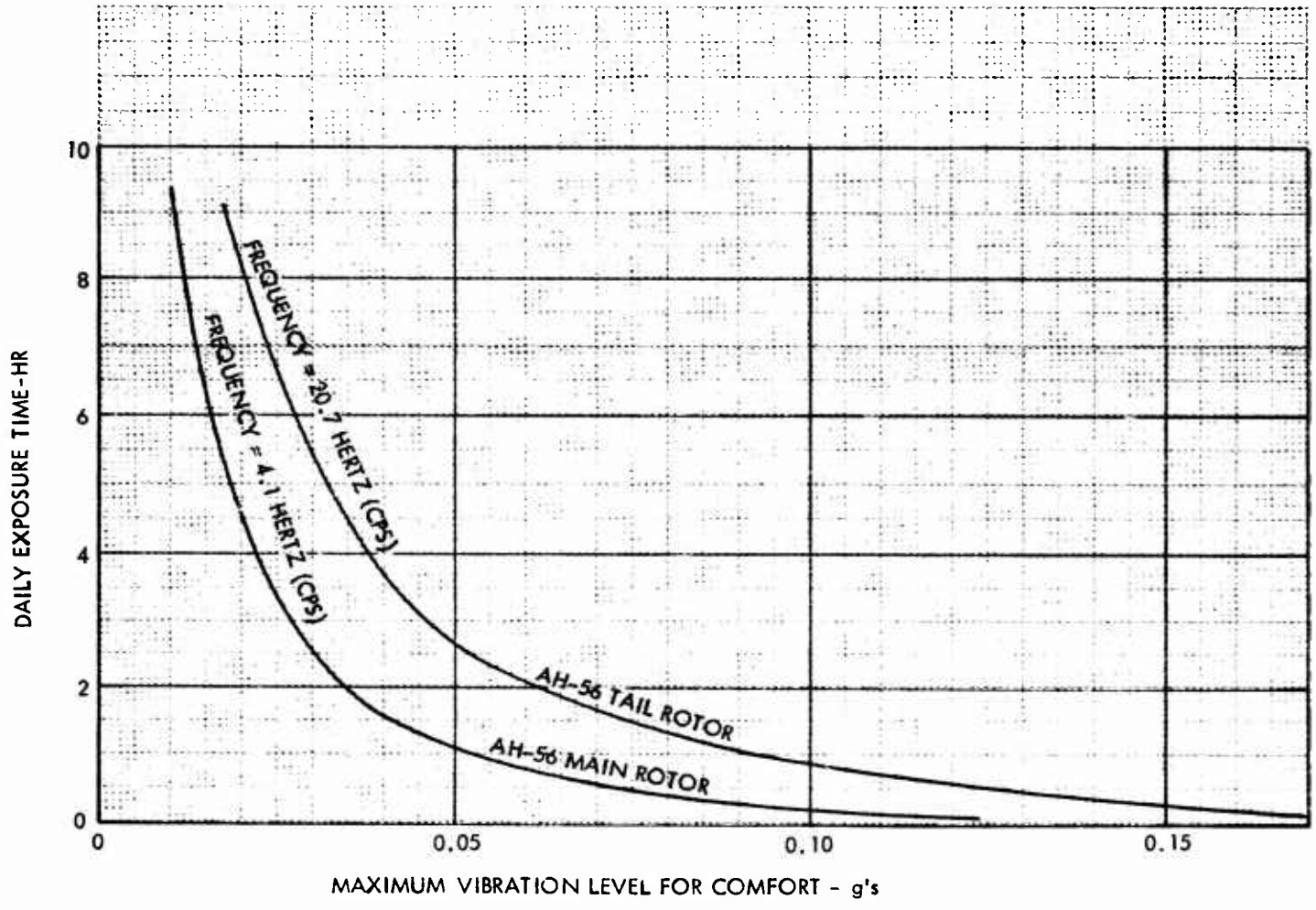

Figure 9. Daily Exposure Time vs Maximum Vibration Level For Comfort.

tions behind an aircraft-tanker or flight tests under natural icing cloud conditions.

References 4 and 5 which report on flight tests of unprotected rotor systems for the Bell HTL-4 and the Sikorsky HO4S-2 at the Ottawa Spry Rig have been reviewed.

Bell HTL-4 Icing Tests

The Bell vehicle had a 35-foot main rotor diameter, a 300-hp Franklin engine, and an all-up weight of 2,180 pounds (includes pilot and observer). Figure 10 is a typical plot from Reference 4, showing the increase in horsepower required while accreting ice; Figure 11 shows the associated ice thickness distribution at the time of landing. At the time these tests were made (1955), NRC did not have a calibration of the icing cloud parameters for the spray rig; thus the only meteorological parameter reported is an ambient temperature of 12°F. In addition to hover tests in the spray rig, five autorotational descents were made with sufficient ice on the blades to make hovering flight marginal without ground effect. The rate of descent was increased as much as 30 percent because of a near-critical ice accretion on the blades (where a critical ice accretion was defined as one just sufficient to make hovering impossible out of ground effect at maximum engine power). Vibrations of an uncomfortable nature were encountered on about a third of the flights (mostly at the higher temperatures). On two occasions they were of sufficient severity to prompt the pilot to discontinue the tests. Generally, the onset of noticeably higher levels of vibrations coincided closely with the event leading to termination of flight (the requirement for full throttle accompanied by a decrease in rotor speed). From Figure 11, it is noted that all of these adverse effects occurred with less than 1/8 inch of ice on the main rotor system, and Reference 4 concluded that "the performance of this type of helicopter is extremely susceptible to small amounts of rotor blade icing over a wide range of conditions."

Sikorsky HO4S-2 Icing Tests

The Sikorsky helicopter had a 53-foot main rotor diameter, a 550-hp Pratt and Whitney Wasp engine, and a design gross weight of 6,490 pounds (some flights were made with takeoff weights up to 7,200 pounds. Figure 12 is a typical plot from Reference 5, showing the increase in power requirements as a function of time. About every 6 minutes there would be typically an abrupt decrease in power required as a result of some shedding (the minor variations are due to wind gusts). Since this aircraft had a larger power margin than the Bell machine, it was possible to achieve flights of up to 1 hour duration at the higher ambients and wind speeds due to frequent self-shedding. (Had no self-shedding occurred, little more than 6 minutes of flight would have been possible due to a limitation of 33.8 inches Hg manifold pressure.) However, the level of vibration rose to such an extent on several occasions that the flight had to be terminated for structural considerations. The most severe vibrations were attributed to asymmetric

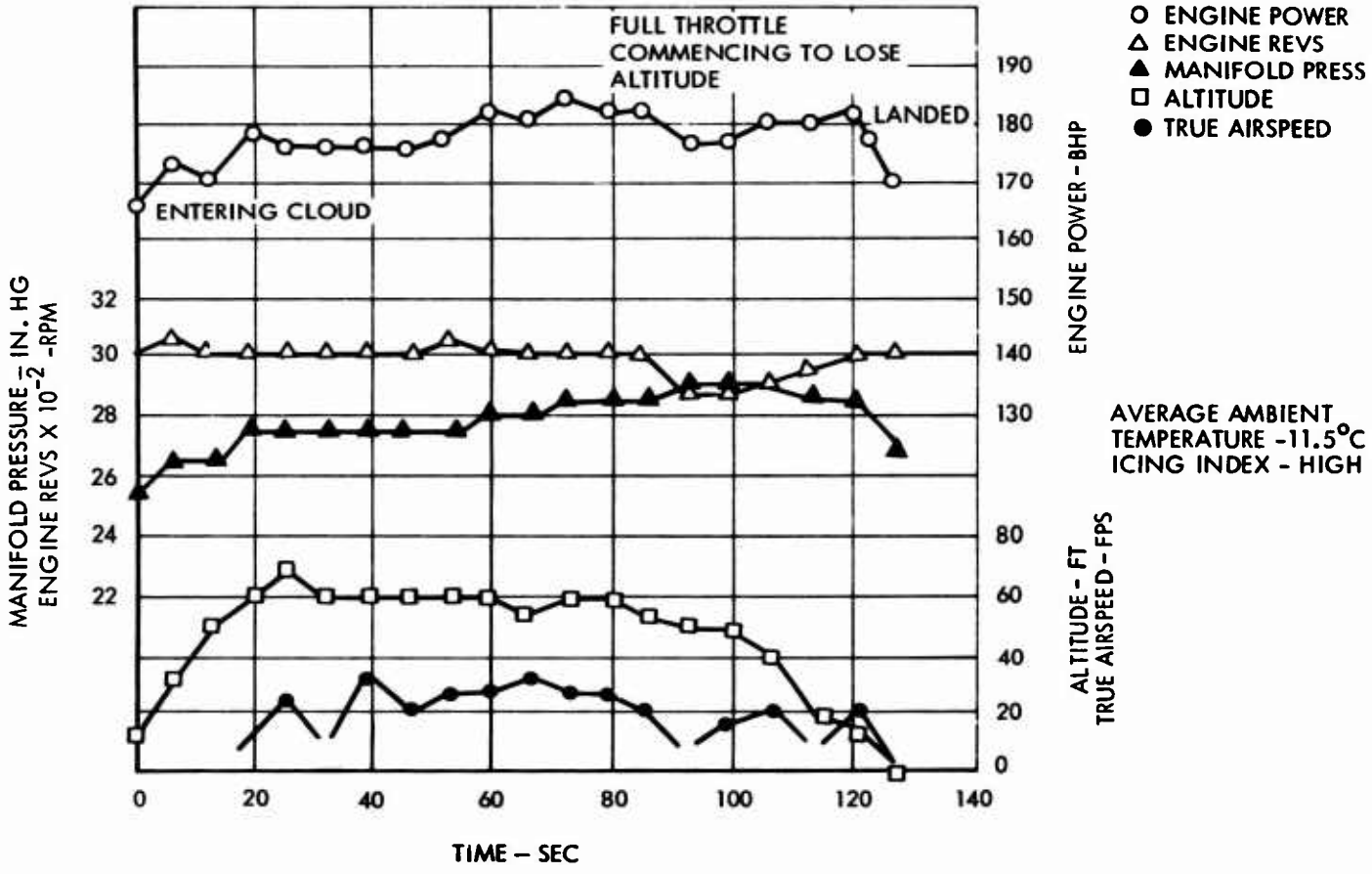

Figure 10. HTL-4 Flight and Engine Operating Parameters During Icing Tests, Flight 11-18.

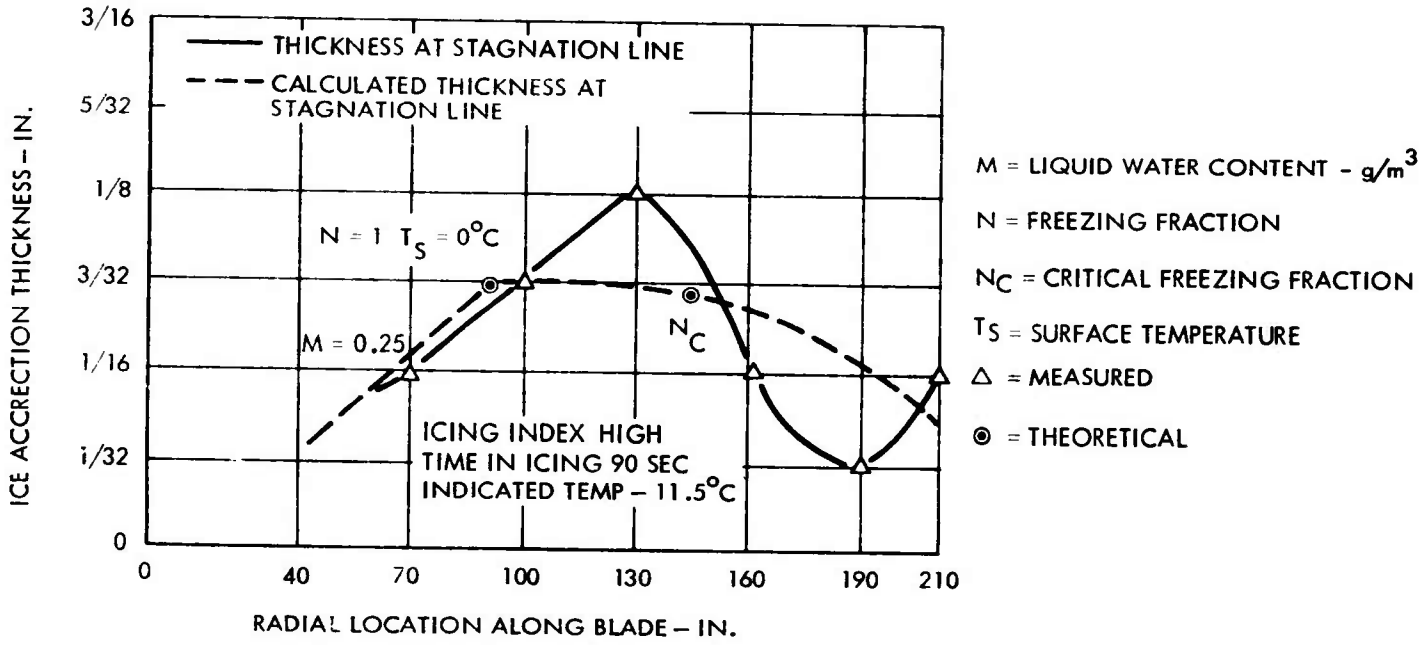

Figure 11. Ice Accretion Characteristics of a Bell HTL-4 Helicopter, Flight 11-18.

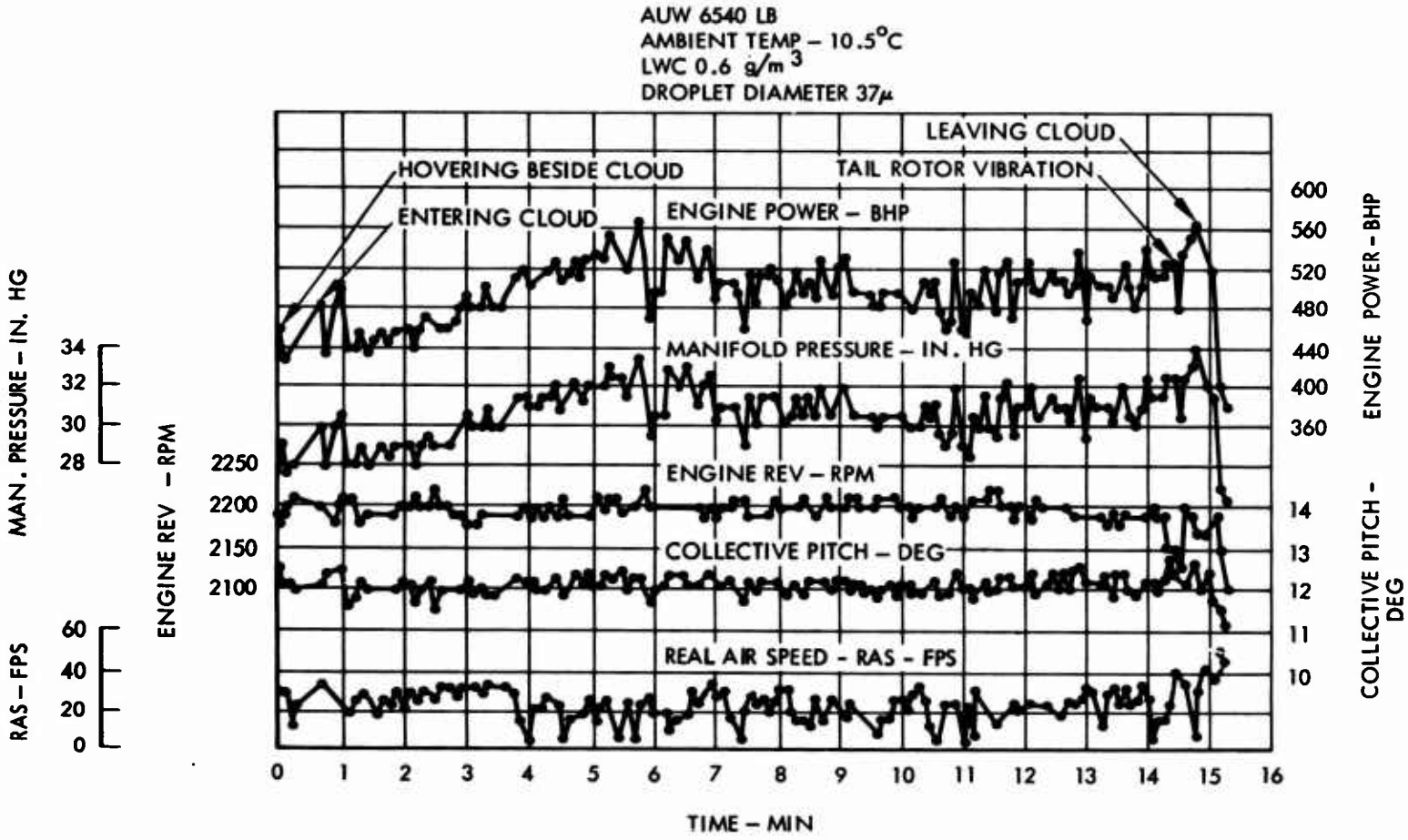

Figure 12. HO4S-2 Flight and Engine Operating Parameters During Icing Tests, Flight 33.

self-shedding of ice from the tail rotor. Unbalance of the main rotor blades did not appear to produce vibrations of an excessively unpleasant nature, owing to the low frequency (about 3 cps) and the fact that asymmetry was never excessive. Greater asymmetry of self-shedding, on the other hand, occurred from the tail rotor. One flight was discontinued when a momentary violent loss of control occurred, during which the helicopter plunged sideways out of the cloud before control was regained.

While no evidence was obtained as to the exact cause of this control loss, two explanations were: (1) early onset of blade stall aggravated by wind gusts; or (2) some ice accreting on the sloppy link of the main servo and subsequently removed by the ensuing motion of the controls. On one occasion, ice thrown from the tail rotor self-shedding had struck and dented the port stabilizer. At the completion of a number of icing flights, some difficulty was encountered with the droop stops on shutting down. With the centrifugal weights of the droop stop mechanism in their extended position in flight, even a light ice accretion on parts of the mechanism prevented full engagement of the stops when rotor rpm was reduced before shutting down. A certain amount of stick stirring by the pilot, however, would overcome the problem. Autorotational descent tests confirmed the 30 percent increase in descent rate observed with the Bell aircraft.

Kaman HU2K-1 Icing Tests

The HU2K-1 helicopter was tested in the Ottawa Spray Rig during December 1960 (Reference 6). The aircraft had a 1/2-inch mesh screen covering the engine inlet. This screen iced very rapidly. The inlet system had alternate blow-in doors that automatically open when the plenum pressure reaches a -10 in. H_2O (of which approximately 6 in. H_2O is due to ice). As seen from Figure 13, this would occur within two minutes. Icing of the pitch locks and droop stops was also a problem. The test aircraft was fitted with a wire embedded heating element in a neoprene rubber blanket for the rotor blades, but a number of runs were made with the system off. The self-shedding ice from the blades did cause damage. Some bad and many small tail rotor dents were caused by ice shedding from the main rotor, and a few dents were made in the main rotor from ice shed from the tail rotor. Some of the dents were severe enough to require blade replacement. Asymmetric tail rotor shedding also caused heavy vibrations, although vibrations from the main rotor were not felt to be serious.

Sikorsky HH-53C Icing Tests

Reference 7 reports Category II icing tests on the HH-53C helicopter in 1971. These tests were conducted behind a KC-130 tanker and in natural icing. For this aircraft (about 30,000 pounds gross weight), vibration levels due to ice accretion on the blades were acceptable, but there was repeated damage to the tail rotor from ice shed from the main rotor. Damage to the main rotor from tail rotor shedding was mimimal.

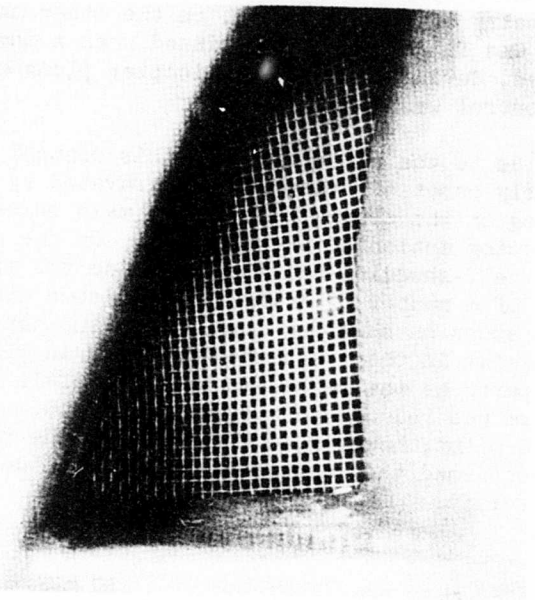

SCREEN ICE SUFFICIENT
TO CAUSE BLOW-IN
DOOR TO OPEN

RUN 7-2
TEMP -7.1° C
L.W.C. 0.5 gm./m.^{3}
TIME IN ICING 2 min.

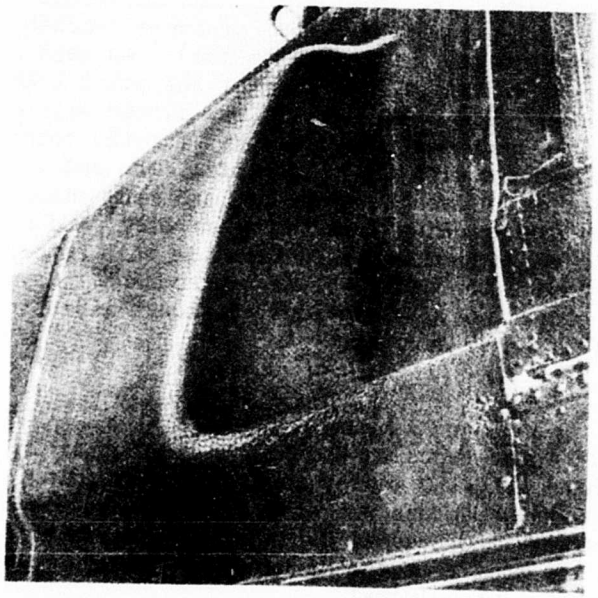

HEAVY SCREEN ICING

RUN 6-4
TEMP -11.0° C
L.W.C. 0.5 gm./m.^{3}
TIME IN ICING 21 1/4 min.

Figure 13. Kaman HU2K-1 Engine Inlet Screen Icing.

Lockheed AH-56A Icing Tests

These tests were conducted at the Ottawa Spray Rig in February 1969 and are documented in Reference 8. The presence of rotor blade ice buildups was readily detectable by the pilot since it was evidenced by a noticeable increase in airframe 1P vibration; there was, however, no deterioration in stability or control power. These ice buildups on the rotor blades were readily controlled by the application of small, rapid cyclic inputs (pitch or roll) to flex the blades and shed the ice. This is a relatively safe procedure for this rotorcraft since the main rotor coning angle is such that ice shed from the blades clears the tail rotor and propeller. Also, the ice was shed upon pilot command while the accumulation was relatively light. As a result, the overall operation of the vehicle was satisfactory within the range of climatic conditions encountered during the test program. The ability of the AH-56A pilot to readily control ice shedding from the rotor blades and thus promote a greater tolerance to icing for the AH-56A as compared to other helicopter models may be due to the unique in-plane and flapping characteristics of the AH-56A rigid-rotor system. Whereas the rigid-rotor system is hingeless and the flapping mode of the rigid-rotor blades is accompanied by considerable flexing of the blades, the other rotor systems incorporate hinges or pins that do not permit blade flexing and result in different flapping and/or in-plane frequencies. In the case of the OH-58 teetering rotor, which is solid with a pin at the hub permitting "teeter-totter" action, the in-plane frequency characteristics are similar to those of a rigid rotor. However, the rotor flapping characteristics are different from those of the AH-56A, and no blade flexing can be induced. In the case of the CHSS-2 and Superfrelon articulated rotor systems, as a result of action of blade hinges, no blade flexing is possible and both the in-plane and flapping blade frequencies are different from those of the AH-56A. Although plausible, available experimental data is not sufficient to fully verify the hypothesis relating to the cause of the different behavior of the AH-56A rotor under icing conditions. To fully resolve this question more testing would be required.

Sikorsky S61N (Commercial Version of SH-3)

BEA Helicopters Ltd. of England conducted extensive S61N flight tests under natural icing conditions during January/April 1971 (Reference 9). As a result of these tests, BEA received official clearance from the British Civil Aviation Authority (BCAA) to operate the S61N in icing conditions down to minus 5°C (23°F). These icing trial tests in 1971 consisted of 18 flights, of which 27 hours were flown in actual icing conditions out of a total of 30 hours 20 minutes. On flights 1 to 9, the aircraft was loaded to approximately 17,500 pounds, and for flights 10 to 18 the takeoff weight was approaching the maximum of 19,000 pounds. Most of the flying was done in stratiform type clouds associated with frontal depression type weather conditions.

Changes in directional control settings were required to remain within the cloud. The vertical height of the icing conditions varied from the 2000-

foot level to 7000 feet and temperatures varied from 0°C (32°F) down to -12°C (10°F). Icing conditions encountered varied from light to severe glazed and/or rime type ice, some moderate snow, and heavy sleet/rain at temperatures just below 0°C (32°F). The icing test flights were performed over the sea to permit descent to warmer temperatures at low altitude where the effect of ice shedding could be observed.

On landing after each flight, the main and tail rotors were found to be clean down to the root ends, but substantial ice deposits were always obvious on pitch change rods, droop stops, damper and bifalar weights. The engine air inlet ice deflector and the anti-icing system were found to be satisfactory for operation in icing environments down to -10°C (14°F). Perhaps the most significant observation made as a result of these tests, which is not found in icing test reports of other helicopters, is that "the weight of airframe ice and drag (due to ice) at high speed may well be an important factor." There was a marked increase in excess power required (with respect to power level for clear air flight) when entering icing conditions at normal cruising speeds. Therefore, to reduce the excess power, it was recommended that during flight in icing, the maximum permissible speed be reduced by 40 to 50 knots and the ability to autorotate be retained at all times. At the high forward speed (110 knots), increased vibration levels were experienced.

On the other hand, the worst case of icing at the slower speed (60 to 70 knots) was not accompanied by increased vibration levels. This suggests that for the S61N, vibration may not be a reliable indicator of the presence of ice on the rotor blades.

The following modifications were considered essential to operate the S61N in icing conditions:

1. Introduction of HF aerial restraint.

2. Introduction of a second more accurate outside air temperature gage.

3. Introduction of the Teddington "Hot Rod" (a small ice detection probe which is mounted in front of the forward windshield. An ice buildup observed on the small-diameter cylindrical probe provides a visual indication of the presence of icing conditions. To monitor the presence or absence of icing conditions and the approximate intensity of such conditions when encountered, the ice accretion on the probe is periodically removed by pilot-activated electric heating).

4. Introduction of rear-view mirrors to enable observation of the pitot mast and front of the engine inlet ice deflector.

General Trend of Icing Test Results as Related to Rotor Icing

Changes in aircraft drag, lift, pitch, roll, controllability, and vibration levels which may be caused by ice formations are important criteria in

establishing the need for rotor ice protection. Another criterion is the degree of potential structural damage that can be inflicted on the main rotor by uncontrolled ice shedding from the tail rotor, or vice versa. Potential damage to the fuselage, flight probes, and engines is another important consideration.

A review of the Ottawa icing flight test results, with respect to airframe and rotor icing, revealed a definite trend which is related to the gross takeoff weight of the rotary-wing aircraft:

1. The larger the vehicle and the higher the available power margin, the more tolerant the vehicle is to ice forming on unprotected rotor surfaces.

2. A helicopter geometry wherein the main rotor coning angle is designed so that ice shed from the blades clears the tail rotor, engine inlet, and other vehicle components is conducive to greater safety during icing encounters.

3. The basic design of the rotor configuration (rigid rotor versus teetering or articulated rotor) may imply the rotor blade ice protection requirements.

For those helicopter designs having a sufficient power margin during cruise and hover, the drag rise caused by icing is, in itself, not considered sufficient justification for ice protection. This is true if it can be demonstrated that the controllability characteristics are not adversely affected, and that the vibration level and potential structural damage, due to uncontrolled rotor self-shedding of ice, are within tolerable limits.

The Ottawa icing flight test results indicate that small vehicles, such as the OH-6 and the OH-58A (which have gross takeoff weights up to approximately 7000 pounds) are ultrasensitive to icing because they experience a rapid degradation in aerodynamic characteristics and handling qualities, and significant increases in vibration levels. These small vehicles cannot tolerate any prolonged icing encounters. For example, Ottawa icing flight tests of the OH-58A were aborted due to unacceptable lift and/or stability and excessive rotor vibrations. Of the five OH-58A flights conducted at Ottawa, one flight in the cloud was as short as 1.0 minute, and the longest was only 7 minutes (Reference 10).

These icing tests revealed that for rotary-wing aircraft with gross takeoff weights in the approximate range between 7,000 and 12,000 pounds, such as for the Bell UH-1 and Kaman UH-2, degradation of the aerodynamic characteristics and handling qualities represents a lesser hazard, particularly for icing encounters of moderate duration. However, for this class of aircraft the vibration levels under icing conditions deteriorated and damage to the main or tail rotor due to icing caused concern (Reference 6). Thus, it appears that for helicopters with a gross takeoff weight in the 7,000- to 12,000-pound category, the vibration level may dictate ice protection provisions for both main and tail rotors.

Finally, on heavy vehicles that were tested at the Ottawa Icing Spray Rig, such as the HH-53, CH-54, and CH-47, the aerodynamic characteristics and vibration levels were found to be within acceptable limits after 0.5 hour or longer in icing. The greater tolerance of larger vehicles to icing during the tests at Ottawa may have been enhanced by the fact that the spray rig cloud diameter is too small to retain the entire rotor within the cloud. However, damage to the main and/or tail rotors due to uncontrolled ice shedding was observed on some of these vehicles. Also, to prevent ingestion of rotor-shed ice into the engine, special Foreign Object Damage (FOD) deflectors had to be installed at the engine inlets of some large vehicles (Reference 7). It is concluded, therefore, that for vehicles with gross takeoff weights in excess of 14,000 pounds, the governing criterion for ice protection appears to be structural damage of the main and tail rotors and the engine due to uncontrolled ice shedding from the blades. The relative location and geometry of the two rotors with respect to one another and with respect to the engine inlet influence to a large extent, the degree of potential damage that can be inflicted.

In summary, experimental data indicate that to assure adequate aerodynamic and handling quality margins, tolerable vibration levels, and elimination of engine and rotor damage due to ice shedding, teetering and articulated rotor systems require ice protection to afford all-weather capability without restrictions. On heavy vehicles this need is largely dictated by the fact that on teetering and articulated rotors, ice shedding is caused solely by centrifugal forces and cannot be controlled without rotor deicing systems. Cyclic deicing on rotor blades is acceptable if the ice buildup thickness between shedding cycles is limited to approximately 1/4 inch. On heavy vehicles with rigid-rotor systems wherein controlled ice shedding can be pilot-induced by a combination of centrifugal forces and blade flexing, rotor ice protection may be deleted without apparent detrimental effects to vehicle safety.

Engine Inlet Icing

Helicopter turbine engine inlets have two unique features which distinguish them from conventional fixed-wing aircraft: (1) a much higher sensitivity to ingestion of ice shed from the basic airframe, and (2) the use of sand and dust particle separators (also, the engines are of smaller scale than those on fixed-wing and commercial aircraft; thus their structural members are generally less rugged). Common practice has been to locate the engine inlet at the top of the fuselage behind the cockpit or flight station. Thus, any ice which slides along the fuselage ahead of the inlet would be ingested. This problem has been noted on the CH-53 and CH-46 aircraft. The approach taken to solve this problem has been the incorporation of FOD deflectors at the engine inlet, bringing the air in at right angles to the airstream. This approach, however, results in serious propulsion performance penalties since there is a negative ram pressure recovery at the engine front face. Moreover, tests in the Canadian NRC spray rig on the SH-3D, CHSS-2 and CH-53 have indicated unsatisfactory large accumulations of ice on certain interior surfaces of the deflectors, thus creating a further hazard.

Ice accretion tests of engine air particle separator systems (EAPS) consisting of multiple inertial separator modules have been run for the design incorporated on the CH-54A/B (Figure 14). The system incorporates the Donaldson filter design, and an inlet assembly was tested in the NASA-Lewis Research Center Icing Tunnel in December 1970 (Reference 11). The unit was tested at a tunnel airspeed of 110 knots, and the ram performance under various icing conditions is shown in Figures 15 and 16. With the protective screens at the filter inlets removed, it is seen that the tunnel results show a "favorable" effect due to icing for an initial period of time (e.g., there is a ram pressure gain in the EAPS plenum over the clear configuration). This very surprising result has been attributed to the growth of the ice forward from the filter inlets causing a ram tunnel type of buildup, particularly at the lower tunnel (total) temperatures as shown in Figure 17.

The HH-53C also had an EAPS filter installed on the engine inlet (Reference 7), and no serious performance effects were noted on the aircraft. In fact, it was reported that "the ice that formed on the EAPS were self-shedding in flight. This was confirmed by simultaneous observations from both the chase helicopter and the photo observer who saw noticeable decreases in the static differential pressure reading as the ice was shed". Another icing flight test with an EAPS system was that on the OH-58A (Reference 10), where the vehicle was tested on the NRC Spray Rig. Unfortunately, that aircraft is so sensitive to main rotor ice accumulation and tail rotor vibration that the limitations of the EAPS could not be determined. Of the five flights conducted at Ottawa, one was as short as 1.0 minute in the cloud, and the longest was only 7 minutes. The Bell tests showed increases in filter pressure drop - averaging about 2 inches of H_2O (a 1-percent loss in engine power).

The design of the vortex inertial separators used with their high efficiency collection surfaces would suggest a high likelihood of rapid icing, particularly in view of experience with screen icing; and while the Navy considers CH-54 flights of up to 1/2 hour in icing safe as a result of the Lewis tests, further testing is recommended to explore a wide variety of icing conditions, especially just below freezing.

Flight Sensors

While anti-iced pitot-static probes are presumably a well-developed component, Reference 12 reports difficulty with the installation during icing tests of the CHSS-2 in 1970. Icing of the probe near the static ports caused airspeed indicator fluctuations and malfunctions of barometric altitude stabilization of the automatic stabilization equipment. The cause of this icing was an installation peculiarity of the probe rather than a defect in its anti-icing capability, and illustrates the need to carefully consider all factors of a component installation in determining the need for ice protection. The probe itself apparently met Military Specification requirements, but a collar around it was cold. This occurrence is worthwhile, however, in demonstrating the need for adequate pitot-static anti-icing.

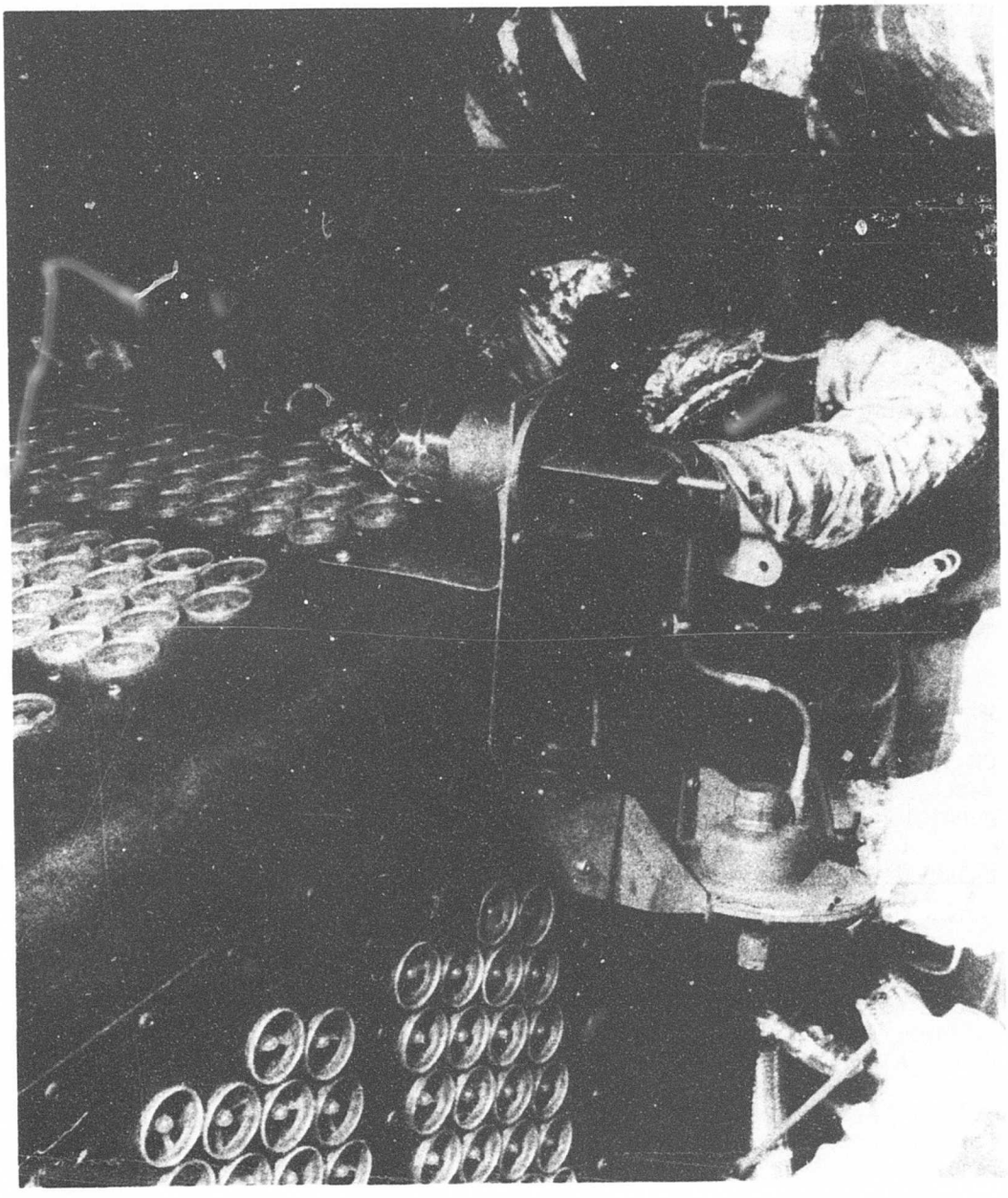

Figure 14. CH-54 EAPS Installation in NASA Icing Tunnel.

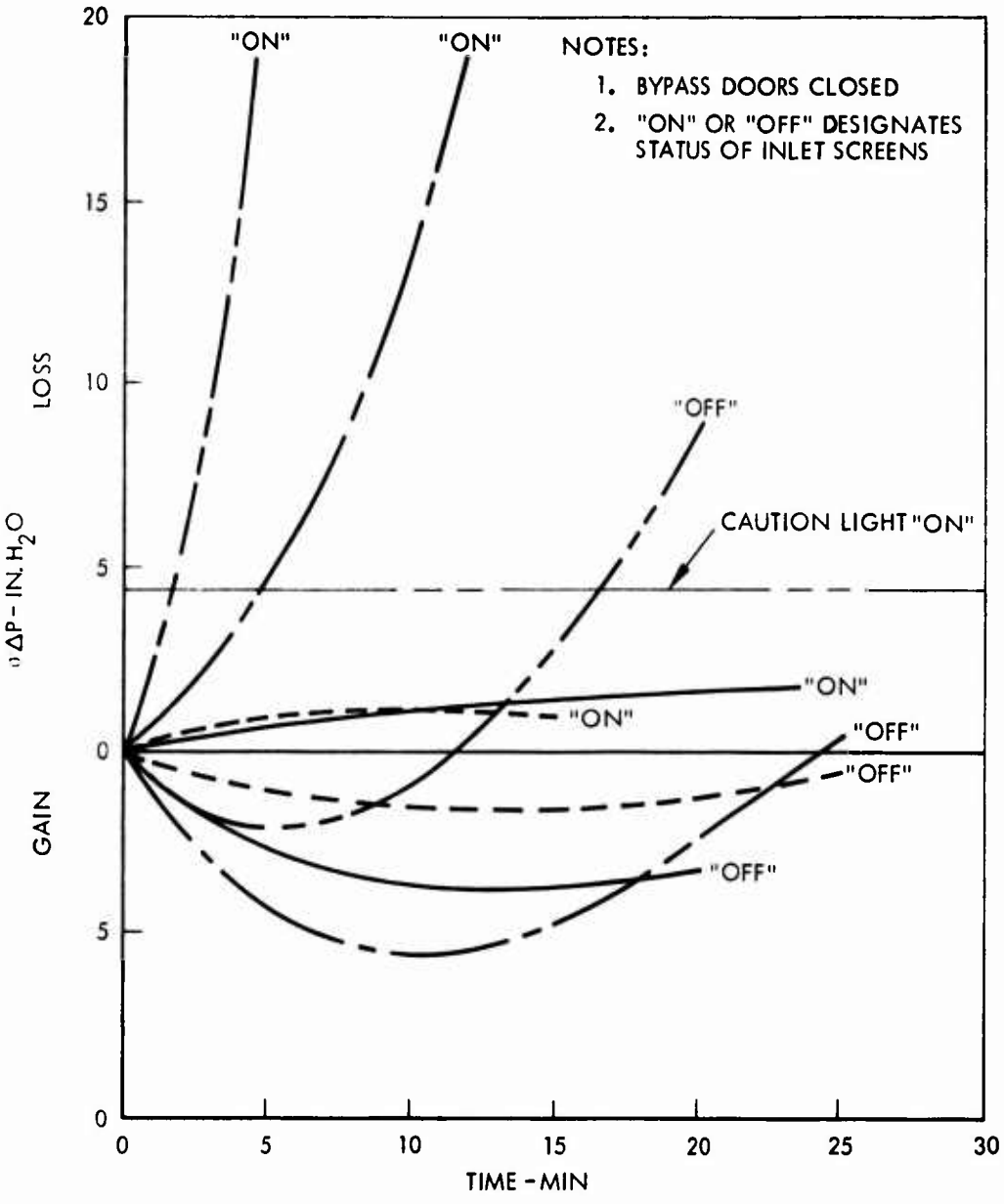

	AMBIENT TEMPERATURE °F	LIQUID WATER CONTENTS – g/m³	DROPLET DIAMETER -μ
- - - -	25	1.62	25.4
———	14	1.54	24.0
— - —	-4	1.44	22.0
— - - —	-18	1.27	19.3

Figure 15. CH-54 EAPS Performance Characteristics (Maximum Intermittent Icing).

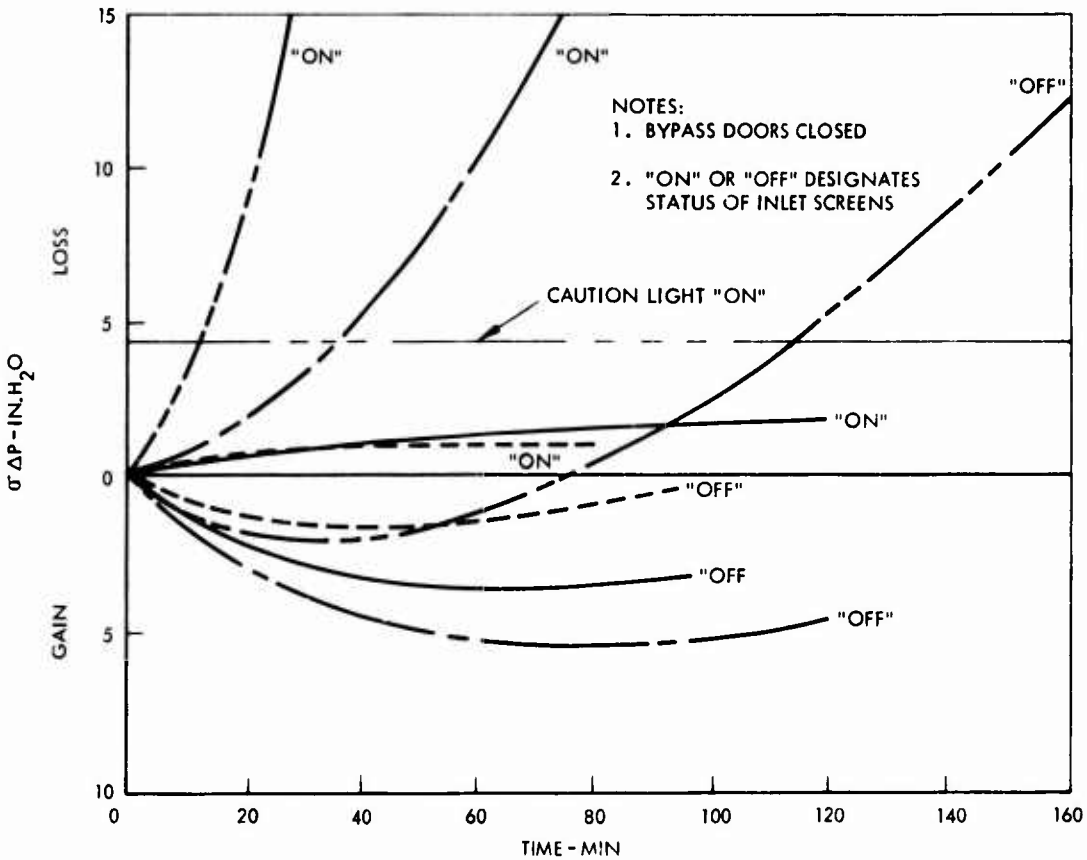

	AMBIENT TEMPERATURE °F	LIQUID WATER CONTENT - g/m^3	DROPLET DIAMETER - μ
- - - -	25	0.41	25.4
———	14	0.31	24.0
— — —	-4	0.19	22.0
— - — -	-18	0.19	19.3

Figure 16. CH-54 EAPS Performance Characteristics (Maximum Continuous Icing).

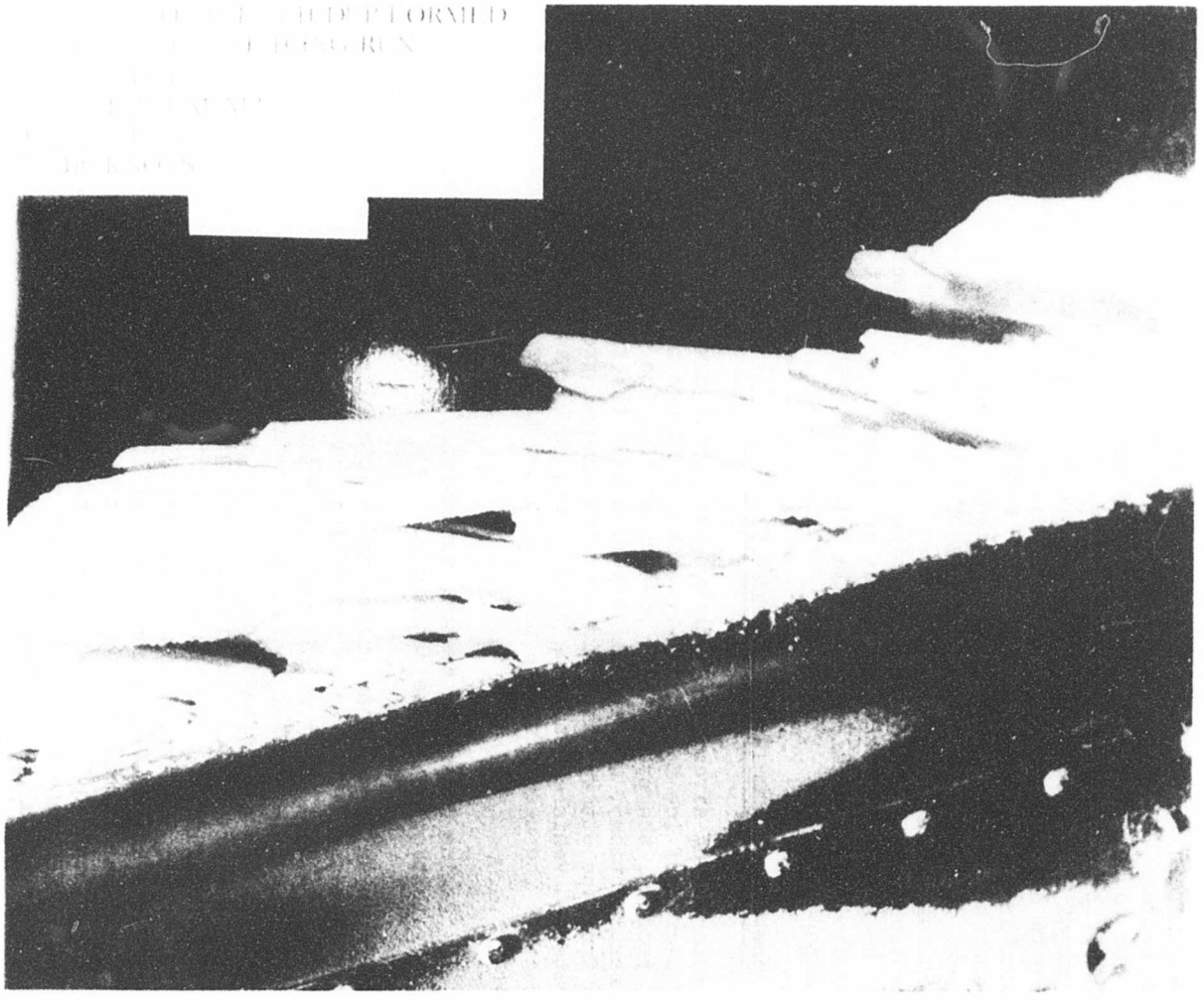

Figure 17. Ice Buildup Formed on a CH-54 EAPS After 40-Minute Icing Run.

2.2 ACCIDENTS CAUSED BY ICING

Information on civil aircraft rotary-wing accidents attributable to icing is shown in Figure 18. A relevant statistic in addition to the data contained therein is the number of Canadian helicopter accidents per year, which average 40. Thus an average of 7 percent of the helicopter accidents were due to icing, with about two-thirds believed due to blade icing. The U. S. civil records for the years 1968 - 1970 showed that approximately 2 percent of the helicopter accidents were attributed to icing (15 icing accidents out of a total of 786 rotorcraft accidents). The bulk of the accidents were believed to be due to carburetor icing, and thus the data are somewhat at variance with the Canadian experiences. In addition to the accident data, the Canadian Ministry of Transport has accumulated 27 pilot reports of "incidents" due to icing. Of these, 7 reported noticeable vibration, and 10 showed deterioration of rotorcraft control effectiveness. There does not appear to be similar information on military aircraft since no models are cleared for flight in icing (apparently chance encounters are not reported).

2.3 COMPONENTS REQUIRING ICE PROTECTION

The rotary-wing aircraft components and surfaces which are subjected to some degree of ice accretion are shown on Figure 19. In view of the accident records, the probability of encountering ice worldwide (discussed in the next section), operational experience in the field, flight test experience from the Ottawa Icing Rig, and the general prohibition of flying unprotected vehicles in icing conditions, conclusions have been drawn with respect to the needs for ice protection and the areas requiring ice protection.

1. Engine induction system, windshield, and flight sensor ice protection should be mandatory.

2. No uniform ground rules can be established on the necessity for main and tail rotor protection, but such a capability should be available on test aircraft in order to provide a high confidence level for flight testing under natural icing conditions. A preliminary determination on the necessity for main and tail rotor protection for individual helicopter models must be based on experimental results from one of the following: the Ottawa Spray Rig, flight in simulated icing conditions behind an aircraft tanker, or flight under natural icing conditions. However, the general trend of sensitivity of helicopters to icing in terms of vibration level, aerodynamic efficiency, and handling qualities is known: (1) the larger the vehicle and the higher the engine power margin, the more tolerant it is to ice forming on unprotected rotor surfaces; (2) a rotorcraft geometry wherein the main rotor coning angle is such that ice shed from the blades clears the tail rotor, the engine inlet, and other vehicle components is conducive to greater safety during icing encounters; and (3) the basic design of the rotor configuration (rigid versus teetering

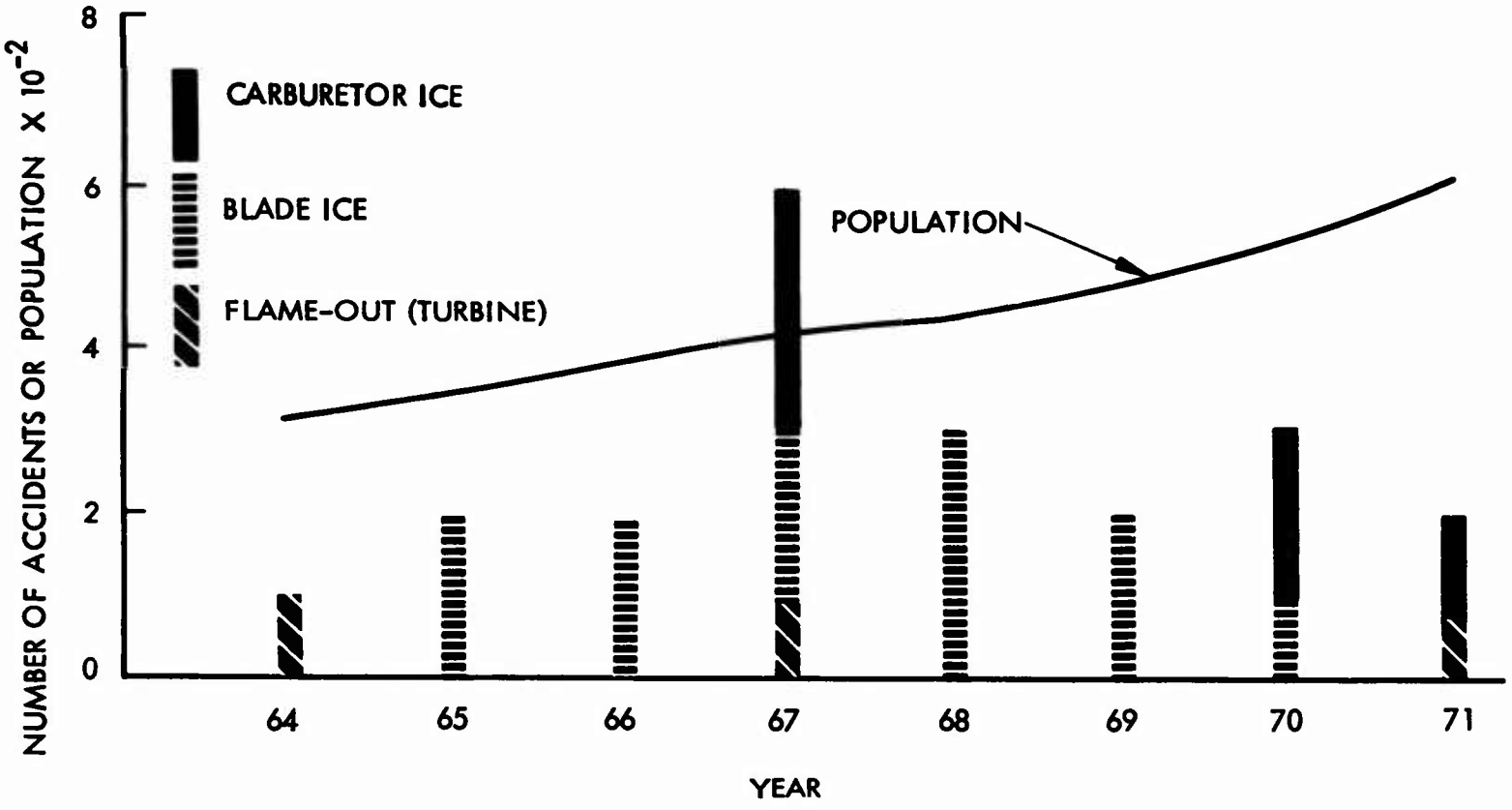

Figure 18. Canadian Helicopter Icing Accidents.

Figure 19. Area Subject to Icing - Rotary-Wing Aircraft.

or articulated) may mean the difference between the need for and the deletion of rotor blade ice protection. This has not been fully substantiated (extensive operational experience in icing may ultimately be required to fully settle the question of rotor ice protection for individual models).

Components and surfaces of rotary wing aircraft that require ice protection are shown in Figure 20.

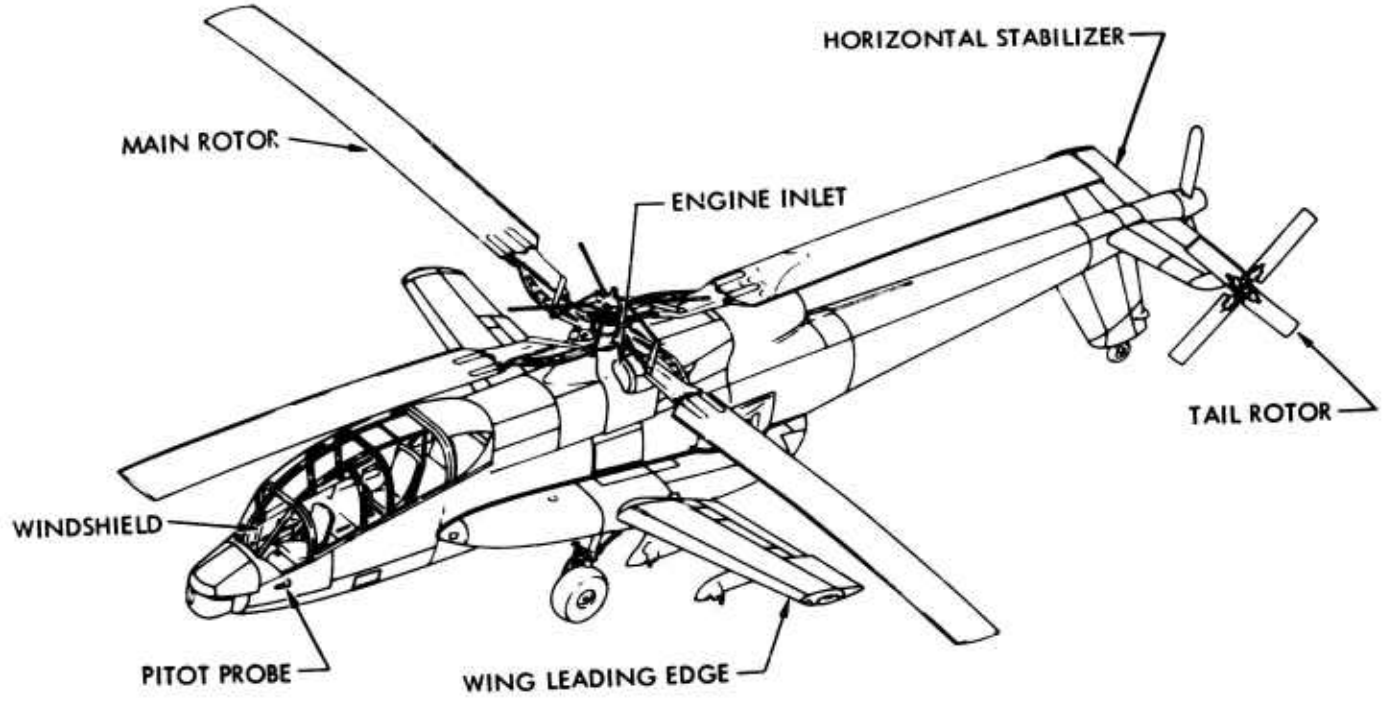

Figure 20. Vehicle Areas Generally Requiring Ice Protection.

SECTION 3 PROBABILITY AND SEVERITY OF ICING CONDITIONS

Of major importance in determining the need for ice protection on Army rotary-wing aircraft is an analysis of the probability of encountering icing in various potential operational theaters. Therefore, this section contains a discussion on worldwide icing probabilities during various times of the year, a discussion of the meteorological parameters pertinent to an analysis of icing severity, a review of statistics on icing severity, and recommendations of meteorological criteria to be used for system design.

3.1 WEATHER CONDITIONS CONDUCIVE TO ICING

The most useful information relating to weather conditions conducive to ice formation on aircraft is found in References 13 and 14. Information from these two sources has been utilized in the following discussion.

Ambient Conditions and Cloud Considerations

Clear and rime ice were observed to form at mountain observatories long before the first aircraft flew. Reference 15, for example, noted that the formation of ice was associated with clouds at ambient temperatures below 0°C and that these clouds consisted predominantly of liquid water drops. Later studies at mountain observatories and on aircraft confirmed that the meteorological factors conducive to icing of aircraft are determined by:

1. supercooled water content
2. temperature and humidity level
3. ice crystal content
4. droplet and crystal size distribution

The atmospheric distribution of potential aircraft icing zones is mainly a function of temperature and cloud structure. These factors, in turn, vary with altitude, synoptic situation, orography, location, and season.

It is widely accepted that aircraft icing is limited to the layer of the atmosphere lying between the freezing level and the -40°C isotherm. Icing has occasionally been reported at temperatures lower than -40°C in the upper parts of cumulonimbus and other clouds. In general, the frequency of icing decreases rapidly with decreasing temperature, becoming rather rare at temperatures below -30°C. The normal vertical temperature distribution in the atmosphere is such that icing is usually restricted to the lower 30,000 feet of the troposphere.

Supercooled droplets have diameters varying from a few microns to a few millimeters. When such droplets impinge upon a surface, freezing is initiated. At surface temperatures near but below 0°C, and especially with large drops, the freezing process may be relatively slow, and the drop has time to spread over the surface before losing all the liberated latent heat and before freezing is completed. This process produces a clear ice formation bonded firmly to the surface and often referred to as glaze ice. At low temperatures most droplets are small and freeze essentially on impact; ice at low temperature is formed in great numbers of discrete particles with air entrapped between the particles to produce a white crystalline deposit known as rime ice. This rime ice has a low apparent density and is easily broken away from the surface. Statistical summaries of flights at 10,000 feet and 18,000 feet indicate that clear ice formed 10 percent at the time, clear-rime mixture 17 percent, rime 72 percent and frost 1 percent.

Aircraft icing can occur in stratiform or cumuliform clouds. Icing in middle- and low-level stratiform clouds is confined, on the average, to a layer between 3,000 and 4,000 feet thick. The intensity of the icing generally ranges from a trace to light, with the maximum values occurring in the upper portions of the cloud. Both rime and mixed icing are observed in stratiform clouds. The main hazard lies in the great horizontal extent of some of these cloud decks. High-level stratiform clouds are composed mostly of ice crystals and give little icing.

The zone of probable icing in cumuliform clouds is smaller horizontally but greater vertically than in stratiform clouds. Further, icing is more variable in cumuliform clouds because many of the factors conducive to icing depend to a large degree on the stage of development of the particular cloud. Icing intensities may range from generally a trace in small supercooled cumulus to often light or moderate in cumulus congestus and cumulonimbus. The most severe icing occurs in cumulus congestus clouds just prior to their change in cumulonimbus. Although icing occurs at all levels above the freezing level in a building cumulus, it is most intense in the upper half of the cloud. Icing is generally restricted to the updraft regions in a mature cumulonimbus, and to a shallow layer near the freezing level in a dissipating thunderstorm. Icing in cumuliform clouds is usually clear or mixed (Reference 16). Aircraft icing rarely occurs in cirrus clouds, some of which do contain a small proportion of water droplets. However, icing of light intensity has been reported in the dense cirrus anvil-tops of cumulonimbus, where updrafts may maintain considerable water at rather low temperatures.

Frontal Systems

In general, frontal clouds have a higher icing probability than other clouds. It has been estimated that 85 percent of the observed aircraft icing occurs in the vicinity of frontal zones. Usually, the greatest horizontal extent of icing is associated with warm fronts, and the most intense icing with cold fronts.

Warm frontal icing may occur both above and below the frontal surface. Moderate or severe clear icing usually occurs where freezing rain or freezing drizzle falls through the cold air beneath the front. This condition is most often found when the temperature above the frontal inversion is above 0°C and the temperature below is below 0°C. Icing above the warm-frontal surface, in regions where the cloud temperatures are lower than 0°C, is usually confined to a layer less than 3,000 feet thick. Jones (Reference 17) found a definite possibility of moderate icing, usually mixed or clear, within 100 to 200 miles ahead of the warm-front surface position. This was particularly noticeable for fast-moving, active, warm fronts. Light rime ice was noted in the altostratus up to 300 miles ahead of the warm-front surface position.

Whereas warm-frontal icing is generally widespread, icing associated with cold fronts is usually spotty (Reference 18). Its horizontal extent is less, and the areas of moderate icing are localized. Clear icing is more prevalent than rime icing in the unstable clouds usually associated with cold fronts (Reference 17). Moderate clear icing is usually limited to supercooled cumuliform clouds within 100 miles to the rear of the cold-front surface position and is usually most intense immediately above the frontal zone (Reference 19). Light icing is often encountered in the extensive layers of supercooled stratocumulus clouds which frequently exist behind cold fronts. Icing in the stratiform clouds of the widespread anafront type of cold-front cloud-shield is more like icing associated with warm fronts.

Icing conditions associated with occluded and stationary fronts are similar to those of a warm or cold front, depending on which type the occlusion or stationary front most resembles. Moderate icing conditions are frequently associated with deep, cold, low-pressure areas in which the frontal systems are quite diffuse (Reference 19).

Icing is more prevalent in maritime than in continental air masses, and is more hazardous in regions of instability (Reference 20).

Effect of Dew Point and Precipitation

Statistics from a number of sources suggest that the spread between the dew point and the dry bulb temperature at flight level can be used as an indicator of aircraft-icing occurrence. Table II shows the probabilities of icing occurrence and intensity as related to the dew-point spread, the flight-level thermal advection*, and the presence of building cumuliform clouds. Considering only the dew-point spread, there was an 84 percent probability that there would be no icing if the spread were greater than 3°C, and an 80-percent probability that there would be icing if the spread were less than 3°C.

*Advection is defined here as the rate at which the isotherms appear to be transported by the upper-level contours, i.e., $-(v.\nabla T)$ at flight level.

TABLE II. ICING INTENSITY AS RELATED TO TEMPERATURE DEW-POINT DIFFERENCE (PROBABILITY IN PERCENT)

Condition of Flight Level	Temperature Dew-Point Difference						
	<3°C					>3°C	
	No Icing	Trace Icing	Light Icing	Moderate Icing	Severe Icing	No Icing	Trace Icing
Cold-Frontal Zone*	0	18	45	35	2	67	33
Cold-Air Advection	10	33	44	13	0	54	46
Neutral Advection	22	46	29	3	0	100	0
Warm-Air Advection	67	20	13	0	0	100	0
Building Cumulus	0	6	70	24	0	-	-
Overall	20.5	30.5	35.5	13.0	0.5	84.0	16.0

*Most intense cold-air advection occurs in cold-frontal zone.

The type of thermal advection or the presence of building cumuliform clouds, taken in conjunction with the dew-point spread, showed a definite association with the occurrence and intensity of aircraft icing. When the dew-point spread at flight level was 3°C or less in areas of warm-air advection, there was a 67-percent probability of no icing, 20-percent and 13-percent probabilities of trace and light icing, respectively, and no probability of moderate icing. By contrast, when the dew-point spread was 3°C or less at flight level in a cold-frontal zone, the probability of icing approached 100 percent. There was also nearly 100 percent probability of icing in building cumuliform clouds when the dew-point spread was 3°C or less.

With a dew-point spread greater than 3°C, trace icing was about 40 percent probable in regions of cold-air advection while there was almost 100 percent probability of no icing in regions of neutral or warm-air advection.

During NACA flight tests (Reference 21) to measure the physical properties of icing, a trace of ice was reported in 80 percent of the observations in clouds over steady precipitation areas, and light icing was reported in only 20 percent of the observations. In stratiform clouds over areas without precipitation, the observed percentages were just the reverse. However, Air Force investigators (Reference 19) found that the presence of precipitation does not necessarily mean that the icing will be trace. If the vertical motion caused by frontal slopes, terrain, or surface heating is sufficient to maintain a constant supply of supercooled water droplets, light or even moderate icing can be present in clouds over areas of steady precipitation. Table III based on flight-test data (Reference 19), shows

TABLE III. ICING INTENSITY AS RELATED TO THE PRESENCE OF PRECIPITATION (REFERENCE 20)
(PROBABILITY IN PERCENT)

Condition at Flight Level	Temperature Dew-Point Difference ≤3°C									
	Precipitation Absent					Precipitation Present				
	No Icing	Trace Icing	Light Icing	Moderate Icing	Severe Icing	No Icing	Trace Icing	Light Icing	Moderate Icing	Severe Icing
Cold-Frontal Zone*	0	32	55	13	0	0	5	35	56	4
Cold-Air Advection	15	18	52	15	0	3	50	37	10	0
Neutral Advection	41	38	21	0	0	9	52	34	5	0
Warm-Air Advection	75	13	12	0	0	11	67	22	0	0
Building Cumulus	0	0	77	23	0	0	25	50	25	0
Overall	32.5	22.5	37.0	8.0	0.0	5.5	40.5	34.5	18.5	1.0

*Most intense cold-air advection occurs in cold-frontal zones.

the probabilities of various intensities of icing when the dew-point spread at flight level is 3°C or less and precipitation is present. Icing occurred in 67.5 percent of the cases when there was no precipitation and 94.5 percent of the cases when there was precipitation.

Geographical and Seasonal Considerations

High or steep terrain, particularly mountains, causes icing to be more intense than is usual under identical conditions over low, flat terrain (References 17 and 22). Icing is greater over the ridges than over valleys and greater on the windward side than on the leeward side. Moderate icing, usually clear, is experienced in convective clouds over mountainous terrain.

Windward, mountainous coasts in winter are especially subject to extensive aircraft-icing zones. The lifting of the fresh maritime polar air by the mountains results in the formation of more-or-less continuous supercooled clouds. Also, the orographically-induced updrafts permit the air to support larger cloud droplets than otherwise, so that the icing is more intense.

There is a wide variation between geographic areas in aircraft-icing potential due to area-to-area variations in temperature and available moisture. For example, icing during the winter season is very frequent over the warm-water areas off the east coast of continents, to the lee of large inland water bodies, and over those western portions of continents where winds transport ample moisture inland from the oceans (References 20, 23, 24, 25, and 26). Because of the comparatively small amount of moisture in winter arctic air and the small liquid-water content of clouds, icing is seldom regarded as a serious problem in the arctic in winter (Reference 27).

The distribution of Air Force aircraft accidents in which icing was a factor is shown in Figure 21 for the 13-year period ending 31 December 1958 (Reference 28). The greatest number of such accidents occurred in the Central United States while the Northern Rockies and Plains ranked second. An NACA study (Reference 25) of icing reports by civilian airlines in the U.S. showed similar results.

Generally speaking, winter is the season of maximum, and summer the season of minimum, aircraft-icing frequency. A similar seasonal variation is also evident in the incidence of Air Force aircraft accidents involving icing. Of the 114 aircraft accidents occurring from 1946 through 1958 in which icing was a factor, 56 occurred in winter, 6 in summer, 25 in spring, and 27 in fall.

At 10,000 feet in the vicinity of this pressure surface, there is relatively little seasonal variation over the northern portions of the North Atlantic and North Pacific Oceans, which have a relatively high climatological frequency of icing. However, comparatively large seasonal

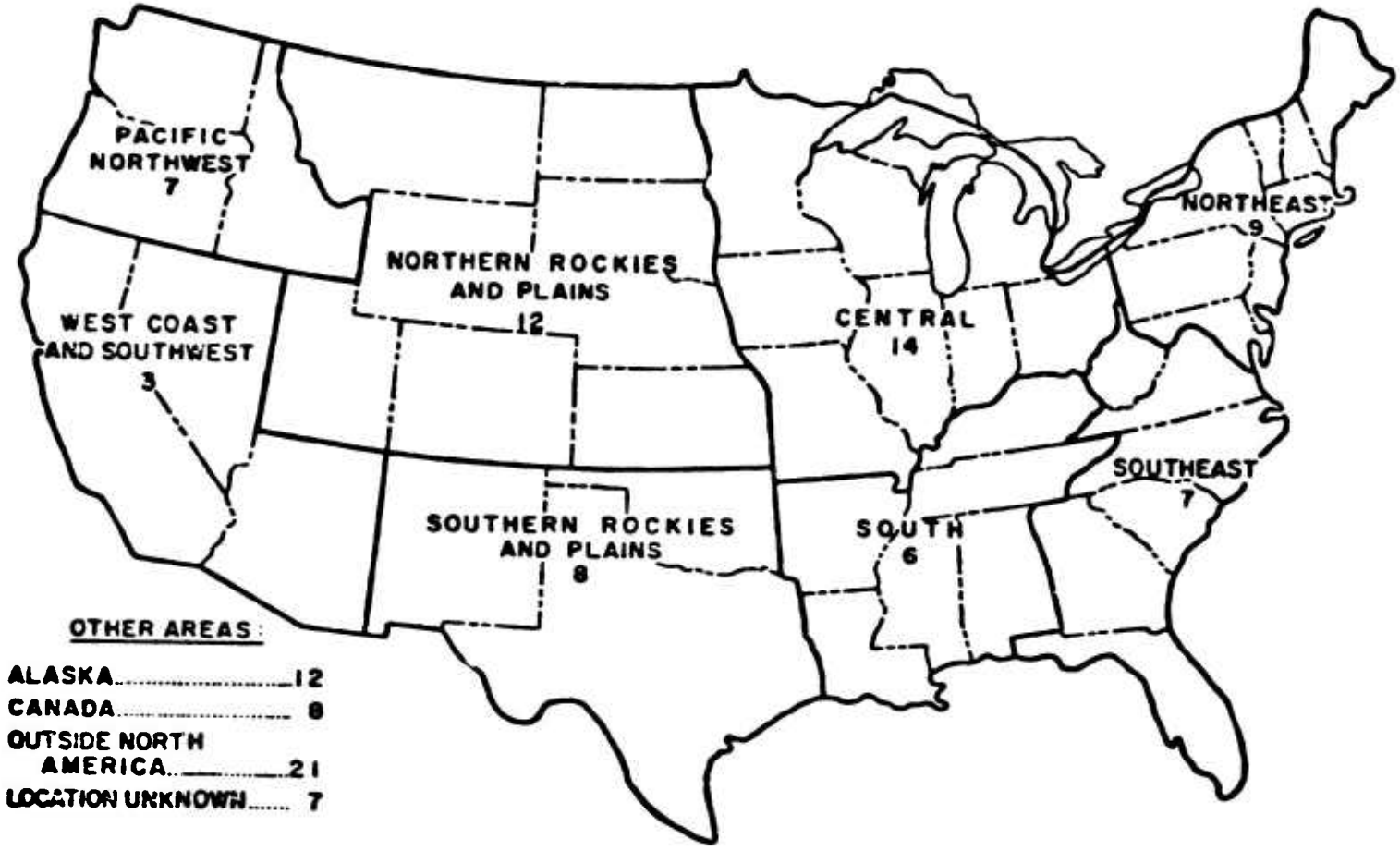

Figure 21. Geographical Distribution of USAF Aircraft Accidents in Which Icing Was a Factor, 1 January 1946 Through 31 December 1958.

variation is found over the other ocean areas. Winter is the season of maximum icing (more suitable temperatures) in these other areas, except over the Arctic Ocean which has the maximum in summer (Reference 30) (temperature and moisture too low in winter).

Because temperatures are almost always below freezing at 18,000 feet, seasonal variations of icing at altitudes near this pressure surface are more dependent on the seasonal variations of moisture than of temperature. The summer-season icing maximum over the Arctic Ocean and the northern and western portions of the North Atlantic and North Pacific Oceans results from the higher moisture content of the air in summer than in the other seasons. On the other hand, the maximum icing over the eastern ocean areas is found in the fall, the season of greatest cyclonic and convective activity.

3.2 WORLDWIDE ICING PROBABILITIES

3.2.1 Potential Icing Conditions

The climatology of icing conditions for aircraft in flight is generally categorized in terms of potential icing conditions, reports of actual icing encounters, and the probability of icing conditions. Potential icing conditions are defined as the presence of a cloud at a temperature $\leq 0^{\circ}C$ and $> -30^{\circ}C$. The probability of icing is defined by Katz (Reference 30) and Heath (Reference 31) as the product of the probability of potential icing condition and the probability that icing would occur given the existence of potential icing conditions. Each of these three aspects of the climatology of icing are discussed in this section.

A necessary but not sufficient condition for the formation of ice on a helicopter is the presence of a supercooled cloud. Hence, maps indicating the frequency of occurrence of supercooled clouds also indicate the occurrence (Reference 32) of potential icing conditions. Such maps have been published by Jailer (Reference 32), Figures 22-25; Ingram and Gullion (Reference 33), Figures 26-29; Guttman (Reference 34); and Briggs and Crawford (Reference 35), Figures 30-35. The significant differences between these estimates are, in part, attributable to the differing altitudes and time intervals used, but most of the differences are probably associated with different interpretations of meager data. None of the authors are explicit on the procedures used for determining the isopleths. All, however, caution that the charts should be used in a qualitative sense only.

The basic problems associated with the construction of maps such as are given in Figures 22-35 are discussed in the following paragraphs. First, it is important to know that the various National Weather Service meteorological stations do not directly measure or report the temperature in clouds or whether the clouds consist of water droplets, ice crystals, or a mixture of both. The maps of the frequency of occurrence of supercooled clouds are made by combining the data on the relative frequency of below-freezing temperatures with the data on the frequency of occurrence of

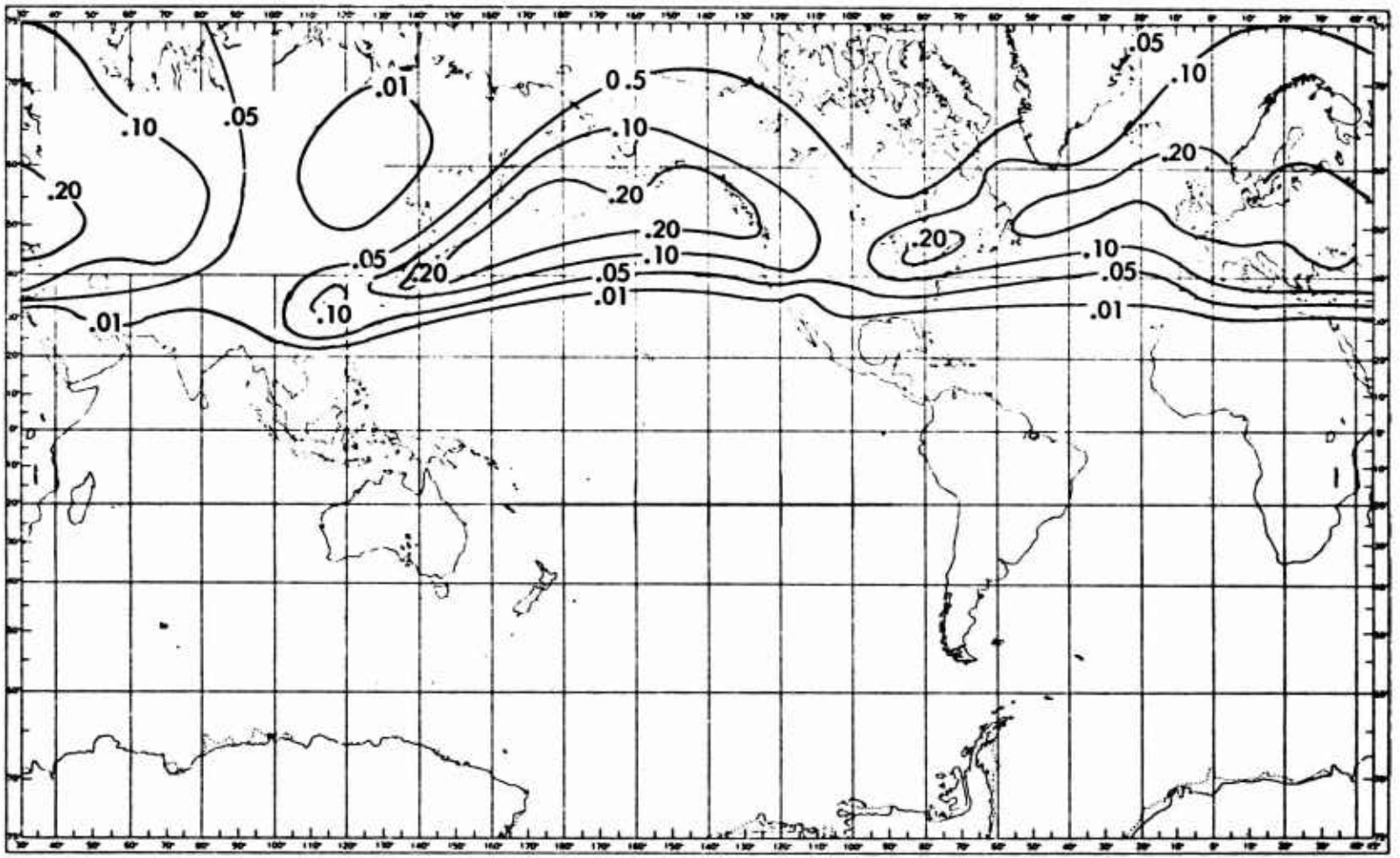

Figure 22. Potential Icing Probabilities, Surface to 10,000 Feet in Winter (Ref. 33).

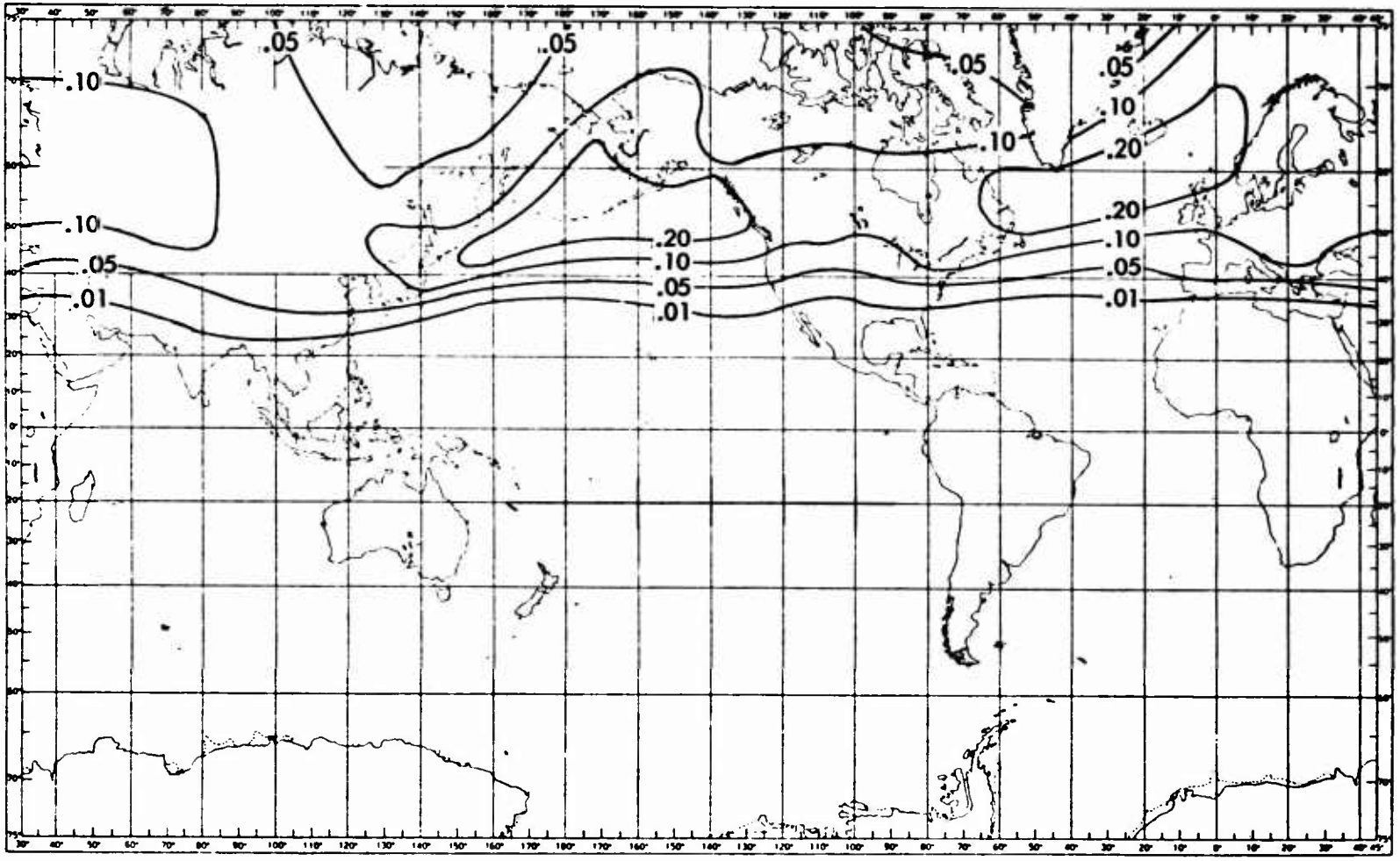

Figure 23. Potential Icing Probabilities, Surface to 10,000 Feet, Spring (Ref. 32).

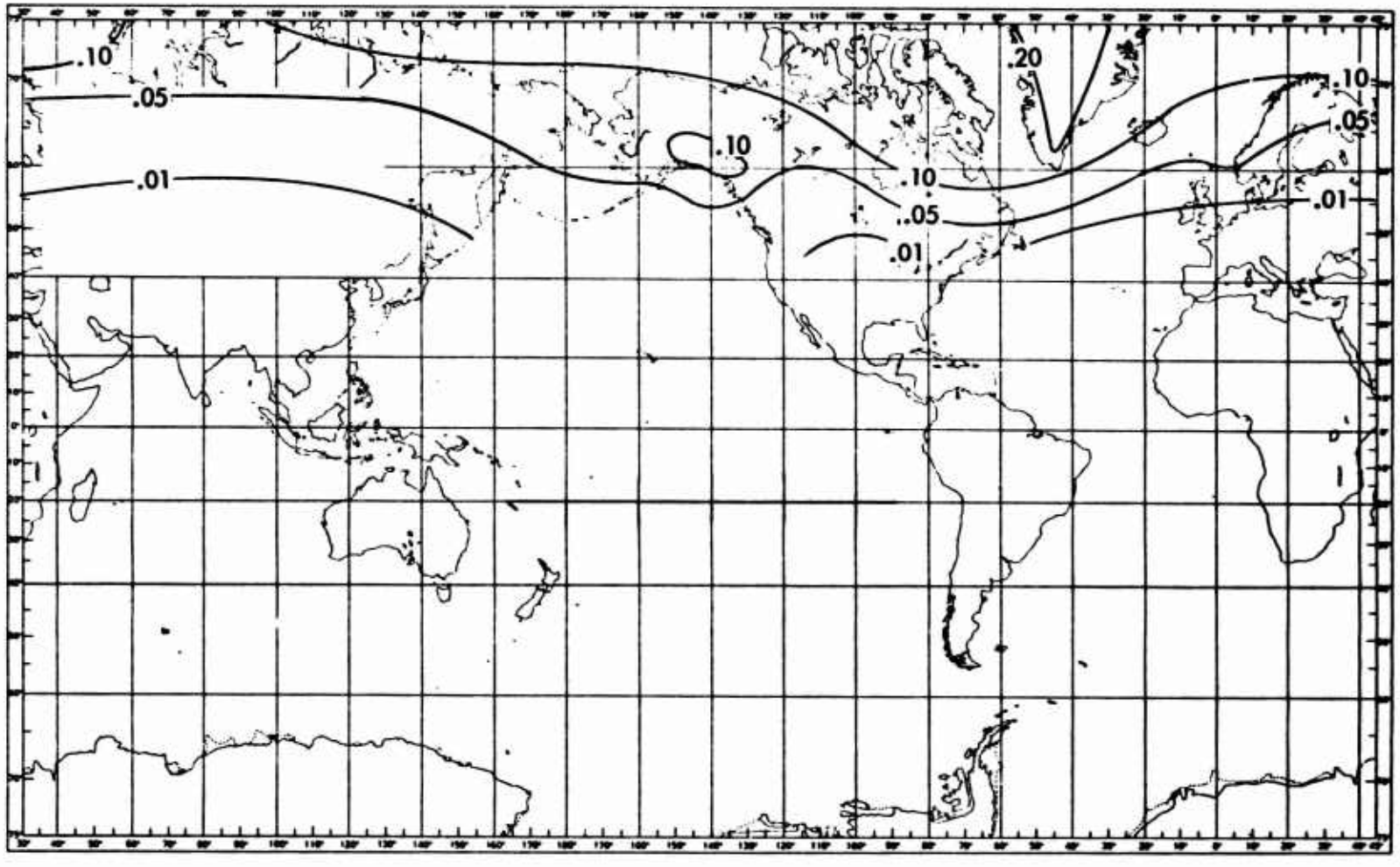

Figure 24. Potential Icing Probabilities, Surface to 10,000 Feet, Summer (Ref. 32).

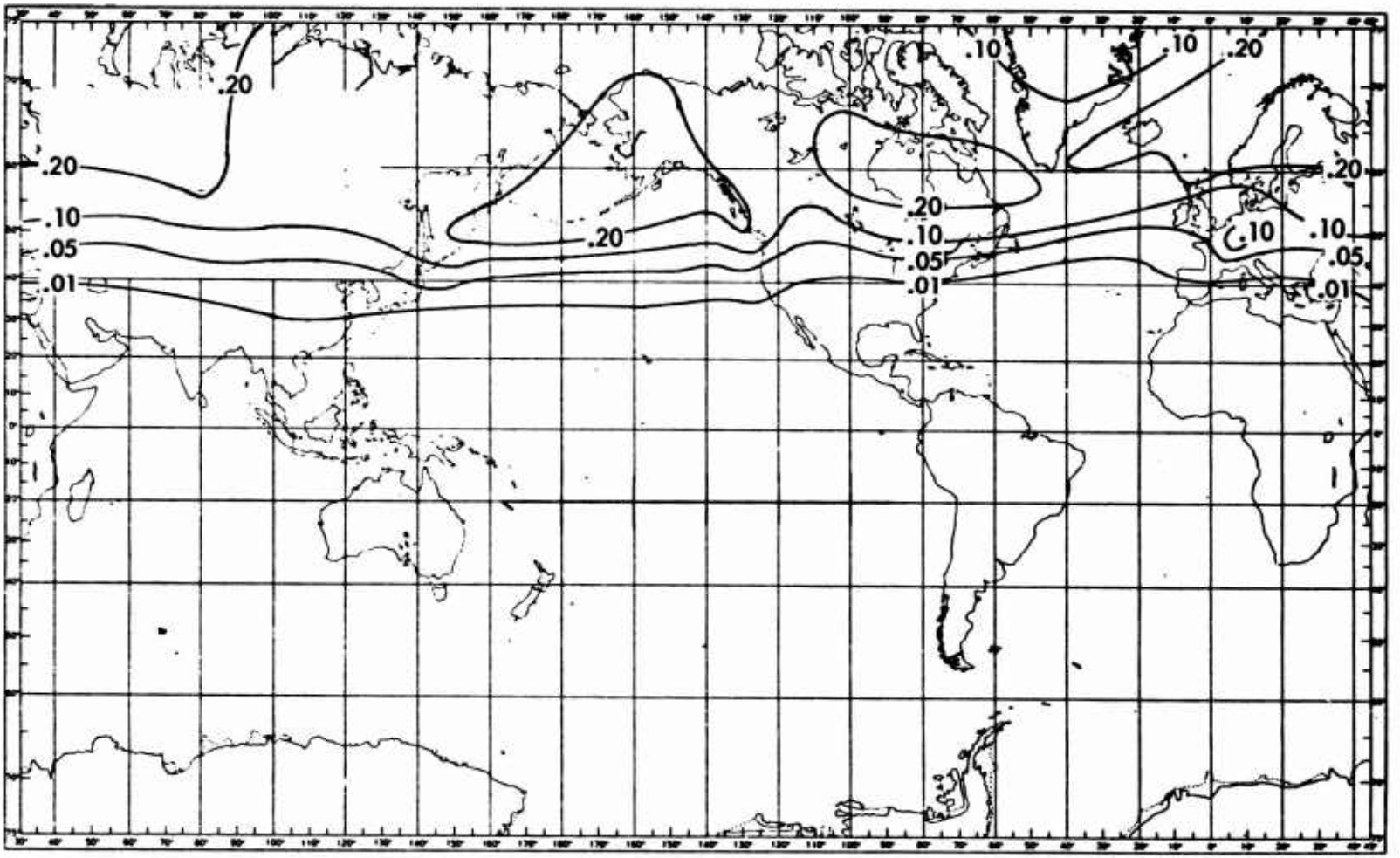

Figure 25. Potential Icing Probabilities, Surface to 10,000 Feet, Autumn (Ref. 32).

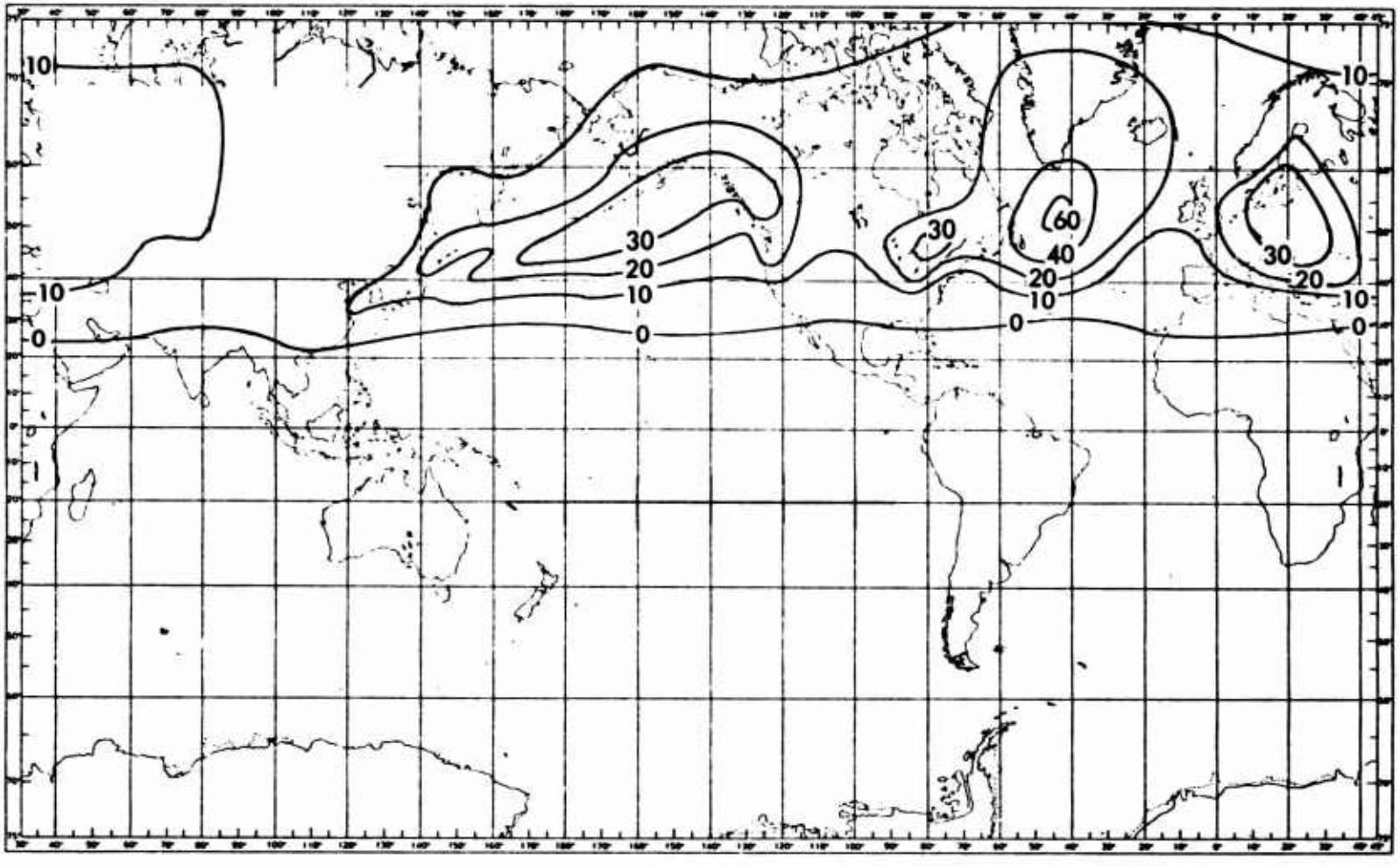

Figure 26. Percentage of Frequency of Potential Icing Conditions (Ref. 33), January, 5,000 Feet.

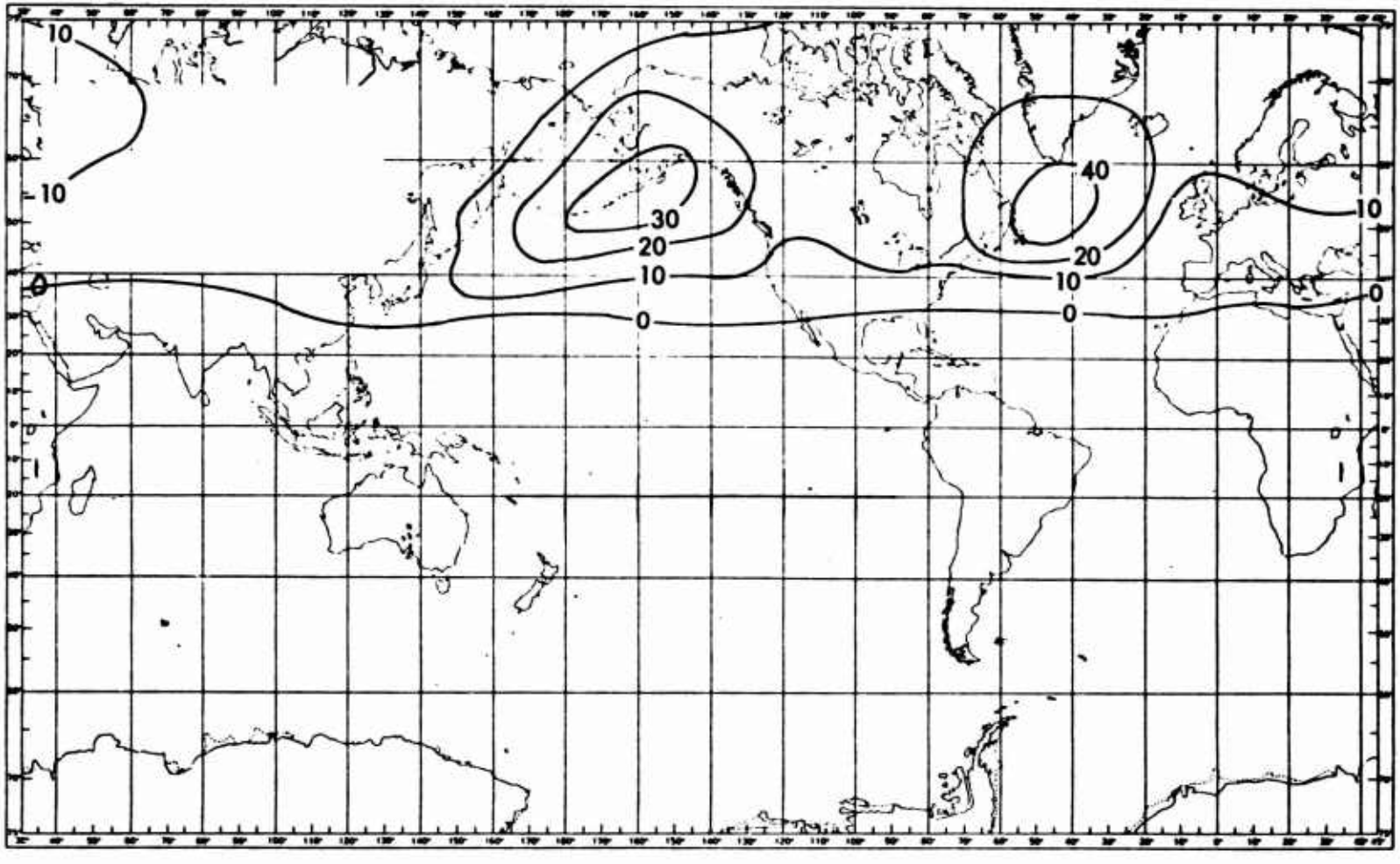

Figure 27. Percentage of Frequency of Potential Icing Conditions, April, 5,000 Feet (Ref. 33).

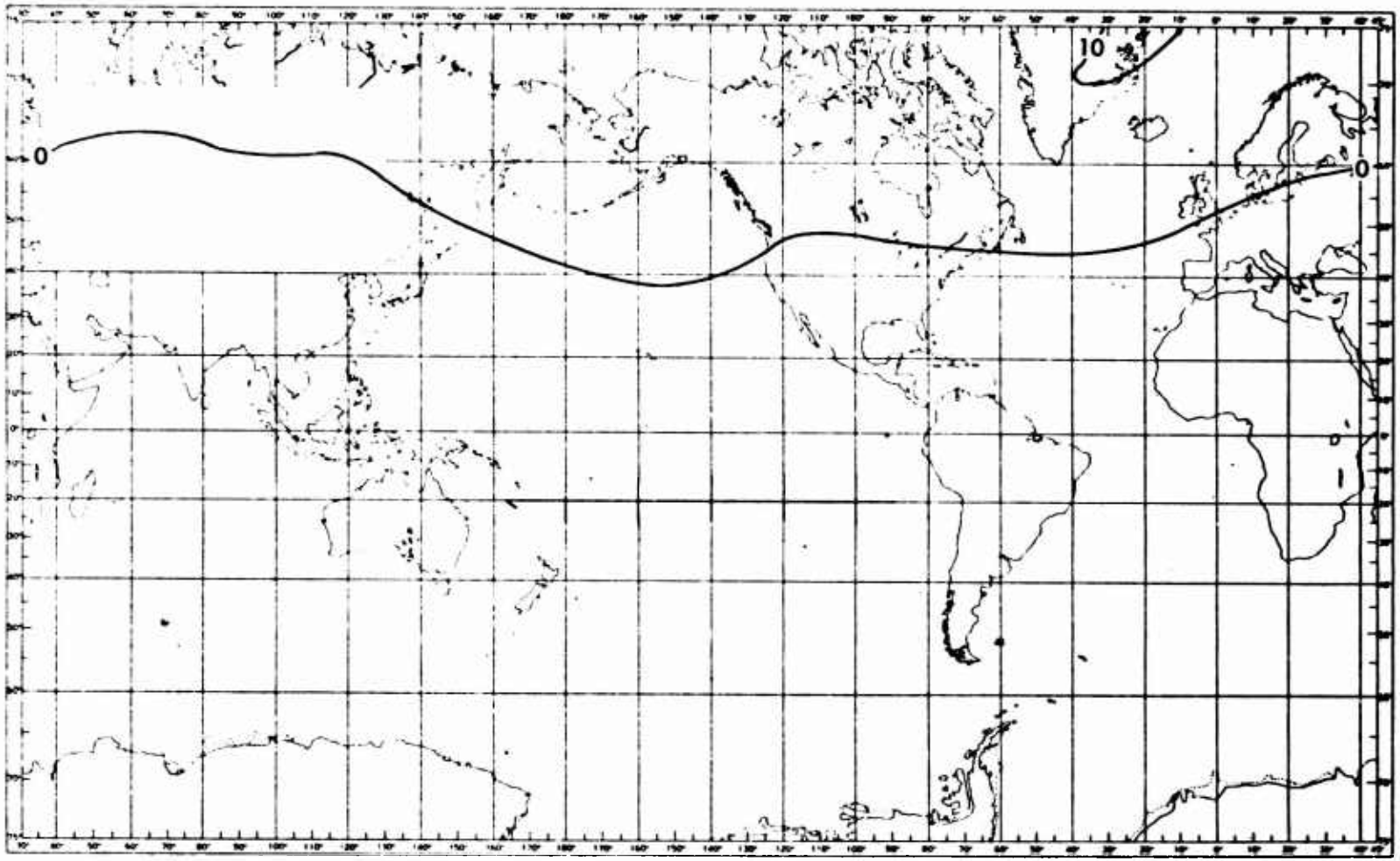

Figure 28. Percentage of Frequency of Potential Icing Conditions, July, 5,000 Feet (Ref. 33).

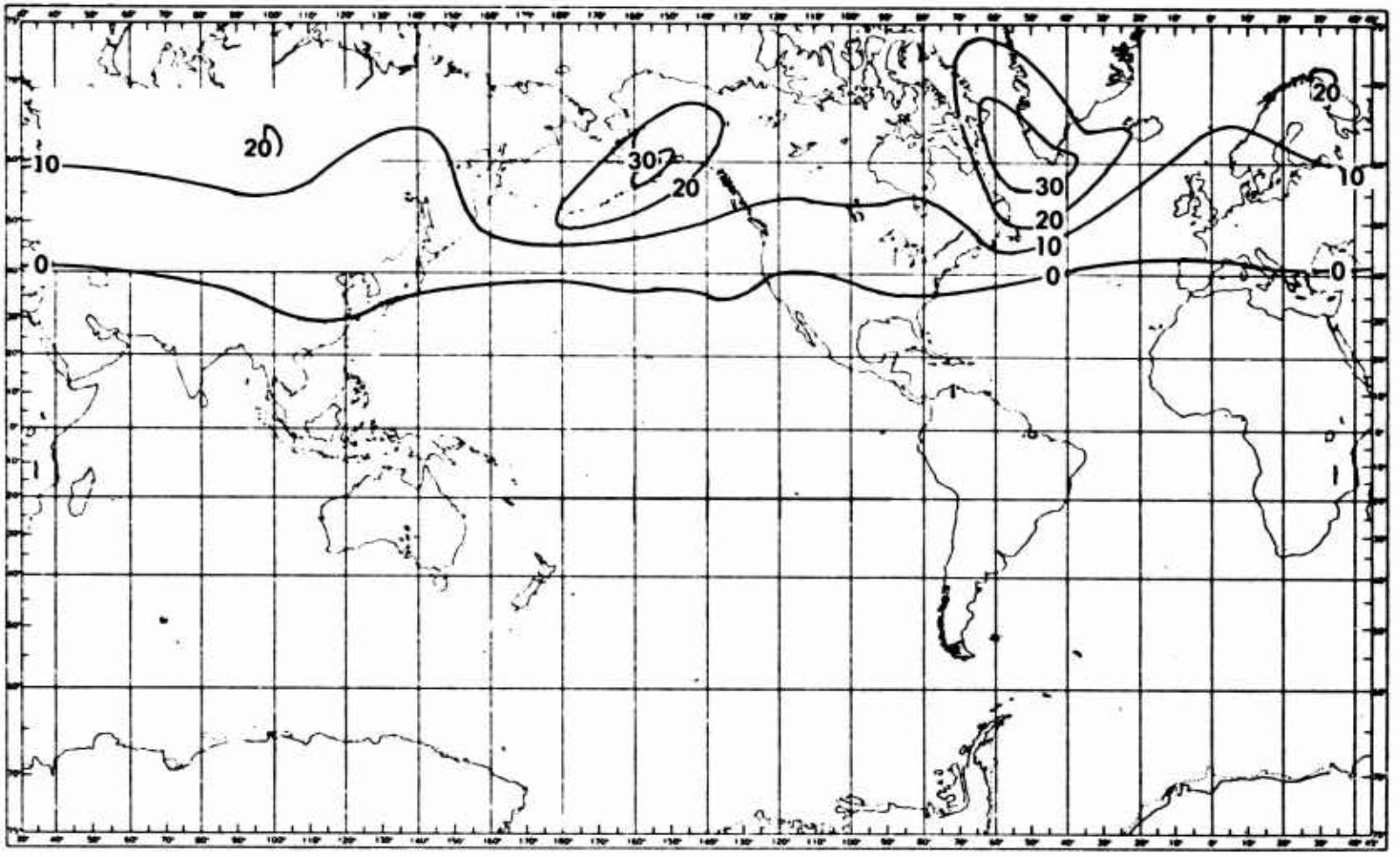

Figure 29. Percentage of Frequency of Potential Icing Conditions, October, 5,000 Feet (Ref. 33).

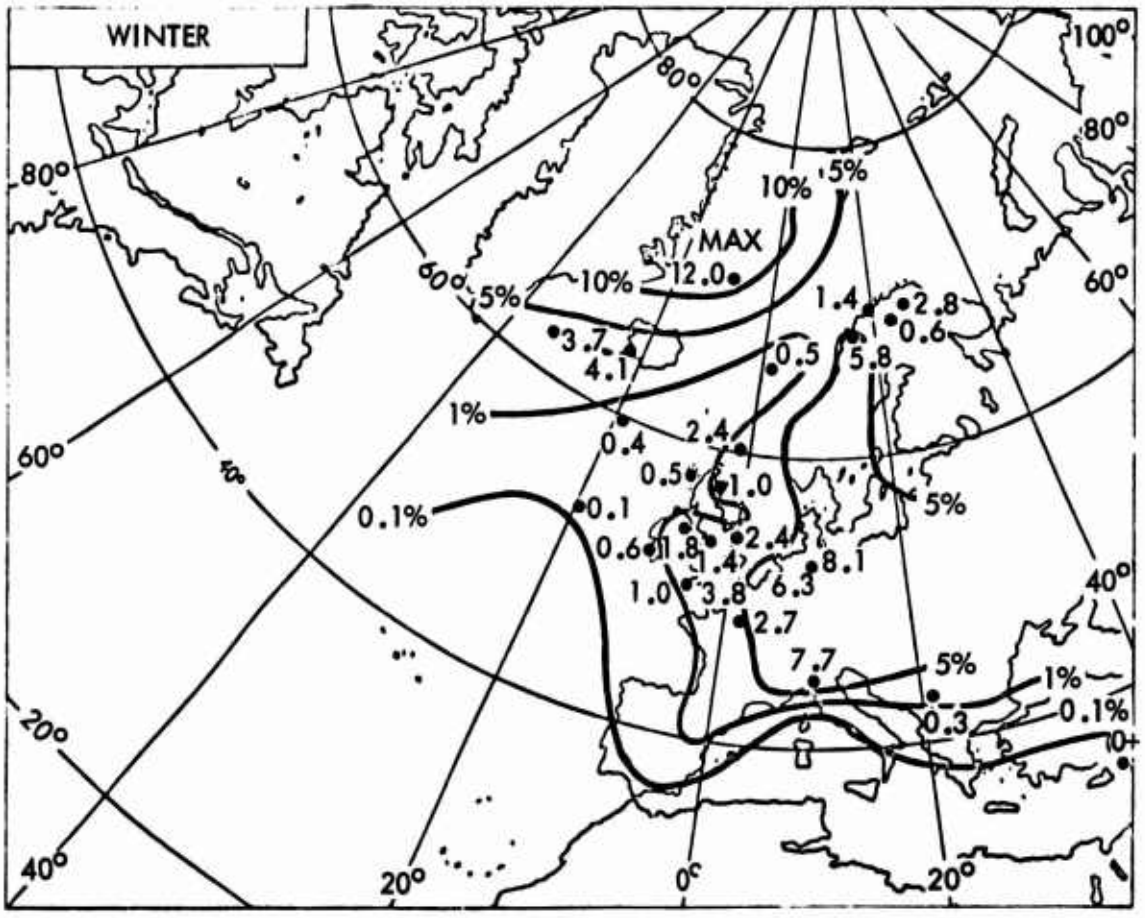

Figure 30. Winter Percentage of Probability of Temperature ≤0°C Combined With More Than Half Cover of Cloud (Averaged 0-1000 Feet) (Ref. 35).

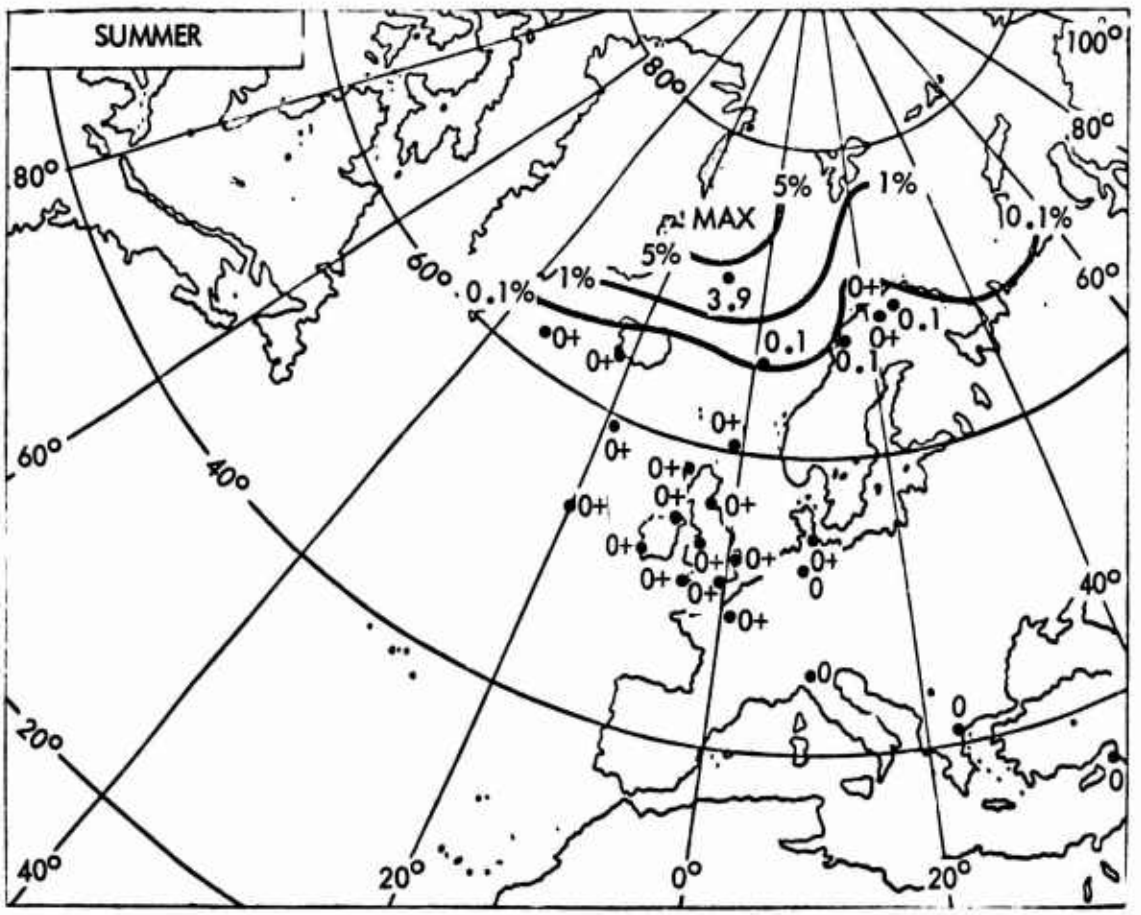

Figure 31. Summer Percentage of Probability of Temperature ≤0° C Combined With More Than Half Cover of Cloud (Averaged 0-1000 Feet) (Ref. 35).

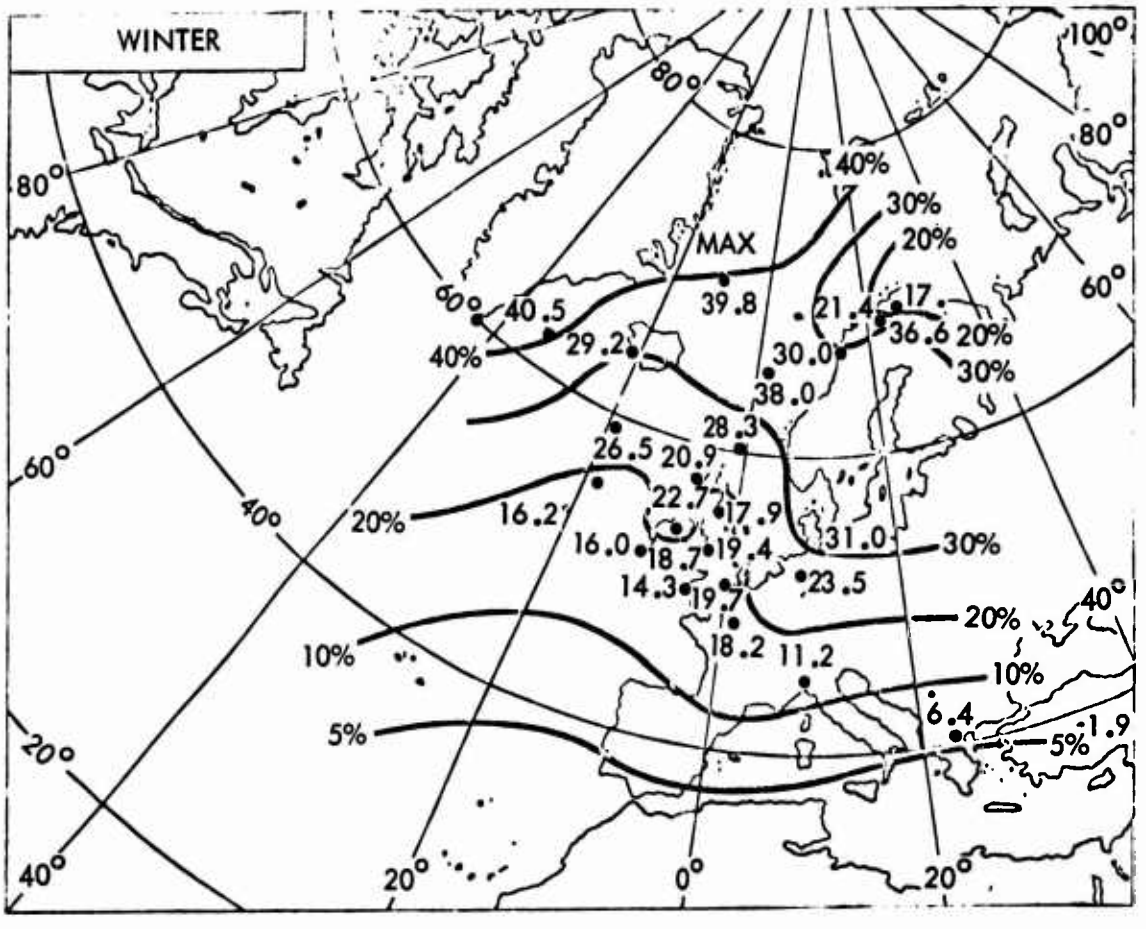

Figure 32. Winter Percentage of Probability of Temperature ≤0°C Combined With More Than Half Cover of Cloud (Averaged 2000-5000 Feet) (Ref. 35).

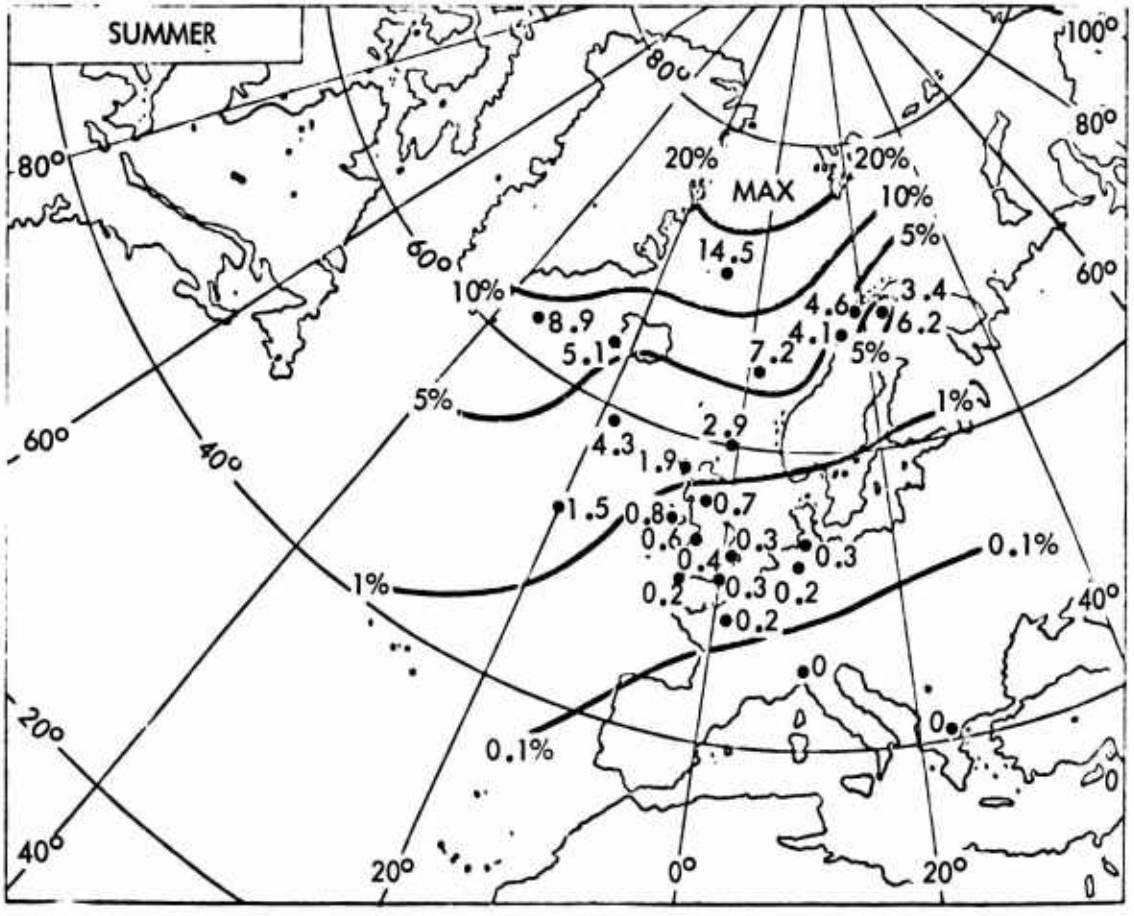

Figure 33. Summer Percentage of Probability of Temperature $\leq 0°C$ Combined With More Than Half Cover of Cloud (Averaged 2000-5000 Feet) (Ref. 35).

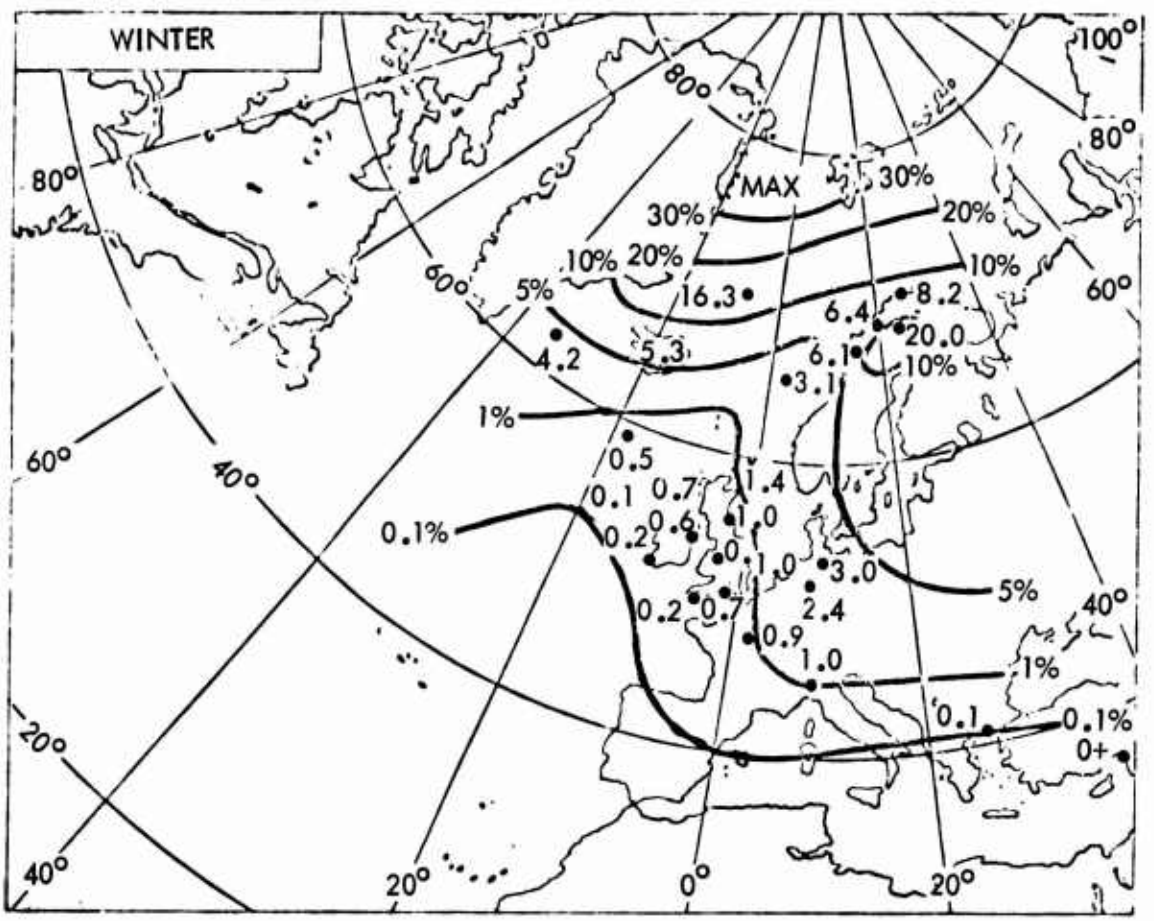

Figure 34. Winter Percentage of Probability of Temperature ≤-10°C Combined With More Than Half Cover of Cloud (Average 2000-5000 Feet) (Ref. 35).

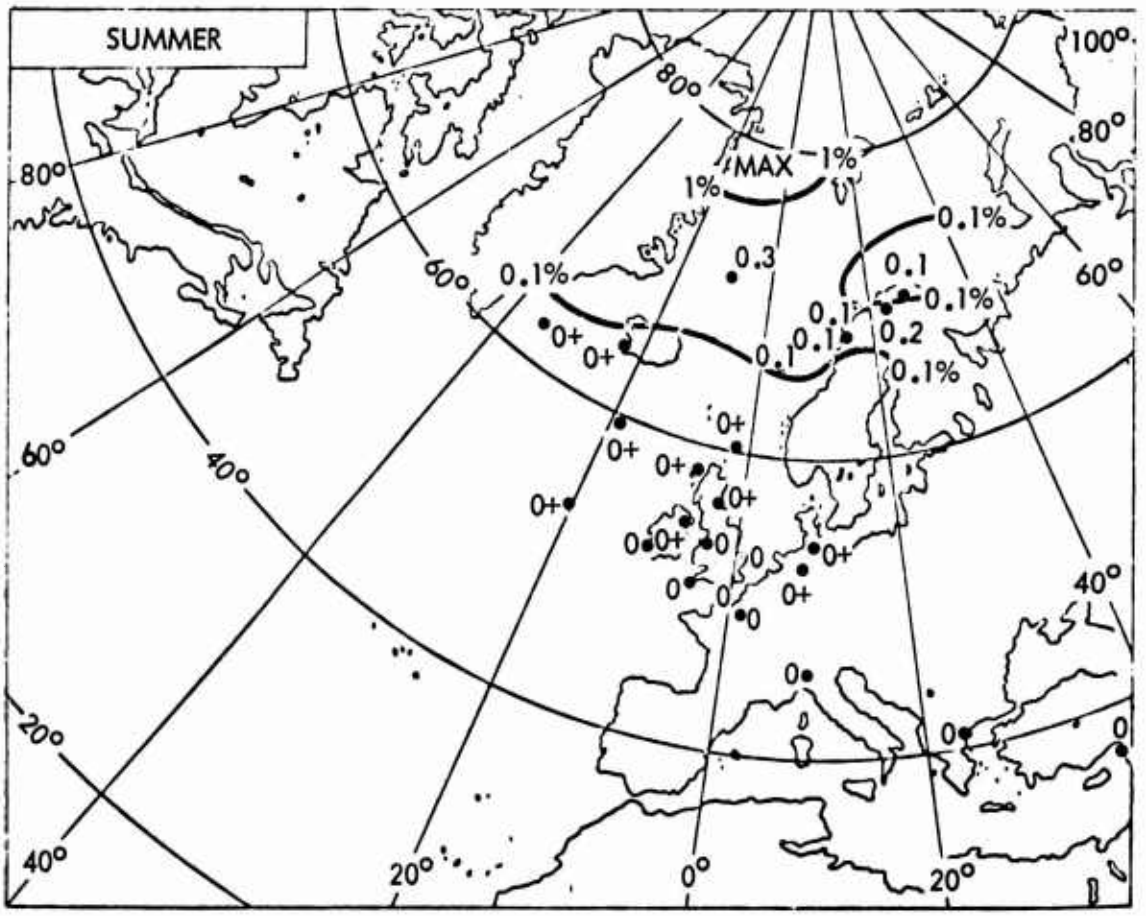

Figure 35. Summer Percentage of Probability of Temperature ≤-10°C Combined With More Than Half Cover of Cloud (Average 2000-5000 Feet) (Ref. 35).

clouds presumed to consist of water droplets. The frequency of occurrence of temperatures below 0°C is assumed to be independent of the frequency of occurrence of clouds. The probability of occurrence of supercooled clouds is the product of the probability of temperatures below freezing at a given altitude and the probability of the occurrence of clouds at this same altitude.

There are major difficulties in determining both the probabilities of the occurrence of below-freezing temperatures and the presence of clouds. The temperatures in the atmosphere are almost entirely obtained through the use of radiosondes carried aloft by balloons. The distribution of radiosonde stations is probably adequate over North America and Europe to prepare maps showing mean monthly isotherms over these regions. However, over the rest of the world, the distribution of radiosonde stations is sparse and the maps showing the mean monthly temperatures are based upon interpolations of unknown accuracies. The locations of the oceanic and coastal radiosonde stations are as given by Crutcher and David (Reference 36) and are shown in Figure 36. Many of these stations have records for only two to five years.

The most recent and complete summaries of upper air temperatures over the world are those published by Crutcher and Meserve (Reference 37) and Taljaard, et al., (Reference 38). One of the sets of their charts gives the mean monthly temperatures at 850 mb (4800 feet msl on the U.S. Standard Atmosphere scale). Figures 37-40 show the positions of the 0°C isotherm as indicated on charts of References 37 and 38. Figures 37-40 also indicate an estimate of the northernmost and southernmost positions that would be exceeded in only 1 percent of the daily observations. At latitudes greater than the highest latitude line, the temperature at 4,800 feet msl may be expected to be below 0°C in at least 99 percent of the days. At latitudes less than the lowest latitude line, the temperature at 4,800 feet msl may be expected to be above 0°C for 99 percent of the days. The conclusion does not apply to areas where the ground elevation is near or above 4,800 feet msl or in the arctic winter. The northern and southern limits of the daily 0°C isotherm were estimated from the frequency distributions given by Ratner (Reference 39) for the United States. Figures 37-40 may be used to indicate areas in which the helicopter icing would not be a problem and areas where it may always be a problem. Extreme positions of the 0°C isotherm were estimated by combining the temperature frequency distribution data published by Ratner (Reference 39) with Crutcher and Meserve's, and Taljaards charts (References 37 and 38). Ratner's data (Reference 39) for the U.S. indicated that when the monthly mean 4,800-foot temperature was 8°C, a temperature 0°C was reached approximately 1 percent of the time; and when the monthly mean was -12°C, a temperature of 0°C was reached approximately 1 percent of the time. On the assumption that this relationship is valid for the rest of the world, the -12°C and +8°C isotherms as given by References 37 and 38 were used as the northern and southern boundaries, respectively, of the 0°C isotherms. For altitudes 1,000 feet above the ground to 4,800 feet msl, the 0°C isotherms are slightly poleward of the positions shown in Figures 35-38. In general, the temperature in this altitude range decreases with altitude. Near the ground, temperature inversions complicate the presentation of temperature data.

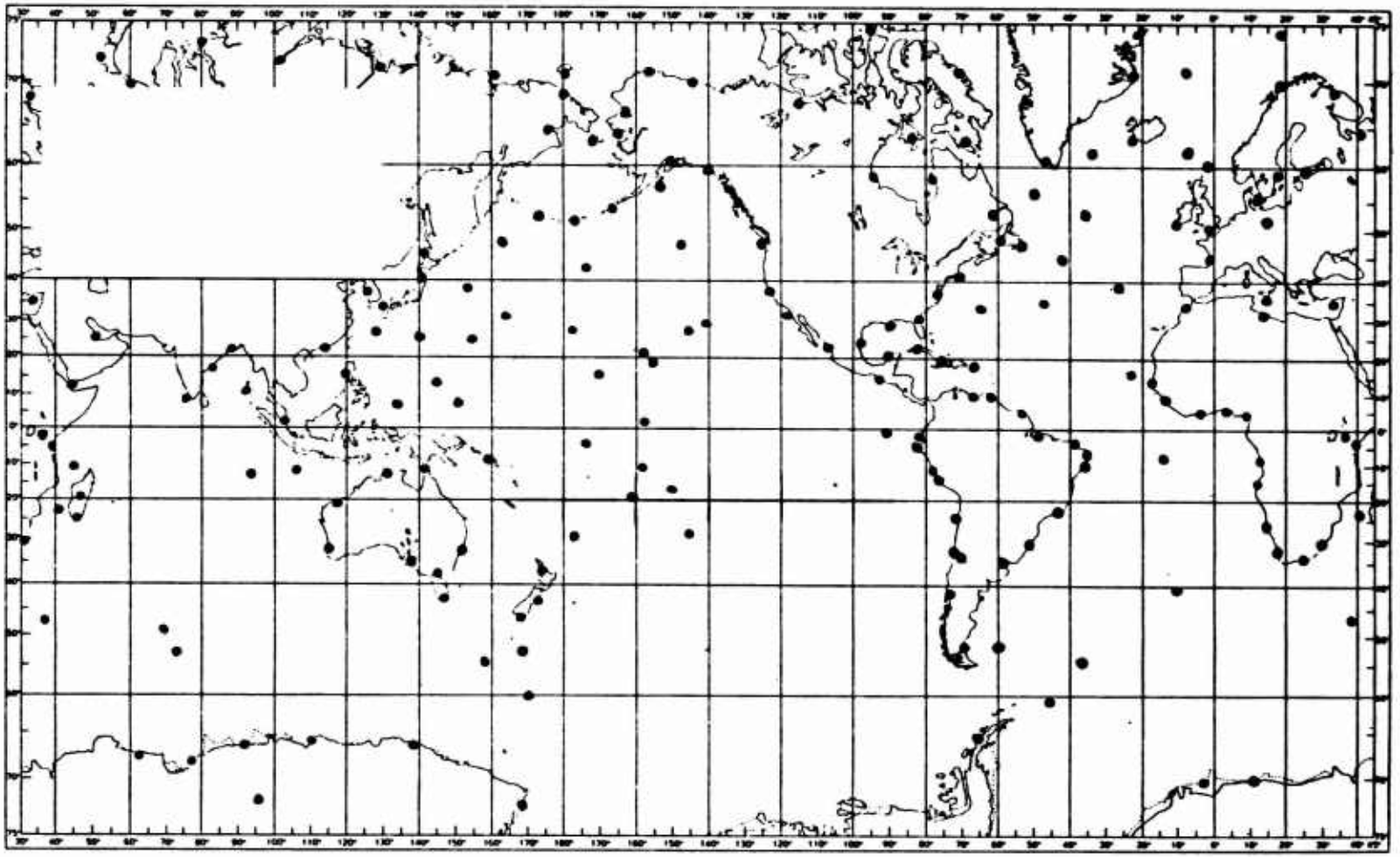

Figure 36. Coastal and Oceanic Radiosonde Stations. (Ref. 36).

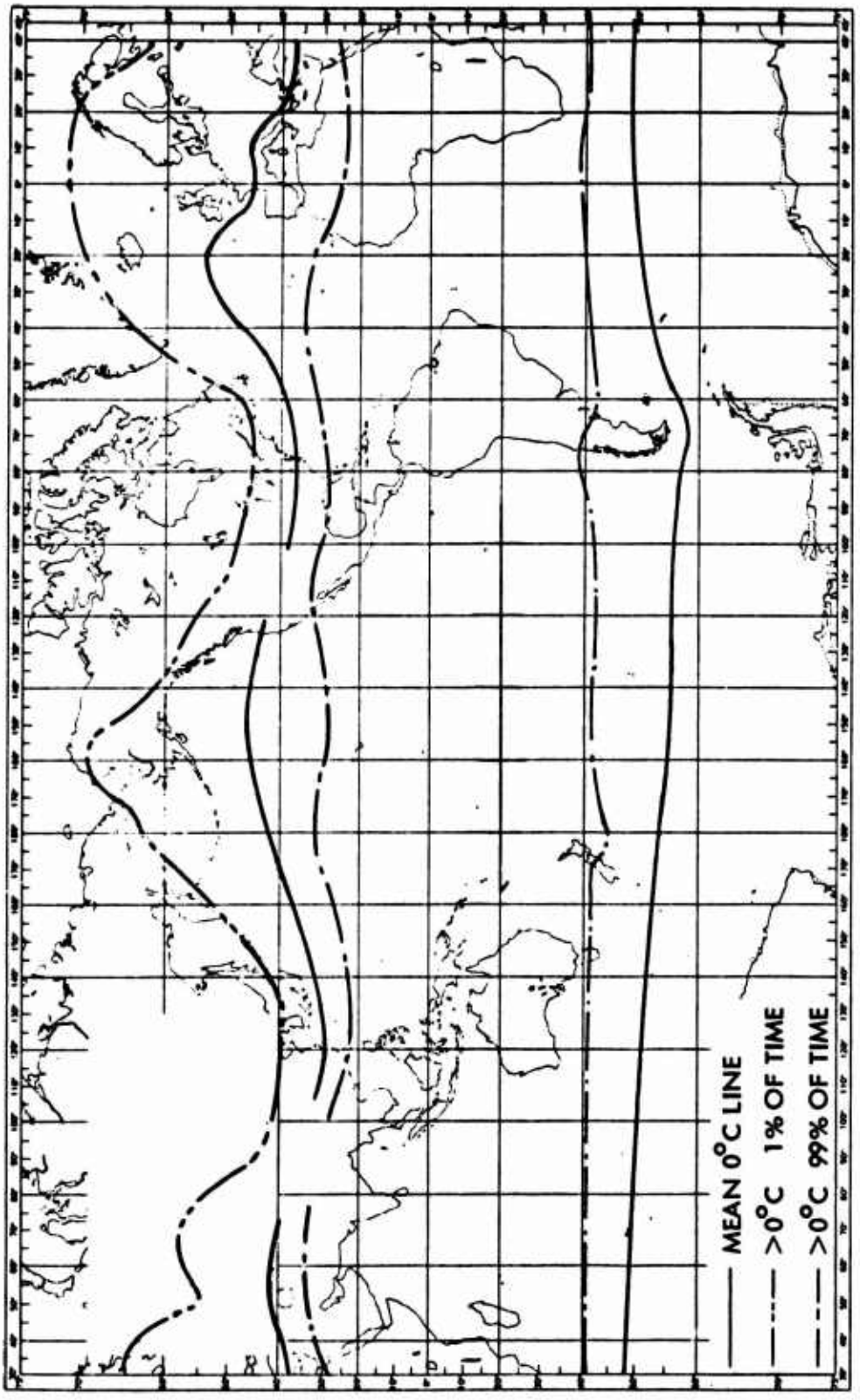

Figure 37. Mean and Extreme (1% and 99%) Positions of 0°C Isotherm at 850 mb (4,800 Feet Standard Atmosphere) for January.

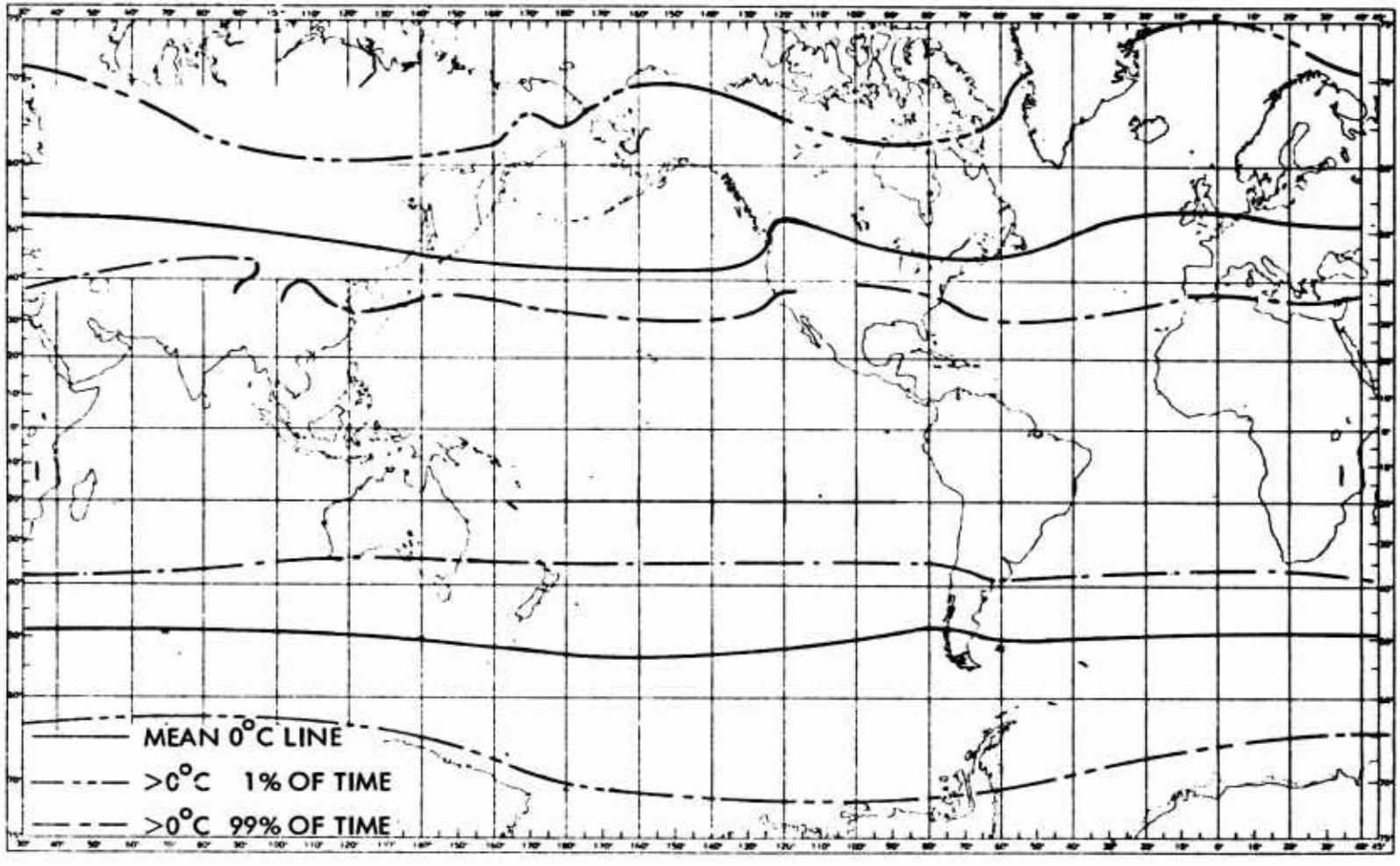

Figure 38. Mean and Extreme (1% and 99%) Positions of 0°C Isotherm at 850 mb (4,800 Feet Standard Atmosphere) for April.

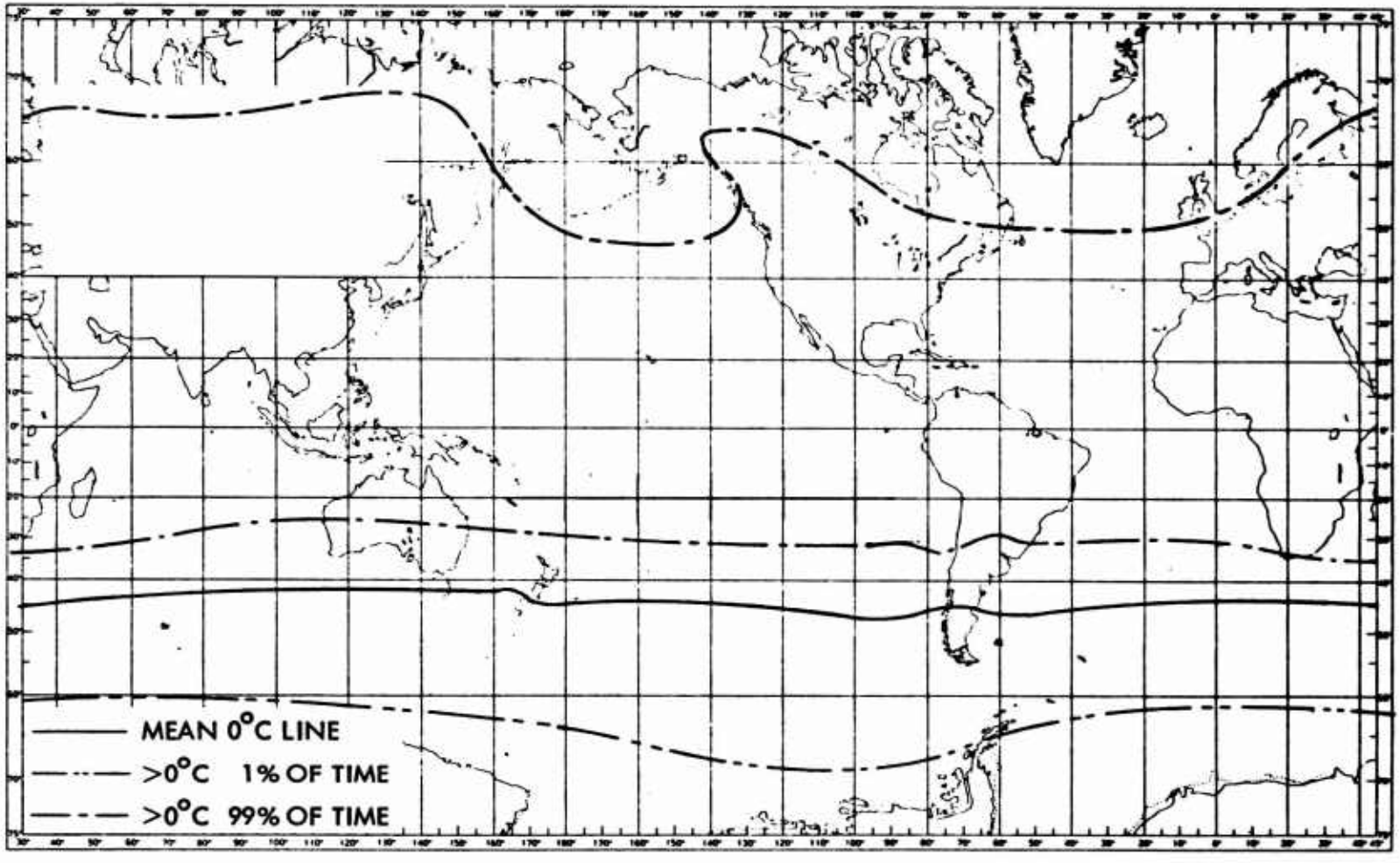

Figure 39. Mean and Extreme (1% and 99%) Positions of 0°C Isotherm at 850 mb (4,800 Feet Standard Atmosphere) for July.

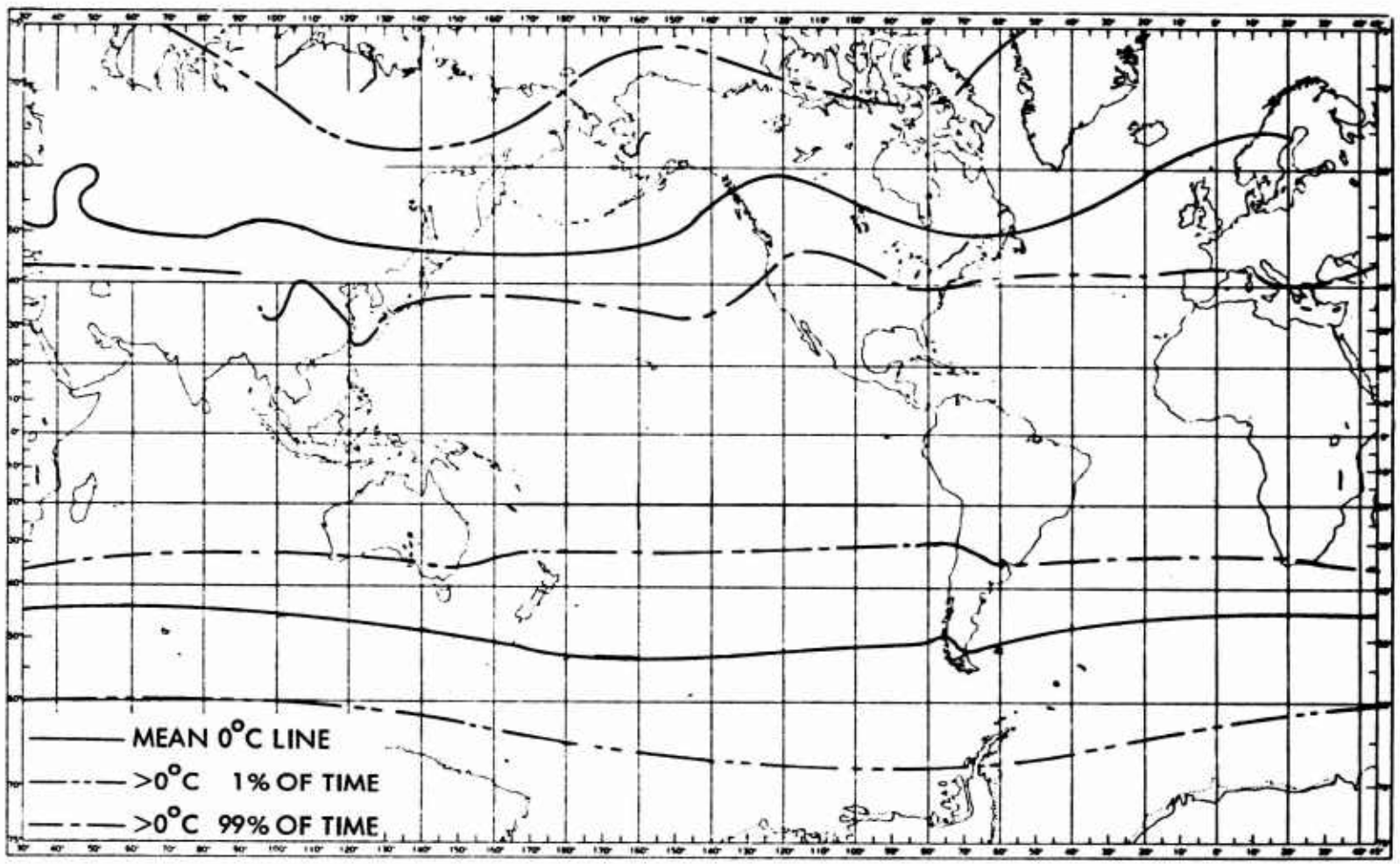

Figure 40. Mean and Extreme (1% and 99%) Positions of 0°C Isotherm at 850 mb (4,800 Feet Standard Atmosphere) for October.

To arrive at maps of potential icing conditions, it is necessary to expand the information given in Figures 35-38 by drawing lines for probabilities other than 0.01 and 0.5 (mean). Such lines are not indicated on Figures 37-40 because these figures are presented only to illustrate the method of arriving at potential icing charts.

To determine the relative frequency of potential icing conditions, data relative to the frequency of occurrence of low clouds are combined with information analogous to that presented in Figures 37-40. Maps indicating the frequency of occurrence of low clouds covering $\geq 5/8$ of the sky (and $> 7/8$ of the sky) have been published by Crutcher and Davis (Reference 36) for the whole world. Solomon (Reference 40) published charts of the northern hemisphere giving the percentage of frequency of 0/10 through 3/10 cloud cover and 6/10 through 10/10 cloud cover at altitudes less than 5,000 feet. The heights refer to cloud bases only. Figures 41 and 42 are taken from Crutcher and Davis (Reference 36) to illustrate the nature of the data. These charts are marine charts only. They do not portray the cloudiness over the continents. The principal purpose of presenting the charts is to show that the available cloud summaries do not give the detail on the vertical extent of the clouds and the altitude of the base of the clouds necessary for a relatively complete summary of potential icing conditions. References 32, 33, and 34 do not indicate how they determined the temperature frequencies for specific altitudes or how they determined the probability that the clouds were at the altitudes where the temperatures were freezing or below. However, the temperature and cloud data illustrated in Figures 37-40 indicate that the information presented in Figures 22-35 may be used as satisfactory qualitative guides to the frequency of occurrence of potential icing conditions. It is important to realize, however, that these charts do not give any indication of the possibility of avoiding icing by flying either at an altitude where there are no clouds or at an altitude at which the temperature is above freezing. Figures 21-35 do not indicate that the potential icing conditions exist throughout the altitude range considered (0 to 5,000 feet, for example).

3.2.2 Statistical Summaries of Icing Reports

Statistical summaries of reports of aircraft icing may be used to estimate the probability of encountering icing, but the interpretation of these statistics is difficult. The reasons for the difficulty is clearly and succinctly stated by Jones in the World Meteorological Organization report on ice formation on aircraft (Reference 13). His statement of the problem and summary of statistical results is:

"Since it has become obvious that the accurate determination of supercooled water content in clouds in any easy and routine way is virtually impossible, considerable interest has been expressed in statistics of icing experiences themselves. At first sight this seems the most logical thing to do since we are only interested in the supercooled water content by virtue of the icing which it may cause. There are several pitfalls to avoid, however,

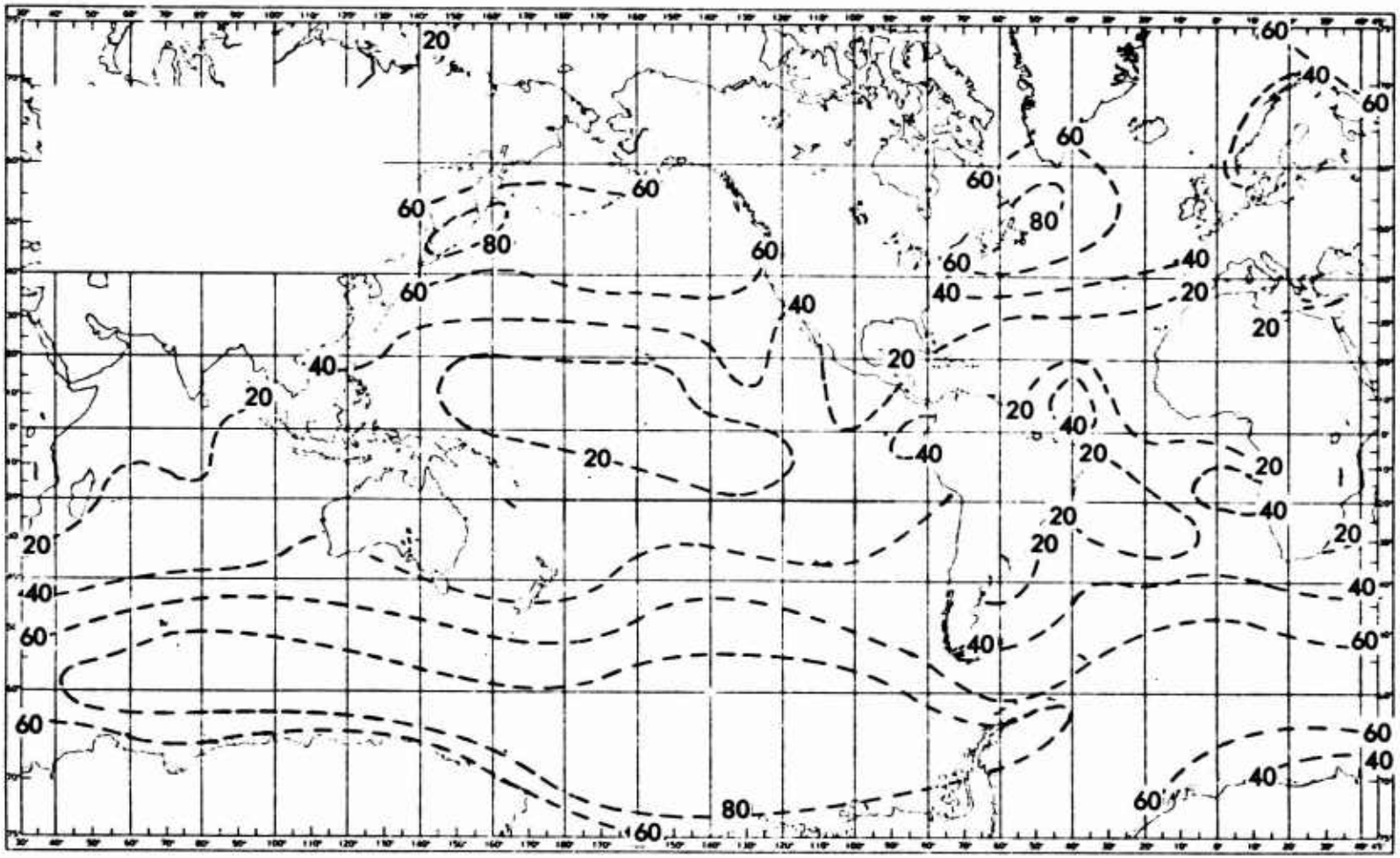

Figure 41. Percentage of Frequency of Low Clouds ≥5/8 Cloud Cover, January (Ref. 36).

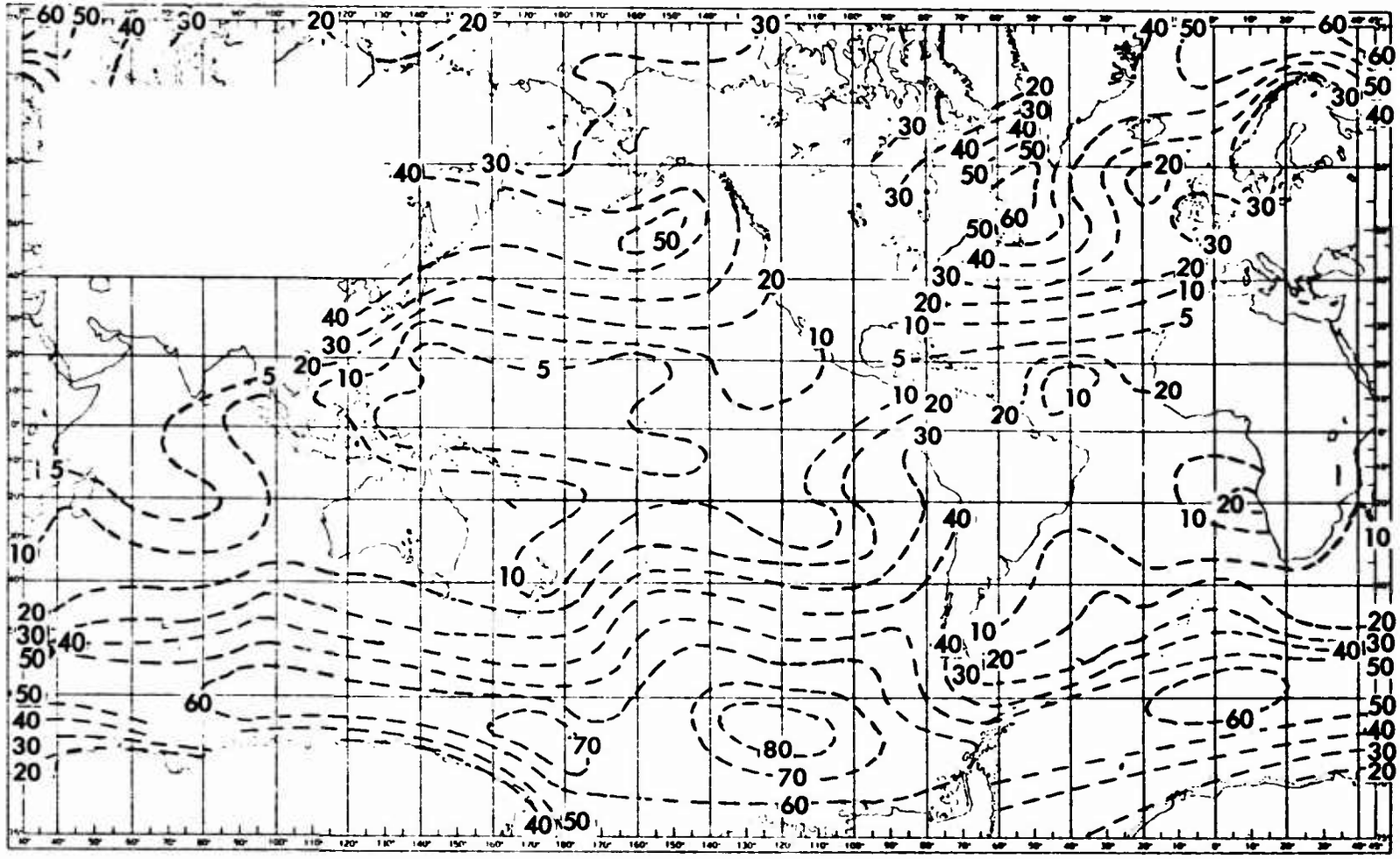

Figure 42. Percentage Frequency of Low Cloud >7/8 Cover, January (Ref. 36).

and as true statistics the observations leave much to be desired. Icing experiences of a particular aircraft are greatly influenced by the characteristics of the aircraft itself and the frequency with which a particular aircraft is exposed to the risk of icing depends on the operating practice of the organization responsible for the operation of the aircraft. Statistics obtained by a particular airline operating a certain route with one type of aircraft are no doubt valuable to the airline but cannot reliably be extrapolated to cover other aircraft, even operating the same route, and certainly cannot be applied with any real prospect of success to other routes."

The most extensive study of aircraft icing statistics to date has been done under the sponsorship of the National Advisory Committee for Aeronautics (NACA), Washington, later the National Aeronautic and Space Administration (NASA), and published in a number of reports (see, for example, References 41, 42, 43 and 44).

Reference must be made to the individual reports for details, but the following summary of results from Perkins (Reference 44) is typical of the information obtained. In reading this summary, it must be remembered that a large proportion of the data was obtained on routine airline operations and is, therefore, subject to the limitations discussed above.

The supercooled water contents were estimated from the rate of ice formation on a probe mounted on the aircraft, and would be subject to the same limitations as most measuring instruments; i.e., there will be a maximum value in the range 1-2 g/m^3, beyond which water contents cannot be measured. The results show that:

1. Icing is not continuous within a cloud; icing encounters in a single cloud may be separated by period of no-icing of varying length. If the period of no-icing exceeded 10 minutes the next experience of icing was regarded as a separate encounter.

2. Along airways within the United States, across the North Atlantic, along the Pacific air route to Alaska and Japan, and over wide areas of the Pacific and Arctic oceans, 3,200 icing encounters were recorded.

3. Frequency distributions of measured icing parameters gave the following statistics:

    a. Liquid water content (averaged over 1-minute intervals of ice buildup, i.e., over distances of the order of 5-7 km) of 0.3 g/m^3, 0.6 g/m^3, and 1.1 g/m^3 was exceeded on 33 percent, 10 percent, and 1 percent of the intervals respectively.

    b. Distances of 42 km, 85 km, and 193 km traveled within icing clouds (cumulative distance in icing throughout an encounter)

were exceeded on 33 percent, 10 percent, and 1 percent of icing encounters, respectively.

c. Depths of icing-cloud layer (460 m, 820 m, and 1430 m) were exceeded on 33 percent, 10 percent, and 1 percent of icing-cloud layers, respectively.

d. Temperatures within icing clouds (below -12°C, -20°C, and -32°C) were exceeded on 33 percent, 10 percent, and 1 percent of icing encounters, respectively.

4. Water contents were estimated to be about two-thirds of the theoretical values from adiabatic lifting.

The statistics concerning depth of icing-cloud layer must be regarded as dubious since they are merely based on the recorded difference of heights between the height of commencement of icing and the height of cessation. They do not, therefore, represent at any time a true vertical depth at a point and it is easy to imagine conditions (e.g., entry and exit from a vertical column containing supercooled water) under which the recorded depth is a very substantial underestimate of the true vertical depth. In a substantial number of icing encounters, of course, the aircraft continued without change of height.

The statistics do not give the probabilities of encountering an icing cloud, but this has been attempted for the 10,000-foot and 18,000-foot levels over ocean areas in the northern hemisphere by Perkins, Lewis, and Mulholland (Reference 42). The data, of course, show geographical variations depending on the frequency of clouds and the temperature variation at these levels. At the 18,000-foot level, the frequency of clouds ranges from a value of about 1.5 percent over the Arctic Ocean in winter to 18 percent on the Western Pacific in spring, while the frequency of icing clouds is usually around 1 or 2 percent but reaches as high as 7 percent in the region of the East China Sea in summer and hardly ever occurs over the Arctic Ocean in winter and spring. At the 10,000-foot level, the highest frequency of icing clouds (6.5 percent) is in the Western Pacific, while icing has not been reported at this level in the region of the Azores.

Two analyses of reports received from civil aircraft on the trans-Atlantic route have been made by Rohan and Ohoonghusa (Reference 45) and by Crossley (Reference 46). Reference 45 analyzed 37,746 reports received at Shannon during the period October 1953 to September 1954. Only 582 (1.5 percent) reported ice, with a higher frequency in the winter months than in the summer. The maximum frequency of icing reports was in the region of -5°C to -7°C and 95 percent of reports were in the temperature band from 0 to -25°C. The lowest temperature at which icing was reported was -42°C. About one-third of all reports of icing were associated with warm fronts and about one-third with cold fronts or occlusions; of the remaining one-third, the large majority (about 75 percent) were in a cold air mass.

Three percent of all icing reports were described as severe icing, 21 percent as moderate icing, and the remainder as light in intensity.

Reference 46 analyzed POMAR and AIREP reports received as routine reports at London Airport from trans-Atlantic aircraft in the months of January and July 1955-57. In January, 3.8 percent of the observations made at temperatures at or below 0°C reported icing. The maximum number of reports were received in the temperature band from -22°C to -25°C, but this merely reflected the fact that a high proportion of the flying was taking place around this temperature. Correction for this bias shows a maximum frequency of 10.4 percent of flying time in the -6° to -7°C band in icing conditions with a broad spread at 4 to 6 percent of flying time in the temperature band from -8°C to -25°C. When the observations were related to the reports of flying in clouds, it was found that 43 percent of all flights in clouds in the temperature band -4°C to -7°C experienced icing, falling off irregularly to a minimum of 7 percent at -36°C to -39°C and then, surprisingly, rising again to 20 percent in the range from -40°C to -44°C, the latter temperature being the lowest temperature at which icing was reported.

In July, icing was less frequent (1.7 percent of observations) and is attributed by Crossley (Reference 46) to the lower frequency of convection clouds over the sea compared with the winter. The frequency of icing in clouds is about 20 percent from -4°C to -11°C and falls to a minimum of 8 percent at -20°C to -23°C. As in January, there is again a second maximum, of 13 percent, in the region of the lowest icing temperatures reported, but this now occurs in the temperature range from -24° to -27°C, although the height range, 18,000-24,000 feet, is the same. Crossley (Reference 46) suggests that this secondary maximum is associated with flight near the tops of cumulonimbus clouds. It may be that the anvil cloud is on occasions so extensive as to obscure the more active core of the cloud which at lower heights would be visually avoided.

Perkins (Reference 43) and Samuels (Reference 47) have presented data on icing of aircraft during climb and descent. Data on aircraft icing at altitudes below 5,000 feet taken from these reports are given in Table IV.

Fighter-interceptor aircraft were used at Duluth and Seattle, and very low speed aircraft were used at the other four locations. The data are not adequate to justify the preparation of probability of exceedance values for icing of given intensities. Further, none of the data are from helicopter flights.

The total number of icing encounters reported by Perkins in Reference 44 is shown in Table V as a function of altitude.

Heath's recent Air Force work (Reference 31) has also been evaluated. He has published charts indicating the probability of encountering icing conditions in the northern hemisphere at 850 mb (5,000 feet msl). These charts are shown in Figures 43 through 46. Heath directly used only

TABLE IV. AIRCRAFT ICING AT ALTITUDES ≤ 5,000 FEET

Date	Reference	Locations	Total No. Flights	Flight With Icing
Duluth, Aug 55 - Jun 56 Seattle, Nov 55 - Sep 56	44	Seattle and Duluth	1174	15
29 Oct 31 to 1 Jun 32	48	Chicago, Cleveland, Dallas and Omaha	864*	71

*Maximum possible number of daily flights. No data reported on the number of flights cancelled because of weather.

TABLE V. THE DISTRIBUTION OF AIRCRAFT ICING BY ALTITUDE

Altitude Interval (feet msl)	No. of Reports of Icing
0 - 1000	13
1100 - 2000	59
2100 - 3000	74
3100 - 4000	110
4100 - 5000	143
>5100	2801

temperature and aircraft icing data. The differences between the ambient air temperature and the dew point were used to infer the presence or absence of clouds. The statistical test of the validity of this approach was weak in that the test did not require that the cloud height correspond with the predicted cloud height. The use of aircraft data indicating the probability of icing in a supercooled cloud does, however, add a significant factor. Table VI shows the values used by Heath and Table VII shows for comparison values cited by Briggs and Crawford of the United Kingdom (Reference 35). The data in these tables is useful in providing at least a trend in the relation between the potential threat of icing and the probability of encountering icing in flight.

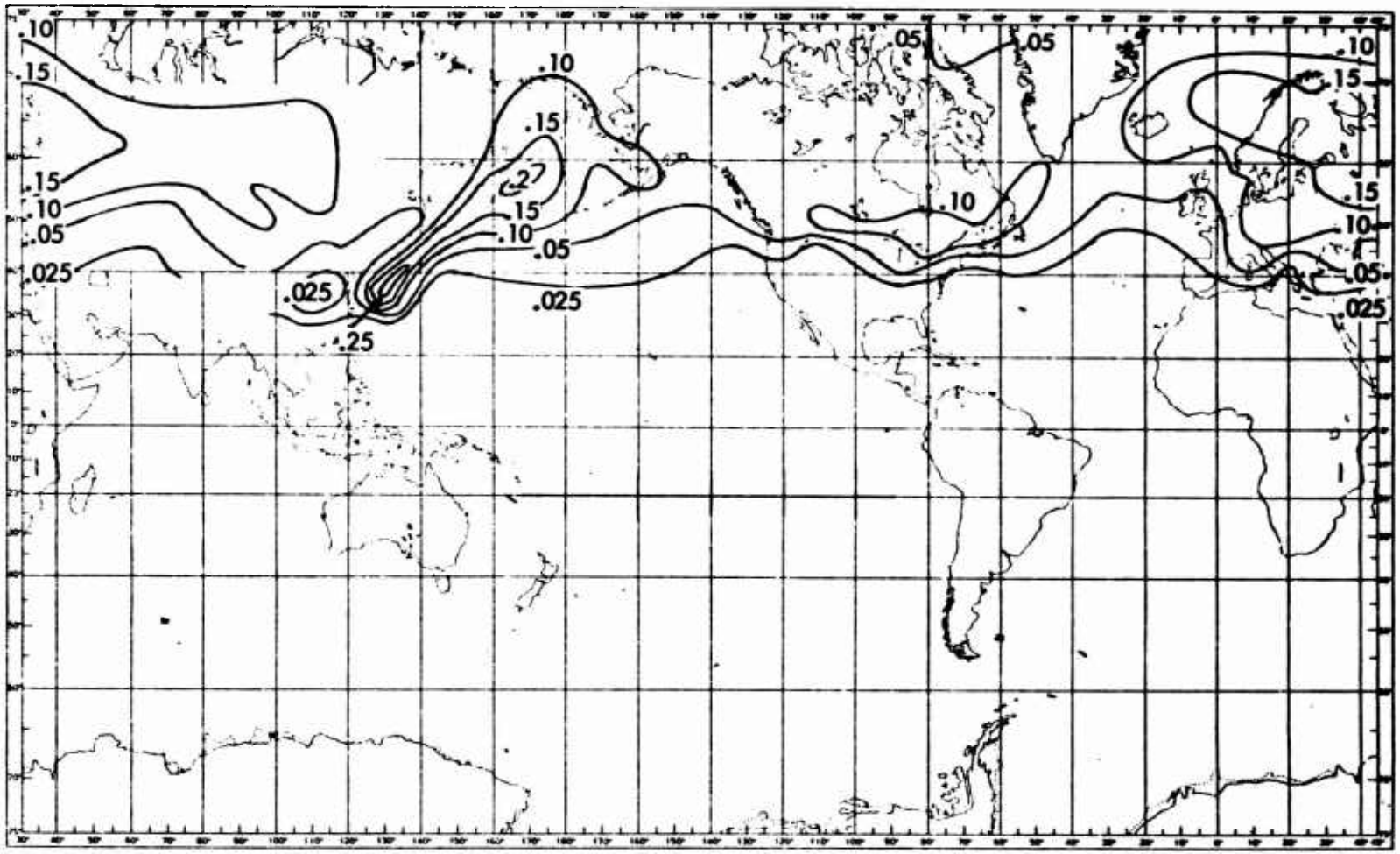

Figure 43. Probability of Encountering Icing Conditions at 5,000 Feet, January.

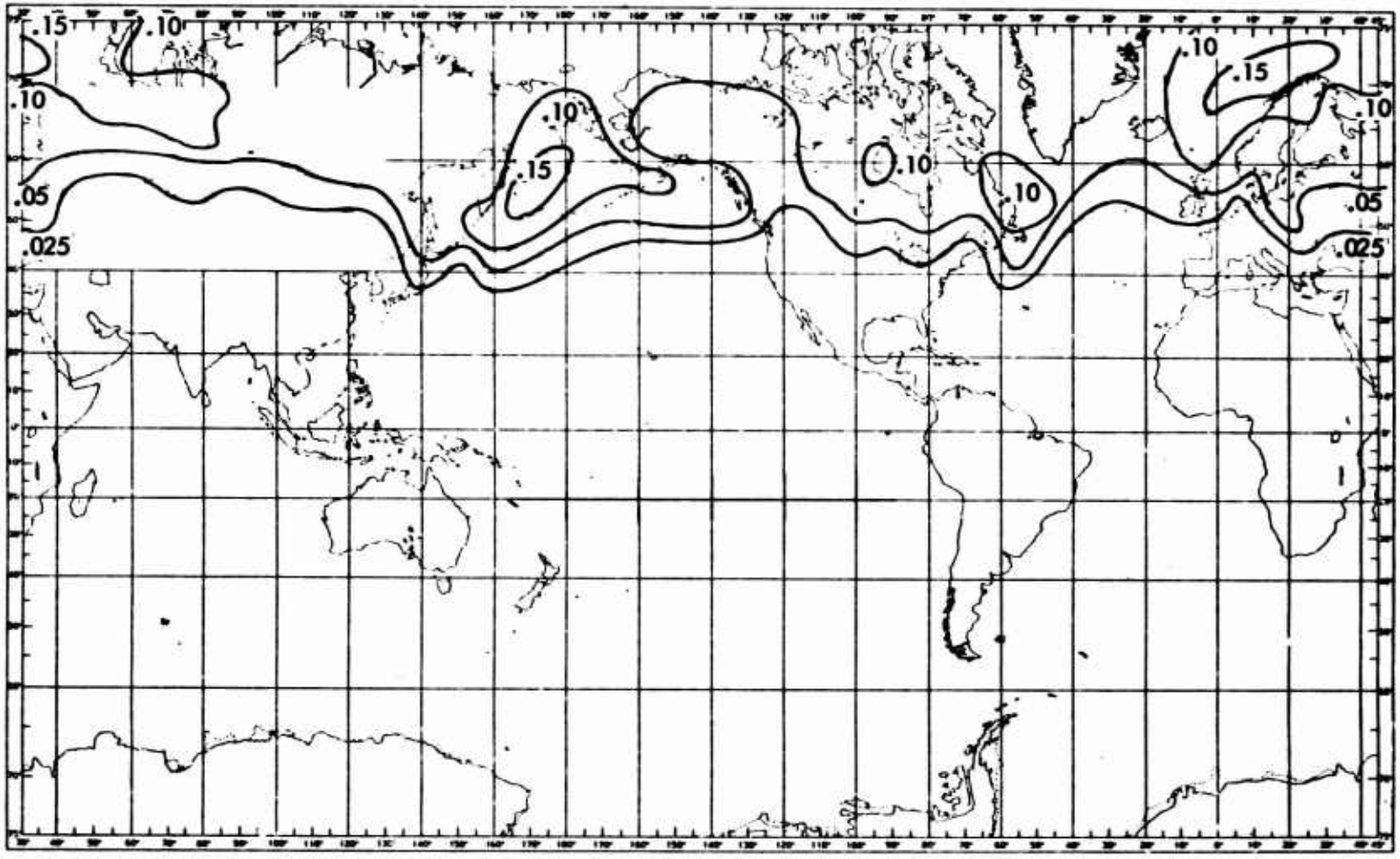

Figure 44. Probability of Encountering Icing Conditions at 5,000 Feet, April.

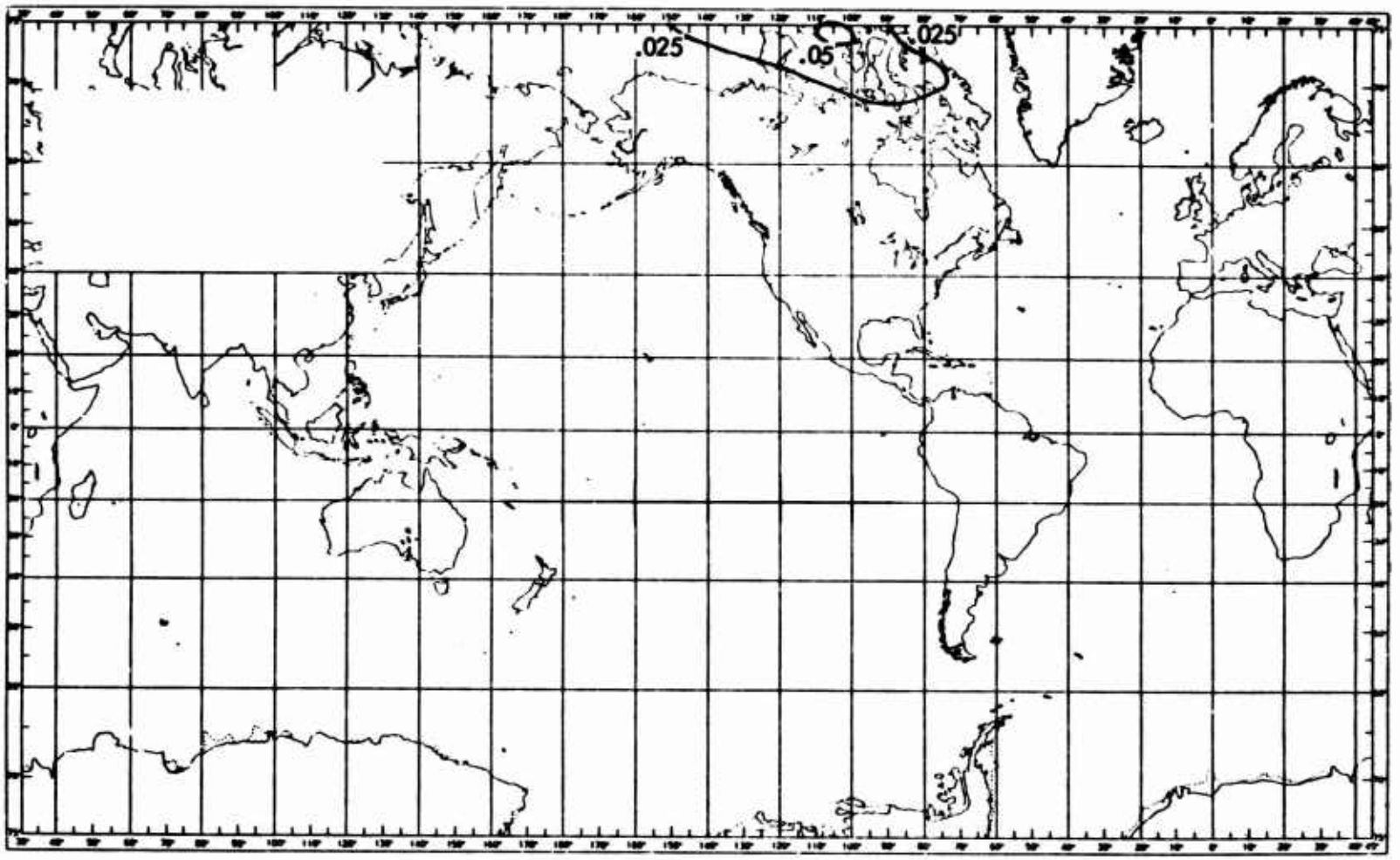

Figure 45. Probability of Encountering Icing Conditions at 5,000 Feet, July.

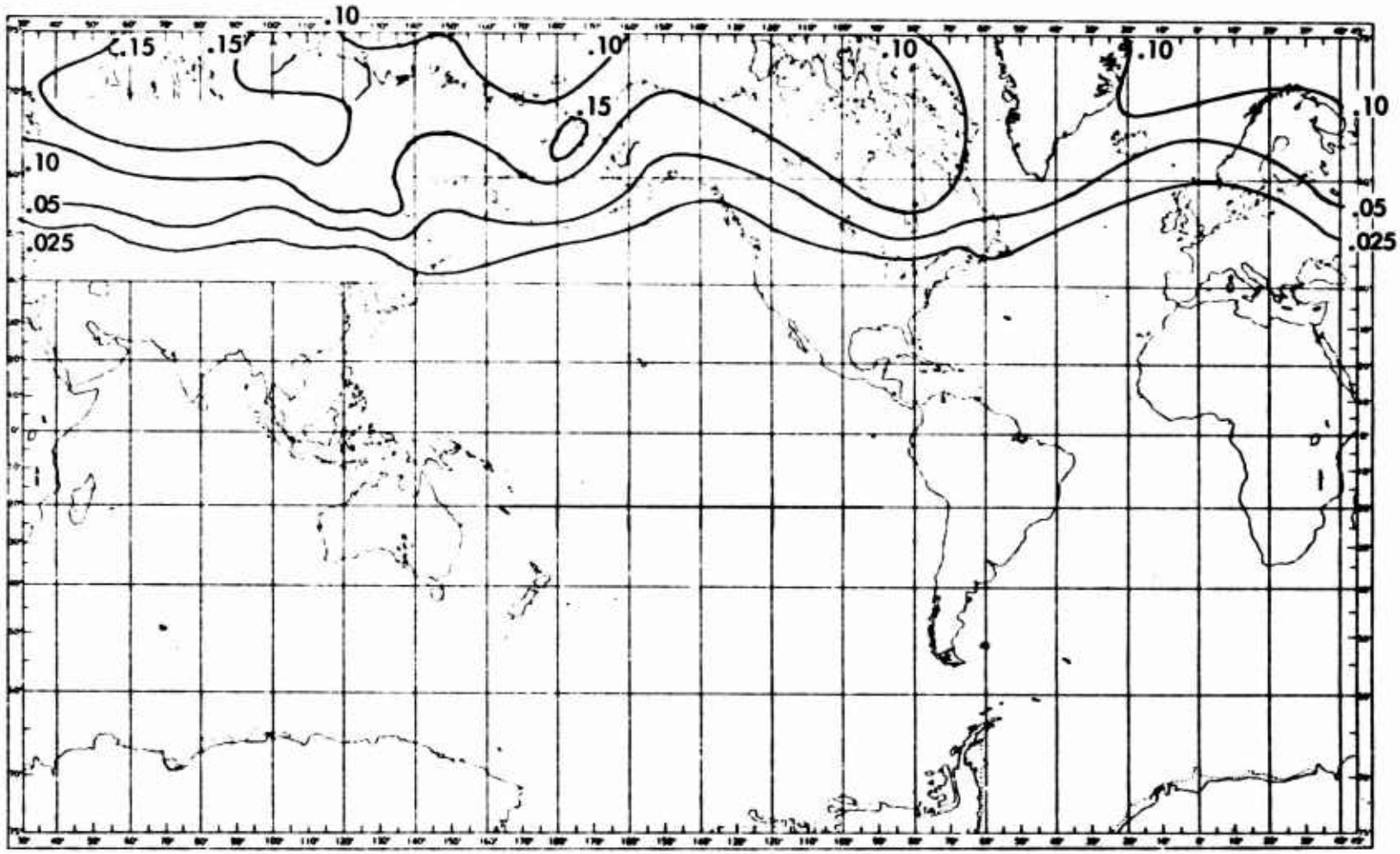

Figure 46. Probability of Encountering Icing Conditions at 5,000 Feet, October.

TABLE VI. FREQUENCY OF AIRCRAFT ICING IN SUPERCOOLED STRATIFORM CLOUDS AS A FUNCTION OF TEMPERATURE

Ambient Air Temperature °C	No. of Icing Cases	% Frequency of Icing
0 to -2	49	17
- 3 to -7	600	49
- 8 to -12	450	39
-13 to -17	252	18
-18 to -22	141	17
-23 to -27	43	11
-28 to -32	15	8
Total	1550	28

TABLE VII. FREQUENCY OF AIRCRAFT ICING IN SUPERCOOLED STRATIFORM CLOUDS AS A FUNCTION OF MONTH

Month	Jan/Feb	Mar/Apr	May/Jun	Jul/Aug	Sep/Oct	Nov/Dec
Percentage of Icing	33	33	50	75	80	56

Direct comparison of the data cited by Heath (Reference 31) and those cited by Briggs and Crawford (Reference 35) is not possible because one summary is by temperature and one is by season; but, on the whole, the percentage of flights in supercooled clouds that produced icing appear to be significantly higher for the British data given by Briggs and Crawford. Thus, from this standpoint, Heath's data may yield a low probability of icing. In any event, the actual criteria for vehicle dispatch will probably be "icing potential" and not "probability of encountering icing in flight" because there is no way of forecasting the actual condition in a cloud once the "potential" has been established. Thus, an unprotected vehicle would not be permitted to fly into any condition as long as there is danger of icing (clouds at below-freezing temperatures).

In any event, the data presented in Tables VI and VII should be used only as a qualitative guide for helicopter icing because of the significant difference in altitude range and speed of the aircraft. (It is suspected that heating effects due to airspeed have not been properly accounted for in the data, and that "true" icing conditions will occur more frequently for lower speed vehicles.)

Extensive research programs on icing have been conducted at the observatory on the summit of Mount Washington, New Hampshire. During the period 1942-1948 measurements were made on the characteristics of the icing and the associated cloud every 3 hours during icing conditions. The average number of such observations in a winter month was approximately 300. Conrad (Reference 48) published a statistical review of these measurements. A summary of these results is given in Table VIII.

TABLE VIII. MEAN AND STANDARD DEVIATIONS OF ICING VARIABLES

	Mean	Standard Deviation
Liquid water content, g/m^3	0.472	0.269
Diameter of drops, microns	12.96	5.14
Rate of ice accumulation at 200 mph on a nonrotating cylinder 7.62 cm (3 in.) in diameter, in./hr	1.45	1.29
Number of droplets per cm^3	625	624
Ambient air temperature, °C	-10.65	6.63

The seasonal and diurnal linear correlation coefficients shown in Table IX are significantly different. These differences may be associated with "chance" or with the seasonal means of some other important variable such as temperatures having a narrower range of values than the daily temperatures. The correlation coefficients clearly indicate that, for a particular case, the rate of icing is not simply a linear function of the liquid water content of the cloud.

TABLE IX. CORRELATION COEFFICIENTS

Elements	Seasonal Correlation Coefficients	Diurnal Coefficients
Rate of icing and liquid water content of clouds	+0.934	+0.405
Rate of icing and drop diameter	+ .752	+0.266
Liquid water content and drop diameter	0.509	0.013

Table X indicates that the liquid water content of the clouds on the summit of Mount Washington was significantly higher than the liquid water content

of the clouds that produced aircraft icing. This suggests that helicopters flying near the ground in mountainous or hilly terrain may be subjected to more severe icing than those flying over level terrain.

TABLE X. PROBABILITY OF LIQUID WATER EXCEEDING GIVEN VALUES

Probability of Exceeding	.90	.75	.50	.33	.25	.10	.01
Liquid Water Content of Cloud (g/m^3) (Conrad)	0.14	0.26	0.45	0.58	0.66	0.80	1.22
Aircraft Measurements (Ref. 13)				0.33		0.6	1.1

The exceedance probabilities of various ice accumulation rates shown in Table XI may be useful as a guide for helicopter studies, but it is probable that icing rates in clouds not adjacent to a mountain would be slightly lower.

TABLE XI. PROBABILITY OF RATE OF ACCUMULATION OF ICE ON NONROTATING 3 INCH-DIAMETER CYLINDER AT 200 MPH

Probability of Exceeding	.64	.48	.31	.17	.10	.01
Rate of Accumulation, in./hr	0.64	1.28	1.92	2.56	3.19	5.76

3.2.3 Probability of Icing

The probability of aircraft icing at a specified altitude in the atmosphere is the probability that an aircraft at that specified altitude will, in fact, experience icing. A supercooled water cloud amount ≥ 0.6 of the sky is a necessary, but not a sufficient, condition for aircraft icing; hence, the probability of icing is, in general, less than the probability of potential icing conditions existing. Briggs and Crawford (Reference 35) state that the correction factor to convert potential icing probability to "actual" icing probability is between 0.5 and 0.75 and that the factor is nearer 0.5 in the colder winter months and nearer 0.75 in the warmer summer months. References 30 and 31 used U.S. Air Force data on the occurrence of icing to determine the correction factor, which was expressed as a function of the ambient air temperature minus the dew-point temperature. Figures 47-50 illustrate the final results obtained by Katz (Reference 30). These charts differ significantly from those shown in Figures 22-39 in that Katz indicates a secondary maximum of icing in the tropics near longitude 120°E. The secondary maximum appears entirely unreasonable if the data illustrated in Figures 30-35 are a reasonable approximation to the actual air temperatures. Figures 51-54 illustrate Heath and Cantrell's (Reference 31) estimate of the probability of icing. They derived their charts from temperature

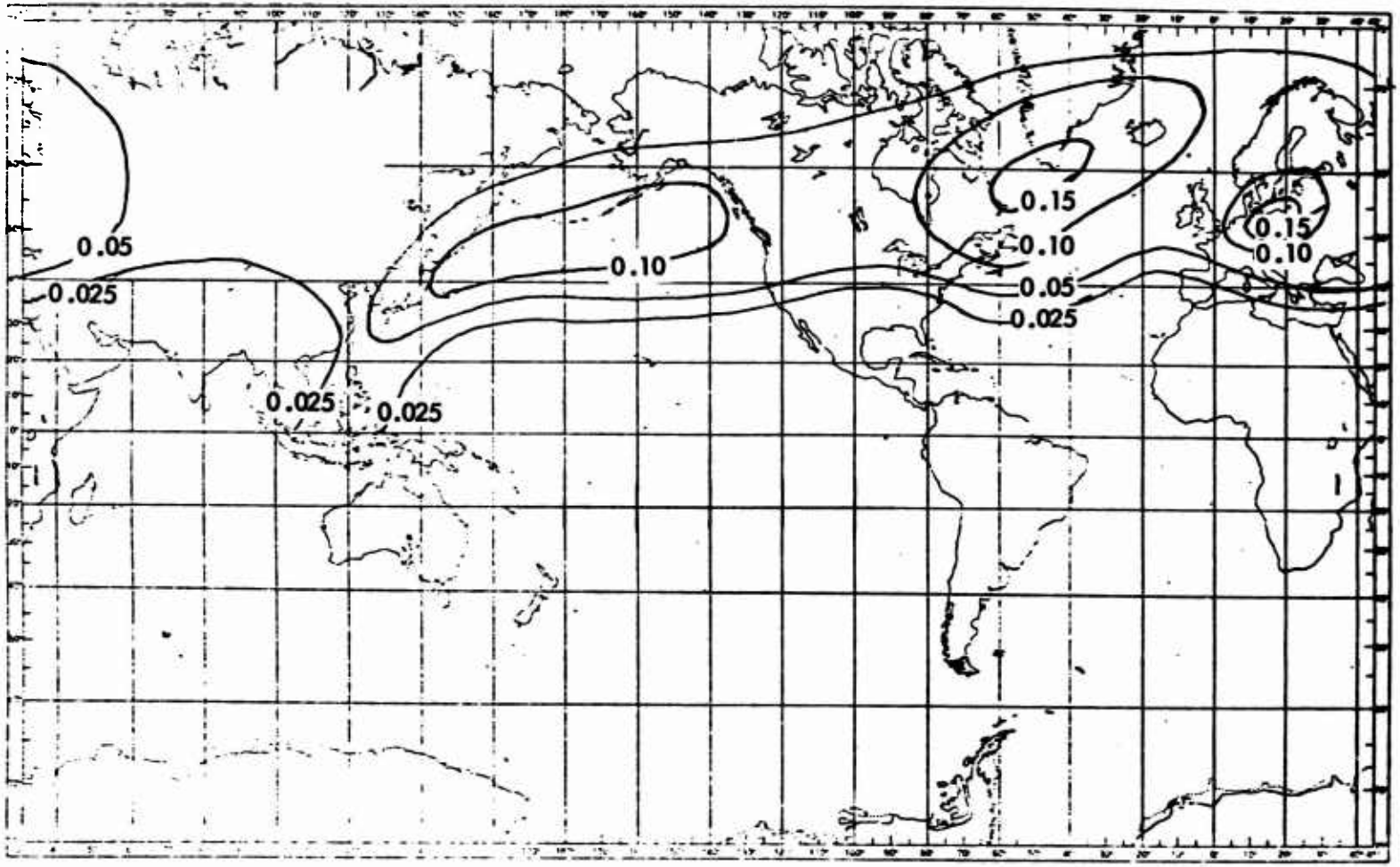

Figure 47. Probability of Encountering Icing Conditions, Winter, 5,000 Feet (Ref. 30).

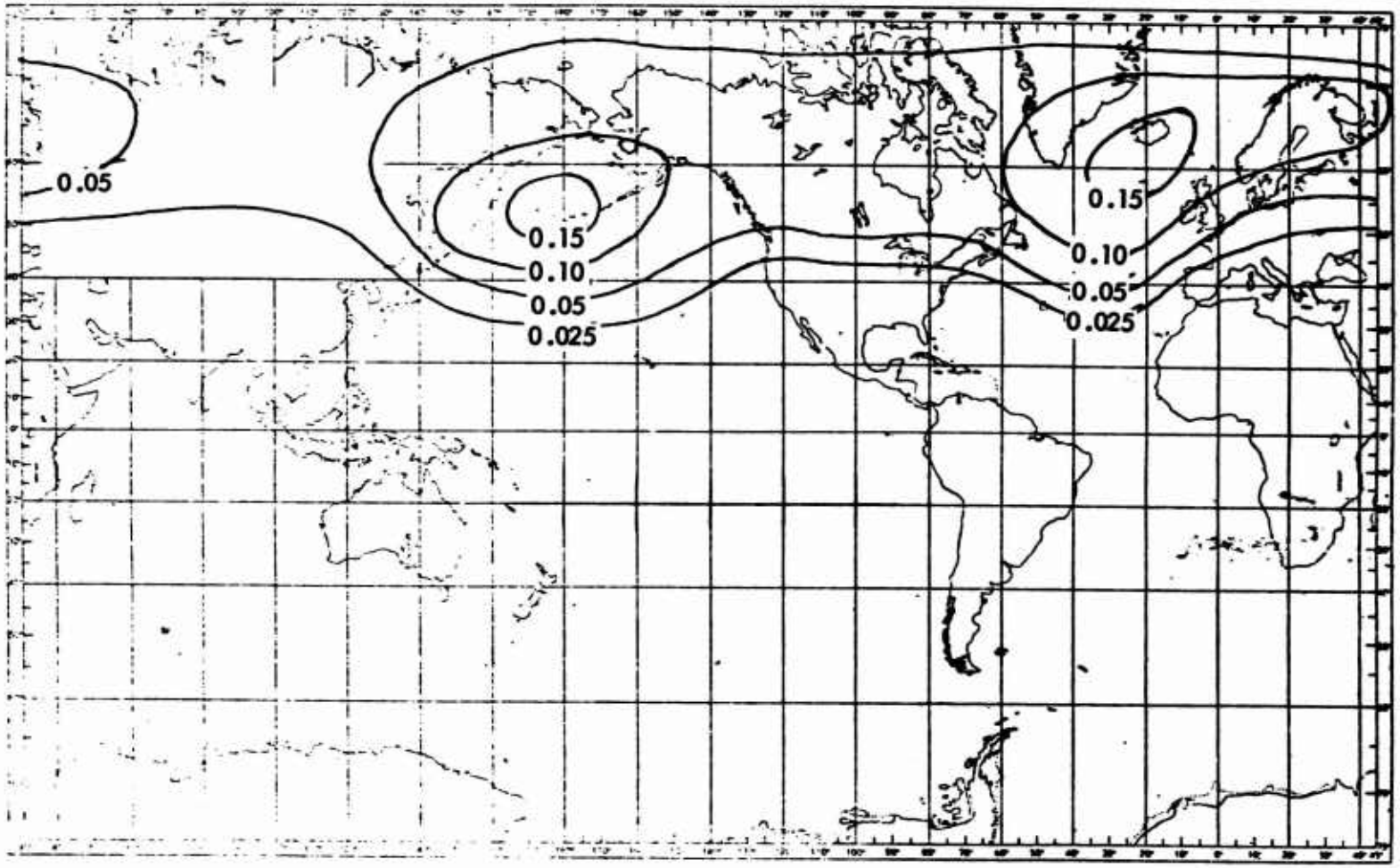

Figure 48. Probability of Encountering Icing Conditions, Spring, 5,000 Feet (Ref. 30).

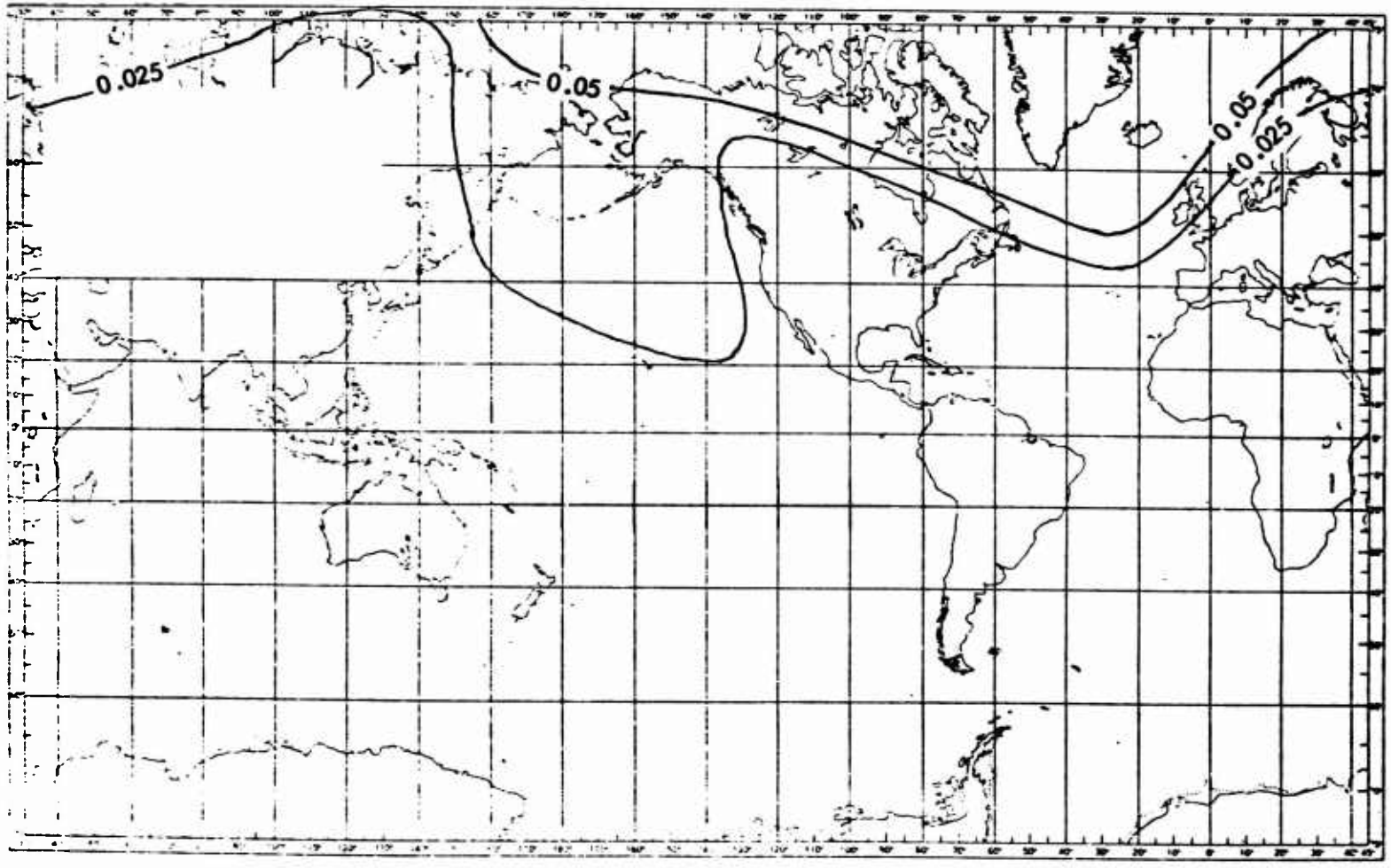

Figure 49. Probability of Encountering Icing Conditions, Summer, 5,000 Feet (Ref. 30).

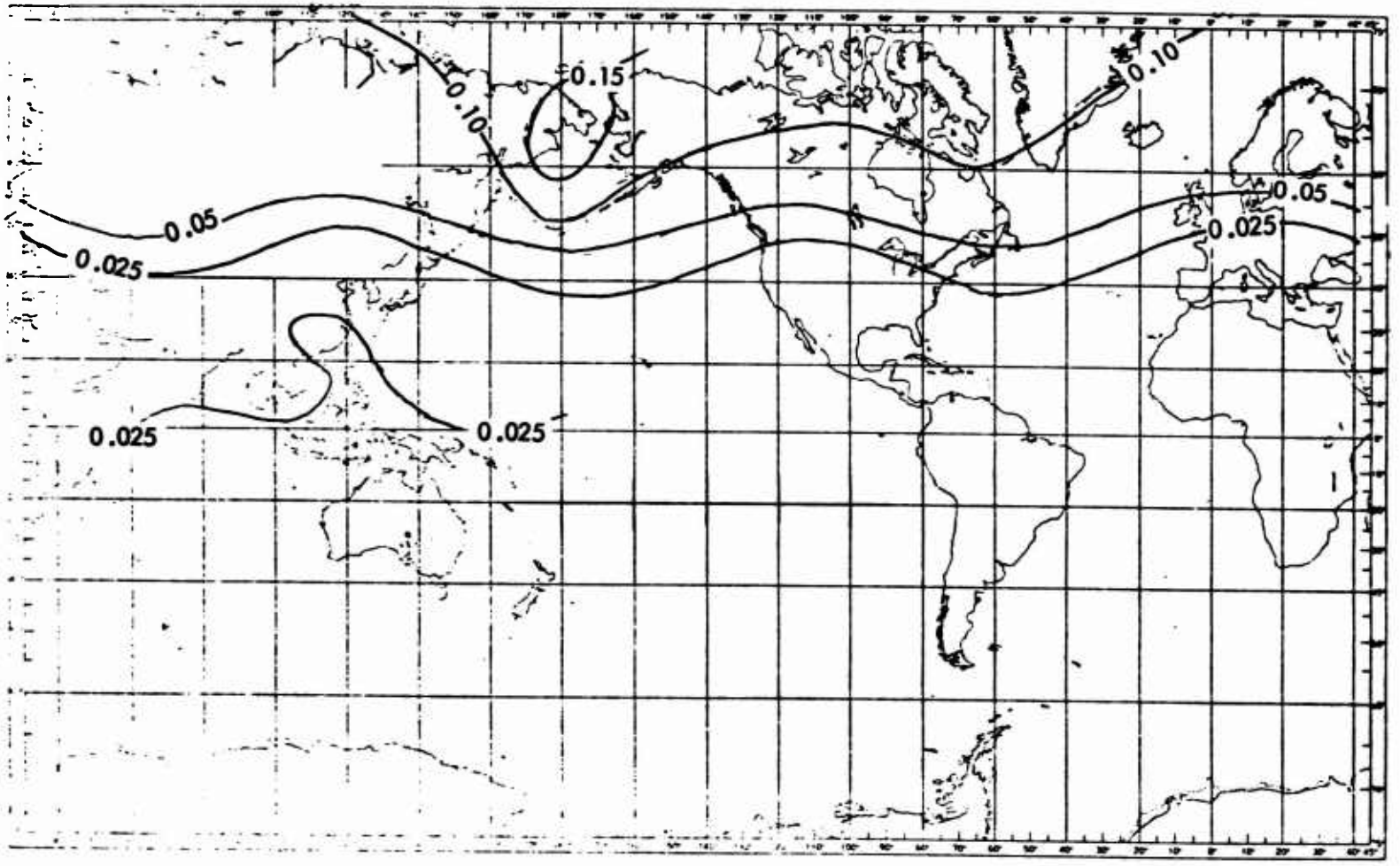

Figure 50. Probability of Encountering Icing Conditions, Autumn, 5,000 Feet (Ref. 30).

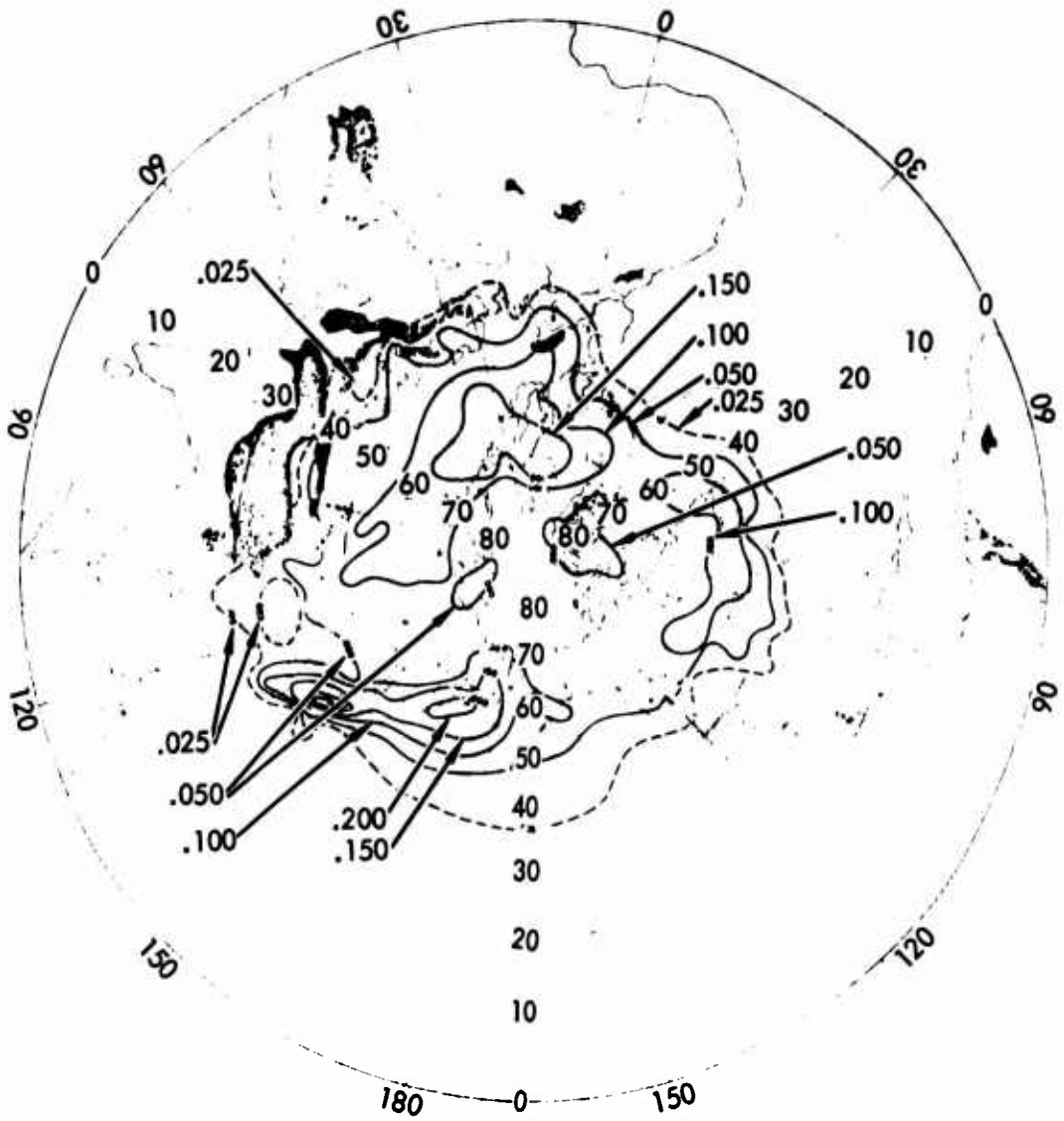

Figure 51. Probability of Encountering Icing Conditions, 5,000 Feet, January.

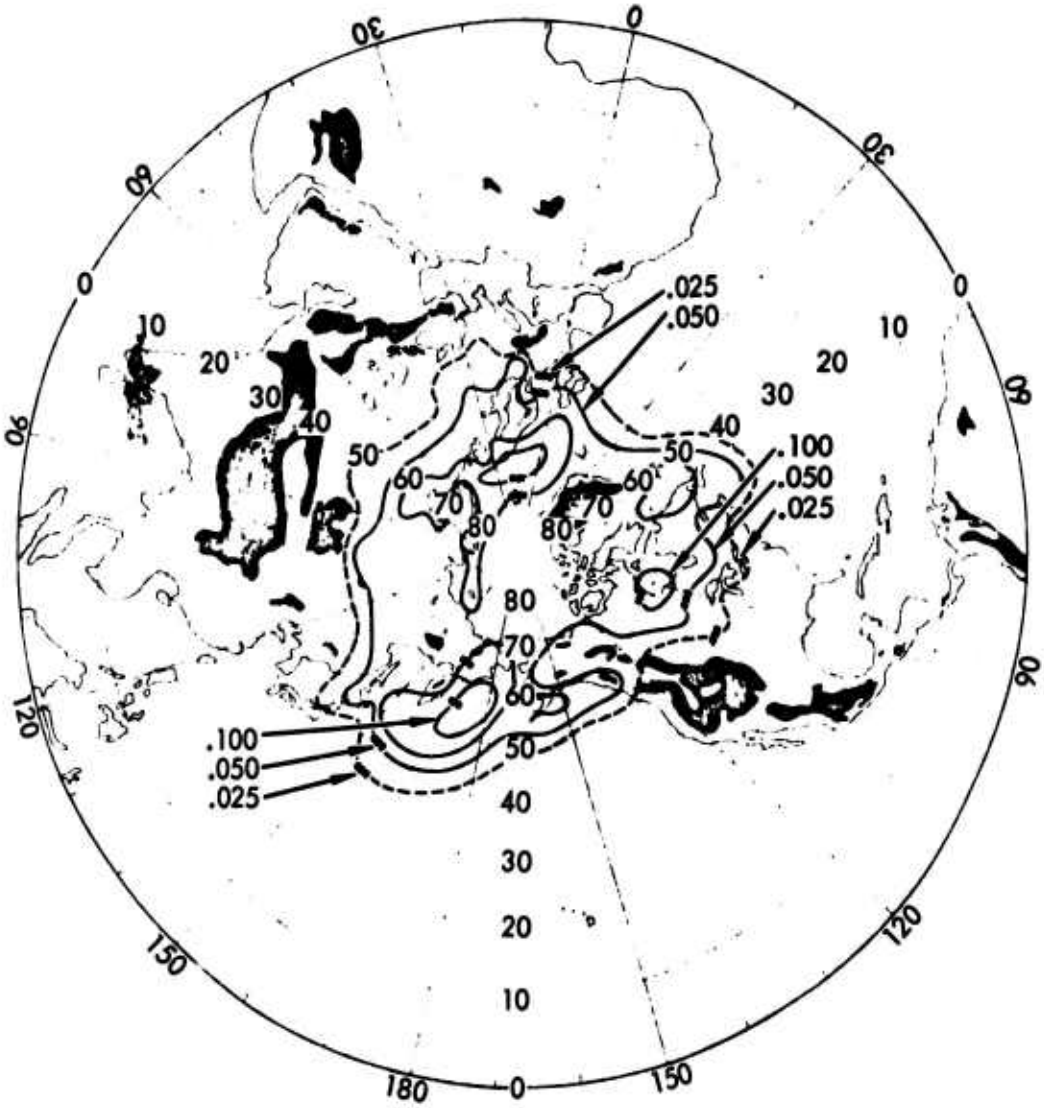

Figure 52. Probability of Encountering Icing Conditions, 5,000 Feet, April.

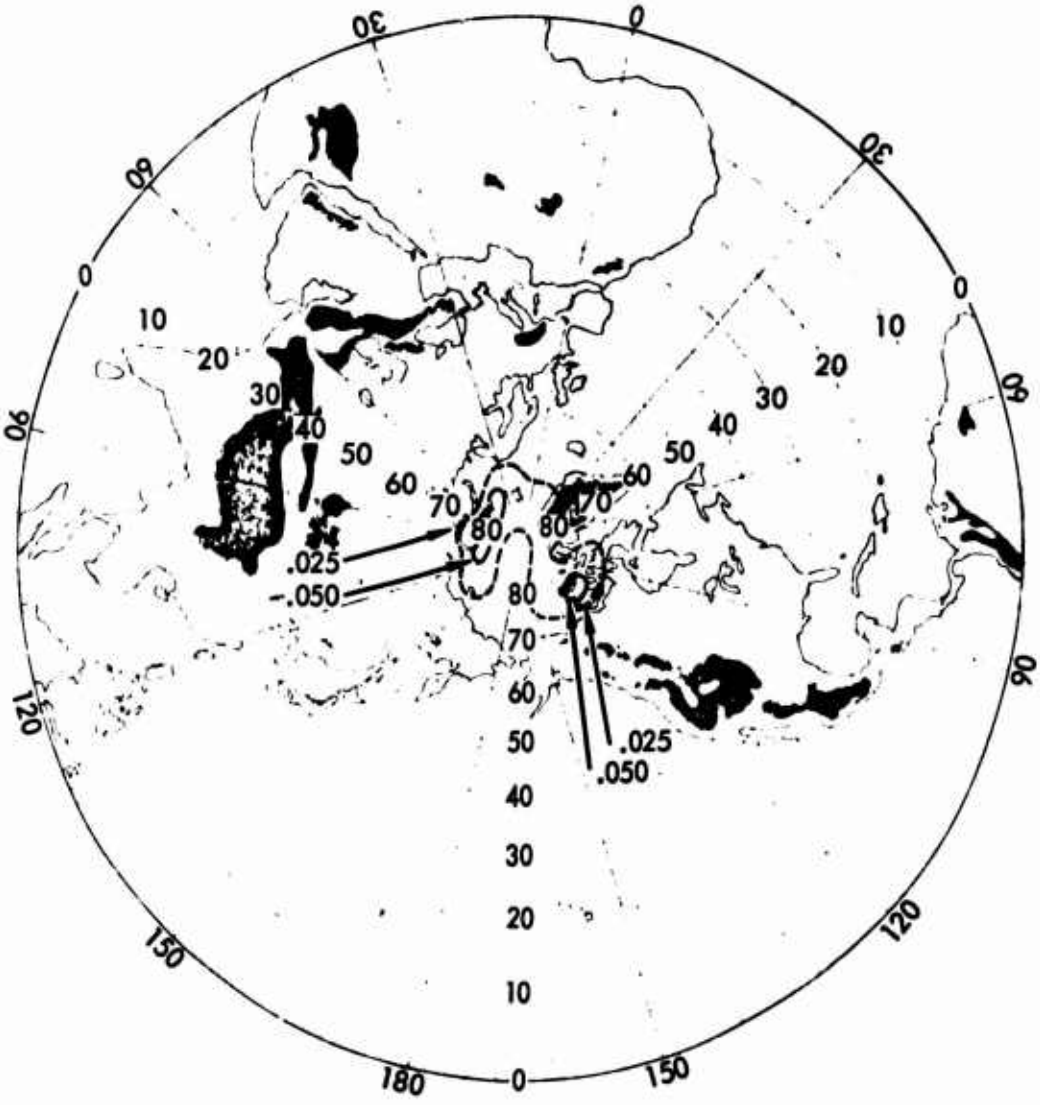

Figure 53. Probability of Encountering Icing Conditions, 5,000 Feet, July.

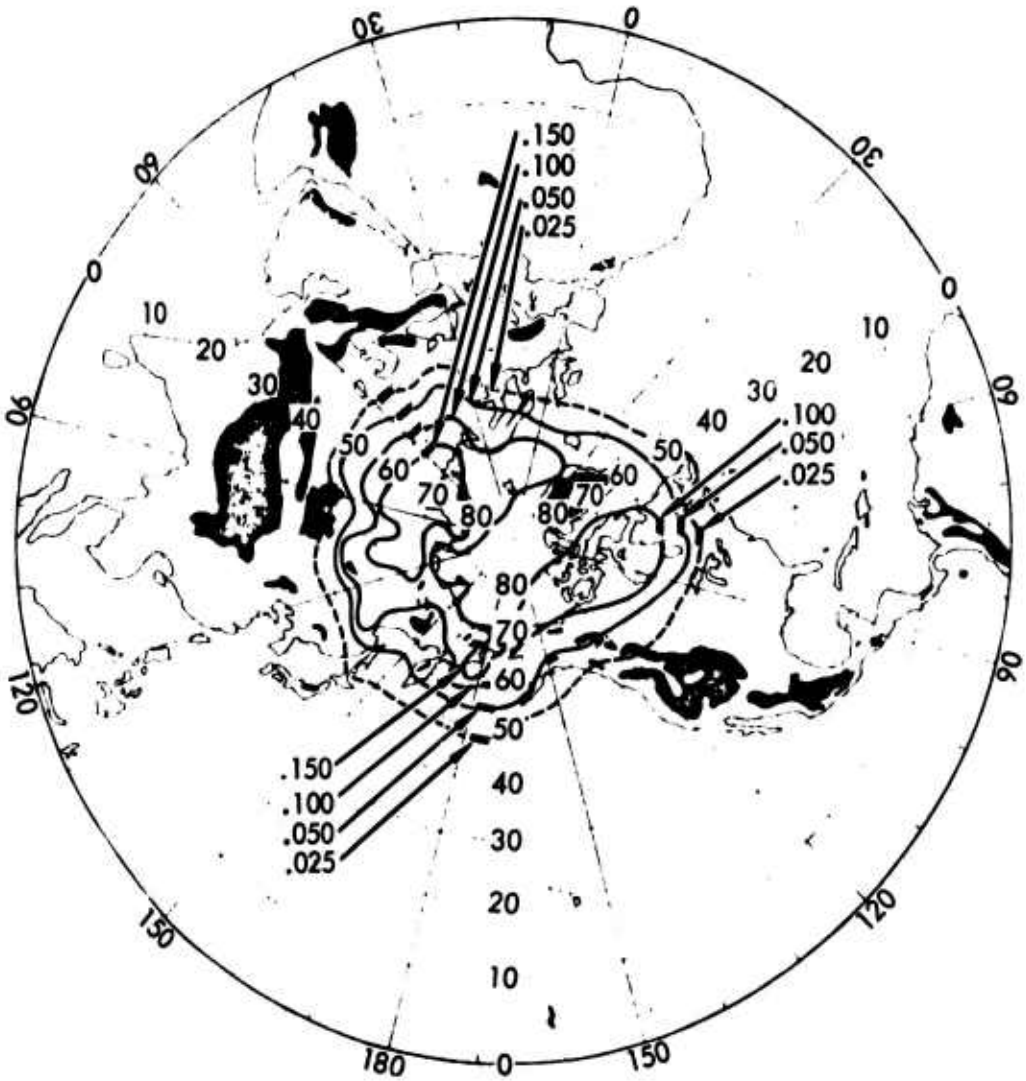

Figure 54. Probability of Encountering Icing Conditions, 5,000 Feet, October.

and dew-point data. Cloud cover data were not used directly. As pointed out earlier herein, the statistical validity of using the dew-point spread approach alone is debatable because it may result in unrealistically high probabilities.

3.2.4 Summary and Conclusions on the Probability of Icing

Three different methods have been used to obtain estimates of the probability of icing. One is based upon the frequency of occurrence of low clouds at temperatures between 0°C and -40°C; the second method is indirect and uses the difference between dew-point and dry bulb temperature as a criterion instead of observing the actual presence of clouds; and the third method is based upon reported icing occurrences. The first two methods require a correction factor because aircraft do not always encounter icing when flying in supercooled clouds. Direct comparison of the results that have been obtained through use of the first two methods is difficult because some authors have used a single altitude (such as 5,000 feet), some have used a specific altitude interval, and others have used a nonspecific altitude interval (such as low stratus or cumulus covering 0.6 or more of the sky). Statistical summaries of icing occurrences of commercial aircraft usually apply to altitude intervals above that of principal interest for helicopter flights. Figure 55 presents a comparison of published frequencies of occurrence for the North Atlantic and Northern Europe. Some authors have used monthly averages and some seasonal averages. If the estimates of potential icing are multiplied by the suggested 0.5, then the differences in the estimates are significantly reduced.

All of the data show that the regions of highest frequency of potential icing conditions are the Pacific Ocean between Kamchatka and the Aleutians and in the vicintiy of Japan, Lake Erie to Iceland, the Baltic area in the northern hemisphere winter, and southern oceans near the 60th parallel in the southern hemisphere winter. During winter, potential icing at the 5,000-foot msl altitude may be expected to occur at latitudes as low as the 25th parallels. An examination of the data and the various estimates for the northern hemisphere indicate that a reasonable working hypothesis is that the probable icing to 5,000 feet above the surface in the winter is 10 percent to 15 percent in Northern Europe and from Japan to the Aleutians and 10 percent from the Great Lakes to the southern tip of Greenland. These figures should be reduced by at least one-half to allow for reasonable icing avoidance flight procedures (flying below the clouds). These percentages are for icing of all types and intensities. Of the total occurrences of icing, approximately 75-80 percent may be expected to be light, 20 percent moderate, and less than 3 percent severe.

In the summer, no aircraft icing may be expected at altitudes below 5,000 feet msl except in the Arctic and Antarctic. Probable icing percentages for an arctic region (Alaskan Tundra) are shown in Figure 56.

The frequency of occurrence of potential icing conditions may be modified through the use of statistical summaries of ceilings. Such summaries have

Sources of Data

Potential Icing:	Surface to 10000 ft (Ref. 33) at 5000 ft (Ref. 34) Supercooled Low Clouds (Ref. 35) Clouds 2000 to 5000 ft (Ref. 36)
Probable Icing:	at 5000 ft (Ref. 31) at 850 mb (4800 ft) (Ref. 32)

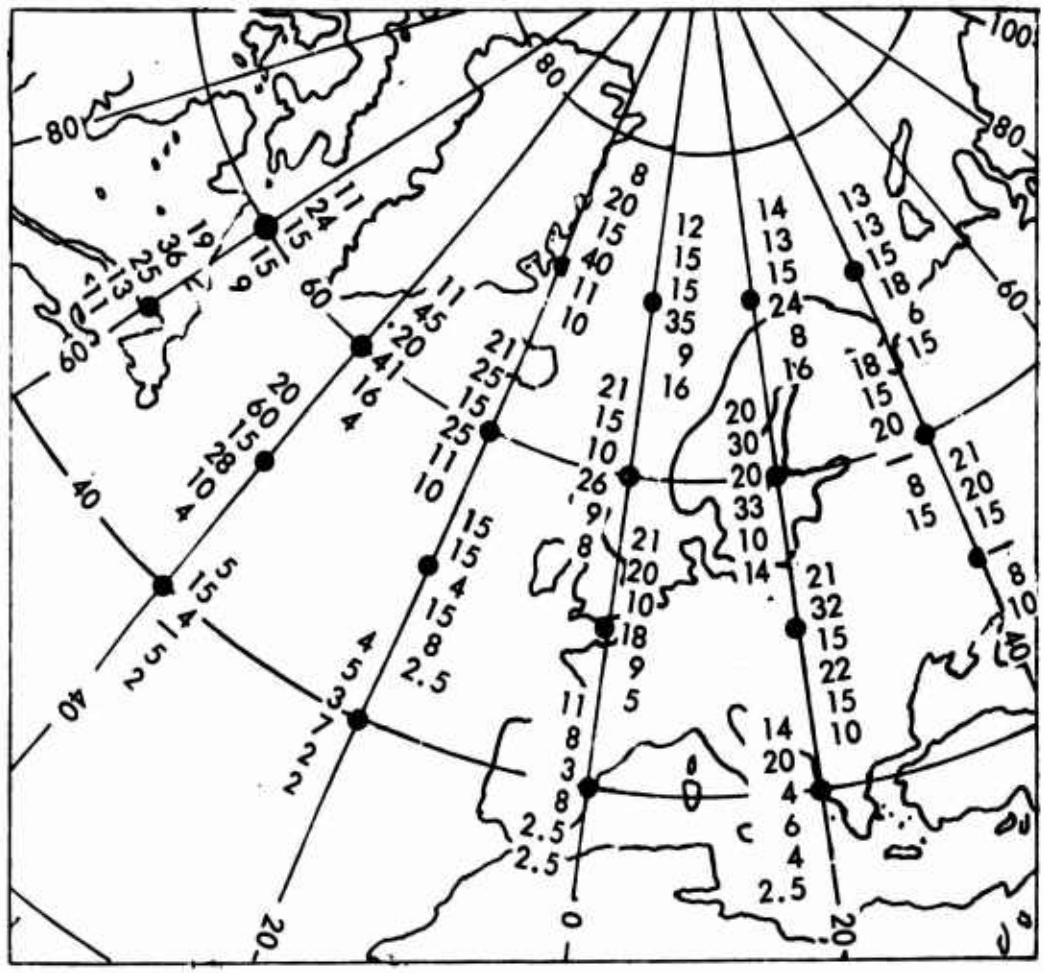

Figure 55. Potential and Probability of Icing Expressed in Percentage of Total Time for Winter Season.

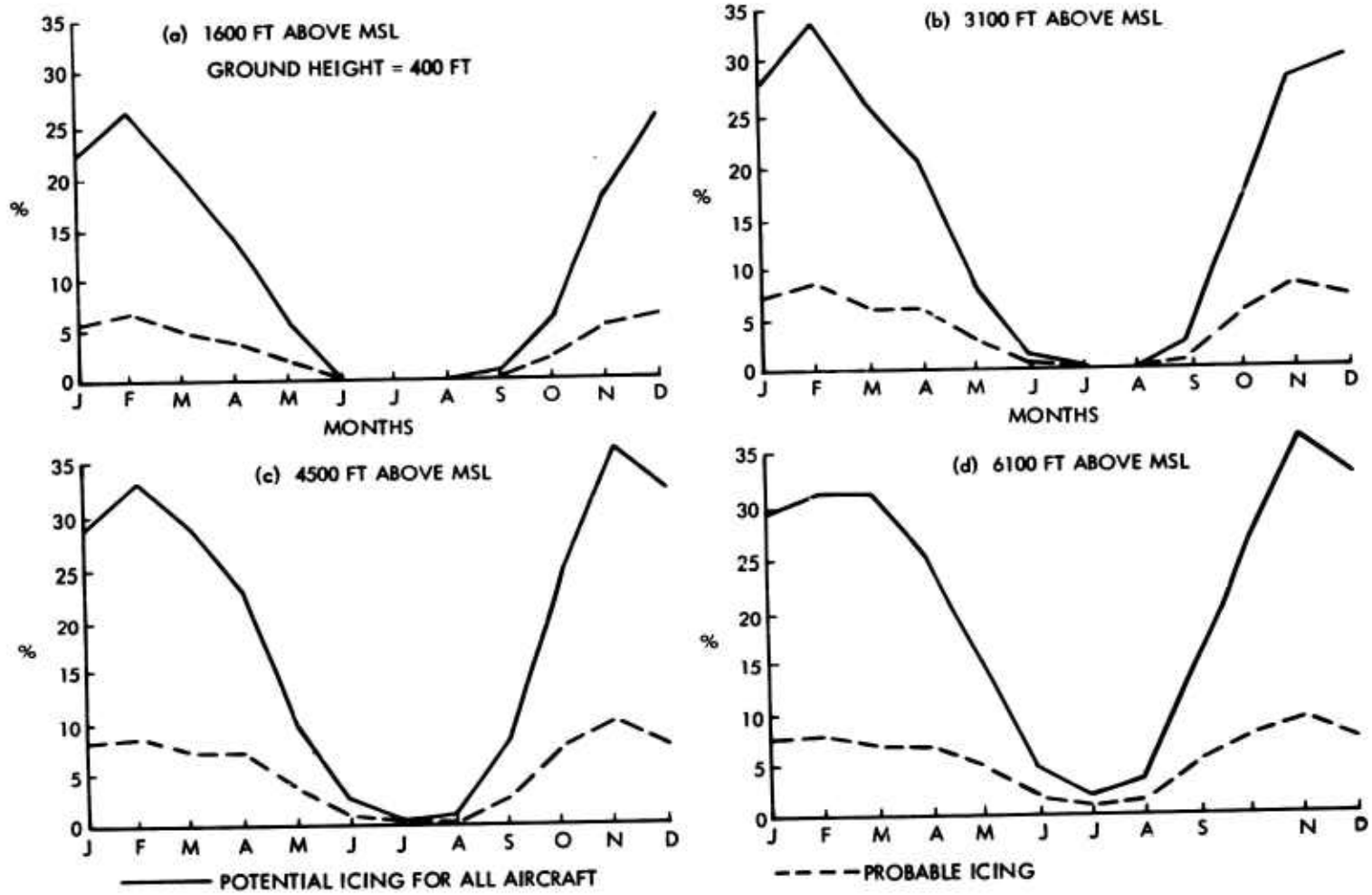

Figure 56. Percentage of Frequency of Occurrence of Potential Icing and Probable Icing for Alaskan Tundra Climate.

been published for the principal airports in the United States (Reference 49). If it is assumed that helicopters may operate safely with a ceiling of at least 900 feet and that low clouds are defined as clouds whose bases are 4,000 feet or less, then potential icing conditions with cloud base ≥ 1000 feet can be subtracted from the total potential frequencies. In the major regions of icing potential in the United States, approximately one-third of the ceilings ≤ 4,900 feet that are ≤900 are shown in Table XII.

TABLE XII. RATIO OF CEILINGS ≤900 FEET AND ≤1900 FEET TO CEILINGS ≤ 4900 FEET FOR SELECTED U.S. AIRPORTS FOR JANUARY

Airport	Ratio ≤ 900 ft	Ratio ≤ 1900 ft	≤4900 ft
Mobile, Ala.	.44	.67	.36
Anchorage, Alas.	.31	.50	.29
Fairbanks, Alas.	.12	.38	.226
Phoenix, Ariz.	.03	.15	.06
Fresno, Calif.	.49	.65	.32
Spokane, Wash.	.52	.74	.54
Los Angeles, Calif.	.35	.61	.23
Denver, Colo.	.30	.67	.11
Milwaukee, Wisc.	.28	.61	.46
Atlanta, Ga.	.44	.66	.36
Pittsburgh, Pa.	.26	.54	.62
Baltimore, Md.	.37	.52	.27
Reno, Nev.	.17	.38	.20
Salt Lake City, Ut.	.16	.38	.21
Des Moines, Ia.	.38	.70	.34
New Orleans, La.	.41	.66	.32
Portland, Me.	.44	.60	.34
Detroit, Mich.	.26	.55	.55
Minneapolis, Minn.	.25	.66	.33
Omaha, Neb.	.35	.66	.29
Buffalo, N. Y.	.21	.52	.62
Bismark, N. D.	.22	.63	.31
Cleveland, O.	.26	.57	.63
Portland, Ore.	.16	.42	.55
Philadelphia, Pa.	.33	.51	.30

Alternatively, if it is conceded that helicopters would not fly with ceilings <1500 feet, then the figures given in Table XII could be modified by linear interpolation between 900 and 1900 feet.

3.3 METEOROLOGICAL ICING CLOUD PARAMETERS

3.3.1 General Statement

Although ice invariably starts to melt at 0°C if heat is added, water droplets in the atmosphere never freeze instantaneously at 0°C. Laboratory experiments indicate that freezing of droplets is initiated by the presence of motes within the drops. The number of motes that become active at a given temperature increases as the temperature is lowered. The temperature at which a drop will freeze is also a function of the size of the drop. Drops of rain, 1 mm (1000 microns) or greater in diameter, usually freeze at temperatures from -15° to -20°C. Cloud droplets, 10-20μ diameter, freeze instantaneously at approximately -30°C. Even the smallest drops freeze at -40°C. Icing of aircraft caused by the impact with supercooled water drops is, therefore, confined theoretically to a temperature band 0° to -40°C.

The maximum free-water content of ascending air is simply calculated if it is assumed that the ascent is adiabatic and that the products of condensation are retained within the ascending air mass and there is no dilution of the ascending air by mixing with other air. The results for the adiabatic lifting theory are shown in Figure 57.

In general, the liquid water content of the cloud increases with distance above the base of the cloud, but the increase is usually one-third to one-half that expected from adiabatic lifting theory (values of 5 gm/m^3 or higher can be predicted from adiabatic lifting theory as shown in Figure 57).

Supercooled water in the atmosphere is distributed over a large range of drop sizes, and the amount of water collected by an aircraft will depend on this drop size distribution. For clouds of greater depth, larger droplets are present in greater numbers, and for a given depth of cloud, larger droplets are more frequent in layer clouds than in convection clouds. The median volume diameter in most clouds lies in the range from 10 to 20 μ.

Based upon measurements of Reference 50, Figures 58 and 59 show liquid water content and droplet size distribution for two separate typical cumulus clouds. As can be seen from these figures, droplet size and LWC tend to increase with cloud height as predicted by the adiabatic lifting theory. However, variation of LWC within the cloud is significantly more pronounced than variation of the volume mean droplet size.

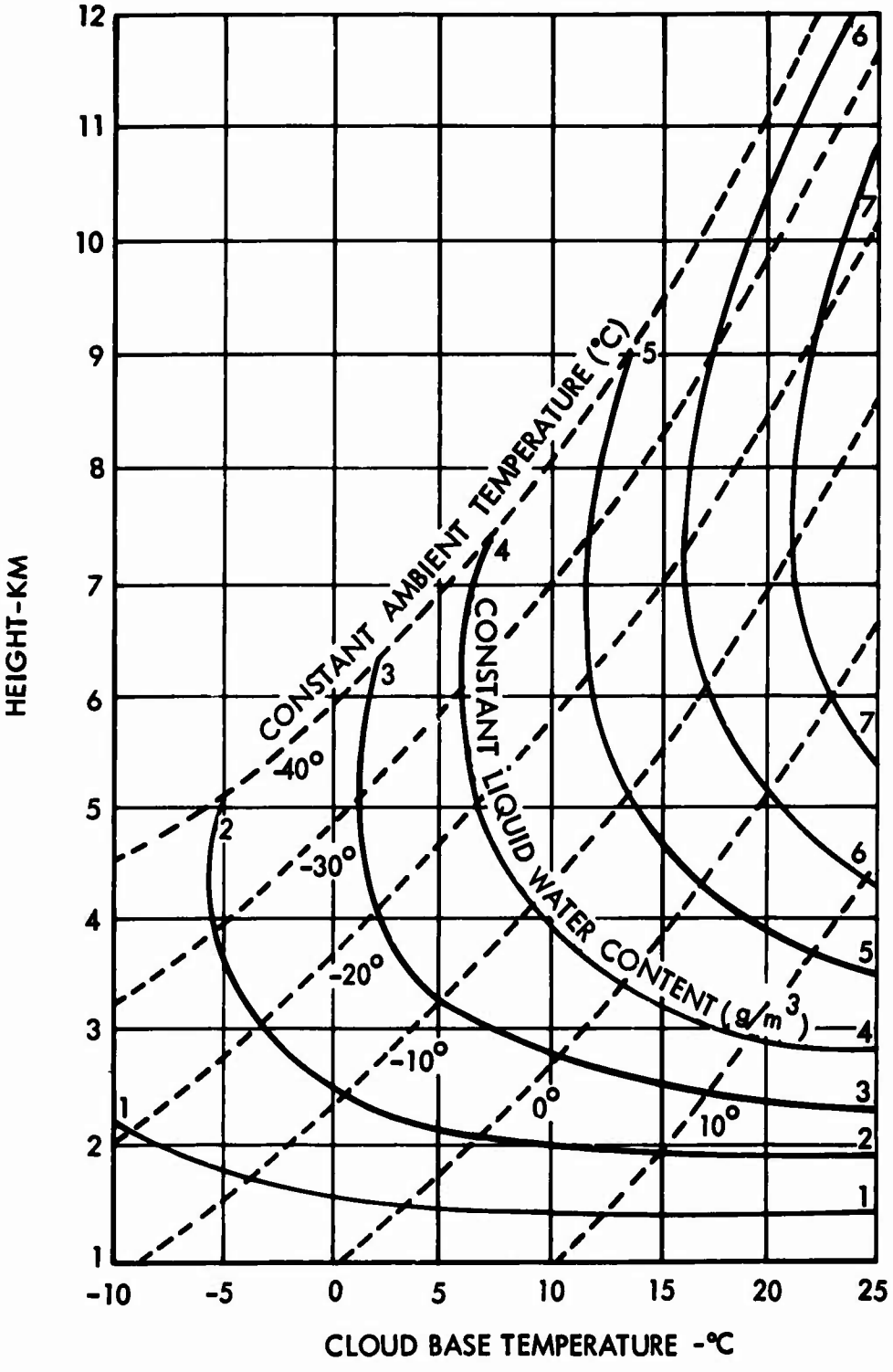

Figure 57. Concentration (in g/m^3) of Liquid Water Condensed During Adiabatic Ascent From a Condensation Level at 900 mb (About 1 km Above the Ground), as a Function of Height and Temperature at the Condensation Level (Ref. 13).

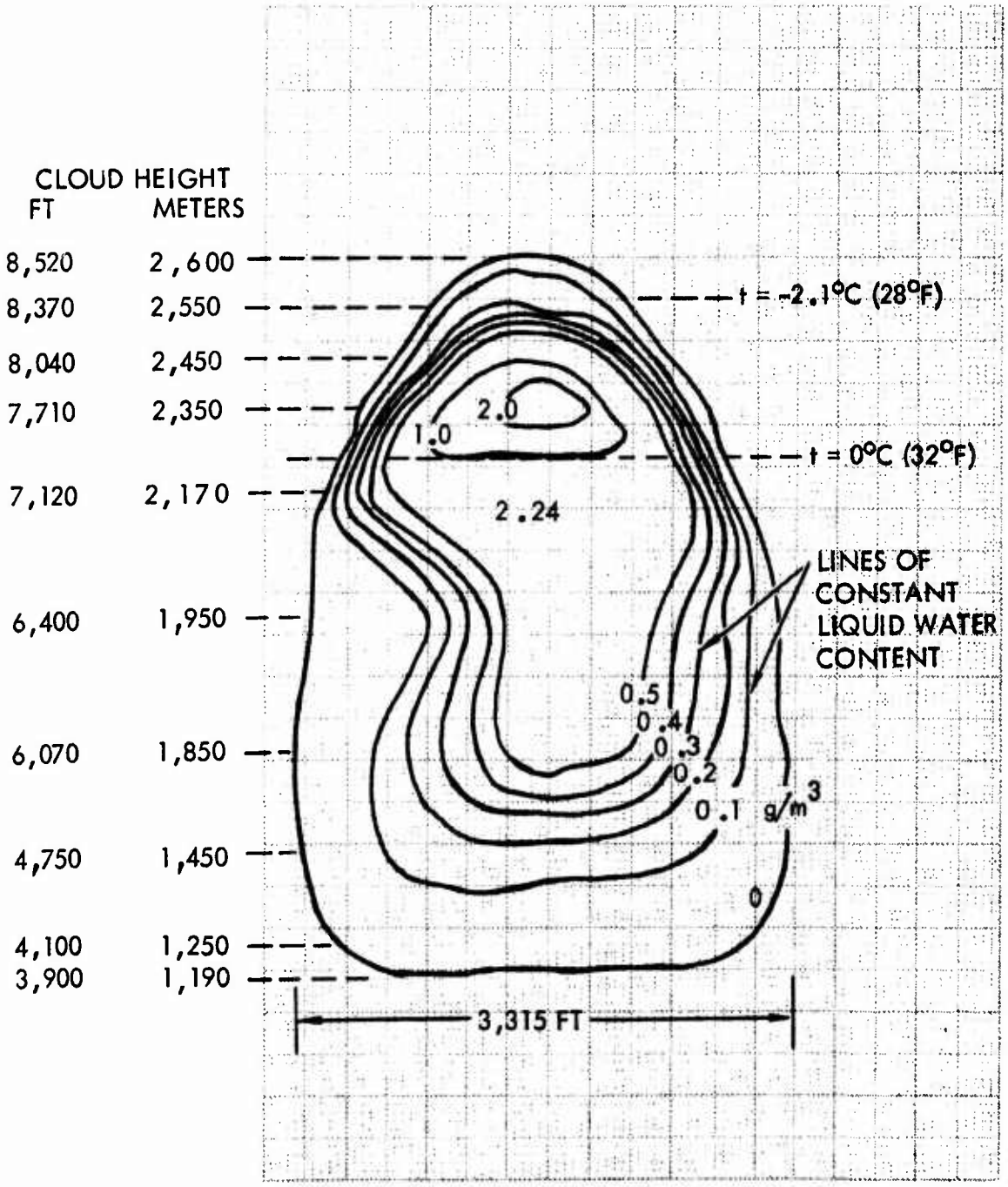

Figure 58. Properties of Typical Cumulus Congestus Clouds - LWC, Drop Size, Temperature, Vertical and Horizontal Dimensions (From NRC-TT-395, Ref. 50).

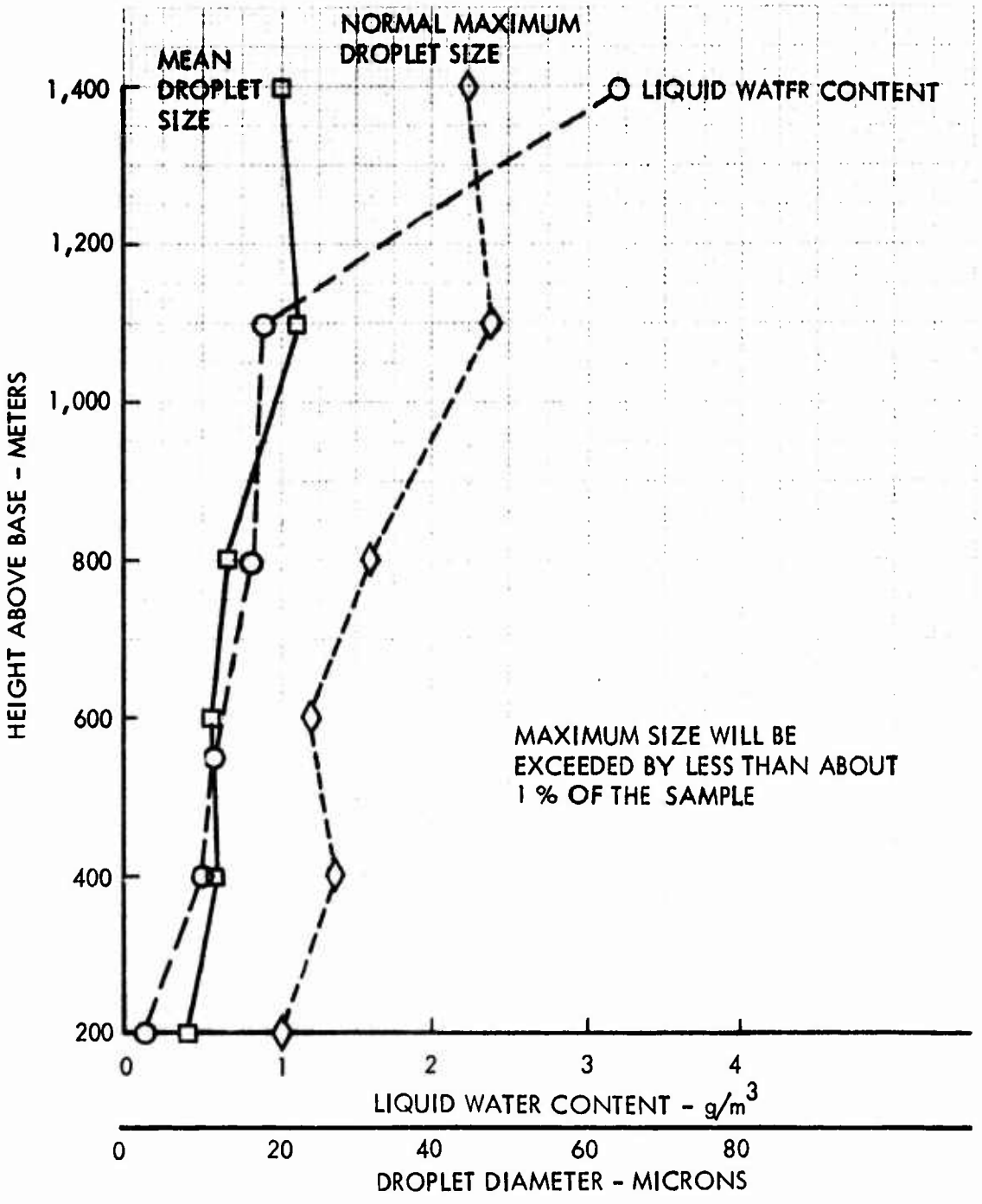

Figure 59. Properties of Typical Cumulus Congestus Clouds - LWC, Drop Size, Temperature, Vertical and Horizontal Dimensions (From NRC-TT-395, Ref. 50).

3.3.2 Liquid Water Content Distribution

Measurements of the liquid water content of supercooled clouds have been made by research aircraft in the United States, Canada, Great Britain, Australia, and Russia, but the observations are scattered throughout the literature and it is difficult to summarize the results adequately. All measuring devices give mean results over periods corresponding to the response time of the instrument, and most instruments have an upper limit to which the water content can be measured - a limit that increases as the temperature decreases. It is unfortunate that a great deal of the information obtained so far has been acquired by instruments incapable of measuring the highest water concentrations and with a considerable response time, so that average values over distances of several kilometers were usually obtained. Results obtained with rapid-response instruments have mostly been used for limited physical studies but are all unanimous in indicating the extreme variability of water content during passage through a cloud. The variability is most marked in cumuliform clouds, but substantial variability also exists in stratiform clouds. Such measurements suggest that values approaching the full theoretical value may exist over limited distances (e.g., 1 km or less) in moderate-sized cumulus clouds but that average values over the whole traverse of a cumulus cloud are considerably less than the theoretical. For obvious reasons, however, accurate measurements have not been made within the most active parts of the most vigorous convection clouds.

A summary of a number of flights made for the National Advisory Committee for Aeronautics has been given by Lewis in Reference 51, and is shown in Table XIII.

It should be emphasized that these are mean results over about 1 minute (3-5 km) in cumuliform clouds and 3-5 minutes (10-25 km) in stratiform clouds by instruments for which the upper limit of measurement was in the region of 1-2 g/m^3.

A valuable addition to these data has been provided by Minervin, Magin, and Burkovskaya (Reference 52). They give comprehensive tables, of which the following are extracts:

(1) Stratus, (2) Stratocumulus, (3) Altocumulus, (4) Altostratus,

(5) Cumulus, (6) Cumulonimbus

It will be seen that the values of Tables XIII and XIV are not inconsistent, although the maximum contents measured in Russia are greater, probably reflecting a shorter averaging time.

They concluded that the mean values of water content in air-mass clouds depend essentially on temperature and height above the cloud base, increasing with increase of these factors. This is, of course, in complete

TABLE XIII. OBSERVED FREQUENCY OF VARIOUS VALUES OF LIQUID WATER CONCENTRATION IN CLOUDS

Liquid Water Concentration g/m^3	①② St, Sc 327 obs %	③④ Ac, Ac-As 264 obs %	⑤⑥ Cu, Cb 342 obs %
0.00 - 0.09	12	50	31
0.10 - 0.19	32	32	
0.20 - 0.29	22	13	26
0.30 - 0.39	16	4	
0.40 - 0.49	12	1	22
0.50 - 0.59	5	0	
0.60 - 0.69	0.3	0	10
0.70 - 0.79	0.6	0	
0.80 - 0.89	0.3	0	7
0.90 - 0.99	0	0	
1.00 - 1.19	0	0	2
1.20 - 1.39	0	0	1.0
1.40 - 1.59	0	0	0
1.60 - 1.79	0	0	0.7
	g/m^3	g/m^3	g/m^3
Lower quartile	0.13	0.05	0.15
Median	0.22	0.10	0.34
Upper quartile	0.35	0.17	0.55
Maximum	0.80	0.41	1.71

TABLE XIV. SUPERCOOLED WATER CONTENT (g/m^3)

Cloud Type St, Sc, Ac					
Temperature (°C)	-25 - 20,	-20 - -15,	-15 - -10,	-10 - -5,	-5 - 0
Mean	0.08 - 0.14	0.06 - 0.14	0.11 - 0.22	0.14 - 0.24	0.20 - 0.27
Maximum	0.08 - 0.33	0.12 - 0.33	0.41 - 1.47	0.53 - 0.99	0.76 - 1.53
Cloud Type Ns*, As					
Mean	0.09 - 0.15	0.09 - 0.30	0.14 - 0.32	0.12 - 0.21	0.61 - 0.34
Maximum	0.16 - 0.27	0.14 - 0.48	0.21 - 0.67	0.38 - 0.74	0.49 - 1.11

*Nimbostratus

accord with simple theory, but they find that the gradient of water content starting from a certain height above cloud base is less than, but proportional to, the theoretical value. The factor of proportionality was 0.65 to 0.68 in Sc, less than 0.4 in Cb, and less than 0.2 in Ns*. Above a certain level in the cloud (usually situated in the upper third of the cloud), the water content gradient becomes negative; while in the lowest tens of meters of the cloud, the gradient is usually considerably higher than theoretical.

These conclusions are quite explicit in terms of the factors discussed in paragraph 3.3.1. The smaller factor of proportionality in Cb than in Sc is no doubt accounted for by entrainment of dry air, the presence of ice crystals, and precipitation, while the very low factor for Ns suggests a considerable effect from ice crystals and precipitation. The negative gradient in the upper part of the cloud indicates depletion by precipitation and possibly also entrainment through the top of the cloud, and the large gradient in the bottom tens of meters is due to the effect of precipitation or settling down of larger droplets.

Pettit (Reference 53) has summarized the results of Canadian flight experience amounting to 1182 measurements at temperatures below 0°C on 84 flights. There were no flights in cumulonimbus clouds. Maximum liquid water contents, which are averages over 13 seconds, equivalent to about 1.2 km, are quoted as well as average liquid water contents on complete traverses exceeding 52 seconds (about 5 km). Once again, the absolute maximum values at temperatures higher than about -10°C reflect more the inability of the instrument used to measure higher values than the true values which might be encountered. The limiting values were about 1.0 g/m^3 at -6°C increasing to 1.4 g/m^3 at -9°C, and values at least up to these values were encountered on the flights; but at lower temperatures the limiting values were not approached, the highest liquid water content measured at -30°C being 0.29 g/m^3.

The most frequent values of average liquid water content encountered appear rather low, probably reflecting the fact that the aircraft was mostly searching for low-temperature icing and possibly also a low cloud-base temperature. The values were 0.17 g/m^3 for cumuliform cloud and 0.10 g/m^3 for stratiform cloud, with maximum values in each case of 0.8 g/m^3.

The horizontal icing extent reached as high as 64 km in cumuliform clouds and 370 km in stratiform clouds, but 90 percent of icing extents did not exceed 8 km and 58 km, respectively.

The foregoing show clearly that average values of water contents in clouds do not approach the theoretical but that witin limited regions of a cloud

*Nimbostratus

the theoretical values may well be achieved. Any successful estimate of water content, even in qualitative terms, must take account of the factors discussed in the preceding paragraphs.

3.3.3 Droplet Size Distribution

Relevant meteorological factors affecting the size of supercooled liquid water droplets (and also the LWC) in icing clouds are:

1. The effect of coexistence of water droplets and ice crystals.

2. The effect of the strength of the up-current.

3. The effects of turbulence and entrainment.

When ice crystals and water drops coexist in the cloud, the ice crystals grow at the expense of the water drops because of the difference in vapor pressure over an ice surface and a water surface. The size of the drops that will be supported in the atmosphere is a function of the strength of the updraft because the terminal velocity of the drop is a function of drop size. Turbulence increases the probability of coalescence of the drops, and entrainment of drier air increases evaporation of the drops. Thus, it is seen that many physical processes are involved in producing the liquid water content and drop size distribution of clouds.

The most reliable indication of drop-size distribution and of the mean drop size can be obtained by the rotating cylinder method. The instrument consists of a series of cylinders (often five) of different diameters arranged to be slowly rotated with the axis of the cylinder normal to the wind. From a comparison of the relative amounts of ice collections on the several cylinders, the mean drop size and a measure of the drop size distribution can be obtained. Unfortunately, for routine applications, the multicylinder measuring technique is suitable only for laboratory conditions. The most direct means for the measurement of drop size and drop size distribution in flight is the collection and photomicrography of a sample of the drops utilizing a slide, the surface of which is covered with a layer of oil. Because of the finite size of the slides, there is discrimination against the smaller drops. In addition, large drops tend to fracture on impact at high airspeeds. In spite of these difficulties and limitations, this general method is the only one which permits the nearly instantaneious determination of the drop-size distribution. Another indirect technique to determine the approximate mean drop-size diameter in flight, utilizes a fixed cylinder of a large diameter (at least 6 inches) to estimate the droplet impingement limits on the cylinder, and thus, the maximum drop size; the mean droplet diameter is then derived from the measured maximum drop size.

As already stated, an indication of the breadth of the drop-size distribution can be obtained from the multicylinder data. The general form of the distribution curve must be assumed. The evidence available suggests that

the majority of drop-size-distribution curves are of the general form assumed, although there are occasional curves with multiple maxima. For convenience, nine standard volume-distribution curves have been adopted, identified by the letters A through J (I is omitted). The A distribution corresponds to complete uniformity and the succeeding letters to distributions of increasing breadth as shown in Table XV.

TABLE XV. STANDARD VOLUME-DISTRIBUTION CURVES USED IN THE MULTICYLINDER METHOD

Percentage of Liquid Water in Each Group	Ratio of diameter of group to volume-median diameter for each distribution								
	A	B	C	D	E	F	G	H	J
5	1.0	.56	.42	.31	.23	.18	.13	.10	.06
10	1.0	.72	,61	.52	.44	.37	.31	.27	.19
20	1.0	.84	.77	.71	.65	.59	.54	.50	.42
30	1.0	1.00	1.00	1.00	1.00	1.00	1.00	1.00	1.00
20	1.0	1.17	1.26	1.37	1.48	1.60	1.73	1.91	2.22
10	1.0	1.32	1.51	1.74	2.00	2.30	2.64	3.04	4.01
5	1.0	1.49	1.81	2.22	2.71	3.30	4.02	4.93	7.34

As seen from Table XV, each distribution is made up of seven different drop diameters, each representing the percentage of the total water indicated in the first column. The drop sizes are represented as the ratios of the drop diameter to the volume-median diameter so that the distributions may be applied to any volume-median diameter. The frequency of occurrence of the nine drop-size-distribution types at Mount Washington for the months of November 1946 through May 1947 is indicated in Table XVI.

TABLE XVI. OCCURRENCE OF DROP-SIZE-DISTRIBUTION CURVES BY TYPE AT MOUNT WASHINGTON, N.H.

Distribution curve type	A	B	C	D	E	F	G	H	J
Number of occurrences	241	96	47	21	13	5	2	4	7

The predominance of narrow size distributions is striking. This is probably due in part to the high frequency of cloud-cap conditions which do not favor the nonuniform rates of lift apparently required to produce broad size distributions. For this reason Table XVI cannot be taken as typical of the clouds of the free atmosphere. It is also apparent from Table XVI that a significant number of broad distributions occur (E through J), which certainly cannot be explained on the basis of uniform lift.

Experimental icing tunnel data is based upon a water spray cloud having approximately a "D" distribution.

Diem (Reference 54) has reported the most extensive set of drop-size-distribution data from the free atmosphere. His measurements were made from aircraft by exposing a small oil-covered slide to the airstream for about 1/50 second. The slides were photomicrographed within a minute of collection. The slides undoubtedly discriminated against the smaller drops. Diem states that the collection was satisfactory down to a diameter of 3μ, but there is reason to believe that the discriminatory effect started at a somewhat larger diameter. Diem gives the most frequent drop diameters for six cloud types (Table XVII). Fair-weather cumulus, altostratus and stratocumulus show the sharpest distributions. The other three cloud types exhibit broad size distributions. It is interesting to note that, in general, the cloud types associated with precipitation have broad distributions. Very few of Diem's size distributions would fall in types A and B of Table XV. The difference between Diem's data and the Mount Washington data in this respect is doubtless due in part to the different methods of measurement.

TABLE XVII. DATA FROM COMPOSITE DROP-SIZE-DISTRIBUTION CURVES (REFERENCE 54)

Cloud Type	Prevalent Diameter (μ)	Range of Curve (μ)
Dense cumulus	14.5	3-40
Fair-weather cumulus	8.5	2-20
Stratocumulus	7.9	2-24
Nimbostratus	13.2	2-42
Stratus	12.9	2-42
Altostratus	10.6	2-30

It should be noted that all theoretical water catch data for airfoils or bodies are based upon a uniform drop size. A volume median droplet size is normally used in design work, rather than calculating the water catch for each of the several size ranges that make up an icing cloud. The mean droplet size (often called the mean effective drop size) as used in this

report and nearly all icing literature is a volume median drop size. It is defined as that diameter (for a given sample of cloud) for which half the total volume of liquid water is contained in drops larger than the volume median drop size and half in drops smaller than the volume median. In aircraft design work, use of mean drop size gives an adequate approximation of water catch for most airfoils, and it is, therefore, universally used for this purpose.

3.4 ICING SEVERITY CRITERIA

3.4.1 Horizontal and Vertical Extent of Icing Clouds

Lewis' data shown in Figures 60 and 61 (taken from Reference 55) represent the best statistical summary of the horizontal and vertical extent of icing conditions. While the data are based upon the average of all meteorological encounters — rather than just the lower altitude condition — and the measurements were made 20 years ago, Lewis' data is consistent with the previously cited Canadian flight data summarized by Pettit (Reference 53). Since Lewis' data has stood the test of time and has been corroborated by other sources, it is still considered valid. These data show that, for the mission times associated with army airmobile operation (see Section 2.1.2), relatively long periods of time (maximum durations between one-half and one hour) could be spent under continuous icing conditions. The data of Reference 55 is reflected in the commercial FAR 25 and MIL-E-38453 requirements.

3.4.2 Icing Severity in Terms of Cloud Parameters

Data on the characteristics of icing clouds have been obtained from a variety of locations around the world, covering diverse time periods, flight conditions and sensing equipment. The Lewis data of Reference 56 has 1038 points from the continental USA. A summary of icing severity data compiled by Lewis is shown in Figures 62-65. Perkins' report (Reference 44) has 3,200 points from the continental USA as well as trans-Atlantic and -Pacific routes. The 1972 Briggs and Crawford data (Reference 35), discussed earlier, was for 1,550 icing cases in the British Isles. A 1965 report by Trunov (Reference 57) presents the results of 5,785 cases pertaining to the European portion of the USSR. Finally, the extensive treatise by the Russians V. S. Savin, et al., (Reference 58) analyzes 7,899 data points, but it is not clear if these are only from the USSR or are a worldwide total.

The last report observes, however, "We must note very close agreement of water content measurements in the temperate zone of the United States, the Soviet Union, and Canada." For stratus clouds, the probability curve derived by Lewis in 1952 from the mid-'40s data is superimposed on the probability curves from Savin's data for six times the data and 20 years more experience. These curves are reproduced herein as Figure 66 and do, indeed, show close agreement.

An alternative method of considering icing severity probability is shown in Figures 67 and 68, which are calculated from the data shown in Reference 59.

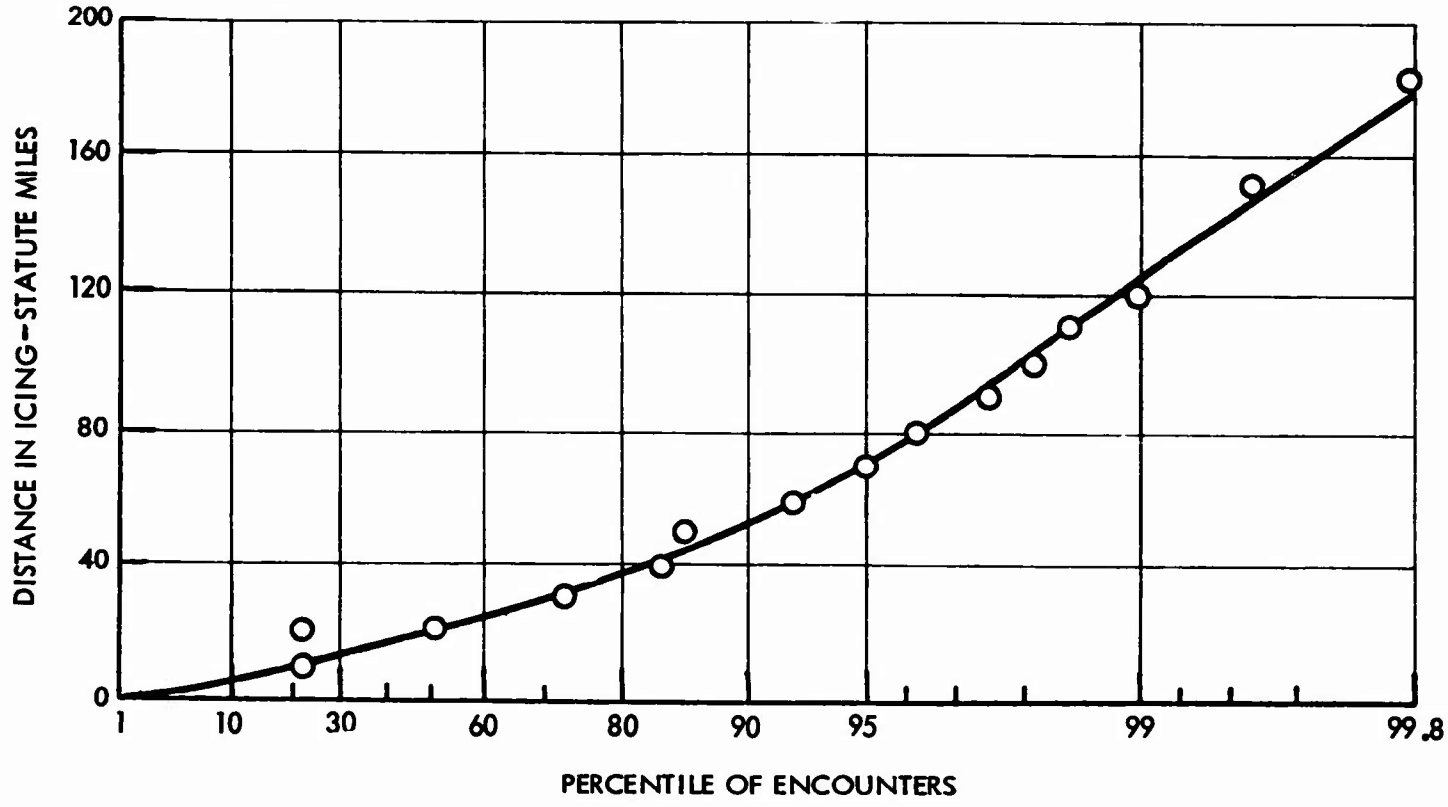

Figure 60. Frequency Distribution of Distance in Icing-Airline Data.

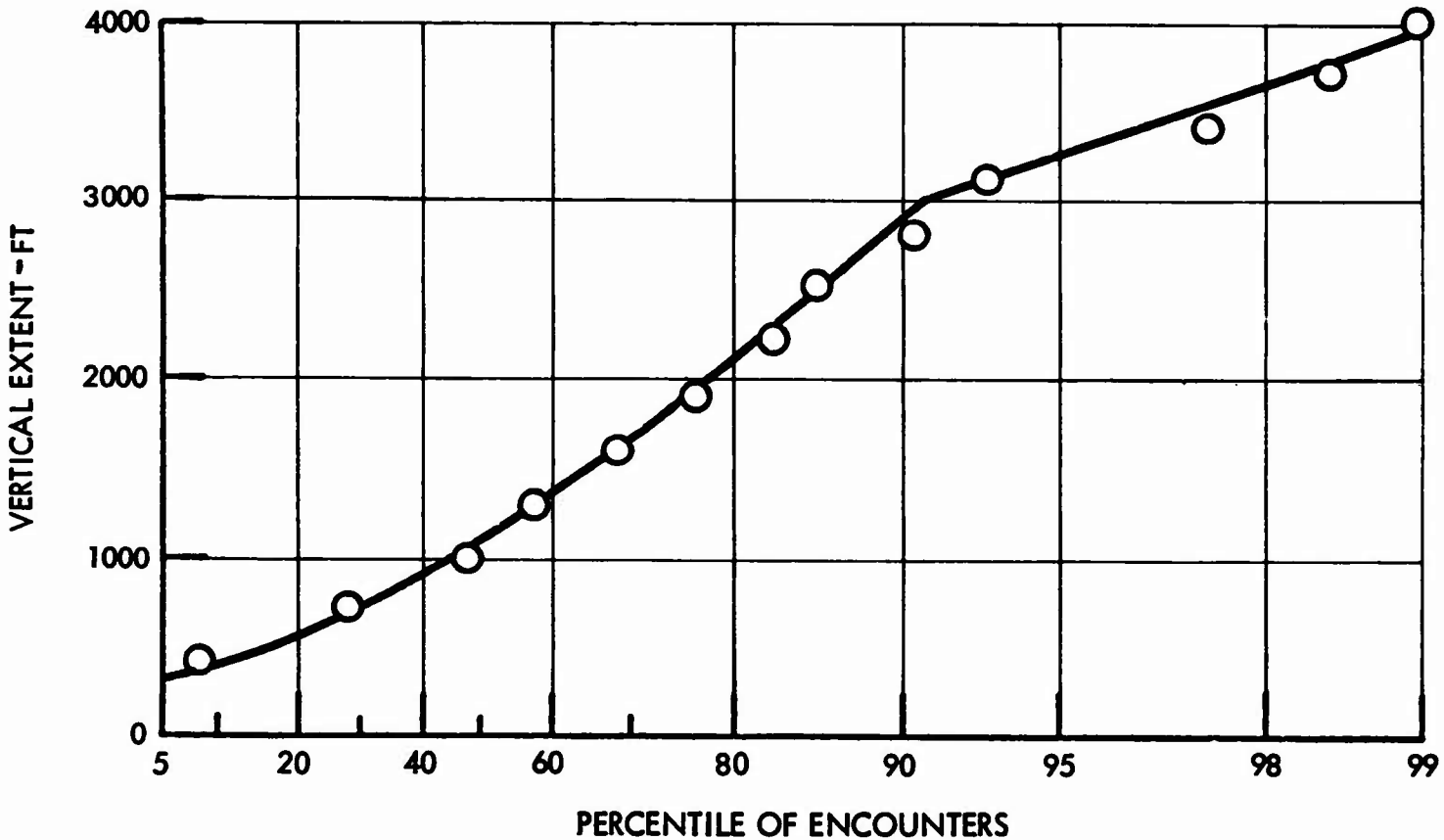

Figure 61. Frequency Distribution of Vertical Extent of Icing.

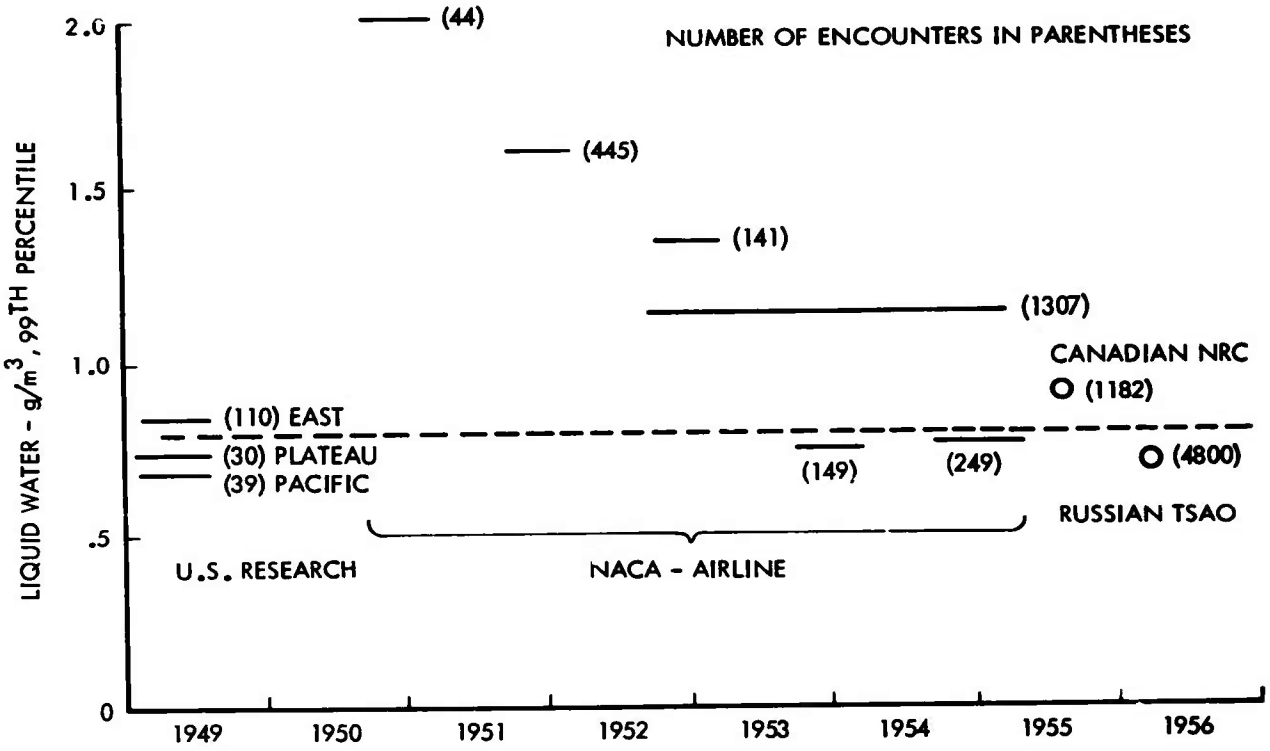

Figure 62. Historical Comparison of Data on Liquid Water.

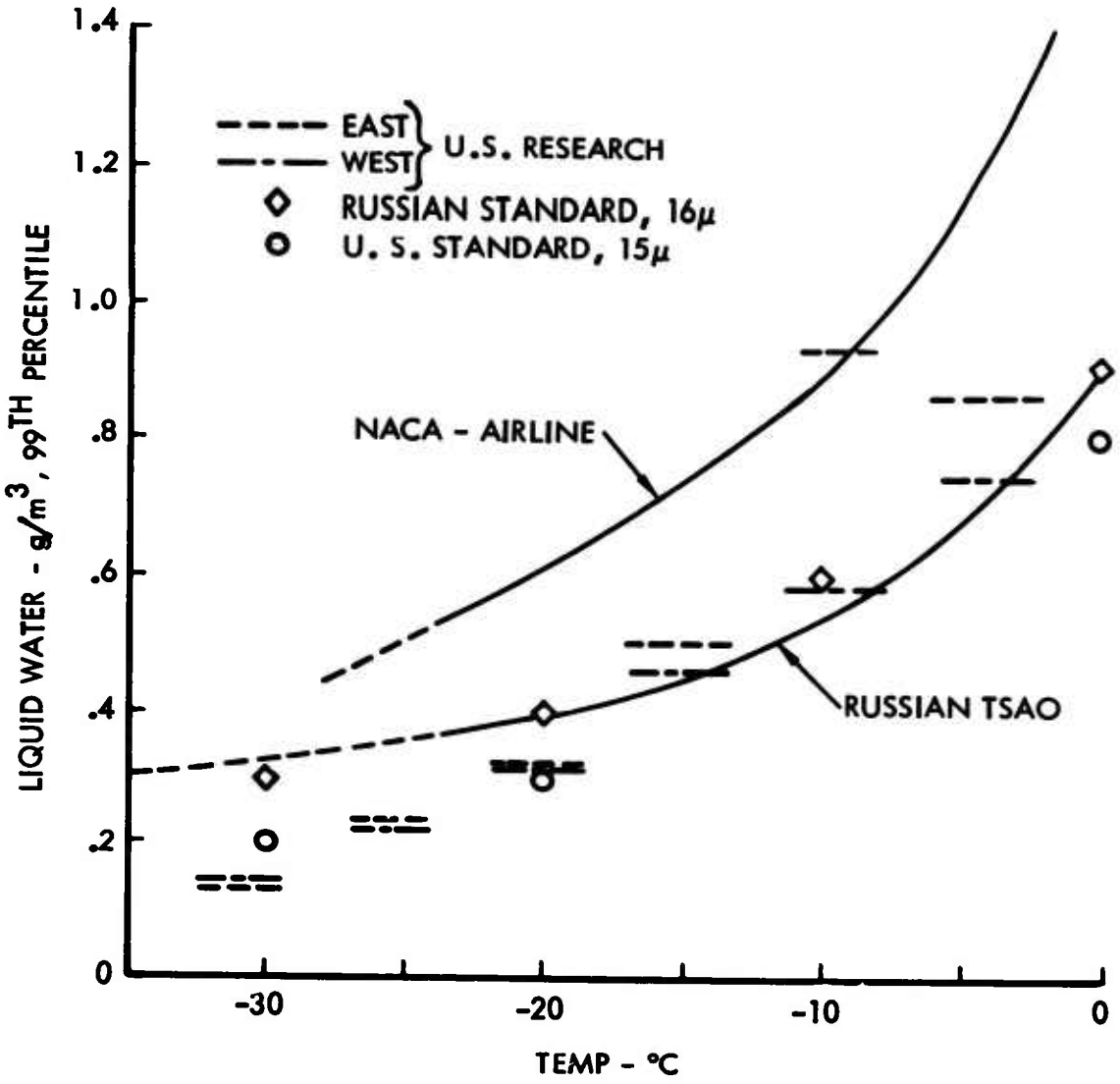

Figure 63. Variation of Liquid Water With Temperature-Layer Clouds.

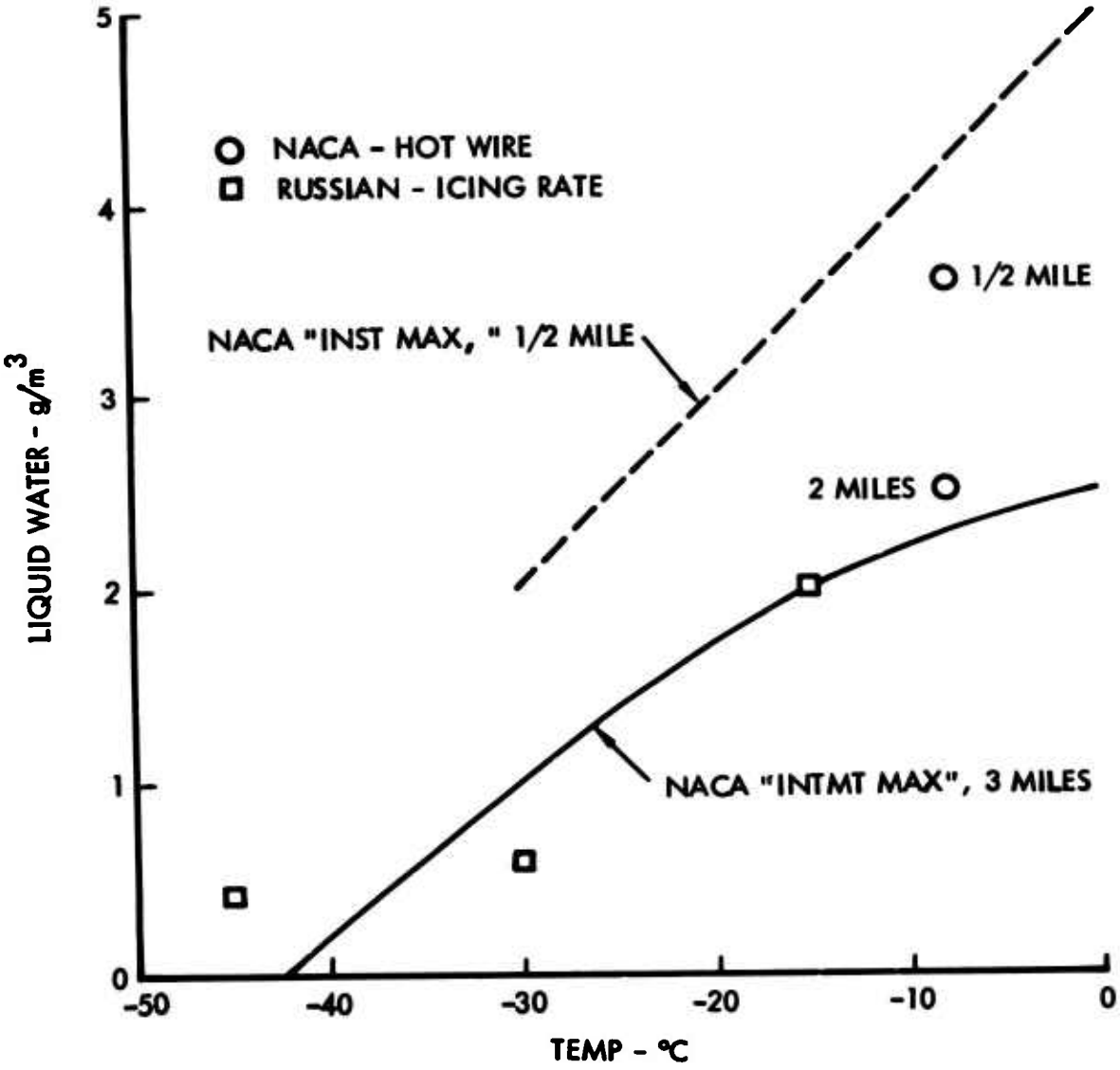

Figure 64. Extreme Values of Liquid Water.

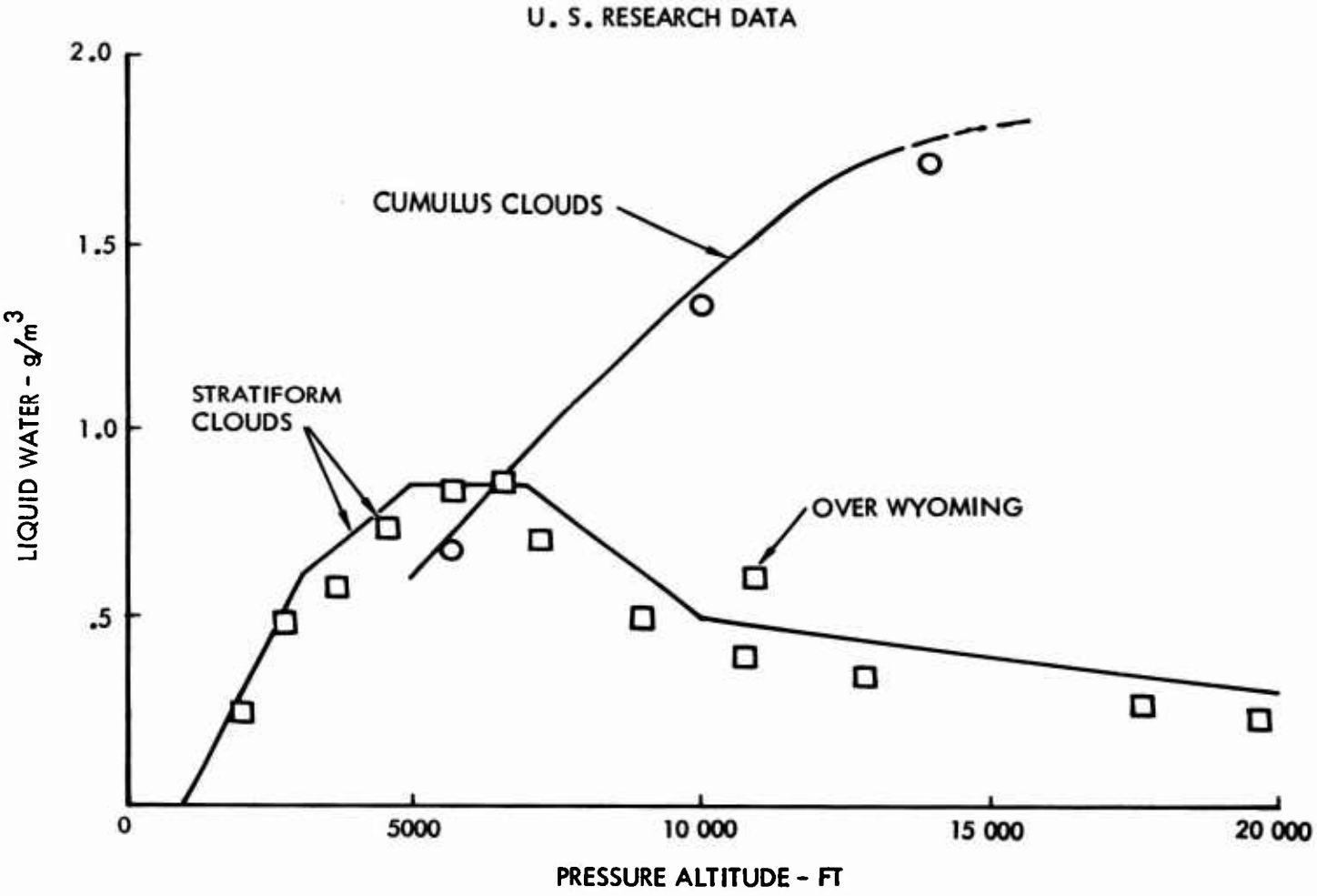

Figure 65. Envelopes of Liquid Water vs. Altitude.

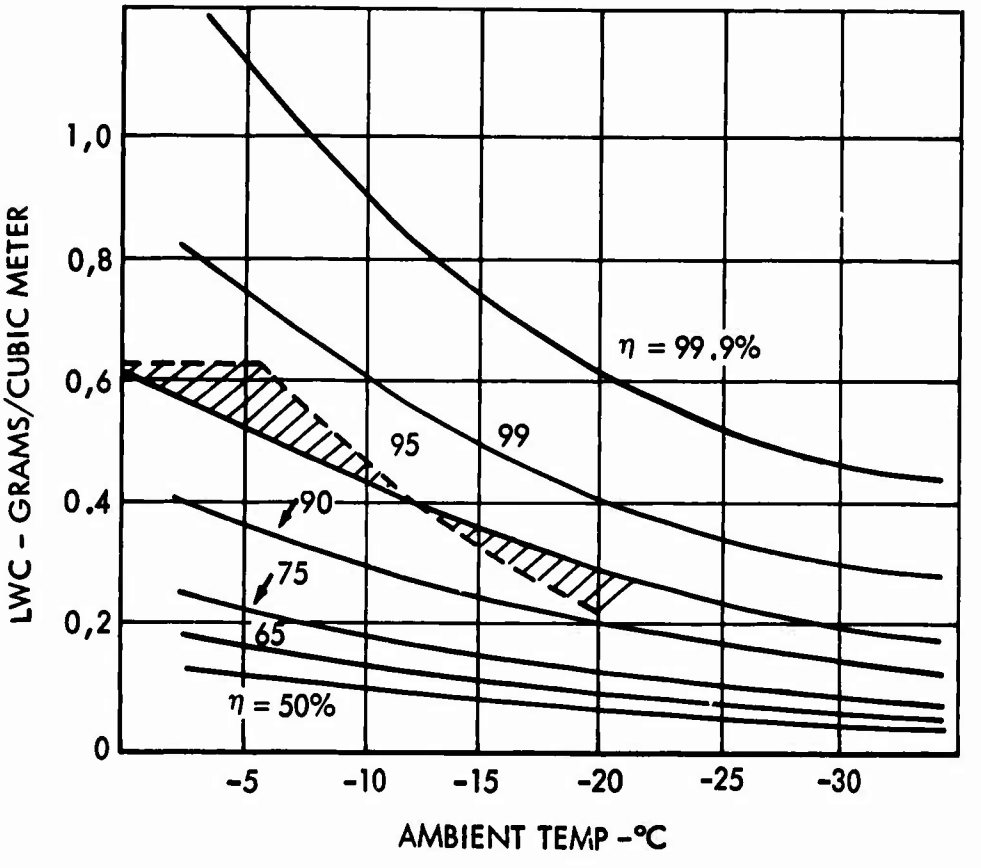

LEGEND: - - - 95% PROBABILITY LINE FROM NACA TN 2738 (REFERENCE 56)

Figure 66. Water Content as a Function of Ambient Temperature at Different Water Content Quantities (Stratus Clouds).

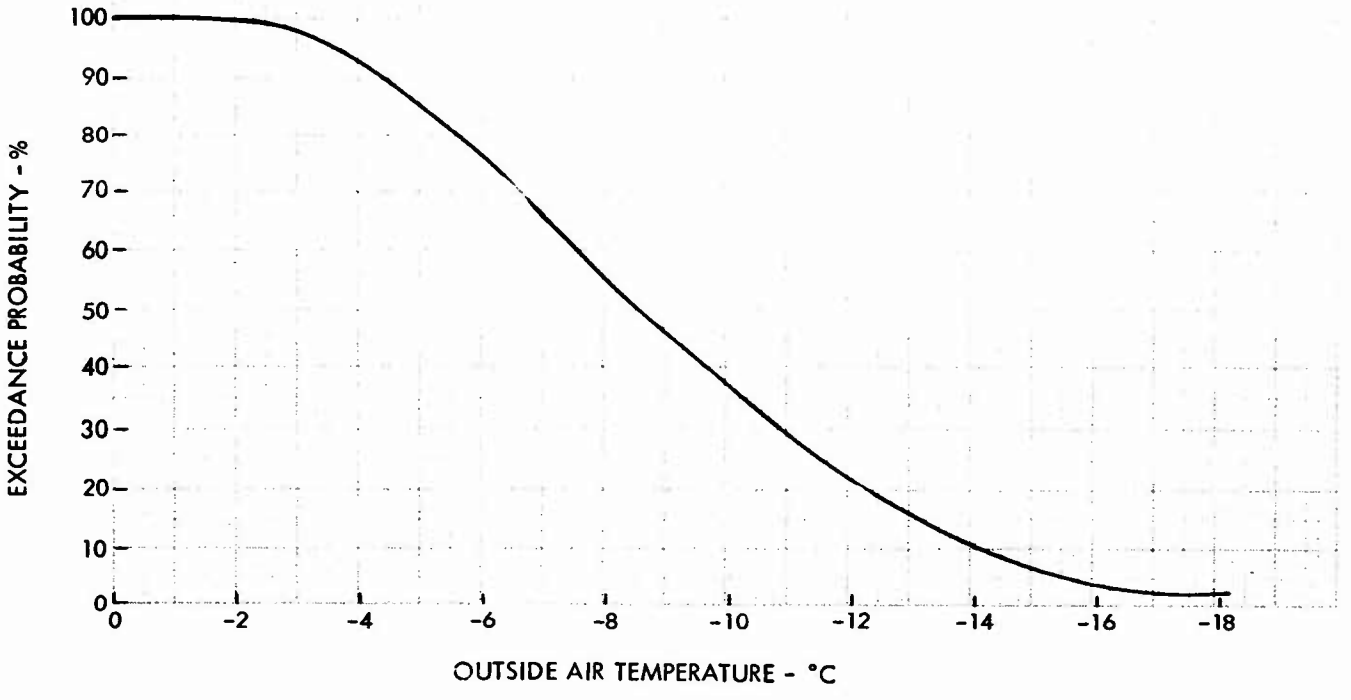

Figure 67. Outside Air Temperature Exceedance Probability.

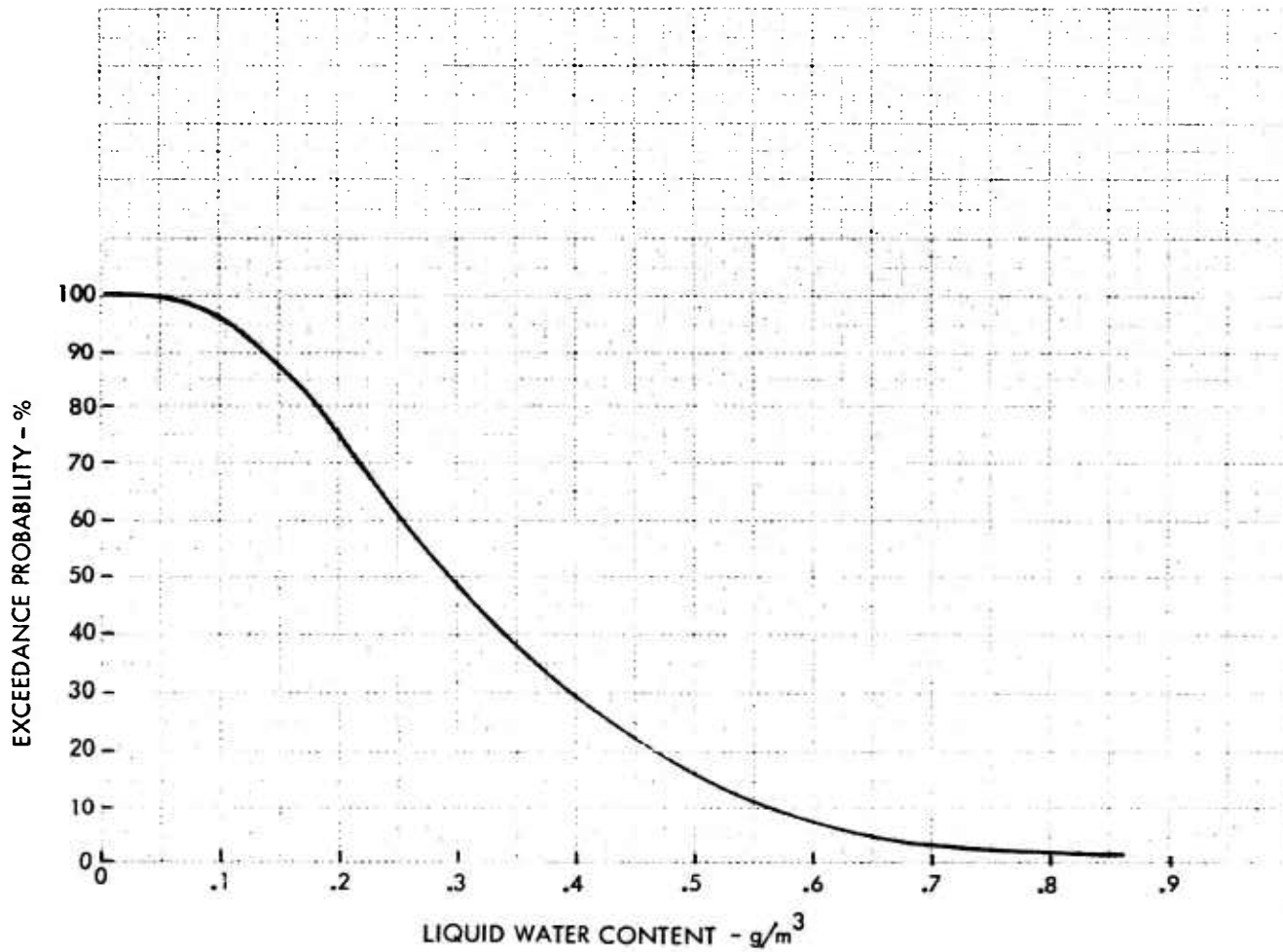

Figure 68. Liquid Water Content Exceedance Probability.

These show independent probability of icing temperature and liquid water content below 10,000 feet. The relationship between droplet size and liquid water content, liquid water content and altitude, and droplet size and altitude is shown in Figures 69-74 for both cumuliform and stratiform clouds. The cumuliform data would be applicable to a consideration of intermittent maximum conditions, and the stratiform data are applicable for the continuous maximum requirement.

By and large, the statistical data from the various sources on the severity of icing encounter are consistent, and as far as the aircraft designer is concerned no new trends different from those reflected in FAR 25 and MIL-E-38453 have come to light.

3.4.3 Definition of Degree of Icing Severity

There have been a variety of operational definitions for "icing severity" (from the point of view of the aircraft operator or pilot). These have included attributes of vehicle performance when exposed to icing, but these attributes correspond to far different liquid water content (LWC) or temperature environments from vehicle to vehicle. Another set of operational definitions refers to ranges of LWC. Still another set of definitions refers to the ice buildup rate on "typical" unheated probes. There is, of course, an interaction among all of these variables. However, in view of the fact that the tolerance of an aircraft to icing is a function of its size, power margin, and airframe/rotor/engine inlet configuration operational attributes are unappropriate to use as aircraft design standards, especially to define predicted or experienced meteorological conditions.

The location of an unheated "small" probe is quite important since different flight attitudes can promote either shading of the probe from the cloud or the development of heavy boundary layers yielding a typical ice catch result. In addition, the operational icing terminology has been inconsistent.

As far as U.S. Army regulations are concerned AR 95-1 (Reference 60) paragraph 3-5c states: "Flight into icing conditions: Army aircraft will not be flown into known or forecast severe icing conditions. If flight is to be made into known or forecast light or moderate icing conditions, the aircraft must be equipped with adequate deicing and/or anti-icing equipment."

Specific definitions for severe, light, moderate, and heavy icing are not given in the U.S. Army regulations (Reference 60). The probable definitions are either those established in February 1964 by the National Coordinating Committee for Aviation (published in the Nov. 1964 issue of the Naval Aviation Center and the Dec. 1964 issue of Aerospace Safety) or those of Reference 15. Table XVIII presents the 1964 definitions. Table XIX compares the earliest (1956) accepted terminology from Reference 61 with the 1964 and the most recent (1969) terminology of Reference 14. The qualitative description of the latter is reproduced in Table XX.

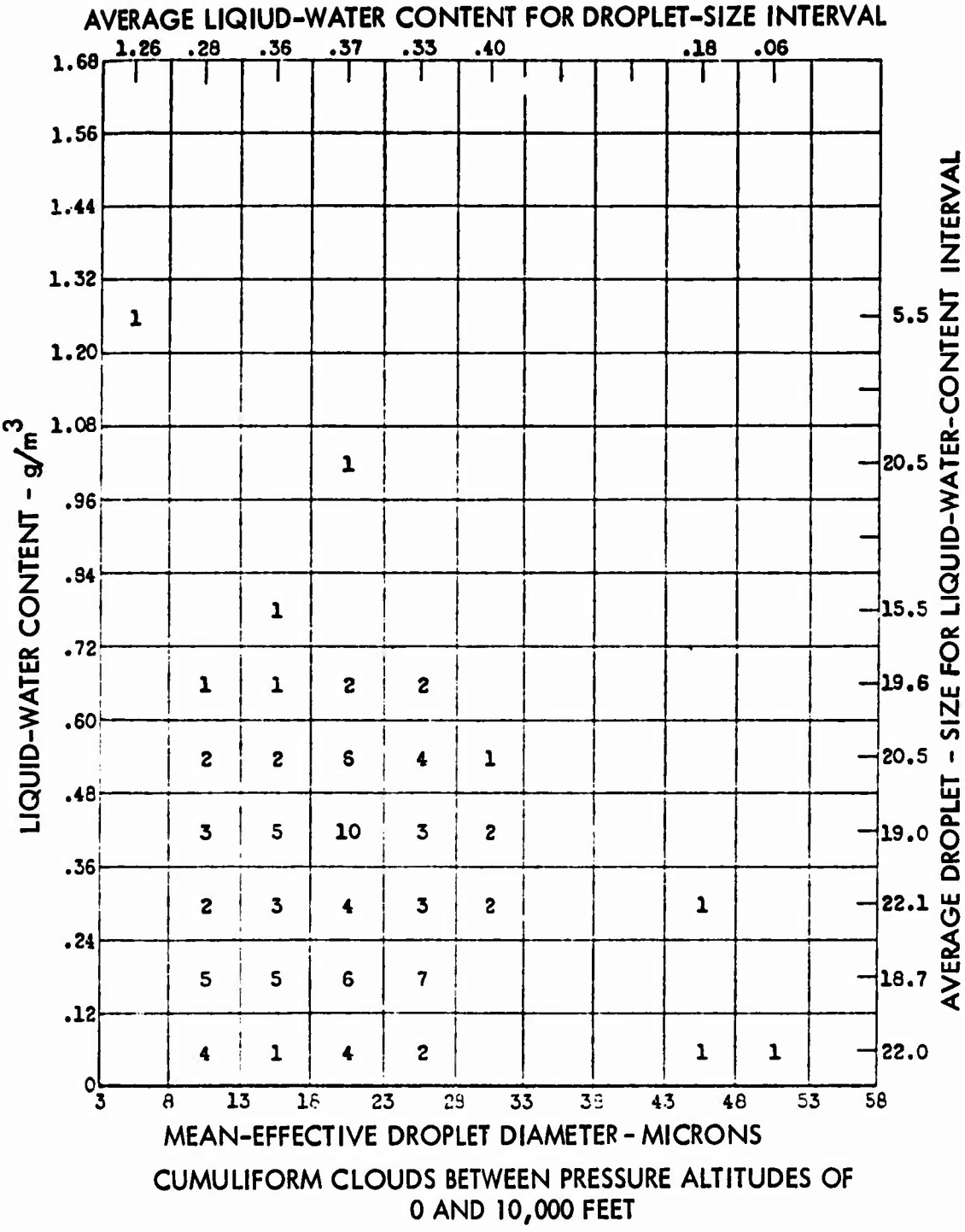

Figure 69. Frequency Distribution of Icing Observations for Various Increments of Liquid-Water Content and Mean-Effective Droplet Diameter. (Numbers given indicate number of icing conditions observed with these conditions.)

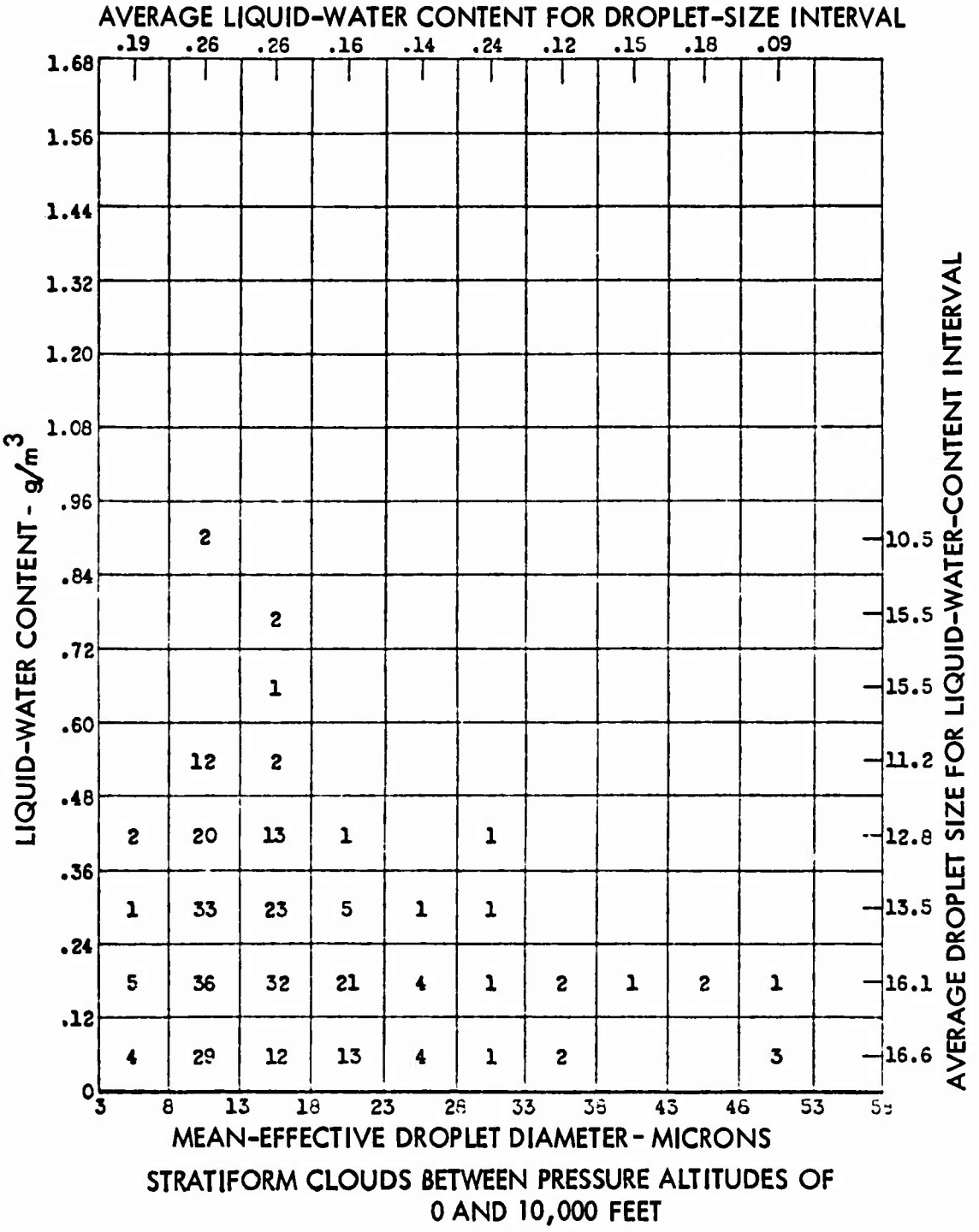

Figure 70. Frequency Distribution of Icing Observations for Various Increments of Liquid-Water Content and Mean-Effective Droplet Diameter. (Numbers given indicate number of icing conditions observed with these conditions.)

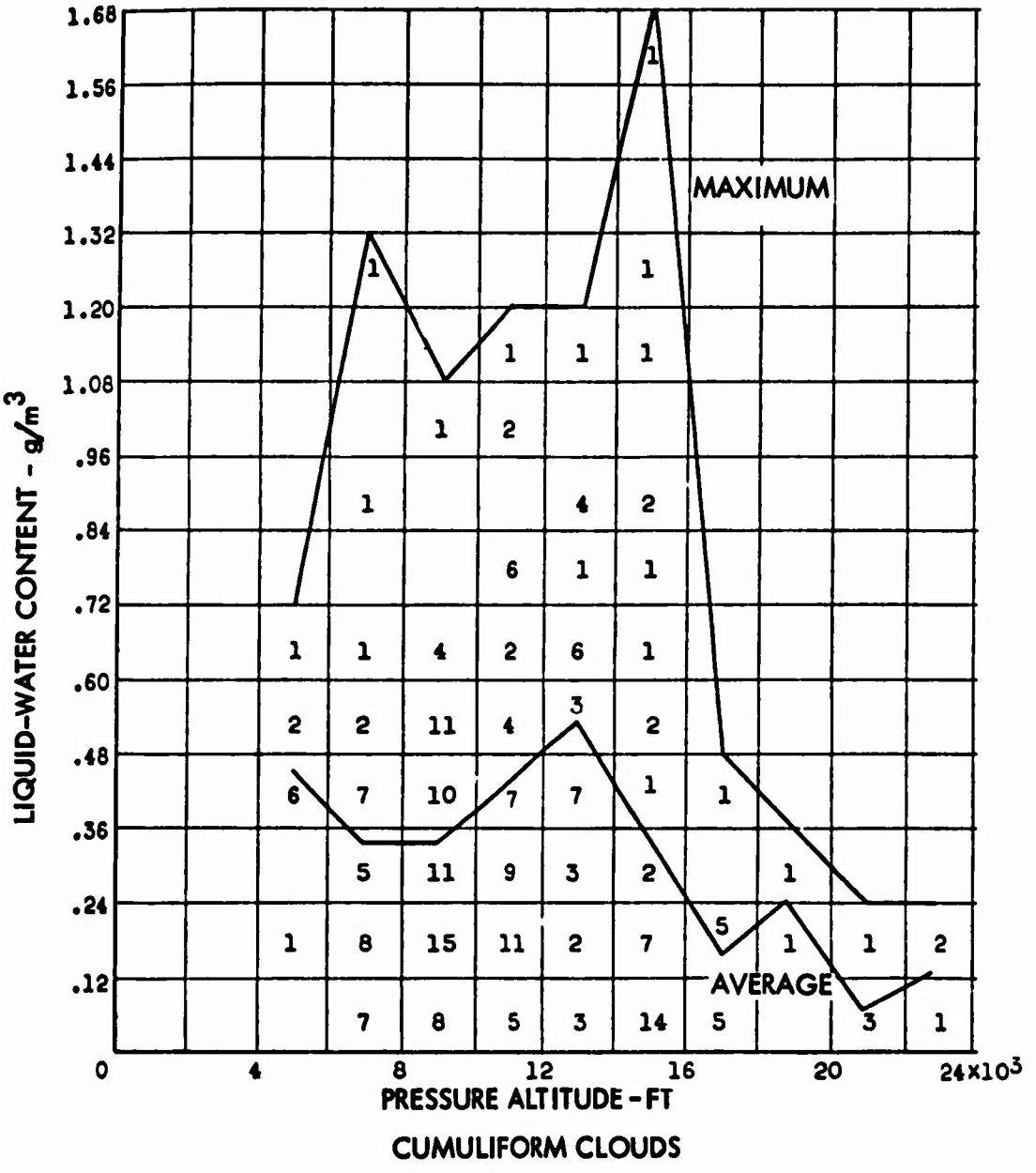

Figure 71. Frequency Distribution of Icing Observations for Various Increments of Liquid-Water Content and Pressure Altitude. (Numbers given indicate number of icing conditions observed with these conditions.)

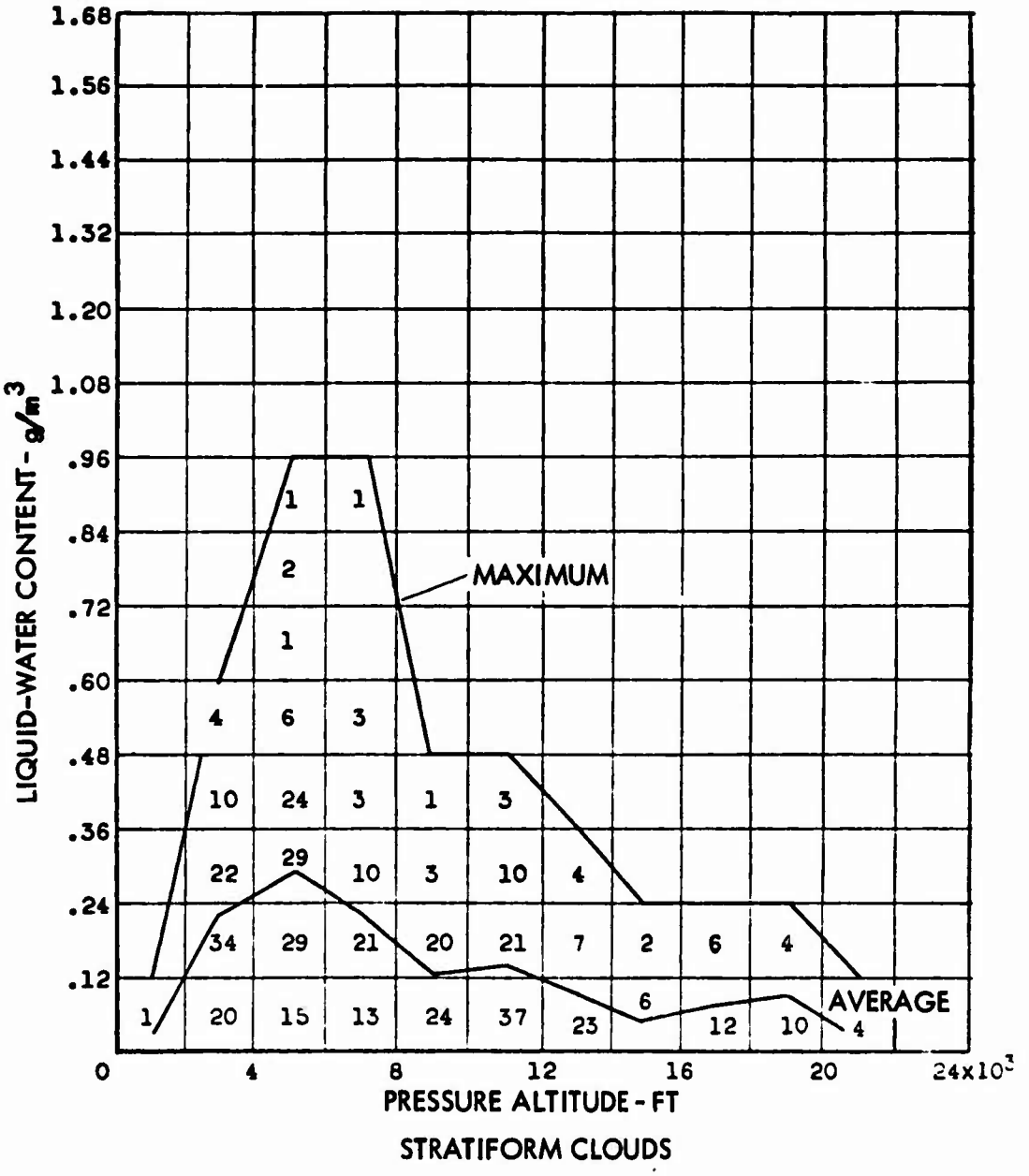

Figure 72. Frequency Distribution of Icing Observations for Various Increments of Liquid-Water Content and Pressure Altitude. (Numbers given indicate number of icing conditions observed with these conditions.)

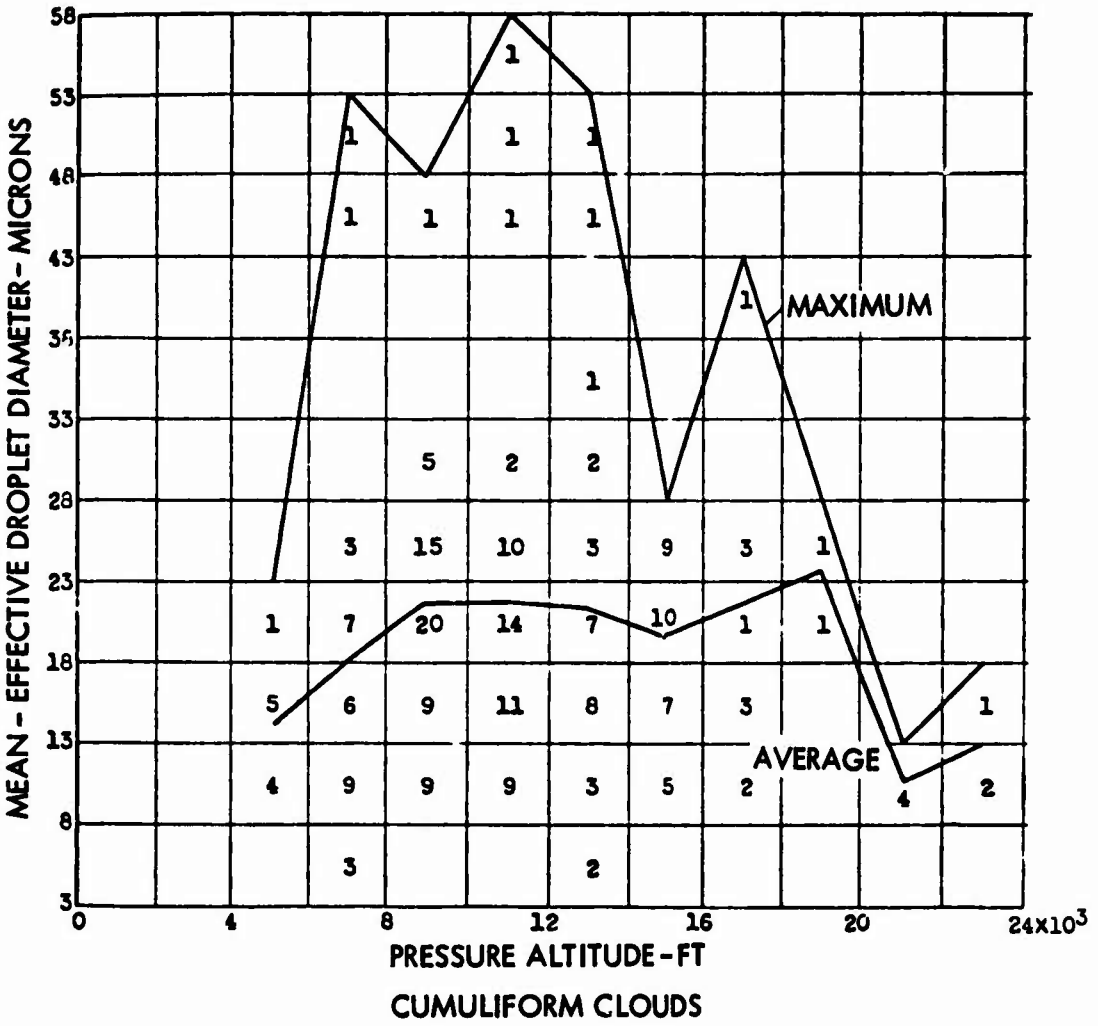

Figure 73. Frequency Distribution of Icing Observations for Various Increments of Mean-Effective Droplet Diameter and Pressure Altitude. (Numbers given indicate number of icing conditions observed with these conditions.)

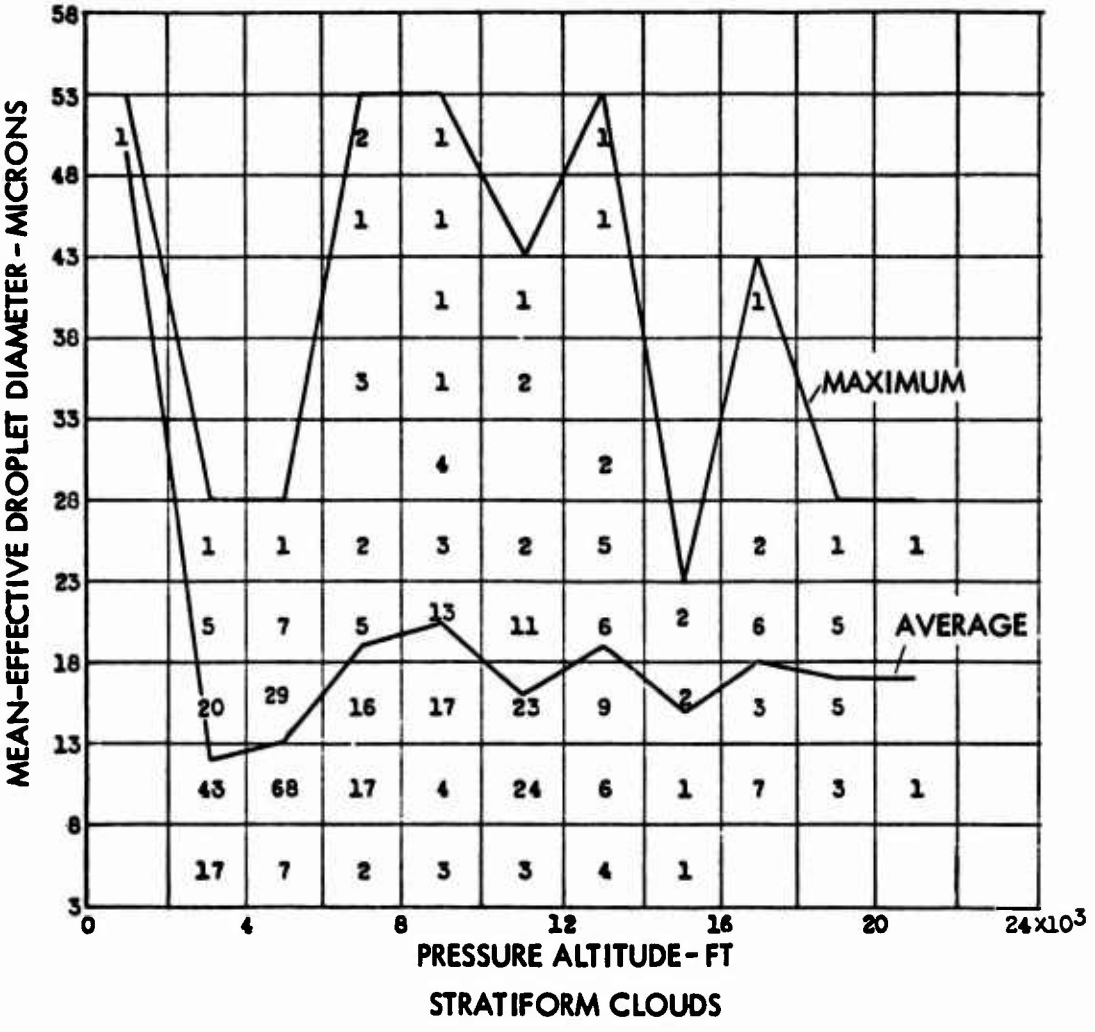

Figure 74. Frequency Distribution of Icing Observations for Various Increments of Mean-Effective Droplet Diameter and Pressure Altitude. (Numbers given indicate number of icing conditions observed with these conditions.)

Some important differences in Tables XVIII and XIX should be noted. Each of the previously accepted (Reference 61, 1956) terms is related to the current (Reference 14, 1969) ones by being displaced one term. For the same word descriptors, the 1964 collection rate in miles per 1/2 inch of ice is essentially the same as the one defined in 1956, but the associated liquid water content and the aircraft performance criteria are almost exactly one term different. Thus, as Reference 62 warns the pilots, "the new terms Trace, Light, Moderate, and Heavy generally correspond to the old (1956) terms Light, Moderate, Heavy, and Severe. Each pilot must become familiar with the current terminology to assure the existing conditions do not compromise with safe flight."

A report (Reference 63) prepared by the Rosemont Corporation for the U.S. Navy correlates the LWC experimentally determined (corresponding to 150 knots) at various ambient temperatures to the ice buildup on a small (1/2-inch-diameter hollow aluminum) probe. This correltation is shown on the upper portion of Figure 75. The correlation of these tests with the assumed variations of the previous and current definitions is shown on the lower portion of Figure 75.

It is obvious that the 1969 Rosemount tests correlate far better with the superseded 1956 terminology and attributes than with the current definitions. Unless other tests contradict these results, it would appear preferable to reinstate the earlier descriptions.

TABLE XVIII. 1964 ICING DEFINITIONS

Trace Icing - Accumulation of one-half inch of ice on a small probe per 80 miles. The presence of ice on the airframe is perceptible but the rate of accretion is nearly balanced by the rate of sublimation. Therefore, this is not a hazard unless encountered for an extended period of time. The use of deicing equipment is unnecessary.

Light Icing - Accumulation of one-half inch of ice on a small probe per 40 miles. The rate of accretion is sufficient to create a hazard if flight is prolonged in these conditions but insufficient to make diversionary action necessary. Occasional use of deicing equipment may be necessary.

Moderate Icing - Accumulation of one-half inch of ice on a small probe per 20 miles. On the airframe, the rate of accretion is excessive, making even short encounters under these conditions hazardous. Immediate diversion is necessary or use of deicing equipment is mandatory.

Heavy Icing - Accumulation of one-half inch of ice on a small probe per 10 miles. Under these conditions, deicing equipment fails to reduce or control the hazard and immediate exit from the icing condition is mandatory.

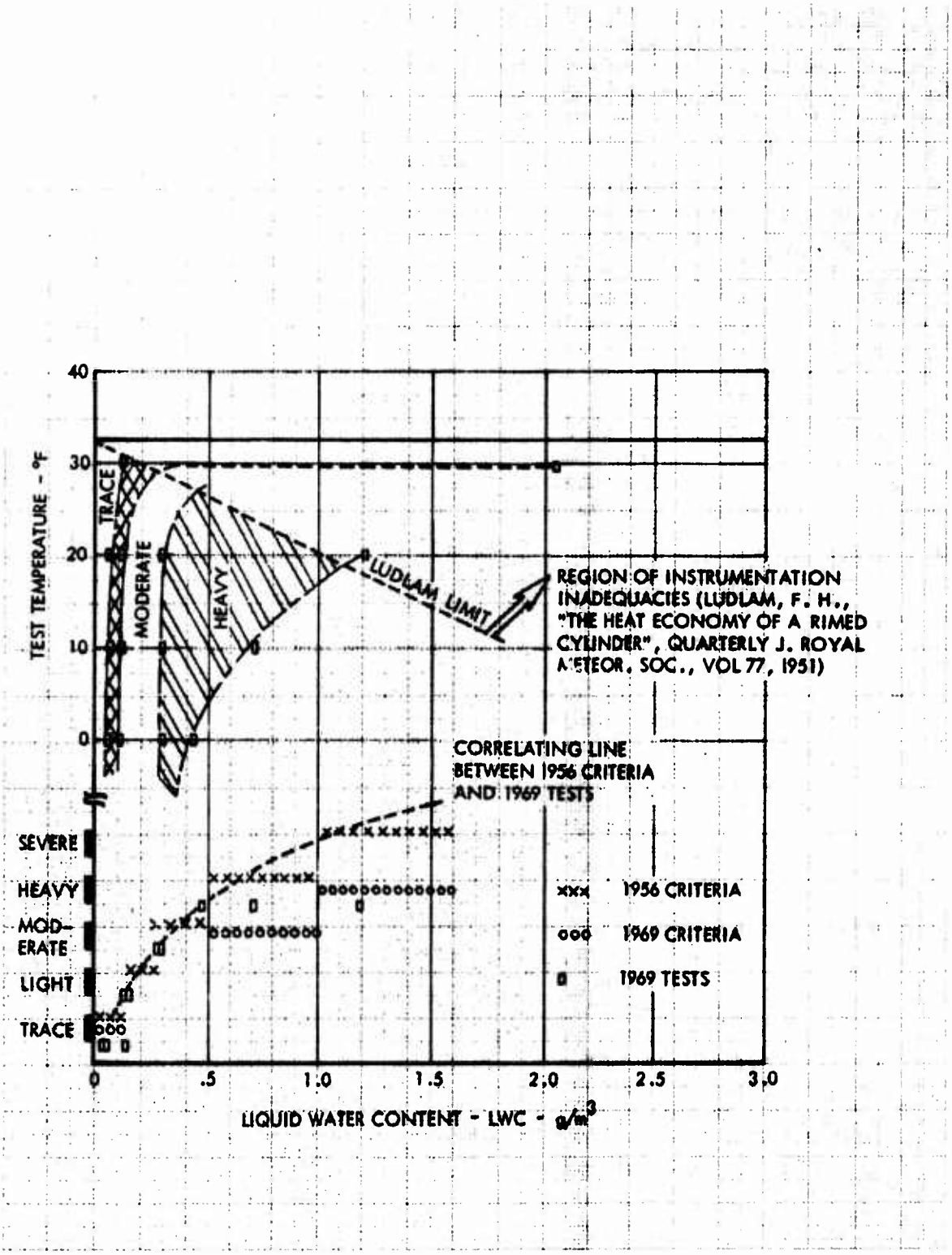

Figure 75. Comparisons of Various Icing-Severity Criteria.

TABLE XIX. COMPARISON OF 1956 ICING DEFINITIONS WITH THOSE OF 1964 AND 1969

AERONAUTICAL ENGINEERING REVIEW — JULY 1956				
Descriptive Terminology	Aircraft Performance Criteria	Liquid Water Content (Grams Per Cubic Meter)	Ice Collection Rates on Small Probes	
			Inches Per 10 Miles	Miles Per 1/2 Inch
Trace	Barely perceptible ice formations on unheated aircraft components	0 to .125 $(0 < .1)_a$	0 to .09	58 to Maximum $(80)_b$
Light	Evasive action unnecessary. (No perceptible effects on performances.)	.125 to .25 $(.1 < .5)_a$	.09 to .18	28 to 58 $(40)_b$
Moderate	Evasive action desirable. (Noticeable effects on performance.)	.25 to .50 $(.5 < 1.0)_a$	.18 to .36	14 to 28 $(20)_b$
Heavy	Eventual evasive action necessary. (Aircraft is unable to cope with icing situation and extended operation is not possible.)	.50 to 1.00 $(> 1.0)_a$	.36 to .72	7 to 14 $(10)_b$
Severe	Immediate evasive action is required. (Aircraft uses climb power to hold altitude and continued operation is limited to a few minutes.)	1.00 to Maximum $(----)_a$	.72 to Maximum	0 to 7 $(--)_b$

( )$_a$ 1969 Criteria (Reference 14)

( )$_b$ 1964 Criteria

TABLE XX. 1969 AIRFRAME ICING REPORTING TABLE

Intensity	Ice Accumulation	Pilot Report
Trace	Ice becomes perceptible. Rate of accumulation slightly greater than rate of sublimation. It is not hazardous even though deicing/anti-icing equipment is not utilized, unless encountered for an extended period of time - over one hour.	A/C Ident., Location, Time, (GMT) Intensity of Type*, Altitude/FL, Aircraft Type, IAS
Light	The rate of accumulation may create a problem if flight is prolonged in this environment (over one hour). Occasional use of deicing/anti-icing equipment removes/prevents accumulation. It does not present a problem if the deicing/anti-icing equipment is used.	Example:
Moderate	The rate of accumulation is such that even short encounters become potentially hazardous and use of deicing/anti-icing equipment or diversion is necessary.	Holding at Westminster VOR, 1232Z Light-Rime Icing, altitude six thousand, JetStar IAS 200 kts
Severe	The rate of accumulation is such that deicing/anti-icing equipment fails to reduce or control the hazard. Immediate diversion is necessary.	

*Rime Ice: Rough, milky, opaque ice formed by the instantaneous freezing of small supercooled water droplets.

Clear Ice: A glossy, clear or translucent ice formed by the relatively slow freezing of large supercooled water droplets.

From the foregoing definitions of icing severity, "moderate" icing fundamentally implies the need for ice protection equipment for continued safe flight. Therefore, moderate icing conditions can be considered as being equivalent to those used for system design purposes.

3.4.4 Recommended Design Meteorological Conditions

Sufficient information on icing probabilities has been presented to make a recommendation related to meteorological design conditions for rotorcraft.

Earlier Suggestions

A proposal was made in 1963 (Reference 64) on a design envelope of liquid water content versus ambient temperature. The uppermost curve in Figure 76 is an updated version of this envelope and is based on all the available icing statistics for all cloud types, altitudes, and geography. As such, it is applicable to helicopters that are either pressurized (none produced yet) or have oxygen provisions. A second curve has been developed for the typical helicopter that is restricted to 10,000 feet altitude or less.

The first (>10,000 feet) of these curves is essentially the one presented in Reference 64 as the sole recommended standard (at that time) and represents the case of the overall average of worldwide icing encounters for a probability of .001 (one case in a thousand) for more extreme combinations of icing conditions (it thus includes instantaneous maximum as well as continuous maximums). The second curve (≤10,000 feet) is based on the same probability but considers only those icing conditions that occur at less than 10,000 feet altitude. The data for this condition were presented earlier as Figures 67 and 68. Figure 76 also includes the NRC (and U.S. Navy) design envelope. This curve is based upon a 0.001 probability of exceedance for the "continuous maximum" conditions.

Practical Considerations

Considering a practical limit to certifying an ice protection system on the basis of flight test experience, the Canadian Forces in Reference 65 observed: "AETE's conclusion that their tests cleared the system to -11°C (12°F) only, and their recommendation that further qualification to 0°F (-17.8°C) be undertaken, was outside the strict terms of reference of this project directive. As a practical matter, the probability of encountering natural icing below -11°C is so remote that a test program could go on for years without generating the necessary data. It is worth noting that in the past three years of natural icing tests, AETE have not encountered a single test point below this temperature." This quotation illustrates the problem that system evaluators face in certifying the ultimate performance of a system in terms of available test conditions and predicted performance.

A review of ice protection design criteria for the P-3, C-130 and C-141 have indicated that the electrical running wet and cyclic deicing systems have been designed for protection to 0°F while the bleed air systems have been

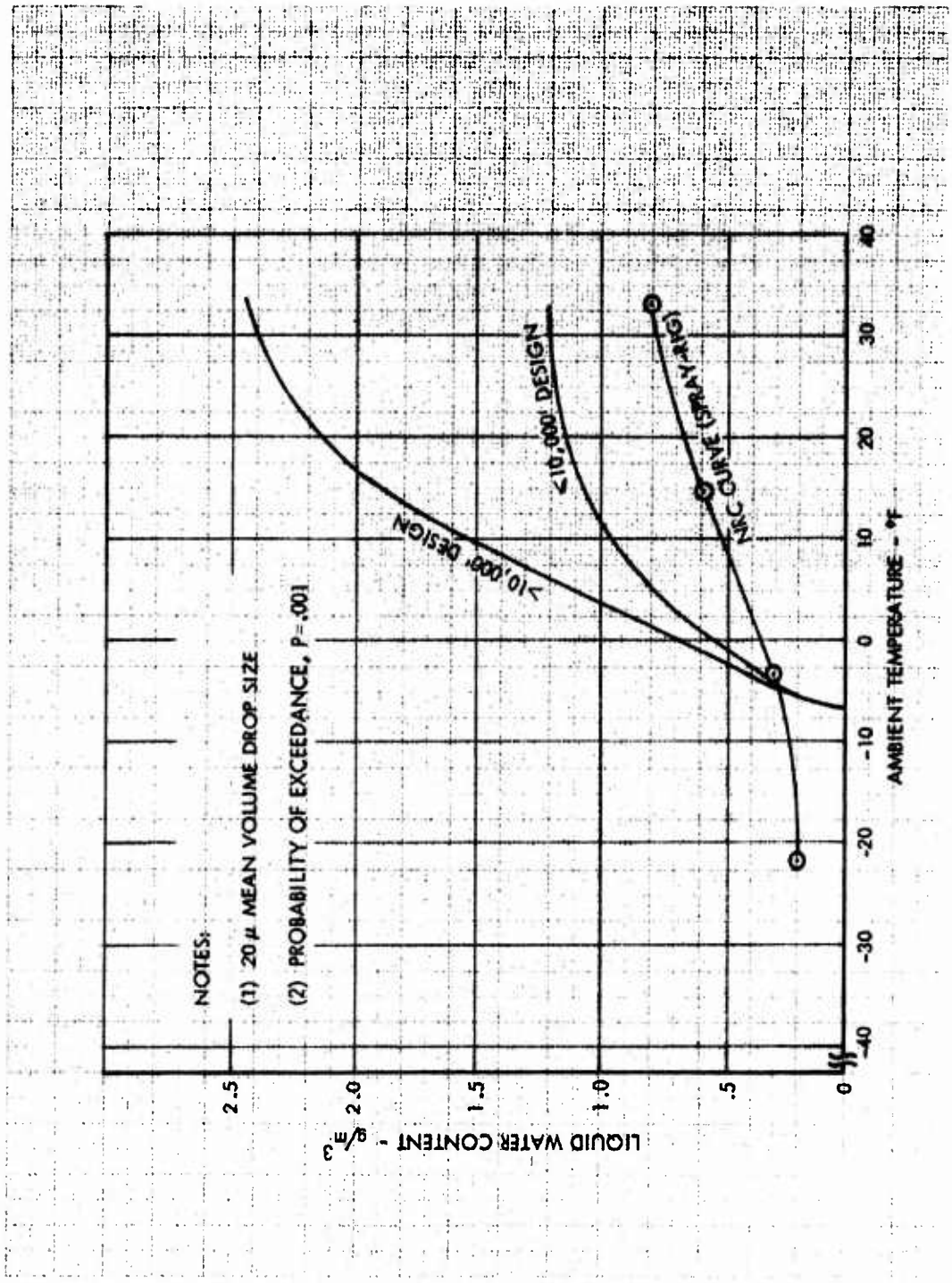

Figure 76. Helicopter Icing Criteria

designed to provide protection to -22°F. To our knowledge, there has never been a problem of inadequate heating capability with any of the electrical systems. Moreover, it is extremely difficult to find natural icing conditions for proof testing below 0°F. And, as a practical matter, it is futile to establish a performance requirement for a condition more severe than for which the system can be flight tested in natural icing conditions. MIL-A-9482 recognizes this fact and specifies an ambient temperature of 0°F as the design criterion for running-wet ice protection. The AVSCOM specification for engines specified a minimum icing temperature of -4°F (Tables IX and X of AV-E-8593B). Thus, it would appear that the principal value of designing to lower ambients would be to achieve a measure of conservatism in the design and perhaps to assure that the system does indeed work to 0°F. However, the problem of obtaining a design that truly meets the specification (and this is a problem) should be separated from the specification meteorological requirements themselves. (Perhaps this situation can be controlled by specifying the design and analysis procedures to be used.)

Icing Design Criteria for Rotary-Wing Aircraft

Presently, the principal criterion for ice protection of any all-weather U.S. Army or commercial airplane is safe flight in icing conditions for durations compatible with the expected aircraft flight envelope and based on icing intensities defined by FAR 25 (or MIL-E-38453). The governing objective of FAR 25, as presently formulated, is simply: achievement of safe flight in icing conditions. FAR 25 and MIL-E-38453 do not prescribe any specific method of protection, nor even consider whether active ice protection is required at all on a particular aircraft; instead, they provide a rational definition of the icing environment as it is likely to occur in nature and permit the aircraft designer to judge if, and in what form, protective measures are necessary to meet the criterion of safe flight. The requirements of these two documents are identical.

No new icing severity measurements have been reported since 1952. However, foreign icing severity data collected more recently confirmed the validity of the U.S. data. Therefore, it is recommended that the existing FAR 25 curves which show the interrelationships between ambient temperature, LWC and median droplet size be utilized for helicopter design purposes except that the low temperature limit be 0°F instead of -22°F. These curves are shown in Figures 77-80. Since these requirements have stood the test of time for all types of fixed-wing aircraft, and since there is little operating experience in icing with rotary-wing aircraft, there appears to be little justification for recommending a change in design criteria.

For individual helicopter models, the sensitivity to and consequences of ice formations on airframe elements cannot be readily predicted. It is, therefore, recommended that experimental procedures, similar to those required by the FAA, be specified for determining the need for ice protection on airframe components of rotary-wing aircraft. It is recommended that the need for fuselage nose, rotor, and engine inlet ice protection be established

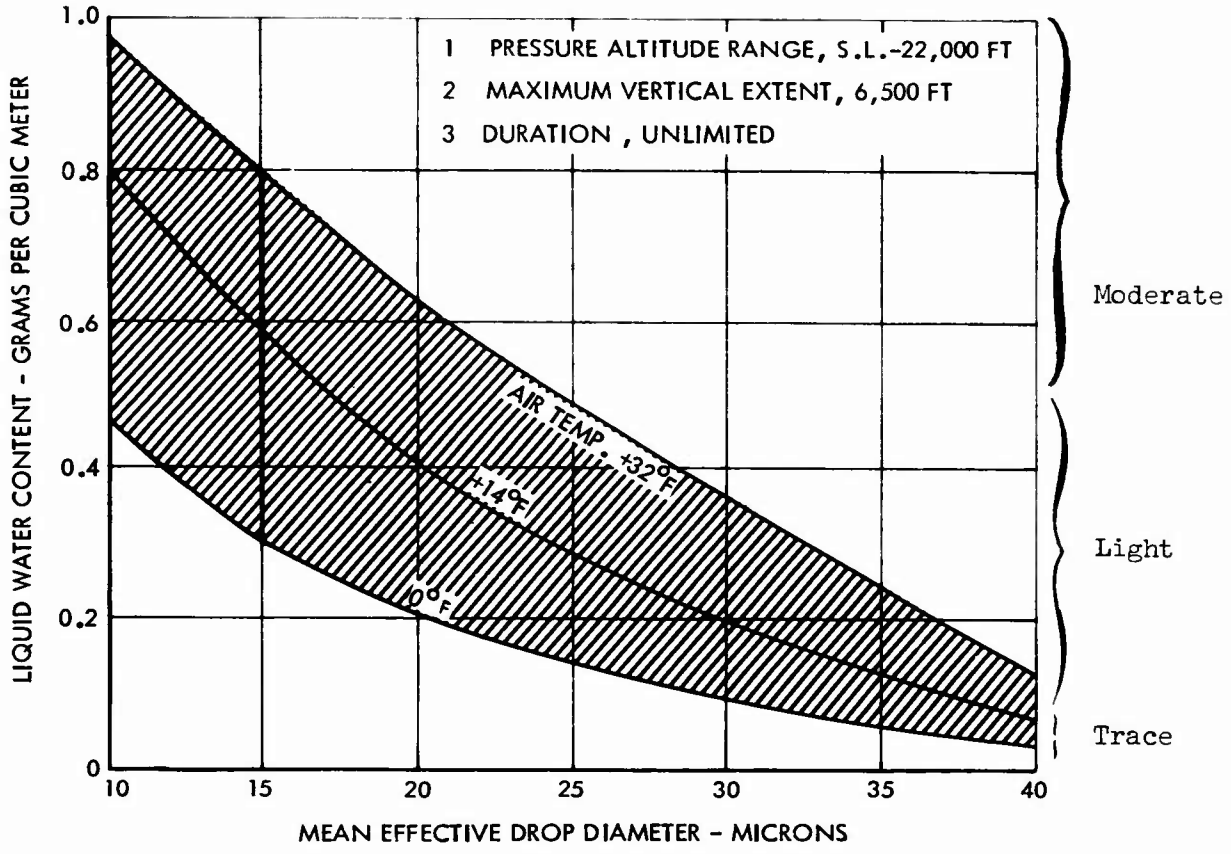

Figure 77. Recommended Continuous Maximum (Stratiform Clouds) Atmospheric Icing Conditions, Liquid Water Content vs. Mean Effective Drop Diameter.

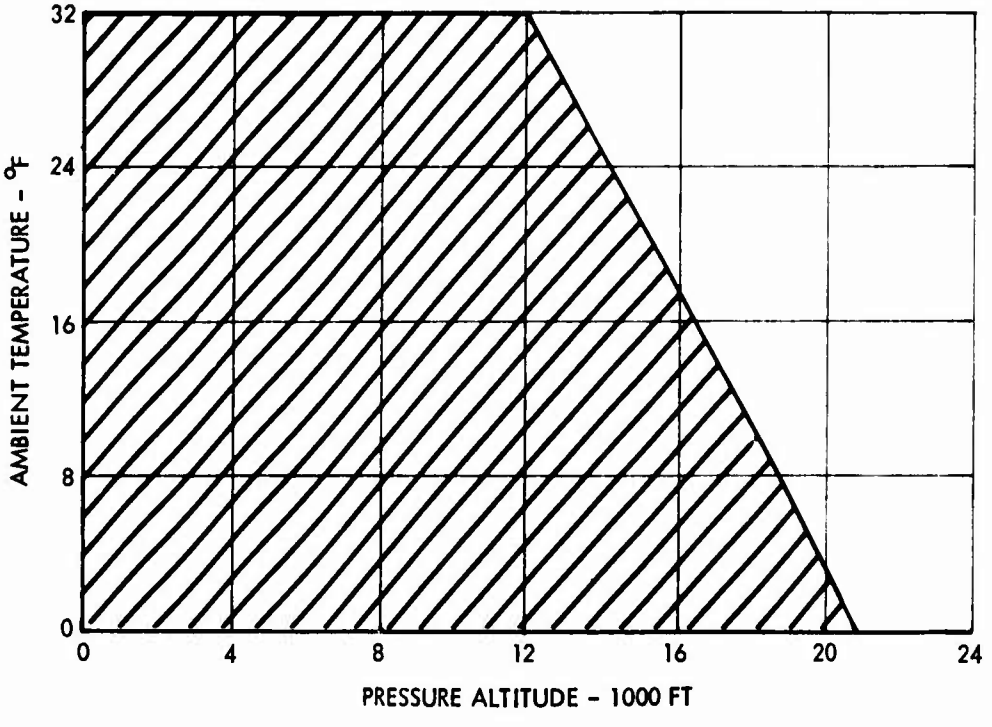

Figure 78. Continuous Maximum (Stratiform Clouds) Atmospheric Icing Conditions, Ambient Temperature vs. Pressure Altitude.

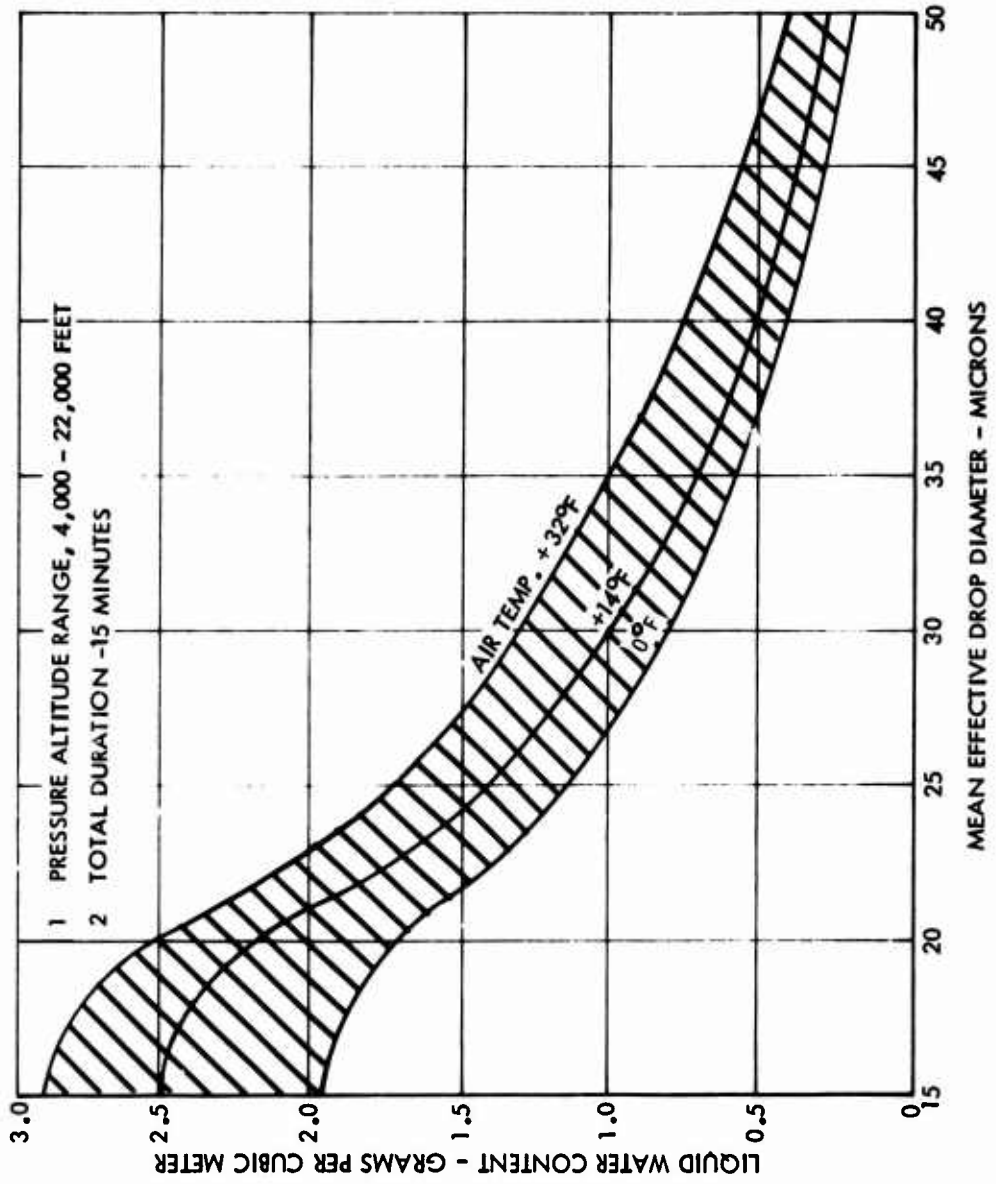

Figure 79. Intermittent Maximum (Cumuliform Clouds) Atmospheric Icing Conditions, Liquid Water Content vs. Mean Effective Drop Diameter.

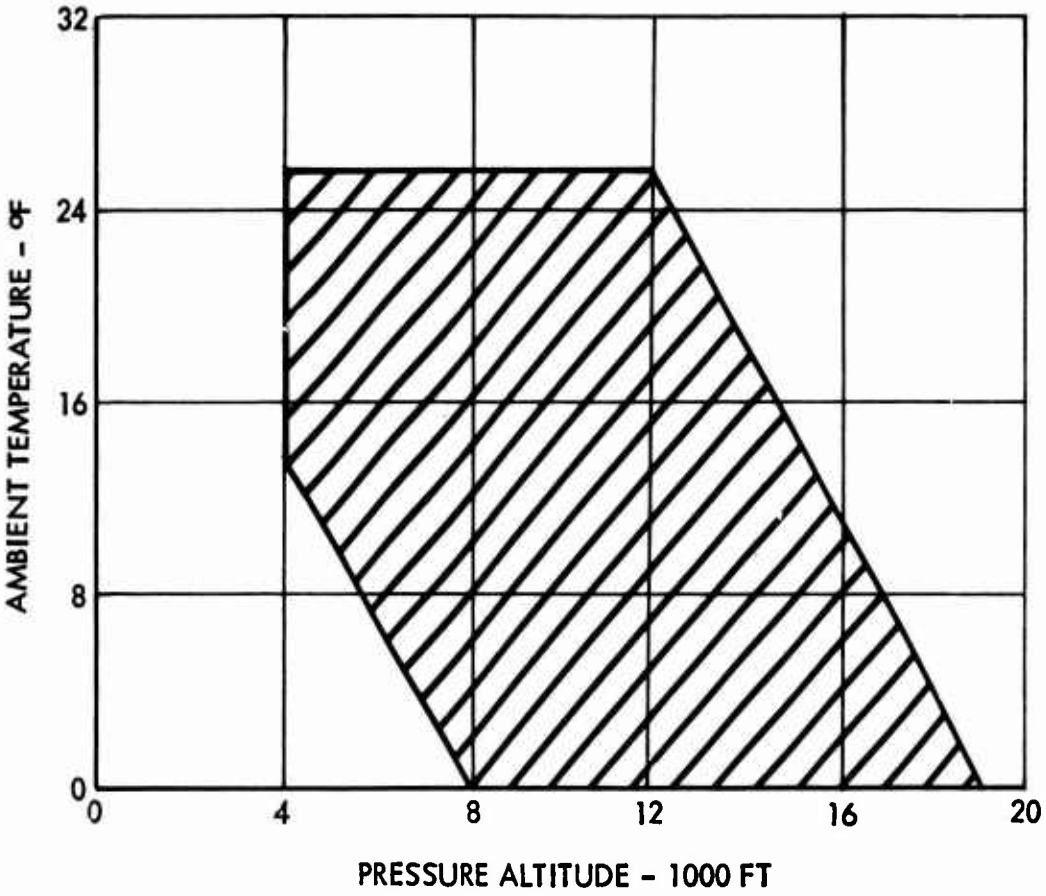

Figure 80. Intermittent Maximum (Cumuliform Clouds) Atmospheric Icing Conditions, Ambient Temperature vs. Pressure Altitude.

by flight testing the aircraft for at least one hour in FAR 25 (MIL-E-38453) continuous maximum icing conditions down to 0°F ambient (Figures 77 and 78). This duration is conservative when viewed in light of meteorological considerations discussed in this section and airmobile mission considerations discussed in Section 2. The required flight testing of the helicopter in icing can be accomplished at the Ottawa spray rig facility where a cloud of the required continuous maximum icing intensity can be obtained. However, these test requirements are not adequate to demonstrate the tolerance of the engine inlet duct to intermittent maximum icing conditions. Due to the dynamic characteristics (continuous motion due to lifting forces, wind vectors, etc.) of cumulus clouds, wherein intermittent maximum icing conditions occur, and due to the limited horizontal extent of such clouds, exposure to such conditions is relatively short, even during prolonged hover.

Statistical icing frequency data summarized in Figures 58 and 59 indicate that cumuliform icing clouds associated with intermittent maximum icing intensities (Figures 79 and 80) occur under natural conditions only above 4,000 feet (above S.L.) and the probability of encountering such clouds is greatest above 8,000 feet. This phenomenon is reflected in FAR 25 requirements for commercial aircraft and also in Figure 3 of MIL-E-38453. The typical liquid water content distribution in cumulus clouds increases with altitude such that occurrence of icing encounters with design intermittent maximum intensities is remote at altitudes below 7,000 feet above S.L. It has been concluded that rotary-wing aircraft will be subjected to intermittent icing severities (shown in Figures 79 and 80 or in Table IX of AV-E-8593B) for no more than 5 minutes. Even this number is conservative because of the inherent dynamic characteristics of clouds. Also, there is no data from fixed-aircraft experience to indicate that these icing severities prevail for longer than 5 minutes. To provide a large positive performance margin, it is recommended that the need for engine inlet ice protection be established on the basis of meeting requirements of paragraph 3.23 of AV-E-8593B after a 0.5-hour test under maximum intermittent icing conditions down to an ambient temperature of 0°F. To substantiate this capability, special engine inlet duct icing tests are required in an icing tunnel.

Once the need for and the degree of ice protection on helicopter surfaces are determined, the criteria for system design are evaluated. The minimum recommended icing design temperature of 0°F is not applicable in those cases where the engine inlet duct surfaces are heated sufficiently to achieve fully evaporative performance. Unlike cyclic deicing systems or continuous running wet systems, the heating capacity of which is dictated by the minimum ambient temperature, evaporative systems are sized for the maximum possible water catch rate. Considering the FAR 25 (MIL-E-38453) requirements, the maximum possible catch would result at ambient temperatures associated with the highest liquid water content. Consequently, for evaporative performance at low altitude, the criterion for engine inlet duct protection is governed by the ambient temperature that yields a surface equilibrium temperature of 32°F. In all commercial and military applications, FAR 25

(MIL-E-38453) continuous maximum icing intensities have been used successfully for many years as the design criterion for evaporative ice protection not only of airframe but also engine inlet duct surfaces. It is recommended that for evaporative engine inlet systemr, the same criteria for evaporative protection (Figures 77 and 78) be retained for rotary-wing aircraft airframe, rotor, and engine inlet duct.

Where engine inlet duct protection is based on providing running-wet protection, i.e., maintaining the surface just above freezing, it is recommended that the 0°F minimum icing design temperature be applied in conjunction with FAR 25 (MIL-E-38453) intermittent intensities. These curves are shown in Figures 79 and 80. Use of the intermittent maximum intensities minimizes the possibilities of frozen runback, yet does not impose excessive heating requiremnets. For a running-wet design, the energy requirements are not significantly influenced by the liquid water content because these requirements are governed by convective heat losses.

As will be described in Section 5, evaporative and cyclic systems can tolerate, for extended periods of time, conditions substantially more severe than the design conditions. While running-wet systems are more sensitive to ambient temperature rather than to icing severity, systems which have been designed to a 0°F limit appear to be satisfactory. It should also be remembered that the system designer does not consider a single-point design for the aircraft but must meet the worst combination of ambient temperature, volume median droplet size, and liquid water content for each system on the aircraft. Retaining this design requirement thus provides a substantial amount of flexibility which will be of benefit by providing a somewhat conservative design over a single-point criteria. However, it is recommended that for the purpose of computing the aft impingement limits a maximum (rather than median) droplet size of forty microns be used.

As far as ice protection of transparent areas is concerned, it is recommended that the requirements of MIL-T-5842, which are based on running-wet protection for intermittent maximum icing intensities, be retained without changes. Windshield heating on all fixed-wing and rotary-wing aircraft has been based on these requirements since the advent of transparent, electrically conductive coatings, and in-service experience has confirmed the validity of these requirements.

The rationale for the icing severity criteria relating to protection of flight probes (pitot-static tubes, total temperature probes, etc.) is different from that for the airframe and rotors. As discussed earlier, and also in Section 5, a slight compromise in protecting the airframe and rotor is justified because it does not jeopardize the safety of the aircraft even in extremely remote cases of very severe, short-duration icing encounters. For protection of flight probes, the entire envelope of potential icing conditions must be covered, regardless of icing duration or severity, and

no compromises, no matter how slight, can be accepted. It is recommended, therefore, that the criteria for ice protection of flight sensors, as specified in MIL-P-26292, be retained without changes. Provisions of flight probes with electrical heaters offering a running-wet capability at intermittent maximum icing intensities of MIL-P-26292 had stood the test of time and provides a large positive performance margin. It does not impose large power requirements because of the small area of the heated probe surfaces.

SECTION 4 VEHICLE ICE ACCRETION RATES

With the establishment of icing severity criteria identified in the previous section, it is possible to calculate the rate of ice accretion on vehicle surfaces and to estimate the initial ice shapes. By varying the meteorological parameters (ambient temperature, droplet size, liquid water content, etc.) the amount of ice accumulated on a surface can be determined. This information is required in order to determine when and where ice protection is required and how much energy is required to provide anti-icing/deicing. The following paragraphs describe the methods for determining water catch rates and calculations for estimating ice shapes, which will assist in determining the critical design point for an unheated airfoil.

4.1 DROPLET IMPINGEMENT THEORY

For a two-dimensional airfoil the total water catch, or more precisely, the total rate of water catch, is defined as the amount of water impinging on a unit span per unit time. If the water droplets traveled straight to an unswept 2-D airfoil, at zero angle of attack, the amount of water intercepted by the airfoil in 1 hour would be

$$R_W = 0.38 \times d \times V \times LWC \qquad (1)$$

where R_W = total water catch, lb/hr ft-span

d = maximum thickness of airfoil, ft

V = free-stream velocity, knots TAS

LWC = liquid water content, gm/m^3

0.38 = conversion factor for units

V x 1 hr

Any water droplets in the air and in the path of an object will tend to travel straight to the object, due to droplet inertia. However, the air streamlines tend to deflect the droplet from its path due to drag forces, so that each droplet actually has a curved path or trajectory as it approaches the airfoil as shown in Figure 81. There will be one droplet trajectory on each side of the stagnation point which will just graze the airfoil. All water droplets which follow trajectories within these two

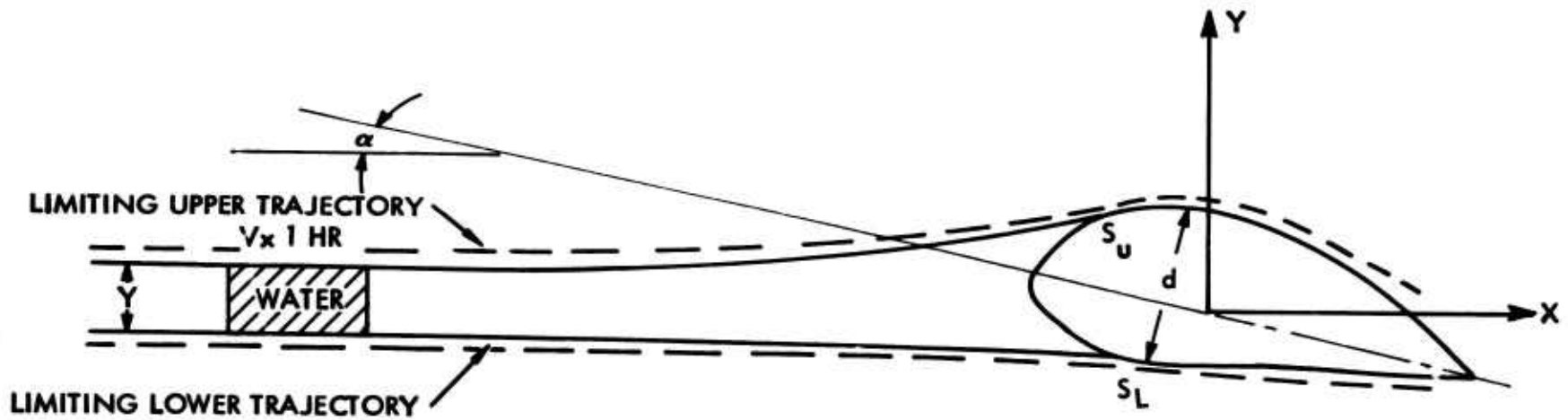

Figure 81. Water Droplet Trajectory in an Airfoil Flow Field and Illustration of Impingement Terminology.

limiting trajectories will impinge on the object; all droplets outside the limiting trajectories will not impinge. The total ordinate, "Y", divided by the maximum airfoil thickness, "d", is called E_m, the efficiency of water catch. Figure 81 depicts the droplet trajectories around a 2-D airfoil at an angle of attack α.

From Figure 81, the total rate of water catch is

$$R_W = 0.38 \times d \times V \times LWC \times E_m \qquad (2)$$

where E_m = collection efficiency, dimensionless

Since E_m is based on airfoil thickness, an airfoil at angle of attack might have a water collection efficiency greater than unity. (In Reference 66, E_m is based on projected height; therefore, in Reference 66, E_m is always less than unity.) For swept airfoils of infinite span, the 2-D water catch can be computed for an airfoil cross section normal to the leading edge by replacing the free-stream velocity with the free-stream velocity multiplied by the cosine of the sweep angle.

Langmuir and Blodgett (Reference 67) were the first to present the mathematical equations for determining water droplet trajectories. They solved the trajectory differential equations for a cylinder by using a mechanical differential analyzer. Langmuir and Blodgett also proved that the water droplet trajectories (or collection efficiency) for similar airfoil shapes were similar, provided that any two of the following dimensionless parameters were specified:

1. The Reynolds number of the water droplet, which compares the inertial and viscous forces on the water droplet:

$$R_U = 2a\gamma_a U/\mu_a g \qquad (3)$$

where a = radius of water droplet, ft

γ_a = density of air, lb/ft^3

U = free-stream velocity, ft/sec

μ_a = viscosity of air, $lb\text{-}sec/ft^2$

g = gravitational constant, 32.17 ft/sec^2

2. The water droplet inertia parameter, which includes the effect of the inertia of the water droplet:

$$K = 2a^2 U\gamma_d/9C\mu_a g \qquad (4)$$

where γ_d = density of water droplet, lb/ft^3

C = airfoil chord length, or characteristic length, ft

3. The impingement parameter, which accounts for the deviation of the water drop drag forces from Stokes' Law:

$$\phi = R_u^2/K$$

4. The scale modulus, which "scales" the airfoil size to the droplet size:

$$\psi = R_u/K$$

Langmuir and Blodgett utilized these similarity parameters in presenting the collection efficiency data for cylinders in the K and ϕ format of Figure 82. Later NACA investigators used the R_u and ψ format also shown in Figure 82.

The use of a modified water droplet inertia parameter K_o permits consolidation into only a few graphs of most of the published water drop trajectory data. The representation was suggested by Dr. Irving Langmuir (Reference 67) and first shown by Dr. Myron Tribus, whose report (Reference 68) contained water droplet trajectory data for a cylinder, sphere, ribbon, and several airfoils.

The term K_o is obtained from the relation $K_o = (\lambda/\lambda_s)K$, where (λ/λ_s) is a function only of the water droplet Reynolds number R_u, as shown in Reference 66. λ is the true distance a water drop will travel when injected into still air, and λ_s is the distance the water drop will travel if released in still air when its drag coefficient obeys Stokes' Law. Since $K = R_u/\psi = \lambda_s/C$, then $K_o = (\lambda/\lambda_s)\,K = \lambda/C$, and K_o is thus the actual range of a water droplet expressed in units of the body characteristics length (C).

Presentation of Tribus' data using the K_o parameter showed the close grouping of data points instead of the usual family of curves. A mean line through the K_o curves showed that the deviations in efficiency of water catch and limits of ice impingement were generally about 10 percent or less. (Exceptions were E_m data for the cylinder and ribbon at low K_o values for which the deviations from the mean line were higher than 10 percent.) This is accurate enough for most preliminary calculations involving the heat requirements for anti-icing an airfoil.

A more detailed analysis of the K_o correlation was made in Reference 69, and similar results were obtained in reducing the theoretically determined

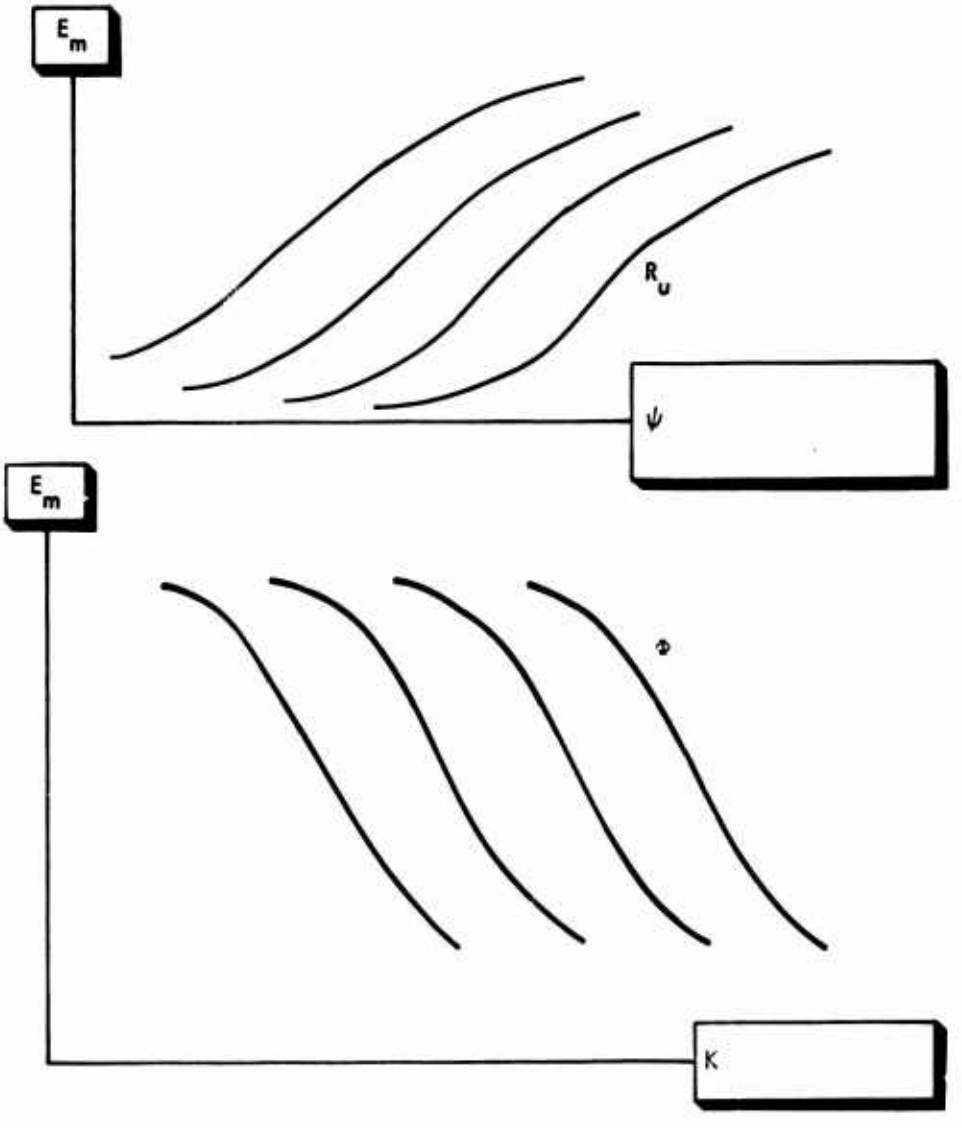

Figure 82. Exact Methods of Representing E_M.

water drop trajectory data for all other published information on airfoils and geometric shapes. The extension or interpolation of experimental as well as analytical data points over a wide range of the pertinent variables (water drop size, body size, speed, and altitude) is greatly aided by this K_o parameter, even though no complete theoretical proof of its significance or validity is available.

Figure 83 shows how the sets of curves in Figure 82 are reduced to a single curve by the K_o correlation.

Many investigators solved the water drop trajectory equations and determined the impingement limits (the points on the body where the limiting tangent trajectories impinge) and the collection efficiencies for a variety of airfoil shapes. It was found that the accuracy of their solutions was very much dependent on how accurately they could predict the air streamlines. For Joukowski airfoils, cylinders, ellipses, and spheres, exact potential flow solutions exist, and the agreement between analytical and experimental impingement data is good. However, a great majority of practical airfoils do not have exact potential flow solutions, and the analytical and experimental water impingement data for these airfoils did not agree as well. Since the previous water catch data for bodies with exact potential flow solutions agree well with experimental data, while the previous water catch data for bodies that require an approximate potential flow solution do not agree well, it follows that the water catch calculations are very sensitive to the air flow-field.

The K_o correlation for determining water catch on an arbitrary airfoil or engine inlet requires interpolation of the impingement data from airfoil shapes which approximate the design airfoil shape. Since the water droplet trajectories are very sensitive to the air streamlines, interpolation of water catch data for different airfoil contours might be grossly inaccurate. It is thus desirable to have an economical method for solving the basic water droplet trajectory equations for an arbitrary airfoil.

A computerized technique for solving the water droplet trajectory equations for reasonably shaped, 2-D and swept airfoils and axisymmetric engine inlets at angle of attack has been utilized. It solves the water droplet trajectory equations by a numerical technique and then uses the water drop trajectory results to calculate the water catch data; i.e., local efficiency distributions, local water catch distribution, impingement limits, total collection efficiency, and the total water catch. The method outputs all of the water catch data discussed above, given the body coordinates, angle of attack, free-stream velocity, altitude, free-stream temperature, chord length, thickness of the body, droplet size, and liquid water content.

The accuracy of the water droplet trajectory is greatly influenced by how accurately the local air velocity can be computed as a function of position. Many of the previous investigators performed their calculations for cylinders, ellipses, or Joukowski airfoils for which there exists an exact

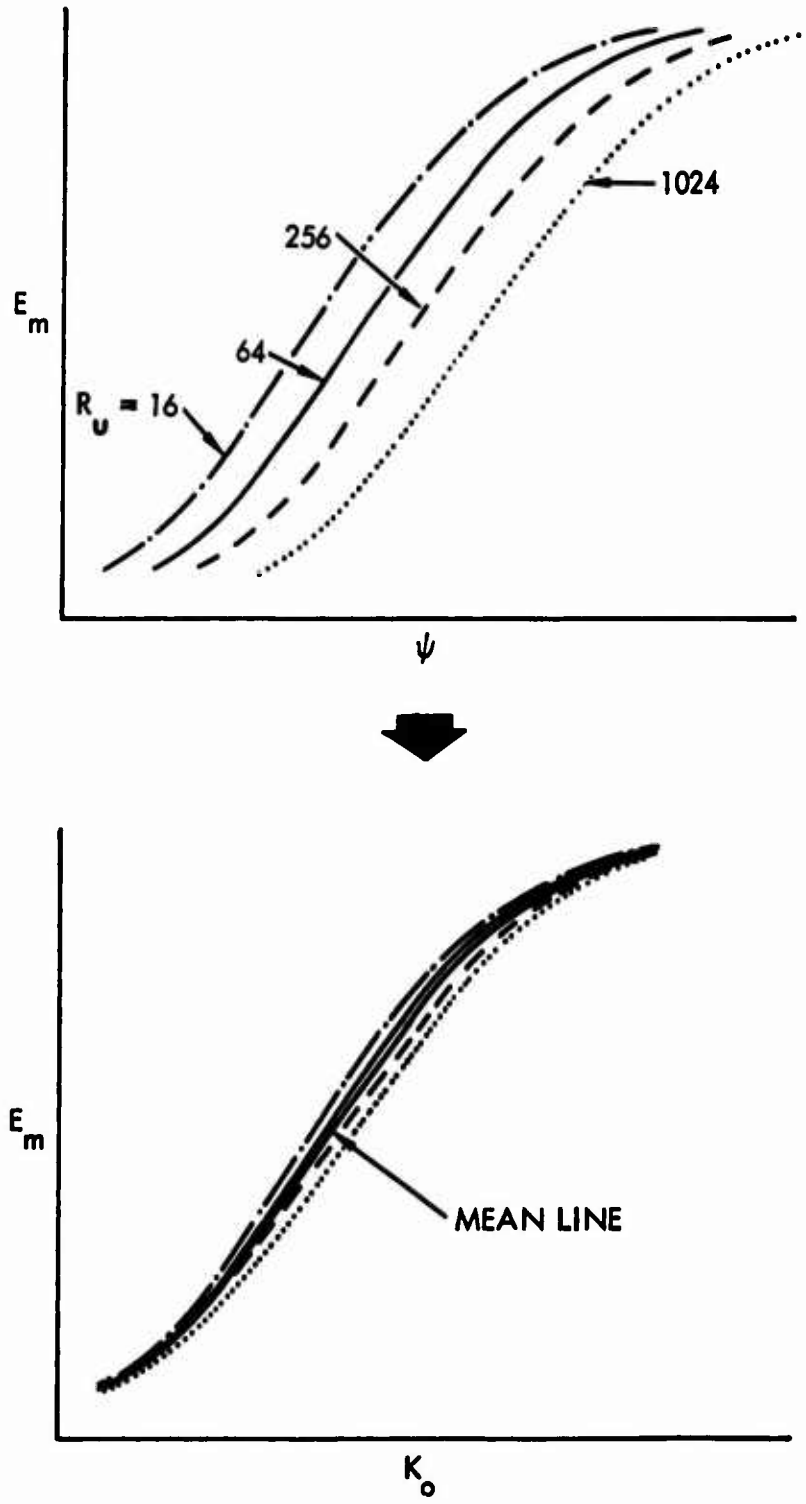

Figure 83. K_o Approximation for Representing E_M.

potential flow solution for local air velocity. For an arbitrary body which does not have an exact potential flow solution, there are two ways to calculate local air velocity: (1) a numerical solution of Laplace's potential equation by a relaxation technique, and (2) a vorticity substitution technique which can calculate the local air velocity off the body, given the body pressure distribution.

Of the two methods, the vorticity substitution technique provides more accurate data for a given computational effort. Thus, the inviscid incompressible pressure distribution, given the body coordinates and angle of attack, have been calculated by a computer program which uses the vorticity substitution technique off the body, and interpolation near the body. Another computer program was used to calculate local air velocity components at any point in the flow field, given the body coordinates and angle of attack.

The droplet trajectory analysis considers the drag on the droplet relative to the air-stream, and the conventional form for the drag force on a spherical water droplet moving in a fluid is

$$D = 1/2\ \rho_a\ \pi\ a^2 \bar{V}^2\ C_D \tag{5}$$

where ρ_a = density of air, slugs/cu ft

a = droplet radius, feet (3.048×10^5 microns)

$\bar{V}$ = local vector difference between velocity of the droplet and velocity of air, ft/sec

C_D = drag coefficient for droplets in air, dimensionless

D = drag force, lb

If Reynolds number is defined as

$$R = \frac{2a\ \rho_a\ \bar{V}}{\mu} \tag{6}$$

Equation (5) may be rewritten:

$$D = \frac{C_D\ R}{4}\ \pi\ a\ \mu\ \bar{V} \tag{7}$$

where μ = viscosity of air, slugs/ft-sec

Newton's second law implies that the motion of a spherical water droplet is a function of drag only, if buoyancy and gravity effects are neglected. In the X-direction, the equation of motion may be written

$$4/3\ \pi\ a^3\ \rho_w \frac{d\ V_x}{dt} = \frac{C_D\ R}{4} \pi\ a\ \mu(U_x - V_x) \qquad (8)$$

where V_x = x-component of water drop velocity, ft/sec

U_x = x-component of local air velocity, ft/sec

ρ_w = density of the water droplet, slugs/cu ft

x-axis = chord line of the body

y-axis = a line perpendicular to the x-axis at the mid chord point

t = time, sec

In this analysis, the coordinate system is fixed and the air and droplets are moving relative to a stationary body (see Figure 84).

Define U = free-stream velocity, ft/sec

C = characteristic length, ft

$v_x = V_x/U$, dimensionless

$u_x = U_x/U$, dimensionless

$|\bar{v}| = |\bar{V}/U| = \sqrt{(u_x - v_x)^2 + (u_y - v_y)^2}$, dimensionless

K = inertia parameter $= \frac{2}{9} \rho_w \frac{a^2 U}{\mu C}$, dimensionless

τ = time scale $= t\ U/C$, dimensionless

R_U = free-stream Reynolds number $= \frac{2a\ \rho_a\ U}{\mu}$, dimensionless

Using the above definitions, equation (8) can be written in dimensionless form.

$$\frac{dv_x}{d\tau} = \frac{C_D R}{24K}(u_x - v_x) \qquad (9)$$

Similarly, the y-component of the motion equation may be written in dimensionless form.

$$\frac{dv_y}{d\tau} = \frac{C_D R}{24K}(u_y - v_y) \qquad (10)$$

The total collection efficiency is

$$E_m = \frac{(S_{y_{o,u}} - S_{y_{o,l}})}{d} \qquad (11)$$

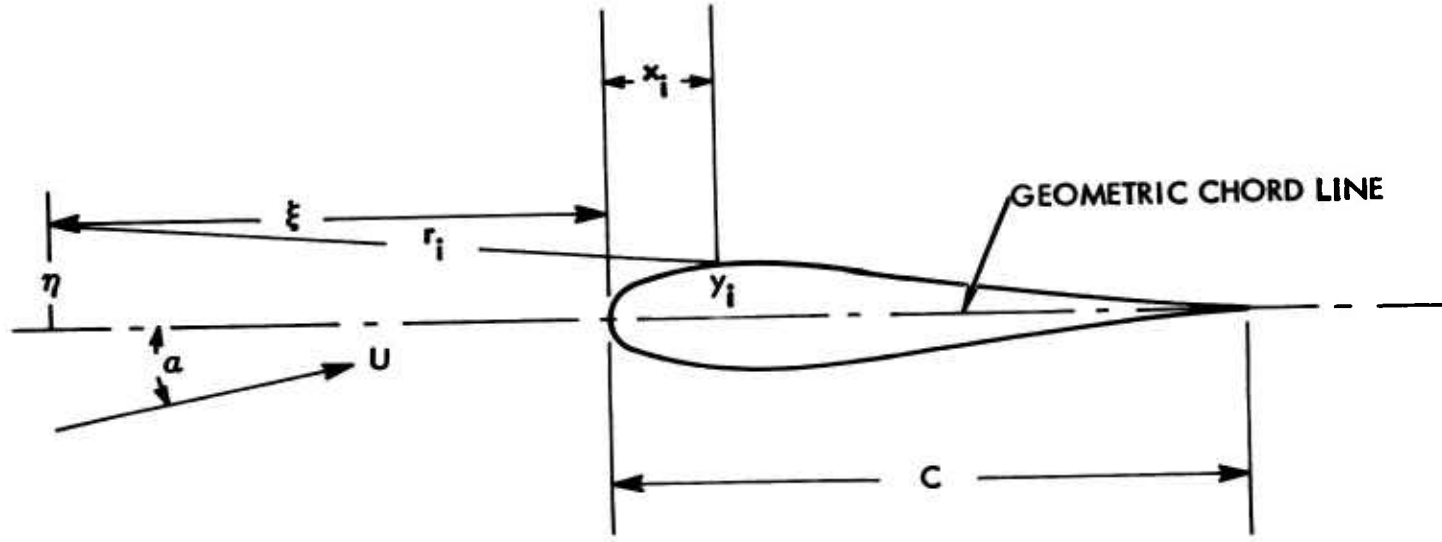

Figure 84. Coordinate System Used Computing Flow Field Velocities.

where $S_{y_{o,u}}$ = largest value of S_{y_o} for which a droplet will impinge, ft

$S_{y_{o,\ell}}$ = smallest value of S_{y_o} for which a droplet will impinge, ft

d = frontal thickness of the body, ft

The ratio of the local collection efficiency to the total collection efficiency as a function of body position is defined as follows:

$$E/E_m\ (\hat{S}) = \frac{S_{y_o} - S_{y_{o,\ell}}}{S_{y_{o,u}} - S_{y_{o,\ell}}} \tag{12}$$

where $\hat{S}$ = the distance along the body from the leading edge to the impingement point of the droplet which started at S_{y_o}, nondimensionalized by the chord length

S_{y_o} = an arbitrary ordinate, within the impingement limits, for the droplet in question

The local catch at a body position $\hat{S}$ is defined as follows:

$$R_{w_{local}} = R_{w_{total}} \times \frac{d}{d\hat{S}} (E/E_M\ (\hat{S})) \tag{13}$$

The local impingement efficiency, β, can be related to the local catch as follows:

$$\beta = \frac{dy_o}{d\hat{S}} = \frac{y_{o,u} - y_{o,\ell}}{R_{w,\ total}} R_{w_{local}} \tag{14}$$

where $y_o = S_{y_o}/C$ = starting ordinate value, nondimensionalized by chord length

$y_{o,u} = S_{y_{o,u}}/C$ = starting ordinate value of upper impingement limit, nondimensionalized by chord length

$y_{o,\ell} = S_{u_{o,\ell}}/C$ = starting ordinate value of lower impingement limit, nondimensionalized by chord length

The results of this analysis were programmed and used to generate water catch data.

4.2 THERMODYNAMICS OF ICE SHAPES

The estimation of ice shapes is a very complex procedure, involving a heat and mass transfer balance at the airfoil surface. For rotor blades this is

further complicated by the variation in local velocity, total temperature, and blade angle of attack from root to tip. Also, once an airfoil has collected ice, it becomes a new shape with different local flow fields and catch efficiencies.

The first step in estimating the ice shape on an unheated airfoil, e.g., rotor blade, is to estimate whether the surface temperature is at or below the freezing point. A graphical method has been developed (Reference 70) of estimating the unheated surface temperature subjected to water impingement given the local ambient temperature, water catch rate, velocity, and heat transfer coefficient. Depending upon the relative magnitude of these parameters, the unheated equilibrium temperature may be less than or more than the local recovery temperature, which is calculated as

$$T_r = T_\infty + \left(\frac{V^2}{2gJCp}\right) r \qquad (15)$$

where T_∞ = ambient temperature, ^oF

V = local velocity, fps

J = Joule's constant, 778 ft-lb/Btu

Cp = specific heat of air

r = recovery factor (0.85 for laminar flow and 0.9 for turbulent flow)

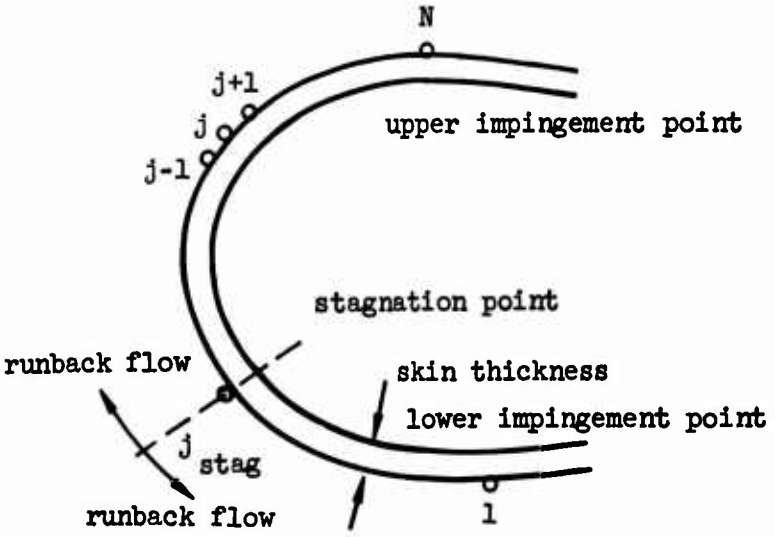

Messinger (Reference 70) was the first to present the heat balance equation for ice accretion at a point j. The heat balance equation of Reference 70 tacitly assumed that the equilibrium surface temperature and freezing fraction at a point j are independent of the heat balance at other points along the airfoil contour.

The surface of an unheated airfoil moving through an icing cloud will assume an equilibrium temperature distribution as determined by a thermodynamic balance. In order to determine the equilibrium surface temperature distribution, N heat balance equations must be solved along an airfoil contour. The equilibrium temperature is determined by a heat balance where:

q sources = q sinks

q sources = all heat delivered to the surface, tending to raise its temperature

q sinks = all heat absorbed at the surface, tending to lower its temperature

The following modes of heat transfer are included in the heat balance of Reference 70 (see Figure 85):

Heat Sources

1. Convective (aerodynamic and frictional) heat delivered by boundary layer inner limit at adiabatic wall temperature to skin at temperature t_{se} to a surface of area A (The heat transfer coefficient is h, Btu/hr-ft^2-^{o}F)

$$q = hA(t_\infty + \frac{rV^2}{2gJCp} - t_{se}) \qquad (16)$$

2. Latent heat of fusion delivered to skin when fraction n of the impingement water freezes

$$q = nR_W AL_f \qquad (17)$$

where $0 \leq n \leq 1.$ and L_f is the latent heat of fusion of water (approximately 144 Btu/lb).

The freezing fraction, n, is the percentage of impinging water which freezes upon impact. When the surface temperature is below freezing, all of the impinging water freezes, resulting in ice shapes which are streamlined and conform roughly to the airfoil contour. As the local ambient temperature and/or velocity increase, and the surface temperature reaches 32^{o}F, not all the impinging water freezes on impact; but rather a portion of it (1-n) runs back and freezes elsewhere. Increased local impingement rates also tend to raise the equilibrium surface temperatures and reduce the freezing fraction.

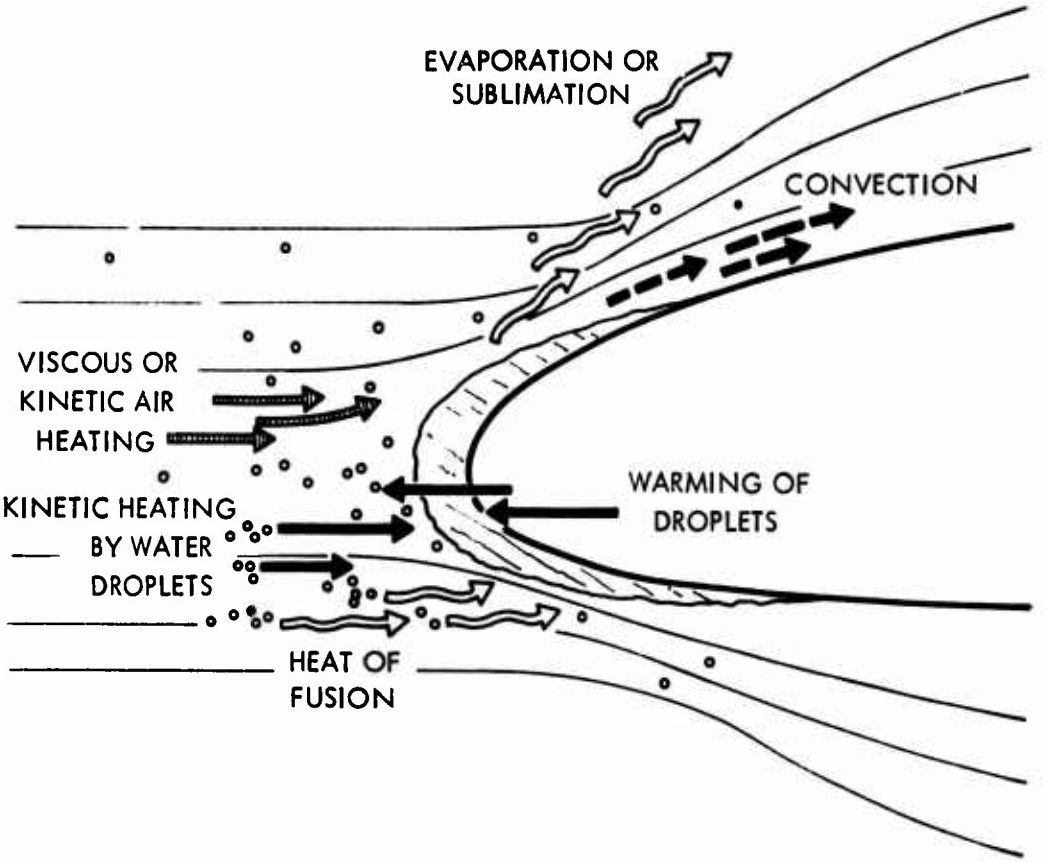

Figure 85. Modes of Energy Transfer for an Unheated Airfoil in Icing Conditions.

3. Sensible heat delivered to skin when ice cools from $32^{\circ}F$ down to t_{se} (if $t_{se} < 32$).

$$q = R_w AC_i(32 - t_{se}) \tag{18}$$

4. The kinetic energy of the droplets, delivered to the surface when they impinge.

$$q = R_w AV^2/2gJ \tag{19}$$

Heat Sinks

1. Sensible heat absorbed by impinging supercooled water, as it is warmed from t_∞ to $32^{\circ}F$ or to t_{se}, whichever is higher.

$$q = R_w AC_w(32 - t_\infty) \tag{20}$$

or

$$q = R_w AC_w(t_{se} - t_\infty)$$

whichever is greater.

2. Latent heat of sublimation absorbed by vapor leaving dry surface of ice ($n = 1$, $t_{se} \leq 32^{\circ}F$).

$$q = 2.9h\ AL_s(p_{se} - p_\infty)/B \tag{21}$$

where p = partial pressure of water vapor (at t_{se} or t_∞)

B = barometric pressure

L_s = latent heat of sublimation (approximately 1020 Btu/lb)

3. Latent heat of evaporation absorbed by vapor leaving wet surface ($n<1$, $t_{se} \geq 32^{\circ}F$).

$$q = 2.9h\ AL_e(p_s - p_\infty)/B \tag{22}$$

L_e is the latent heat of vaporization of water (approximately 1060 Btu/lb)

In addition to the above modes of heat transfer there are two phenomena which will couple the N heat balance equations that were not considered in Reference 70.

Runback - if the temperature at point j-1 is greater than or equal to $32^{\circ}F$, some fraction of the impinging water which did not freeze on impact between the stagnation point and point j - 1 will run back to point j (see above sketch). The following terms enter the heat balance due to runback, when the water runback rate is defined as R_w' ($lb/hr\text{-}ft^2$).

Latent heat of fusion when fraction n of the runback freezes.

$$q = nR_w'AL_f \tag{23}$$

Sensible heat delivered to skin when runback ice cools from $32^{\circ}F$ down to t_{se} ($t_{se} < 32^{\circ}F$).

$$q = R_w' AC_w(32 - t_{se}) \tag{24}$$

Sensible heat absorbed by runback as it is warmed from $t_{se_{j-1}}$ to $32^{\circ}F$ or t_{se}, whichever is higher.

$$q = R_w' AC_w(32 - t_{se_{j\pm1}})$$

or

$$R_w' AC_w(t_{se} - t_{se_{j\pm1}}) \tag{25}$$

whichever is greater.

Conduction - the temperature at a point j is influenced by conduction from points j-1 and points j+1.

Conduction from j-1 to j

$$q = kA_x(t_{se_{j-1}} - t_{se})/(S_{j-1} - S_j) \tag{26}$$

Conduction from j+1 to j

$$q = kA_x(t_{se_{j+1}} - t_{se})/(S_{j+1} - S_j) \tag{27}$$

In the conduction equations, the temperature gradient is approximated by finite differences.

Of the parameters mentioned above, those having the most significant effects are aerodynamic heating and the latent heats of fusion and vaporization. Aerodynamic heating tends to increase the equilibrium temperature at all times. The effect of the latent heat of fusion is to raise the surface temperature if it is below $32^{\circ}F$, while above $32^{\circ}F$ it has no effect. The

latent heat of vaporization tends, at all times, to lower the surface temperature. This is due to the evaporation of water off the surface as shown in equation (22).

The local water catch distribution for an arbitrary airfoil can be obtained analytically by the methods previously discussed. The external heat transfer coefficient distribution must be calculated by a different method in each of the three distinct regions: (1) stagnation region, (2) laminar flow region, and (3) turbulent region. In the stagnation region, the heat transfer coefficient is calculated by assuming that the flow is similar to flow normal to the axis of a cylinder. The Eckert Wedge Analogy is used for heat transfer calculations in the laminar region. In the turbulent region, the heat transfer coefficient is computed by a flat plate analogy. The above three techniques for calculating heat transfer coefficients are discussed in Reference 71.

4.3 ICE BUILDUP RATES

Water catch calculations, for a main rotor blade, during hover, were performed using an NACA 0012 airfoil with a 28-inch chord as shown in Figure 86. Calculations of impingement limits, water catch, and ice shapes were done for the "average" angle of attack of 4.6 degrees. (For a 20,000-pound vehicle, in hover, the angle of attack, as presented in Figure 87, is nearly constant along the entire blade.) The blade tangential velocity is shown in Figure 88 and varies linearly from 195 feet/second at the root to 660 feet/second at the tip.

The refinement of the airfoil description and establishment of valid flow field "grids" is quite sensitive to the "roughness" of the blade contour, having a direct effect on local water catch efficiency, β, air streamlines, and water droplet trajectories. The water droplet trajectories and, therefore, β are highly sensitive to the blade contours and tangencies. To avoid discontinuities of the water droplet trajectories, the blade contour is described by 52 sets of points (26 on each surface) defined to eight significant places, with the majority of the points concentrated in the forward 20 percent of the chord. The flow field calculation requires a definition of the local airfoil pressure coefficient distribution. Figure 89 shows the pressure coefficient, C_p, distribution along the upper and lower surfaces, for the main rotor blade at 4.6 degrees angle of attack. This is the C_p distribution associated with the data presented in Figures 90 through 99.

Water droplet trajectories and local water catch efficiency data have been generated for the hover condition, for the rotor blade root, tip, and a mid-span station for water droplets of 10-, 15-, 20-, and 40-micron diameters. The 40-micron-diameter droplets are used to determine the maximum water droplet impingement limits on the upper and lower blade surfaces, while the 20-micron drops are used to estimate the total water catch.

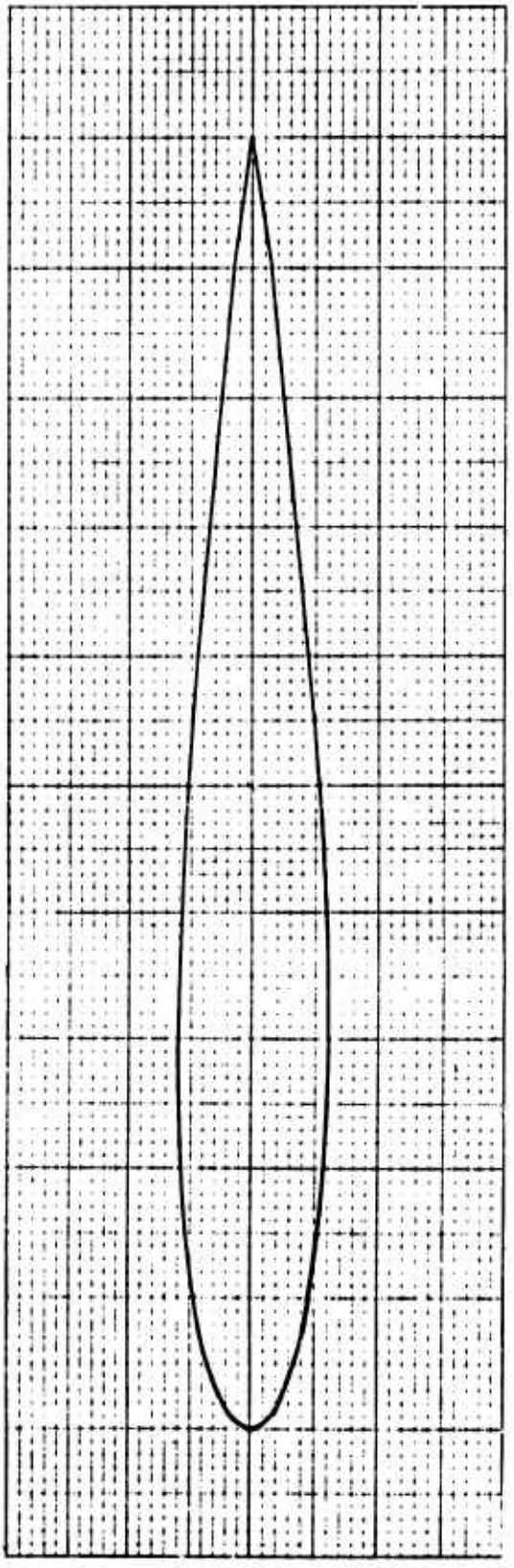

Figure 86. NACA 0012 Symmetrical Airfoil.

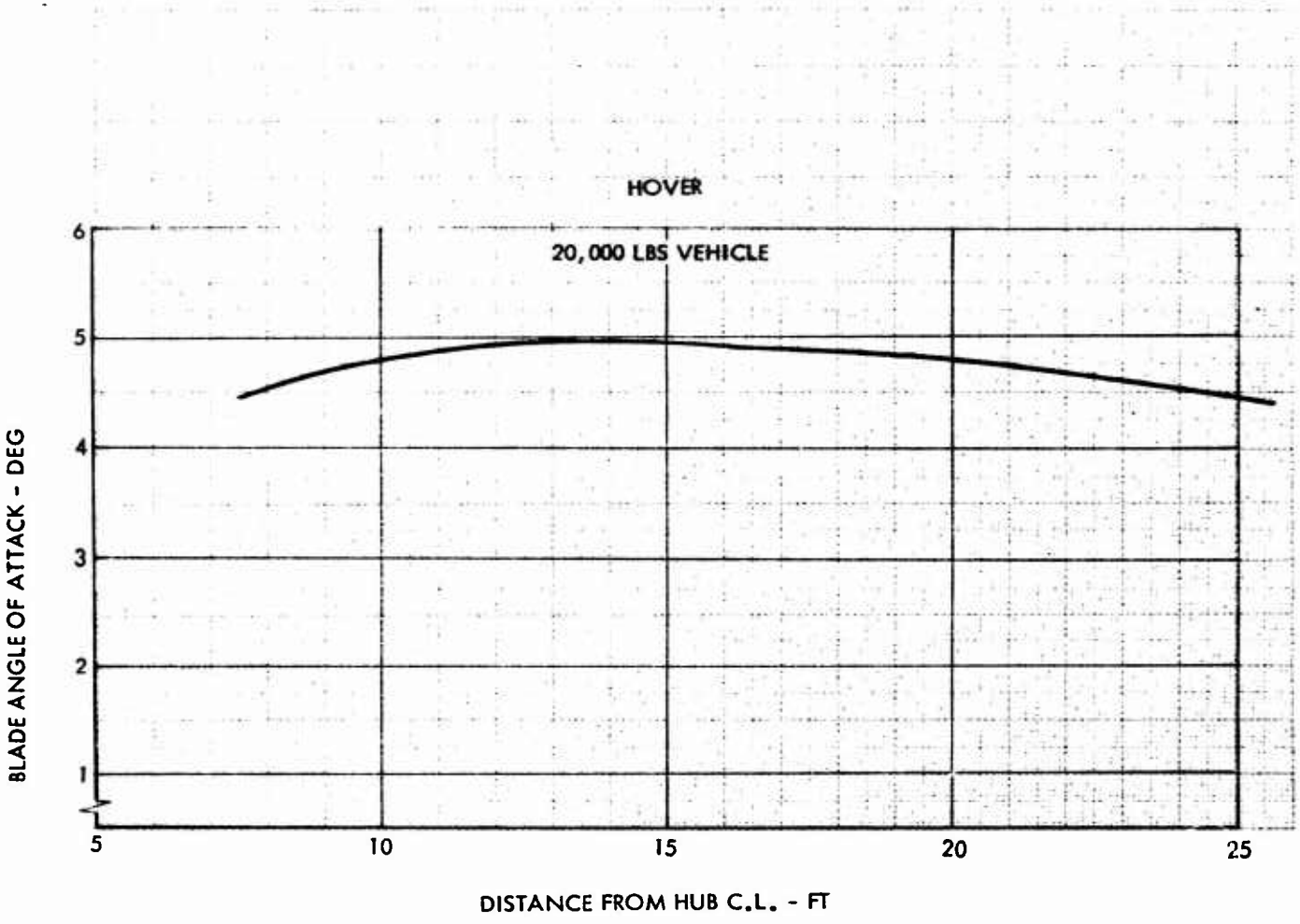

Figure 87. Angle of Attack vs. Blade Station.

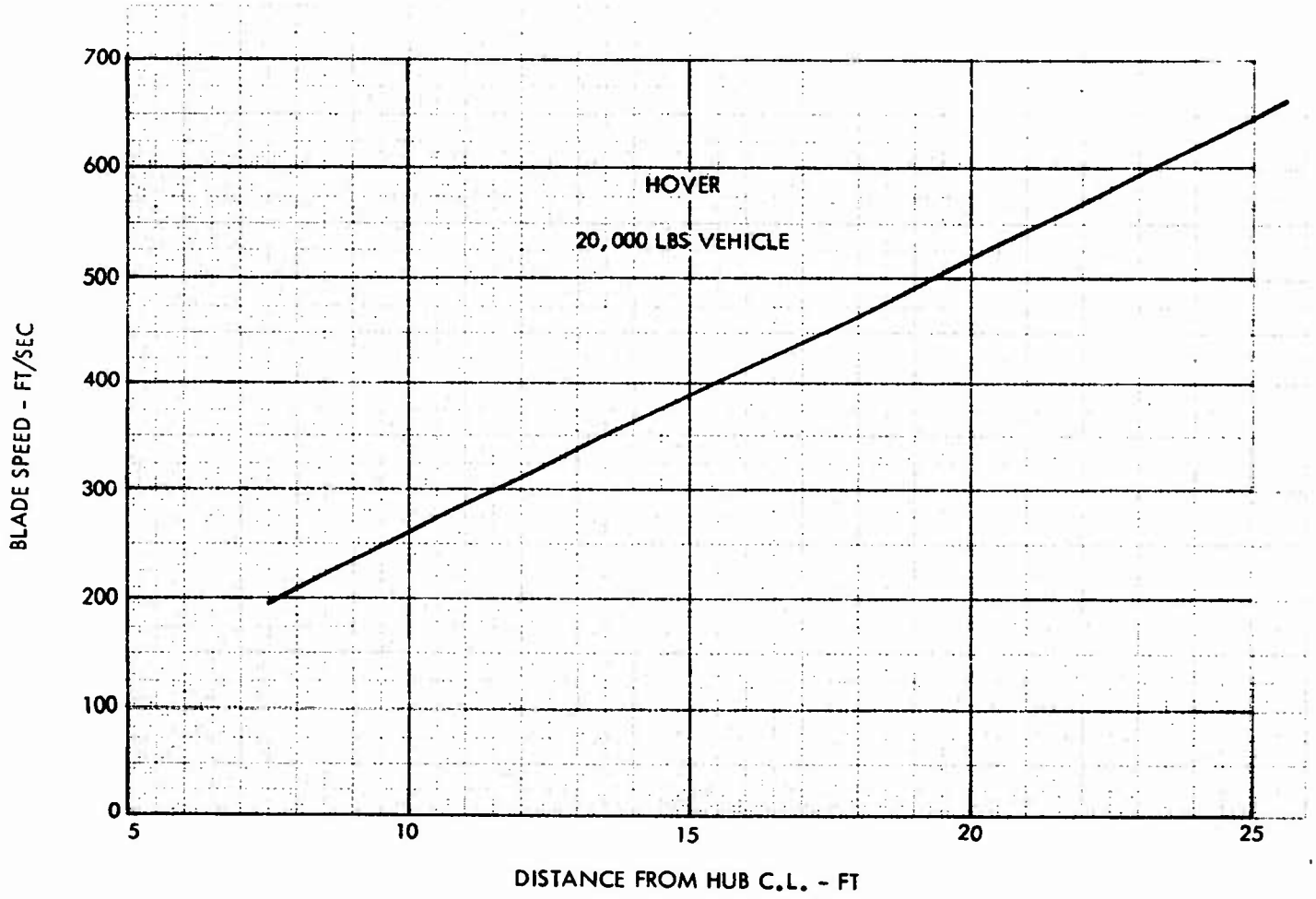

Figure 88. Blade Speed vs. Blade Station.

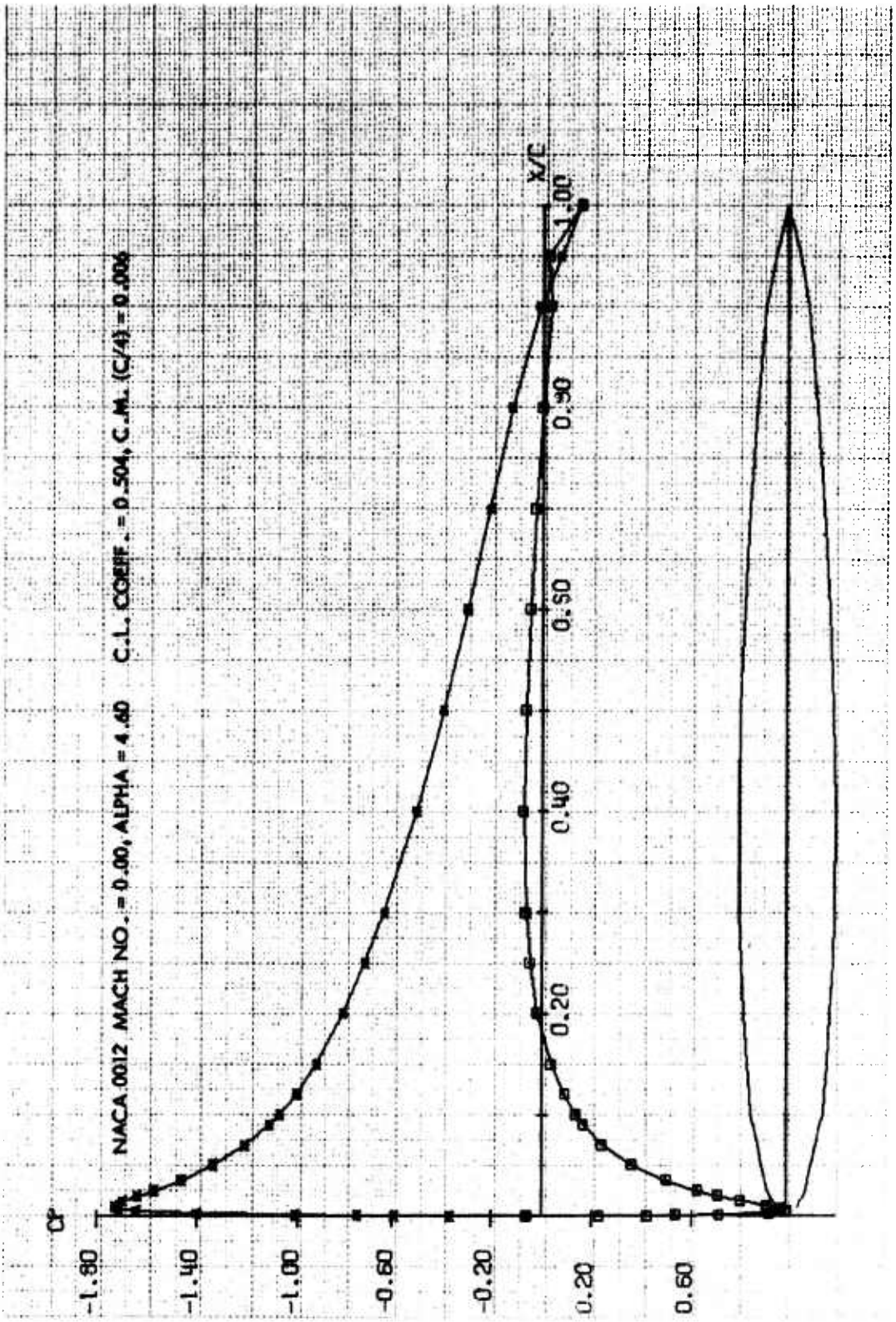

Figure 89. C_p Distribution, $\alpha = 4.6^0$.

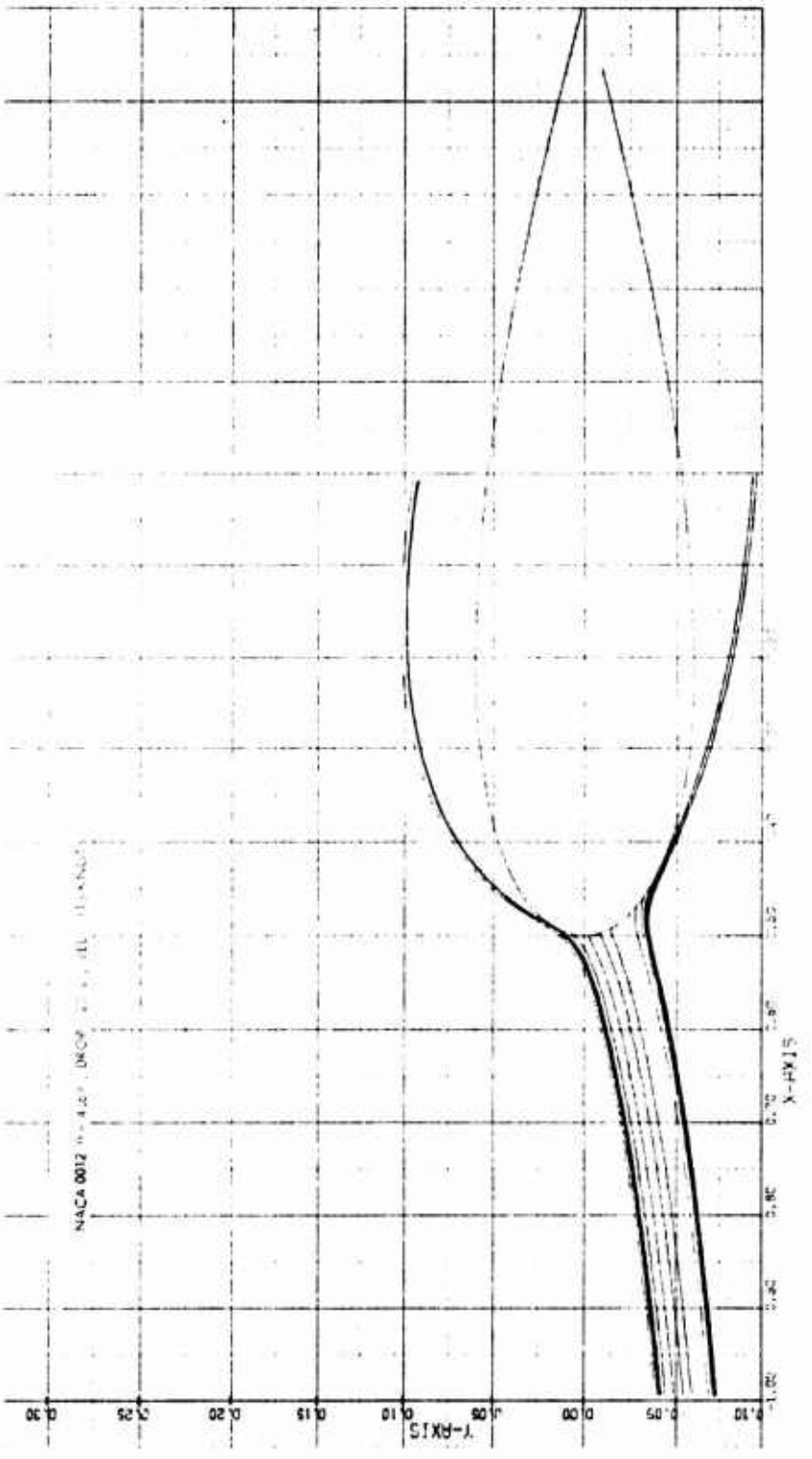

Figure 90. Water Droplet Trajectory - Root.

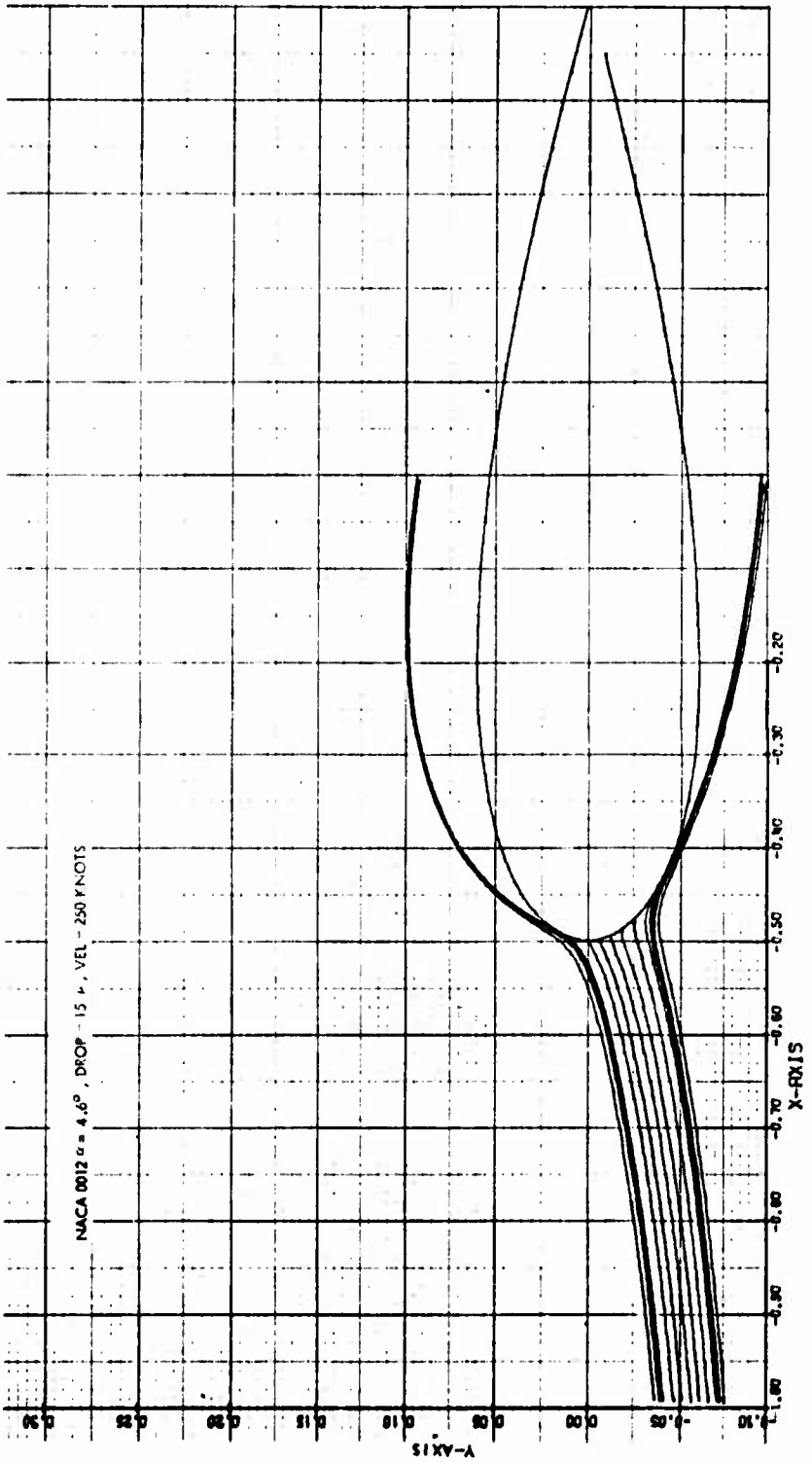

Figure 91. Water Droplet Trajectory - Mid-Span.

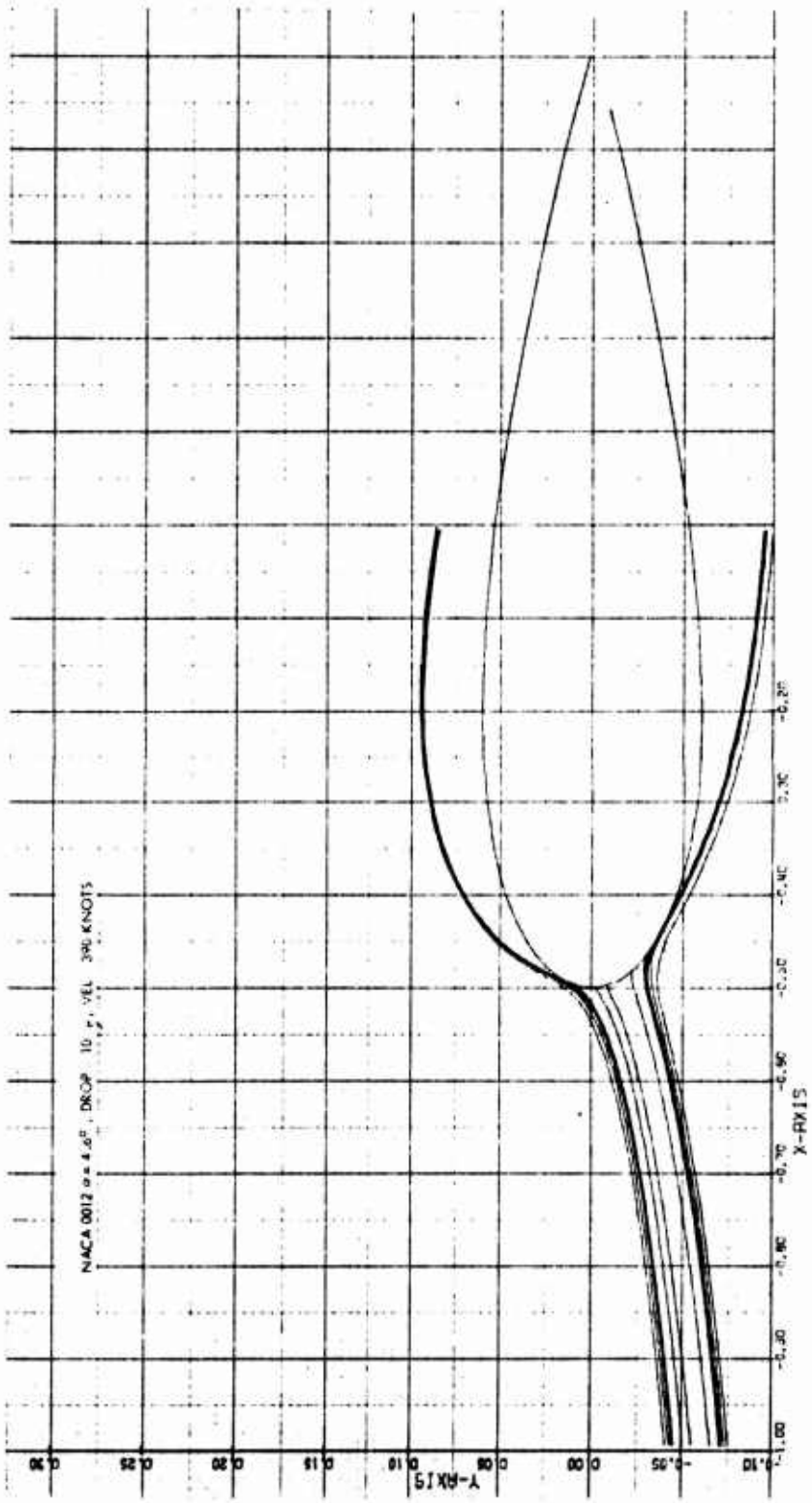

Figure 92. Water Droplet Trajectory - Tip.

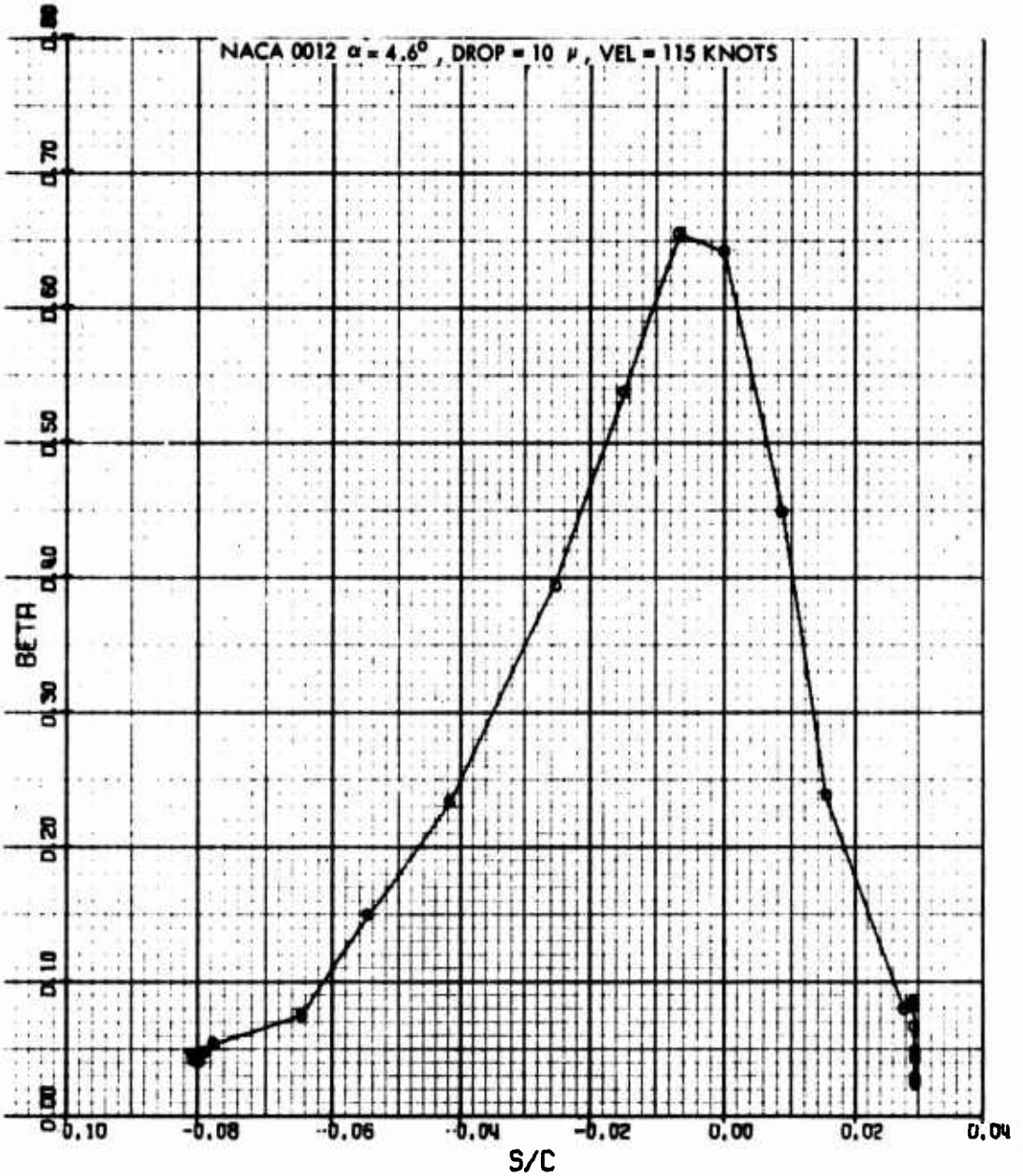

Figure 93. Water Catch Efficiency - Root.

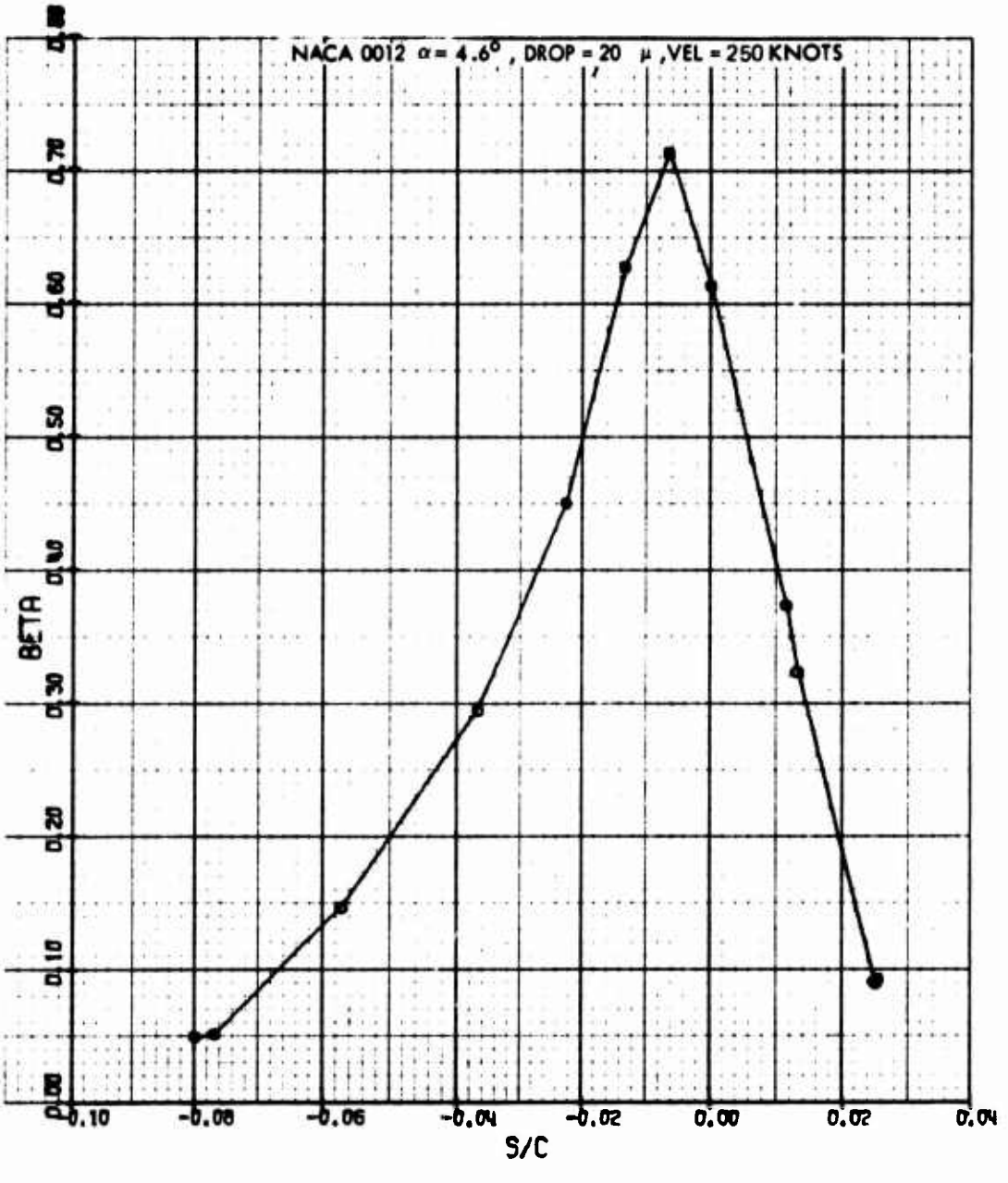

Figure 94. Water Catch Efficiency - Mid-Span.

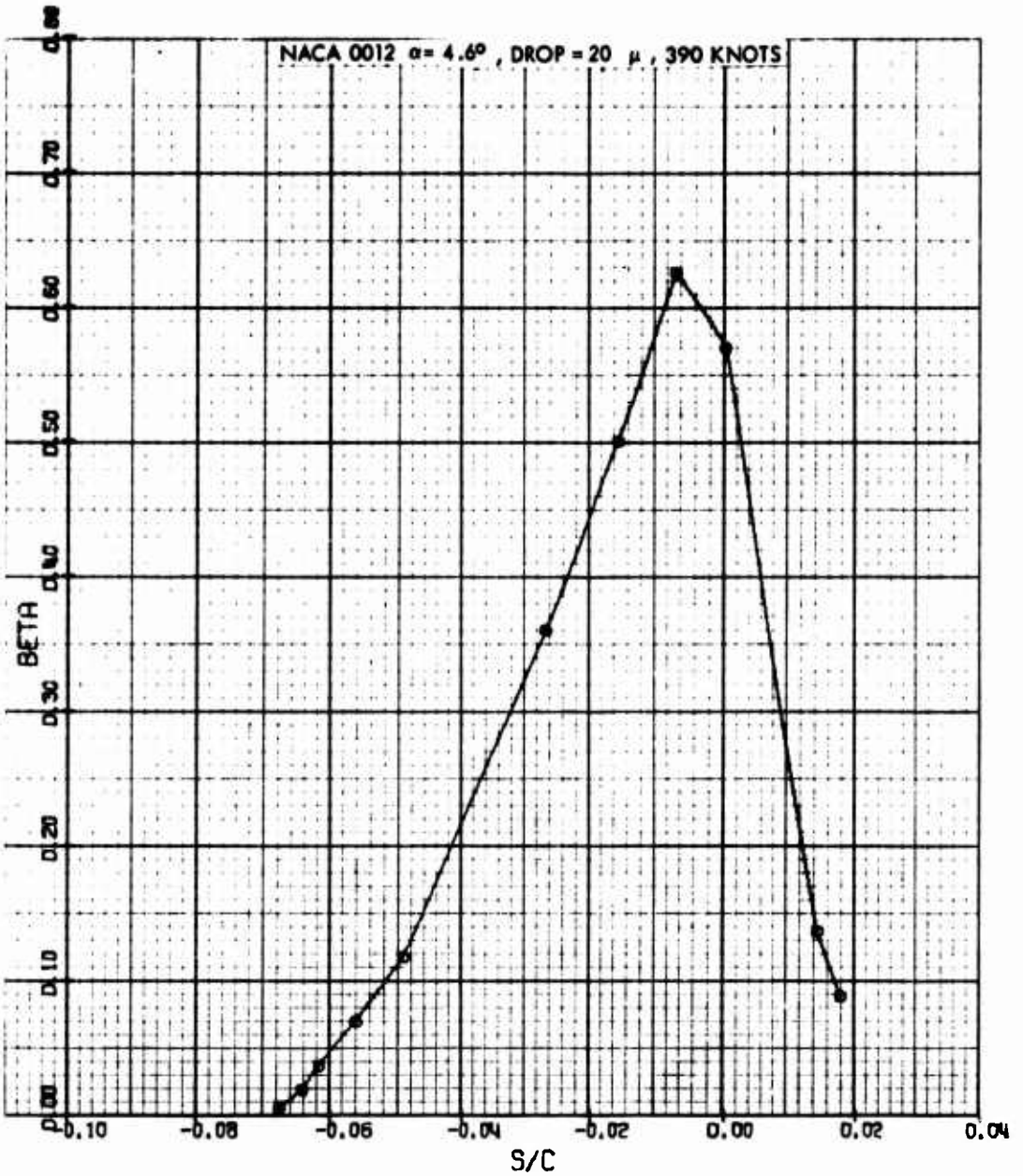

Figure 95. Water Catch Efficiency - Tip.

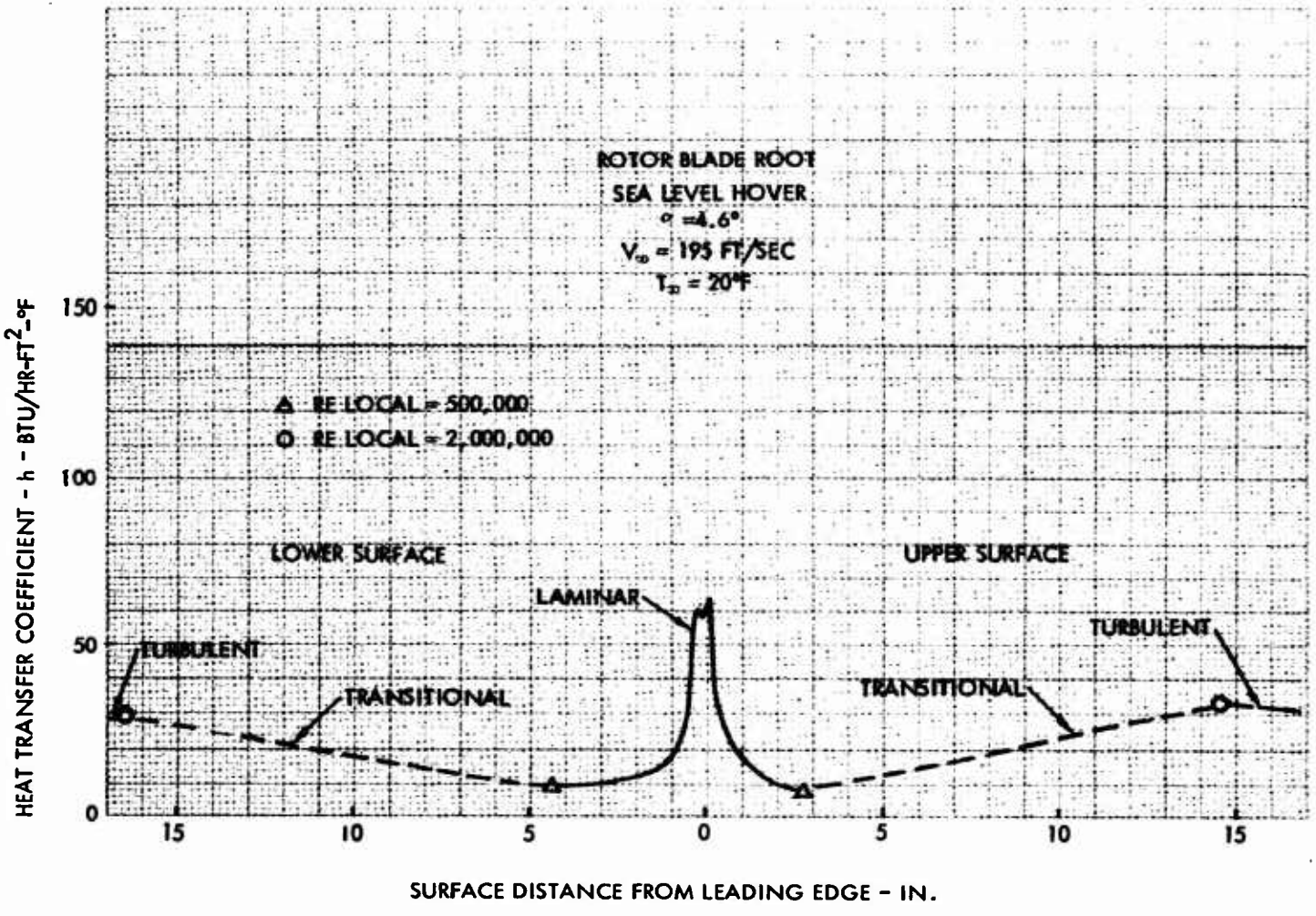

Figure 96. Heat Transfer Coefficient Distribution - Root.

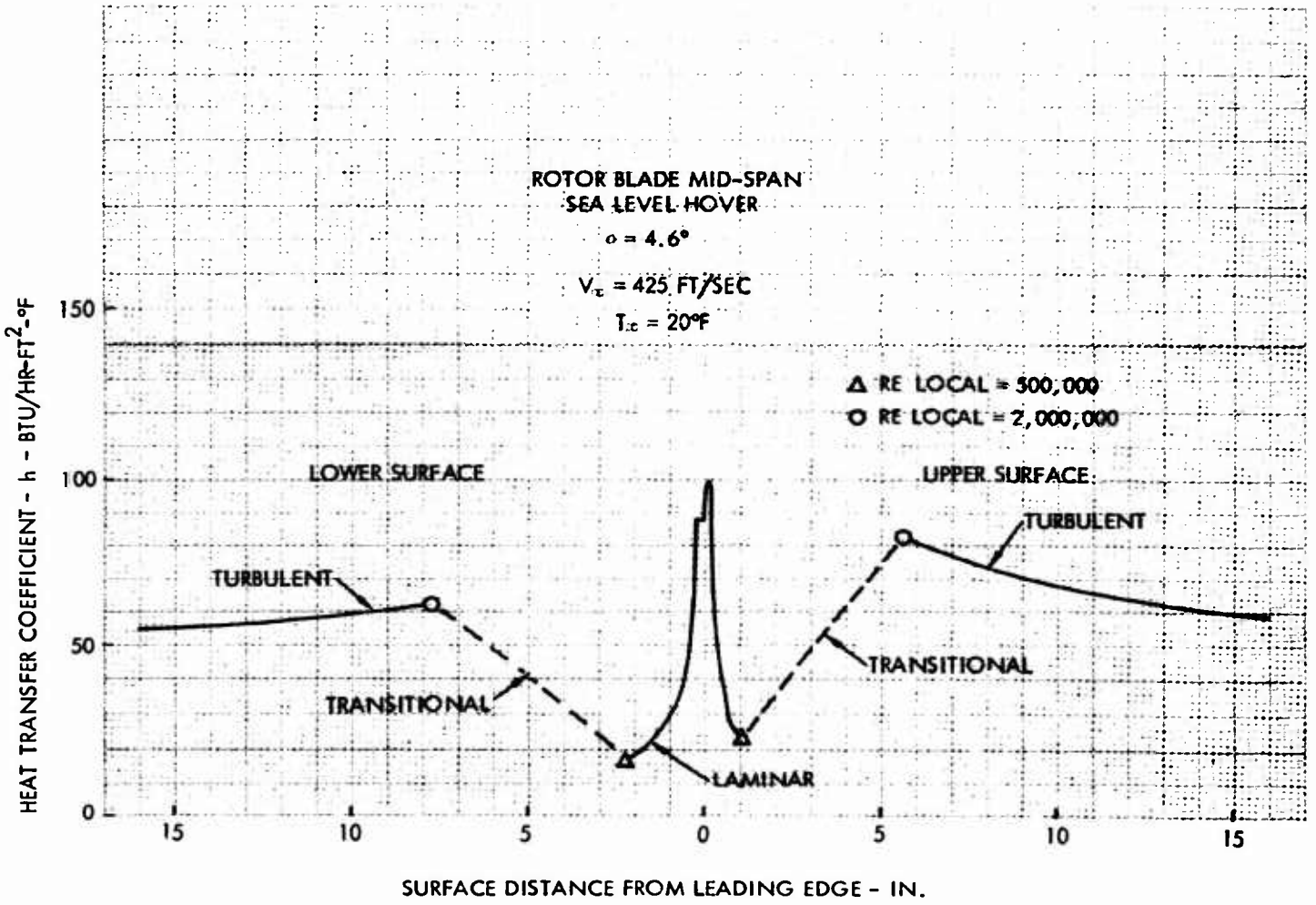

Figure 97. Heat Transfer Coefficient Distribution - Mid-Span.

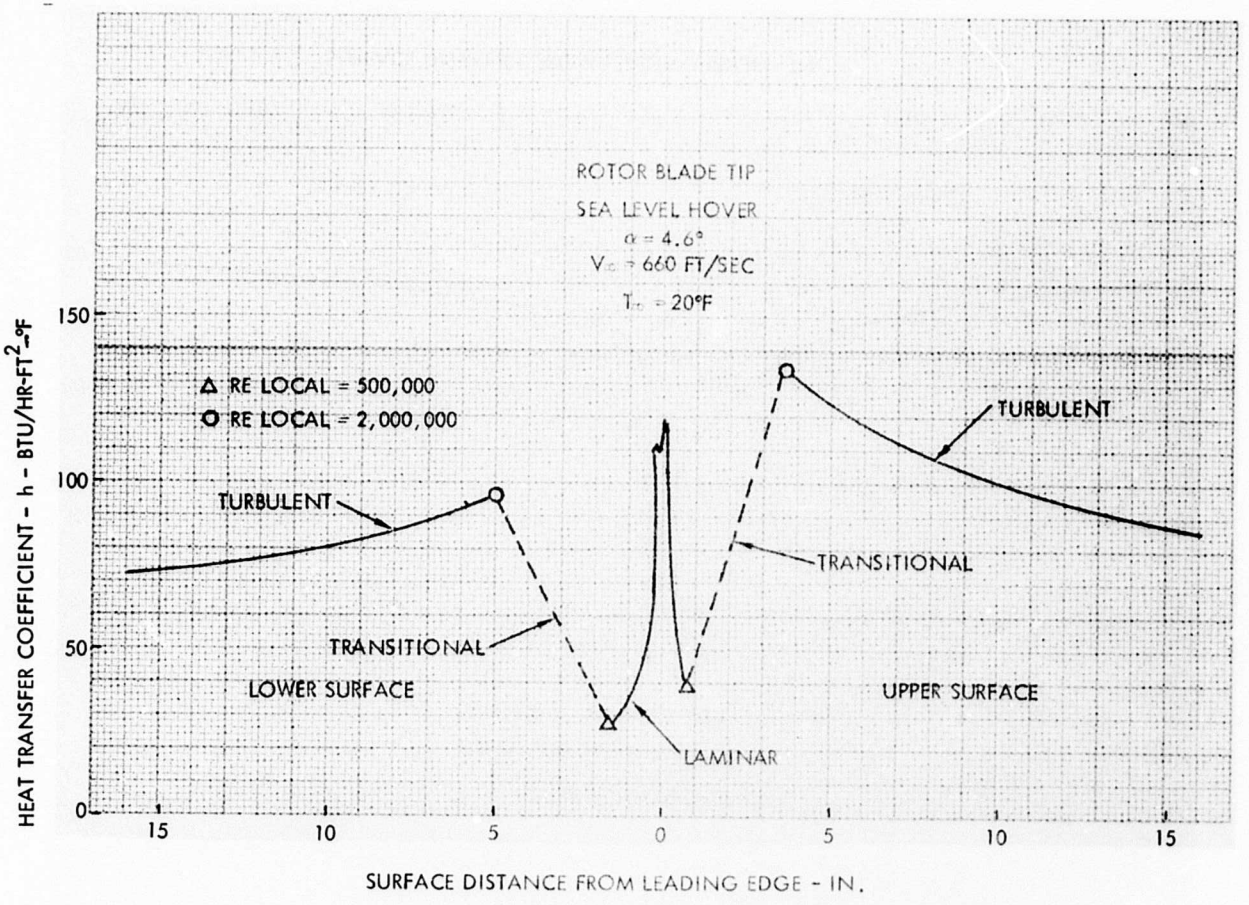

Figure 98. Heat Transfer Coefficient Distribution - Tip.

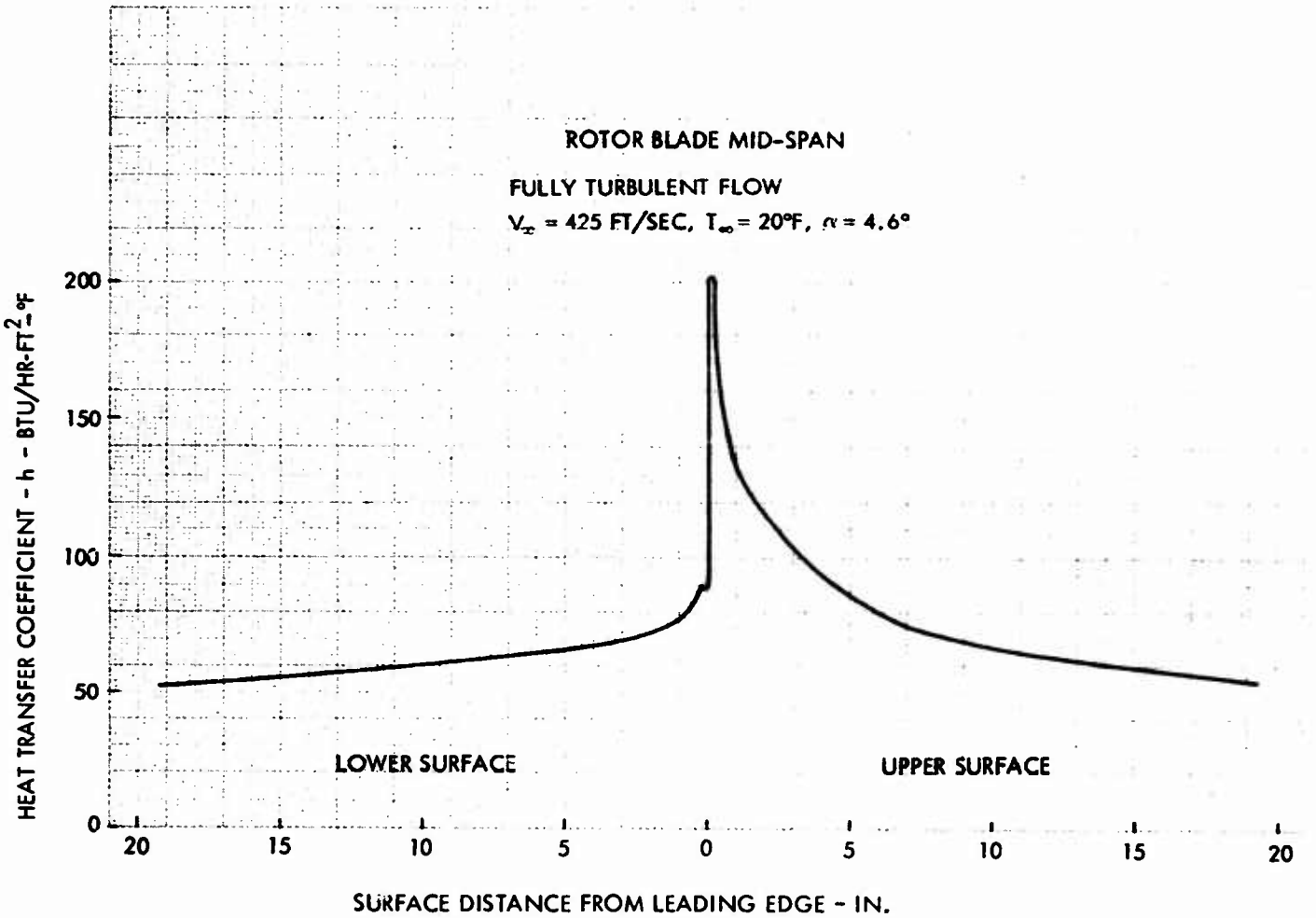

Figure 99. Mid-Span Heat Transfer Coefficient Distribution.

Table XXI tabulates the upper and lower impingement limits for all main rotor cases. Figures 90-92 show typical water droplet trajectories generated for the main rotor, while Figures 93-95 show their respective local water catch efficiencies. At positive angles of attack, more water impinges and is collected on the lower surface of the blade increasingly.

TABLE XXI. MAIN ROTOR IMPINGEMENT LIMITS

Blade Location	Droplet Diameter (Microns)	Upper Impingement Limit S/C	Lower Impingement Limit S/C
ROOT	10	+ 0.005	- 0.058
	15	+ 0.012	- 0.074
	20	+ 0.029	- 0.080
	40	+ 0.053	- 0.144
MID-SPAN	10	+ 0.012	- 0.066
	15	+ 0.025	- 0.080
	20	+ 0.039	- 0.110
	40	+ 0.057	- 0.183
TIP	10	+ 0.018	- 0.068
	15	+ 0.025	- 0.092
	20	+ 0.032	- 0.115
	40	+ 0.062	- 0.178

Local heat transfer coefficients over the upper and lower surfaces of the rotor blade have also been determined for the three rotor stations. Figures 96 - 98 show the heat transfer coefficient distribution at the rotor root, mid-span, and tip stations, respectively.

Laminar flow normally occurs for local Reynolds numbers up to 500,000, while the flow is fully turbulent at Reynolds numbers above 2,000,000; flow between these values is transitional. Laminar heat transfer coefficients are computed using the technique of Appendix C of Reference 72. This method assumes that the laminar heat transfer coefficient at any point on an airfoil is the same as that on a wedge at the same distance from the stagnation point, provided that the stream velocity and its gradient on the wedge and on the airfoil are the same at the given location. Turbulent heat transfer coefficients are calculated from flat plate theory

using local velocity which is a function of the local pressure coefficient, C_p. Stagnation point heat transfer coefficients are calculated using cylinder theory. Heat transfer coefficients are undetermined in transitional flow. Figure 99 shows the heat transfer coefficient distribution at mid-span, assuming fully turbulent flow, and compares directly to Figure 97.

For unheated surfaces with ice, boundary layer transition is uncertain, and a comparison has been made to determine the effect of a full turbulent flow from the leading edge on ice shapes and freezing rates.

Using the heat transfer coefficient and C_p distributions, as well as impingement limit and local water catch data, initial ice shapes and freezing rates are calculated for the sea-level hover condition at the rotor blade root, mid-span, and tip. Figures 100, 101, and 102 indicate the initial ice shapes and freezing rate for the root, mid-span, and tip sections, respectively. Four ambient temperatures (10°, 15°, 20° and 25°F) are used at each section to determine the variation in temperature effect along the span. Freezing rates and ice shapes are calculated using previously computed water catch rates for 20-micron-diameter water droplets and the maximum impingement limits associated with 40-micron-diameter droplets.

The shape of the ice formation is influenced by location on the rotor blade span, ambient temperature, and external heat transfer coefficient over the blade. At the root (Figure 100), at lower temperatures (10° and 15°F), the ice freezes in a single spike formation typically characteristic of rime ice shapes. As the ambient temperature rises (i.e., 20°F and higher), the blade surface temperature also rises, and runback and refreezing occur along the surface of the blade.

Figure 101 shows the mid-span ice shapes and indicates a definite change in ice shape to a much more "turbulent," almost triple-horn form. At 10°F, the ice shape on the lower surface strongly resembles the heat transfer coefficient distribution, while on the upper surface the catch is limited to about 8 inches. As the ambient temperature rises, the blade surface temperature also rises, and runback and refreezing occur on the upper surface. The freezing patterns at 15° and 20°F are almost identical to the heat transfer coefficient pattern and show extensive runback. As the ambient temperature continues to rise, more ice is melted and less remains frozen, until at 25°F only a small amount of ice accumulates on the first 2 inches of the lower surface.

At the blade tip, the higher speeds of the advancing blade result in both higher heat transfer coefficients and warmer skin temperatures. These two effects combine to reduce the amount of ice accumulation on the blade. Figure 102 shows the ice pattern at the tip. At 10°F there is a thin layer of almost streamline shape along the airfoil, with little or no ice accumulating above 15°F.

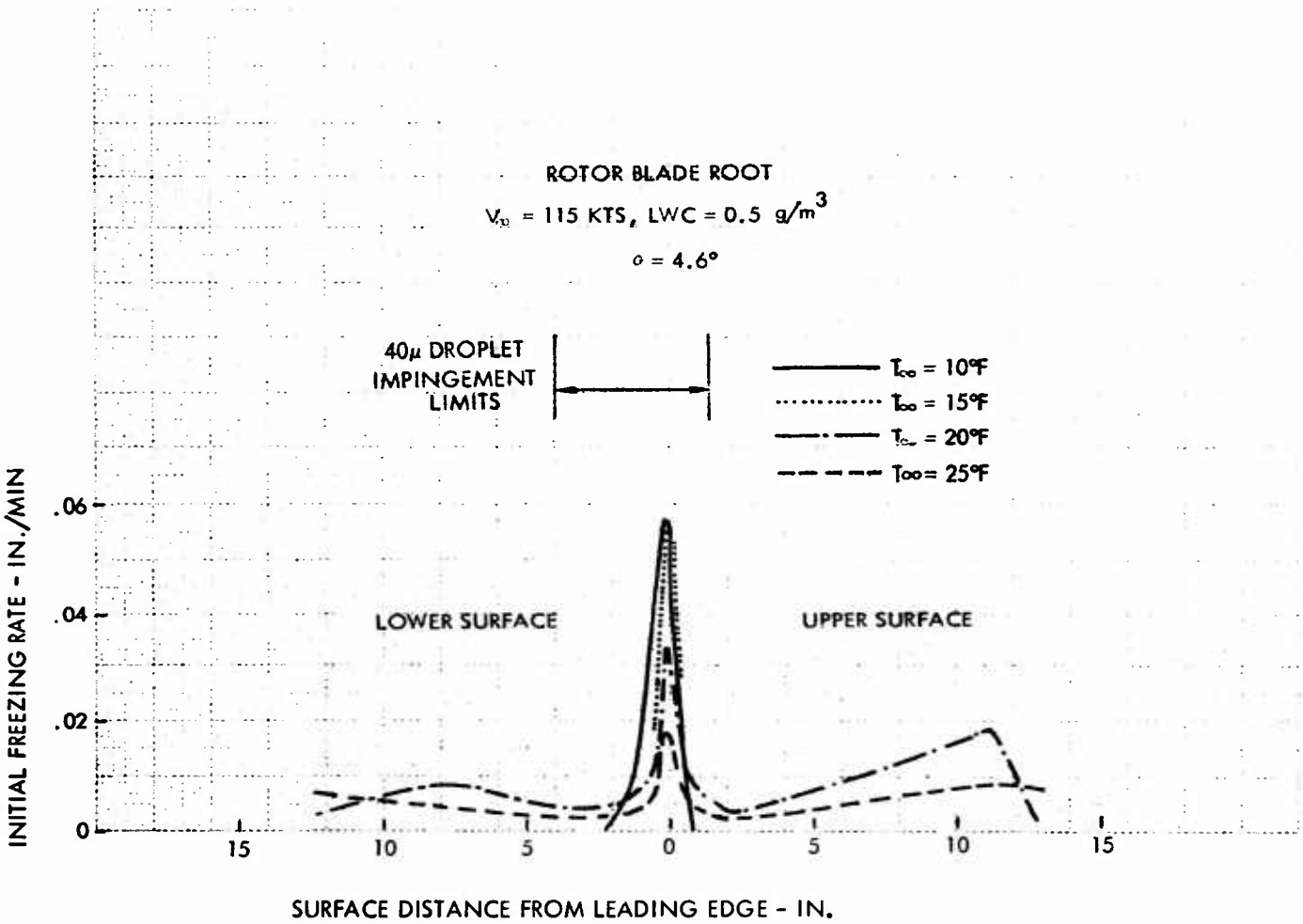

Figure 100. Rotor Blade Root Initial Freezing Rate.

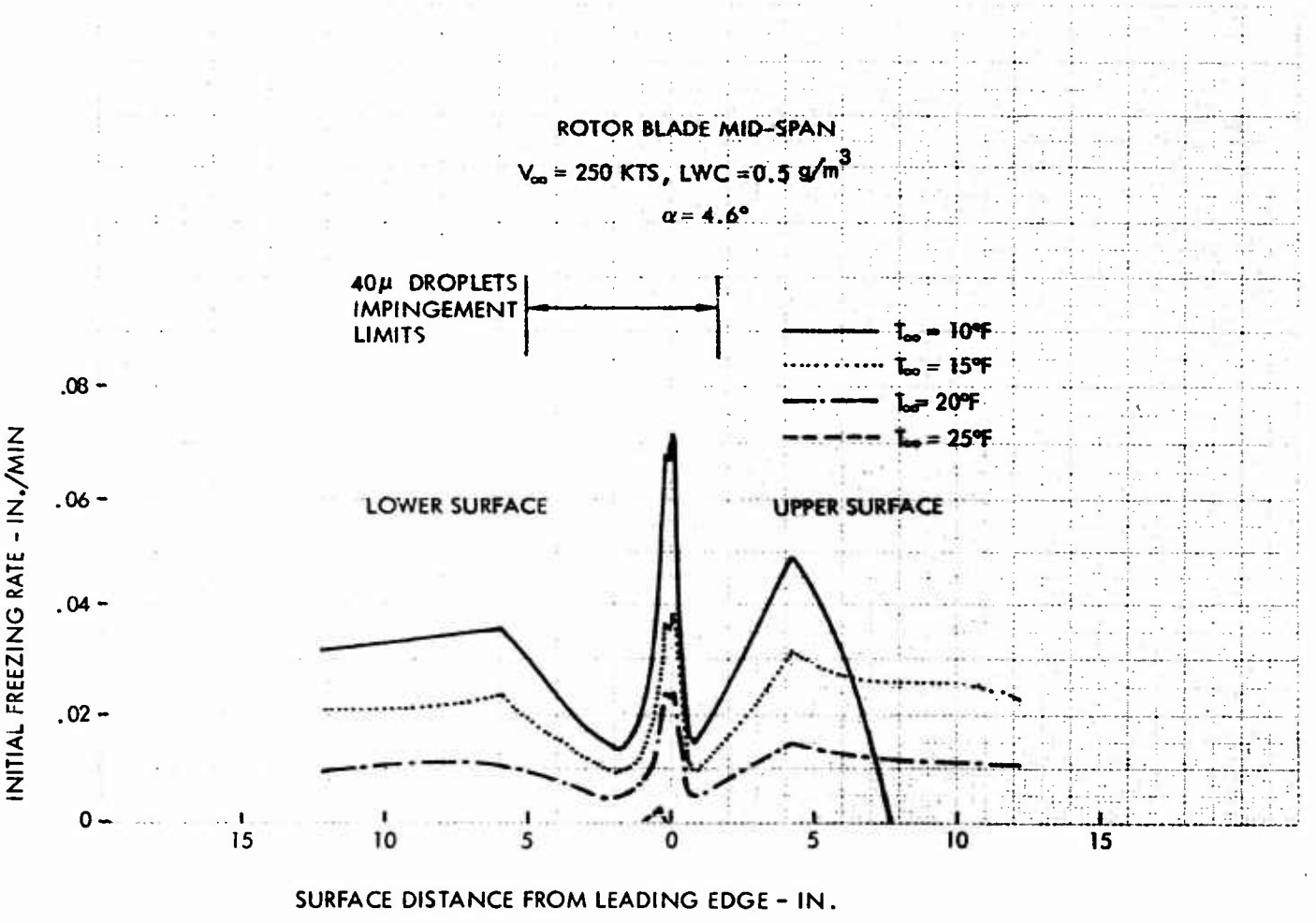

Figure 101. Rotor Blade Mid-Span Initial Freezing Rate.

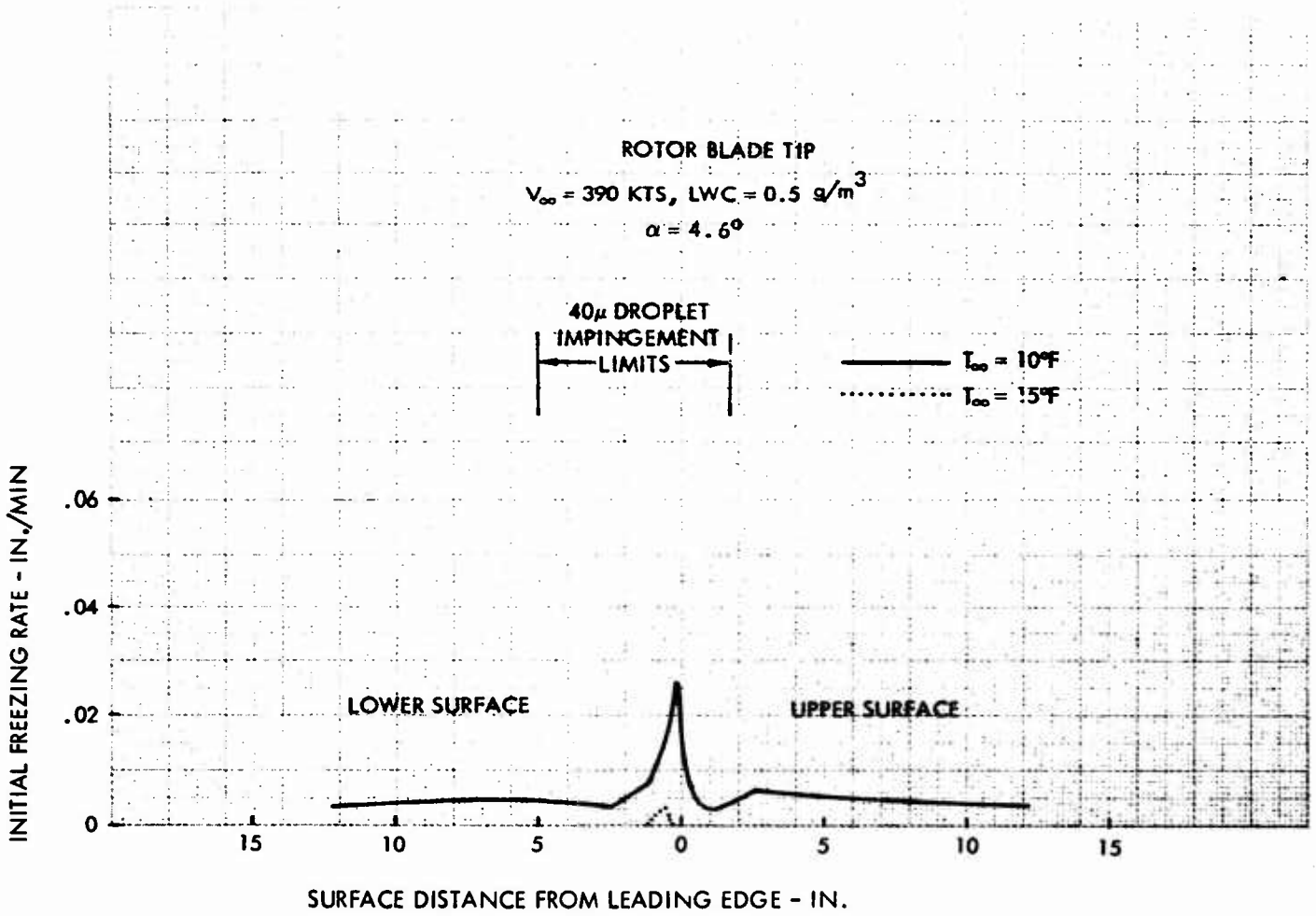

Figure 102. Rotor Blade Tip Initial Freezing Rate.

To evaluate the effect of laminar versus turbulent airflow on the shape of the ice at the mid-span position, Figure 99 was generated based upon all turbulent flow over the blade instead of laminar flow up to a local Reynolds number of 500,000 and then transition to turbulent flow at a local Reynolds number of 2,000,000. Figure 103 shows the mid-span ice shapes for fully turbulent flow. At 10°F, the double-horn shape is prominent, indicating large disruptions in the airflow pattern around the blade and large drag increments. At 15°F, runback and refreezing occur on the lower surface and the double-horn shape, while not so prominent, shifts to the very front of the upper surface. By 20°F, runback has become dominant and the freezing pattern closely resembles that of the turbulent heat transfer coefficient distribution. At 25°F, the skin temperature is high enough that there is no refreezing along the surface.

The pattern indicated by Figures 100-103 clearly show that runback and refreezing are significant and that, under most instances, ice will accumulate over the forward 40 percent of the blade. The thickness of the accumulation aft of the impingement limits, however, does not appear to be severe enough to cause any problems.

One of the significant distinctions between the main and tail rotor is that, at hover, there is a large change in tail rotor angle of attack (α) as blade station changes. Figure 104 shows the angle of attack of the tail rotor versus blade station. As the percentage of radius increases the blade angle decreases over 50 percent. Using this information, pressure coefficient distributions over the tail rotor blade were generated for angles of attack of 11.7, 8.9, and 5.1, corresponding to the root, mid-span, and tip sections, respectively. Figures 105, 106, and 107 show the pressure coefficient distribution for these stations. These data were generated for an NACA 0012 airfoil with a 14-inch chord (one-half the size of main rotor) and a radius of 5 feet. These data were also used to calculate the heat transfer coefficients along the blade surface. Due to the location of the tail rotor and the considerable influence upon it by both main rotor downwash and engine exhaust gas impingement, only fully turbulent flow was assumed for the heat transfer coefficients. Heat transfer coefficients for the three tail rotor locations are shown in Figures 108-110.

Water droplet trajectory and local water catch efficiency curves were generated on the tail rotor for the three blade stations and four water droplet diameters. Table XXII tabulates the inboard and outboard impingement limits for the tail rotor cases. Tail rotor water droplet trajectory runs are similar to those presented for the main rotor and, thus, are not presented.

Figures 111-113 show typical water catch efficiencies at the three tail rotor stations.

The initial ice shape and freezing rates at the three blade locations are shown in Figures 114-116. Figure 115 shows these data for the mid-span

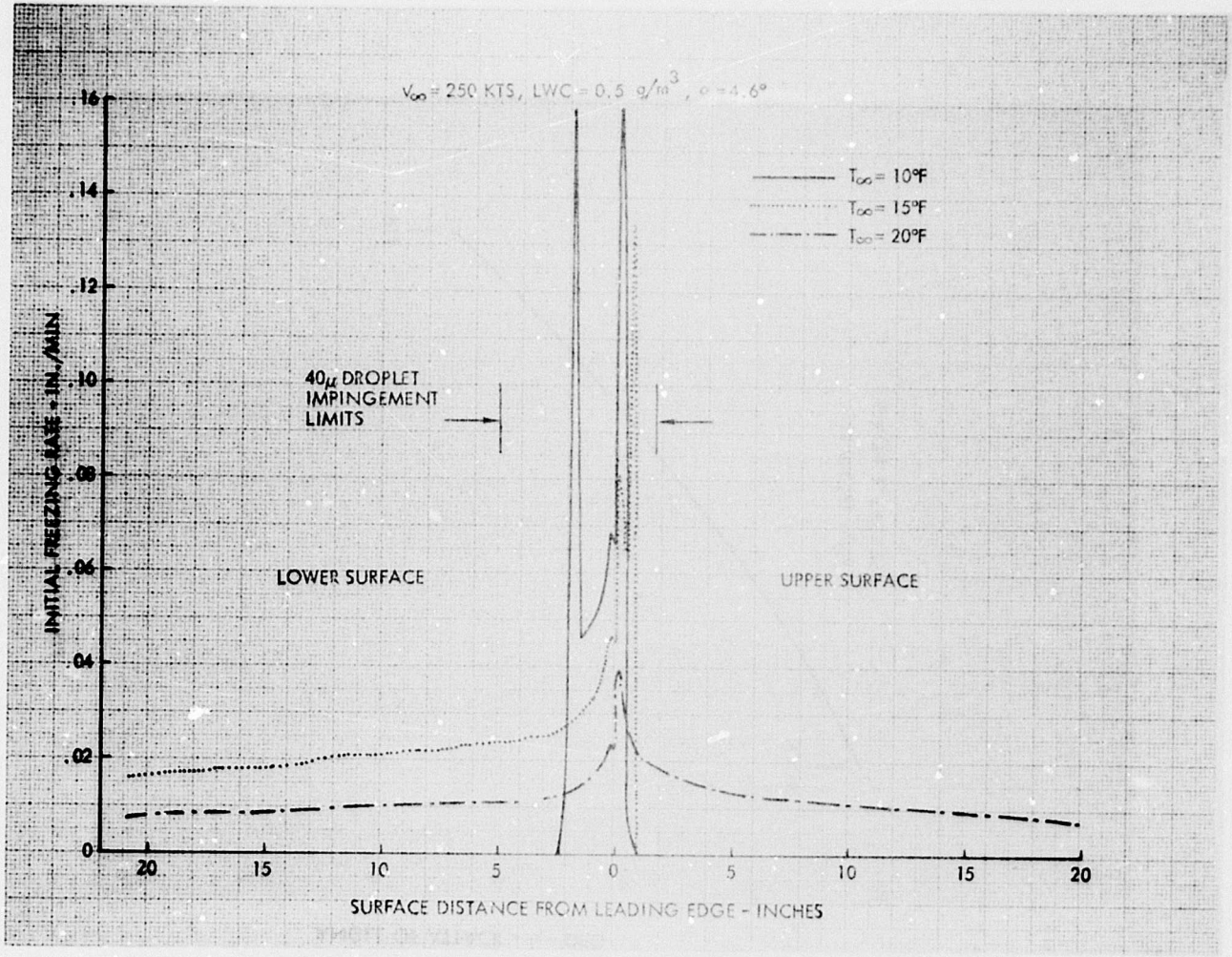

Figure 103. Rotor Blade Mid-Span Initial Freezing Rates - Fully Turbulent Flow.

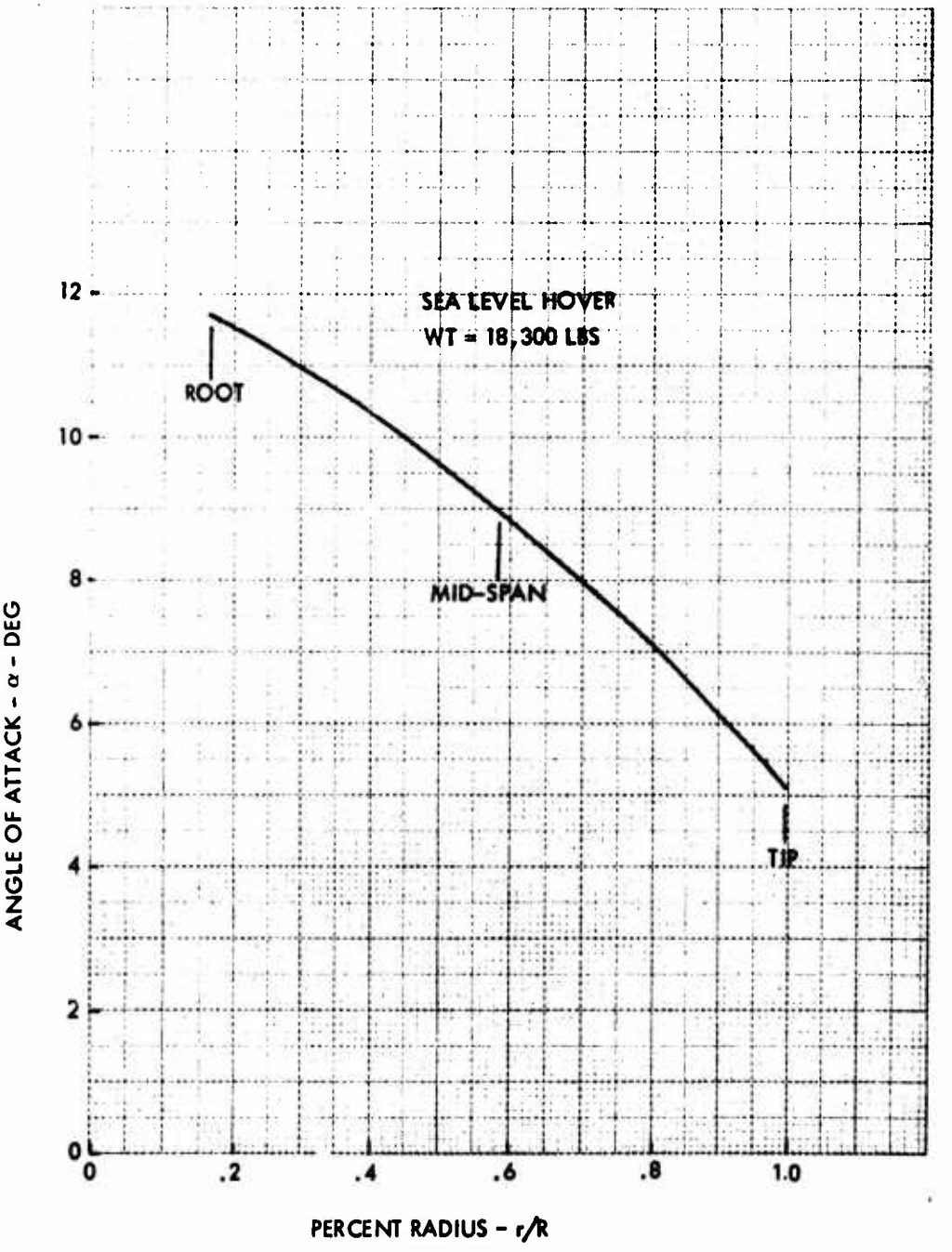

Figure 104. Tail Rotor "α" Distribution.

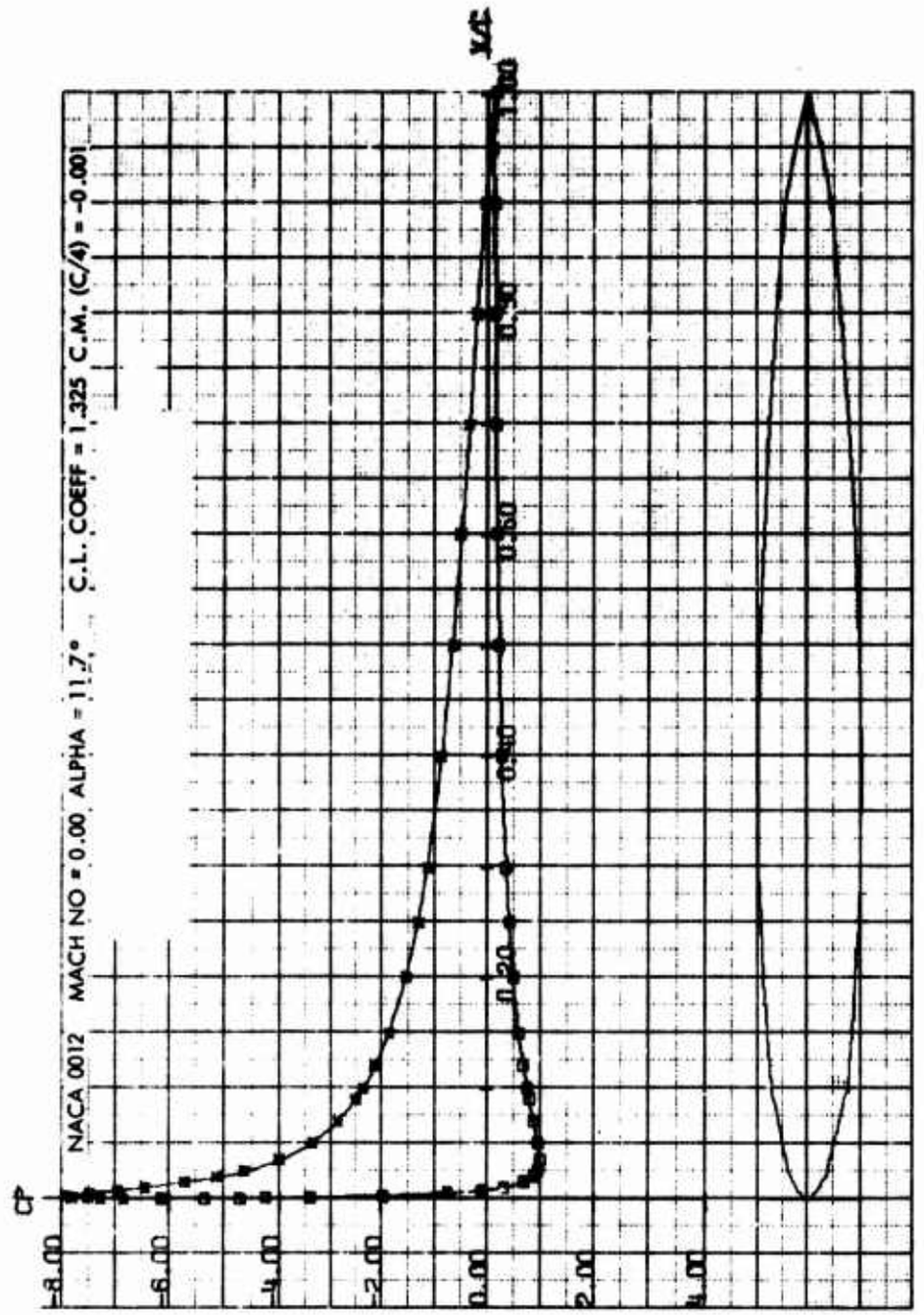

Figure 105. C_p Distribution, $\alpha = 11.7^{\circ}$.

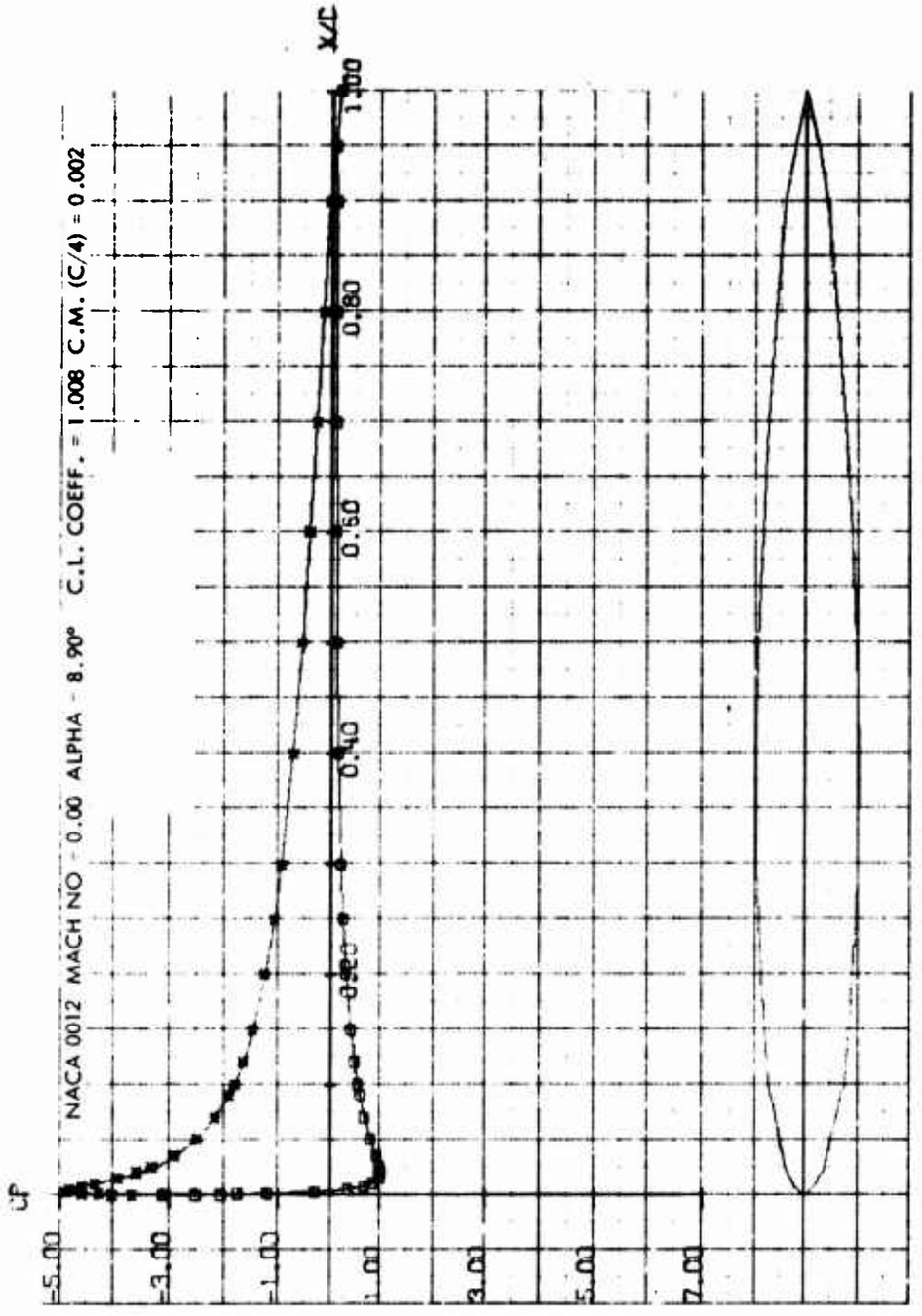

Figure 106. C_p Distribution, $\alpha = 8.9^\circ$.

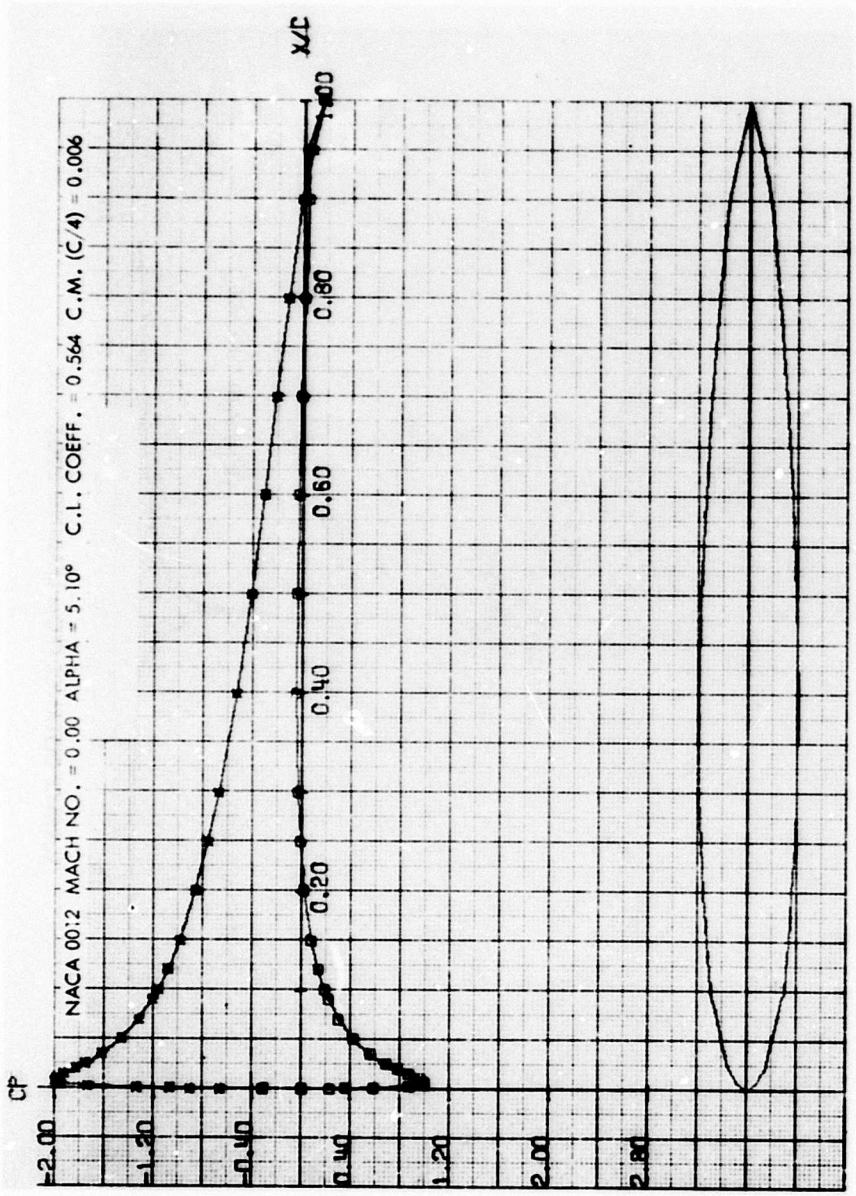

Figure 107. C_p Distribution, $\alpha = 5.1°$.

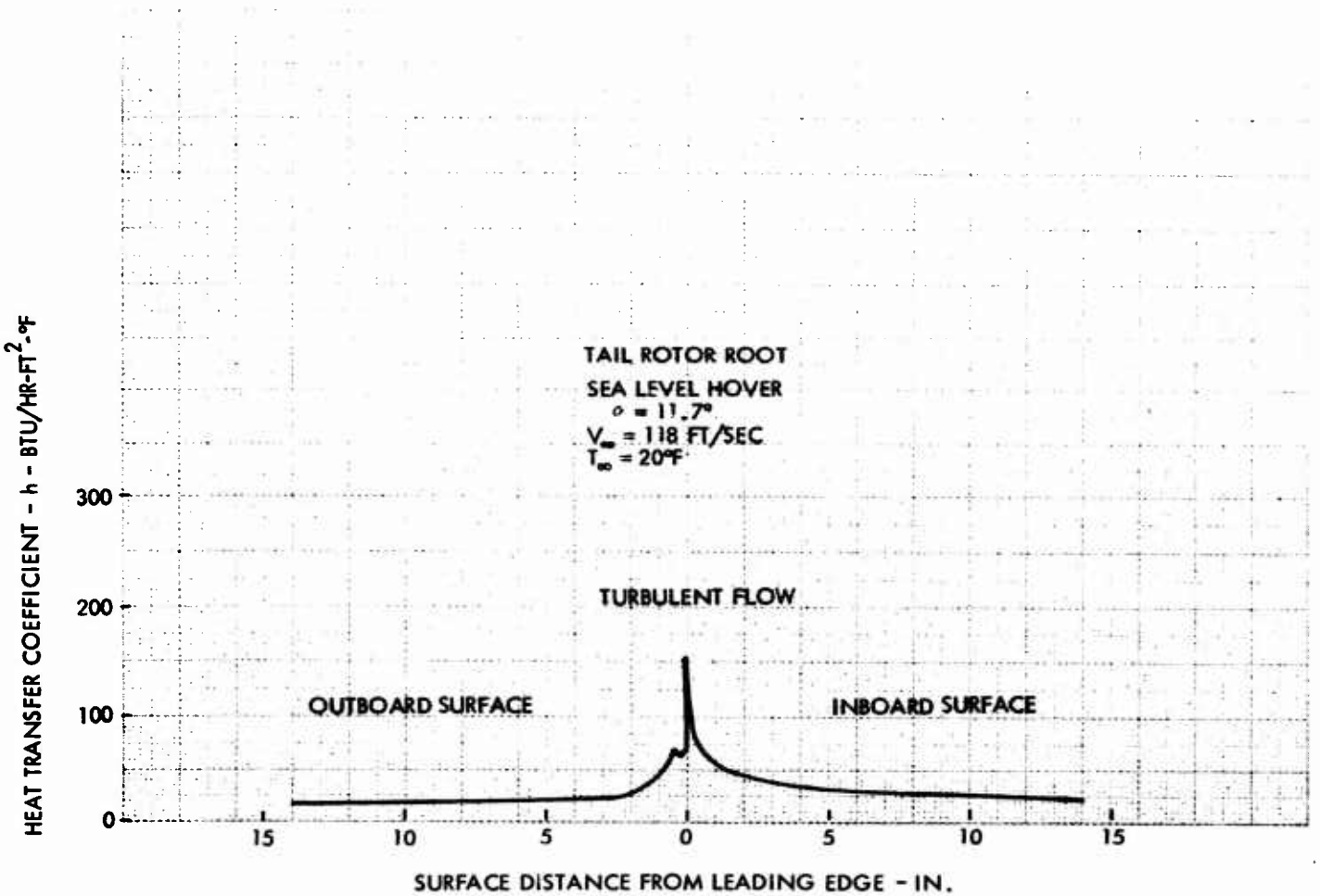

Figure 108. Tail Heat Transfer Coefficient Distribution.

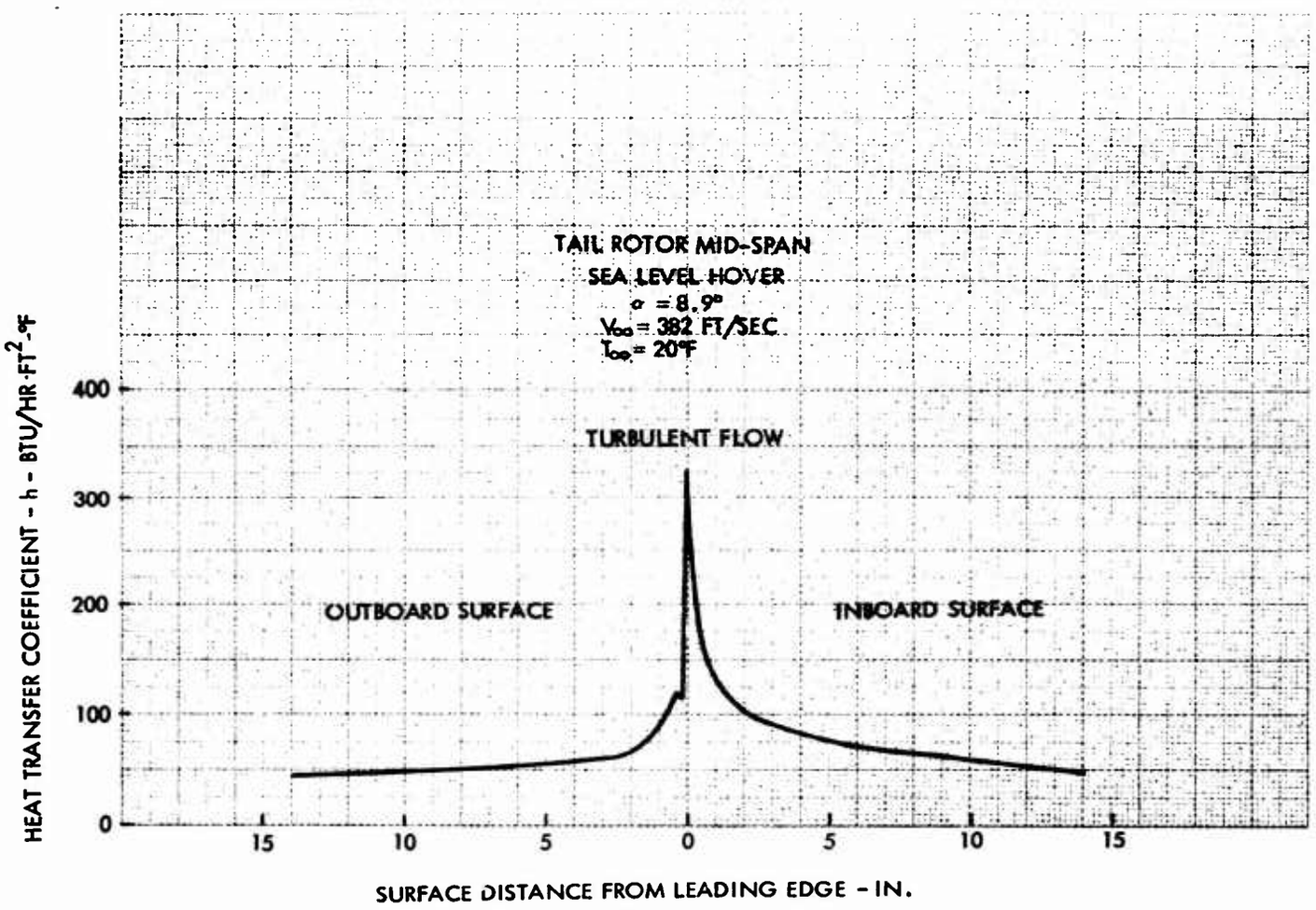

Figure 109. Tail Heat Transfer Ccefficient Distribution.

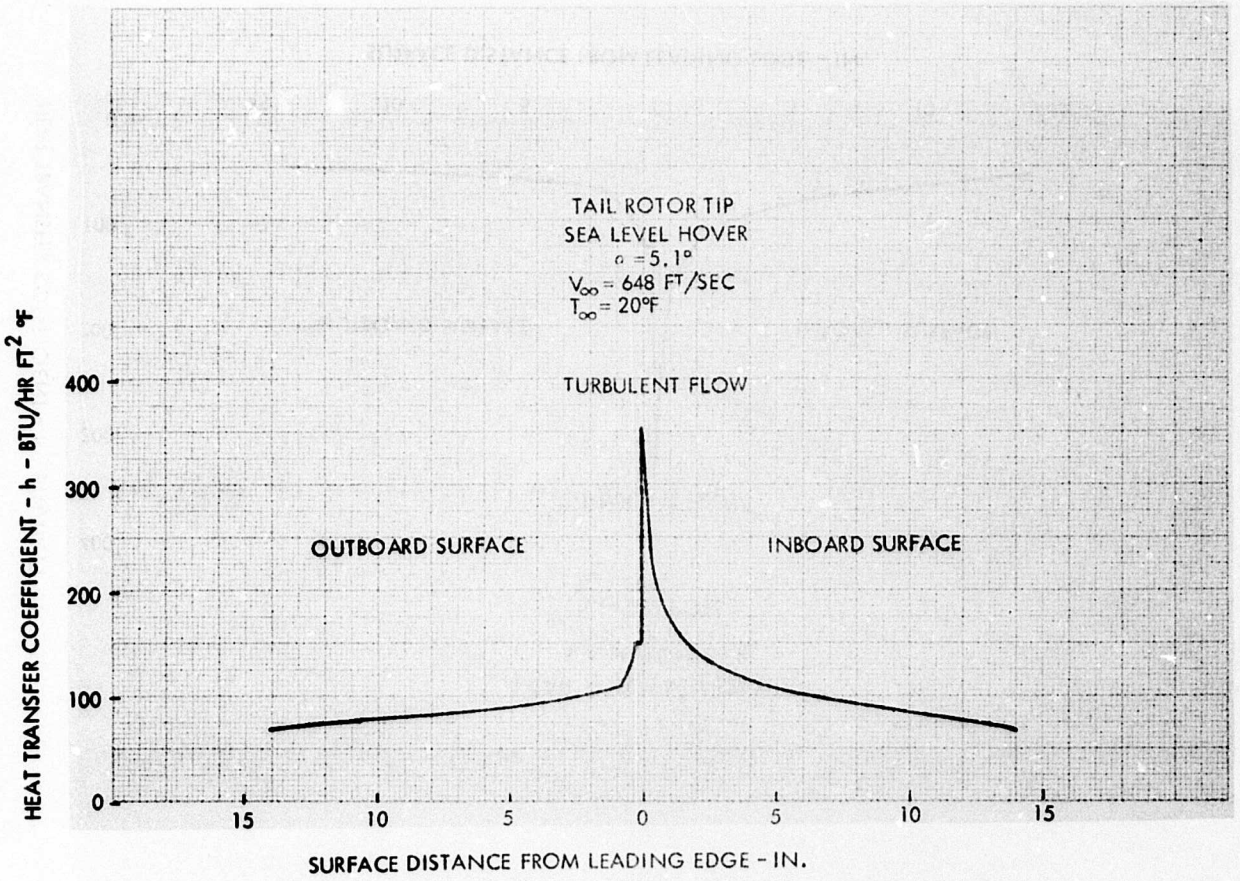

Figure 110. Tail Heat Transfer Coefficient Distribution.

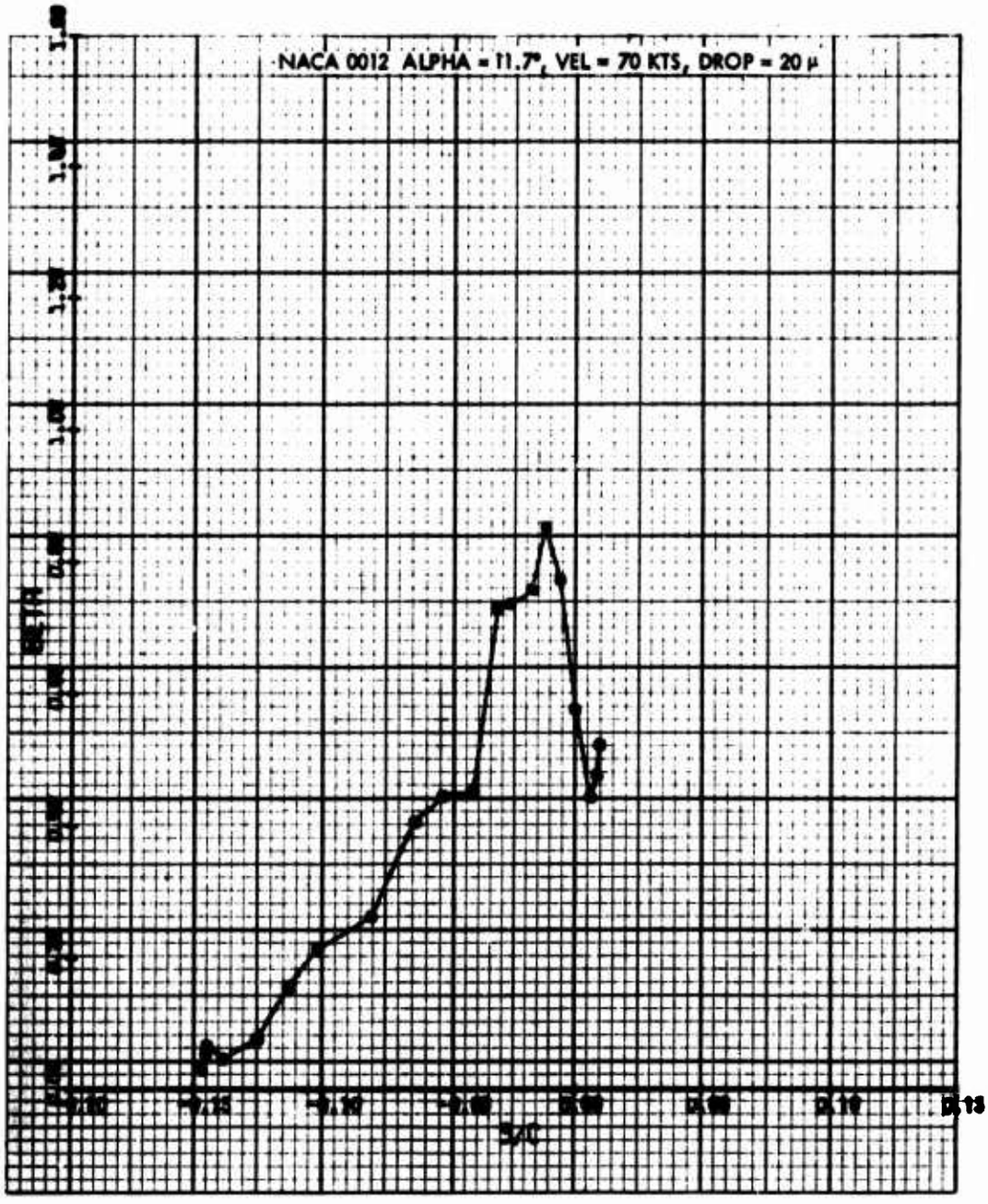

Figure 111. Tail Water Catch Efficiency - Root.

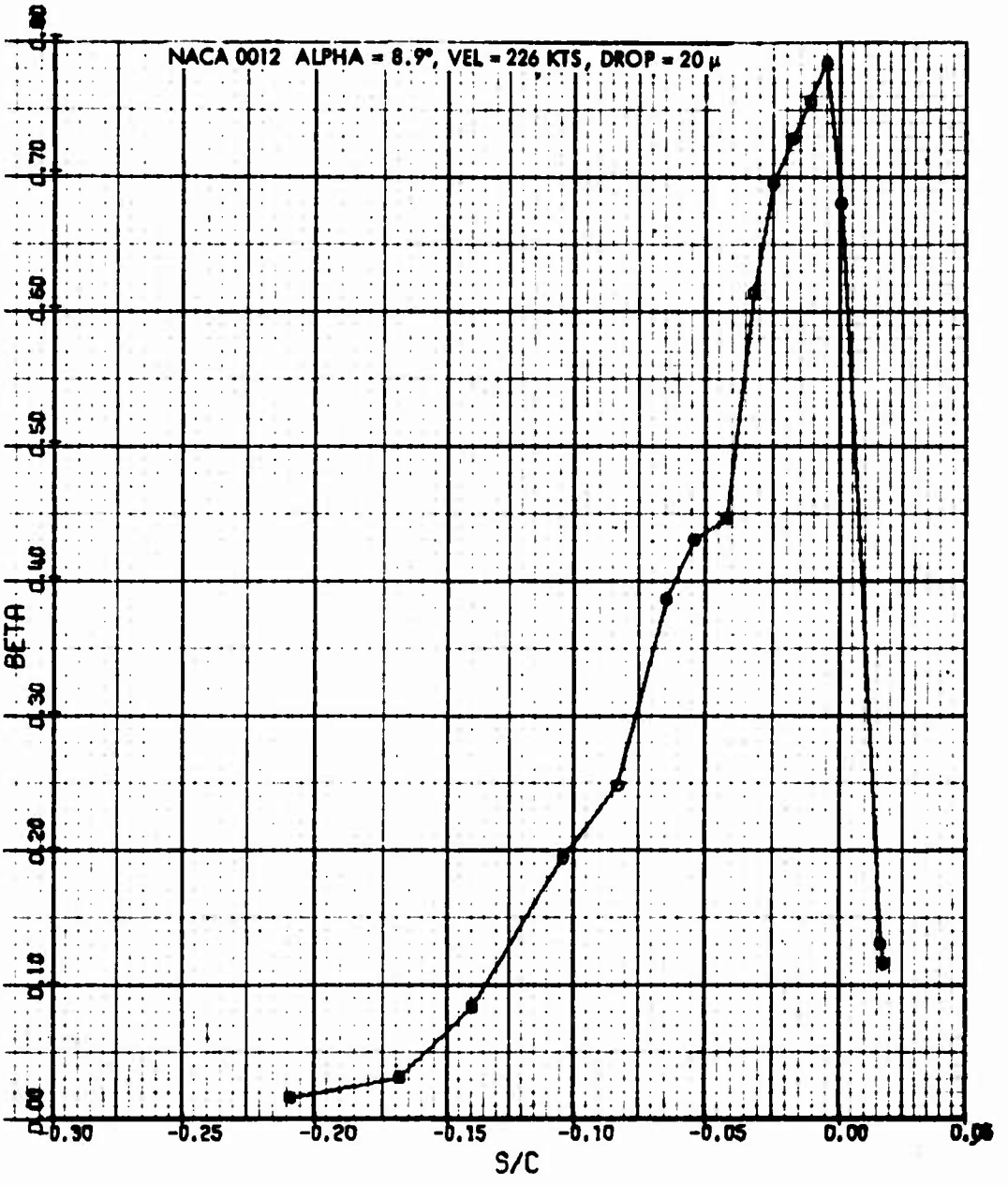

Figure 112. Tail Water Catch Efficiency - Mid-Span.

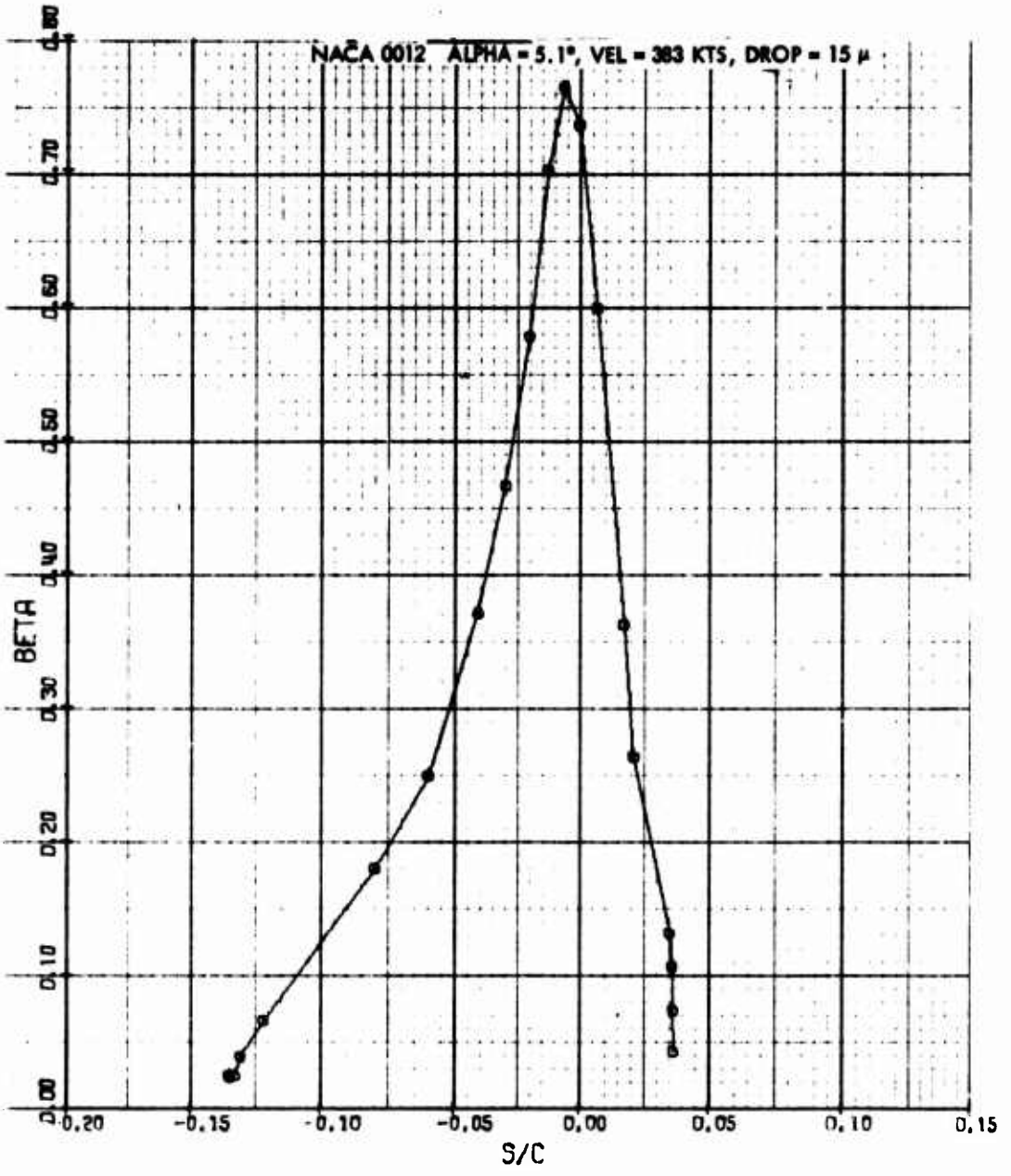

Figure 113. Tail Water Catch Efficiency - Tip.

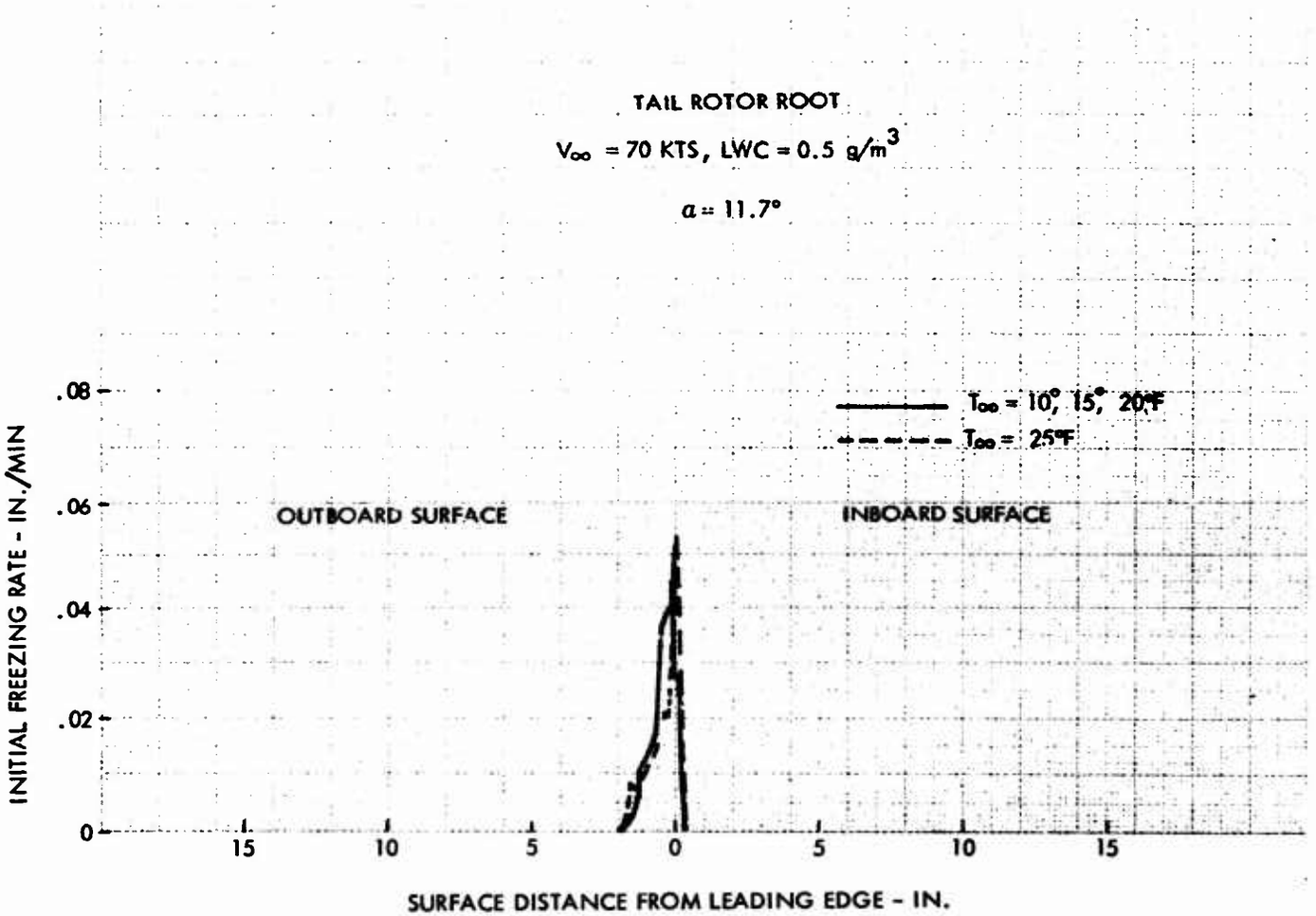

Figure 114. Tail Rotor Root Initial Freezing Rate.

V_∞ = 226 KTS, LWC = 0.5 g/m^3

α = 8.9°

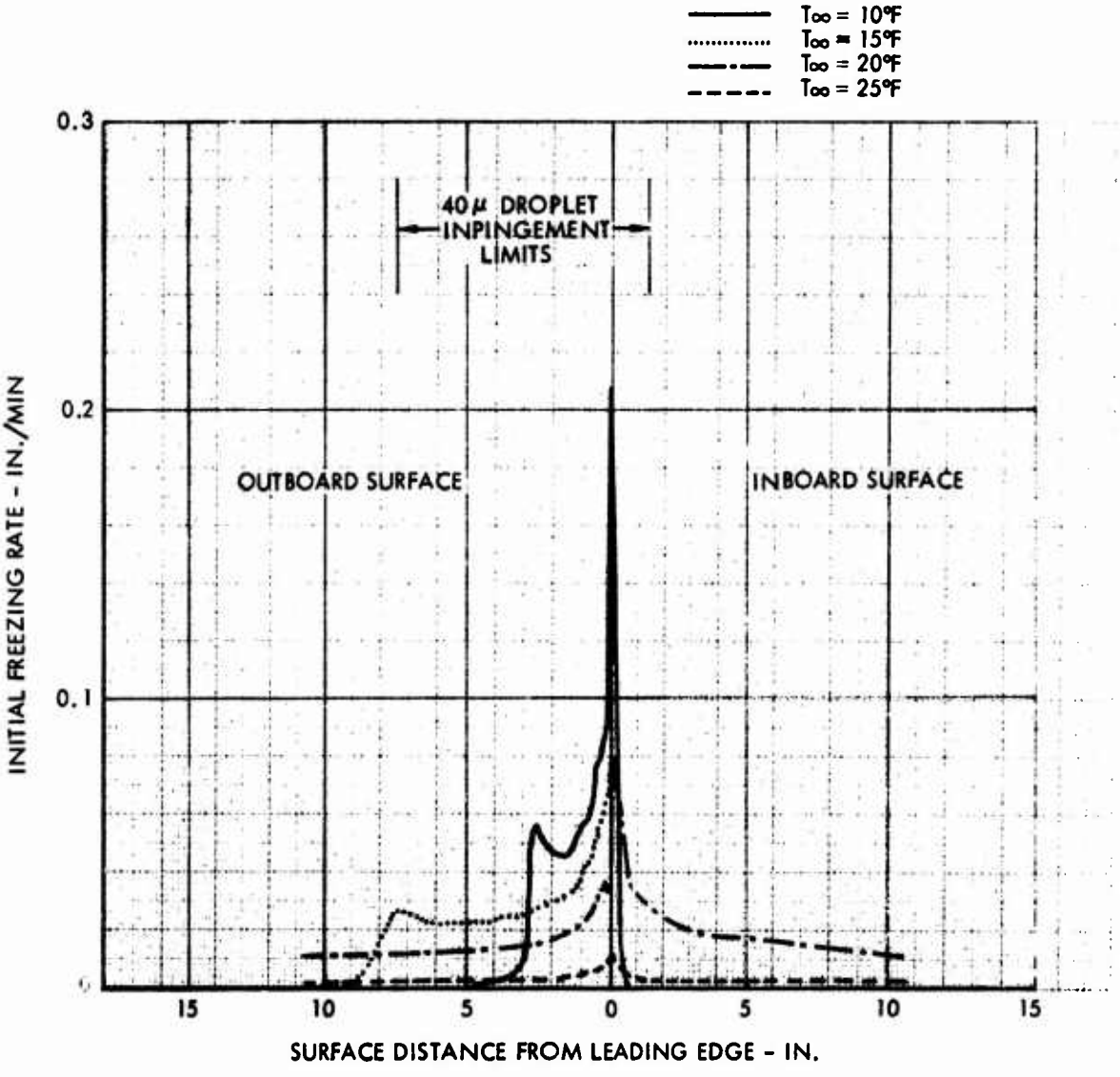

Figure 115. Initial Freezing Rate - Tail Rotor Mid-Span.

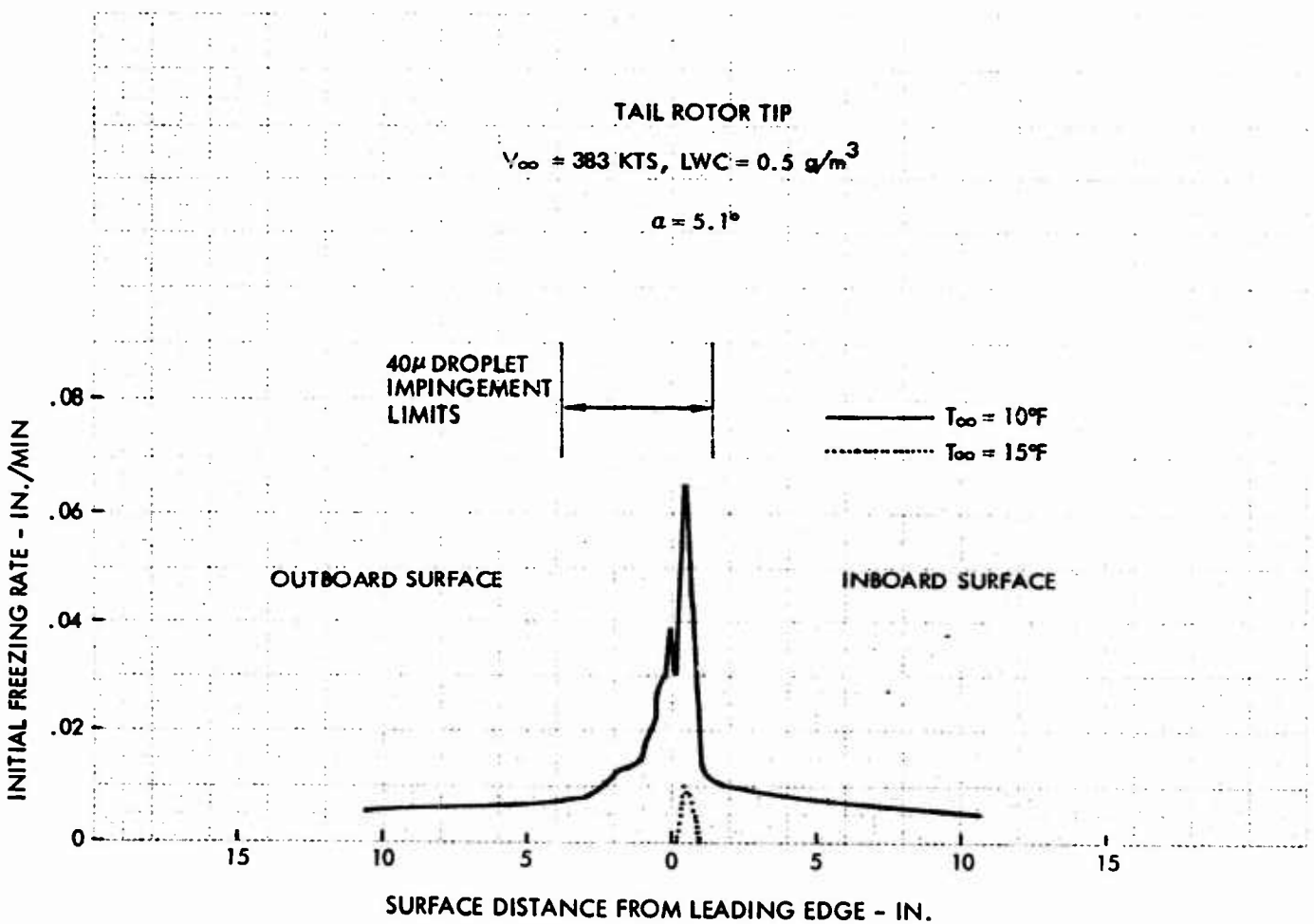

Figure 116. Tail Rotor Tip Initial Freezing Rate.

TABLE XXII. TAIL ROTOR IMPINGEMENT LIMITS			
Blade Location	Droplet Diameter Microns	Outboard Impingement Limit S/C	Inboard Impingement Limit S/C
ROOT	10	- 0.100	+ 0.020
	15	- 0.130	+ 0.017
	20	- 0.146	+ 0.010
	40	- 0.247	+ 0.025
MID-SPAN	10	- 0.103	+ 0.018
	15	- 0.155	+ 0.013
	20	- 0.208	+ 0.017
	40	- 0.305	+ 0.058
TIP	10	- 0.130	+ 0.020
	15	- 0.135	+ 0.037
	20	- 0.173	+ 0.053
	40	- 0.273	+ 0.098

location at four ambient temperatures (10°, 15°, 20°, and 25°F) to determine variation due to temperature effect. Freezing rates and ice shapes were calculated using previously computed water catch rates for 20 micron diameter water droplets and the maximum impingement limits associated with 40 micron diameter water droplets.

Figure 115 shows the mid-span ice shapes and indicates a "turbulent" form in that there are definite indications of a double-horn form at 10°F. The "horn" occurs within a 3-inch region, on the outboard surface, with a peak at the blade leading edge. This peak is due primarily to the influence of the heat transfer coefficient which, as seen in Figure 109, peaks at the leading edge. As the ambient temperature rises, the blade surface temperature also rises, and runback and refreezing occur first on the outboard surface; then as the temperature continues to rise, on both surfaces. At 20°F the freezing pattern is almost identical to the heat transfer coefficient pattern and shows extensive runback. As the ambient temperature continues to rise, the freezing fraction decreases, until at 25°F only a thin layer accumulates over the entire blade chord. This total coverage does not, however, appear to happen in actual icing encounters due to frequent tail rotor ice shedding. A comparison can be made between Figure 115 and Figure 103 which shows the initial ice shapes and freezing

rates for the main rotor at mid-span for turbulent flow. The geometries of the two blades are identical (both NACA 0012 airfoils), with the tail rotor chord being one-half that of the main rotor. At their respective mid-chord positions, however, the angle of attack of the tail rotor is almost twice that of the main rotor (8.9 versus 4.6) while the tangential velocities are similar (226 knots for the tail and 250 knots for the main rotor, respectively). The combination of the effects of blade thickness, angle of attack, and tangential velocities results in total water catch rates which are of similar magnitude (i.e., 3 lb/hr-ft on the tail rotor and 4 lb/hr-ft on the main rotor).

While the peak freezing rate on the tail rotor is of greater magnitude than on the main rotor, at 10°F (approximately 30 percent higher freezing rate) the main rotor double-horn ice shape is more severe in terms of disruption of airflow pattern and increased drag. The total accumulation of ice is about the same for both blades and is, of course, relatively more severe on the tail rotor due to its smaller size. As the ambient temperature rises, the blade surface temperatures also rise; and at 15°F, runback and refreezing are occurring on the lower and outboard surfaces of the main and tail rotor, respectively. At 20°F, the ice accumulations on the two blades are almost identical in shape and magnitude, both resembling the turbulent heat transfer coefficient profile. At 25°F, at mid span, the main rotor blade equilibrium temperature is above freezing, while there is still a thin, streamlined ice shape on the tail rotor. This is due to the higher heat transfer coefficients over the main rotor blade due to the 10 percent higher tangential velocity than the tail rotor has at the respective mid-span locations.

The data presented in this section have all been generated analytically. Figure 117 shows the results of extensive testing of ice formation on rotor blades for various blade stations and various ambient temperatures. The testing was more extensive in that more blade stations were investigated. A comparison of Figure 117 with the data presented shows that the types of ice shapes predicted analytically generally agree with that observed to occur naturally. Figure 117 displays the streamline low-drag shape on the lower surface, the intermediate "spike" shapes, and the double-horn shape associated with airflow field distruption and high drag. Also in agreement is the temperature effect on ice accretion. At lower ambient temperatures (i.e., 0° to 10°F), the ice shape is streamline and tends to follow (roughly) the airfoil contour.

As the surface temperature approaches 32°F, that portion of the impinging water which does not freeze upon impact, freezes elsewhere and results in a bulge which progressively deviates from the airfoil contour. Eventually a limiting condition is reached, at 32°F, where most, if not all, of the impinging water freezes elsewhere, thus resulting in the double-horn or mushroom shape.

The aerodynamic effects of the ice buildups are progressively more severe as the ice shape transforms from the streamline to double-horn shape.

312″ 295″ 275″ 235″ 195″ 155″ 115″ 75″ 50″

STATIONS ALONG BLADE. TEMPERATURE — 15°C.

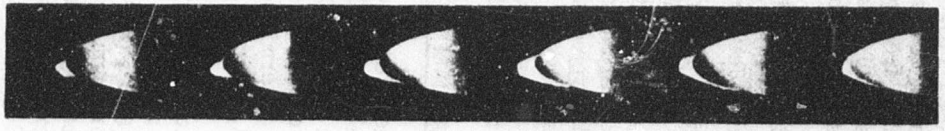

275″ 235″ 195″ 155″ 115″ 75″

STATIONS ALONG BLADE. TEMPERATURE — 8·5°C.

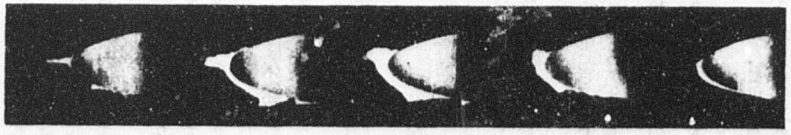

195″ 155″ 115 75″ 50″

STATIONS ALONG BLADE. TEMPERATURE — 2°C.

Figure 117. Rotor Blade Ice Formation at Various Temperatures.

Figure 118 and 119 show the effect of ice buildup on rotor blade aerodynamic characteristics for streamline and mushroom ice shapes, respectively. As expected, the double horn of the mushroom ice shape greatly disrupts the flow field about the blade, thus increasing drag.

When water impinges upon a surface and does not freeze on contact, it runs back along the surface until it refreezes. This runback is shown in Figures 100-103 and in Figures 115 and 116. While runback is usually streamlined and just a thin layer upon the surface, there can be times when it can contribute to aerodynamic drag penalties by building upon itself. The selection of an ice removal system must consider minimizing the runback problem, as will be discussed in Sections 5 and 7.

Figure 120 shows the total collection efficiency, E_m, as a function of modified inertia parameter, K_o, for a Joukowski 0012 airfoil at the angles of attack investigated in this study. As angle of attack increases, so does the collection efficiency and total water catch over the airfoil. These data can be used to calculate total airfoil water catch rates for any combination of meteorological conditions. Figure 120 is good for any NACA 0012 airfoil at, of course, the appropriate angle of attack. A 12-percent airfoil has been the standard rotor blade design for helicopters. Therefore, the work established by this effort is applicable to almost all helicopters and can be used as a standard of design criteria.

4.4 DESIGN ICING CONDITIONS FOR MAXIMUM WATER CATCH

The foregoing analysis was performed for a constant liquid water content (LWC) of 0.5 gram/cubic meter (g/m^3). Droplet trajectory plots, local and total water catch rates, and local catch efficiency were computed at an ambient temperature of 20°F - these parameters being only slightly influenced by ambient temperature. To determine whether or not the most severe icing cases have been investigated, Figure 121 was prepared.

The solid lines in Figure 121 indicate the total water catch at the three rotor blade stations being investigated, at a constant ambient temperature of 20°F, and a constant LWC = 0.5 g/m^3, for droplet diameters of 10, 15, 20 and 40 microns. However, at constant temperatures, the LWC does not remain constant when the drop diameter changes but varies as shown in Figure 77. By interpolating and extrapolating, it can be found that at 20°F and 40 microns the LWC = 0.12 gm/m^3; at 20°F and 15 microns, the LWC = 0.66 gm/m^3; and at 20°F and 10 microns, the LWC = 0.80 gm/m^3. Applying these factors to the solid curves of Figure 121 yields the broken lines shown, water catch being linearly proportional to LWC. Since the LWC = 0.5 gm/m^3 for 20 microns at 20°F, that line does not change.

Figure 121 shows that with respect to the water catch, the 15-micron-diameter case is slightly more severe than the 20-micron-diameter case, with the magnitude of the severity increasing as rotor blade station increases.

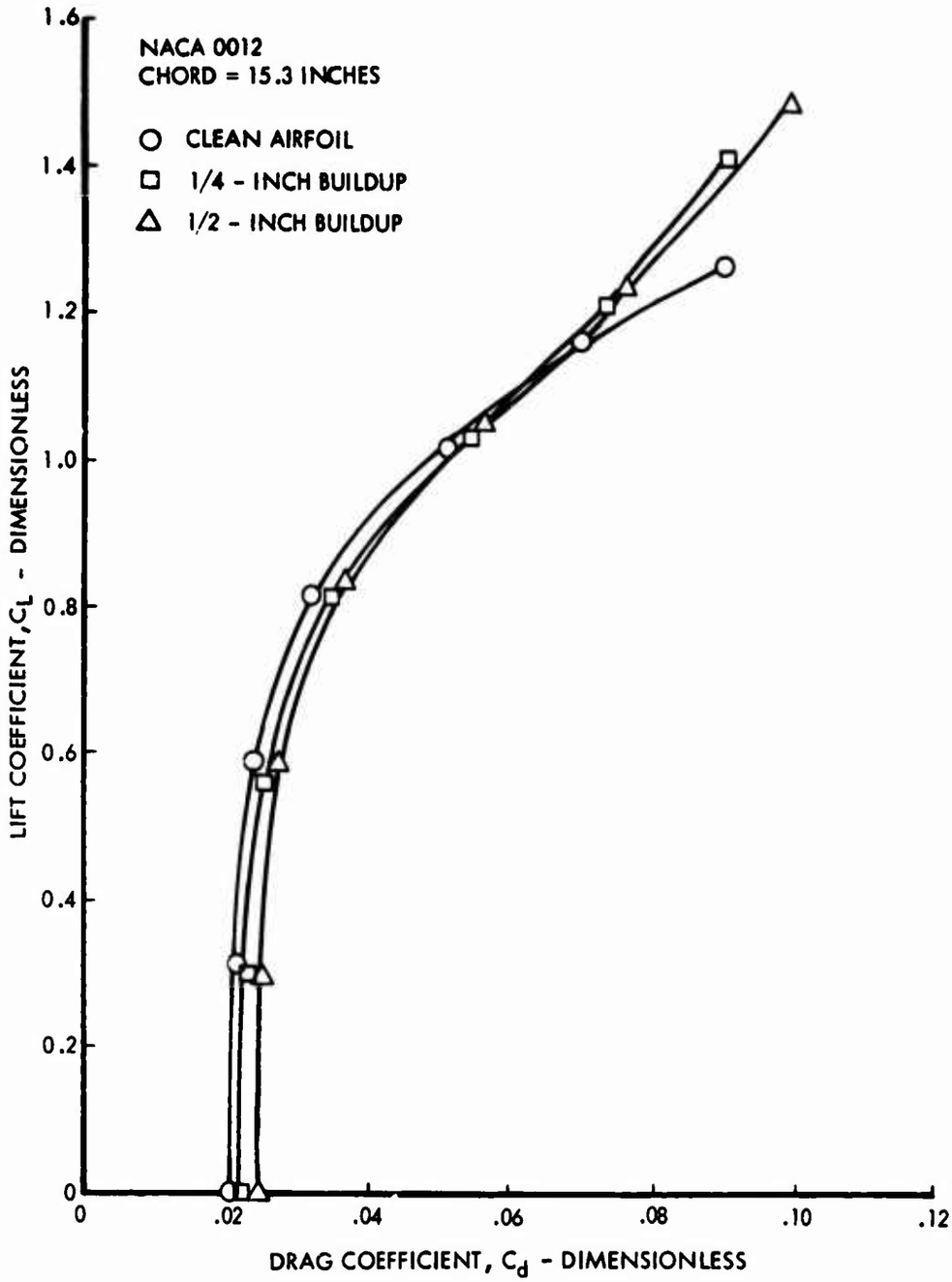

Figure 118. Effect of Streamlined Ice Buildup on Rotor Blade Aerodynamic Characteristics.

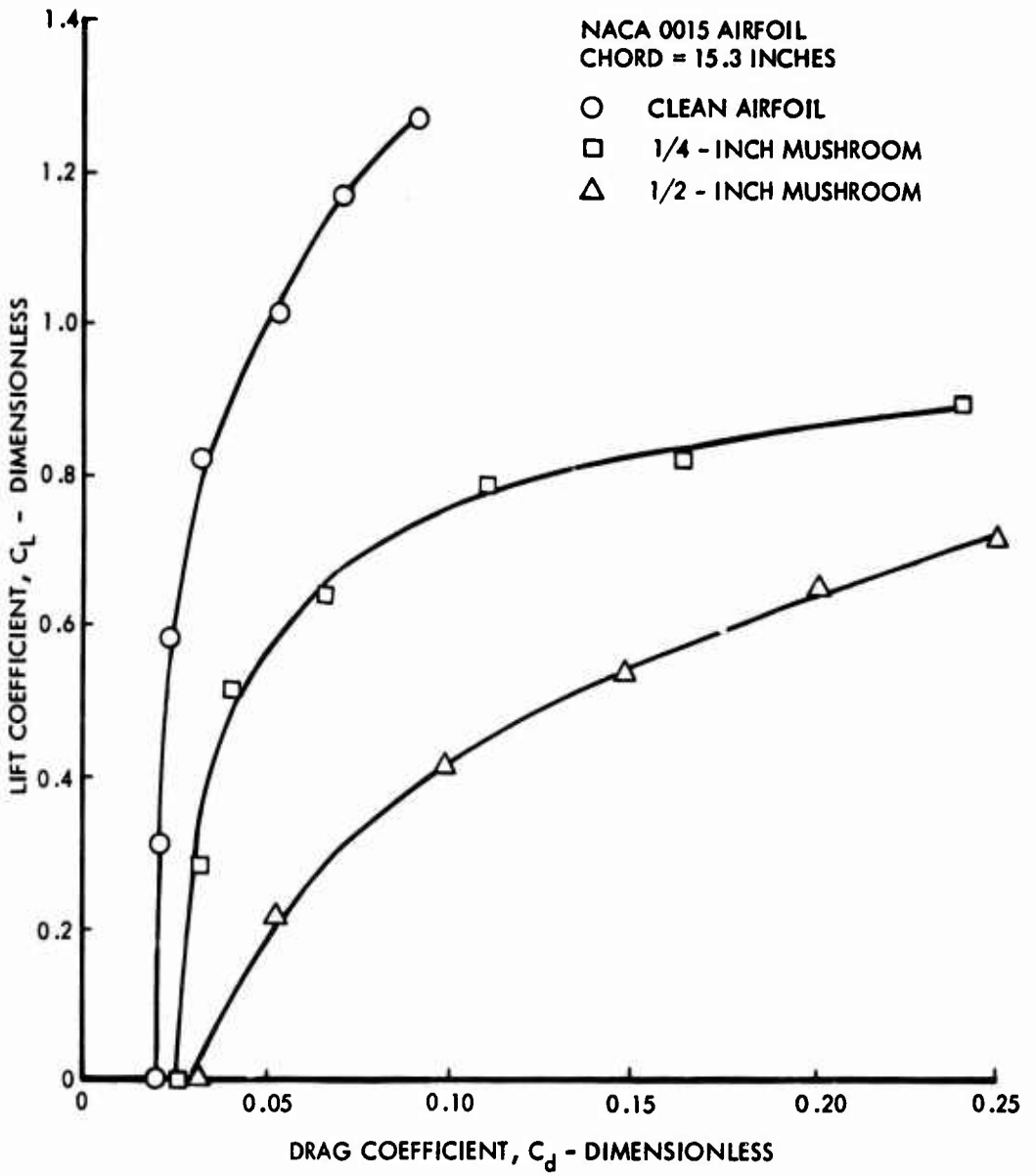

Figure 119. Effect of Mushroom Ice Buildup on Rotor Blade Aerodynamic Characteristics.

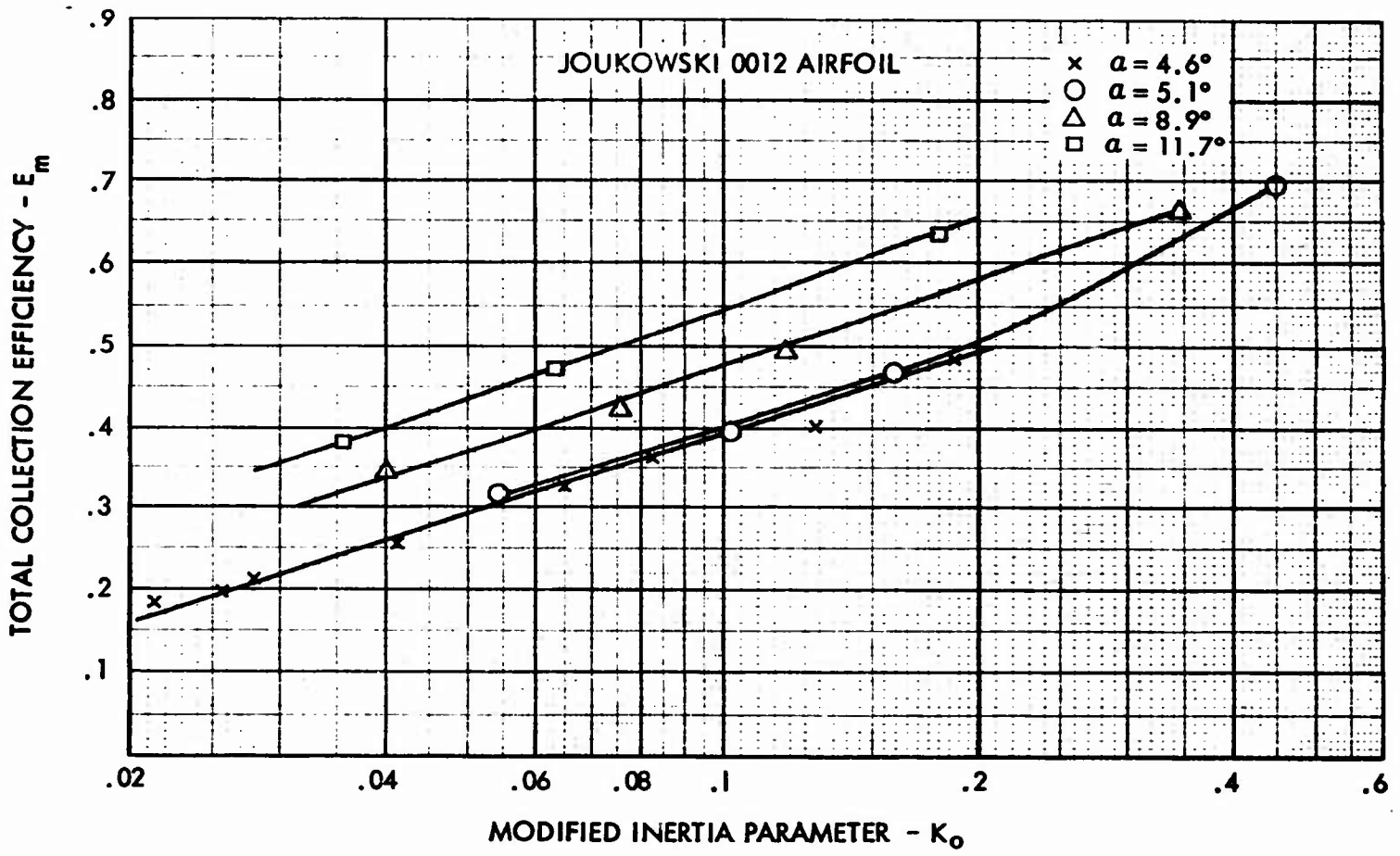

Figure 120. Total Collection Efficiency Versus Modified Inertia Parameter.

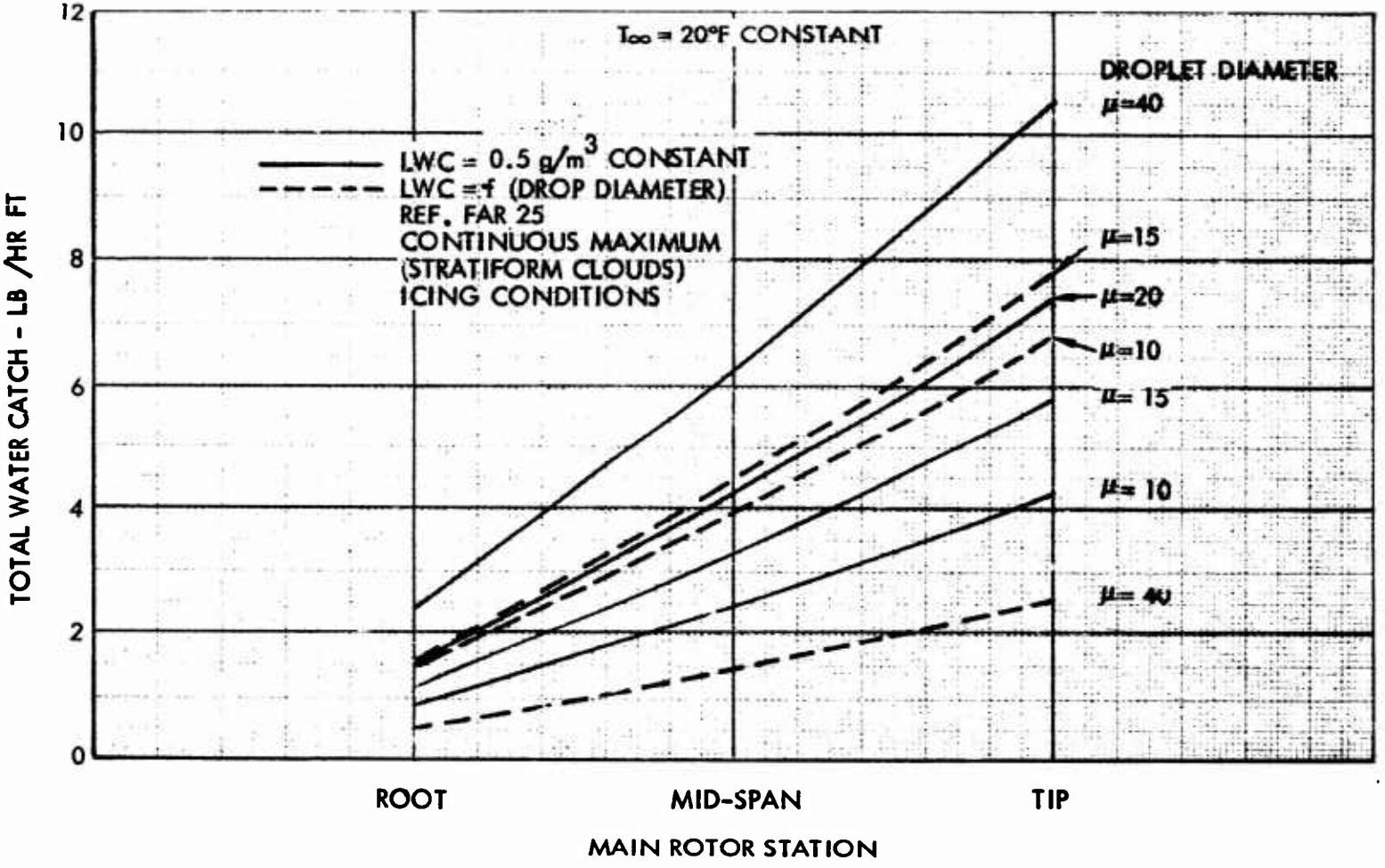

Figure 121. Total Water Catch vs. Main Rotor Station.

At the tip, the total water catch at 15 microns is 7 percent greater than at 20 microns. At mid-span the differential is only 3 percent, decreasing to a zero differential at the root. Since this differential is not large, it was decided to retain the main and tail rotor blade initial freezing rate and ice shape data, done for 20 microns, so that the data would be parametrically consistent.

To be more precise, it is recommended that future icing investigations be performed using water droplet diameters of 15 microns instead of the 20-micron diameter used in this study. However, the accuracy of this investigation should be within 3-4 percent because blade ice shed due to increasing centrifugal force along the blade span was not considered. Ice shed has been empirically observed at rotor blade tips and, more frequently, on the tail rotor.

From this investigation it is concluded that ice protection of the tail rotor is, in fact, as critical as, if not more so than, the main rotor blade ice protection. It is recommended that future helicopter anti- or deicing protection be extended to the tail as well as the main rotor blades.

SECTION 5 ICE PROTECTION SYSTEM DESIGN

This section includes a discussion of weight, reliability, and vehicle performance penalty trends for each type of ice protection system. The appropriateness and applicability of the various concepts to the affected components of rotor wing craft are discussed, along with the sensitivity of the performance to meteorological conditions. The section concludes with a discussion of in-flight measurement of icing severity.

Special attention is given to each of the candidate systems to provide the following:

1. Identification of the basic concepts
2. The principle of operation of the various techniques
3. A general description of the hardware involved
4. The adequacy of the system with respect to meeting specified performance criteria
5. The penalties of the candidate systems in terms of weight and power
6. The in-service reliability of the systems.

5.1 BASIC CONCEPTS

The development of all-weather capability for any aircraft entails consideration of the following factors:

1. The vehicle components to be protected
2. The type of system to be used
3. The energy source

All of these items are interrelated, in that the resolution of one of these factors influences the others. Since past experience shows that aircraft cruising below 20,000 feet encounter icing conditions about once in twenty flights, a slight compromise in completeness of aircraft ice removal but not in flight safety may be considered rational. Primary emphasis in helicopter ice protection design must be placed on safety, simplicity, low cost (both in terms of initial cost and performance penalty to the aircraft), maximum reliability, and a technique which offers a tried and proven design. The technology for all-weather capability for aircraft has evolved to a well-developed state over the past 20 to 25 years. There are a number of

alternate methods for ice protection available which will be discussed in some detail. The background material for assessing the suitability of a given ice protection concept has been accumulated over many years as a result of extensive practical experience in icing tunnels and on actual in-flight installations.

In considering the ice protection design philosophy for an aircraft, it is often desirable to establish the ambient temperatures above which ice will not form. The value of this ambient temperature is dictated by the ram air temperature rise (due to speed) that produces a skin equilibrium temperature of 32°F. This is particularly true for higher speed aircraft. An example of this is shown in Figure 122 for a typical rotor system during hover. Due to the kinetic heating of the rotor blades, there must be a substantial reduction in ambient temperature below freezing before ice will form. For example, the main and tail rotor tips are (just) ice free at 12°F. This information is useful in determining component design conditions, from both a meteorological and a vehicle operating condition standpoint. Surfaces which can remain ice free to relatively low temperatures can be designed to low liquid water content conditions, and severest ice catch and heating requirements will occur at some intermediate speed. These conditions, of course, are a function of a specific vehicle design. In addition to the considerations related to the ambient temperatures above which ice will not form, the design icing point for a given system is dependent upon the type of ice protection system and energy source utilized.

5.1.1 Modes of Ice Protection - Anti-Icing and Deicing

Basically, ice protection systems can be classified as either anti-icing or deicing. With anti-icing, the protected area is maintained free of ice buildups at all times, either by evaporating all of the impinging water or by allowing all or some of it to run back and freeze on noncritical areas. Deicing, on the other hand, is the periodic shedding, by mechanical, chemical, or thermal means, of small noncritical ice buildups by destroying the bond between the ice and the protected surfaces.

The choice between anti-icing and deicing is based upon several factors, among them being the sensitivity of the component and/or vehicle to small ice buildups and the total energy available for ice protection. In general, it takes more energy input per unit area to remove ice once formed than to prevent its formation in the first place. However, since heat is applied in sequence to a large number of cyclic elements during deicing, only a small portion of the vehicle is deiced at any given time; and the total energy requirements for deicing are less than those for anti-icing. Anti-icing systems must also have a certain degree of recovery capability, whereby they must first remove a small ice buildup which may result from the system's inadvertently not being activated until several minutes subsequent to the icing encounter. On the other hand, deicing has associated with it the drag and potential impact damage problem caused by small ice buildups.

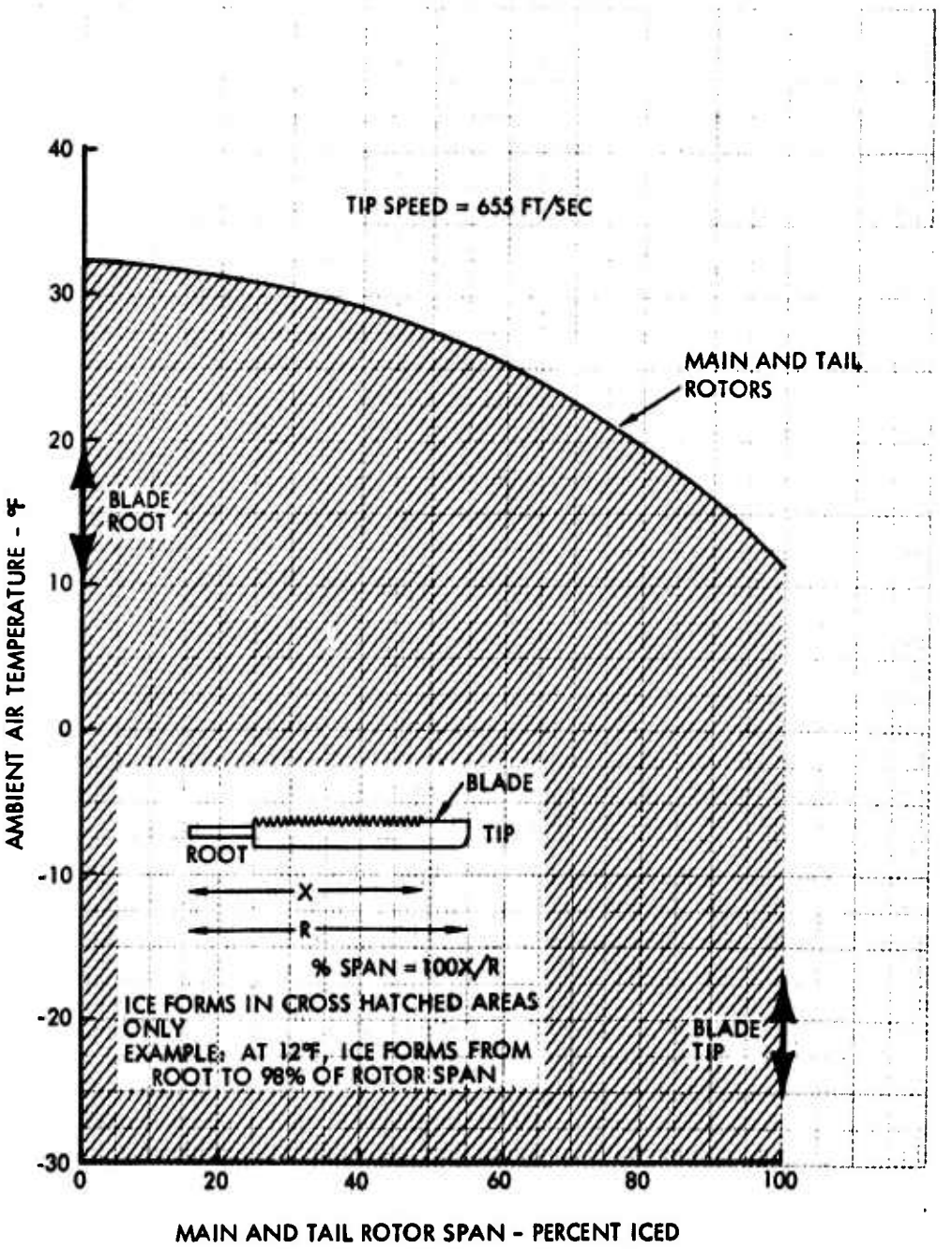

Figure 122. Spanwise Extent of Rotor Icing.

In selecting between anti-icing and deicing, there are no hard-and-fast rules, as each application must be looked at as a separate entity. Therefore, a set of guidelines or design criteria has been established for defining the vehicle areas requiring protection and whether anti-icing or deicing is more appropriate. These criteria are based upon consideration of the mission and anticipated frequency and duration of icing encounters, the vehicle sensitivity to ice buildups, the penalties imposed by a protection system, and the increased mission reliability achieved by airmobile all-weather capability. Based on in-service experience, it has been concluded that the following components basically must be protected by anti-icing (the prevention of ice formations rather than their removal by deicing):

1. Windshields
2. Pitot tubes and other flight probes
3. Carburetors
4. Engine inlets

It should be emphasized, however, that the anti-icing system should have the capability of deicing the protected component. This should be a requirement since the pilot inadvertently may delay turning the system on until after entry into the icing condition. The amount of time in icing before system activation is an arbitrary decision, but the capability of removing a 3-minute accumulation (at the "design" icing rate) is not unreasonable.

Deicing is an acceptable procedure for aerodynamic surfaces (wings, empennages, and rotor systems).

More recently, the overwhelming trend has been to use thermal energy for both anti-icing and deicing. This thermal energy can be obtained in two ways:

1. Hot air, either heated ram (combustion heater) or engine compressor bleed air, passed through passages integral with the surface being heated.
2. Electrical resistance heating elements embedded just below the surface being heated.

With the almost universal use of turbine engines and lightweight three-phase electrical power systems, thermal methods are used almost exclusively for current all-weather aircraft. For comparison purposes, however, other techniques are also presented.

5.1.1.1 Anti-Icing

In an evaporative anti-icing system, sufficient heat must be supplied to counterbalance the heat losses arising from three concurrent processes: (1) convective cooling of the protected surface; (2) sensible heating of

the impinging water (heating of the water droplets to the skin temperature); and (3) complete evaporation of the impinging water. To meet the evaporative anti-icing demand, approximately 65 percent of the supplied heating energy is required to counterbalance the evaporative heat loss, 30 percent to counterbalance the convective loss, and less than 5 percent to counterbalance sensible heating of the water droplets. Therefore, the required heating capacity of a fully evaporative system is governed by conditions associated with the highest possible water catch rate, i.e., the highest liquid water content. In terms of ambient temperature, the design icing point for evaporative protection coincides with the ambient temperature that represents the demarcation point below which ice protection is required.

The design ambient temperature for evaporative anti-icing lies between 15° and 32°F (depending on the speed), the design droplet size is on the order of 15 or 20 microns, and the liquid water content (LWC) range is between 0.45 and 0.8 gram/m^3 (depending on ambient temperature). Evaporative anti-icing involves a discretely heated area, which extends aft of the water droplet impingement limits. In this case the maximum, rather than the median, droplet size is used to determine the aft boundaries of the heated area. Evaporative anti-icing of airfoil and engine inlet lip leading edges requires from 1.5 to 4.0 lb/min of engine bleed air per foot of span. Complete evaporation requires a typical skin temperature range between 80° and 120°F. The precise flow rate depends upon the temperature of the supply air. With respect to the flight regime for helicopters, the design icing point for thermal anti-icing is associated with the minimum power setting that results in the lowest bleed temperatures, bleed pressures and available airflow (the latter being limited by a fixed flow-metering orifice). This design flight condition is frequently referred to as the "bucket" power point on the helicopter power-velocity curves (Figures 123 and 124).

If electrical energy is used for evaporative anti-icing, the required intensity for continuous maximum icing conditions may vary between 6 and 16 watts per square inch, depending upon the size and shape of the airfoil and the local distance from the stagnation point.

In a running-wet system, the water is not entirely evaporated; the principal design criterion is to maintain the surface temperature just above freezing (32° to 40°F). If a limited area is heated for running-wet conditions, the water from the heated area may be carried by the aerodynamic slipstream aft into the unheated area and freeze there, forming "frozen runback". To prevent frozen runback from forming, the entire affected surface must be heated. Most of the heat load in a running-wet system (up to 90 percent) is required to counterbalance the heat loss due to convective cooling. Therefore, the lowest ambient temperature in the recommended icing envelope (i.e., 0°F) determines the required capacity of the running-wet system.

As far as the icing design point is concerned, the "bucket point" criterion applicable for evaporative protection is also valid for running-wet systems

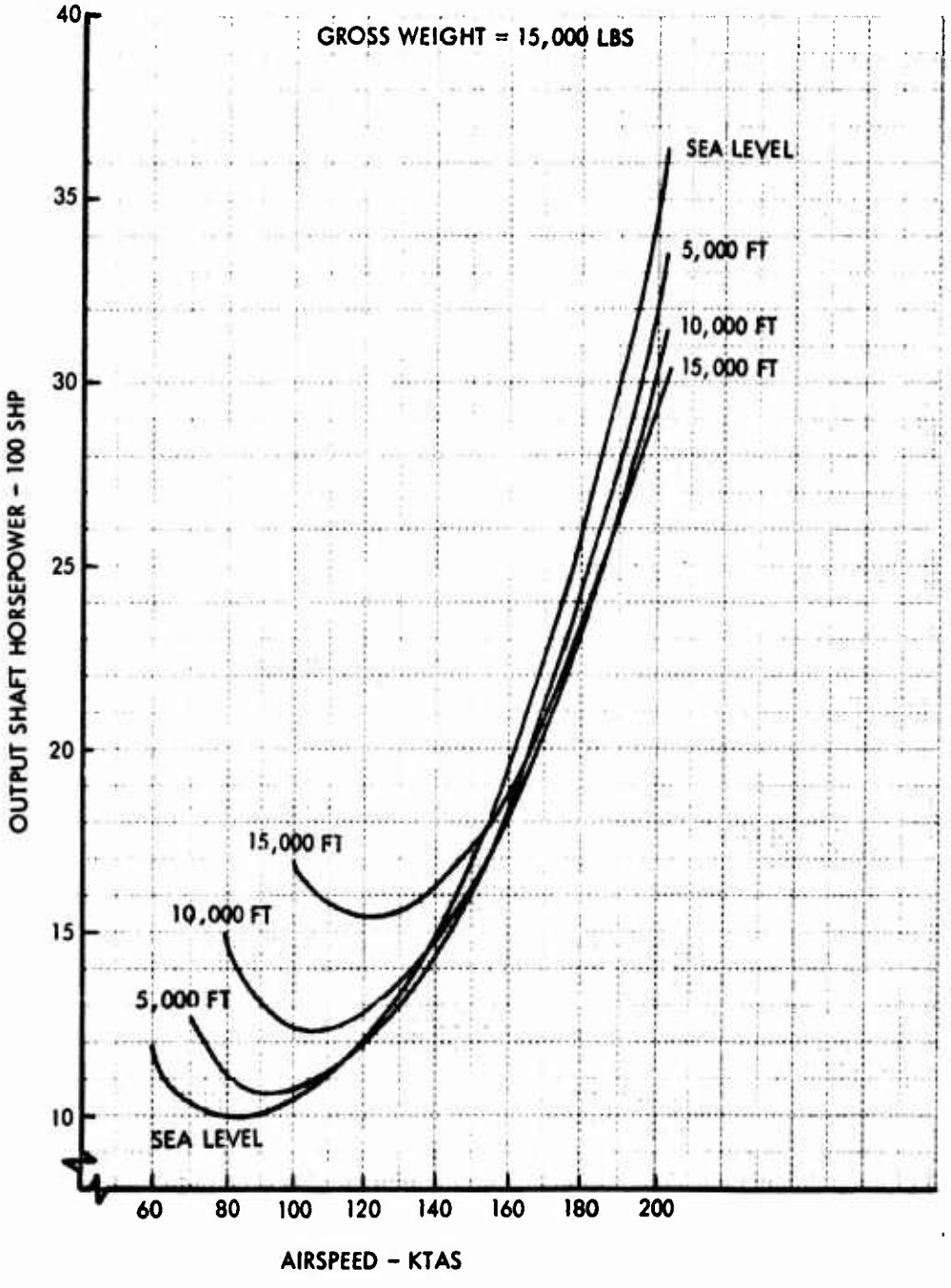

Figure 123. Typical Helicopter Engine SHP Requirements.

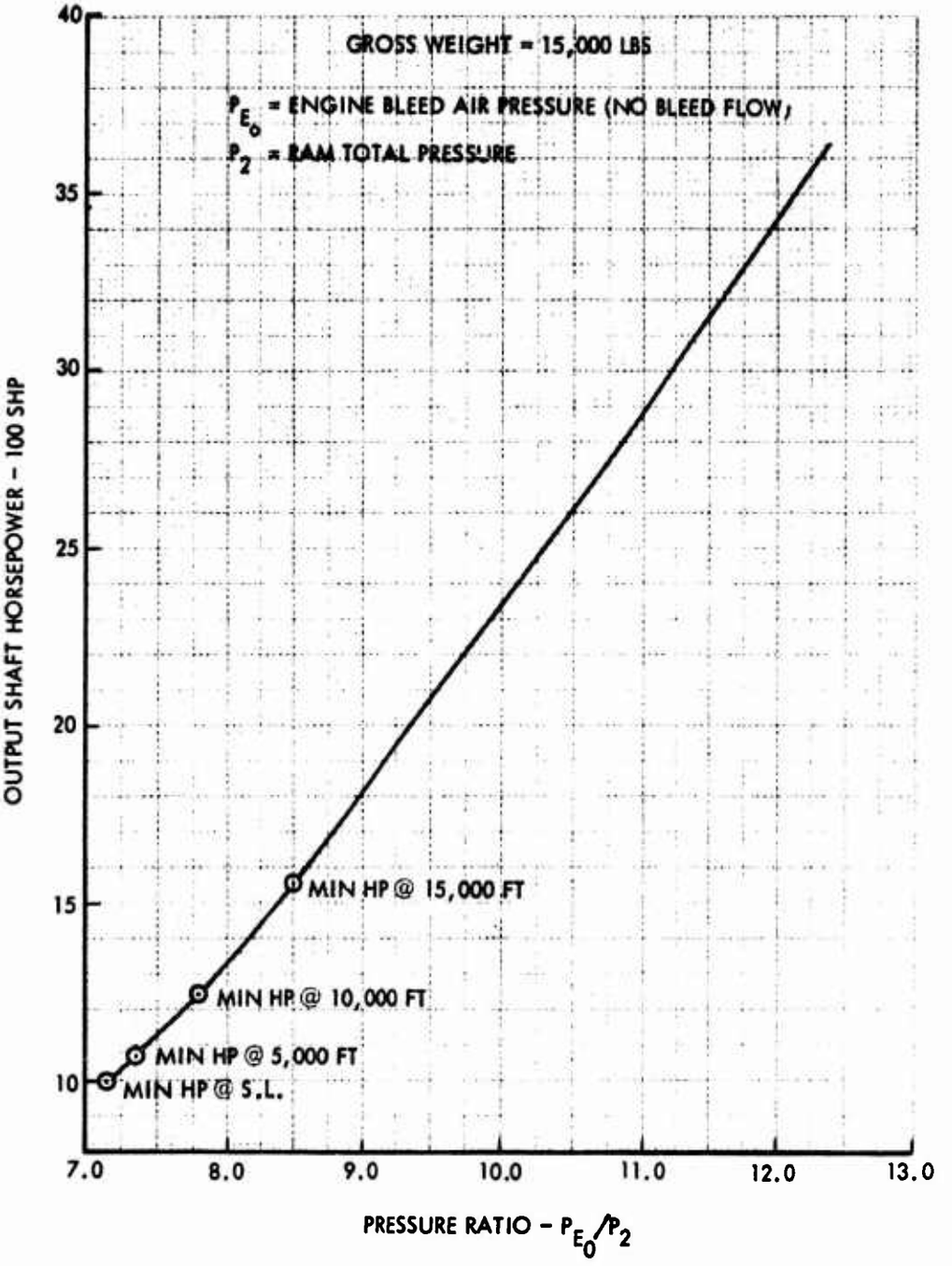

Figure 124. Typical Helicopter Engine Bleed Air Pressure Ratios

utilizing engine bleed air. The design point for electrically anti-iced surfaces is not affected by the engine power setting and is governed solely by the heat losses. Generally, the total heating requirements for a running wet system are considerably smaller than those required for evaporative anti-icing. Evaporative anti-icing systems are usually used for leading edge surfaces of large components, such as large airfoils (wing or tail of fixed aircraft), or for the cowl lip of long engine inlet ducts. In these applications it is not practical to heat the entire surface area. Running-wet systems are used in engine inlet ducts where protection is provided not only for the cowl lip but for the entire inner duct surface, such that any liquid runback enters the engine compressor directly. Other applications for running-wet systems include areas where the runback is not critical; e.g., on external cowl surfaces or on transparent areas, or where the entire surface is heated and liquid runback is blown off by the aerodynamic slipstream, e.g., flight probes and antenna masts.

The amount of bleed-air flow used for running-wet anti-icing depends on the area of the heated surface; for engine inlet ducts this flow may be as much as 40 percent lower than required for evaporative anti-icing of the cowl lip alone. When electrical energy is used for running-wet anti-icing, the required intensity may vary between 2 and 8 watts per square inch for continuous maximum icing intensities, depending on the water catch efficiency of the flight surface and the distance from the stagnation region.

Turbine engine compressor bleed air for engine, engine inlet, wing and/or empennage continuous anti-icing has been favored by designers since the introduction of turbopowered aircraft. Because the bleed air heating method has been so effective, there has been a willingness to pay an ever-increasing penalty for the energy consumed. The increasing bleed air penalty is due to more efficient engine cycles, where bleed air, if extracted, constitutes a larger percentage of the engine gas generator airflow. The high reliability and low maintainability costs are other important advantages of the bleed air anti-icing systems over the other candidate technique-electrothermal anti-icing. In the case of engine and engine inlet cowl anti-icing, the proximity of bleed air points to the anti-iced area, light weight, and ease of integration of the airframe manufacturer's inlet duct protection system with the engine manufacturer's engine anti-ice protection system are other important considerations.

The power requirements for completely anti-icing an aircraft using an electrical power source are prohibitive, and therefore the areas ordinarily anti-iced electrically have been restricted to: (1) running-wet windshield anti-icing by use of an electrically conductive coating (vacuum-deposited tin oxide or gold) within the windshield laminate, (2) narrow parting strips along the stagnation lines of wing or empennage leading edges (as part of a cyclic deicing system), (3) flight probe surfaces, (4) propeller spinners and propellers, and (5) areas remote or inacessible from any hot-air source.

5.1.1.2 Deicing Techniques

Over the years, several different techniques have been used to remove ice buildups on aircraft surfaces. Following is a description of the available techniques:

Inflatable rubber pneumatic boots - Pneumatically operated mechanical deicing boot systems have been in use longer than any other concept, and some improvements in boot design have been incorporated in recent years. The boots, when inflated, break the bond between the ice and the surface, thus allowing aerodynamic forces to blow the ice away. This method is often used for light aircraft because of its simplicity and relatively low first cost. In turboshaft powered aircraft, a pneumatic deicing system can utilize a very small quantity of cooled engine bleed air continuously to provide ejector suction for maintaining the boots in a deflated position (minimizing drag), and intermittently to inflate the boots. The amount of bleed air extraction for deicer boots is small, and the fuel penalty due to engine bleed over a typical airmobile mission is negligible. Thus, in icing conditions the variable fuel penalty of a pneumatically operated boot system is due solely to the drag resulting from ice buildup on leading edges before the ice is shed. In addition to the drag increase due to ice buildup before shedding, the boots may impose a permanent drag increase regardless of whether the flight is performed in clear air (nonicing weather) or whether the helicopter penetrates an icing condition. This permanent penalty is due to the fact that the boot surface, when deflated is not as smooth as a metal leading-edge surface. This permanent drag increase can amount to 2 percent for rotor airfoil sections of helicopters, which is equivalent to an overall drag increase of up to 1.4 percent for the aircraft. Pneumatic boots must be virtually drag-free to show an operational weight advantage over thermal deicing techniques. Modern boots, carefully recessed and bonded to the structure, do minimize or eliminate the drag increase when compared to the old type of installation. As far as aircraft operators and maintainability personnel are concerned, there is generally a negative attitude toward boot installations; logistics problems and high maintenance cost are cited as adverse factors. Even modern pneumatic deicers on commercial transports require replacement every 2 years because of gradual erosion. Inadvertent damage of penumatic boots during maintenance not related to the deicing system and during aircraft ground handling is frequent. Inspection of boots is required almost on a daily basis. Patching of boots is a cumbersome and time-consuming procedure. Solvents, detergents, diester oils (used for engine lubrication), etc., are deleterious to boot material and require masking during cleaning and paint touch-up operations. In addition, some pilots have taken strong exception to the automatic cycling device used for inflating the boots as being a "useless gadget." Reliance on the automatic timer in either light or very heavy icing conditions may cause considerable residual ice on the boots. The ice thickness must be "just right" to afford optimum shedding. Therefore, many pilots resort to manual control to operate the boots, which, of course, requires continuous surveillance of ice formed on affected airframe surfaces. To minimize the cost and problems associated with utilization of pneumatic

boots, there may be some merit in installing the boots as a winter kit for the icing season only.

A schematic of a typical system is shown in Figure 125. Engine bleed air is used in conjunction with a pressure regulator and ejector to inflate and deflate the boots, thus eliminating the need of for a dry-air pump. The bleed air supply line is of a 3/8-inch diameter and the pressure regulator setting is within the range from 15 to 22 psig. During the deflation cycle, the ejector maintains a 6-inch Hg vacuum on the boots. Spanwise or chordwise boot cells are operated alternately and symmetrically about the fuselage, with each of the tubes being inflated for six seconds every three to four minutes, by means of an electric timer. The pneumatic deicer boot is comprised of tubes the width of which may vary between 3/4 and 1-1/4 inches. For high-speed thin airfoils, chordwise installed boots with small tubes are preferred, because they cause less disturbance of airflow over the surface. However, the leading edge radius may be too small to permit inflation of chordwise boots, and in such cases spanwise boots represent the only practical boot installation.

On some installations, the electric timer incorporates a dual setting which permits use of a 60-second cycle during heavy icing and a 3- to 4-minute cycle during light or moderate icing conditions. Such a dual setting requires some caution on the part of the crew because a short cyclic time in light icing conditions results in deformation of the thin ice, with insufficient cracking to cause shedding by slipstream action. The sequencing of inflation (pressure) and deflation (vacuum) of the boots is controlled by the cyclic timer operating either a centrally located distributor valve (as shown on Figure 125) or solenoid operated valves located near the boot air inlets. A pressure relief valve is incorporated to act as a safety valve in the event of a failure of the pressure regulating valve.

Chemical Systems - A second method involves the use of a freezing point depressant (e.g., glycol, alcohol, etc.), which is pumped in a thin film over the protected surface, thus lowering the freezing point and preventing the formation of ice. Although relatively simple in concept, it does have some drawbacks when applied to airfoil anti-icing, such as difficulty in obtaining an even flow distribution in the presence of a variable external pressure field. It is an expendable system which requires resupply; and the sensitivity of the fluid distribution holes to clogging, particularly in a dusty environment, is also a drawback for helicopter operation. Depending upon the width of the fluid expulsion band, the system performance may be sensitive to aircraft attitude (angle of attack). Also, chemical systems have, at best, marginal recovery capability as evidenced by recent icing tunnel tests (Reference 73) on a vendor proprietary fluid anti-icing system. Use of chemical systems is sometimes reserved for windshield ice protection (Twin Otter) and nose radome protection (C-5A). This method offers also one possible means of rotor, wing, and tail surface protection and hence is examined herein.

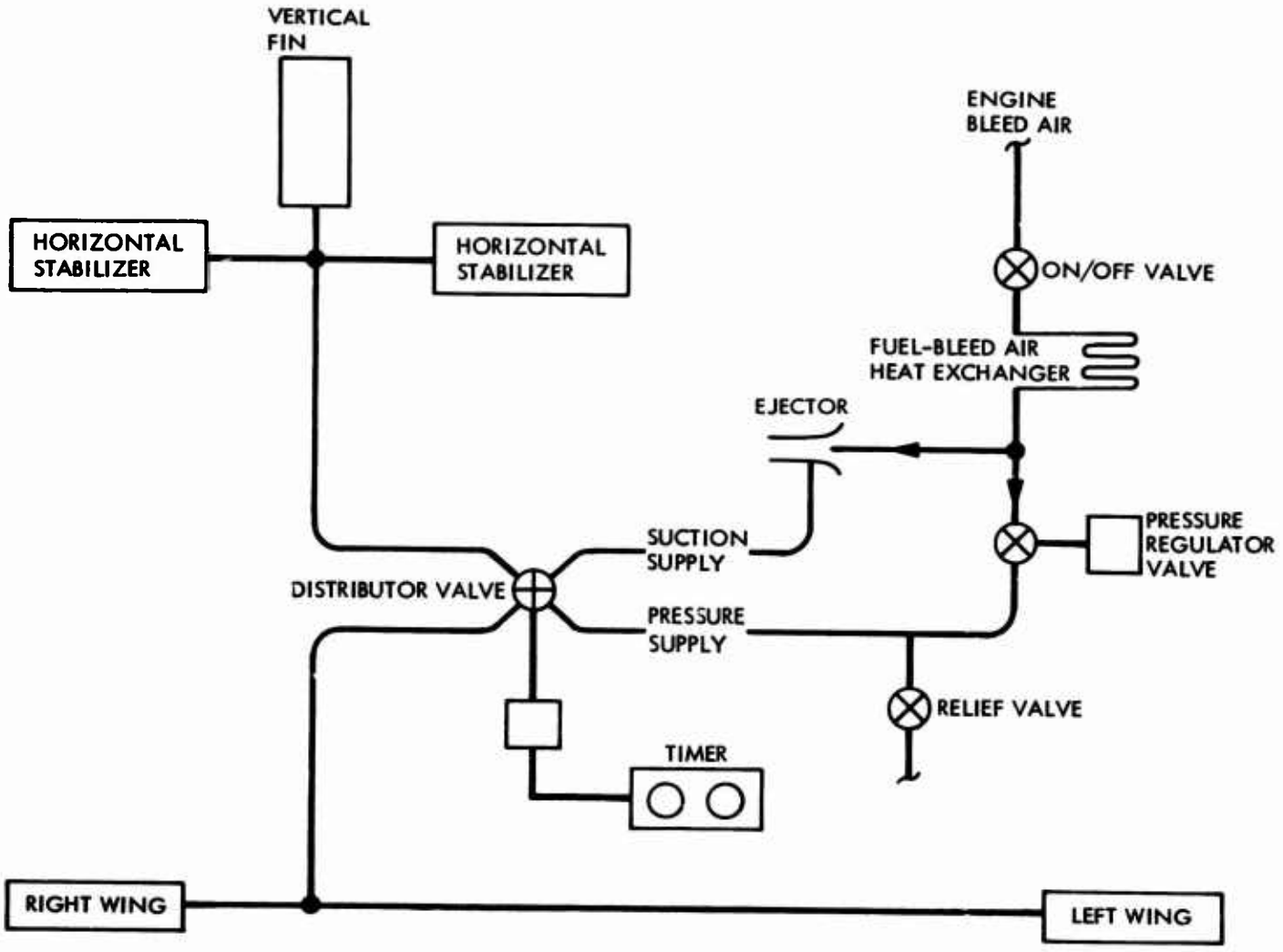

Figure 125. Schematic, Pneumatic Deicing System.

Thermal Deicing - In this technique, discrete elements are cyclically heated in sequence for durations between 7 seconds (electrothermal deicing) and 30 seconds (bleed air deicing). The duration of a complete cycle is on the order of 3 to 4 minutes. Unlike the continuous evaporative or running-wet system, the energy supplied to a thermal cyclic system is not absorbed in the airstream. Instead, most of the energy is used transiently to warm the skin surface and the ice interface to above 32°F; and some of the heat energy is also used to melt a very thin layer of ice. As soon as the thin ice layer is melted, aerodynamic and/or centrifugal forces sweep the unmelted ice from the surface. It can be appreciated that there is a significant saving in heating energy with a cyclic system. Cyclic thermal deicing energy requirements are not appreciably influenced by altitude and severity of icing parameters, but are dictated mainly by the coldest ambient temperature associated with icing. Either compressor-bled hot air or electrothermal heating can be applied for cyclic deicing. The P-3 and C-141 aircraft (horizontal and vertical stabilizer) have examples of electrothermal deicing, and the S-3 (wing and horizontal stabilizer) contains an example of bleed air deicing. Both techniques have been found to be equally acceptable as far as deicing performance is concerned. In terms of reliability and maintainability, however, hot air deicing has proven superior to electrothermal deicing on fixed-wing aircraft. On many aircraft, including the P-3, Electra, and L-1011, the hot-air anti-icing system can be operated manually in a deicing mode.

Rotor deicing by means of hot air has not been found to be feasible because of practical considerations. The problems associated with supplying the hot air to the rotor blades via large rotary seals are very difficult, if not unsurmountable. The leakage problems of such a system, the inherent poor reliability of such seals, and the space allocation requirements of cyclic valves and large-diameter air supply ducts are major disadvantages that render a hot-air deicing system for helicopter rotors unviable. As a result, cyclic rotor deicing by means of hot air has not found application on rotary-wing surfaces, and electrical energy has been found, so far, to be the most practical and acceptable technique for cyclic deicing of main and tail rotors of helicopters. However, this does not imply that the electrical deicing technique offers a satisfactory solution for rotor blade deicing from the points of view of reliability and maintenance. If anything, the in-servicing problems of deicing systems encountered on fixed-wing aircraft are compounded on rotary-wing craft because of the additional complexity introduced by sliprings, sophisticated controls, structural loads, and the sand environment. There is still a great deal of room left for improvement and further development of electrically heated deicers for rotary-wing aircraft.

The maximum ice accretion period (minimum deicing frequency) is related to the ice tolerance (and damage potential from shedding) for the affected surface. The minimum ice accretion period is determined by the total power available for the system, the power requirements and "on time" per unit area for deicing, and the total area to be deiced. It is, of course, desirable to have the largest possible spread between the minimum and maximum rates. The total energy per unit area for deicing (watt-sec/in.^{2})

decreases as the applied power (watts/in.^{2}) increases. Thus, it is more "efficient" to use very high watt densities for deicing, and a typical trade-off is shown in Figure 126. Although this curve was developed from tests in the Lockheed Icing Research Tunnel on a fixed airfoil surface using a continuously heated 1-inch-wide "parting strip" at the leading edge, it correlates very well with two sets of NRC data (References 74 and 75). For a fixed total available power, the number of segments which the protected area must be divided into increases as the power intensity increases; thus, the circuit and controller complexity increases. The final design, therefore, represents a "best judgment" trade-off between number of elements and efficiency. It is seen that, in any event, little is to be gained by using more than about 27 watts/in.^{2} (a power "on" time of 4 seconds). For a reasonable total power level and a cycle time of, say, 2 minutes, 30 segments would be required for a uniform and continuous alternator load. This has been considered an excessive number in the past; and a timer/controller in the rotor will be required to achieve an acceptable number of slip rings (four for three-phase power plus two for the controller).

Aerodynamic Discontinuity Principle (ADP) and Ice Phobic and Passively Deformable Surfaces - The ADP system as set forth in the patent by S. J. Jusyk (#3,173,491 assigned to United Aircraft Corporation) states that an ice phobic material applied discretely to the impingement area of the blade leading edge will prevent the ice accretions which normally handicap a rotary-wing aircraft. This approach to the blade icing problem is commendable for its simplicity, but unfortunately an adequate ice phobic material (a surface with very low ice adhesion) has not yet been found.

A substantial amount of testing has been conducted by various experimenters in the search for a material which exhibits and retains, for a reasonable service life, a low ice adhesion characteristic. The results to date indicate that certain liquids, pastes, and waxes applied to surfaces before icing are effective, but these are easily washed or eroded away and must be reapplied before each flight. Goodrich Icex is an example of such a material used as a temporary means of protecting propeller blades and of increasing the ice shedding effectiveness of pneumatic deicer boots. Icex has been tried on helicopter blades and resulted in insufficient protection after a few shedding cycles.

In 1962, J. R. Stallabrass and R. D. Price, of the National Research Council of Canada, reported on tests of ice adhesion to aluminum, stainless steel, titanium, teflon, and viton, in which they measured the shedding force of ice formed on these materials on a whirling arm (Reference 3). Their tests closely simulated natural icing of rotary wings. The results showed that ice adhesion was substantial on all of these materials, particularly at temperatures approaching 0°F, where helicopter blades typically become iced all the way to the tip. Teflon was the best material at low temperature, but showed an ice removal force per unit area of 15 psi, sufficient to create large unbalanced forces due to asymmetrical shedding (150 pounds to shed 10 square inches from one blade; 1500 pounds to shed 100 square inches). Other plastic materials such as polyurethane and polyethylene have also

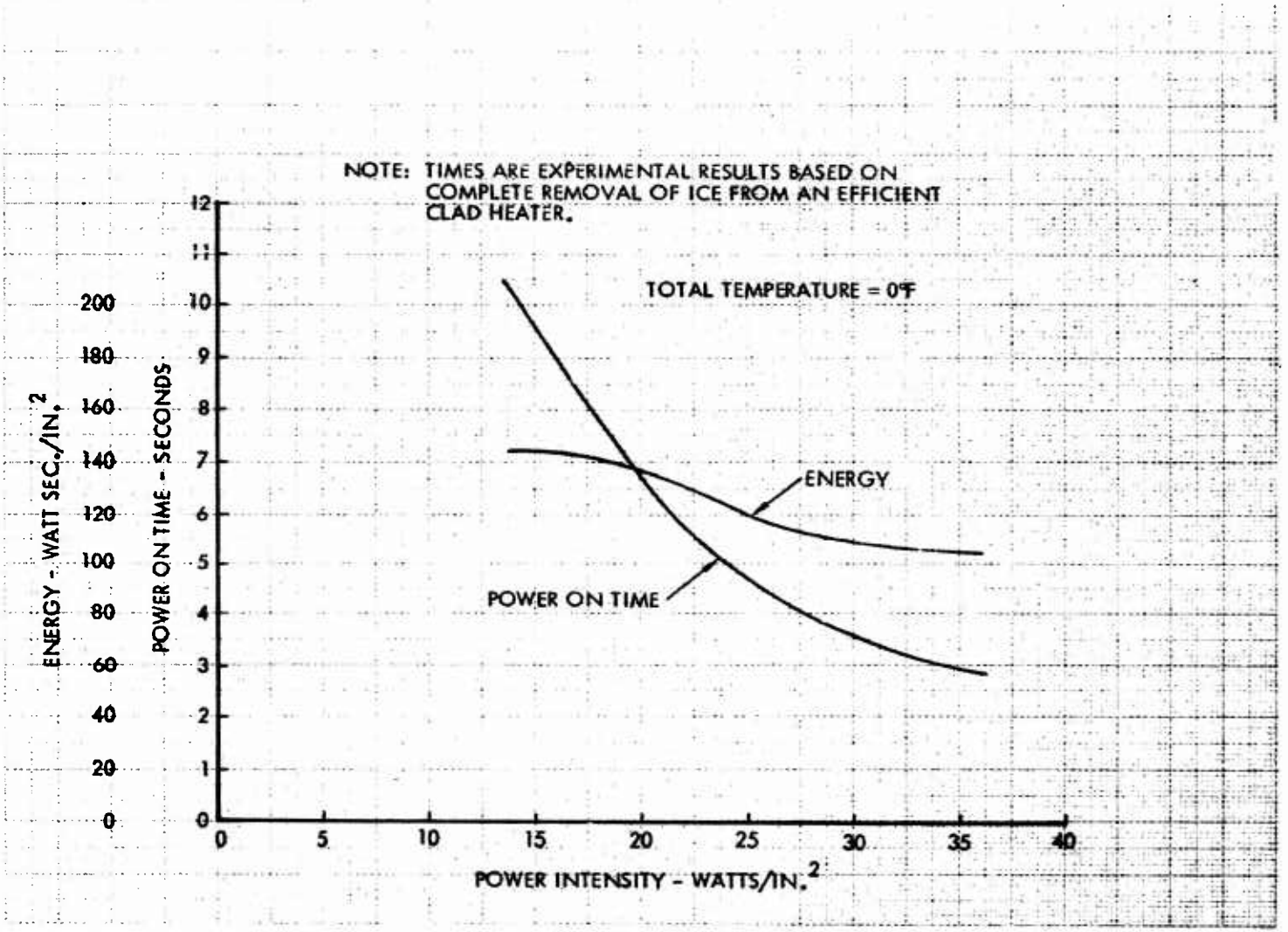

Figure 126. Power On Time and Energy vs Power Intensity for Cyclic Deicing.

been tested and exhibit similar ice release behavior when the material is new. After roughening by erosion, the ice adhesion strength increases, thus producing a higher potential unbalanced force during natural shedding.

In summary, treatment of rotor blade surfaces with different materials, including ice phobic, has not substantiated the claims that such treatment may obviate active ice protection techniques.

Recently, the Polymer Properties Group of the Royal Aircraft Establishment (RAE) at Farnborough (Reference 76) claimed laboratory success in constructing a blade with a passively "deformable surface" that permits tangential shear-stresses to be applied to the ice layer, causing cracks to form with resultant peeling of ice without an active system. The recommended formulation consists of a 1.6 mm thick elastomer, such as sponge rubber, applied to the leading-edge of the blade and covered with a stiff, thin (0.1 mm) plastic (polyurethane) or metal coating. It was claimed that with optimal design the coated elastomer combination is flexible enough to bend under an applied force, yet stiff enough to tend to be restored to its original position, causing a wave to be propagated along the surface. The periodic deformation causes the shedding of the ice.

Operation tests to demonstrate this principle were conducted during the winter of 1970-1971 at the Ottawa NRC icing test facility on a helicopter with two out of four blades coated as described above. The purpose of these tests was to determine the feasibility of applying this technique to the Wessex HU-5 helicopter, which has the same blades as the S-58. During the winter of 1972-1973, operational tests have been completed in Ottawa on helicopters with all blades being coated. Verbal telecon information from the cognizant NRC personnel on the technical merits of this ice-shedding technique revealed that this method remains effective only for the first icing encounter and, in this respect, its effectivity is no different from that of hydrophobic coatings. Erosion of the coating and rapid degradation of the shedding performance after the first icing encounter render the polymer combination useless. For these reasons the use of the polymer combination on the Wessex UH-5 was rejected, and further feasibility for potential application is not considered herein.

5.2 PAST AND EXISTING ICE-PROTECTION INSTALLATIONS ON ROTARY-WING AIRCRAFT

5.2.1 Main and Tail Rotors

5.2.1.1 Hot-Air Protection

With the trend in the direction of ever-decreasing specific air consumptions (lb/sec of air per hp), bleed air extraction becomes a greater percentage of the gas generator airflow; not only does it cause a significant increase in specific fuel consumption, but most important, use of engine bleed air for evaporative rotor blade anti-icing would require a flow rate in excess of the operational limit of the bleed-air quantity usually

specified by the engine manufacture. Therefore, use of bleed air for rotor anti-icing has not found an application on modern helicopters. There are two known cases wherein combustion heaters were used to attempt hot-air anti-icing of rotor blades. This was done on two experimental prototypes and did not involve any production type hardware. A heated air blade anti-icing system was built and tested on a Bell helicopter using combustion heaters mounted on each blade root. The Bell helicopter was a prototype of the HU-1. A similar system was installed on a piston-engine-driven prototype of the Boeing/Vertol H-21. An open-blade construction was required to pass sufficient air spanwise to heat the entire chord. With air at 400°F introduced at the blade root, the Bell system operated as a marginal "running-wet" anti-icing system. Both companies abandoned this effort because the fixed weight, fuel weight, and cost of such a system were not justified in view of the marginal, and often unsatisfactory, anti-icing performance.

5.2.1.2 Chemical Systems

Chemical ice prevention and removal systems have been used in both fixed-wing (References 74, 77 and 78) and rotary-wing applications (References 79 thru 83). The chemical systems used on rotary-wing aircraft are composed of a fluid supply, a pump, a distribution arrangement at the point of icing, switches, control valves and instruments, as shown typically in Figure 127 for the prototype system installed on a UH-1 helicopter. The fluid used as an ice depressant is usually an ethyl alcohol/glycerine mixture.

The distribution system used on the UH-1 helicopter two-bladed main and tail rotor utilized a fluid applicator consisting of grooves milled into the forward and aft surfaces of the rotor nose block, and holes drilled into the stainless steel leading edges. This arrangement is shown in Figure 128 for the protected main rotor blade. The aft grooves supplied fluid to the leading-edge grooves at various locations along the blade span. The leading-edge grooves distributed fluid to the holes in the stainless steel leading edge.

A slinger ring was used to transfer the fluid from a fixed nozzle to the rotating blades, as shown in Figure 127. The fluid was supplied to the blade by centrifugal force resulting from the rotational velocity of the slinger ring. Flexible hoses were used to direct the fluid from the slinger rings to the rotor blades.

A selector switch located on the pilot's panel allowed selection of mode of operation, i.e., continuous flow, cyclic flow, or system off. The main and tail rotor rates of flow were set by adjusting appropriate needle valves to obtain the pressure gage reading corresponding to the desired flow rate. A timer was used in conjunction with a bypass valve to cycle the main rotor flow on and off. The tail rotor flow was kept constant during the main rotor off-on cycle.

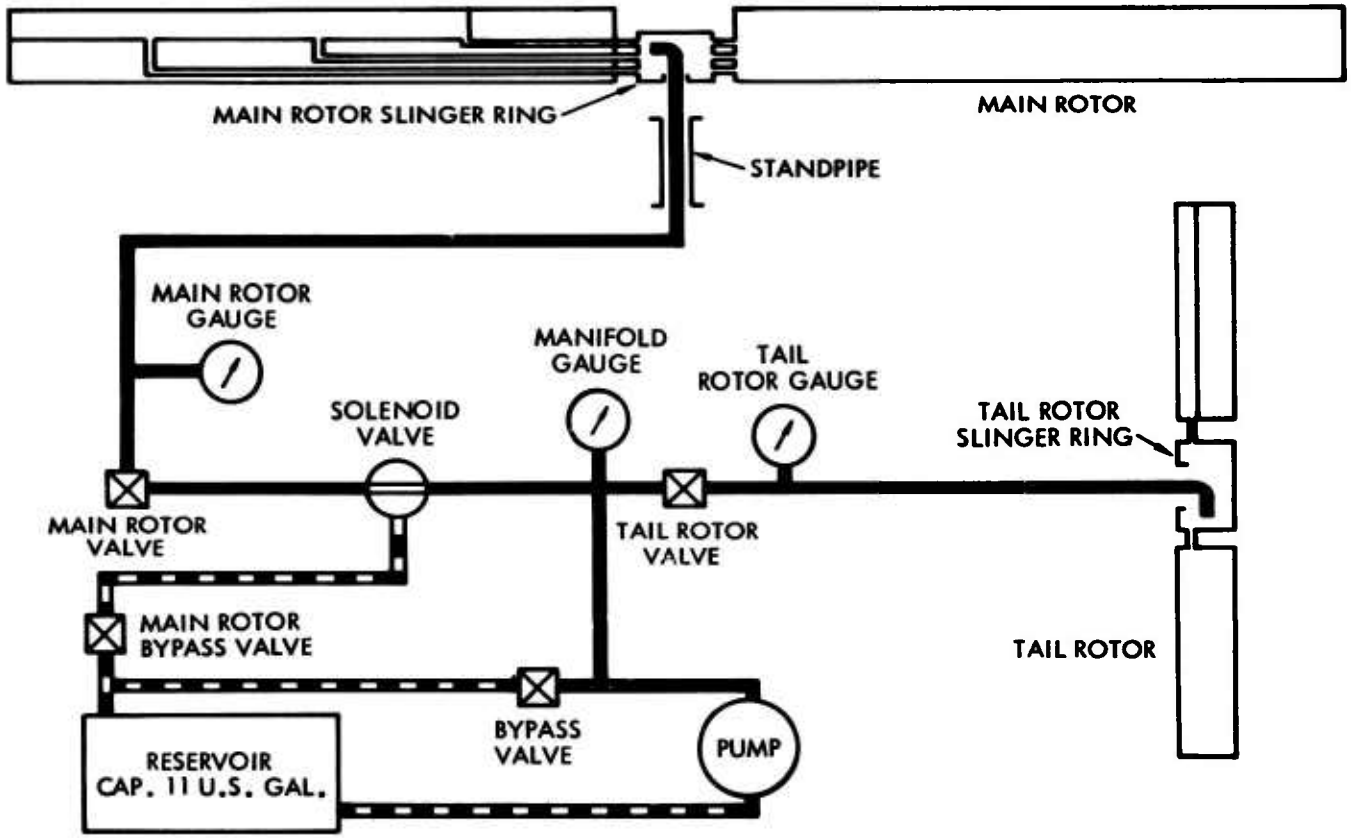

Figure 127. Schematic of Fluid Ice-Protection System.

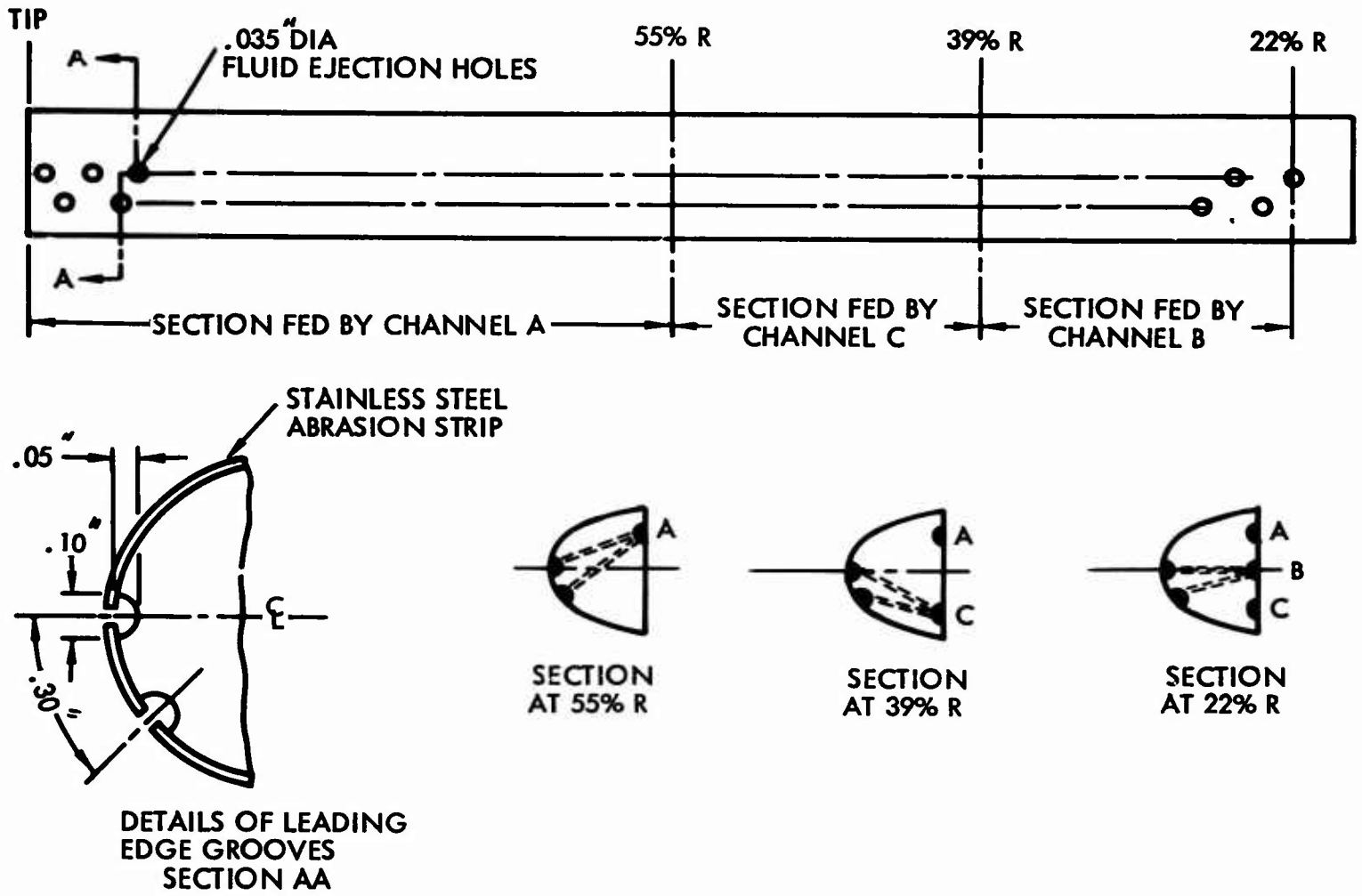

Figure 128. Details of Fluid Ice-Protected Main Rotor Blade.

The fluid reservoir used had a capacity of 11 gallons. The fluid was supplied to the system by a fuel pump at a rate of 43 gal./hr at 15 psi pressure. A similar ice protection system was used on the three-bladed main rotor of a British helicopter, the Sycamore MR 14XE 308 (Reference 83). The main difference in the systems was the distribution method, which consisted of a hollow rubber duct in the leading edge of each rotor blade into which were pressed jet spray nozzles. The nozzles distributed along the blade span each had a specially selected metering hole to effect a suitable fluid distribution and two spray holes to dispense the depressant fluid onto the blade. Good anti-icing and deicing was achieved using a flow rate of 28 gal/hr with a fluid capacity of 30 gallons. The distribution system of this arrangement is shown in Figure 129.

To improve the coverage of the depressant on a surface subjected to icing, porous surfaces have been proposed as the injection device in an effort to uniformly distribute the fluid. The porous surface would be fabricated from furnace welded laminations of woven stainless steel wire. Micronic filters are used in the system to protect against internal pore blockage. Figure 130 shows a porous leading-edge distributor panel which can be manufactured in spanwise lengths up to 36 inches. The fluid deicing system has been tested in an icing tunnel. The model tested was a wing section without leading-edge sweep and rigidly mounted as shown in Figure 131. Although the results from the tests (Reference 73) indicate that shedding of the ice cap was not demonstrated, it is expected that a rotary-wing application would be conducive to better ice removal with the porous surface distribution system.

The rotary-wing installations (as noted above) have consisted of orifices or nozzles in the leading edge of the main and tail rotor blades. These distribution devices were used to inject a freezing-point depressant fluid into the stagnation region airflow to coat the blades for anti-icing protection, or between the ice-airfoil interface to weaken the ice bond to the blade and thus permit aerodynamic or centrifugal forces to remove the ice.

It has been found that, as a deicing means, the chemical systems must be utilized within 2 to 3 minutes of initial ice encounter. This requires continuous system operation until the ice buildup is shed. A cycling of the depressant fluid injection may, thereafter, provide protection. The distribution of the injection holes in the leading edge of the blade is critical as to whether or not ice is shed before sufficient buildup causes a rotor unbalance with subsequent excessive vibrations.

Tests have indicated that good protection can be achieved when adequate fluid is supplied to a surface subjected to icing impingement. However, development is required for each application to obtain a distribution system (whether it be orifices, nozzles or porous panels) to provide the desired fluid coverage, particularly at extremes of the angle-of-attack range. A sensitive ice detection system is also required to ensure that the fluid depressant is turned on as soon as possible after icing is encountered

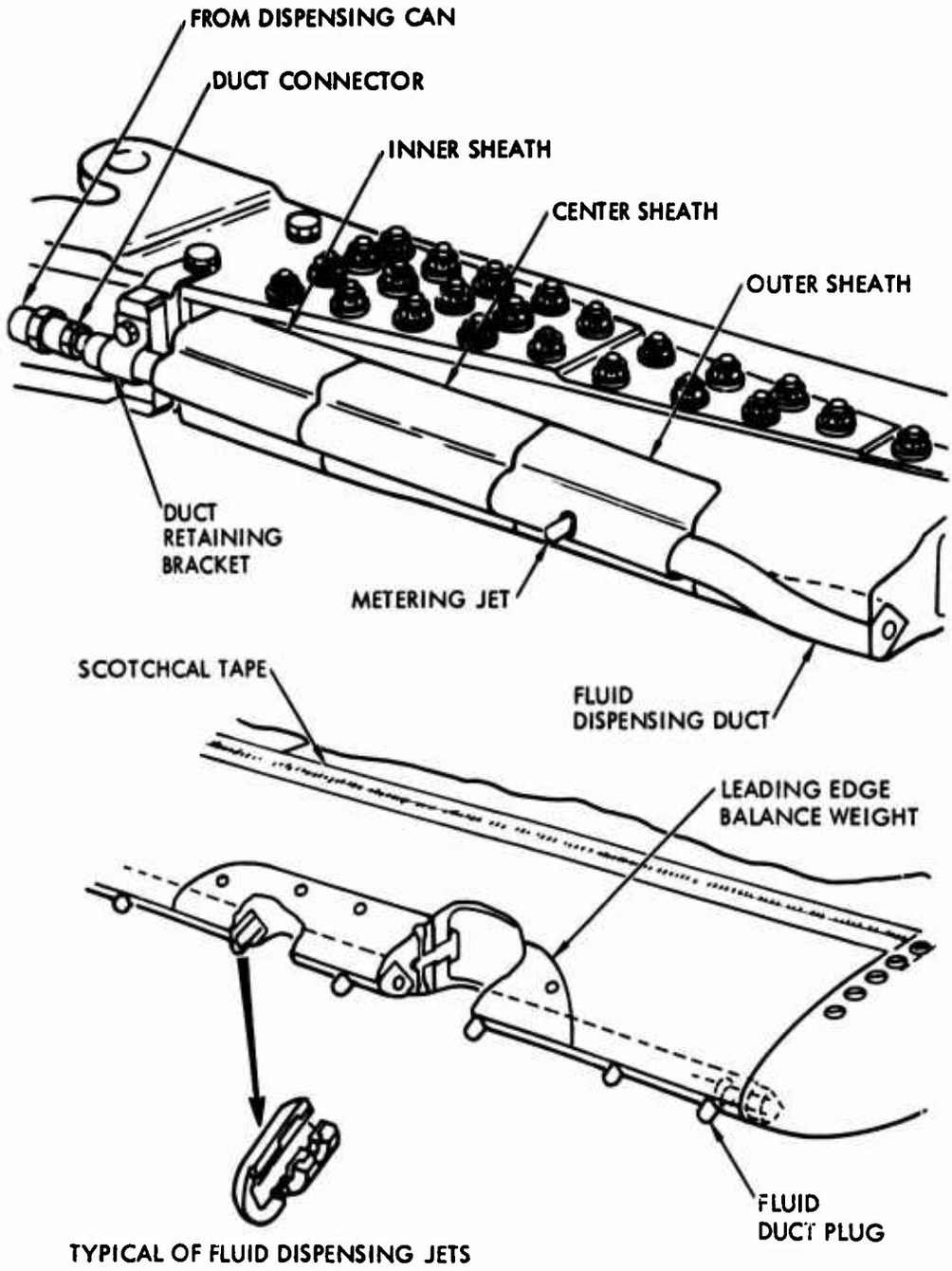

Figure 129. Leading-Edge Fluid Distribution Concept.

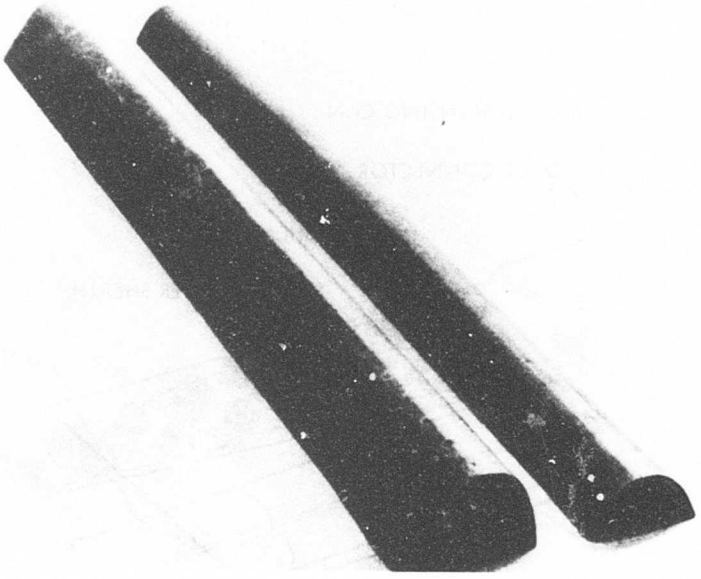

3/4 Front View - Test Panels.
Porous Leading Edge

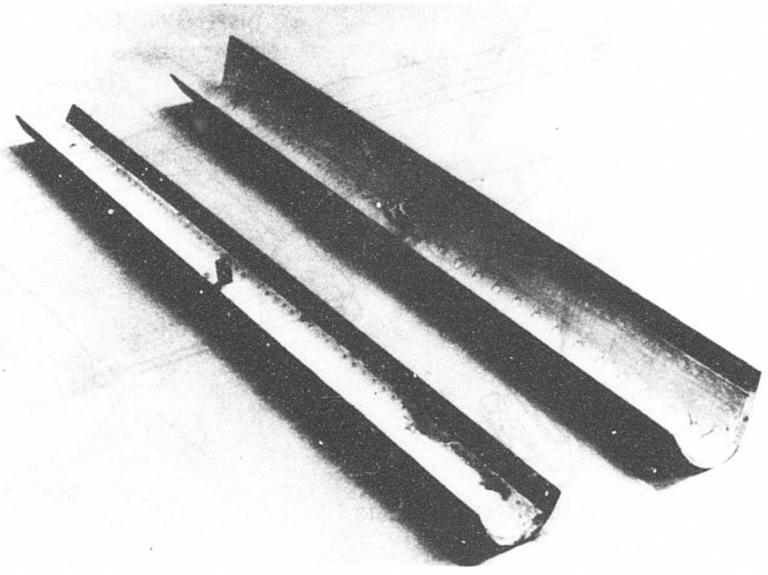

3/4 Rear View - Test Panels.

Figure 130. Porous Leading-Edge Fluid Anti-Icing System.

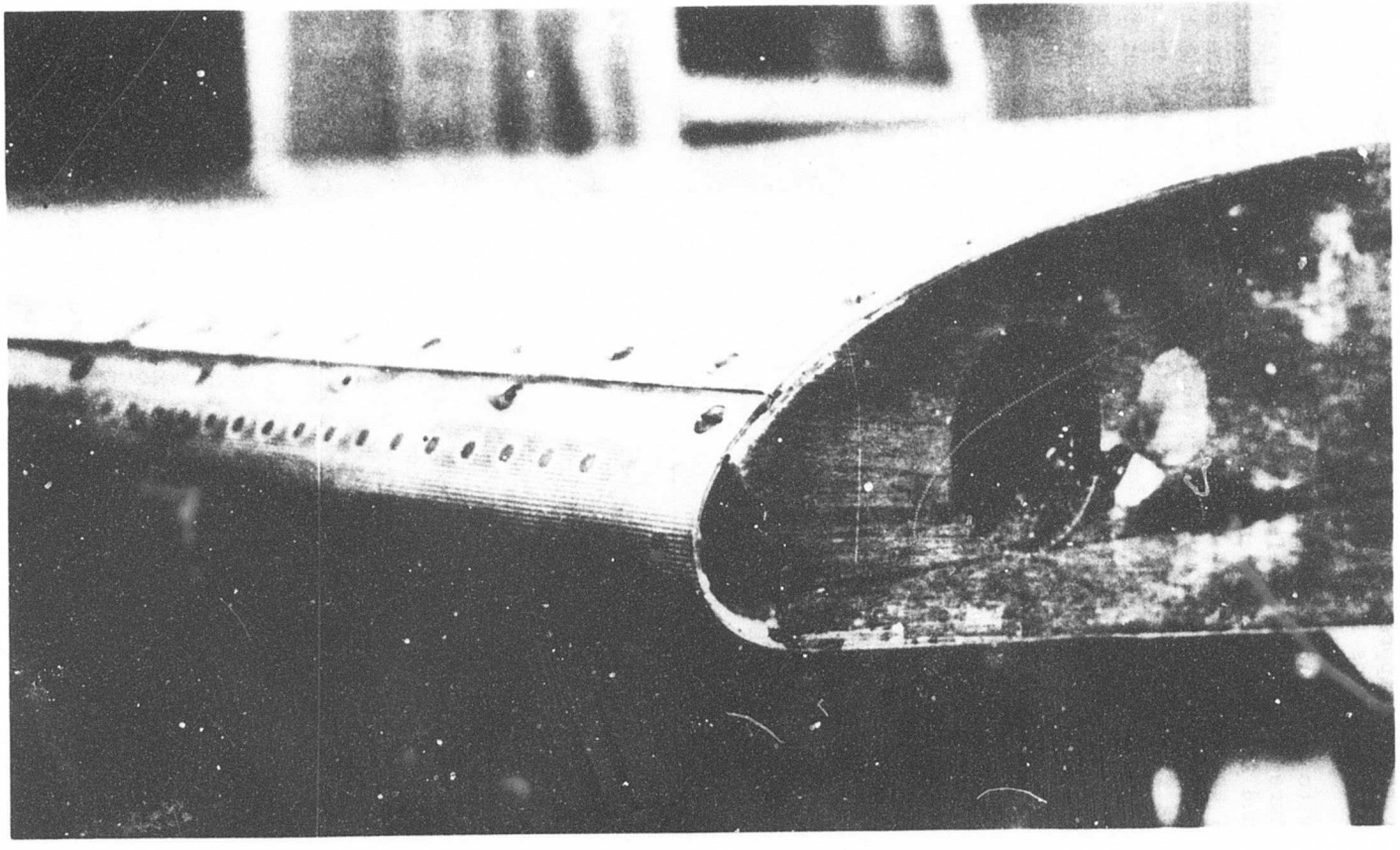

3/4 Front View of Wing Model with First Test Panel Installed.

Figure 131. Porous Leading-Edge Icing Tunnel Model.

in order that no appreciable ice thickness can build on the rotor blades and cause vibrations from asymmetric shedding.

In order to calculate the quantity of liquid depressant required, a datum temperature is used as a reference (Reference 66). The water catch rate is determined from the flight and climate conditions, the configuration of the airfoil, and the collection efficiency, which is also a function of flight and climate conditions as well as geometry of the airfoil. With the selection of a freezing-point depressant (e.g., percentage of ethylene glycol in water) and its relation to the datum temperature, a flow rate of the depressant can be determined to prevent freezing of the mixture of the water catch and depressant. Distribution as described above plays an important factor. The theoretical approach assumes that the depressant completely covers the surface. However, experience has shown that this is not necessarily true, as aerodynamic and/or centrifugal forces can shed ice even though coverage has not been complete. In any case, excess depressant is required to assure that the ice is removed. The equations used in the theoretical approach are summarized as follows:

Datum Temperature (wet air boundary layer temp., t_{ok}, °F)

$$t_{ok} = t_o + \frac{(1.688\ U_o)^2}{2gJCp}\left[1 - \left(\frac{V}{V_o}\right)^2\left(1 - Pr^{1/2}\right)\right] - 0.622\ \frac{Ls}{Cp}\left(\frac{e_{ok}-e_1}{P}\right)$$

Depressant Rate Required To Prevent Freezing (lb/hr-ft span)

$$W_f = \frac{G\ W_M}{X - G}$$

where t_o = ambient temp., °F

U_o = flight speed, kt

V = local velocity along surface, fps

V_o = free stream velocity, fps

Pr = Prandtl number (for air)

Ls = Latent heat of evaporation of water, Btu/lb

e_{ok} = vapor pressure of air at surface of airfoil, in. Hg

e_1 = vapor pressure of saturated air at edge of boundary layers, in. Hg

P = pressure just outside the boundary layer, in. Hg

W_M = water catch, lb/hr-ft span

W_f = weight of freezing depressant, lb/hr-ft span

G = percent of freezing point depressant in final mixture - by weight

X = percent of freezing point depressant in the fluid mixture

Figure 132 contains a typical solution of the datum temperature equation for a specific altitude. Given the ambient temperature and flight speed a datum temperature is selected from this graph. To satisfy the datum temperature for the flight and climate conditions, the experimental data of Figure 133 may be used to determine the percentage by weight of depressant required to prevent freezing. Figure 134 shows the variation of a glycol-water mixture depressant (both theoretical and test results) required with increasing liquid water content for constant flight and climate conditions of a radome surface as reported in Reference 82.

5.2.1.3 Electrothermal Deicing

The Canadian Forces CHSS-2 will have the capability for sustained flight under moderate natural icing conditions due to the electrical cyclic deicing system installed on the rotors. For the rotor system, tests determined that a 1/4-inch ice buildup on the blades was reasonable between deicing cycles, and this could occur in as little as 2-1/2 minutes. This time interval has been established as the element "off" time and is a fixed value regardless of icing severity. Element "on" time is a function of ambient air temperature in accordance with the schedule shown in Figure 135. Also shown in this figure are element "on" times for the Wessex HU5, Vertol 107 (CH113), Kaman UH-2C, CHSS-2, CH124, and Bell 47G2. Since not all systems employ the same element power density, the curves have been redrawn in Figure 136 to show watt-sec/in.^{2} versus ambient temperature.

An early theoretical deicer boot performance map is found in Reference 84. Figure 137 shows a more recent theoretical deicer boot performance comparison. This figure is taken from a 1972 article (Reference 85) and represents analytic time histories of a one-dimensional laminate structure. A cross-plot of the 25 watt/inch^2 power input of Figure 137 is replotted as curve 7 on Figure 136. Two points of interest should be made. The first is the superposition of the Kaman design, curve 4. This vehicle was designed just after Reference 84 became popular. Although it was tested in the NRC spray rig and its icing characteristics were found marginal, the need for improved performance has never been pushed. In fact, the latest vehicles (SH-2D) are without rotor ice protection due to the lack of usage and the typical maintainability/reliability problems. Second, the difference between the rest of the vehicle data and the theory is by factors of from 3 to 5 times greater energy requirements. These differences are treated at some length by the NRC in Reference 85 and are attributed to three main effects: (a) the impact of two-dimensional heat flow in contrast to one-dimensional flow; (b) the impact of delayed heating over the

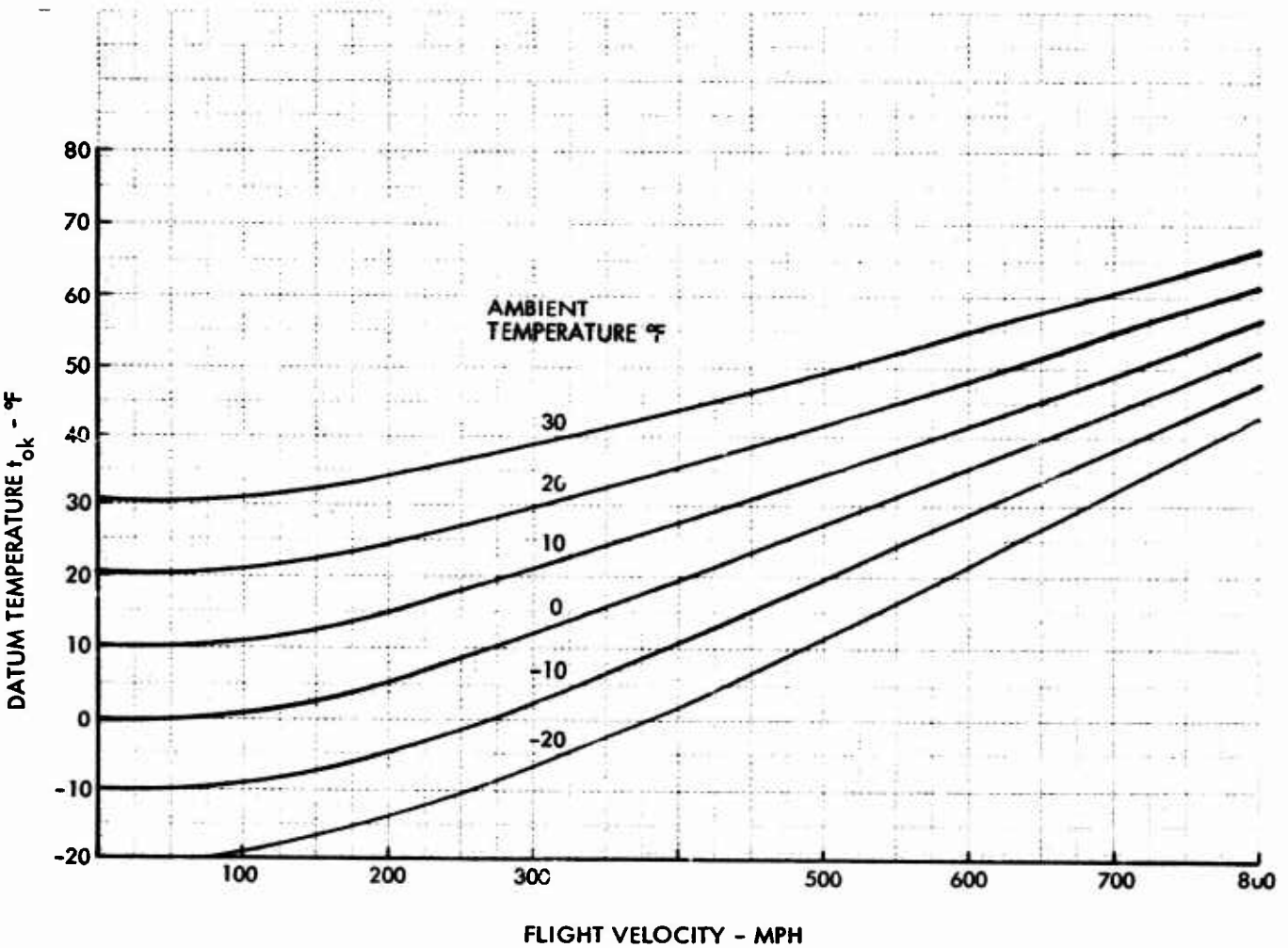

Figure 132. Datum Temperature at 10,000 Ft - Temperature Versus Airspeed.

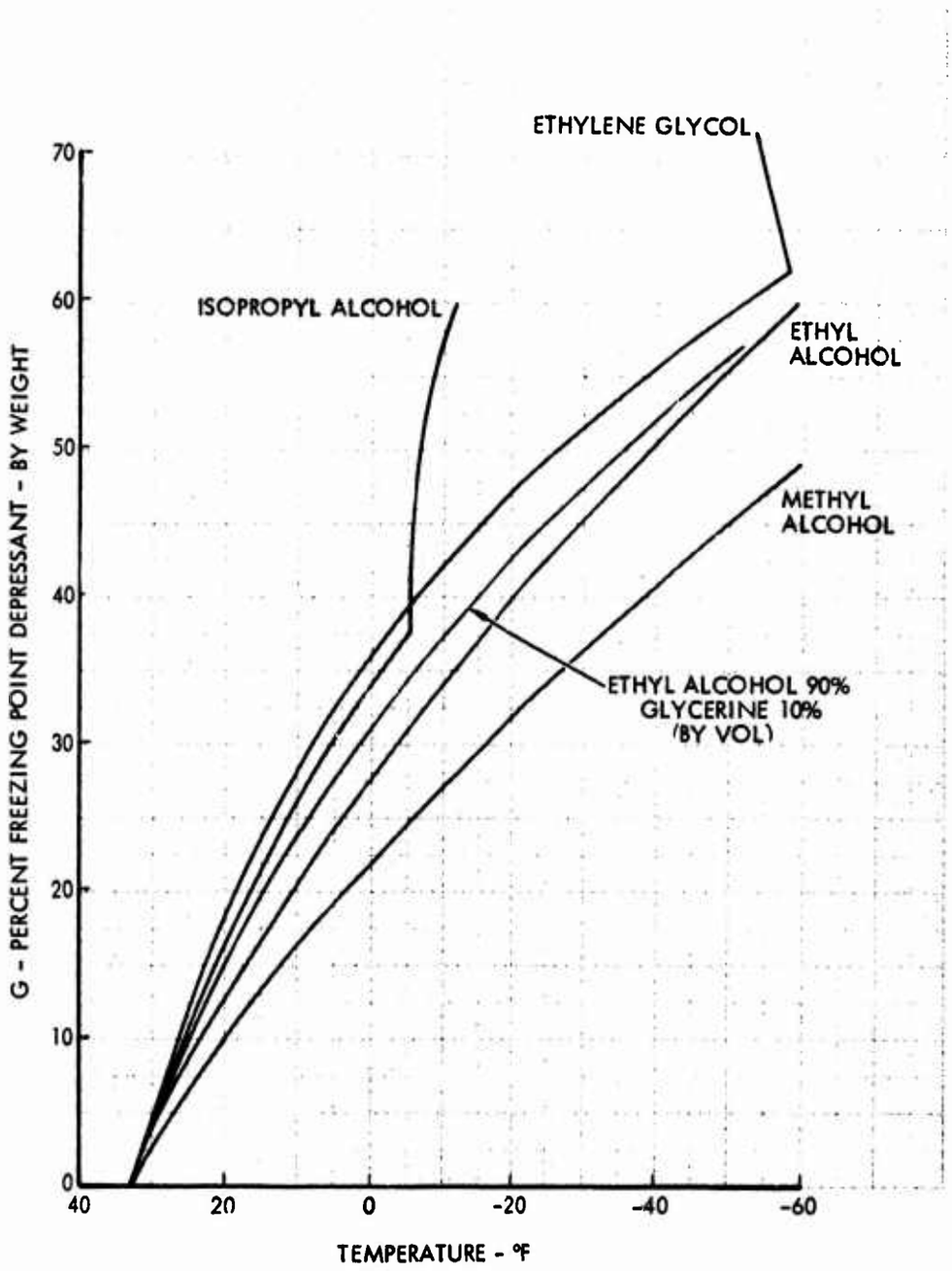

Figure 133. Freezing Point Plots for Aqueous Solutions of Several Freezing Point Depressant Fluids.

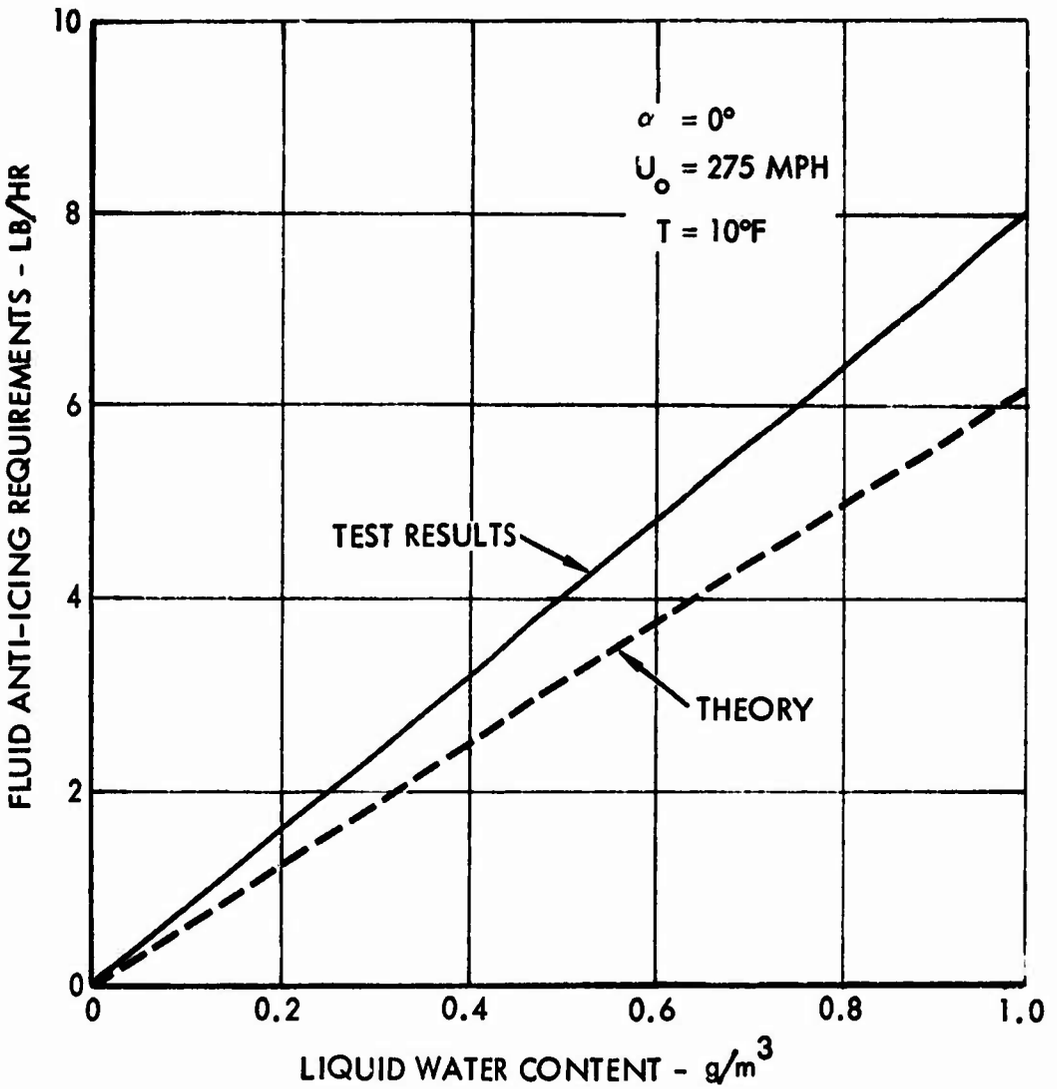

Figure 134. Variation of Fluid Anti-Icing Requirement With LWC.

(1) CANADIAN AETE REPT 68/92 "CHSS-2 AND SH-3D HELICOPTER ICE PROTECTION SYSTEM TRIALS" 23 JULY 1969.

(2) ROTOR LTD. ENGINEERING REPORT, REFERENCE N.E.S. 2473 (22 JULY 1970) "DESIGN STUDY FOR ICE PROTECTION OF THE WESSEX HU5 HELICOPTER ROTORS"

(3) VERTOL DIVISION/BOEING REPORT 107-T-299, ADDENDUM 1 (26 MARCH 1963) "FLIGHT TEST REPORT OF AN EVALUATION OF THE 107-II"

(4) LETTER (8 AUGUST 1971) G.I. HACKENBERGER, JR. (KAMAN) TO J. B. WERNER (LOCKHEED) "UK2C/HH2D ICING SURVEY: ROTORCRAFT PROTECTION"

(5) J. HELICOPTER ASSOCIATION OF GREAT BRITAIN, "CANADIAN RESEARCH IN THE FIELD OF HELICOPTER ICING," VOL. 12, NO. 4, AUGUST 1958.

(6) CANADIAN AETE REPORT 70/89 "CH124 FOD SHIELD ICING TESTS" 7 JUNE 1971.

(7) "THERMAL ASPECTS OF DE-ICER DESIGN," J. R. STALLABRASS, INTERNATIONAL HELICOPTER ICING CONFERENCE, OTTAWA, CANADA 23 - 26 MAY 1972.

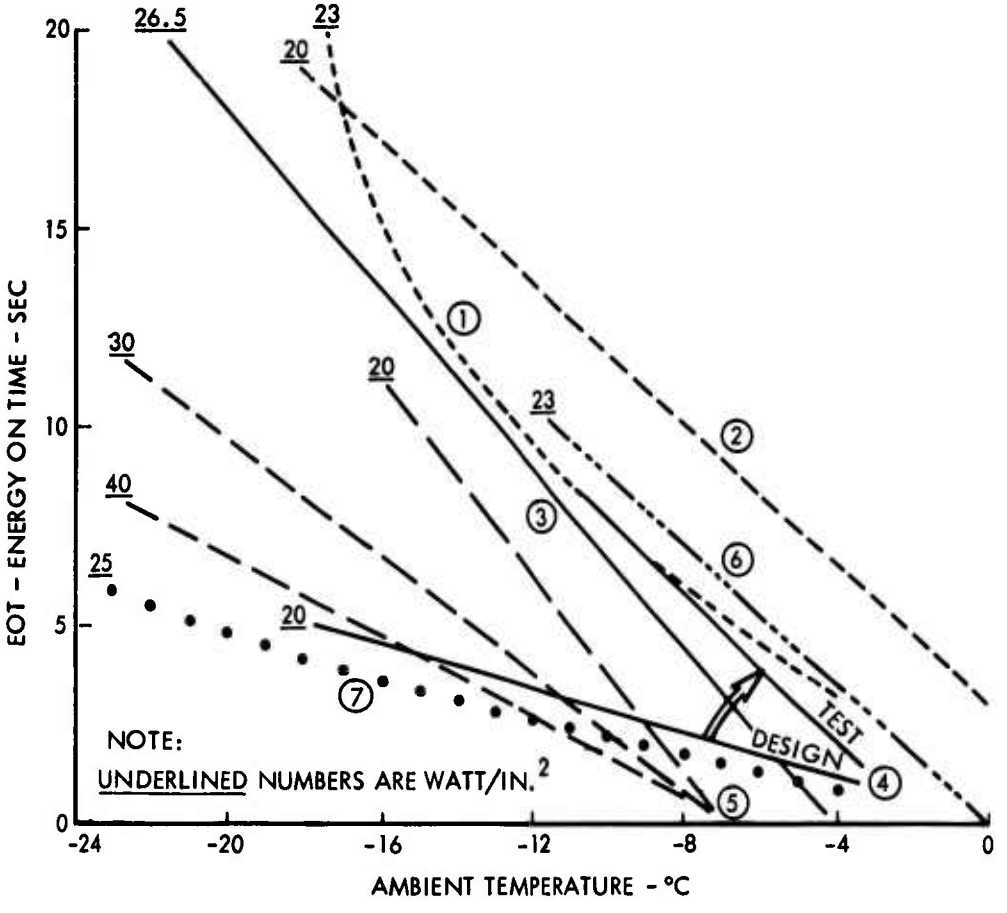

Figure 135. Energy On Time for Helicopter Rotor Blade Deicing

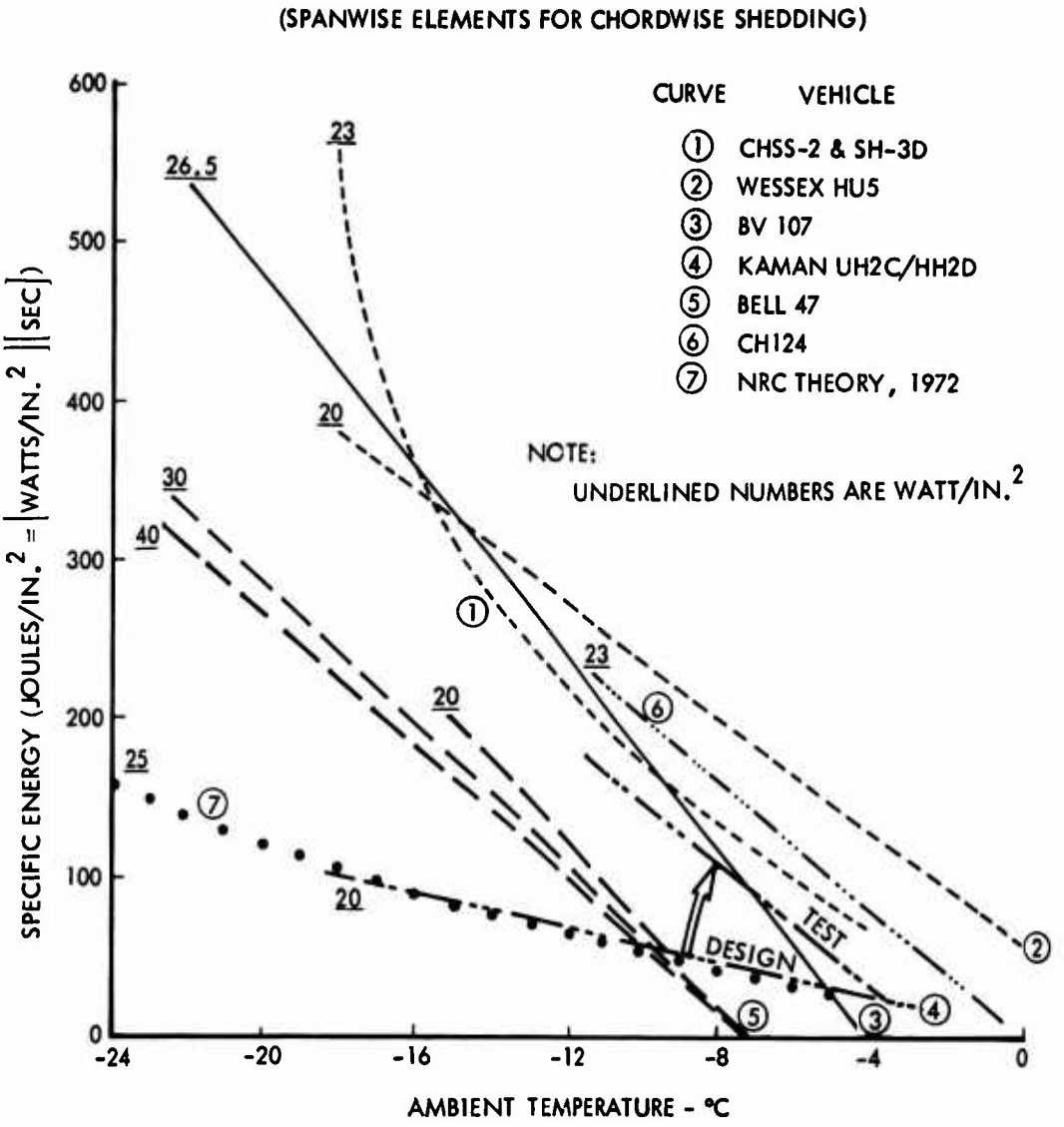

Figure 136. Electrical Deicing Energy for Helicopter Rotors.

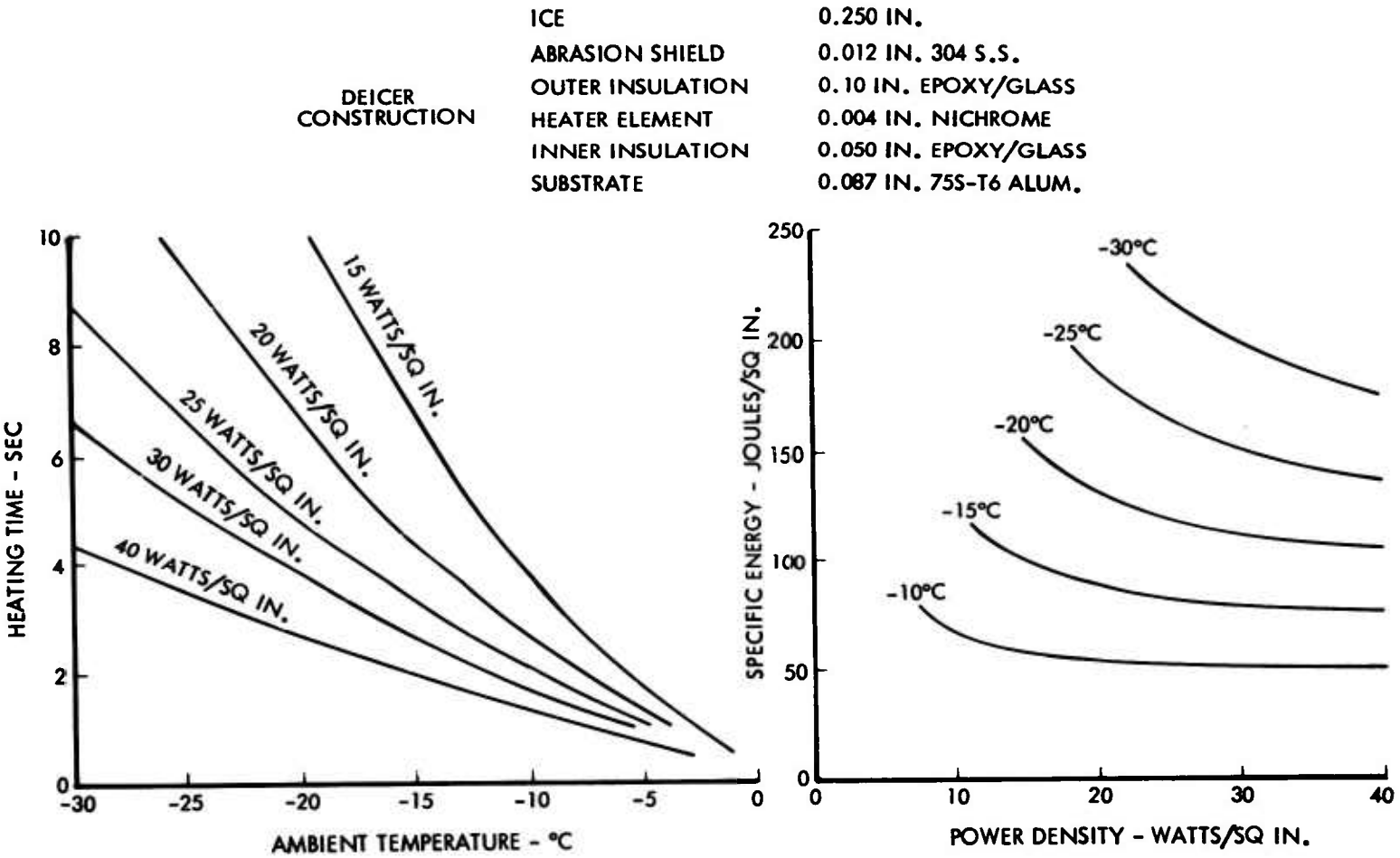

Figure 137. Effect of Power Density on Deicer Performance.

gaps between heater elements, and (c) the one and two-dimensional effects of the melting water interface. The net result of these influences is to increase the energy-on-times (EOT) by a factor of about four, thus explaining the experimentally observed results.

That the geometry of the vehicle/rotor system does affect the energy requirement is also hidden in Figures 135 and 136. All of the vehicles tested were single rotor systems except for curve 3 for the tandem-rotored BV107/CH113/CH46. Vertol attributed the lack of energy requirements in the region -4° to 0°C as being probably due to the aerodynamic slap phenomenon peculiar to this type of vehicle as the forward and aft rotor blades pass over one another. Detailed study of transient blade surface pressures on a larger tandem, the CH-47, indicated a wide span of supersonic flow regions with attendant pulsating shocks to the blades. Thus an attribute that was unfavorable to blade box integrity is probably also unfavorable to ice adhesion, at least under conditions below a minimum adhesion threshold.

On a similar CH-124, as reported in Reference 86, engine torque requirements increased 15 - 20 percent between deicing cycles during natural icing flights (a forward speed of 100 knots, an OAT of 12°F, and a main rotor cycle "off" time of 195 seconds). This note on torque variation represents the only available data on the expected performance penalty with rotor blade deicing. Unfortunately, the liquid water content meter was not operating correctly on the flight; thus, there was no record of icing severity except to note that it was moderate.

There are many factors which enter into good electrical heating element design for a cyclic deicing system, and all must be included before the installation can be considered as satisfactory. (The requirements for a continuously heated running wet system are not as exacting, as will be discussed later.) The factors which determine the efficiency of the heater are:

1. Uniformity of heating

2. Amount of insulation between heater element and structure

3. Amount of insulation between heater element and iced surface

The uniformity of heating is determined by the design of the heating element itself and the conductance of the surface material. Uniformity of heating is desirable in that all areas of the iced surface would reach 32°F simultaneously, and there would be no hot spots to cause undue runback of water rivulets to an unheated area. Ideally, a film type of element with uniform resistance (ohms per square) and of rectangular planform should be used. However, a film of good, uniform resistivity has not been developed. Typically, the resistivity of a windshield type unit is allowed to vary ±20 percent. Also, nonsquare corners cause serious problems since there can be current concentrations in acute-angled corners (resulting in possible overheat problems) and current deficits in obtuse corners. Consequently,

electrical heating elements may be made of closely spaced resistance wires in a rubber or plastic base, ribbons of nichrome or stainless steel, an etched stainless steel foil grid, a spray-on grid pattern, or for small areas, calrods. The best choice of a heater design depends upon the power density required, whether for anti-icing or deicing, the amount of compound curvature, and the number of parts to be made.

Early cyclic deicing boots were made with wire-imbedded rubber heating elements, using either 8 or 16 wires/inch at 20 watts/inch^2. These designs turned out to be unsatisfactory due to excessive thermal gradients: there were large variations in surface temperature between the wires, requiring very high wire temperatures to assure that all parts of the surface would be above freezing (causing burnouts). Control of wire spacing during manufacture also proved to be a problem, and to some extent this can be controlled by incorporating the wire in a cloth weave or knitted fabric. For a deicing system, a very close wire spacing is required (along with metal cladding) to achieve an efficient heater system. A minimum of 20 wires/inch is required, and there is a benefit to an even closer spacing. Metal cladding is also shown to be very beneficial in achieving a more uniform surface temperature (References 87 and 88).

A nichrome ribbon type element has also been utilized, but problems occur at the turnaround at the end of the heating element: if the material is folded to change direction, there will be an increase in material thickness, causing a reduction in resistance and a resultant cold spot. Satisfactory designs have been achieved using an etched foil or a sprayed-on element pattern, with the etched foil design probably having lower manufacturing cost for a high production-rate program and the sprayed element design being easier to apply on surfaces with compound curvature. In any event, it is of crucial importance, when using metal cladding, to obtain a void-free bond between the cladding and the dielectric.

Any voids will cause cold spots on the surface and premature heater element failure. Obtaining the necessary fabrication quality is possible through use of appropriate vacuum bagging bonding techniques, and a very careful inspection is also required to assure that the completed assembly does indeed perform as intended. A technique which can be used for inspection is the use of a wax or paint which changes color at a certain temperature; the assembly is coated with this material and the uniformity (and speed) of temperature change is noted, often by color movies.

Figure 138 is a cross section of a modern heater mat design. While it is highly desirable to have as thin an insulation as possible between the cladding and the heating element, current materials limit the minimum dielectric thickness to approximately 0.010 inch. Typical heating element thicknesses are about 0.003 inch. In general, the thicker the insulation between the heating element and the substructure, the better, as shown in Figure 139, but there is a weight penalty. The usual compromise is to make the backside thickness 2.5 - 3 times that of the front dielectric.

(NOMINAL DIMENSIONS)

NOMINAL WEIGHT (LESS 0.030" SKIN) = 0.48 LB /SQ FT

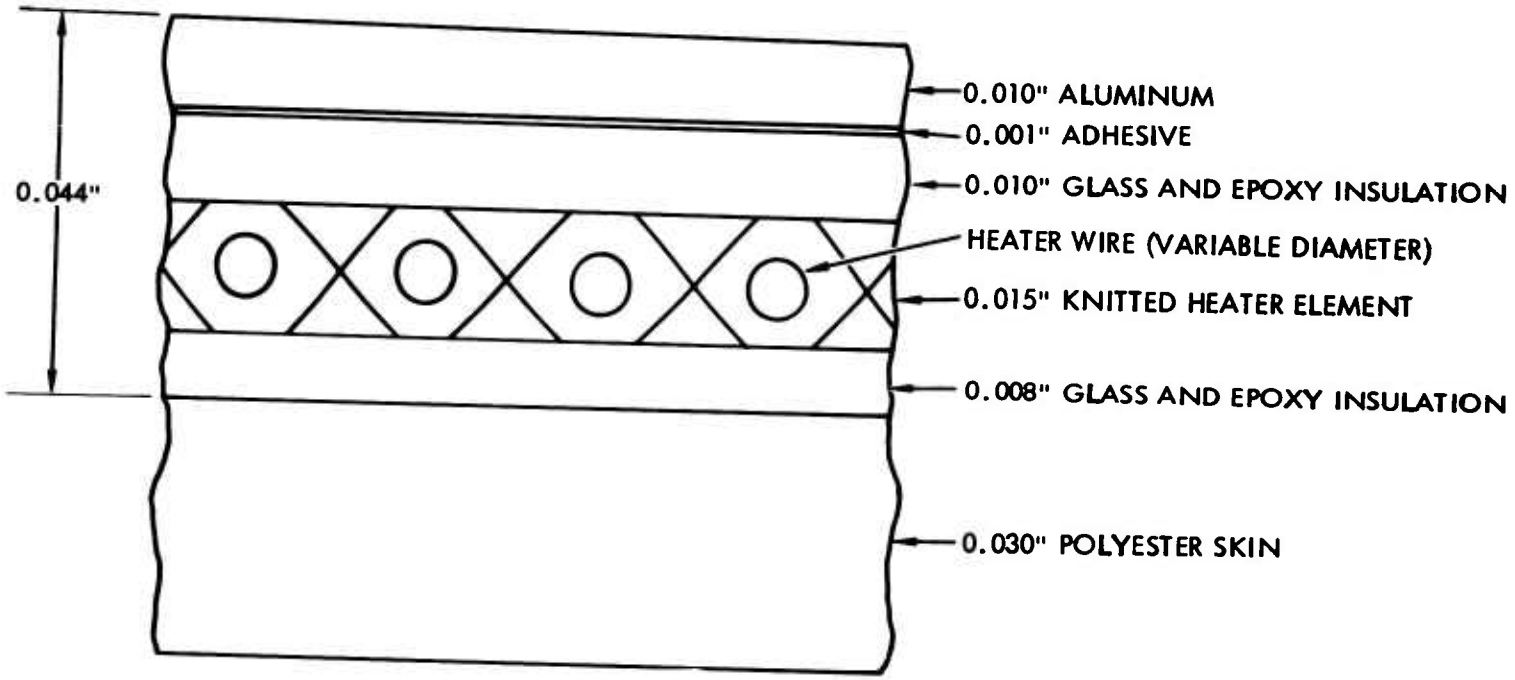

Figure 138. Heater Element Construction.

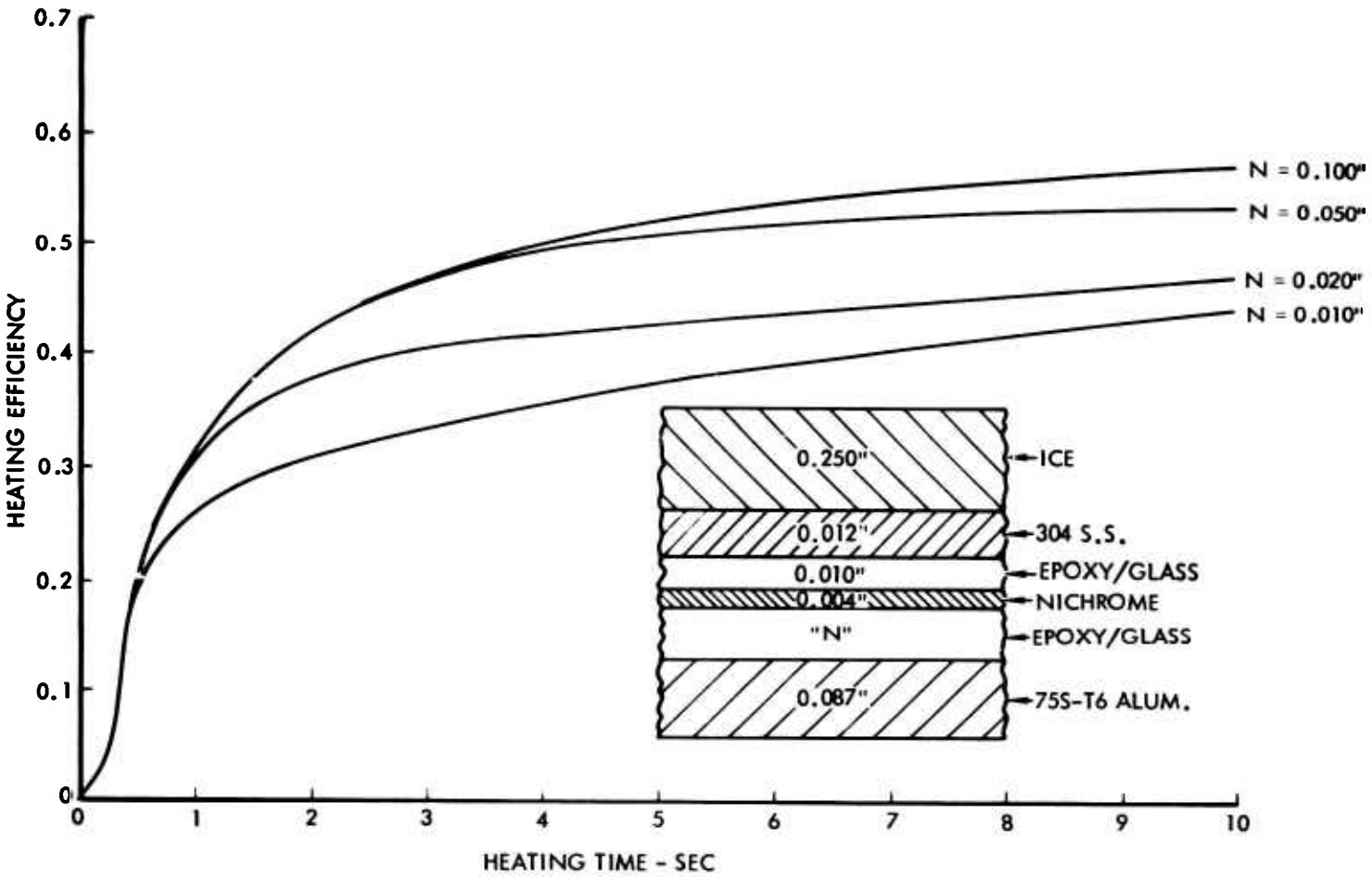

Figure 139. Heating Efficiency vs. Heating Time for Various Ratios of Inner to Outer Insulation Thickness.

In the mid-'60's, some research was being conducted on the use of a Mylar dielectric, which would permit values as thin as 0.003 inch for the outer insulation. However, the bonding problems were not solved, and the idea was dropped. Since substantial thermal, weight, and aerodynamic benefits would occur from a thinner assembly, it is believed that a development program should be revived with this objective.

With respect to rotor blade electrical deicing systems, it is possible to arrange the heater mats so that shedding is accomplished in either a spanwise or a chordwise fashion (Figure 140). Spanwise shedding has the heating element sections so arranged that a whole blade section will deice at one time, with the deicing sequence starting at the tip section and proceeding inboard to the root. Chordwise shedding has the heater arranged so that a fixed percentage of the chord (from root to tip) sheds at one time. Several deicing sequences are possible, and a preferred order would be the leading-edge segment, the upper surface, and then the lower surface segments proceeding aft from the leading edge.

The NRC conducted tests in 1959 (Reference 89) to compare spanwise and chordwise shedding. These tests showed that spanwise shedding of ice was about equally effective as chordwise shedding at temperatures from 32°F down to 14°F but that at colder temperatures the chordwise shedding required greater energy (seconds x watts/inch^2), about 60% at -4°F. The simplicity and the lighter weight of the chordwise construction, however, have made the chordwise system the only produced configuration.

On less than a dozen vehicles has an attempt ever been made to solve the problems of production ice-protection systems, with only about three vehicles (CH-46, HSS-3/CH-3, UH-2) ever seeing relatively high production quantities. Most of those systems have been deactivated or left unused because of various problems encountered in service.

Effect of Icing Conditions Severer Than Design Icing Severity. As noted earlier, Reference 86 brought attention to the 15 to 20 percent torque variations between icing cycles experienced on the Canadian CH-124. (This ship is essentially the same as the Boeing/Vertol 107 II Model reported in Reference 90.) Figure 141 is taken from that report and shows the effect of ice on the power required to hover. The variation in blade lift capability is essentially linear and indicates about 2-1/2 percent torque increase requirement per tenth of an inch ice buildup in the range from .04 to .42 inch of rotor blade ice. The apparent discrepancy between these two pieces of data may be due to two effects. The hover data could probably be doubled since the Vertol vehicles are tandem rotors of such size that only one-half the vehicle was capable of being encompassed by the Ottawa spray rig cloud. This is pointed out by the "note" on the Vertol graph. Thus, at the 3/16 inch (~.2 in.) ice thickness level that Vertol selected as being an optimum ice-release thickness, the adjusted power

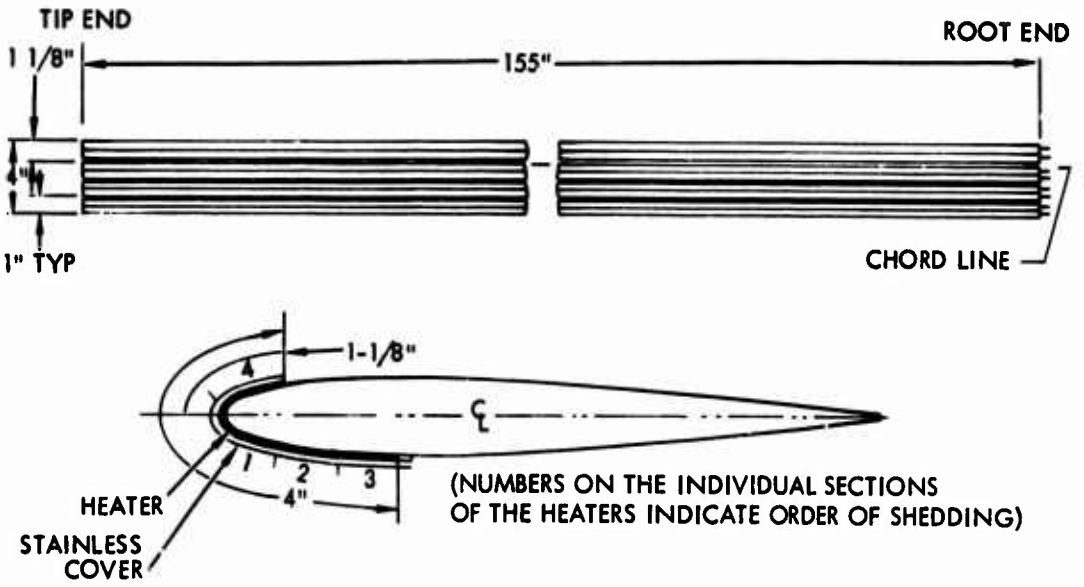

(a) Spanwise Elements for Chordwise Shedding

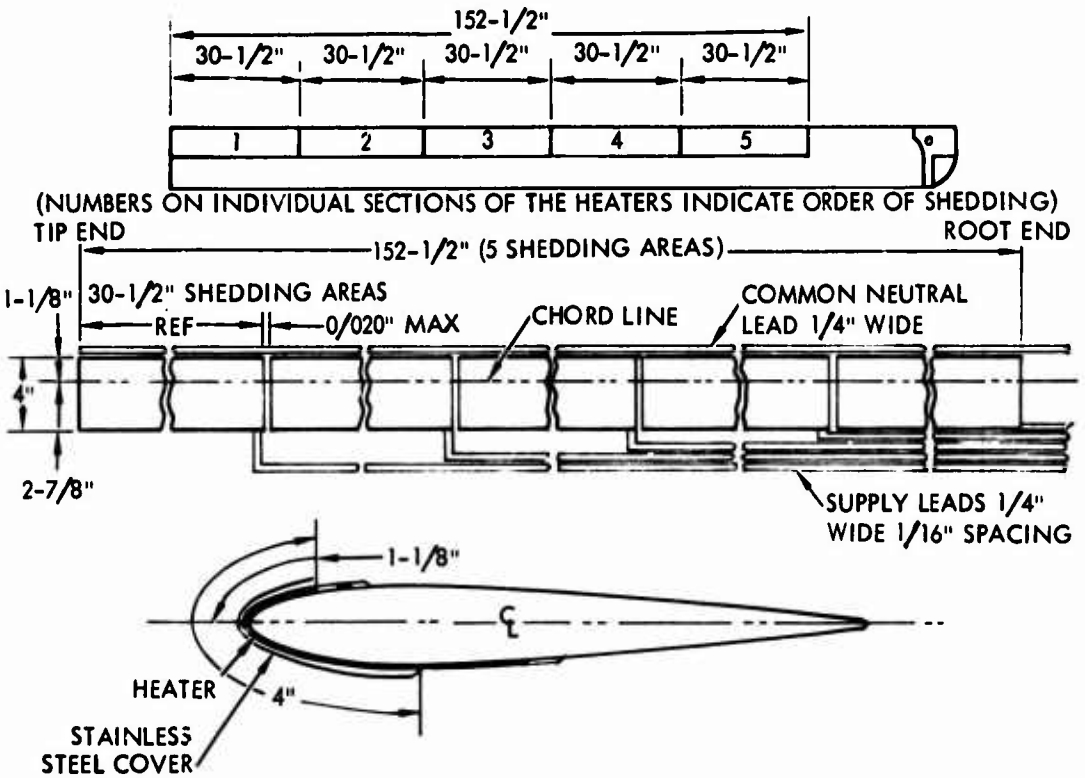

(b) Chordwise Elements for Spanwise Shedding

Figure 140. Electrical Heating Elements for Ice Shedding.

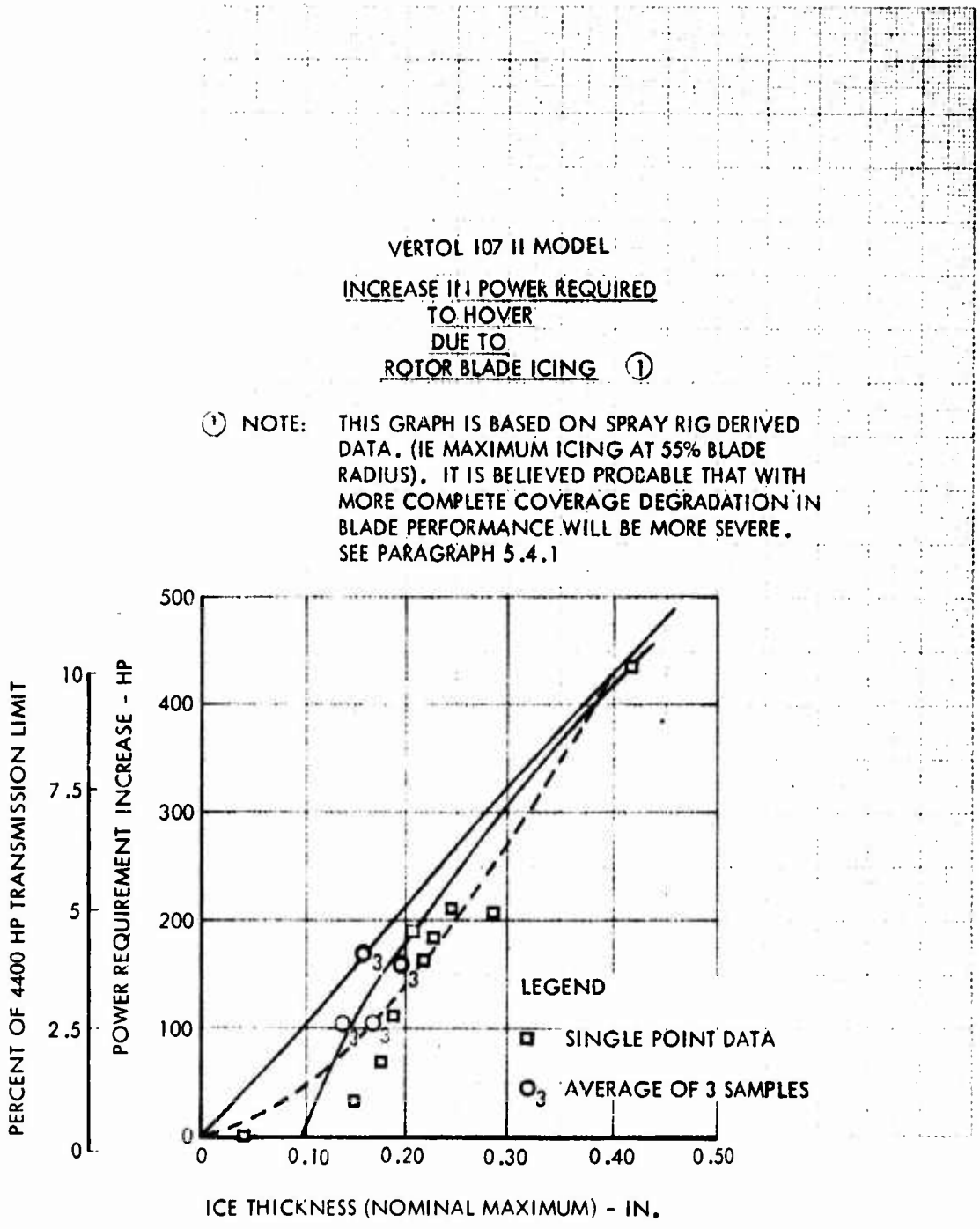

Figure 141. Effect of Ice on the Power Required To Hover.

increase would be about 10 percent. From analyses of blade and fuselage catch characteristics, the weight of ice built up is about 150 pounds. But with an influence factor of 228 pounds gross weight per percent torque change obtained from the flight manual, this effect is only about 1/2 percent.

The remainder of the 5 to 10 percent torque effect seen at 100 knots is due to changes in the airfoil drag characteristics. This effect is developed on the following pages.

An important problem associated with the design of icing protection systems for a helicopter is the effect of more-severe-than-design icing conditions on the performance of the vehicle. This is especially true of evaporative anti-icing systems where runback icing may adversely affect the lift and drag characteristics of airfoils. It may also pose a problem of engine ice ingestion if evaporative anti-icing is selected for the inlet lips or related components susceptible to icing.

Designing for the most severe icing conditions which could conceivably be expected is not acceptable due to the penalty on helicopter performance resulting from the additional weight and higher fuel consumption. An inlet lip anti-icing system has been used as an example of the effect of changing design conditions on its anti-icing performance. The basic design conditions are:

1.	Altitude	15,000 ft
2.	True Airspeed	130 kt
3.	Engine Power	1740 shp
4.	Engine Airflow	16 lb/sec
5.	Ambient Temp	20°F
6.	Water Droplet Size	15
7.	Liquid Water Content	0.66 g/m^3

The conditions that were changed for this analysis were ambient temperature and liquid water content, in that order. For the first case, the ambient temperature was reduced from 20°F to 0°F. The bleed air supply temperature was correspondingly reduced; and although this resulted in slightly increased bleed airflow (for a fixed orifice supply system), the skin temperature of the lip drops below that required for evaporative heating about midway along the flow passage, as shown in Figure 142. For the second case, the LWC was increased from 0.66 to 1.0 g/m^3. The effect was to increase the surface temperature required for evaporation from 99°F to 111°F. The design airflow for 0.66 g/m^3 is, of course, too low and does not supply enough heat to any part of the lip surface for complete evaporation of the impinging water.

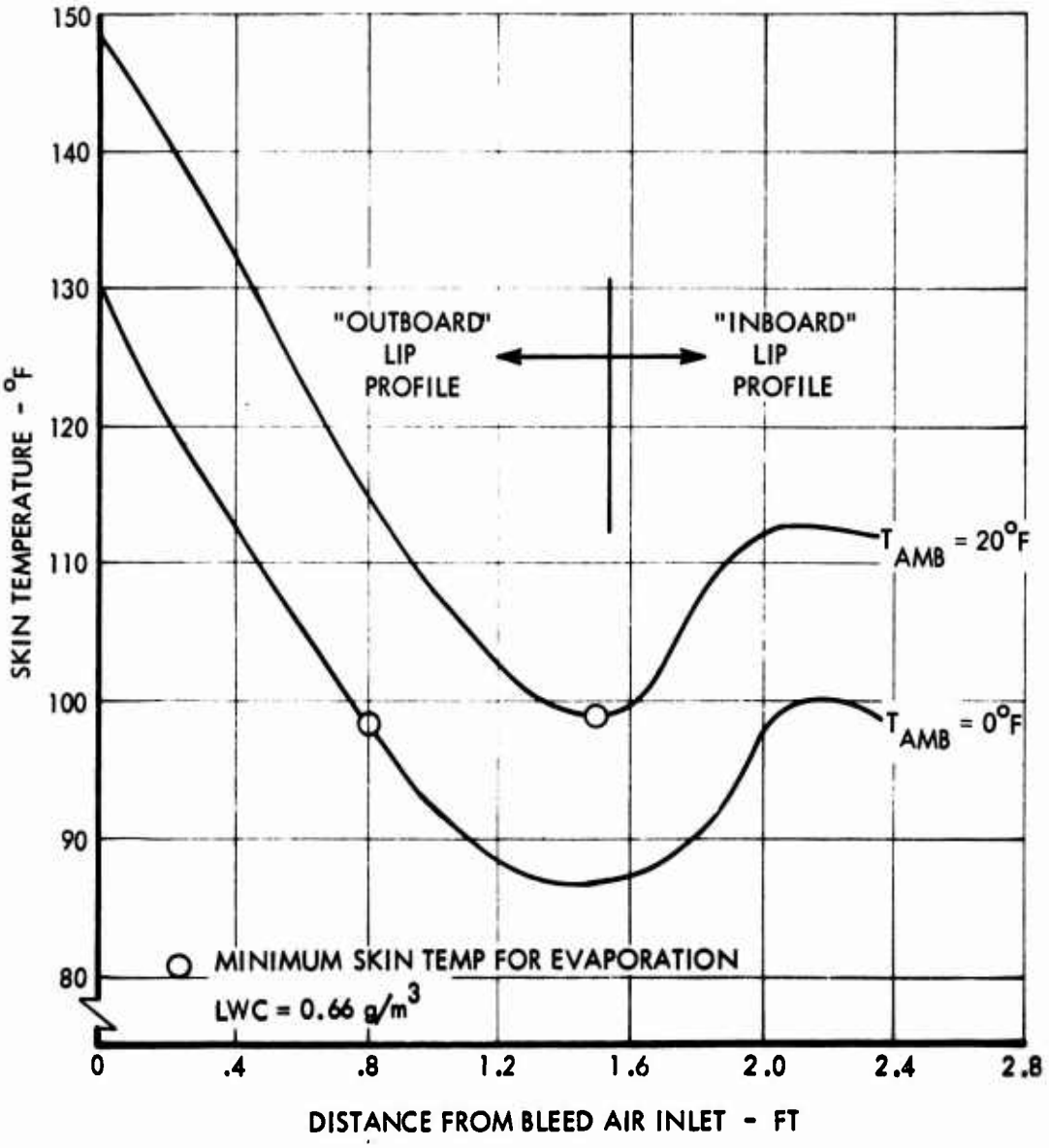

Figure 142. Airframe Inlet Lip Average Skin Temperatures.

The airflow increase required to maintain an evaporative anti-icing system for the more severe icing conditions posed in the two cases discussed above was estimated. For the first case, about a 10% increase in bleed airflow would provide sufficient heating of the lip surface to raise the skin temperature profile up to the original curve (in Figure 142). The second case, however, would require about a 50-percent increase in bleed airflow due to the more than 50 percent increase in liquid water content. Runback icing behind the heated area will occur in the inlet duct, and the problem of most concern then would be the ingestion of this ice by the engine. In the case of wing and empennage leading edges, the runback icing will increase the airfoil drag, may cause stalling at high angles of attack, and may cause damage to other parts of the aircraft when pieces break off. This problem is discussed in the ensuing paragraphs. References 91 and 92 report on icing tunnel tests which have evaluated the effect of runback icing on icing tunnel models when the hot airflow was insufficient.

Reference 91 tests were run on an 11-percent thick wing (with a chord of 60 inches). Bleed airflow rates corresponding to 92 to 23 percent of the flow required for full evaporation were run. Photographs of the runback ice formations at the end of 30 minutes are shown in Figures 143a through 143h. It was judged that aircraft performance would be affected by as little as 60 percent of the bleed airflow required for complete evaporative anti-icing in 99 percent of the icing encounters. (Note: Surface shown in the 143a through 143f photos is the upper side of the airfoil section, and surface shown in 143g and 143h is its lower surface). As can be seen from these photos half of the model was painted to afford a sharper contrast between the ice-free and frozen runback-ice-covered areas. The spanwise parallel marks on the painted half represented runback or ice accretion reference lines, to permit a better assessment of the extent of frozen runback and/or aft ice boundary limits.

Similar evaluations of runback icing for an NACA 65, -212 airfoil using hot air anti-icing systems were reported in Reference 92. In these tests, the drag of the airfoil with runback icing was measured at various angles of attack. The model used was an airfoil section of 8-foot chord spanning the 6-foot height of the Lewis Icing Research Tunnel. Results of these tests are shown in Figure 144, which is reproduced from Reference 92. The heating rates used were about 28 to 45 percent of those necessary for total evaporation of the impinging water. It is seen from Figure 144 that the drag appears to increase more rapidly with time in icing at a high datum air temperature than at a low datum air temperature and at higher angles of attack than at lower angles of attack. Except at the 8-degree angle-of-attack case (LWC = 1.05 g/m^3) where accretion of runback ice formations on the upper surface near the zero chord point caused a severe increase in drag, only moderate drag increases occurred at lower angles of attack, where spanwise ridges of ice were formed on the lower surface aft of the heatable area.

(a) Bleed Airflow = 176 lb/hr-ft (92 percent); Upper Surface.

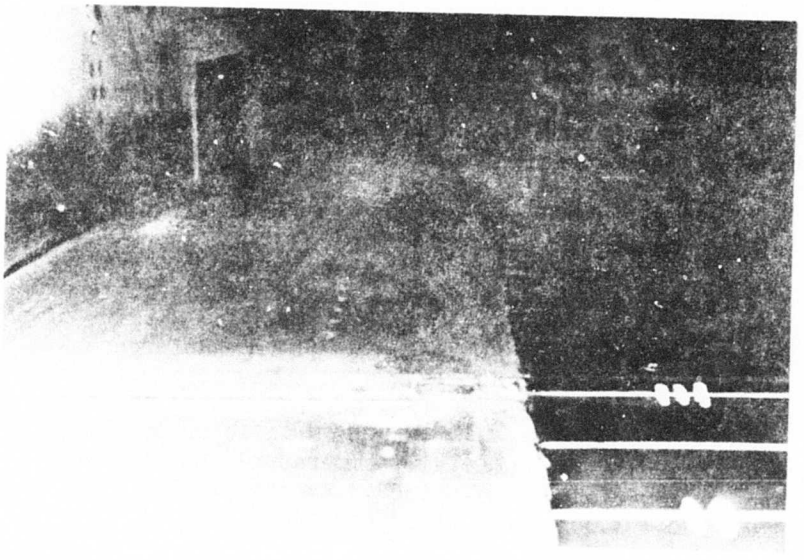

(b) Bleed Airflow = 162 lb/hr-ft (85 percent); Upper Surface.

Figure 143. Effect of Reduced Bleed Airflow on Anti-Icing Runback Ice Formation: Angle of Attack = 0°, Temp = +15 °F, Vel = 150 knots, Altitude = 650 feet, LWC = 1.1 g/m^3, d_m = 20 microns. 30 minutes icing run.

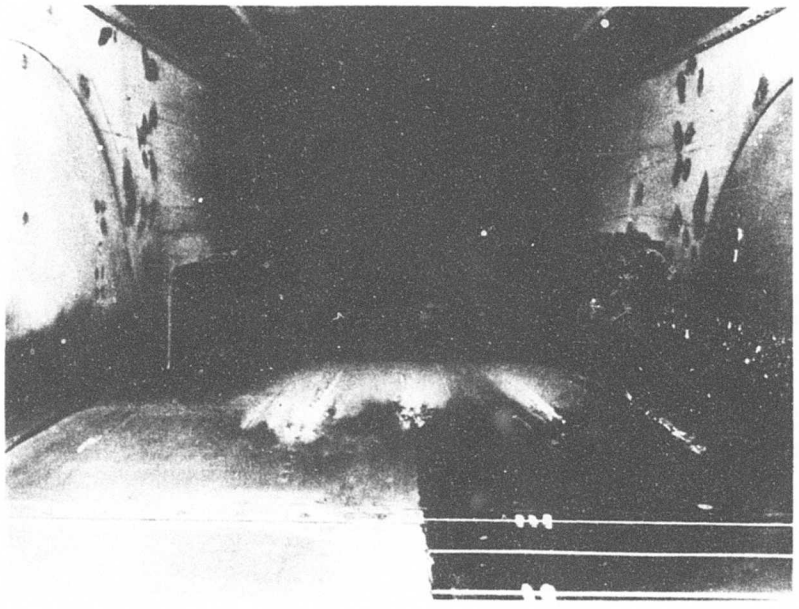

(c) Bleed Airflow = 140 lb/hr-ft (73 percent); Upper Surface.

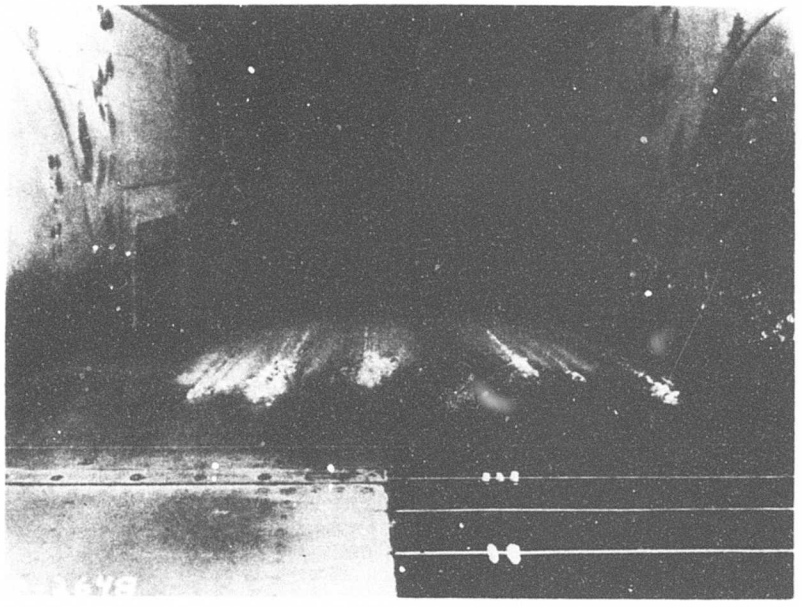

(d) Bleed Airflow = 123 lb/hr-ft (64 percent); Upper Surface.

Figure 143. Continued.

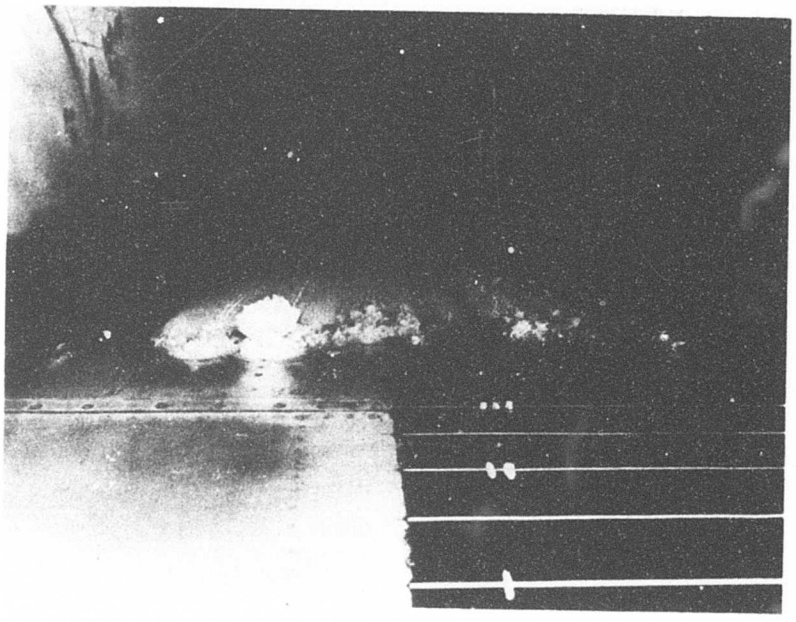

(e) Bleed Airflow = 101 lb/hr-ft (53 percent); Upper Surface.

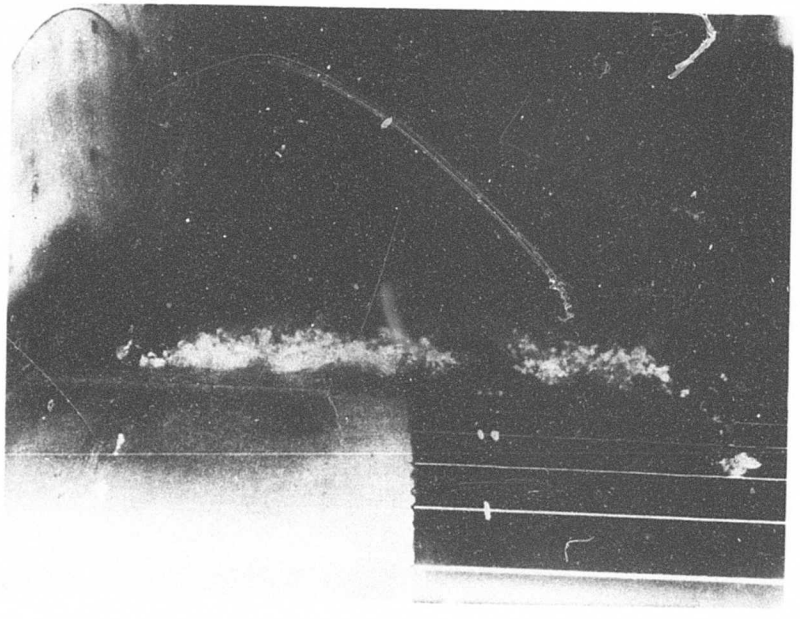

(f) Bleed Airflow = 44 lb/hr-ft (23 percent); Upper Surface.

Figure 143. Continued.

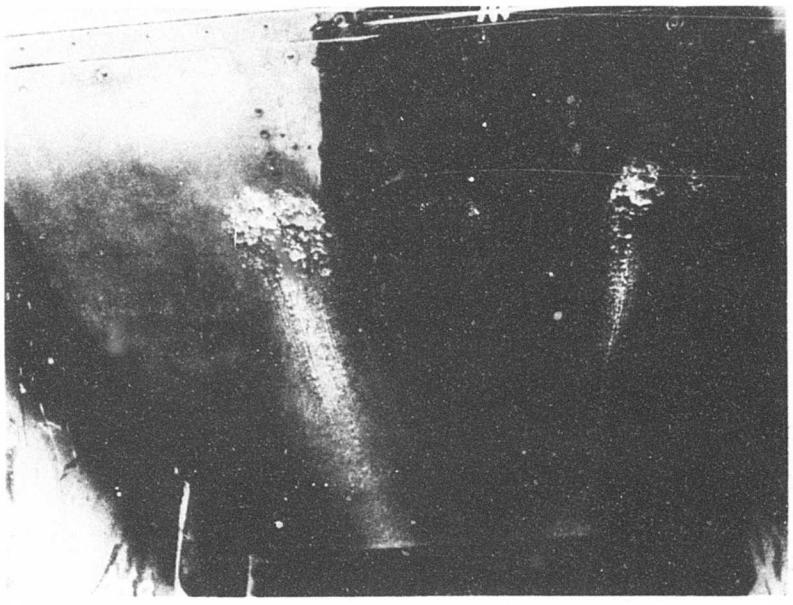

(g) Bleed Airflow = 101 lb/hr-ft (53 percent); Lower Surface.

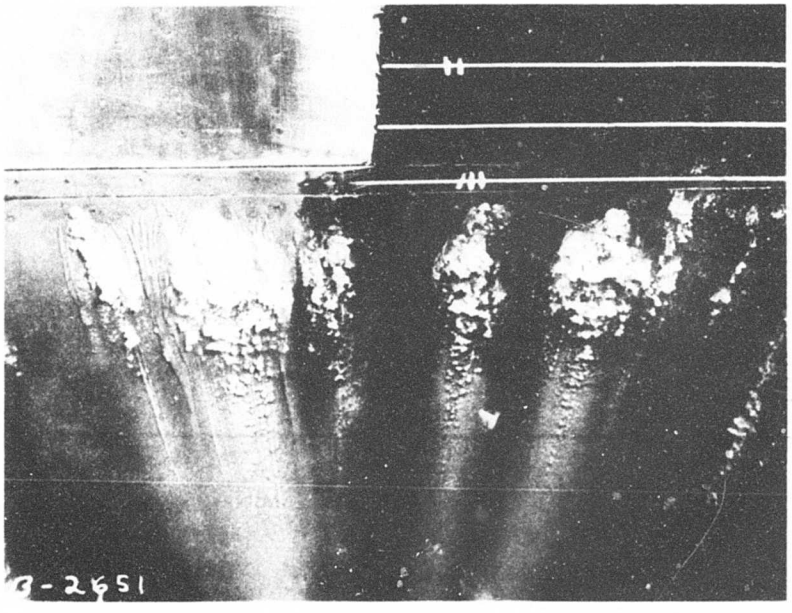

(h) Bleed Airflow = 44 lb/hr-ft (23 percent); Lower Surface.

Figure 143. Continued.

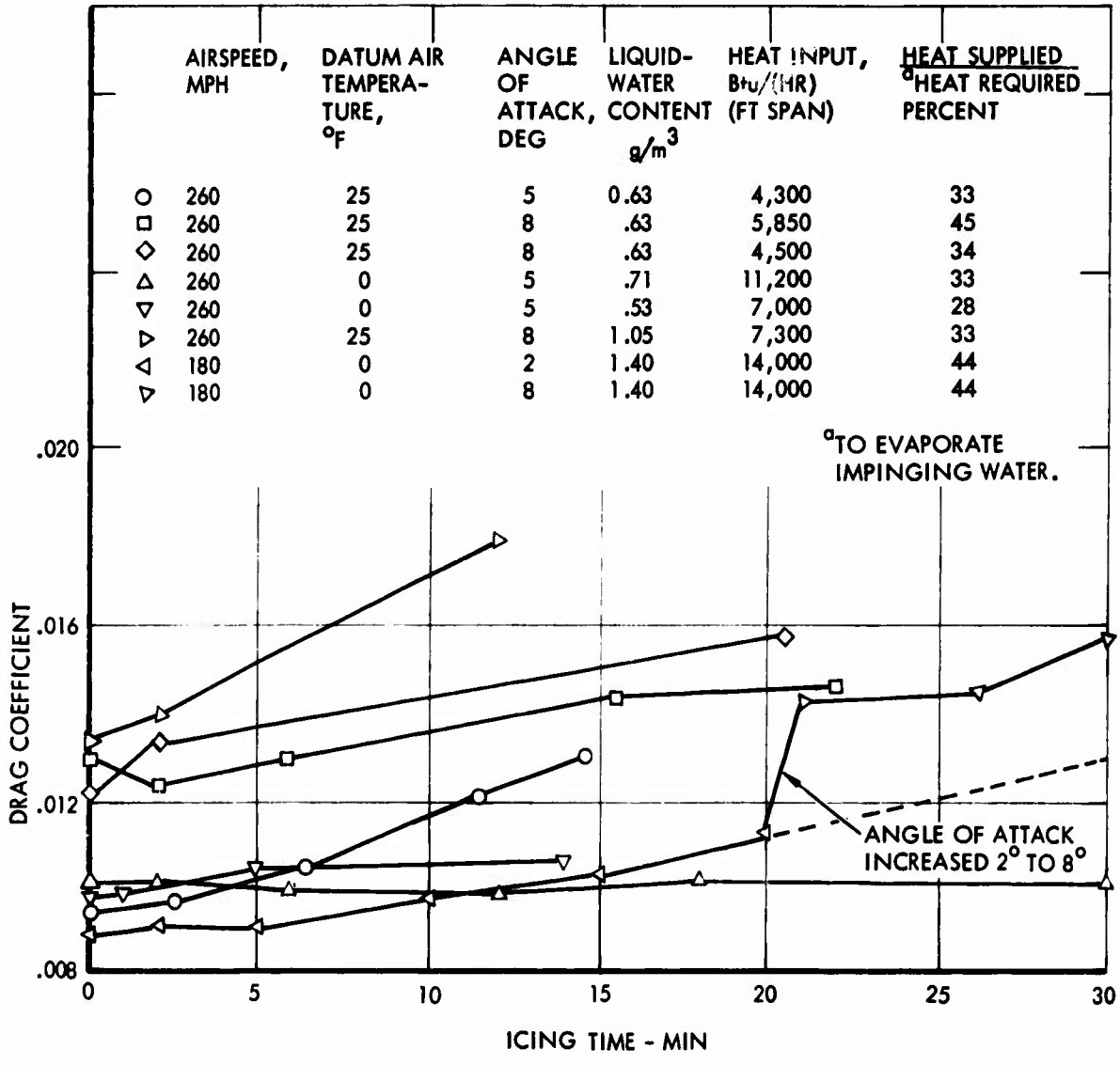

Figure 144. Effect of Runback Icing on Drag Coefficient As Function of Time In Icing With Leading-Edge Section Continuously Heated and No Afterbody Frost Formations.

The above icing tests were run on airfoil sections with similar thickness ratios (11 percent and 12 percent, respectively). The tests of Reference 91 were run at an angle of attack of 0-degree, while the tests of Reference 92 were run over an angle-of-attack range of 2 to 8 degrees. The latter tests, therefore, show a longer extent of icing on the lower surface than on the upper surface. Similar runback icing formations are seen for both airfoils. During the Reference 91 tests, runback icing started progressively forward as the bleed airflow was reduced until, at 23 percent of design flow, a spanwise ridge of ice formed just aft of the heated section on both the upper and lower surfaces. Figure 11 of Reference 92 shows for the NACA test spanwise ridges of ice formed also just aft of the heated section on both upper and lower surfaces at 2-degree angle-of-attack. Since the drag increases in the NACA tests are attributed to the formation of the spanwise ridges of ice, similar percentage increase in drag is predictable for the tests of Reference 91. By extension of the 2° angle of attack line from 20 minutes to 30 minutes icing time as shown in Figure 143, the drag increase is estimated at 50 percent for the 11 percent thick airfoil. The height of the ice ridge is not only due to runback but also to the fact that additional water is caught by the ice formation.

Icing tunnel tests have also been conducted on electrothermal deicing system performance (Reference 93). The basic airfoil section used in the tests was an NACA 0012 series with a chord length of 50 inches. The maximum thickness of 6 inches occurred at the 30 percent chord.

Figures 145 and 146, taken from Reference 93, show the runback icing resulting from the cycling procedure of 8 seconds on and 152 seconds off for three vendor products after the eighth shedding, for tunnel static temperature of 20°F and angles of attack of 0° and -4°, respectively. It is seen from these figures that part of the model was painted black (right side of photo) to obtain a sharper contrast with potential ice formations; the center section of the model was not painted and shows the natural color of the aluminum cladding; and the left side of the photo shows a section of the model painted with the aircraft finish. The spanwise dotted lines delineate the continuously heated parting strip at the leading edge and two chordwise cyclically heated elements aft of the parting strip. The chordwise dotted lines at the center and at the right side extremity of the model represent the boundaries of continuously heated simulated structural chordwise production breaks. At 0-degree angle of attack, the average trend of the drag coefficient with icing time shows a drag increment of only 5 percent for the best performing boot after 32 minutes (Figure 147). At the -4-degree angle-of-attack condition, the heavy catch on the upper surface resulted in appreciable runback which accumulated aft of the protected area and periodically shed. The average trend in drag coefficient for this test condition (Figure 147) showed a rapid increase after about 15 minutes of icing time.

As previously discussed, runback icing occurs for the evaporative anti-icing system because of more severe than design conditions such as lower temperature or higher liquid water content. For the electrothermal deicing system, runback icing is caused by the skin temperature (when periodically raised

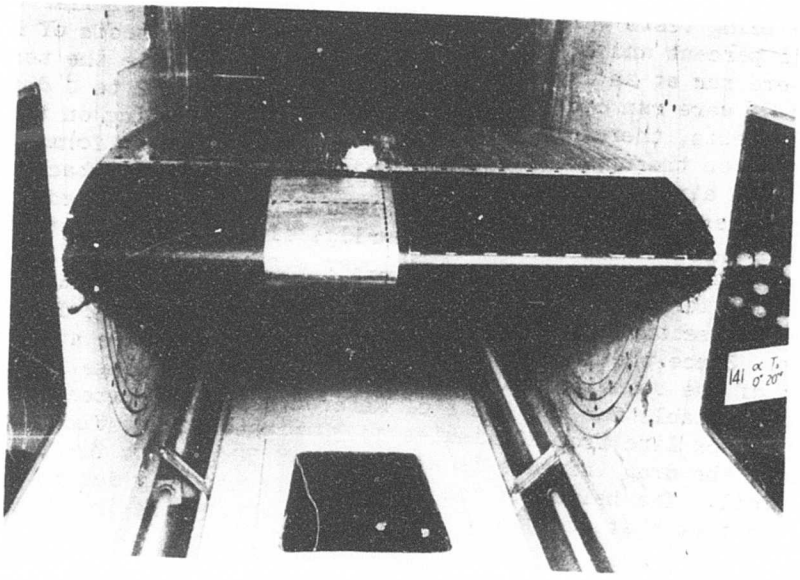

(a) Performance of Spraymat Elements After 32 Minutes of Icing.

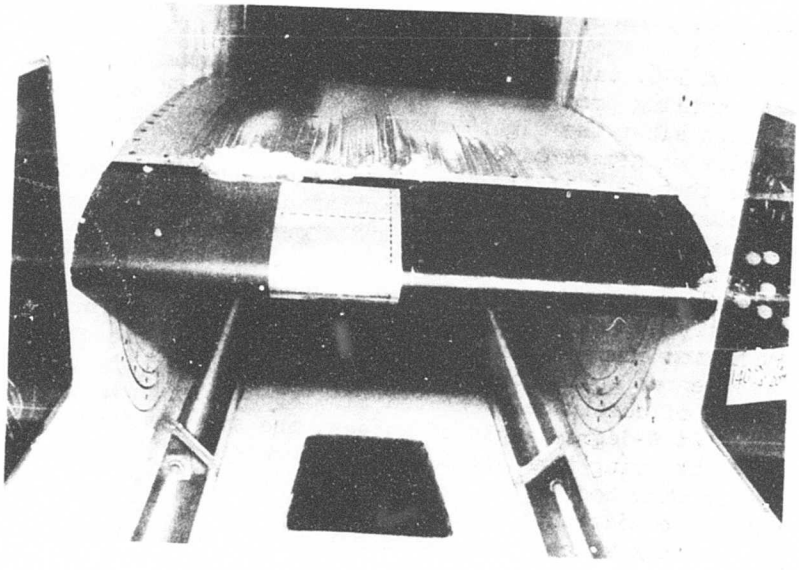

(b) Performance of Spraymat Elements After 32 Minutes of Icing, Angle of Attack = -4°.

Figure 145. Runback Comparisons for Two Zone Upper Surface: Angle of Attack = 0°, Temp = +20°F, Vel = 150 knots, Altitude = 650 feet, LWC = 1.1 g/m^3, d_m = 20 microns; Parting strips at 11 w/in.^{2} continuously and Cyclic Zones at 20 w/in.^{2} for 8 seconds On and 152 seconds Off.

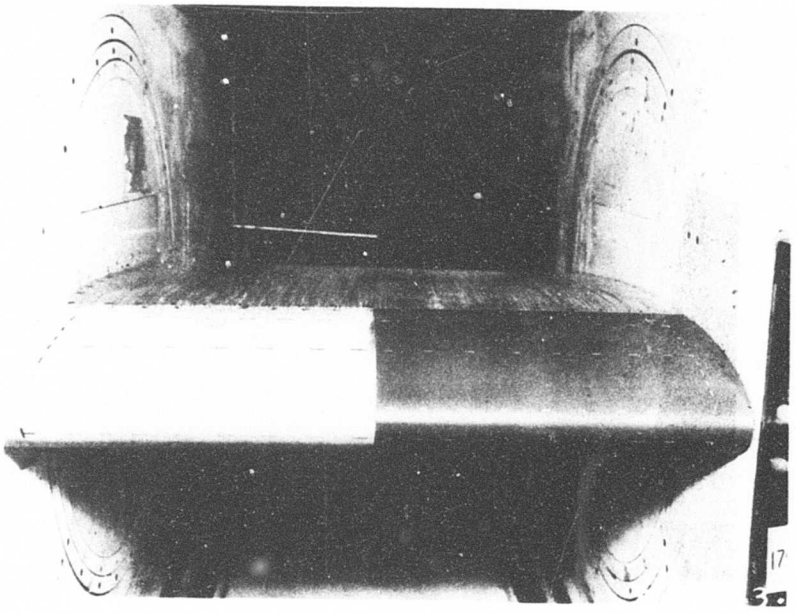

(c) Performance of Woven Wire Elements After 32 Minutes of Icing.

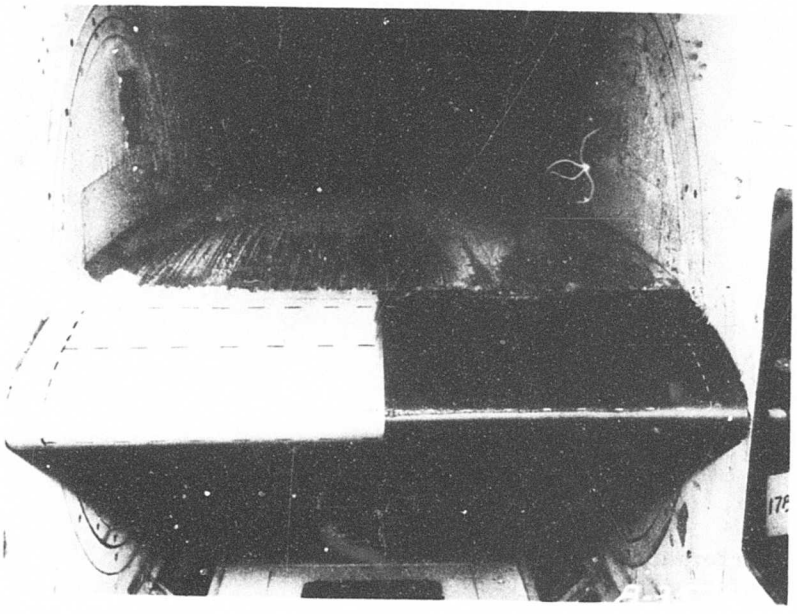

(d) Performance of Woven Wire Elements After 42-1/2 Minutes of Icing, Angle of Attack = -4°.

Figure 145. Continued.

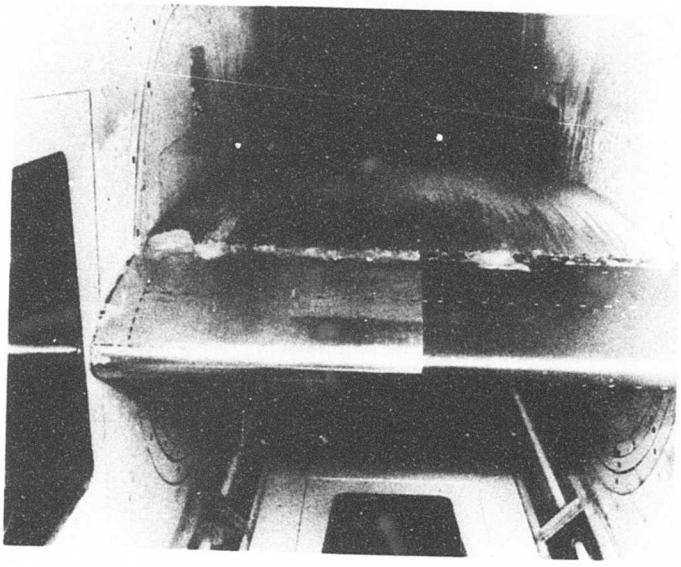

(a) Performance of Etched Foil Elements After 32 Minutes of Icing.

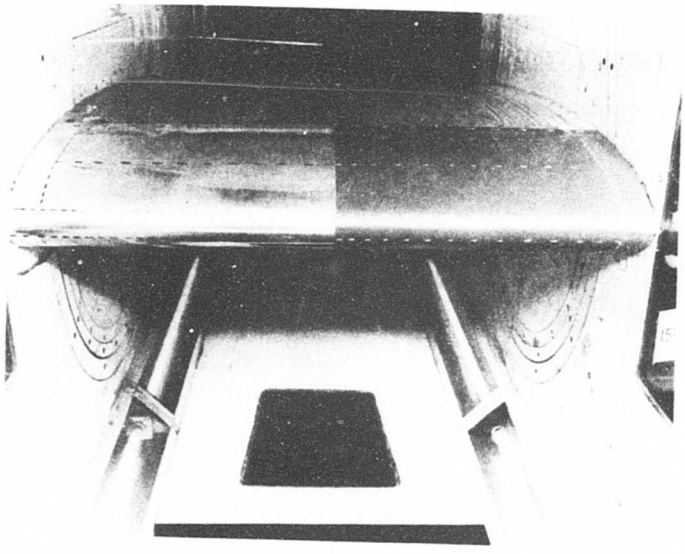

(b) Performance of Etched Foil Elements After 37-1/2 Minutes of Icing, Angle of Attack = -4°.

Figure 146. Runback Comparisons for Two Zone Upper Surface: Angle of Attack = 0°, Temp = +20°F, Vel = 150 knots, Altitude = 650 feet, LWC = 1.1 g/m^3, d_m = 20 microns; Parting strips at 11 w/in^2 continuously and Cyclic Zones at 20 w/in^2 for 8 seconds On and 152 seconds Off.

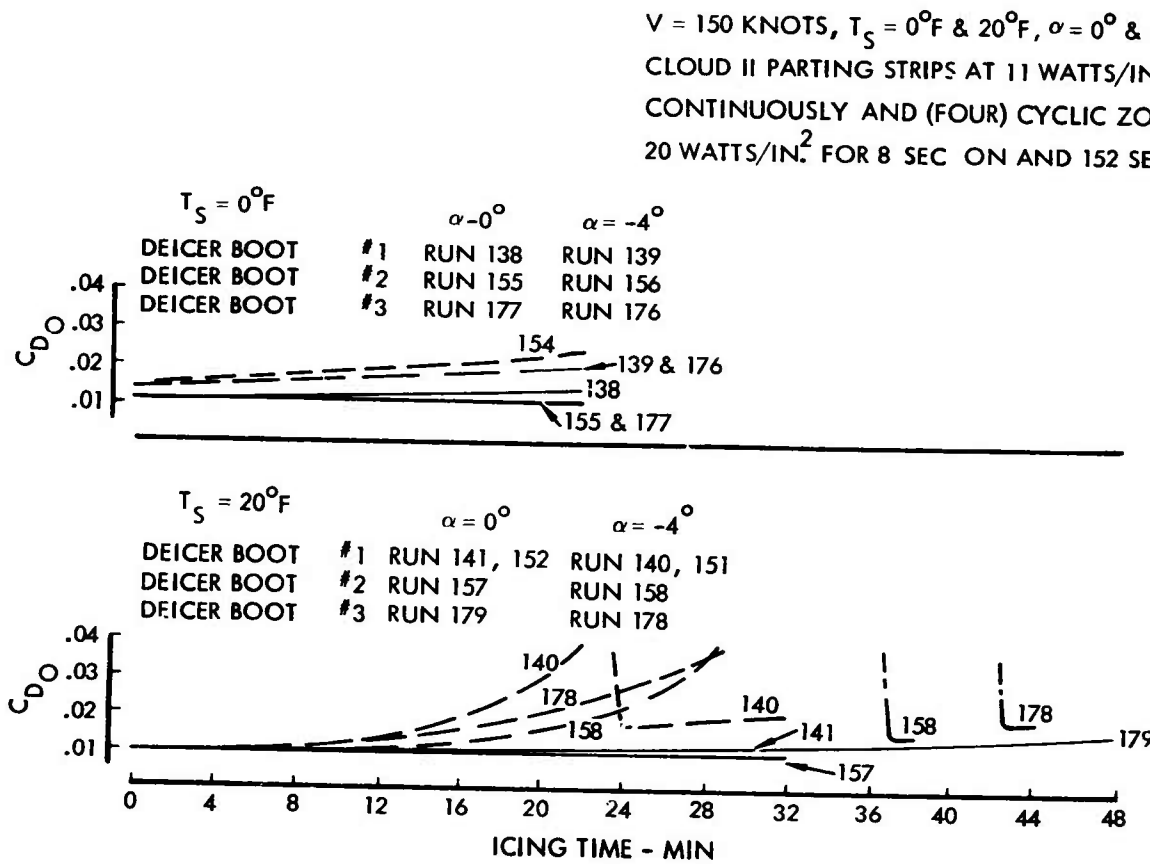

Figure 147. Average Trend of Drag Coefficient vs. Icing Time.

to melt the bond) overshooting the 32°F required and then spending a finite time above 32°F before cooling back to ambient. Water thus freezes aft of protected areas. As these frozen rivulets increase in size, they become subject to additional buildup due to direct droplet impingement. Therefore, while runback icing may not occur for the evaporative system, it is inherent with the cyclic deicing system.

5.2.2 Wing and Empennage

Wing and empennage ice-protection requirements for compound helicopters, such as the AH-56, are not as critical as for the engine inlets, windshields or rotors. Once it is assured that the aerodynamic efficiency and balance of the rotor blades are not significantly affected by prolonged icing encounters of moderate intensity, formation of ice on unheated wing surfaces is not detrimental as far as safety is concerned. For compound rotary-wing aircraft using turboshaft engines with adequate performance margins, the drag rise caused by wing or empennage icing is in itself considered not sufficient cause to justify wing ice protection when it can be demonstrated that the controllability characteristics are not adversely affected. On a compound helicopter, the lift of the rotor blades alone, if not impaired by icing, is sufficient to continue safe flight without dependence on lift augmentation provided by the wings. Of course, the speed of the aircraft will be significantly affected by ice formation on the wings but not its safety.

5.2.3 Transparent Areas

A survey of modern commercial and military airplanes shows that the majority use electrical heat for windshield anti-icing and defogging. Among the major advantages of this method are the following:

1. Minimum weight
2. Simple "on-off" control switch operation
3. Ability to obtain good control of heat distribution
4. Ability to obtain good temperature control of viewing area
5. Independence of the system performance from all aircraft operational modes.

An example of a schematic of the controls for the electrically heated pilot's windshield is shown in Figure 148. As can be seen, in this case the windshield is a laminate consisting of two glass layers with a layer of polyvinyl butyral between the glass layers. The transparent electrically-conductive coating of tin oxide is applied between the external plate of semitempered glass and the polyvinyl layer. The mechanical and thermal properties of tin oxide and semitempered glass are compatible for the deposition of the coating. Also, use of tin oxide as the conductive material results in improved

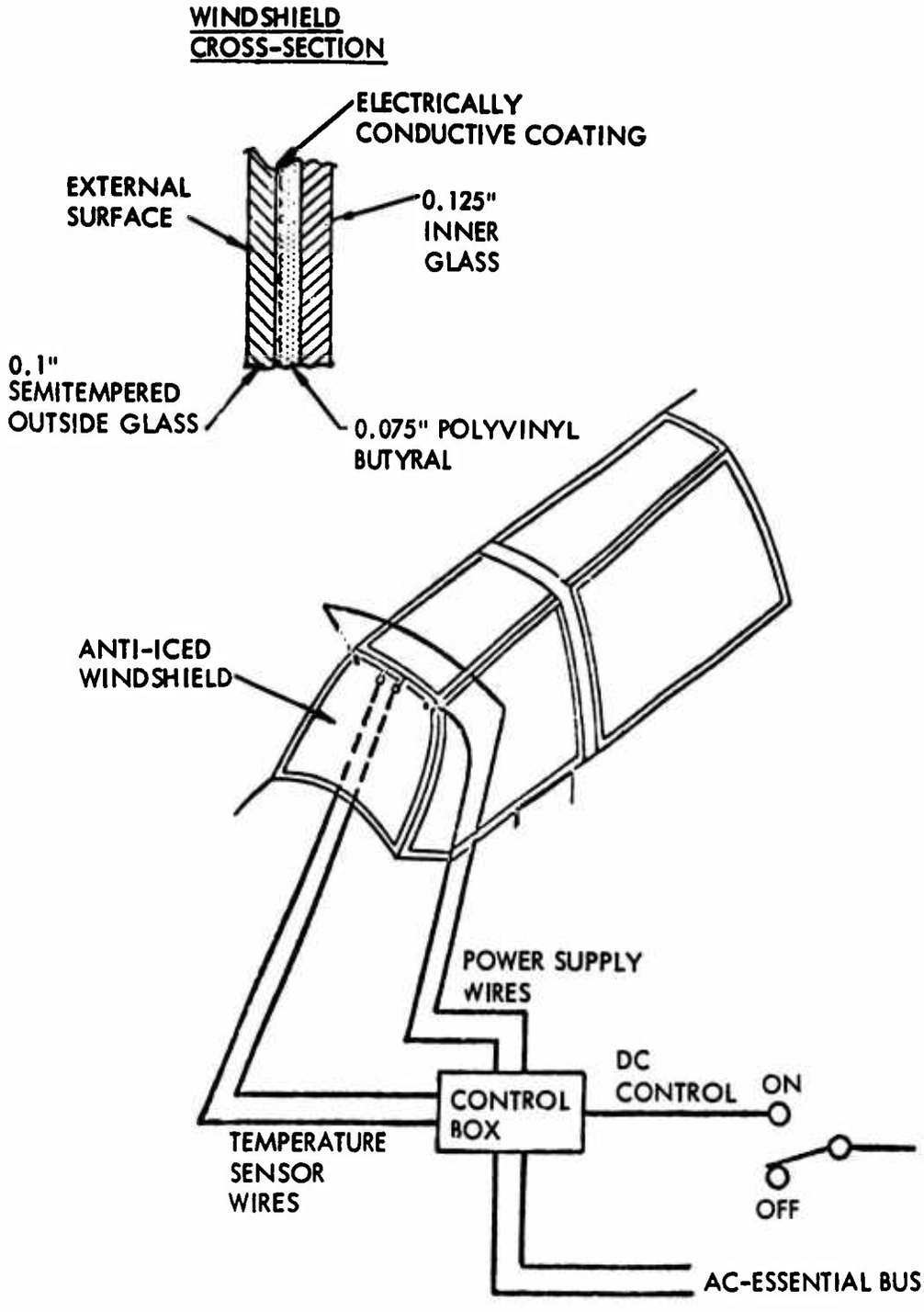

Figure 148. Typical Schematic of Windshield Anti-Icing/Defogging System.

visibility from the optical point of view. The alternate coating material, evaporated gold, yields a higher light reflectivity (by approximately 30 percent) and a lower light transmissivity (by approximately 10 percent). To eliminate potential local hot spots on the irregularly-shaped windshield panel, the conductive-coating thickness is applied nonuniformly to achieve the graduated resistance levels required for achievement of a uniform windshield temperature distribution. A maximum power intensity of 4 watts per square inch provides running-wet ice protection for intermittent maximum icing intensities down to -22°F and is commensurate with requirements of MIL-T-5842. The total power consumption depends on the size of the heated area.

A windshield temperature range between 105 and 115°F is typical for anti-icing/defogging system operation and is not exceeded by automatic ON and OFF cycling of the heat in response to temperature sensors imbedded in the windshield.

5.2.4 Engine and Engine Inlet Anti-Icing

5.2.4.1 Anti-Icing Provisions

The icing threat to the propulsion system is twofold: (1) blockage of airflow by ice accretion on the inlet guide vanes and on the first rotating stage, and (2) damage to guide vanes and rotating blades due to impact of ingested pieces of ice shed from the induction system or from surfaces ahead of the engine inlet duct such as the windshield, fuselage, or the main rotor blades. The first threat is removed by a bleed air system on the engine itself which heats the inlet vanes and the particle separator, if the latter is integral with the engine.

For multiple module type inertial separators (EAPS), anti-icing may or may not be required depending upon the orientation of the face of the particle separator with respect to the free-stream direction. Specifically, when the EAPS face is oriented such that it forms a small angle with, or is parallel to, the free-stream flow direction and the engine installation is "buried" behind the filters, the EAPS may not require anti-icing. This is discussed in some detail in Section 2, where experimental data is presented to substantiate this conclusion. In engine installations where the air is admitted into the engine by means of a discrete full ram air inlet duct, the inner duct surfaces require protection to eliminate the second threat.

For a full ram air inlet duct, two heating methods have been used:

1. In cases wherein the maximum engine bleed temperature reaches 800°F or higher, and an evaporative system is used, only the cowl lip is heated. In this case the cowl is constructed of a high-temperature material such as titanium or stainless steel, thus preventing structural overheating for inadvertent hot-day operation, control valve failure, or for normal operation in light icing. Special overheat protection is not required. Figure 149 shows an example

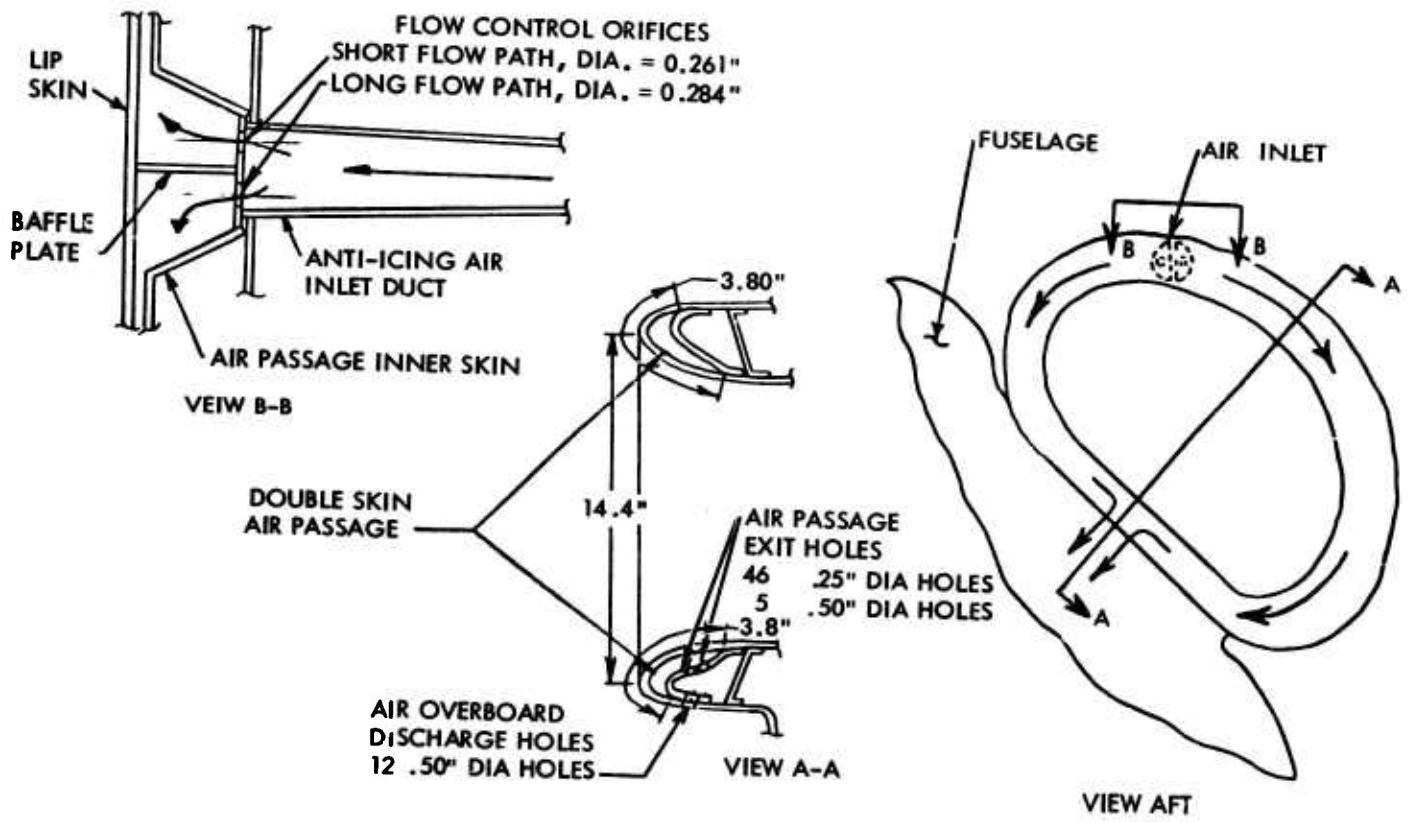

Figure 149. Air Frame Inlet Lip Anti-Icing System.

of such a stainless steel inlet lip anti-icing system. Compressor bleed air enters at the top of the inlet through two flow-measuring orifices and flows circumferentially around each side of the inlet in a double-skin air passage. The air discharges overboard at the bottom of the inlet through holes in the air passage inner skin and lip cowl skin. Airflow to the lip is controlled by an ON-OFF (nonpressure regulating) solenoid valve that is designed to fail open for an electrical failure.

2. In cases wherein the maximum engine bleed air temperature is 700°F or lower, a running-wet system is feasible. The entire inner surface of the inlet duct is heated to the engine face. In view of the lower heating intensities required to maintain the surface just above freezing, the valve failure mode requirement can be met with a conventional aluminum alloy structure. Figure 150 presents a schematic of such a system. To conserve bleed air at high engine power settings, this system may feature a pressure regulator valve (set at 26 psig) which also incorporates the ON-OFF function. The air is ducted into the inlet cowl lip distribution manifold, which represents a circumferential duct located inside the cowl lip at a distance of 1-1/2 inches from the inner surface of the cowl lip leading edge. The hot air is discharged from the 0.75-inch-diameter distribution manifold into a D-shaped plenum by means of in-line multiple jets; 0.08-inch-diameter holes at 0.5-inch centers are drilled in the manifold for this purpose. From the plenum which extends 5 inches aft of the leading edge, the air flows through longitudinal 0.065 inch deep chem-milled passages on the internal skin of the engine duct inlet. The spent anti-ice air is discharged through an annular outlet into the engine inlet duct at the front face of the engine.

5.3 EFFECTS ON ENGINE OPERATION CAUSED BY BLEED AIR AND POWER EXTRACTION

Bleed air extraction penalties due to operation of an ice-protection system have been calculated for nine engines, and the results are summarized in Figure 151. This figure summarizes the impact on maximum power available or on cruise fuel consumption when engine bleed-air is used. Maximum power is reduced by about 2.8% for each percentage point of bleed airflow. This high penalty exists since the output power of a turboshaft engine represents only about one-third of the input power, the other two-thirds being necessary to drive the engine compressor. The upper portion of the figure shows that cruise fuel consumption is increased by about 1.45 pounds per hour of fuel flow for every pound per minute of bleed airflow.

Table XXIII summarizes pertinent data for various engines. The tabulation shows that the engines represent a variety of possible groupings such as: all axial, all centrifugal, or mixed axial/centrifugal compressor stages, low compression ratios of 6 to 9 or moderate ratios of 13-15.

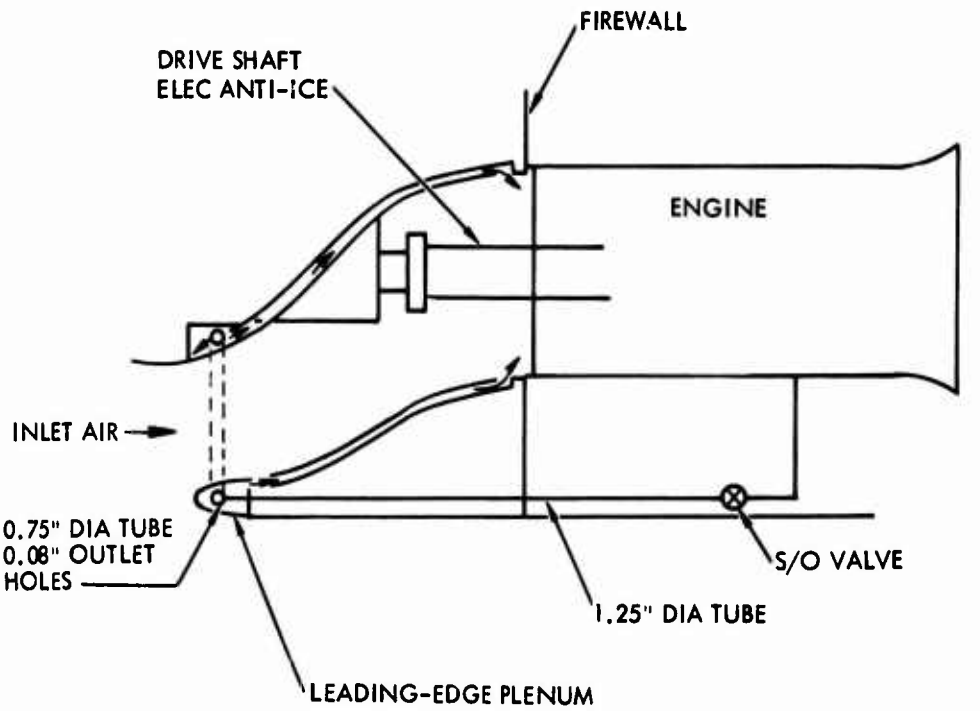

Figure 150. Engine Inlet Anti-Icing System Schematic (Running Wet Protection).

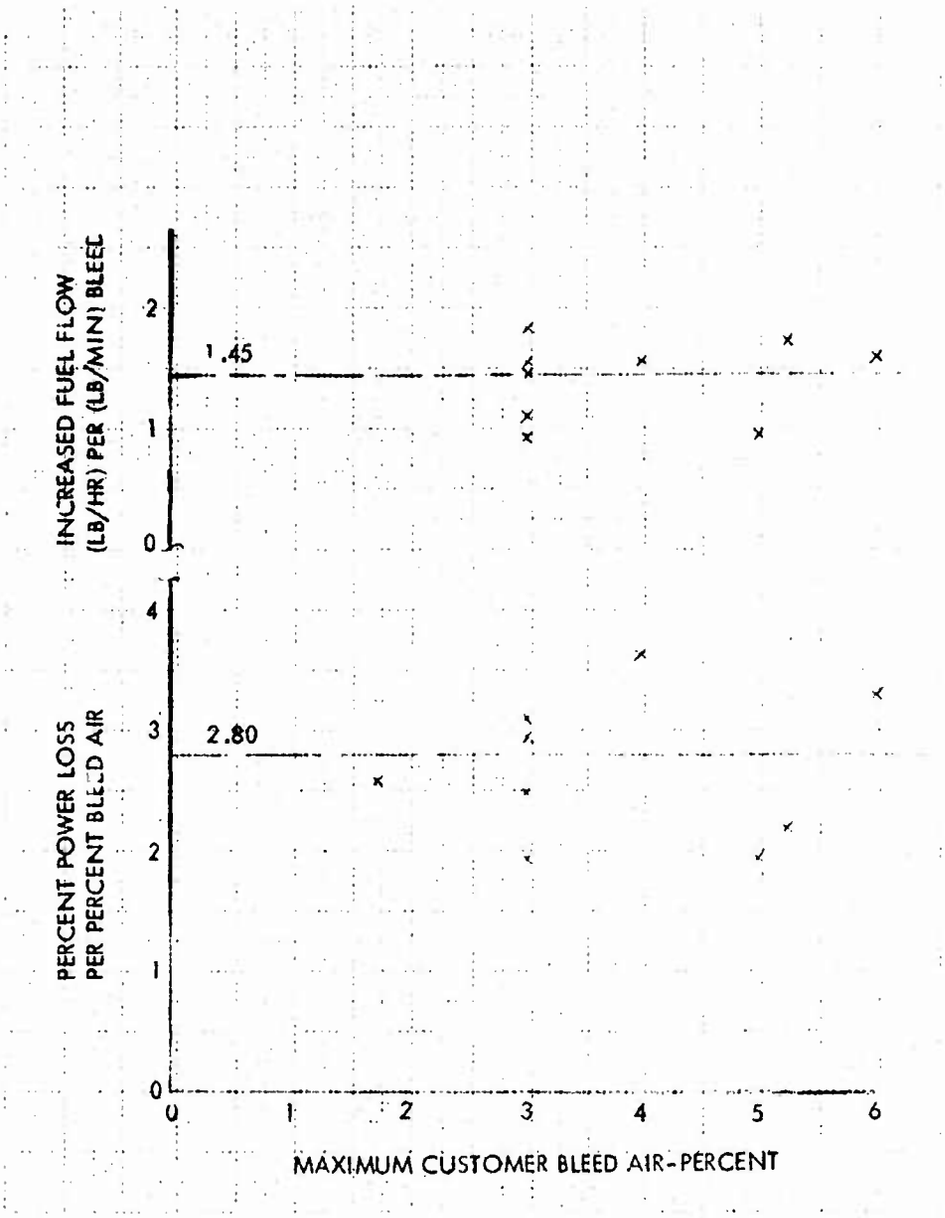

Figure 151. Impact on Free-Turbine Engine Performance When Using Engine Bleed Air.

No single grouping appears to explain the scatter in impact factors seen in the previous figure.

TABLE XXIII. BLEED CHARACTERISTICS OF VARIOUS ENGINES

Max SHP	Compr Stages	PR	Max % Bleed	Total Bleed LB/Min
(1)	(2)	(3)	(4)	
730	3A,1C	7.0	5.25	20.6
1500	2C	6.2	5.0	22.6
1100	5A,1C	6.0	3.0	25.4
2850	7A,1C	7.0	3.0	38.2
1400	10A	8.4	3.0	24.0
317	6A,1C	6	4.0	7.85
3925	14A	13.0	6.0	95.0
474	2C	9	5.0	9.5
1500	5A,1C		5.0	27.2
4500	14A	15	3.0	48.6
			1.75	
1600	11A		3.25	

Notes: (1) Max SHP is "Maximum," which may be rating for 5, 10, or 30 minutes.

(2) "A" represents axial stages, "C" represents centrifugal stages.

(3) This is overall pressure ratio of engine.

(4) This is for majority of power spectrum; maximum power may have reduced limitations.

Figure 152 shows two major ideas: (1) the use of engine bleed is most penalizing when least power is available--on a hot day when the engine T_5 (Turbine Inlet Temperature) is limited. The engine is least penalized when most power is available on cold days, when the engine is N_G (Gas Generator Speed) limited; and (2) there is almost as much variation in impact factor between engines for one model (from 3 to 4 percent, or a spread of 1 percentage point) as in the 8 or so models in the figure (from 1.95 to 3.60 percent, or a spread of 1.6 percentage points).

Until a few years ago, there was little use of engine bleed from turboshaft engines except during icing weather or in cold ambients when plenty of reserve power exists; and as noted previously, the penalty for using bleed air is at a minimum. Since the accuracy of impact factors for bleed-air was previously not too critical, this may explain some of the observed variations between engine manufacturers. With the recent trend to more extensive use of turboshaft bleed for cockpit and avionics cooling, infrared suppressor vane cooling, ejector-induced scavenging of engine air filters, etc., the characteristics of engine bleed and its impact on engine performance are receiving more detailed attention by the manufacturers of turboshaft engines.

The ability of turbine engines to deliver bleed air varies considerably. As shown in Figure 151, engine allowable bleed varies from 1.75 percent to 6.00 percent. This has been extended to 6.50 percent for engine I in Table XXIV. Because of proprietary clauses on many of the engine specifications, identification of specific engines has been deleted.

This table is based on standard sea level uninstalled conditions, as was Table XXIII. That table was based on the maximum (be it 5, 10, or 30 minutes duration), while Table XXIV is based on 100 percent normal rated power conditions. This change was made in order to facilitate comparison with SAE AIR 984 (Society of Automotive Engineers, Aerospace Information Report).

The salient features of AIR 984 are reproduced in Figure 153, which shows "the helicopter bleed air requirements which may be obtained through compressor extraction, and is intended as a guide to engine designers." At the standard sea level temperature of 59°F, this figure shows that the engine designer should provide at least 128 "Btu hour bleed air per shp" (based on 100 percent normal rated power). For convenience, let the quoted parameter be called "K".

The relative heat availability parameter K is tabulated in Table XXIV, and it varies from a low of 87 to a high of 392. Of interest is the division of levels. Engine C, with a level of 209, is one of the oldest engine lines in the list but is of the same vintage as engine D and H, with levels of 113 and 110. Engine F is one of the newer engines, however, and it has a disappointing level of 96. Engine N, the latest growth of an intermediate aged engine line, has a K of 392, or 206 percent in excess of the minimum design recommendation. And yet, according to users of this engine, even more bleed capability was desired.

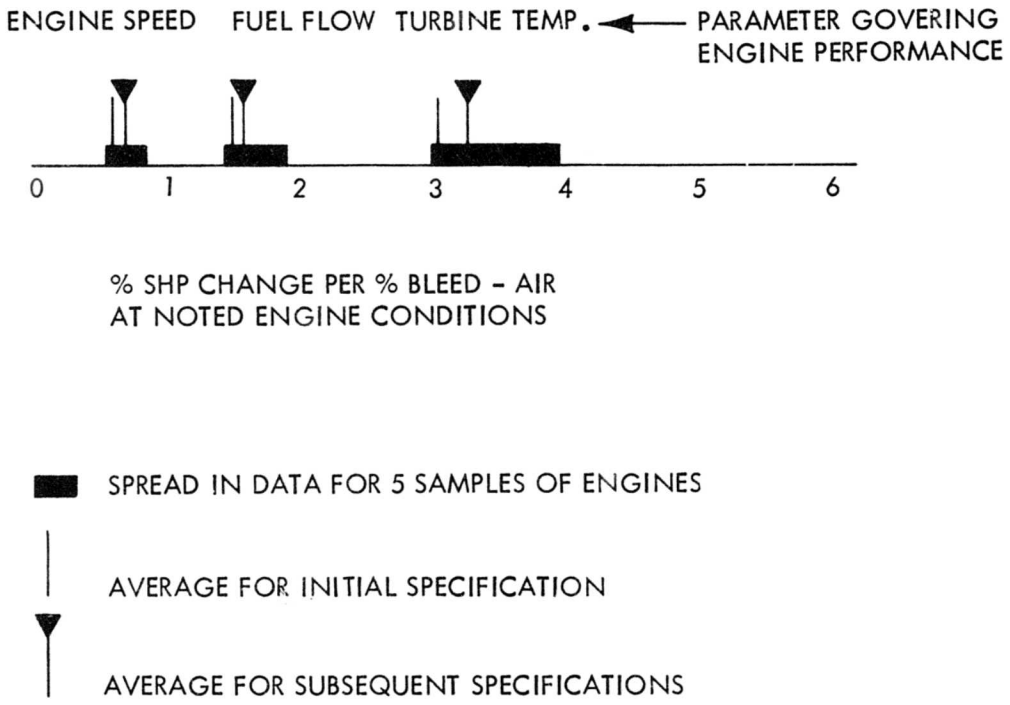

Figure 152. Statistical Variation of Bleed Air Impact Factors.

TABLE XXIV. ENGINE AND BLEED AIR CONDITIONS AT 100% NORMAL RATED POWER, UNINSTALLED STANDARD SEA LEVEL

Engine	SHP	SFC	WA	Max. Bleed	WB	TB	PB	K*	K1**	Comp Stages	ΔHP / % WB	E ΔHP / KW BLEED
-	HP		LB/Sec	%	LB/Hr	°F	PSIA					
A	346		3.28	4	472	540	92	158	128	6A,1C	12.6	4.34
B	403		3.90	5	702	620	130	235	197	2C	10.8	2.61
C	550		5.50	5.25	1040	520	91	209	168	3A,1C	12.1	2.61
D	1000		10.60	3	1145	470	83	113	88	5A,1C	29.0	3.77
E				1.75								
F	1250		7.52	5	1354	436	75	96	73	2C	24.4	5.09
G				3.25						11A		
H	1250		13.25	3	1431	469	119	110	85	14A	31.3	3.36
I	1250		8.74	6.50	2045	413	63	139	103	5A,1C	25.6	4.30
J	1500		12.10	4	1742	540	106	134	109	5A,1C	43.5	4.46
K	1660		9.20									
L	2400		21.20	3	2290	440	49	87	66	7A,1C	70.7	4.96
M	3230		26.40	6	5700	701	171	272	234	14A	106.5	3.23
N	4110		28.70	6	6200	765	210	392	341	14A	127.2	3.18
O	4200		24.20									
P	5455		34.50			765	206					
Q	14254		84.50			756	210			15A		

NOTES:* K = Relative Bleedair Availability, as used in SAE AIR 984 =

= (Btu/hour)/shp, Based on (TB-59)°F

** K^1 = Corrected Bleed Air Availability =

= (Btu/hour)/shp, Based on (TB - 150)°F

E = Bleed Penalty per Heating Capability =

= ((ΔHP/% WB)/.01 (WA) (CP) (TB - 150°F)) (1kw/.948 Btu/sec)

= HP/KW

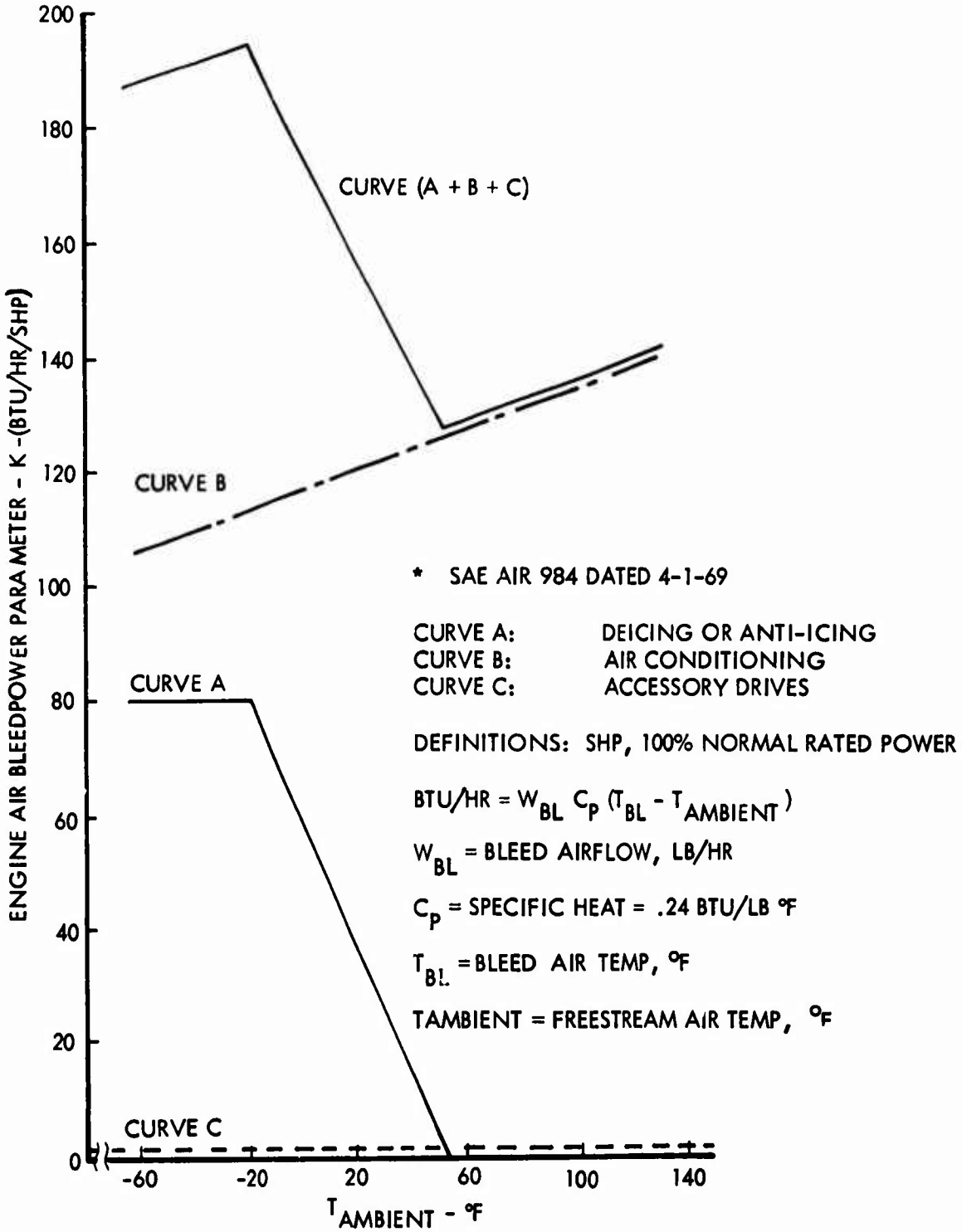

Figure 153. Air Bleed Objective for Helicopter Turbine Engines.

Part of the problem of using bleed air is that of either exceeding turbine temperature limits (Figure 154 shows that full bleed is available only up to 86 percent normal rated power on one engine) or limiting combustor temperature profile distortion (as shown by the cutouts in the typical bleed air diagram of Figure 155).

Another problem is the assumption that all the bleed air energy is extractable. Shown in Table XXIII is the modified relative heat availability parammeter K^1 which assumes that the discharge bleed air is a more appropriate 150°F instead of 59°F. For a low bleed temperature, as for engine I, the K factor is optimistic by 34 percent, while for a high bleed temperature, as for engine N, the K factor is optimistic by 15 percent.

To evaluate the loss in available power (shp), another parameter has been included in Table XXIII. This is the column labeled "E" and represents the loss in shaft horsepower per kilowatt of heat transfer using bleed air (based on 150°F discharge air temperature from the ice protection system). The lowest value is 2.61 shown by engines B and C, one of the newest and one of the oldest engine lines. The high value of 5.04 is for another of the newer engines. These levels are compared to 1.8 to obtain the same thermal energy transfer via an electrical generator. If it were not for the fact that electrical generators are heavy and their capacity is sized almost exclusively by the vehicles icing needs, electric energy is 1.45 (= 2.61/1.8) to 2.83 (=5.09/1.8) more efficient than using engine bleed air.

5.4 CONCLUSIONS RELATED TO TRADE-OFF RESULTS

This section recapitulates trade-off considerations relating to the choice of the optimum ice protection system for the critical helicopter surfaces. For illustration purposes a compound helicopter with a four-blade main and tail rotor system and a gross takeoff weight of 17,000 pounds is used as an example (Figure 20). A brief description and discussion of each approach to ice protection are given for the engine, rotors, windshield and fixed aerodynamic surfaces, followed by a tabulation of advantages and disadvantages. Eight integrated ice protection systems, incorporating logical combinations of these methods for each critical area, are then compared to show the relative weight penalties and lead to a final configuration.

5.4.1 Main Rotor Systems

Protection methods examined for the main rotor are as follows:

1. Chemical freezing point depressant (alcohol)
2. Mechanical pneumatic deicers
3. Electrical cyclic deicing
4. Bleed air anti-icing
5. Heated liquid anti-icing
6. Ice-phobic surfaces and the "Aerodynamic Discontinuity Principle".

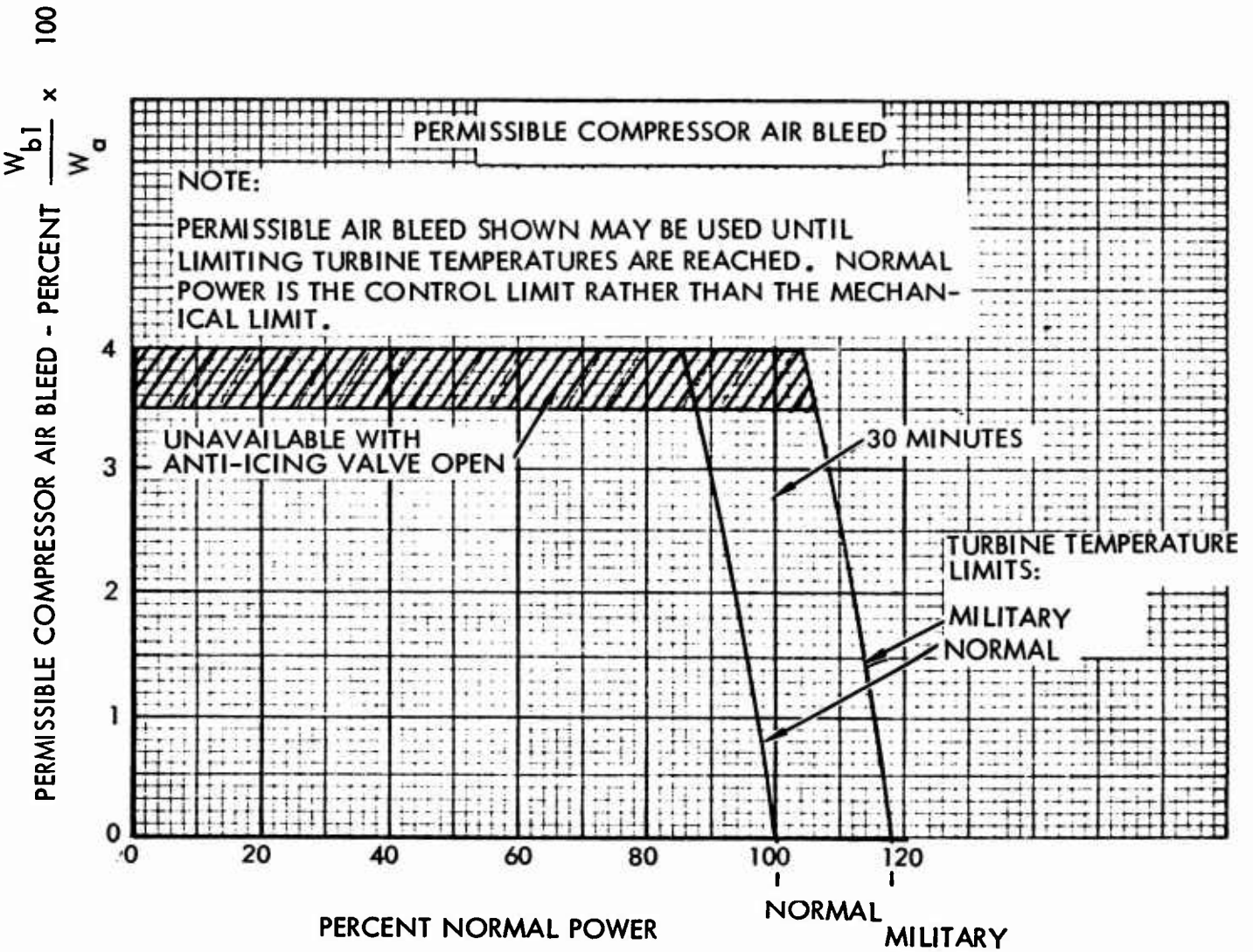

Figure 154. Permissible Compressor Air Bleed.

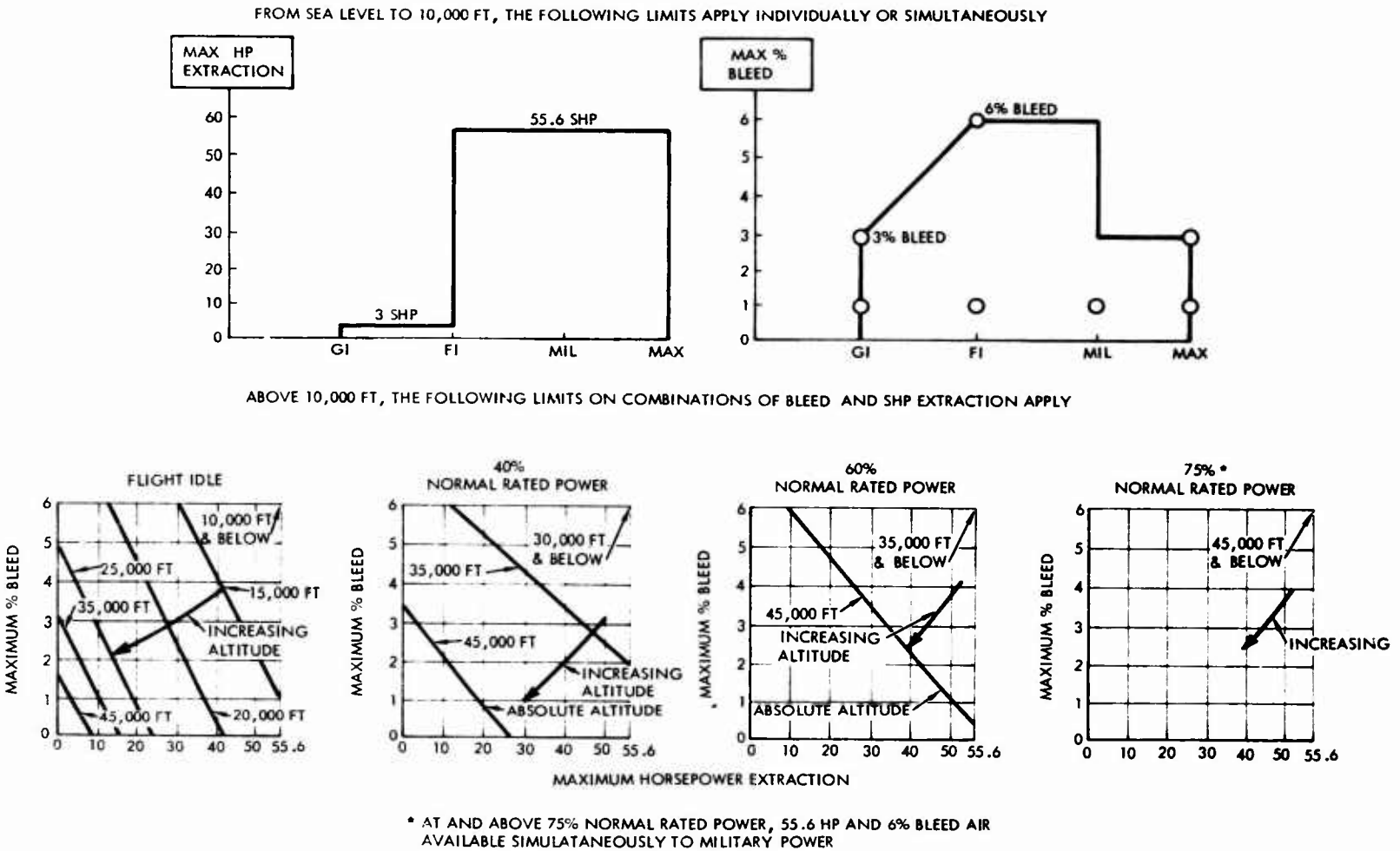

Figure 155. Gas-Generator Horsepower and Bleed Extraction Limits.

Several of these candidate protection methods are summarized in Table XXV. All but chemical and electric deicing are rejected, for reasons set forth previously and elaborated on in the following paragraphs. Finally, the selection of an electric system in preference to the chemical system is made for the following reasons:

1. Deicing effectiveness of the electric system is superior to that of an alcohol system.

2. Sufficient electric power is available for a small weight increase if a two-generator system is provided to meet other requirements.

3. The size and capacity of the generators need not be increased because in subfreezing weather the capability of air-cooled generators is considerably in excess of their nominal rating.

4. Flight safety is improved and the logistics problem is reduced by eliminating alcohol (190 proof) from the air vehicle.

5. The electric system weight compares favorably with the "dry" weight of the alcohol system. When ready for use, the alcohol system weight exceeds the electric system by 120 pounds (1 hour supply of alcohol).

TABLE XXV. MAIN ROTOR BLADE TRADE-OFF SUMMARY

	Operating in Fair Weather Regions		
	Alcohol	Pneumatic	Electric
Flight Safety	Good	Good	Good
Weight, lb	50	36	56
Power, hp	0	30 (drag of boots)	0
Maintenance	Fair	Fair	Fair
Relative Cost/Ship, *	1	2	4
Development Cost	Moderate	Moderate	Moderate
Development Risk	Moderate	High	Moderate

* Higher numbers denote greater cost

TABLE XXV. Continued.

	Operating in Icing Weather Regions		
	Alcohol	Pneumatic	Electric
Ice Protection Effectiveness	Fair	Poor-Fair	Good
Flight Safety	Fair	Good	Good
Vulnerability	Poor	Good	Fair
Weight, lb	156	36	56
Power, hp	1.0	32	30
Reliability	Fair	Good	Good
Maintenance	Fair	Fair	Fair
Logistics/GSE	Poor	Good	Good

5.4.1.1 Chemical Deicing System

An alcohol-glycerin mixture (90 percent/10 percent) is distributed over the blade surfaces through leading-edge holes to depress the freezing point, thereby preventing icing and/or removing small accretions. The manifolds and holes must be carefully tailored experimentally to provide uniform fluid distribution over the blade surfaces. As discussed earlier, the system has been applied only on U.S. development rotors for the Bell UH-1 and the Vertol CH-47 Chinook. No production helicopters are equipped with this system in the USA, but it is in use on Russian helicopters such as the MI-4 and on the British Sycamore. The system is extensively used on fixed-wing vehicles such as the Vickers Viking, DeHaviland Dove and Heron, Hawker-Sidley DH-125, and the Short Brothers Skyvan.

Advantages

1. Fair protection, as demonstrated by Bell, Vertol, and the USAF Adverse Weather tests

2. The system imposes a dry weight penalty (no alcohol) which is slightly less than an electric deicing system when operating in clear weather.

3. Negligible blade drag in fair weather

4. Control system relatively simple compared to electric deicing

Unfavorable Aspects

1. Flight Safety

   a. Increased aircraft vulnerability and decreased safety due to the flammability of stored alcohol (20 gallons) when icing is anticipated

   b. Severe blade unbalance could result from faulty liquid distribution (holes plugged in one blade, trapping liquid at tip, or leakage of liquid into the structure of one blade as occurred on the UH-1B in early tests at Dayton).

2. Performance - does not shed cleanly because necessary uniformity of liquid distribution cannot be achieved. Permits appreciable vibration increase due to uneven shedding, according to References 79 and 80. Ice prevention tends to be unreliable and slow; recovery performance (ice removal after delayed system activation), is unsatisfactory.

3. Operating Weight - Weight of the system charged with alcohol for 1 hour of operation greatly exceeds the electrothermal system weight.

4. Maintenance

   a. Blade distribution holes become plugged with dirt and may also be peened shut due to impact of dirt particles. The fluid distribution system must be flushed with alcohol periodically to remove glycerin and dirt.

   b. The outer surfaces of the blades must be washed with alcohol after each use of the system to remove traces of glycerin which gather dirt.

   c. Sintered metal leading edge distributor is subject to erosion due to rain, dust and dirt.

5. Logistics - Must supply large quantities of alcohol to theaters of operation where icing is anticipated.

5.4.1.2 Mechanical Deicers (Pneumatic Boot)

No development work has been done in this area, mainly due to the fear of adverse aerodynamic effects of inflated tubes on small, thin airfoils and also to the possibility that the boots may be damaged or completely torn off by the centrifugal forces developed by the high rotor rpm.

Advantages of the Pneumatic Boot

1. Low power penalty and moderate weight - Approximately 36 pounds installed on main rotor (consisting of 4 pounds net increase per blade and 20 pounds of mechanical inflation and control equipment)

2. Inexpensive system development, production, and maintenance

3. Good blade leading-edge protection against sand and dust erosion (boots are 0.10 inch thick)

4. Control system simplicity

Unfavorable Factors

1. The ice-shedding performance at low temperature, where the ice bond is highest, is suspected to be only fair, based on past fixed-wing experience. However, centrifugal force of the rotor blade might make some improvement.

2. Leading-edge radius is critically small for inflation of chordwise boots.

3. Rain abrasion resistance is uncertain, but judging from applications on high-speed business aircraft, it may permit acceptable boot life.

4. No development and operating experience is available as applied to helicopter blades.

5. The fair-weather power increase (in hover) due to wavy leading-edge drag is estimated to be 35 horsepower, which is equivalent to 215 - 300 pounds of weight. Aerodynamic distortion of airfoil may be unacceptable at a condition of high angle of attack of retreating blade.

6. Uncertainty of the integrity of the rubber boot bond when subjected to strong centrifugal forces.

7. Retractability of the inflated tube is questionable near the tip in the 700 to 800 g field.

5.4.1.3 Electric Cyclic Deicing

This system has been in production in Vertol, Kaman, and Sikorsky helicopters, and is the only system to have seen operational use in the U.S. Edler Industries, Goodyear, and other companies furnish the leading-edge electric boots, which are plastic laminates protected by thin steel abrasion shoes. The systems have been made quite sophisticated from a control standpoint in an effort to obtain optimum ice-shedding performance. If the systems are

properly designed and operated, the ice-shedding performance is potentially excellent. This type of system is also currently in operation on the large Russian helicopters, the MI-6 and the MI-10, and on the British Westland Wessex and will be on the Canadian CHSS-2.

Advantages

1. Excellent ice-removal characteristics, providing minimum vibration increase and best flight characteristics while in icing conditions, as reported by Stallabrass (Reference 85).

2. Negligible power required to overcome blade drag in fair weather.

3. Many system components are developed and are available from suppliers, and much development experience is available.

4. For large helicopters, the weight penalty compares favorably with the dry weight of chemical systems.

Unfavorable Factors

1. Nominal power requirement of 30 horsepower to generate 23 kilowatts for protection of 51-foot-diameter main rotor during operation of the system. For small helicopters, the weight and power penalty may be relatively heavy.

2. Development and maintenance costs relatively high, due to complexity of power distribution and control systems mounted on vibrating rotor.

3. Operation in an erosion-conducive environment may pose an erosion-resistance problem for the outer 40% of the rotor radius because the element is close to the external surface due to the rapid transient response required.

4. Need for further development to improve reliability and perfect construction and controls.

5.4.1.4 Air Thermal Anti-Icing

A heated air blade anti-icing system was built and tested on a Bell helicopter using combustion heaters mounted on each blade root. An open blade construction was required to pass sufficient air spanwise to heat the entire chord. With air at 400°F introduced at the blade root, the system operated as a marginal running-wet anti-icing system. For the example design helicopter, assuming that only the blade leading edge is open and unobstructed from root to tip, and that the inlet air temperature is limited to 250°F by structural bond, an airflow of 7 lb/sec is required to supply the 600,000 Btu/hr required for a fully evaporative anti-icing system. This is a prohibitive bleed air consumption. If bleed air at 500°F were injected

in a recirculating system (similar to that in use on the C-130 or P-3 aircraft), the bleed flow required would be 2 lb/sec or about 2 percent more than the 6 percent maximum allowable extraction from a typical turbine engine. A carefully tailored thermal insulation system would be required within the blade to isolate the bonded structure from the 500°F air, and to assure that sufficient energy is delivered to the outer span of the blade where anti-icing heat requirements are maximum.

The extremely high operating power penalty due to bleed consumption, and the high air temperature requirements during operation are sufficient reasons to exclude the bleed air approach from further consideration on the basis of flight safety.

The use of combustion heaters is rejected due to their weight and bulk as well as the large ducts necessary for the low-pressure air.

5.4.1.5 Anti-Icing With Heated Liquid

This type of system was recently analyzed and was found to be technically feasible. It was proposed to circulate heated liquid through tubes inside the blade leading edge to provide fully evaporative anti-icing protection for the main rotor. Heat was supplied by an engine exhaust gas heat exchanger, and the heat transport liquid was to be either ethylene glycol engine or transmission oil.

Although the weight penalty for the installed system was shown to be competitive with an electric deicing system, the liquid system is not desirable because of the consequences of leakage in the blades and the maintenance implied to insure against leakage. The potential rotor unbalance which can be produced by a fluid leak which empties the liquid tubes in one blade was found to be 1000 pounds on a small 4200-pound helicopter. This crippling imbalance would be even higher on a 17,000-pound vehicle. Vulnerability to blade damage due to gunfire makes the system undesirable, but it is interesting to note that it is the only candidate for a fully effective anti-icing system.

5.4.1.6 Aerodynamic Discontinuity Principle and Ice Phobic Tapes

Flight tests of the aerodynamic discontinuity principle (ADP) tape system on the CH-3 helicopter by the USAF Adverse Weather Branch of the Flight Test Division and other test organizations did not substantiate the value of the ADP system as a blade protection system. Therefore, the ADP and ice phobic surface system is rejected in favor of a positive ice removal system.

5.4.2 Tail Rotor Ice Protection

The requirements and system evaluations for the tail rotor are essentially identical to those for the main rotor.

5.4.3 Propeller Ice Protection

An aft-located pusher propeller may be adequately protected by impinging engine exhaust gas which provides sufficient blade heating to prevent the formation of significant amounts of ice. Otherwise, the propeller can be protected in the same manner as the main or tail rotor.

5.4.4 Wing and Empennage

The choices include no protection, pneumatic inflatable boots, bleed air anti-icing, and electrothermal deicing. No protection is necessary for flight safety, but if it is desired to minimize drag for ferry flight, the lightest, simplest, and least costly icing protection kit to use is pneumatic deicing boots.

5.4.5 Engine Induction Systems

The bleed air heating system was selected over the only practical alternative, which is an electric anti-icing system, mainly on the basis of superior durability and reliability. The weights of the two systems are comparable when considering an aluminum duct with electric heaters applied versus a double-walled steel duct with bleed air heating. The electric heating elements located in the duct are somewhat more vulnerable to damage by flying objects (ice chunks) than is the double-walled steel duct. Experience with turbine engines using the bleed air system has demonstrated the rugged reliability of the bleed air heated system.

5.4.6 Integrated Ice Protection Systems

Table XXVI illustrates the major ice protection methods investigated for the various critical surfaces of the vehicle. The boxes marked "OK" indicate suitable protection methods for each of the surfaces. The reasons for the "Insufficient Protection" label are noted. For example, an engine inlet deicing system is not sufficient due to potential engine damage from even small pieces of ice which are periodically shed into the engine; an ice prevention (anti-icing) system must be used for the engine and induction system. The "Impractical" label is attached to such methods as electric or bleed air anti-icing of the rotor blades, which requires excessive power consumption.

Using this table, eight ice protection systems were synthesized for the air vehicle. These are shown on Table XXVII, which includes total weights of the permanently installed portions of each system (fair-weather weight penalty). Flight safety, logistics, installed weight, and ice protection effectiveness are the primary factors in final system selection.

Systems 1 and 2 use alcohol on the rotors and on the windshield. The use of pneumatic boots instead of bleed air for the fixed aerodynamic surfaces provides a large weight reduction for system 2, which is one of the lightest at 122 pounds (without alcohol or boots on board).

TABLE XXVI. APPLICABILITY OF ICE-PROTECTION METHODS FOR VARIOUS AERODYNAMIC SURFACES

	Main Rotor Blades	Tail Rotor	Wing	Empennage	Engine Inlet	Windshield
Alcohol Anti-Icing) Deicing)	OK	OK	OK	OK	Insufficient Protection	OK (Inferior Visibility)
Electro-thermal Deicing	OK	OK	OK	OK	Insufficient Protection (engine damage)	Insufficient Protection (visibility)
Electro-thermal Anti-Icing	Impractical (Excessive power)				OK	OK
Bleed Air Deicing	Impractical (Excessive temperature)		OK	OK	Insufficient Protection (engine damage)	Insufficient Protection (visibility)
Bleed Air Anti-Icing	Impractical (Excessive temperature)		OK	OK	OK	Impractical (glass damage)
Pneumatic Deicing	OK (no test data avail.)	Impractical (small air-foil)	OK (marginal at low speeds)	OK (marginal at low speeds)	Insufficient Protection (engine damage)	Impractical (visibility)
No Protection	Insufficient Protection (vibration)	Insufficient Protection (vibration)	OK	OK	Insufficient Protection (engine damage)	Insufficient Protection (visibility)
Ice Phobic Surfaces	Such materials have not proven worthy of consideration					
Heated Liquid	OK	OK	OK	OK	OK	Not Applicable

TABLE XXVII. FAIR-WEATHER WEIGHT PENALTIES FOR VARIOUS ICE-PROTECTION SYSTEMS

Protected Surface \ System	1	2	3	4	5	6	7	8
Main Rotor	Alcohol	Alcohol	Electric	Electric	Electric	Pneumatic	Pneumatic	Electric
Tail Rotor	Alcohol	Alcohol	Electric	Electric	Electric	Electric	Electric	Electric
Wing	Bleed	Pneumatic*	Electric	Bleed	(None)	Bleed	Pneumatic*	Pneumatic*
Empennage	Bleed	Pneumatic*	Electric	Electric	(None)	Electric	Pneumatic*	Pneumatic*
Engine Inlet	Bleed	Bleed	Electric	Bleed	Bleed	Bleed	Bleed	Bleed
Windshield	Alcohol	Alcohol	Electric	Electric	Electric	Electric	Electric	Electric
Total Installed Weight	199	122*	193	187	126	169	114*	136*
Total Wt. Due to Drag	0	Negligible	0	0	0	215**	215**	Negligible

* Add 20 lb to install boots.

** May go as high as 300 lb if surface waviness on rotor boot is more pronounced than assumed.

System 3 is all-electric and weighs 193 pounds. A small weight saving is made by substituting electric deicing for bleed anti-icing on the empennage and engine inlets, as shown for system 4 at 187 pounds.

System 5 shows a substantial weight reduction over system 4 by deletion of ice protection from the wing and empennage. A weight reduction of 61 to 67 pounds is realized compared to systems 3 and 4, due to deletion of the fixed surface protection.

Systems 6 and 7 are similar to each other except for deletion of wing and tail protection on 7. The potential weight advantage of the pneumatic boot main rotor protection method is apparent in system 7 which, at 114 pounds, shows the lightest installed weight of all systems. However, a substantial weight penalty due to increased rotor drag (power consumption) is imposed by the wavy surface of the inflatable boot, even though it is in the deflated position. The drag was calculated from high-speed wind tunnel test data on rotor blade sections which were modified to represent booted airfoils. Unless the boot can be fabricated and maintained as smooth as a steel leading edge, it appears unfavorable from an increased drag standpoint.

5.4.7 Final Selection

System 8 was selected as the best combination. It uses electric deicing for the main and tail rotors, engine exhaust wake and aerodynamic heating for an aft-located propeller, bleed anti-icing for the engine and its inlet duct and debris separator, pneumatic inflatable boots (kit) for the wing and empennage, transparent electrical film for the windshield; and submerged inlets (requiring no protection) for the engine compartment and oil cooler inlets.

An ice detector and automatic controls with manual overrides will operate the integrated system, activating it in icing conditions while protecting it from inadvertent operations leading to overtemperature or to rupturing pressures. The integrated system weighs 136 pounds, and with the fixed surface pneumatic boot kit installed, the weight is 156 pounds or about 1.37% of the vehicle empty weight. Although other systems were moderately lighter, none provided the superior protection and reduced logistics of system 8.

5.5 WEIGHT TRENDS

Icing protection system weights, covered areas, and component weights have been obtained for 46 aircraft (18 rotary-wing and 28 fixed-wing vehicles) as shown in Figure 156. Using the same vehicle identification numbers the total system weight is tabulated in Table XXVIII, as are the individual component weights for the wings, tail, engines, propellers, windshields (canopy), rotors, radomes, and antennas. The protected areas for these components are presented in Table XXIX, as are the specific weights (lbs/sq ft). Further weight breakdowns in Table XXX provide information on the boots, supports, controls, etc.

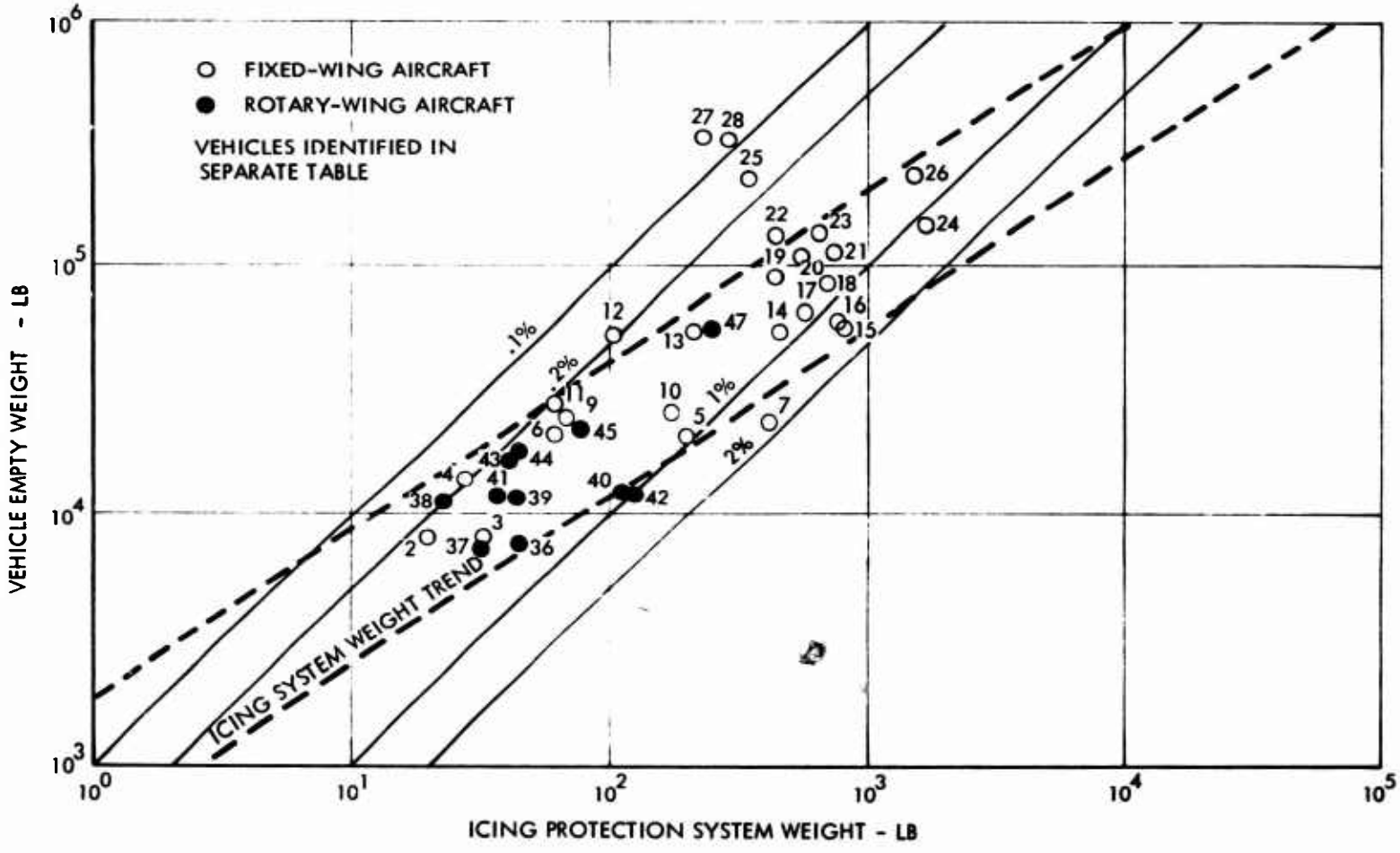

Figure 156. Icing System Weight Trend As a Function of Vehicle Empty Weight.

TABLE XXVIII. ICING PROTECTION WEIGHTS OF SELECTED FIXED- AND ROTARY-WING AIRCRAFT

	Model	Mfgr	Wings	Tail	Engine	Prop	Antenna Radome	Canopy	Rotor	Pitot etc	Total wt	Empty x 1,000 lb
1	T37B	Cessna									6	4
2	F5B	Northrup									20	8
3	T33A	Lockheed									33	8
4	F104G	Lockheed									29	14
5	Jetstar	Lockheed	108	59				33			200	21
6	F100F	NAR									61	22
7	F27A	Fairchild									436	24
8	F105B	Rupublic									9	25
9	F106B	Convair									70	25
10	S3A	Lockheed	95	44	21			12		1	173	26
11	F101B	McDonnell									62	28
12	B58A	Boeing									102	54
13	737-200	Boeing									212	55
14	DC9-30	Douglas									472	55
15	188C	Lockheed									854	57
16	C130E	Lockheed	312	145	169	63	31	66			785	61
17	P3C	Lockheed	348	76	44	80		88			586	66
18	880-22M	Convair									714	85
19	707-200	Boeing									444	91
20	707-120B	Boeing									579	111
21	990	Convair									755	112
22	C141A	Lockheed	181	144	82			40			446	131
23	DC8-62	Douglas									666	135
24	VC10	Vickers									1714	144
25	L1011	Lockheed	102		169		27	49			354	222
26	XB70A	NAR									54	231
27	C5A	Lockheed			195			38			233	323
28	747-21F	Boeing									299	323
*31	OH-6	Hughes									1	1.1
32	OH-58	Bell									1	1.6
33	OH-5	Hiller									2	2.5
34	HH-43	Kaman									0	4.5
35	UH-1	Bell									1	5.0
36	UH-2B	Kaman									56	7.4
37	UH-2D	Kaman			12		2	18			32	7.6
38	SH-3A	Sikorsky									23	11.5
39	SH-3D	Sikorsky									45	11.8
40	CH-46	Vertol									114	12.2
41	CH-3C	Sikorsky			14			21	2		37	12.3
42	CHSS-2	Sikorsky			14			21	93		128	12.3
43	AH-56A	Lockheed	3		34			6			42	17.0
44	CH-47	Vertol									44	18.0
45	CH-53	Sikorsky			66			11			77	22.4
46	CH-54	Sikorsky										26.7
47	MIL-6	Russian									250	58.0
48	HU-5	Wessex									111	7.7

* lines 29 and 30 are omitted.

TABLE XXIX. ICING PROTECTION SURFACE AREAS AND SPECIFIC WEIGHTS

Item	4	5	10	15	16	17	22	25	40	44
Vehicle	F104G	Jetstar	S3A	188C	C130E	P3C	C141	L1011	H46	H47
Mfgr.	L	O	C	K	H	E	E	D	VERTOL	
Ft^2 Wing		71		218		218		195	-	-
Ft^2 Tail		42		62		72		-	-	-
Ft^2 Engine	13	53		54		54		127	16	29
Ft^2 Canopy		17						37	10	6
Ft^2 Prop/Rotor	-	-	-	11	-	11	-	-	59	-
Lb/Ft^2 Wing		1.52				1.59		.53	-	-
Lb/Ft^2 Tail		1.05				1.06		-	-	-
Lb/Ft^2 Engine		.39				.82		1.33		
Lb/Ft^2 Canopy		.72						1.32		
Lb/Ft^2 Prop/Rotor	-	-	-		-		-	-	-	-

TABLE XXX. ICING SUBSYSTEM WEIGHTS (WING)

Valves	7	20		56	59	6	
Ducts			145	213		66	
Shroud		46	83	14	76		
Insulation		2	33	28			
Boots	49	11					
Controls	15	15	30	27	12	15	
Supports	6		21	11	26	14	
Plumbing	30				8		
Total Lb	108	95	312	348	181	102	
Total Ft^2	71			218		195	
Lb/Ft^2	1.52			1.59		.53	

The overall system weights of selected vehicles have been plotted in Figure 156 as a function of the vehicle empty weights. Not included in this figure are any vehicles for which less than 10 pounds was attributed to anti-icing group equipment in the weight statements (such as vehicles 1, 8, 31, 32, 33, and 35). Actually there is a possibility of discrepancies in the order of 40 pounds, due mostly to the problems of conflicting bookkeeping:

1. Electrical wiring and harnesses are sometimes attributed to the electrical system and sometimes to the pertinent group. Such a difference is 42 pounds out of a total of 92 for the CHSS-2 (vehicle 42).

2. The electrically heated rotor boots for the CHSS-2 (vehicle 42) are tabulated as 67.5 pounds "component weight" but only 5.5 as "added weight". For the Kaman H2 (vehicle 37) the electrically heated boots weigh 58.5 pounds but represent zero "added weight." The boots fulfill the blade counterbalance requirements, evidently, for most blade applications.

Although the data of Figure 156 (and Table XXVIII) represents quite a diverse variety of icing system protection requirements, capabilities, and vehicle types, several generalizations can be made:

1. Except for the newest wide-body jets (vehicles 25, 27 and 28), the icing protection system weight varies from 0.2 percent to 1.5 percent of the vehicle empty weight, with an overall trend of increasing weight percentage with increasing vehicle weight.

2. Independent of size, no more than 1,000 pounds need be assigned to icing protection. Vehicles 7, 24, and 26 appear to be overly heavy and would probably be suitable contenders for a weight reduction design.

3. The biggest vehicles have achieved a size such that the radius of curvature of the wing leading edges has reduced the ice collection efficiency to negligible levels, thus permitting omission of those ice protection systems.

4. From heaviest to lightest percentage ratios, the sequence is:

   Business jets

   ASW patrols and trainers

   Commercial-transports and helicopters

   Fighters and bombers

   Jumbojets

5. There is a strong chronological influence as indicated by:

C130 (vehicle 16) Lockheed cargo ship (early '50s)

C141 (vehicle 22) Lockheed cargo ship (early '60s)

C5A (vehicle 27) Lockheed cargo ship (late '60s)

and 188C Electra (vehicle 15) Lockheed commercial (late '50s)

L1011 Tristar (vehicle 25) Lockheed commercial (early '70s)

Similar trends are exhibited by the Boeing, Douglas and Convair data. As part of a questionnaire sent to the rotary-wing airframe manufacturers there was a request for information on the area of the protected surfaces and the subsystem weights. Little information was received, so the area and specific weight data in Table XXIX and the subcomponent weights in Table XXX are primarily for fixed-wing applications. Available excerpts from official weight tables gave only the total weight values shown in Table XXVIII for both the fixed- and rotary-wing vehicles. From the limited data available, however, there appears to be an indication of a range from 0.4 to 1.6 pounds per square foot of protected area.

To give an indication of the difference in actual and effective (or listed) weight panalties, the weight breakdown for the 12,300 lb CHSS-2 (62-foot-diameter rotor) is printed here as Table XXXI. Similar information for the 7700 lb Wessex HU5 (56-foot-diameter rotor) is shown in Table XXXII. Table XXXIII compares on a single page the various electrically heated rotor system components from several vehicles.

5.6 RELIABILITY

B. F. Goodrich Co. data on their current pneumatic boot designs and also reliability and service experience on these boots are shown in Table XXXIV. Table XXXIV shows MTBF data from their F-27 fleet. The average deicer service life is claimed to be 5.188 years, or 10,000 flight hours based upon a utilization rate of about 2,000 hours per year per aircraft.

Tables XXXV through XLVII summarize the reliability and maintainability investigation for all types of systems. All numbers are compared to total flight hours and equipment population.

These data are quick to point out problem areas and places where improvement should be made or, that the component cannot be improved, an indication that a high degree of accessability and quick disconnect functions should be provided. Referring to Tables XLIII and XLIV, data source 1, code 22333, data source 2 code 23LAB are such examples. Further, an investigation as to the manufacturer of the most successful hardware, and careful selection of this hardware would be important in improving maintenance and reliability.

TABLE XXXI. COMPONENT LIST AND WEIGHT BREAKDOWN

The components of the rotor blade de-icing system, as well as their approximate sizes, weights, manufacturer's name, and the UACL specification numbers are given in the table headed Component List. The adjacent table shows the breakdown of the installed weight. It should be noted that the main rotor heating boots involve no weight penalty since the additional weight per blade can be compensated for by reducing the blade balancing weight. Only part of the weight of the main rotor slip ring assembly is included since the CHSS-2 is normally fitted with a slip ring/roller assembly for automatic blade folding.

The position of components in the aircraft is shown below.

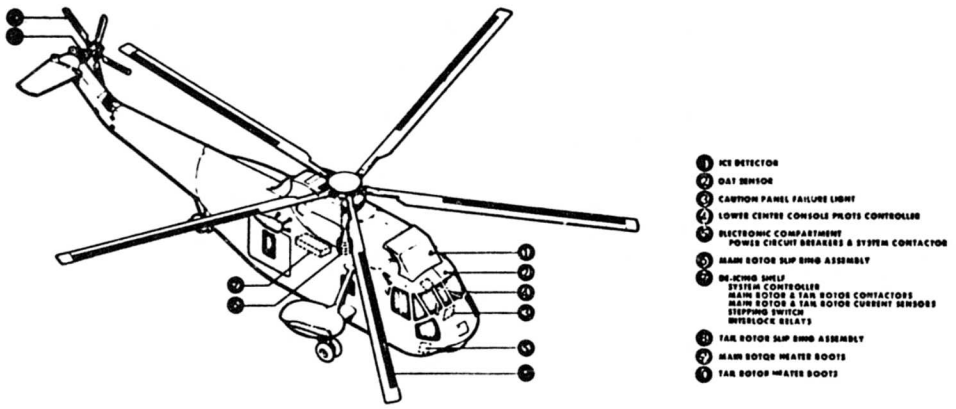

COMPONENT LIST

COMPONENT	SIZE (Inches)	WEIGHT	MANUFACTURER	UACL SPEC.
Controller	6.75 x 4 x 4.2	5 lbs 2 oz	Rosemount Eng.	HES 1004
Stepping Switch	7.55 x 5.5 x 5.5	6 lbs	Marsland Eng.	HES 1002
OAT Sensor	5/32 dia. x 1	1 oz	Rosemount Eng.	
M/R Contactor	5.23 x 3.94 x 4.0	3 lbs 4 oz	Hartman	
T/R Contactor	2.59 x 2.44 x 1.75	14 oz	Hartman	
M/R Current Transformer	3.25 x 3.5 x 1	2 lbs	Apollo Electronics	
T/R Current Transformer	3.25 x 3.5 x 1	2 lbs	Apollo Electronics	
Pilot's Control Panel	4.5 x 3.25 x 3	1 lb 8 oz	UACL	0155-61101-041
Ice Detector	—	1 lb 7 oz	Rosemount Eng.	
M/R Slip Rings	13¾ dia. x 7½ deep	12 lbs	Engelhard	0135-20100
T/R Slip Rings	9 dia. x 3½ deep	3 lbs	Engelhard	0135-66100
M/R Heater Boots	37.2 heated length	12.4 lbs/ blade	Goodyear	S6115-20905 (Sikorsky)
T/R Heater Boots	37.2 heated length	1.1 lbs/ blade	Goodyear	S6115-30905 (Sikorsky)

INSTALLATION WEIGHT BREAKDOWN

		Added Weight (lbs)	
GENERAL	Pilot's Controller	1.5	
	System Controller	5.0	
	Warning Lights and Switches	1.5	
	Wiring & Connectors	43.5	
	Sundries	10.0	
			61.5
MAIN ROTOR	Heater Boots	0.0	
	Slip Ring Assembly	9.0	
	Stepping Switch	6.0	
	Contactor	3.3	
	Current Transformer	2.0	
			20.3
TAIL ROTOR	Heater Boots	5.5	
	Slip Ring Assembly	3.0	
	Contactor	.9	
	Current Transformer	2.0	
			11.4
		TOTAL	93.2

TABLE XXXII. WESSEX HU-5 ESTIMATED WEIGHT OF A PRODUCTION SYSTEM

	Pounds
Transmission and Structural Alterations	3.3
Main Blade Spraymat Penalty	14.0 *
Tail Blade Spraymat Penalty	3.3
U.C.C. Ice Accretion Meter System (Prototype) (comprising probe control unit and icing computer)	7.0 **
Cyclic Distributor	20.0
Master Contactor	2.7
Fault Analyser Unit	3.0
Current Transformers	1.2
Slip Rings	21.0
Cables, Clippings etc.	14.8
Rotor Oil Reservoir Penalty	2.0
Alternator and Control Unit	34.0
Total	126.3 lb

* The Spraymat on the main rotor blades is forward of blade C of G balance position and can therefore be used in place of some of the blade balance weights. The weight penalty quoted above is based on previous applications to the Wessex. However, a recent Spraymat application to S58 (same blade as Wessex) with proper removal of balance weights, resulted in a weight penalty of only 119 gms (0.263 lb) per blade. For production aircraft the 14 lb quoted could therefore be reduced to 1.1 lb.

** On the production system the weight of the U.C.C. ice accretion meter system is estimated to be reduced to 5 lb.

TABLE XXXIII. ROTOR ELECTRICAL DEICING WEIGHTS

	Wessex HU5	Kaman HU2	Sikorsky CHSS2	Lockheed AH56	Vertol CH46
Vehicle Alterations	3.3				
Main Blade Boot Penalty	1.1	0 (58.5)	0 (62.0)	(44.0)	
Tail Blade Boot Penalty	3.3		5.5	8.0	
Ice Accretion Meter System	5.0			1.7	
Cyclic Distributor	20.0	1.5	6.0	13.5	
Master Controller	2.7		4.2	3.5	
Fault Analyser	3.0				
Current Transformer	1.2		4.0	2.2	
Slip Rings	15.0	(6.8)	12.0 (15.0)	14.0	
Cables, Clippings, etc.	14.8		43.5	20.0	
Rotor Oil Reservoir Penalty	2.0				
Alternator and Control Unit	34.0				
Timer		.4			
Temperature Sensor		.2	.1	.2	
Power Supply Box		4.6			
Circuit Breakers and Wiring		9.5			
Pilot's Control Panel			1.5	4.5	
Controller		.4	5.1	10.5	
Sundries			10.0	5.0	
Autotransformer				10.0	
Total Attributed Weight, lb	111	32	93		114
Total Actual Weight, lb	126			137	170

NOTE: Total weights are from spec summaries; part weights from brochures.

( ) ... indicates actual weight of previous line item

TABLE XXXIV. PNEUMATIC DEICER SERVICE EXPERIENCE FOR F-27 AIRCRAFT
PERIOD COVERED: AIRCRAFT LIFE THRU DEC. 31, 1967

	(1)	(2)	(3)	(4)	(5)	(6)	(7)	(8)	(9)	(10)	(11)	(12)
	Aircraft								Deicers Used			
Airline	No In Use	Average Age In Years	Aircraft Years (1)=(2)	Replacement Deicers Purchased	Deicers On Inventory	Purchased Deicers Used (4)-(5)	Total Deicers On Aircraft (1)x15*	Adjustment Factor** Partially Used Deicers (7)/2**	Total Pieces (6)+(8)	Sets/ Aircraft (9)+(7)	Average Deicer Life In Years (2)/(10)	Deicer Life Weighted By Aircraft NO (1)x(11)
Bonanza	15	6.833	102.495	239	44	195	225	112.5	308	1.369	4.991	74.865
Northern Consolidated	3	8.867	26.601	67	0	67	45	22.5	90	2.000	4.433	13.299
Ozark	5	7.049	34.245			104 x 5/7 = 74***	75	37.5	112	1.493	4.721	23.605
	*** 2			138	34	104						
Pacific	13	6.589	85.657	140	21	119	195	97.5	217	1.113	5.920	76.960
Piedmont	8	8.442	67.536			188 x 8/10 = 150****	120	60	210	1.750	4.824	38.592
	**** 2			215	27	188						
Quebecair	5	8.967	44.835	27	0	27	75	37.5	65	.866	10.354	51.770
West Coast	12	8.191	98.292	596	30	566	180	90	656	3.644	2.247	26.964
Wein Alaska	3	7.887	23.661	18	0	18	45	22.5	41	.911	8.657	25.971
Total	64		484.322						1699			332.026
Average Per Aircraft All Airlines			7.57						26.55			5.188

* 15 deicers required per aircraft.

** Adjustment is based on assumption that 50% of useful life of currently installed deicers has been utilized.

*** 2 leased aircraft were used for part of the period - adjustment was made to column (6) and calculations based on 5 aircraft.

**** 2 aircraft maintained for other corporations.

Average Deicer Life = 5.188 years

Median Deicer Life = 4.874 years

TABLE XXXV. SUBSYSTEM: WINDSHIELD DEFOGGING/ANTI-ICING (ELECTRICAL)

Data Source	Code	Component Description	MTUR (Hr)	MTUR (Hr)	MTBF MMH/CA @ 90% C_L	MTBF (Hr)
1	41541	Relay	85,638	256,916	16.5	513,832
1	41542	Rheostat	128,458	-	1.0	128,458
1	41543	Thermistor	4,429	-	2.5	4,429
1	41544	Transformer	10,704	32,114	12.0	64,329
1	41545	Control Box	1,735	51,383	3.1	55,000
1	41546	Heating Element	1,167	-	3.1	100,000
1	41547	Other	14,273	-	3.6	14,273
		Subsystem Complete	543	18,518	6.0	55,500
2	41551	Relay, High/Norm	96,280	320,936	3.3	Infin
2	41552	Control Box	5,842	26,163	2.8	60,175
2	41553	Transformer	35,397	200,585	6.3	601,755
2	41EDE	Wiring	6,656	19,969	5.5	19,969
2	41EDO	Heating Element	1,163	74,468	4.7	Infin
		Subsystem Complete	2,785	10,416	4.5	>14,492
3	41VDA	Switch	6,656	-	13.8	Infin
3	41VDE	Control Box (Side)	19,969	39,938	7.6	Infin
3	41VDF	Control Box (Windshield)	59,907	-	2.5	Infin
3	41VDG	Xfmr. (Side)	13,313	39,938	11.7	39,938
3	41VDH	Xfmr. (Windshield)	19,969	39,938	10.1	Infin
3	41VDL	Relay	19,969	-	5.9	Infin
3	41VDM	Wiring & Connectors	1,996	-	5.4	Infin
		Other	19,969	19,969	18.0	Infin
		Sub System Complete	1,060	8,000	9.4	39,938

TABLE XXXVI. SUBSYSTEM: BLEED AIR DISTRIBUTION - WING ANTI-ICING AND EMPENNAGE ANTI-ICING

Data Source	Code	Component Description	MTBM (Hr)	MTUR (Hr)	MTBF MMH/CA @ 90% C_L	MTBF (Hr)
1	41421	Valve-Isolation	1,173	7,556	8.2	25,691
1	41424	Valve-Anti-Icing, Wing	4,714	10,932	8.9	22,340
1	41425	Valve-Check	17,718	32,114	12.4	128,458
1	41427	Valve Anti-Icing, Empennage	3,425	11,170	7.7	32,114
1	4143B	Expansion Bellows	18,351	128,458	9.1	Infin
1	4143C	Insulation Blanket	3,471	39,525	3.5	Infin
1	4143D	Ducting	340	1,976	11.6	25,691
1	41432	Tubing	4,757	64,229	6.9	Infin
1	41433	Compensator	45,877	214,096	8.6	Infin
		Subsystem Complete	202	1,107	8.5	6,173
2	41432	Valve, Check	137,544	481,404	4.1	Infin
2	41433	Valve, Wing Isolation	2,407	5,470	7.5	17,193
2	41511	Valve, Modulating	4,689	1,668	5.5	42,476
2	41512	Sensor, Temp. Control	80,234	103,158	5.5	361,053
2	41517	Duct, Diffuser	112,327	1,684,914	3.3	Infin
2	41521	Camp, Duct	29,176	148,124	4.7	213,957
2	41522	Insulation Blanket	5,014	12,035	3.8	30,087
2	41453	Ducting	54,705	200,585	10.9	601,755
		Subsystem Complete	1,102	2,710	5.7	8,000

TABLE XXXVII. SUBSYSTEM: EMPENNAGE DEICING (ELECTRICAL)

Data Source	Code	Component Description	MTBM (Hr)	MTUR (Hr)	MTBF MMH/CA @ 90% C_L	MTBF (Hr)
2	41531	Controller	530	1,972	2.8	8,596
2	41532	Heater, Leading Edge	9,347	26,744	8.4	962,808
2	41533	Relay	962,808	962,808	1.7	925,616
2	4153	Indicator Light Assy & Wiring	6,334	60,175	7.2	Infin
		Subsystem Complete	464	1,779	5.0	8,475

TABLE XXXVIII. SUBSYSTEM: ENGINE INLET ANTI-ICING (BLEED AIR)

Data Source	Code	Component Description	MTBM (Hr)	MTUR (Hr)	MTBF MMH/CA @ 90% C_L	MTBF (Hr)
1	41551	Valve	28,546	64,229	6.2	128,458
1	41552	Probe/Ice Detector	12,234	27,043	4.3	42,819
1	41553	Shut-Off Valve (Motor Oper)	64,229	171,277	9.7	Infin
1	41555	Duct	36,702	513,832	5.5	Infin
1	41557	Other	64,229	-	4.4	Infin
		Subsystem Complete	5,681	16,393	6.0	32,258
2	23LBA	Valve, Anti-Ice	3,902	13,539	5.7	31,915
	23LB1	Duct, Nacelle Nose Cowl	15,677	74,468	10.0	893,620
	23LRC	Relay	127,660	Infin	1.9	
	23LRE	Rectifier, Engine A/I	223,406	Infin	4.2	
	23LRF	Actuator/Valve Eng. Inlet	3,786	10,154	6.7	24,822
	23RRJ	Actuator, Nacelle A/I	29,787	81,238	5.1	223,405
	23LS0	Ducting	7,415	223,405	2.7	
		Subsystem Complete	1,307	4,975	5.2	

TABLE XXXIX. SUBSYSTEM: PROPELLER, ANTI-TORQUE AND DEICING SYSTEM (ELECTRICAL)

Data Source	Code	Component Description	MTBM (Hr)	MTUR (Hr)	MTBF MMH/CA @ 90% C_L	MTBF (Hr)
1	4151B	Element Assy., Nose			1.0	Infin
1	4151F	Heater Assy., Cuff			1.0	Infin
1	4151G	Element-Heater, Spinner	18,351	128,458	4.8	Infin
1	41511	Control Panel	64,229	-	2.0	140,658
1	41512	Transformer	128,458		2.0	Infin
1	41513	Relay	856,386		7.6	Infin
1	41515	Timer	64,229		2.2	35,164
1	41517	Boot - Blade	5,677	293,618	5.9	Infin
		Subsystem Complete	3,584	90,900	3.3	28,131

TABLE XL. SUBSYSTEM: ICE DETECTION SYSTEM

Data Source	Code	Component Description	MTBM (Hr)	MTUR (Hr)	MTBF MMH/CA @ 90% C_L	MTBF (Hr)
1		Relay	214,076	321,145	2.8	
1		Interpreter	32,114	64,229	8.9	85,638
1		Rectifier	256,916	770,748	8.5	Infin
1		Detector	10,276	21,409	4.6	28,546
1	41529	Other	64,229	-	18.8	-
2	41EAA	Detector	613	1654		3723
2	41EAB	Switch, Control	31,915	111,702		223,405
		Subsystem Total	376	1573	3.9	3603
3	41XAA	Detector	799	3117		5195
3	41XAD	Switch, Test	10,391	31,175		-
		Subsystem Total	465	2834	7.0	5195

TABLE XLI. SUBSYSTEM: RADOME ANTI-ICING (PNEUMATIC)

Data Source	Code	Component Description	MTBM (Hr)	MTUR (Hr)	MTBF MMH/CA @ 90% C_L	MTBF (Hr)
1	41531	Valve, Pressure Relief	21,409	128,458	2.9	128,458
1	41532	Valve Modulating	2,214	6,760	5.9	25,691
1	41533	Regulator	6,760	64,229	6.3	Infin
1	41535	Thermostat	15,112	85,638	8.1	Infin
1	41536	Ejector	18,351	128,458	3.2	Infin
		Subsystem Complete	1,153	5,208	5.3	21,276

TABLE XLII. SUBSYSTEM: COMPRESSOR BLEED AIR, ENGINE COMPONENTS

Data Source	Code	Component Description	MTBM (Hr)	MTUR (Hr)	MTBF MMH/CA @ 90% C_L	MTBF (Hr)
1	2233A	Valve, Sensitive	562,632	Infin.	4.4	Infin.
1	22333	Valve, Speed Sensitive	1,649	2305	7.3	3091
1	22334	Valve, Comp Bleed	20,838	112,526	4.5	Infin.
1	22335	Valve, Bleed Control	33,096	187,544	6.7	Infin.
1	22336	Valve, Solenoid, 3-Way	281,316	562,632	-	Infin.
1	22337	Valve, Solenoid	56,263	281,316	4.1	281,316
1	22338	Valve, Anti-Ice	40,188	112,526	6.8	140,658
1	22339	Miscellaneous	28,131	Infin.	1.6	Infin.
		Subsystem Complete	1,300	2,183		2,985

TABLE XLIII. SUBSYSTEM: COMPRESSOR BLEED AIR, ENGINE COMPONENTS

Data Source	Code	Component Description	MTBM (Hr)	MTUR (Hr)	MTBF MMH/CA @ 90% C_L	MTBF (Hr)
2	23LAA	Valve Assy., Compressor Field	3197	23,829	4.8	198,582
2	23LAB	Actuator Control, Comp. Bleed	1528	4,536	7.0	10,154
2	23LAC	Governor Assy., Comp. Bleed	10,513	25,532	11.0	54,158
2	23LAD	Screen, Governor/ Air	32,495	595,746	4.2	737,270
2	23LAL	Control, Comp. Bleed Reset	9,212	24,822	6.3	81,238
2	23LA9	Miscellaneous	15,957	44,681	6.3	Infin.
		Subsystem Complete	789	2,740		7,407
3	23SAA	Manifold Compressor Design	1,084	9,592	7.0	62,350
3	23SAG	Valve, Temp. Augment.	483	2,226	7.9	9,592
3	23SAC	Sensor, Temp. Augment. Valve	923	1,833	6.6	4,618
3	23SAD	Manifold, Bleed	1,022	2,226	9.6	31,175
3	23SAF	Valve, Engine	605	1,312	11.5	2,078
3	23SAG	Tubes, Anti Ice	2,587	20,783	3.0	623,500
		Subsystem Complete	141	424		1,174

TABLE XLIV. SUBSYSTEM: ROTARY-WING PECULIAR COMPONENTS

Data Source	Code	Component Description	MTBM (Hr)	MTUR (Hr)	MTBF MMH/CA @ 90% C_L	MTBF (Hr)	Remarks
Predicted		Heating Element Assy. Main Rotor Blade	3,000	10,000	4.0	20,000	Elect.
		Heating Element Assy. Anti-Torque Blade	1,000	2,000	3.5	15,000	
		Slip Ring - Main Rotor	2,000	18,000	4.0	30,000	
		Slip Ring - Tail Rotor	1,000	10,000	4.0	30,000	
		Brush Block - Main Rotor	1,500	18,000	1.0	25,000	
		Brush Block - Tail Rotor	1,000	8,000	1.0	25,000	
		Air Division Door (Air Filter)	1,500	8,000	2.0	10,000	
		Torque Shaft Heater	1,200	3,500	1.0	5,000	
		Wiring and Installation For Above	5,000	15,000	1.0	50,000	

TABLE XLV. SUMMARY OF SUBSYSTEM TOTALS, AND APPLICATION OF ROTARY-WING PREDICTIONS

Data Source	Code	System Description	MTBM (Hr)	MTUR (Hr)	Max MMH/CA @ 90% C_L	MTBF (Hr)	Remarks
1	415	Windshield Anti-Icing	500	15,000	6.5	25,000	Electrical
2	415	Windshield Anti-Icing	2,500	8,500	4.7	10,000	Electrical
3	41V	Windshield Anti-Icing	1,000	6,000	10.3	30,000	Electrical
		Rotary Wing Prediction	500	7,500	7.0	8,000	Electrical
1	414	Wing/Empennage Anti-Ice	1,200	6,500	4.5	10,000	Pneumatic
2	414	Wing Anti-Ice	7,000	12,000	3.7	12,000	Pneumatic
2	415	Empennage Deice	300	1,500	3.0	10,000	Electrical
		Rotary Wing Prediction	4,000	8,000	3.5	10,000	Pneumatic
			300	1,500	3.0	10,000	Electrical
1	415	Engine Anti-Ice	5,500	15,000	6.0	30,500	Pneumatic
1	236B	Engine Anti-Ice	1,200	4,000	5.2	9,000	Pneumatic
		Rotary Wing Prediction	1,500	8,000	5.5	15,000	Pneumatic
1	415	Propeller Anti/Deicing	1,500	10,000	4.9	15,000	Electrical
		Rotary Wing Prediction	1,500	10,000	4.9	15,000	Electrical

TABLE XLV. CONTINUED

Source	Code	System Description	MTBM (Hr)	MTUR (Hr)	Max MMH/CA @ 90% C_L	MTBF (Hr)	Remarks
1	4152	Ice Detection	5,000	10,000	8.7	15,000	Temp. and Moisture
2	41EA	Ice Detection	300	1,000	3.9	2,500	Temp. and Moisture
3	41XA	Ice Detection	300	2,500	7.0	3,500	Ultrasonic
		Rotary Wing Prediction	300	1,000	4.0	2,500	Temp. and Moisture
1	4153	Radome Anti-Icing	1,000	4,500	5.3	16,000	Pneumatic
		Rotary Wing Prediction	1,000	4,500	5.3	16,000	Pneumatic
1	2233	Engine Components, Bleed Air	1,300	2,000	4.4	2,500	Pneumatic/ Electric
2	23LA	Engine Components, Bleed Air	700	2,500	6.6	7,000	Pneumatic/ Electric
3	23SA	Engine Components, Bleed Air	140	400	7.6	1,000	Pneumatic/ Electric
		Rotary Wing Prediction	1,200	1,500	6.6	3,000	Pneumatic/ Electric

TABLE XLVI. PREDICTION SUMMARIES - ROTARY WING

System Description	MTBM (Hr)	MTUR (Hr)	MAX MMH/CA @ 90% C_L	MTBF (Hr)	Remarks
Windshield Anti-Ice	500	7,500	7.0	8,000	Electrical
Lead Edge Anti-Ice	4,000	8,000	3.5	10,000	Pneumatic
	300	1,500	3.0	10,000	Electrical
Engine Anti-Ice	1,500	8,000	5.5	15,000	Pneumatic
Propeller Anti/Deice	1,500	10,000	4.9	15,000	Electrical
Ice Detection	300	1,000	4.0	2,500	Temp. & Moisture
Radome Anti-Ice	1,000	4,500	5.3	16,000	Pneumatic
Engine Components - Bleed Air	1,200	1,500	6.6	3,000	Pneu./Elec.
Rotary Wing Peculiar (No Data Source)	Predicted				
Main Rotor Blade Heater	3,000	10,000	4.0	20,000	Electrical
Anti-Torque Blade Heater	1,000	2,000	3.5	15,000	Electrical
Slip Ring Assy. - Main Rotor	2,000	18,000	4.0	30,000	Electrical
Slip Ring Assy. - Tail Rotor	1,000	10,000	4.0	30,000	Electrical
Brush Block - Main Rotor	1,500	18,000	1.0	25,000	Electrical
Brush Block - Tail Rotor	1,000	8,000	1.0	25,000	Electrical
Air Diversion Door (Air Filter)	1,500	8,000	2.0	10,000	Electrical
Torque Shaft Heater	1,200	3,500	1.0	5,000	Electrical
Wiring and Installation - Rotary Wing Peculiar	5,000	15,000	1.0	50,000	

TABLE XLVII. ANTI-ICING DEICING SYSTEM RELIABILITY ANALYSIS - COMPONENT MALFUNCTION TABULATION - MOST TROUBLESOME COMPONENTS

Component Description	Observed Malfunctions	Distribution %
Valve, Motor Operated - Empennage and Wing Anti-Ice System	Binding or Jammed	11.5
	Failed to Operate	12.3
	Internal Failure	26.2
	Leakage Internal or External	43.8
	Wire or Connector Fault	6.2
Control Box - Windshield Deice/Anti-Icing	Switch/Key Broken	48.3
	Failed to Operate	19.3
	Internal Failure	16.5
	Wire or Connector Fault	4.5
	Overheated/Intermittent	1.2
	Attachment Failure	10.2
Heating Element - Windshield	Broken Element	29.8
	Contacts/Connector Defective	37.2
	Burned or Overheated	1.6
	Torn Element	17.8
	Broken Bonding Wire	1.6
	Shorted	3.2
	Open Fault	4.8
	Deteriorated Insulation	4.0
Ice Detector/Interpreter	Switch/Key Broken	23.6
	Internal Failure	54.0
	Other	32.4
Ice Detector Head	Switch/Key Broken	10.0
	Internal Failure	61.0
	Other	29.0

TABLE XLVII. CONTINUED

Component Description	Observed Malfunctions	Distribution %
Boot, Propeller Blade Deicing	Worn, Chafed or Frayed	10.5
	Broken/Cut	9.4
	Current Incorrect	6.4
	Cracked	.4
	Nicked	3.6
	Shorted	.4
	Broken Bonding Wire	1.4
	Torn	5.5
	Burned or Overheated	62.4
Ducting - Bleed Air Distribution	Chafed	2.4
	Broken	2.3
	Burst/Ruptured	.7
	Attachment Failures	27.0
	Deteriorated, Corroded	13.4
	Cracked	19.0
	Leakage External	27.0
	Punctured	4.2
	Alignment Improper	4.0
Valve Modulating and Shut-Off - Radome and Engine Inlet Anti-Icing	Binding or Jammed	5.9
	Failed to Operate	33.5
	Internal Failure	23.2
	Leakage Internal or External	7.6
	Broken	4.9
	Attachment Failures	24.9
Controller - Empennage Deicing	Switch/Key Broken	71.1
	Failed to Operate	13.4
	Internal Failure	11.1
	Contacts/Connector Defective	4.4

Most of the present-day ice-protection equipment was developed in the late 1950's and has had little improvement since that time. Bleed air systems exhibit chronic failures in valves and ducting; controllers have switching problems; ice detector heads have internal failures dependent upon the type; and electrical heater boots burnout for various reasons, mostly from impact with foreign objects. Therefore, ice protection installed on any airplane adds significantly to unreliability and higher maintenance hours. This will be amplified in the rotary-wing environment.

Table XLV is a compilation of the subsystem totals generated in Table XXXV thru XLIV and allows deduction to be made as to the reliability and maintenance parameters that could be expected if this same equipment were installed in a helicopter. The following items were considered for these predictions:

1. An Army helicopter (either attack or transport).

2. Front line operation and frequent base changes.

3. Operational maintenance; no sophisticated ground support equipment.

4. Combinations of severe environmental conditions; extreme hot and cold with alternate dust and precipitation.

5. Higher vibration levels.

6. Unimproved forward areas but improved pads.

7. Mission capability in icing conditions.

Table XLVI summates the rotary wing predictions from Table XLV, and these numbers can now be used for the further evaluation of rotary wing ice protection systems. It is noted that more of the reliability estimates or data account for foreign object or battle damage. All numbers presented here are best estimates, based on past experience, particularly where no data source exists.

While the figures in Table XLVI on the surface appear acceptable, these are based on total flight hours and not by ice protection "on" time. To understand the impact of continuous operation of the ice protection system, Figure 157 has been prepared showing the number of primary failures that may be expected in 100,000 missions of varying ice encounter time durations. These curves consider that any failure to the system would be cause for mission abort and do not include failures to the generators or bleed air ice protection power supplies.

Referring to Table XLVII, it may be seen that a large percentage of the total failures are the result of only one or two failure modes within the equipment:

	Percentage
Motor operated valves	
Internal failure	26.2
Leakage	43.8
	70.0
Controllers, Windshield	
Switching problems	48.3
Attachments	10.2
	58.5
Windshields	
Defective connections	37.2
Broken element	29.8
	67.0
Ducting	
Attachments	27.0
Leaks	27.0
	54.0
Controllers, deicing	
Switching problems	71.0
Modulating valves	
Internal and operational failures	56.7
Attachments	24.9
	81.6
Ice Detector Interpreters	
Switching	23.6
Internal components	54.0
	77.6

These failure modes are not insurmountable; mechanical attachment and switching arrangement problems should be easily overcome. It is estimated that improvements in all of these areas could reduce the number of failures by at least 50 percent, and as integrated into an ice protection system, the system failures could be lowered from 20 to 30 percent. Therefore, the curve slopes in Figure 157 would lower substantially. (Failures would decrease from approximately 145 failures in 100,000 missions of 1-hour ice encounter each to approximately 100.)

Again, from Figure 157, ice detection systems and engine-mounted bleed air components are responsible for over 50% of the total number of failures in the system. Deletion of the ice detection system and reliance on crew observation would be desirable from the reliability and maintainability aspect. The high temperatures to which engine bleed air components are subjected account for a large number of these failures. The use of improved materials, a strong development program, followed by a well executed preventive maintenance program, with design improvements previously discussed, would no doubt bring the reliability of this system in line.

Improvements to the bleed air mechanical components would place bleed air systems at the top of reliability and maintainability preference. However, the weight penalty for this improvement is not currently known.

Electrical systems are more often destroyed by the environment in which they operate; i.e., dust, oil, dirt, and water cause arcing and wear of slip rings and brushes. Foreign objects and blade flexure cause electrical boots to be short lived.

Figure 158 shows the number of maintenance actions expected in 100,000 missions with varying ice encounter times. As with similar reliability curves in Figure 157, the maintenance action slopes will lower with equipment improvement. The top curve in Figure 158, electrical leading-edge protection (for the C-141), is inordinately high compared with the same reliability values.

While not clear from the data, it appears as though maintenance actions are not the result of reliability problems, but more of operational problems. Another aircraft (the P-3) exhibits maintenance actions on electrical deicers approximately half those of the C-141.

In the case of rotating equipment requiring slip rings and brushes, more maintenance is required to keep these operational. Therefore, designs incorporating self-cleaning slip rings, redundant or dual brushes, brush lifting devices, and arc barriers are almost mandatory. There are other ways in which maintenance may be reduced. The following examples are a few:

Windshield System

1. Threaded power and control terminals
2. Dual heat sensors and more rugged leads
3. "Cushioned" windshield installation

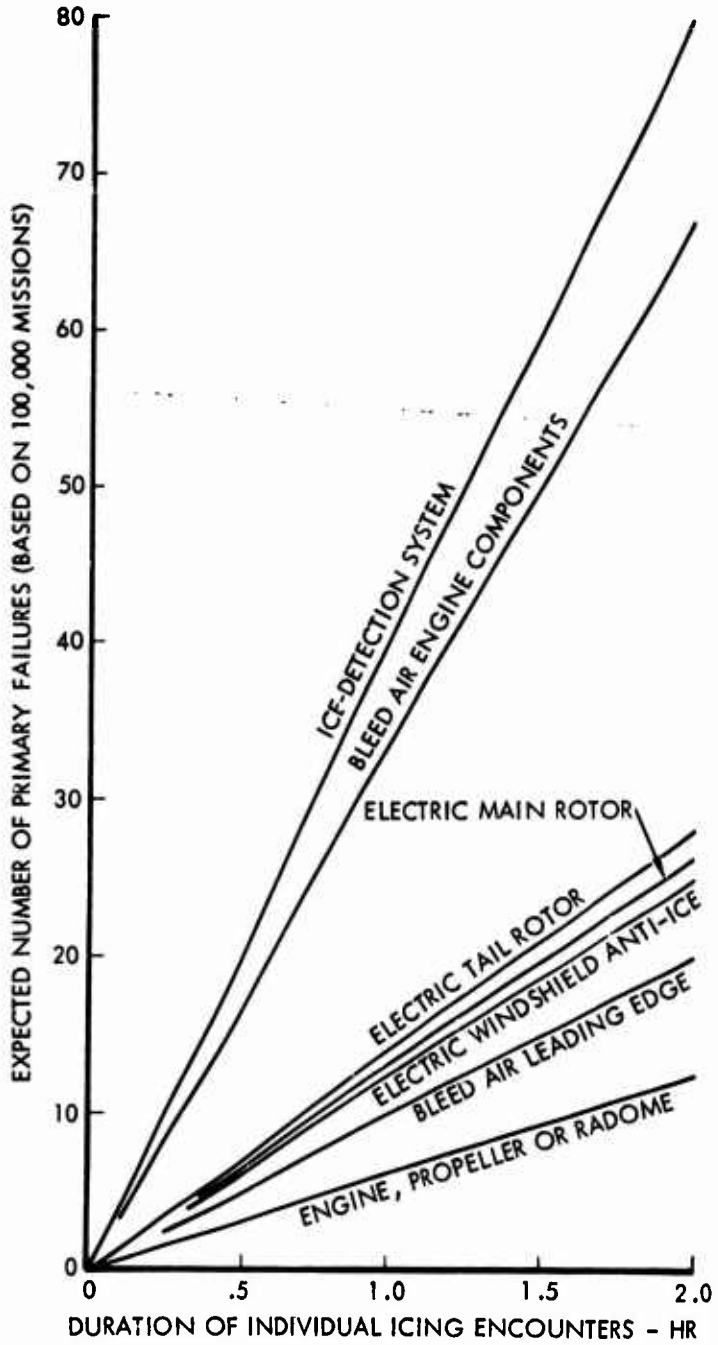

Figure 157. Rotary-Wing Failure Rates.

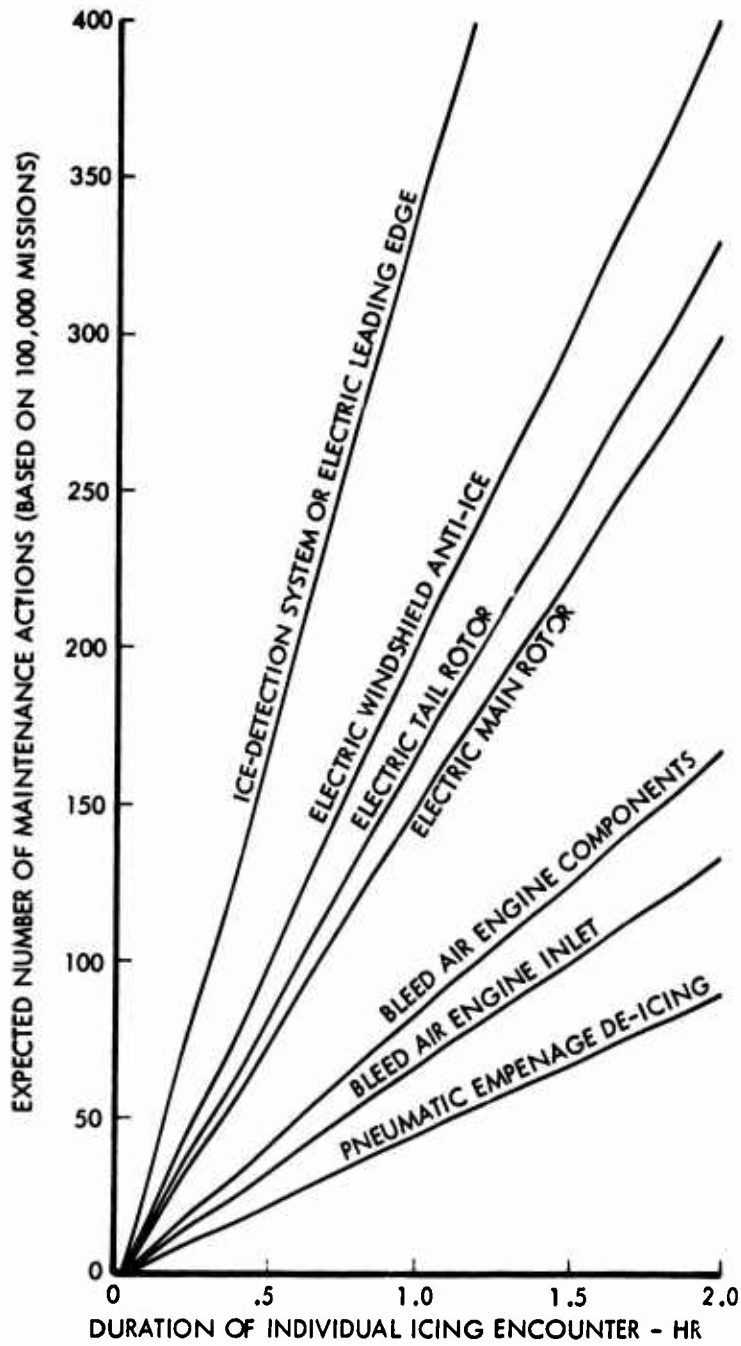

Figure 158. Rotary-Wing Maintenance Rates.

4. BITE equipment or controllers.

5. Controllers designed to fail "off" to prevent overheat of the windshield.

Valves

1. Design mounting flanges to prevent breakage through stress.

Ducts

1. Provide QAD (quick attach-detach) ring.

2. Provide adequate bellows (use internal smooth liners and design as "tension" system rather than "compression" system).

Boots

1. Take advantage of production breaks.

2. Use mechanical fasteners rather than adhesive where possible.

3. Provide adequate protection against stone and hail damage.

4. Use reliable electrical connectors rather than "pigtails".

Detection System

1. Mount detector head away from direction of potential damage by bumping.

2. Provide BITE on controller.

Design system so that it may be easily activated, or deactivated for summer and tropical climates.

All maintenance (less adhesive application) should be capable of being performed with the conventional aircraft mechanic's tool kit.

Locate valves and electronic equipment for maximum accessibility and provide electrical and mechanical quick disconnect feature.

The role of the Army helicopter (to attack the enemy and to replenish troops and supplies under adverse weather conditions) dictates that ice protection systems be designed for maximum reliability and maintainability and that a high degree of repairability be inherent.

Mechanical bleed air components such as valves and regulators must be easily replaceable. This may be accomplished by incorporating quick-detach features rather than nuts and bolts. In those instances where bolts or screws must be used, self-locking features rather than safety wire must be used.

Battle and foreign object damage cannot be ignored and must be part of the design criteria. From a repairability viewpoint, bleed air systems are more desirable than boots. They may be repaired under adverse weather conditions in that no gluing is required. Crude, temporary patches may be used in plenums and ducts, thus improving vehicle availability and readiness. Further, ground checks of hot air systems may be accomplished without additional equipment. Electrical boot systems must be checked with lowered voltages in that operating voltages will overheat the boots (during static conditions) in a matter of seconds.

When electrical boots are used, repair and restoration are important considerations. Table XLVIII has been prepared to provide an overview of the various types of electrical deicers and appropriate restoration techniques. Generally, electrical rubber boots cannot be repaired if the element is separated or shorted. Superficial repairs may be made with "tire patches"; however, these may induce ice accretions by acting as cold spots. In all instances of repair, dry and protected areas are required. While repairs may be made directly on the aircraft if these conditions exist, it is generally not practical. For a front-line operational helicopter, organizational replacement of the component rather than repair will restore the vehicle to operational readiness in a shorter period of time. Direct maintenance may be accomplished on small damage at the squadron level. Major replacement must be accomplished at general or depot levels, especially to metal sheaths.

The design and manufacture of main rotor and tail rotor blades should be controlled to the point where individual blades may be replaced without the necessity of rebalancing or retracking.

In general, regardless of the type or types of systems used, reliability, maintainability, and testing programs must be imposed. Developmental data, and the requirements to test the ice protection components and systems during engine and vehicle development, will highlight problem areas prior to the production of the vehicle, allowing design or quality changes to be incorporated.

Table Explanation, Tables XXXV through XLIV

Column 1. Data Source.

Data Source 1. C-130E aircraft, 140,658 flight hours as of January 1972

Data Source 2. C-141A aircraft, 223,405 flight hours as of December 1971

Data Source 3. C-5A aircraft, 31,175 flight hours as of January 1972

TABLE XLVIII. REPAIRABILITY CHART ANTI-/DEICING BOOTS

Boot Type	Type or Restoration	Method of Restoration Repair Facilities	Maint Level
Electrical: Rubber, Fine Wires	Replace 1	1. Replace affected component 2. Shelter ⚠ adhesives, etc., to replace boot	Org
Rubber, Ribbons	Replace	1. Replace affected component 2. Shelter ⚠ adhesive, rollers, welders/solder equip to replace boot	Org Gen +
Rubber, Impregnated Elements	Replace	1. Replace affected component 2. Not generally repairable	Org
Laminate, Wire Mesh	Replace	1. Replace affected component 2. Not generally repairable, may be soldered with difficulty	Org
Laminate, Sprayed Elements	Replace 1, Repair 2	1. Replace affected section 2. Shelter ⚠ repair kit, heat lamp, paint brush or spray	Org Direct
Laminate, Impregnated Elements	Replace 1	1. Replace affected component 2. Not generally repairable	Org

⚠ Dependent on weather and surrounding environment (dust free)

TABLE XLVIII. CONTINUED

Boot Type	Type or Restoration	Method of Restoration Repair Facilities	Maint Level
Pneumatic:	Repair 1, Replace 2	1. Repair kit, dry conditions 2. Remove and replace boot	Org/Dir
Chemical:	Repair 1, Replace 2	1. Repair kit, dry conditions 2. Remove and replace boot	Org/Dir Gen +
Sheath, Metal	Repair	Requires cutting out damaged section, preparing patch, and cementing in place. Dry and dust free conditions required. Heat lamp or 24 hr cure.	Org/Dir
	Replace	Boot is destroyed, new sheath must be applied over new boot. Pressure fixture and heat required.	Depot
Supporting Structure		Electrical shorts can cause sustained arcing and burning if undetected by the crew, thereby resulting in structural damage. Pneumatic and chemical boots are free from this failure mode.	Dir/Gen

Column 2. Code.

Identifying data number of that component measured. (Used in lieu of part number.)

Column 3. Component/Subsystem description.

Column 4. MTBM - hours

Mean-time-between-maintenance

TOTAL HOURS/TOTAL MAINTENANCE ACTIONS

Column 5. MTUR - hours

Mean-time-to-unscheduled-replacement

TOTAL HOURS/TOTAL UNSCHEDULED REPLACEMENTS

Column 6. MMH/CA 90% C_L

Maintenance man-hours per corrective action at the 90% upper confidence limit. That is, 90% of all corrective actions will require a fewer number of man-hours than the man-hours shown in this column.

Column 7. MTBF - hours.

Mean-time-between-failures

FLIGHT HOURS X PART POPULATION/TOTAL INDEPENDENT FAILURES

Subsystem complete.

The summation of the total experience, including all components.

Table XLIV predicts maintenance and reliability parameters for items peculiar to rotary-wing craft where no data source was available. This information came from previous calculations for equipment considered for use on the AH-56A helicopter.

5.7 IN-FLIGHT DETERMINATION OF ICING SEVERITY

Ever since the development of all-weather aircraft, designers have desired to be able to provide the pilot with a real-time display of the presence of icing or, better still, an indication of the intensity of the encounter. The benefits which such would provide are:

1. A signal which activates, either automatically or manually by pilot action, the aircraft systems.

2. A warning that the encounter possibly exceeds the capabilities of the installed systems.

3. A signal which could be used to modulate the system behavior as a function of the icing severity.

Icing can occur only in clouds below freezing, and hence any such condition would indicate a high potential for icing. Data presented in Section 3 show that if an aircraft is flown through clouds with below-freezing ambient temperature, the probability of icing ranges up to 40 percent. Under such conditions, the pilot would be well advised to activate the windshield, engine, and inlet systems as a guarantee against troubles arising from icing of these areas. Another way icing is often detected is by buildups on some unprotected component in easy view of the pilot. Common examples are windshield posts, windshield wiper blades, or strategically located radio antennas.

However, it is not always desirable to activate all vehicle systems simply because there is a potential icing condition. System activation results in performance and fuel penalties which should always be minimized. This is particularly critical with chemical systems which use an expendable fluid, as unnecessary usage wastes fluid. On the other hand, chemical systems have mediocre recovery capability and should be activated just before they are needed. Therefore, with chemical systems some form of icing indicator, or ice detector, is desirable. On aircraft with thermal anti-ice systems, an ice detector could enhance the thermal fatigue life of the primary structure by minimizing use of the anti-ice system under non-icing conditions.

The purpose of any ice detector is to inform the pilot of the presence of, or, better yet, the severity of an icing encounter. Consequently, any ice detector must be representative of a critical aircraft component. For rotary wing aircraft, this is usually either/or both the engine and rotor systems. The question, then, is which should the detector simulate; this in turn will dictate its location on the aircraft.

Ice detector location has always presented a problem, even on fixed-wing aircraft. Due to the phenomenon known as the "shadow effect", the probe must extend far enough away from the aircraft to "see" the true external environment. On rotary-wing aircraft the problem is complicated by the lack of aircraft forward velocity during hover, thus making fuselage mounting impractical. If engine icing is the critical item, the probe must be located in the inlet duct both to assure adequate velocity over the probe and to sense the inlet conditions to the engine. If rotor icing is a problem, then the detector may be located in the inlet duct as before or on the rotor itself. However, rotor mounting greatly complicates installation because of the added slip rings on the rotor mast. Wherever the detector is mounted, it should account for the spanwise variation in rotor blade buildups in order to represent the actual rotor icing characteristics.

All of these factors, plus those arising from a variable-speed rotor, must be accounted for in locating an ice detector for a rotary-wing aircraft.

One of the great difficulties occurring in attempting to modulate system performance with icing severity is the rapidity with which liquid water content (LWC) varies during natural icing. This is illustrated in Figure 159 which shows LWC plotted versus time for two Grumman Gulfstream II flights (curves a and b) and one Lockheed Electra flight (curve c). It is not practical to have a timer response to these rapid variations; thus an averaging device will be required. It is, of course, not possible to forecast future icing intensity. There is also not a good correlation between (ground based) forecasts of icing and what a pilot is likely to experience. Icing is a highly transitory phenomenon within a given cloud. Thus, it appears likely that a rotorcraft must be able to withstand a moderately severe icing condition if it is to be permitted to fly into an icing cloud.

Canadian flight test experience has shown that rotor deicing efficiency is independent of icing rate, and, therefore, their fleet of CHSS-2's will only have the rotor blade heater "on" time modulated with ambient temperature. Flight experience on the Electra, P-3, and C-141 with electrothermal cyclic deicing systems has not shown a need for system modulation.

Over the years, numerous ice detectors have been designed, with many of them being installed on operational aircraft. These units have taken many forms, depending upon the basic theory behind their operation. As a class, ice detectors have been far from satisfactory and in many cases are either removed or just not replaced when they malfunction. However, in theory, some concepts show promise of overcoming past difficulties.

Of the candiate ice detector concepts, the ones which have reached operational status are the differential pressure, temperature/moisture sensor, beta radiation, and ultrasonic. In the differential pressure type, two sets of orifices are exposed to the airstream. Either by having a larger orifice or by being continuously heated, one set remains open while the other ices over. By sensing the resultant pressure differential (the iced set reads essentially static and the open set total pressure), a signal is generated which can be used to flash a light or to activate the engine systems. This signal also energizes a heater which deices the probes. The frequency of the icing signal is a rough indication of the icing severity.

Differential pressure ice detectors have been installed on the Electra, C-130, and P-3. In general, their performance has not been satisfactory. For example, icing conditions can exist during which the probe leading edge is clear while ice forms elsewhere (due to the freezing fraction being zero at the leading edge, allowing the impinging water to run back and freeze elsewhere); thus no icing signal would occur. A more serious deficiency is the tendency of the small orifices to clog with dirt, bugs, etc., and thus give a false signal of an icing condition. Still another

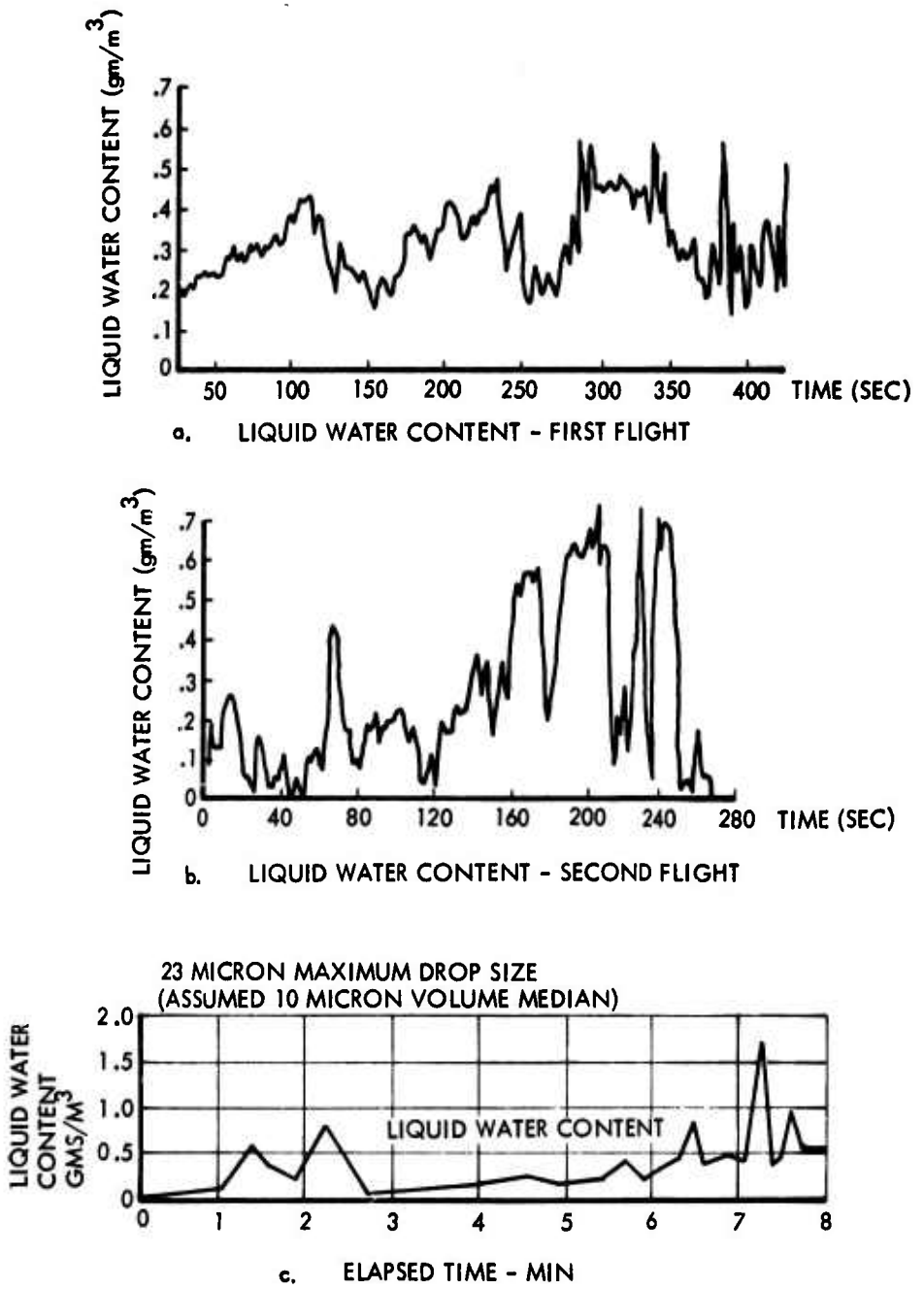

Figure 159. Typical Natural Icing Water Content Variation.

problem has been freezing of water in the plumbing; this, too, causes false or spurious signals. Since this signal also energizes the probe deicing system, a false signal can result in the heater being on for an extended period of time. Because of this, and because of the extremely high heat concentrations required to deice small probes, these units have experienced heater element burnouts. (This latter problem is not unique to this type of detector and has been noted on several designs.)

The temperature/moisture type has been used for years as a laboratory instrument and for flight test. A similar unit is installed on the C-141. This type uses a heated probe to sense the cooling effect of both ambient temperature and moisture. In one type, a single wire is used and the power required to maintain it at a given temperature is measured. Another design uses two heated probes, one of which is directly exposed to the airstream and the other screened by a shroud which nominally keeps water from impinging on it. The two probes are maintained at the same temperature, and the difference in power inputs to the "wet" and "dry" probes is measured. Either unit provides a signal which can be made proportional to the icing severity.

Again, performance of these units has not lived up to expectations, especially as regards serviceability. The heated wire type in particular is quite delicate and cannot withstand the rigors of operational aircraft use. The twin probe type has seen some flight service, including tests on several helicopters and transports. Experience to date with the twin-probe unit has been limited and inconclusive, but it does show signs of being sensitive to vibration.

The beta radiation unit employs a radioisotope beta source and collector so arranged at opposite ends of a probe that any ice which forms interrupts the radiation beams and generates an icing signal. This type of detector suffers from the same problems as the differential pressure type, in that ice can form along the sides without triggering an icing signal. This type has been flown on the Northrup F-5 and Boeing-Vertol CH-46.

Sikorsky reported that the Sundstrand radioisotope unit is not installed overseas on CH-55 aircraft due to the political sensitivity of the radioisotope material (even though Sundstrand claims less radiation than a wrist watch). For U.S. service, only two failures have been reported in 17,000 flight hours. However, it must be remembered that the aircraft does not fly under icing conditions, and the unit's reliability as an ice detector is basically unevaluated.

A fairly recent development has been the ultrasonic type consisting of a vibration rod excited at a resonant frequency of 40 kHz by a magnetic field. As ice forms anywhere on the probe, and not just at the leading edge, the resonant frequency lowers, the rate of which can be calibrated against icing severity. This type is installed on the UH-1N helicopter, on the C-5 and L-1011 transports and on the F-111 fighter-bomber. Although this Rosemount-developed unit has seen extensive service on the F-111, the UH-1N,

and the C-5A, information obtained from Rosemount indicates that the reliability still is not satisfactory to them. Each model has had either improved circuitry or installation location. On the F-111, reliability has suffered because of the high-temperature (supersonic) environment of the probe. The unit on the C-5A has been subject to drift of the oscillator circuitry (an L-C circuit is used), and an improved version for the L-1011 uses a liquid crystal in the oscillator. Basically, a 40-kHz signal is used to drive the detector probe, and a 200-hertz change in probe frequency (due to ice accumulation) triggers the ice warning circuit. It is the accuracy of measurement of this 200 hertz change which is critical to the performance of the unit. Icing rate is measured by determining the time rate of change of probe frequency, as indicated by the derivative of the output voltage.

Operational reliability data was reviewed on the C-5A ultrasonic probe from actual flight experience. The current MTUR (Mean Time Between Unscheduled Removals) is approximately 3,000 hours. Rosemount reported the return of twelve units in their current fiscal year (beginning November 1, 1971). Of these twelve, seven had broken or bent probe units, two had been inadvertently painted (shifting their vibration characteristics), one had a broken wire, and two had shifts in oscillator frequency. The broken probes occurred during aircraft assembly and would not be considered in the MTUR calculations. Thus, Rosemount's records probably do not coincide with the USAF reliability records.

Reference 7, on the HH-53C, contained a discussion of the reliability of the Rosemount ultrasonic ice detector. The sensor was mounted in the cabin heater inlet duct, behind a screen that tended to ice. It was reported that an excessively long period of time in icing (8 minutes during "light" icing) was required to activate the system, and there were a number of false warnings in clear air. While a poor choice of installation location may be the problem with its relative insensitivity, that should not be the cause of false warnings.

A marketing survey of ice detectors was conducted in 1963 by a marketing class student (professionally employed as an engineer). He contacted all of the aerospace prime contractors and some of the engine companies. As of that period, the radioisotope unit was the overwhelming first choice among the following candidates:

1. Pressure-sensitive type
2. Electromechanical (a feeler on a rotating disk)
3. Radioisotope
4. Heated wire

The (Rosemount) ultrasonic type was not developed at that time.

Although the survey report is quite detailed, it was not noted whether the respondents' selection of the best detector was based upon experience or theory. Considering the relatively restricted service application of the radioisotope unit, it is suspected that the first choice of the radioisotope unit was based upon theory whereas the other units were downgraded based upon operating experience. It would appear at this time that the primary failure of the radioisotope unit to achieve wider application in the industry was primarily due to lack of marketing effort by the manufacturer.

An icing severity meter can be developed as a modification of the ultrasonic ice detector. The severity meter measures the rate of change of vibration frequency, which is proportional to changing mass on the sensor head. The cockpit gauge would be a meter calibrated to read "trace," "light," "medium," and "heavy" icing. The unit will weigh 2 pounds more than the conventional detector.

In conclusion, there are very few companies currently engaged in manufacturing ice detectors, and none of the designs has really exhibited acceptable dependability. (Although an MTBF of 43,000 hours is claimed on the C-130 for the pressure-sensitive Cook Electric Company ice detector, industry experience and known thermodynamic limitations of the design do not support that number). While the ultrasonic probe type detector seems to currently offer the best potential for a dependable concept, operating experience to date (with older control circuit designs) has not yet validated the promise.

Pilots of fixed-wing aircraft generally rely on watching for ice accretion on some portion of the aircraft. The favored component is the windshield wiper blade, as it has a high catch efficiency and is, of course, easily visible from the cockpit. A reasonable criterion, moreover, for engine inlet system actuation is the presence of clouds and below-freezing temperatures.

As pointed out earlier, the systems likely to be applied to the critical components do have an inherent overload capability. Thus, since the recommended meteorological conditions encompass over 98 percent of expected encounters, an in-flight severity measurement will not be required from a flight safety standpoint. Also, as discussed, icing severity changes rapidly and by large amounts in a cloud, and it is not possible to forecast icing severity.

It has, however, been suggested that a rotor blade deicing system have its "off" time modulated by icing severity so as to maintain a constant ice thickness before deicing regardless of icing severity. As discussed earlier, testing in Canada on the CHSS-2 and also on fixed-wing aircraft (P-3, C-141) has indicated that this refinement appears to be unnecessary. It is recommended, nevertheless, that such a feature be added to an advanced development test configuration so as to resolve the issue by testing on other than the Sikorsky CHSS-2 design.

SECTION 6 OPERATIONAL LIMITATIONS OF CURRENT HELICOPTERS

Current ice protection systems - their capabilities and limitations - were discussed in the previous section. This section deals with the operational limitations imposed upon current helicopters by these systems. Also included is a discussion on the ice ingestion capabilities of current engines.

6.1 AIRCRAFT OPERATIONAL LIMITATIONS

The principal aircraft in the Army inventory, plus selected aircraft operated by other civilian and military agencies, including Canadian, were analyzed and categorized as to their ability to fly in an icing environment. To achieve this objective, the various flight and/or maintenance manuals were surveyed. Also, comments on vehicle ice protection were solicited directly from other helicopter manufacturers via a survey, the results of which have been incorporated into this presentation.

Flight and/or maintenance manuals were obtained for most of the rotorcraft currently flying in various military services. These documents were searched to obtain: three-views; empty and normal gross weights; details of icing protection for the main and tail rotors, windshields, and engine air induction systems; and aircraft operational limitations. Typical of the vehicles so researched are: UH-1A, B, D, F, P; HU-1B; AH-1G; TH-1F; HH-2C, D; SH-3A, D; CH-3C; HH-3F; OH-6A; HH-43B, F; CH-46A, F; UH-46A; CH-47A, B, C; QH-50D; CH-53A; CH-54A; AH-56A; OH-58; and CH-113.

The limitations of contemporary helicopters for flights in icing conditions are shown in Table XLIX. The limitations have been taken, insofar as possible, from the flight or operational manuals, and are supplemented by responses gained from the industry-wide survey. Direct quotations from the manuals are presented later in this section.

In limiting the operation of a vehicle there are usually three major types of restrictions: (1) vibration or damage from rotor ice shedding, (2) reduction in rotor lift, and (3) engine air induction system limitations.

The engine induction systems are about equally protected with either double-walled thermal ducts using engine bleed air or electrically heated blankets powered by rotor-driven alternators. The electrical protection is usually limited by the quantum jumps in generator sizes (i.e., 20, 30, 40 kw) and leads to most systems being qualified to about 0°F. The bleed systems, however, frequently will provide protection down to -22°F and thus match the engine's own qualification level. For some vehicles an additional engine problem is posed by the ingestion of shed ice from the pilot's canopy, the vehicle body, or the rotors.

TABLE XLIX. ICING LIMITATIONS OF U. S. TURBINE-ENGINE HELICOPTERS

DOD MODEL	MFGR	CIVIL MODEL	ENGINE	ENGINE DUCTS	ENGINE FILTERS	ROTORS	FIXED SURFACES	HEATED PITOT	ICE DETECTOR	WINDSHIELD	IFR AR 95-1	ICING TESTS	ICING LEVEL	LIMITS
UH 1	Bell	204/209	6,53,55	U	SF	T(8)	N	Y	Y	T(8)	Y	abcd	II l	VIB
UH 2	Kaman	–	58	U	U	N	N	U	N	U	Y	b	II l	VIB
SH 3	Sik	61	58	E/B	N	Y(3)	Y(4)	Y	N	U	Y	abcd	II m	FOD
OH 4(1)	Bell	206	63	N	SF	N	N	U	N	U	U	U	IV	
OH 5	F-H	1100	63	U	U	N	N	U	N	U	N	d	III	FOD
OH 6	Hughes	369	63	N	D	N	N	U	N	B	N	abd	III	LIFT VIB
XH 39(1)	Sik	59	Artouste	N	N	N	N	N	N	N	N	N	IV	
UH 43	Kaman	–	53	U	D	N	N	U	N	U	N	U	IV	
CH 46	B/V	107/113	58	E (2)	SC	E	Y(5)	Y	Y(7)	E	Y	abd	II m	ENG
CH 47	B/V	114	55	B	S	T(8)	Y(5)	Y	N	E	Y	acd	II l	RI
QH 50	Gyro	–	50	U	U	E	N	U	U	N	N	U	U	
XH 51(1)	Lock	186	6	N	S	N	N	N	N	N	U	N	IV	
HH 52	Sik	62	58	U	U	N	U	U	N	U	U	U	U	
CH 53	Sik	65	64	E(2)	D	N	U	Y	N	U	Y	ab	II m	RI
CH 54	Sik	64	12	E	D	N	N	Y	N	U	Y	a	II l	RI
AH 56	Lock	800	64	B/E	D	N	Y(6)	Y	N	E	Y	ab	II l	T
OH 58	Bell	–	63	N	P	N	N	Y	N	U		ab	III	LIFT VIB

LEGEND

a Icing Tunnel
b Spray Rig
c Tanker
d Natural Icing

I No Icing Restriction
II Limited Operation in Icing
III Inadvertent Icing
IV Unsafe in Icing

t trace icing
l light icing
m moderate icing
h heavy icing

6 C P&W PT6
12 P&W JFTD 12
50 Boeing T50
53 Lycoming T53
55 Lycoming T55
58 GE T58
63 Allison T63
64 GE T64

ENG Induction limitations
FOD Engine "FOD" protection mandatory
LIFT Loss in rotor lift capability
RI Damage from shed rotor ice
VIB Excessive vehicle vibration
T Test down to +11°F

Sik . . . Sikorsky
F-H . . . Fairchild-Hiller
B/V . . . Boeing/Vertol
Gyro . . . Gyrodyne
Lock . . . Lockheed

B Bleed-Air
C Company Design
D "Donaldson"
E Electric
F Foam Sponge
N No
P "Porous Media"
S Screen
Y Yes
U Unknown
T Test Only

NOTES

(1) Only prototypes built and flown
(2) 0°F inlet due to generator capacity
(3) Ice-phobic tape
(4) Engine "windshield"
(5) "SAS" ports
(6) Pneumatic boots, wing and tail
(7) "United Control"
(8) Fluid deicing

In the following descriptions of vehicle icing limitations, the underlined words are not underlined in their original source; this is done here to facilitate the data recognition.

UH-1A/UH-1B (TM55-1520-211-10, Chapter 10, Section II, page 2-7): "This helicopter is restricted from flight in moderate to heavy icing conditions under provisions of AR 95-2*. Caution. Continuous flight in light icing conditions is not recommended because the ice shedding induced rotor blade vibrations add greatly to the pilot work load." *(The reference to AR 95-2 is probably a typographical error. Nothing was found in the current -2, (dated 8 May 1970), or its predecessors. However, there is an icing restriction in AR 95-1.)

UH-1F (AD486740; ASD-TR-66-7; "Category II Adverse Weather Tests of the UH-1F Helicopter", page 9, paragraph 33): "As a result of these flights (under artificially created and natural icing conditions) the UH-1F is considered suitable for flight in light icing conditions for a period not to exceed 30 minutes. The UH-1F is time limited in icing conditions because of no windshield anti-icing or deicing capability. Continuous flight in icing conditions results in ice shedding which induces main rotor and tail rotor blade vibrations which add greatly to the pilot workload".

UH-1F/TH-1F (T.O. 1H-1(U)F-1, 30 December 1969, page 9.5): "This helicopter is restricted from flight in other than trace icing conditions. Continuous flight in trace icing conditions is not recommended, because the ice shedding induces rotor vibrations which add greatly to the pilot workload. Caution. If flight in icing conditions results in ice accumulation on the helicopter, enter the information on Form 781, as the engine must be inspected for ice ingestion damage when this occurs."

AH-1G (TM55-1520-221-10, 30 April 1969, page 10-8): "Continuous flight in light icing conditions is not recommended because the ice shedding induces rotor blade vibrations, adding greatly to the pilot's workload."

HH-2C/HH-2D (NAVAIR 01-269HCC-1, 1 September 1970, page 6-9/6-10): "Flight through known or forecast icing conditions is not recommended. However, the aircraft is equipped with rotor deicing and turbine and windshield anti-icing equipment."

CH-3C, CH-3E, HH-3E (T.O. 1H-3(c) c-1, 15 October 1971, page 9-4A): "Do not attempt flight in freezing rain or conditions exceeding moderate icing."

SH-3D (NAVAIR 01-230-HLE-1, 15 June 1968, page 6-8): "This helicopter is restricted from flying in known icing conditions when visible moisture, except dry snow, is present. For vehicles with ice deflector installed.... (a) Flight operations may be conducted when icing conditions are forecast. However, known areas of icing shall be avoided. (b) If icing conditions are encountered in flight, immediately leave area where icing exists."

HH-3P (T.O. 1H-3(H)F-1, 1 February 1972, page 9-8): "During icing conditions, the main rotor assembly and rotor blades will collect ice... To preclude the possibility of ice ingestion failure, the helicopter will not be flown in known icing conditions or in visible moisture when temperatures are at or below 5°C (41°F) without the foreign object deflector installed."

HH-43B (T.O. 1H-43(H)B-1, 1 February 1972, page 7-6): "This aircraft is restricted from flight through known or forecast icing conditions."

HH-43F (T.O. 1H-Y3(H)F-1, 1 February 1972, page 7-6): "This aircraft is restricted from flight through known or forecast icing conditions."

CH-46A/UH-46A (NAVAIR 01-250 HDA-1, 15 July 1969, page 6-3): "The deicing and anti-icing capability limitations, with reference to temperature, are provided in Figure 160. The capabilities of the anti-icing and deicing systems vary with OAT and the severity of the icing conditions."

CH-47A (TM55-1520-209-10, 1966 Chapter 10, Section III, page 10-9): "The CH-47A is equipped with adequate engine anti-icing, pitot tube and yaw port heating, and windshield anti-icing systems to enable safe flight in light icing conditions.... Caution. Areas where moderate to severe icing is known to exist or forecast to occur are to be avoided.... Engine anti-icing should be used in accordance with Table 10-1."* *(This table is reproduced as Figure 161).

QH-50D (NAVAIR 01-150 DHC-1, 15 June 1967, page 84/84): "The drone is not provided with an operable anti-icing system at the time of issue of this manual. Heater mats are installed in the leading edge of the fiberglass rotors for future use."

HH-53B, HH-53C, CH-53C (T.O. 1H-53(H)B-1, 30 September 1971, page 9-2): "Flight in icing conditions is a permissible operation, but should be avoided whenever possible.... In the event icing conditions cannot be avoided, turn on the engine air inlet, engine air, windshield, and pitot heater anti-icing systems prior to entering icing conditions. Note the time ice started to accumulate on the windshield wiper arms, to provide data for an accumulation rate from which icing severity can be determined. If the cruise speed is approximately 140 KIAS and the rate of accumulation does not exceed 1/2 inch in 8 minutes, the mission may be continued.... The limits on vibration, although seldom encountered, are established by the readability of the instrument panel. If this vibration level should be exceeded, or the observed accumulation rate exceeds 1/2 inch in 8 minutes on the windshield wiper arms, diversionary action must be taken immediately. With EAPS (Engine Air Protection System) installed, the same procedures outlined above are followed; however, the EAPS doors must be closed and maintained in the closed position until the helicopter has landed and the engines are shut down. The EAPS doors are to remain closed at all time during flight in known icing conditions."** **(As recommended in FTC-TR-71-26, "Category II Icing Test of the HH-53C Helicopter", June 1971. Also recommends flight up through moderate).

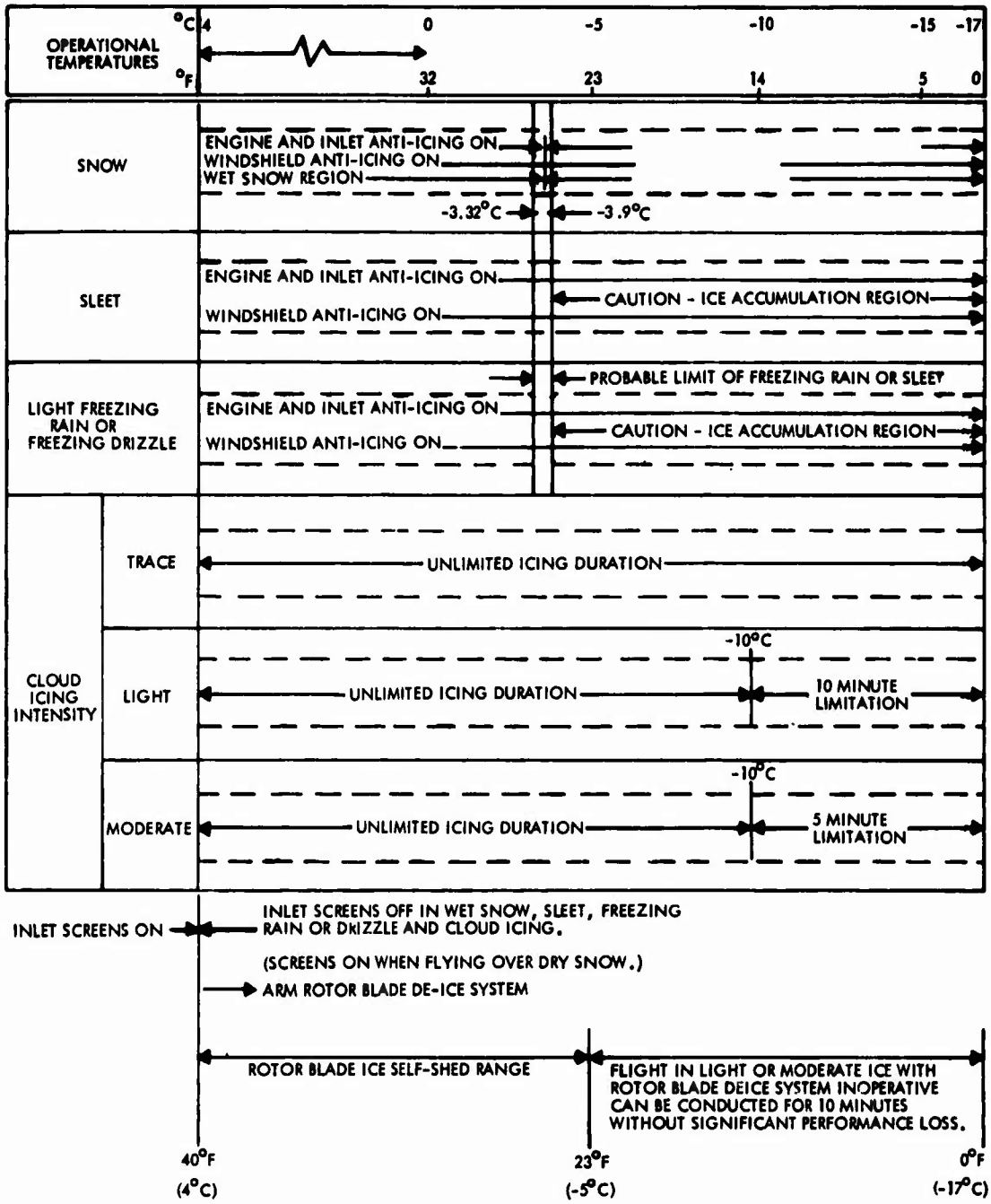

Note: This capability based upon operational rotor blade deicing system. The latest flight manual does not reflect system deactuation order.

Figure 160. H-46 Cold Weather Operation.

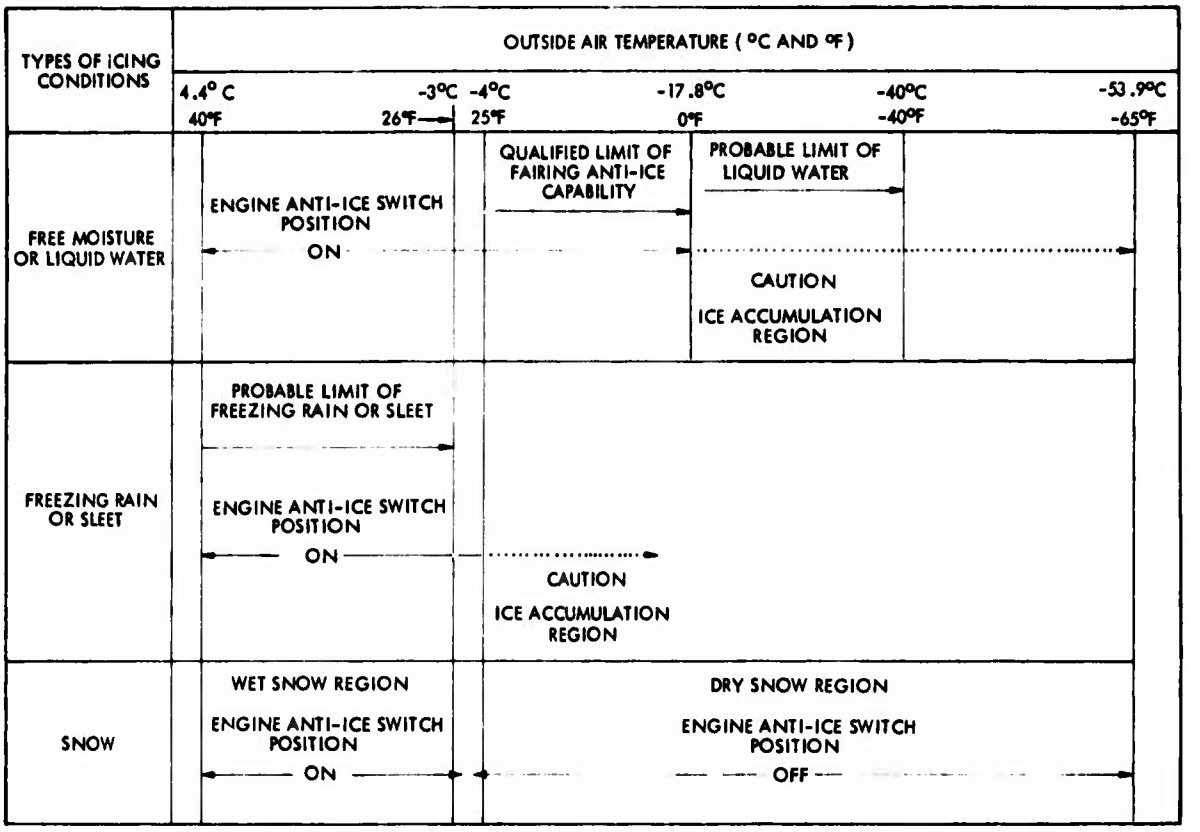

Figure 161. Engine Anti-Ice Requirements CH-47A Outside Air Temperature

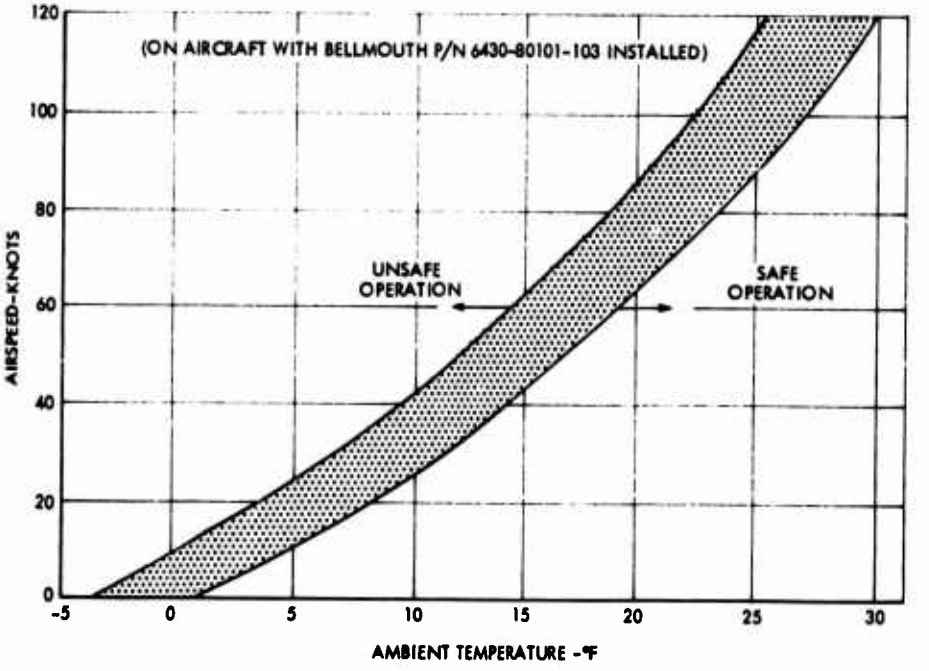

Figure 162. CH-54A Helicopter Operation Limits in Continuous Icing Conditions.

CH-54A (TM 55-1520-217-10/1, February 1969, page 10-8A): "During seasons when icing conditions exist, EAPS should be removed. (See Figure 10-5*). Caution: Should icing conditions arise while EAPS are installed, open bypass doors and land as soon as possible".**. *(This is reproduced as Figure 162.) **(Note the opposing directives for EAPS operation on the Sikorsky CH-53 and CH-54 helicopters. Previously, the CH-53 had a restriction on operating in icing in the EAPS mode. The CH-54 will probably have its EAPS restriction lifted - or in reality changed to a new restriction, that of operating in icing only in the EAPS mode - based on similarity of powerplant induction systems).

The results of this study clearly indicate that, as presently configured, helicopters are not adequately protected against icing hazards and should not be dispatched into known or even forecast icing conditions.

With the exception of the CH-46, flight in icing conditions is limited to emergency operation only (i.e., caught in an icing situation and brief flight out of it). At present helicopters are not provided full icing protection. While the ability to provide full protection exists, ice protection is usually traded off because of weight, cost, and vehicle performance penalties. Full ice protection can be provided if the customer will accept the associated penalties of 1 to 1-1/2 percent of vehicle empty weight and 1/4 percent increase in fuel consumption during system operation.

Engine Ice Ingestion Capabilities

The requirements for turbine engine ice ingestion are of recent vintage, dating from June, 1965 when FAA Advisory Circular 33-1 (Turbine - Engine Foreign Object Ingestion and Rotary Blade Containment Type Certification Procedures) was first issued. Even the latest revision (April 22, 1970) is not too specific, saying "ice should be introduced into an engine operating at cruise conditions to simulate typical ice shedding from inlets and the engine front face because of possible delays in operating ice protection systems. Engine flameout tendencies, reignition, and power capability should be evaluated".

AV-E8593 (Para. 4.5.21) was the first military turboshaft specification to specify ice protection requirements (1972). The ice ingestion test identified in AV-E8593 calls for "one 1-inch-diameter ice ball and one 2-inch-diameter ice ball to be ingested for each 150 square inches of inlet area (or fraction thereof). The ice balls shall have a specific gravity of 0.8 to 0.9 and be at a temperature of -20 ±5°C at the time of ingestion. The ice shall be ingested while the engine is operating at maximum continuous power at conditions simulating a flight speed of 250 knots true airspeed.

For engines produced prior to these documents, the airframe manufactures have adopted some interim solutions. Sikorsky has put a steel "windshield" in front of its T58 engines on the S61 to prevent engine malfunctions due to ice shed from the pilot's canopy. Boeing/Vertol placed a conical screen

ahead of its T58 engines on the CH-46 for FOD in general, due to their "bowling alley gutter" location of the engines at the top aft end of a long fuselage. The British/Sikorsky Sea King with the T58 was fitted with mushroom centerbody deflectors. Canadian Pratt & Whitney has developed a bypass arrangement for its PT6 engine with its annular screen. Other ideas being investigated are the possibilities of flying in the filtered mode for the Sikorsky CH-53 and the Lockheed AH-56A with the T64 engines.

These designs, which diminish ram recovery, are quite detrimental to vehicle performance. The S61 deflector, according to comments made at the 1972 International Helicopter Ice Protection Conference at Ottawa, originally had a 4-percent power loss in hover and a 14-percent loss at 130 knots. By a sophisticated design, the 130 knot loss was reduced to 4 percent; but the deflector weight penalty is 25 pounds per engine, or 7.3 percent of the engine weight. If successful, the variable inlet geometry concepts for the CH-53 and the AH-56A would significantly minimize these losses.

For engines produced since the introduction of ice ingestion requirements, most of the commercial engines desiring icing certification have tried to meet the FAA hail ingestion requirements of 1-inch and 2-inch-diameter ice balls. Frequently, the requirements can be met only at engine rpms greater than that for the required cruise or climb conditions.

The major turboshaft engine producers were contacted to obtain information on their ice ingestion capabilities. The response was disappointing. Not one of the engine companies has ever determined a weight penalty for ice ingestion capability. The only data which they could supply were copies of test reports showing that they pass the FAA hail test (where applicable). There appear to be pieces of information hidden in various reports, especially relating to icing tests at the Ottawa spray rig or the Lewis Icing Tunnel, that give some tolerance levels. For instance, in Technical Report ST 22R-66 from the U. S. Naval Air Test Center (Patuxent River, Maryland) there appears:

> "Thirteen segments of mushroom-type rotor blade ice were intentionally injected into the (T64-GE-6) engine while it was running at cruise power. This ice ranged in size from the smallest, 1 inch wide by 0.125 inch thick and 2 inches long, to the largest, 1.75 inches wide by 1 inch thick and 4 inches long. Three-point power checks were conducted before and after the ice was ingested by the engine; no deterioration in shaft horsepower was detected. The only cockpit indication was a 0 to 5 percent transient drop in engine torque."

To better relate the largest piece of ice ingested, it represented a 0.2 pound piece of ice compared to the 2 inch ice ball weight of 0.12 pound. Since little ice ingestion work has been done, some engine manufactures have limited their ice ingestion tolerance to the lesser of "the weight or kinetic energy equivalent of the FAA hail ingestion tests to which their engines have been demonstrated".

The related areas of snow and water ingestion are similarly not well documented. In general, the small engines have low tolerances and flame-out readily, especially if they have single-nozzle burners. It has been reported that the T63 would flame out with as little as 10 cc of water, while the specification requires 30 cc. The larger T55, however, can ingest water at levels up to 20 percent in excess of the design requirements.

A preliminary summary of ice ingestion capabilities for turboshaft engines indicates: (a) the majority of engines were certified before the existence of criteria for reingestion; (b) ice ingestion tests of more recent vintage are at the discretion of the engine manufacturer since there was no specific requirement. Thus, the T64 engine, in addition to the 0.12-pound hailstones and the 0.20-pound rectangular ice chunk, also was run at 75 percent normal rated power using 1/8 inch to 1/4 inch crushed ice granules. These tests were performed using 1/4-pound bulk, then 1/2-pound bulk, followed by 1-pound bulk. As this engine manufacturer points out, this material identifies only in a general way the limits to which the engines were tested and does not represent the engines' ingestion capability.

Another manufacturer points out that the penalty trade-off for ice ingestion requires heavy-walled blade/guide vane construction for ruggedness compared to the thin-wall design that reduces the engine bleed-air penalty for anti-icing. Design and test requirements for future engines are still biased more to the achieving of anti-icing objectives, which are more specific, than to the nonspecific ice ingestion question.

General Electric Company points out that the stated limit defines only the capability by test to meet a certain (FAA) specification, and the FAA specification continues to change over the years by becoming more severe. Moreover, the FAA does not specify how an ice ball is to be made except for a specification on minimum density. The structural properties (and damage potential) of ice, however, are very much a function of how the ice is made; and the toughest ice balls are those which simulate natural hail (made as layers of ice, like an onion). None of the information provided has described the method of manufacturing the ice balls.

A summary of the various responses to the inquiry on ice ingestion capabilities for various modes is presented to conclude this study.

General Electric's response to the ice ingestion capabilities of the T-58 and T-64 is presented in Table L.

Pratt and Whitney states: "The PT6 turboshaft engine is certified only when used in conjunction with United Aircraft of Canada, Ltd. approved inertial separator system conforming to certified basic dimensions. The inertial separator efficiency has been demonstrated at 100 percent against heavy objects such as ice chunks. As a back-up to inertial separator, the engine has an inlet screen of 1/4 inch mesh."

TABLE L. GENERAL SUMMARY OF INGESTION TESTING AND EXPERIENCE GE TURBOSHAFT ENGINES

Item	CT58	CT64
Water	5% of Engine airflow by weight	5% of Engine airflow by weight
Sheet Ice	No factory testing - Military service experience cited to FAA with slush and ice throw-off conditions (from fuselage and inlet structure)	Crushed ice ingestion tests were run at 75% NRP using 1/8"-1/4" granules. Three tests were performed using 1/4 lb. bulk, then 1/2 lb. bulk followed by 1 lb. bulk.
Anti-Icing	Per FAR 33.67, FAR 25 Appendix "C" and Mil. Spec.	Tested to same Specs, as CT58
Birds	No factory testing - Military service experience over 6-yr. period documented and submitted to FAA (12 strikes from starlings to pelican size - all damage contained)	1 starling @ 117 MPH 1 starling @ 137 MPH 1 starling @ 139 MPH 1 starling @ 206 MPH
Hailstones	Inlet hardware static tests - multiplicity of 1/2" to 2" up to 192 MPH. Operating engine tests consisting of: 170 up to 3/4" dia. @ 120-170 MPH, and 180 up to 3/4" dia. rolled into inlet and/or salvoed through a hopper.	Inlet hardware static test using 18 1" dia. @ 100-190 knots. Operating engine tests at 75% NRP were run using a series of 3-1" snow balls and 2-2" snow balls.
Misc. Ingestion not Planned, But Occured During Development/ Test Program	Nuts, Bolts, Rivets, Lockwire, Rags	Similar experience plus temperature probe, gravel and camera bulb.

The Garrett Corporation (AiResearch Mfg. Company of Arizona) reports: "At the present time, all Garrett production engines for aircraft propulsion are certified in accordance with FAR Part 33, including requirements for Ice/hailstones ingestion capability and inlet anti-icing. In addition, the T76 military turboprop engine was fully qualified per MIL-E-8585 requirements as of June, 1967. For your information, U. S. Army AVSCOM specification AV-E-8593 has been reviewed and AiResearch concurs with the requirements therein for ice ingestion. The AiResearch Model TSE231 engine proposed for the aerial scout program was presented as being able to meet AV-E-8593 ice ingestion requirements."

"The engine design shall be such that ingestion of foreign objects such as birds, snow, ice, and hail will be unlikely to produce flameouts, lengthy power recovery times, or severe sustained power losses although damage of engine parts may occur."

Lycoming reports: "In 1960 a special series of hail-ingestion tests were conducted on the T53 and T55 engines to demonstrate full compliance with FAA requirements in this category." Applicable requirements at the time were: "The effects of ingesting hailstones in sequence should be evaluated to indicate possible critical conditions. Suggested test quantities are one 2-inch stone and two 1-inch stones per engine per each 400 square inches of inlet area."

As indicated by the results of this study, the status of engine ice ingestion capability and requirements is not satisfactory, and a new Army specification in ice ingestion requirements is recommended. The new specification should specify the method of generation of ice balls. From results of this study, it is felt that a 1-inch diameter ice ball is not sufficient to adequately test engine ingestion capabilities and that the use of larger chunks of ice should be considered. At the First International Helicopter Icing Conference held in Ottawa, Canada, May 23-26, 1972, it was brought out that snow ingestion can become a problem as far as engine performance is concerned and, therefore, consideration should be given to the inclusion of a snow requirement as well as hail and ice in the proposed specification.

SECTION 7 ADVANCED CONCEPTS

Since the state of the art for rotor blade ice protection, as presented in Section 5, has not been shown to provide satisfactory weight, reliability, and performance, a study of advanced concepts which are suitable for development, evaluation, and test has been performed. Two candidate concepts are recommended for more detailed evaluation and are described in the following two subsections. The first may be categorized as an electromechanical electropulse deicing system, and the second is an improved electrothermal system.

7.1 ELECTROPULSE DEICING

A new deicing system has been announced by the USSR which offers a potential for a better method of ice protection. This system is known as electroimpulse (EI) deicing. The system has been undergoing flight trials in an Ilyushin 18 and an Ilyushin 62. The Ilyushin 62 is a 180-passenger commercial transport with a gross weight of approximately 300,000 pounds and a range of 6000+ miles; it is powered by four Kuznetsov NK-8 turbofans rated at 21,000 pounds each.

The EI system itself is protected by claims taken by the Russian inventors, and patents have been issued in Russia, France, Italy, Chile, Norway, and the United States. World license interests are also being solicited by Licensingtorg of the Soviet Union.

Electroimpulse deicing is based upon the technology of exerting an impactless mechanical shock to the aircraft skin in such a way that the elastic deformations of the skin result in a mechanical shedding of the ice. In a more discrete definition, it is said that a high acceleration is imparted to the skin by a high pulse of energy in such a way that the ice is shed or precipitated in an inertial fashion. Photographs taken of the test surfaces during the instant of ice shedding show the ice to be almost exploded from the skin surface.

To accomplish the impactless shock, two (or possibly more) ways are considered. In both typical cases, a large quantity of electrostatic energy is used, but in one instance the energy is dumped into one or more electromagnetic coils which are mounted in very close proximity to the aircraft skin. A steep wave-front is then developed in the coils, and this results in the skin moving away rapidly, within its elastic limits, to precipitate the ice. Electrically, the electrostatic energy is obtained from a capacitor bank which is charged over a period of 2 to 3 seconds at a moderately low power level of 3 to 6 kw. The energy, however, is discharged in a period of fractions of a millisecond and the resulting current is measured in thousands of amperes. In the electrical method, the skin must be electrically conductive since the impact is created by a heavy eddy current

inducted in the skin, resulting in a high repulsive reaction force with the magnetic field causing the induction.

In the second method, electrohydraulic technology is used, wherein the electrostatic energy is discharged across electrodes which are immersed in a nonflammable, nonconductive liquid. The liquid is contained in a cavity of which the skin is an integral part. Mechanical shedding in this method is accomplished via the high pressures that are transmitted to the skin by the fluid.

To conserve power and energy in both schemes, individual coils or groups of coils are pulsed sequentially under the control of a commutator or programmer. The control and switching logic are design details that would be determined by the particular installation. In the case of the Ilyushin 18, the aircraft has been used as a test aircraft for about three years, and a hybrid system of conventional and electroimpulse systems has been employed. The electroimpulse system has been installed on the outer main wing sections and also on the horizontal stabilizer portions of the airplane. No definite details are available, but it is understood that there may be some six dozen coils in the Ilyushin 18 aircraft and that the power used is about 3 kw. These coils are estimated to be about three to four inches in diameter, spirally wound, and 3/8 to 1/2 inch thick. They are mounted on a nonmagnetic structure, and the distance from the skin is kept as small as possible, probably 0.040 to 0.060 inch. Figure 163 is a schematic of an electrical circuit of the system, and Figure 164 depicts a possible rotor blade or engine inlet lip design. Details of the programming cycle are not available, but it is understood that the pulse time for each coil is much less than one second and is likely to be in the 0.3- to 0.4-millisecond class. The off-time is a function of the charge time between successive pulses, and, based on this being two to three seconds, the total cycle time would be in the order of two to three minutes.

Very significant weight and power efficiency advantages are claimed for the electroimpulse system. As applied to the Ilyushin 62, it has been estimated that the weight saving is of the order of 400 to 600 kg (or 880 to 1320 lb). These weight differences are presumably based upon a double-walled skin structure (for a bleed air system) and various bleed air penalties such as engine thrust loss and change in specific fuel consumption.

Power estimates for a bleed air system on an Ilyushin 62 type aircraft are given as over 600 kw - compared to about 6 kw for an electroimpulse system. While these are striking differences, the EI system would be better compared to an electrothermal system; and, for the Ilyushin 62, it would appear that this power requirement (for the electrothermal system) would be approximately 45 to 70 kw. The facts, however, are that the differences between the EI and conventional deicing systems are indeed significant. The time-averaged power requirement for electropulse deicing is claimed to be approximately 0.015 to 0.030 w/in.^{2} as compared to 2-4 w/in.^{2} for a conventional electrothermal deicing system.

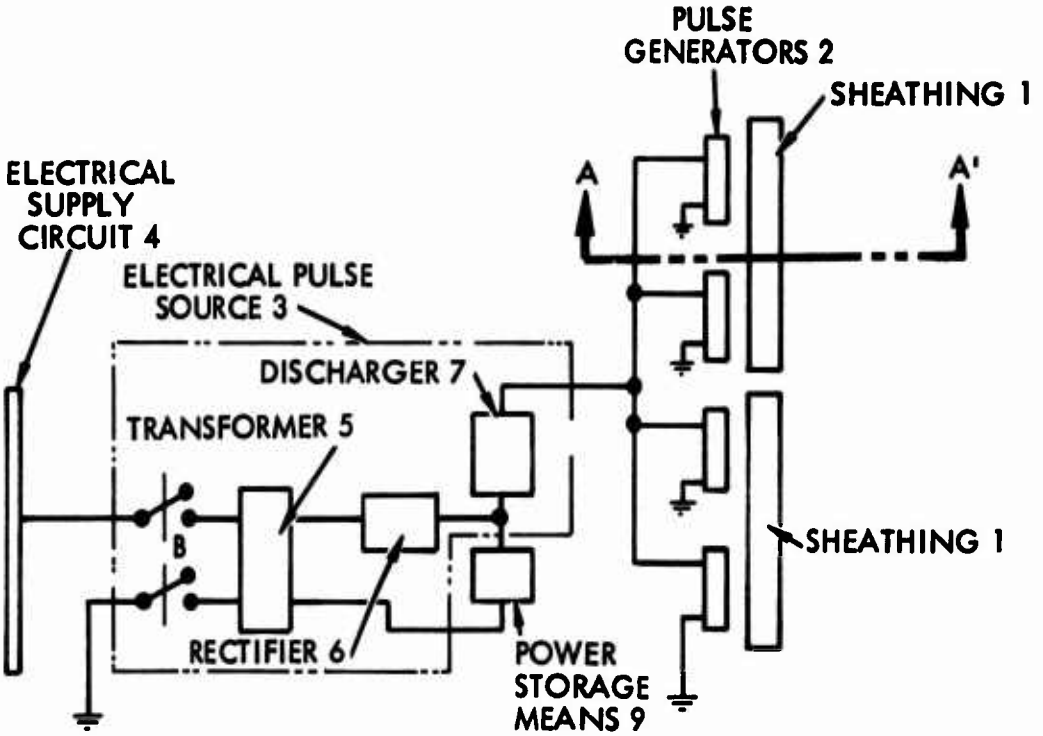

Figure 163. Electroimpulse Deicing-Electrical Schematic.

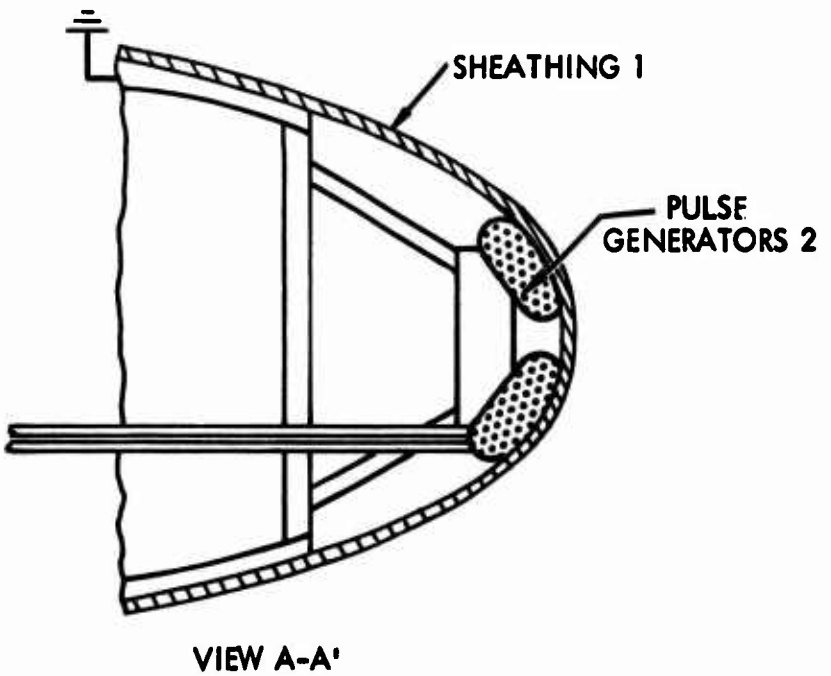

Figure 164. Electroimpulse Deicing-Leading-Edge Arrangement.

The principles of the EI system are basically sound, and they are not new since some sheet-metal-forming processes have used the same principles for many years. However, the main attraction is that the EI system affords an electromechanical method of shedding ice, which means that the skin surface does not have to be heated above freezing - as is the case of the electrical and bleed air systems. As a result, the EI operates almost independently of outside air temperature (OAT) and liquid water content (LWC). However, there is some purpose (in different LWC conditions) in changing the cycle time so as to allow some ice mass to form on the surface before it is shed. It is implicit also in this type of system that there are no runback or insufficient-heat problems which are a legacy of many present deicing systems.

For optimum efficiency, the capacitor discharge time is controlled as a function of the natural frequency of the skin and is usually set to be less than one-fourth of the natural time period. By establishing a sharp wave-front pulse of energy in the electromagnetic coil, the skin is rapidly displaced and caused to vibrate at its own frequency. When displacement is plotted as a function of time, it is seen (from Figure 165) that maximum displacement occurs at one-fourth of the period; also, the ice must be precipitated while the skin is accelerating to its maximum rate during this period. Due to skin elasticity, the elastic deformation wave also travels from the point of its formation opposite the coil along the whole zone of the skin protected by the coil. Figures 166a through 166f are photoframes from a high-speed movie camera showing the deicing sequence (apparently during flight test). Figure 166a shows the ice buildups during the off period of the deicing cycle. Figure 166b shows the ice shedding near the inboard end of the test area (apparently near the location of the coil) and then spreading outboard until the whole section is clear (as shown in Figure 166f). It is also apparent from the blurred motion that the ice leaves the surface at very high speed, which is due to the fact that the ice acquires the velocity of the skin at the time of shedding.

Because of the potential merit of the EI type system, it is recommended that R&D activity be started to explore in more detail the technology of this system. As an integral part of this program, it is further recommended that practical test models be fabricated and icing tunnel tests be accomplished to validate the practical performance of the system. This should be followed by a detailed evaluation of the more practical aspects of a new, or retrofitted, helicopter installation. This would permit physical, electrical, and general installation problems to be explored fully. EMI is one of the problems which would be covered in the electrical evaluation and is one of the items of concern.

7.2 ADVANCED ELECTROTHERMAL DEICING SYSTEM

An advanced electrothermal deicing system design has been conceived, and its application in terms of weight and power requirements has been shown for the AH-56A. Heater coverage would be 10 percent on the upper surface

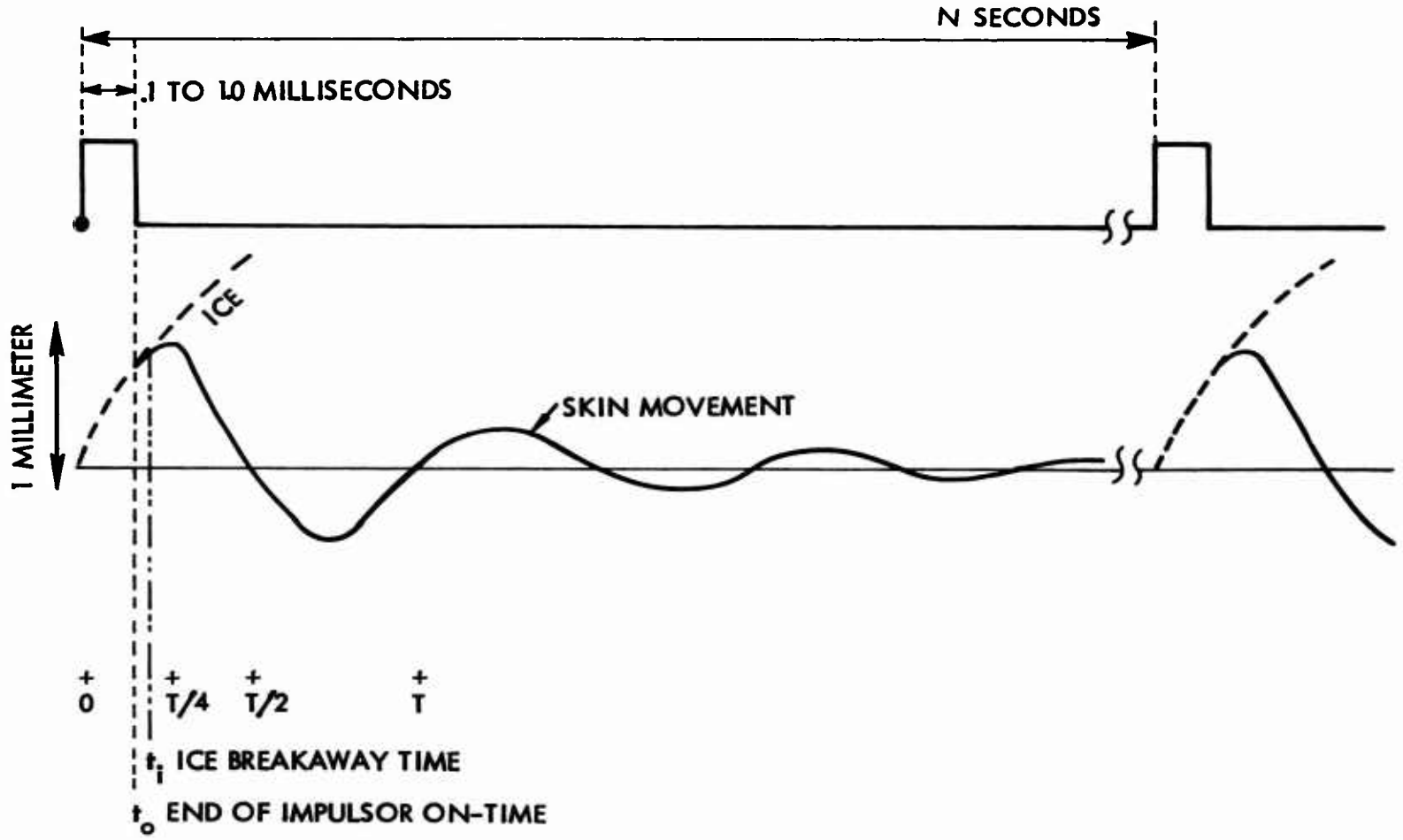

Figure 165. Electroimpulse Time Histories.

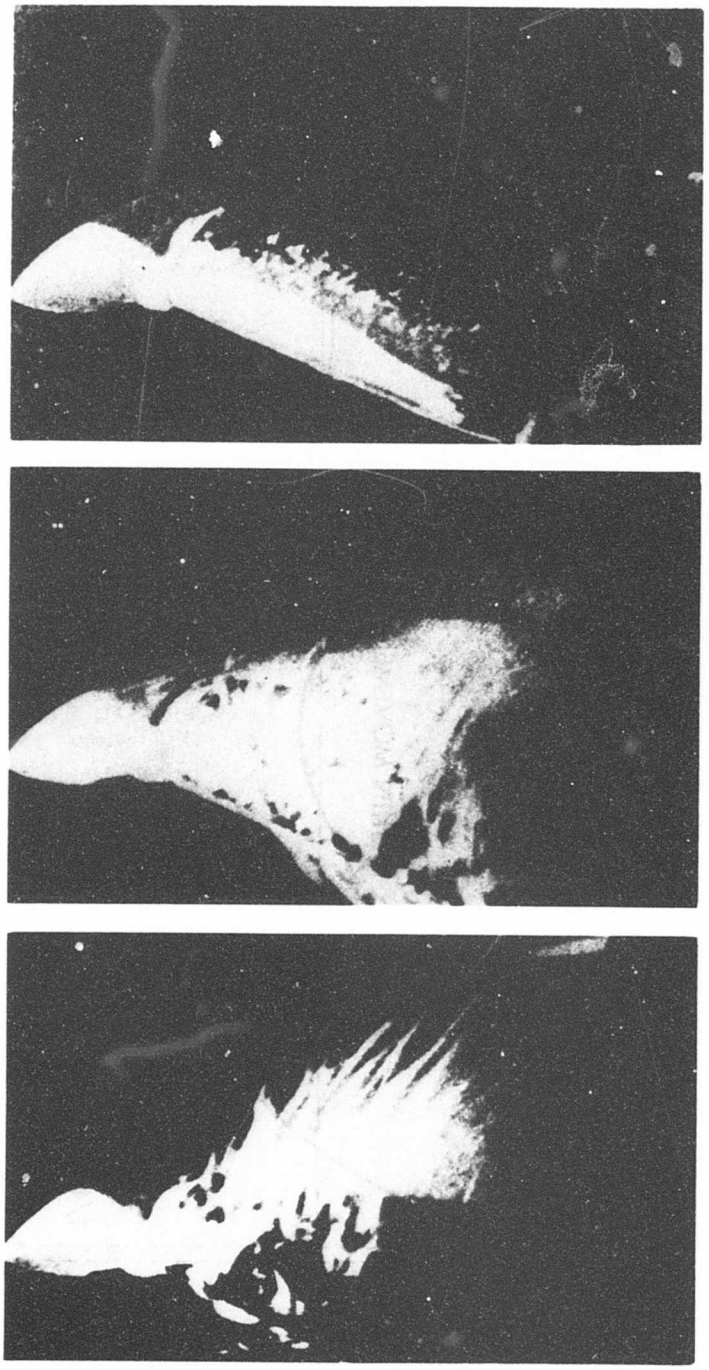

Figure 166. High-Speed Deicing Sequence.

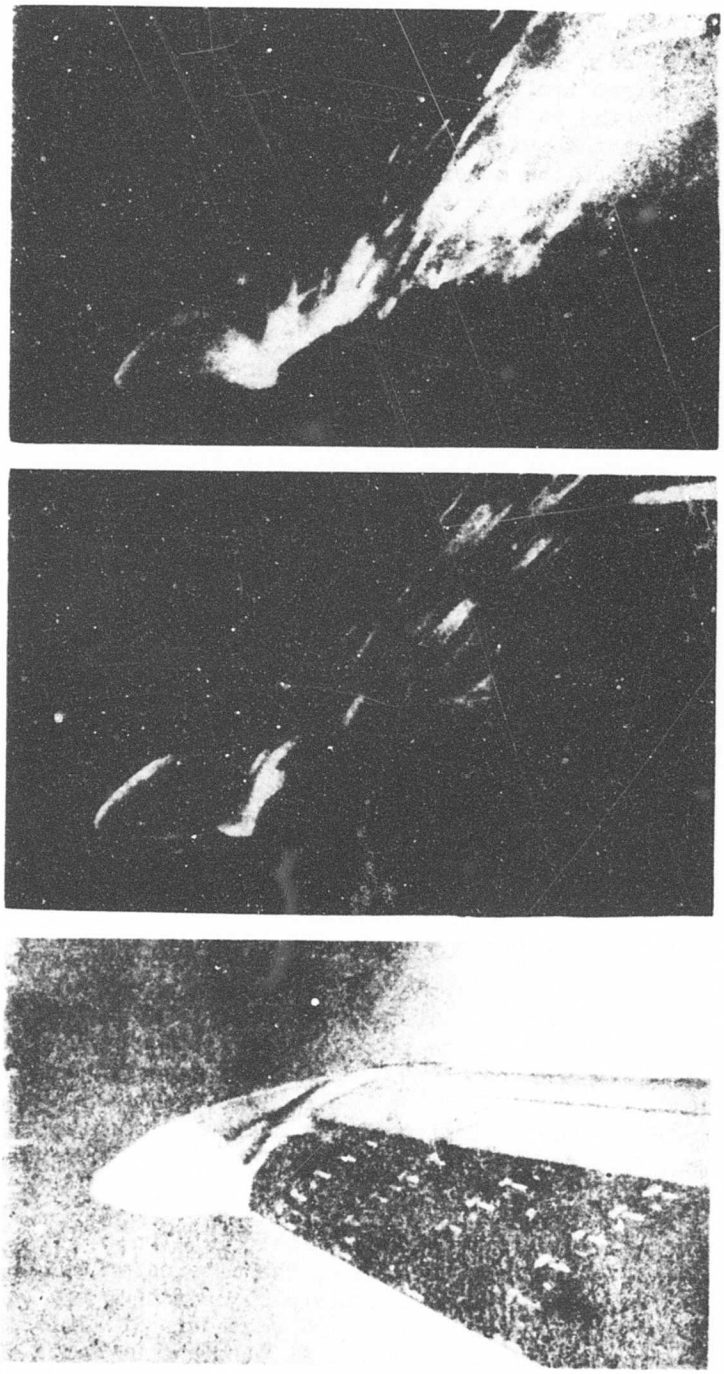

Figure 166. Continued.

of the main rotor and 25 percent on the lower surface (impingement limits for 40μ droplets are 6 percent and 18 percent, respectively; for 20μ droplets, the impingement limits are 4 percent and 11 percent, respectively). Heater coverage on the tail would be 8 percent on the inner surface and 25 percent chord on the outer surface. (Impingement is estimated to extend to 21 percent chord on the outer surface and only 2 percent chord on the inner surface during hover; at forward speed, and thus lower angle of attack, the impingement will extend further back on the inner surface and move forward on the outer surface.) The blade-cladding would be nickel plated over stainless steel and use a mylar dielectric between the cladding and the (etched foil) heating element.

Figure 167 is a schematic of the system. There are six elements per blade, and the concept of spanwise shedding (one element covering the chord) would be used. While past practice has favored chordwise shedding (running the elements the full span of a blade), it is believed that the arguments for that approach are not compelling, mainly being convenience in locating the electric leads at the inboard end and eliminating the need for bussbars running the full span of the blade. Spanwise shedding, however, requires less energy; and, in the event of damage to a single heater element, it would not affect the entire blade, as does the chordwise shedding method. Moreover, it is a convenient method of accounting for blade taper or a graduated power requirement in the spanwise direction.

The total estimated maximum power requirement is 17 kw for the main and tail rotors, and the estimated weight for the system is shown in Table LI. This is 1 percent of the empty weight of the aircraft. It is noted that Table LI contains the allowance for the blade heaters, but the actual weight penalty for the heaters may in fact be zero because of blade balance requirements.

A number of possible combinations of total number of heater elements, w/in.^{2} density, cycle time, and total power requirements are possible for any application. On the AH-56A, the total installed generator capacity consists of two 20/30 kva machines, and the normal power requirement is only 14.5 kw (plus 3 kw for windshield anti-icing). Thus, over 40 kw theoretically could be available for ice protection (the overload capacity rating, 30 kw, can be utilized during the ambient temperatures associated with ice protection). Because of the large available capacity, this particular design would be weighted in the direction of few heating elements for simplicity and minimum weight. For the selected approach, the watt density at the design point (0°F) would be tapered from 21 w/in.^{2} at the root to 10 w/in.^{2} with an average watt-density of approximately 15 w/in.^{2} The nominal element ON time would be 10 seconds. Thus, the alternator would be loaded for only 80 seconds (six main rotor elements plus operation of the tail rotor twice) out of a typical cycle time of 150 seconds. If limiting maximum power consumption were a consideration, as it might be for a different helicopter, then the number of elements per blade could be doubled (to twelve)

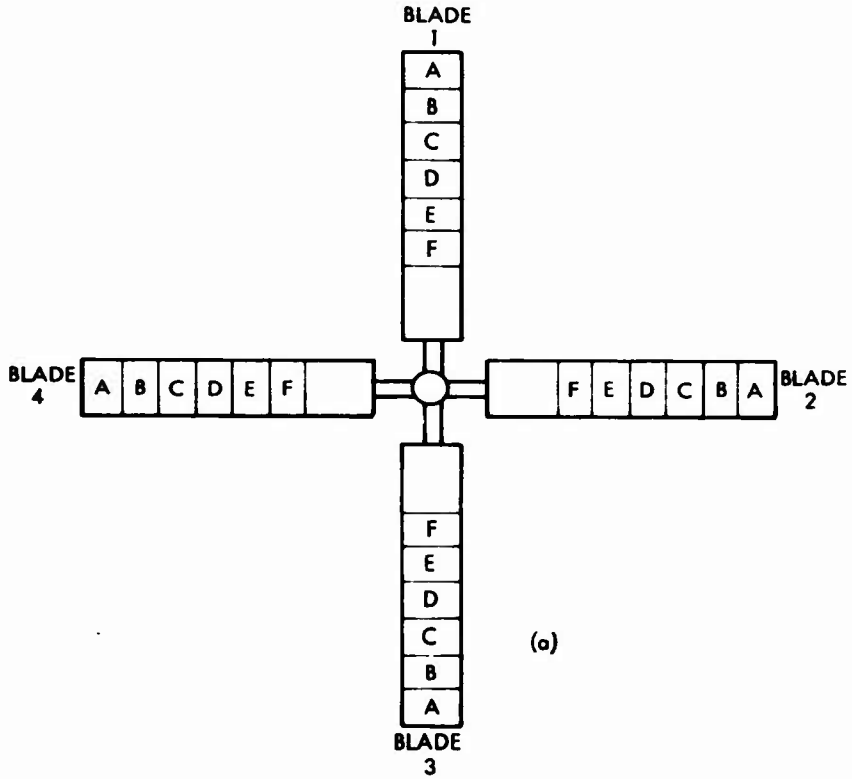

(a)

HEAT SEQUENCE OR PERIOD	BLADES				
	1	2	3	4	
1					TAIL
2	1A	2A	3A	(4A)	
3	1B	(2B)	3B	4A	
4	1C	2B	(3B)	4B	
5	(1D)	2C	3C	4C	
6					TAIL
7	1D	2D	3D	(4D)	
8	1E	(2E)	3E	4D	
9	1F	2E	(3E)	4E	
10	(1F)	2F	3F	4F	

(b)

Figure 167. Four Blade Rotor Deicing Sequence.

and a heat flux of 20 w/in.^{2} for 7 seconds ON could be used. The power consumption would then drop to 15 kw, and the weight requirement would increase by approximately 25 pounds (doubling the controller and rotor wiring weight). As outlined on page 343, the actual element ON time and power requirement could be controlled by icing severity, and the preceding values are to be taken as nominal only. The heating elements are connected to a power distribution switch mounted on the rotor hub as shown in the block diagram in Figure 168. Three phase, 400-cycle, 115v power is applied through three slip rings to the distribution switch. When in operation, corresponding heating elements in three blades are energized simultaneously with a power intensity of from 10 to 21 watts per square inch, depending on location of the element. The cycle begins with the tip elements and progresses inboard as indicated by the table on Figure 167. A small blade unbalance is created on alternate shedding cycles due to the use of three-phase power on a four-bladed rotor. This scheme was tested by J. R. Stallabrass at the Canadian National Research Council (Ref. 89) and found to be completely acceptable from a vibration standpoint, because shedding is repeated with sufficient frequency to prevent large ice accretions. The four-bladed tail rotor is protected by a single heating element on each blade, all four of which are energized at once by the application of 23 kw of power through three slip rings.

TABLE LI. ESTIMATED WEIGHT FOR SYSTEM

		Pounds
1.	Pilots control panel	2.0
2.	Control logic panel	2.5
3.	22.5/30.0 kva auto-trans	10.0
4.	Main deicing relay	3.5
5.	Switching logic/pwr supply	4.5
6.	Protection	2.2
7.	Power switching elements assembly (SCR's, etc.)	13.5
8.	Ice detector and control	1.6
9.	OAT sensor	0.2
10.	T/R timer and logic	6.0
11.	M/R slip rings	10.0
12.	T/R slip rings	4.0
13.	M/R heater mats	44.0
14.	T/R heater mats	8.0
15.	Wiring	20.0
16.	Miscellaneous	5.0
	TOTAL	137.0

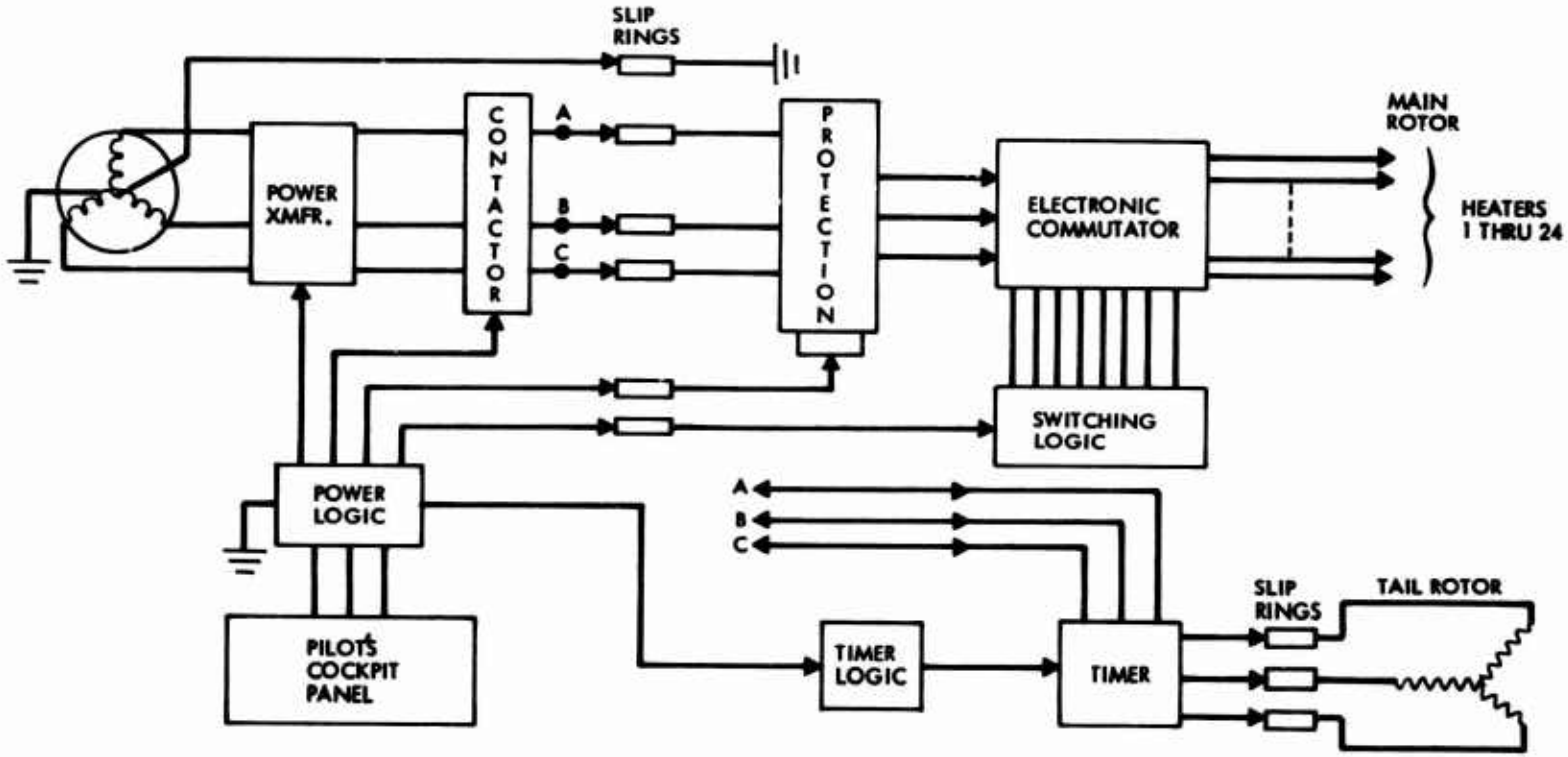

Figure 168. Deicing Control: Simplified Block Diagram.

As indicated in Figure 167, the cycling sequence is programmed to energize the tail rotor twice while the elements of the main rotor are energized once. More frequent shedding of the tail rotor is required because it reaches the point of self-shedding and probable vibration due to unbalanced shedding sooner than the main rotor by virtue of higher centrifugal forces. The probable natural period of self-shedding of the tail rotor is estimated to be about 100 seconds at 0°F ambient air temperature. The recycle period for the tail rotor would be set shorter than this to prevent self-shedding.

The cross section of the recommended heating element design is shown in Figure 169. A thin, etched foil (or equivalent) heating element would be used bonded to a mylar dielectric, which, in turn, would be bonded to a nickel-plated stainless steel cladding. Mylar is an outstanding dielectric material, and as little as 0.003 inch would be sufficient. However, considering adhesive requirements, thicknesses of 0.005 and 0.012 inch have been assumed for the performance analysis. The insulation thickness behind the heating element is conservatively taken to be three times the front dielectric, or 0.015 and 0.036 inch, respectively.

An advanced electrothermal deicing system has been analyzed for a four blade main rotor system. The system consists of stainless steel heating strips imbedded in mylar dielectric and protected from abrasion by a stainless steel-nickel cladding. Figure 170 is a schematic of the deicing boot including dimensions.

An analysis was performed to determine the effects on ice shedding of various heating rates and configuration dimensions. A thermal analyzer computer program was used to solve for detailed temperature histories of the nodal network representation of the system. The network, (see Figure 171), assumes one-dimensional heat flow and infinite thermal conductivity for all metallic portions of the covering. Lines of symmetry were used to bound the network at the centerlines of the heater strip and the separating space.

All configurations and heating rates were evaluated on the basis of the heating time required to shed the ice buildup. The criterion for shedding was arbitrarily chosen as the time at which the ice-cladding interface reached 32°F. Actual shedding times may be smaller because aerodynamic and centrifugal forces on the ice tend to overcome the ice adhesion bond strength at some temperature lower than 32°F.

The modes of heat transfer included in the analysis are: conduction through the mylar dielectric, ice, and into the honeycomb core; external air convection due to blade rotation; evaporative and sensible cooling on the exterior surface due to water catch; and heat generation by the strip heaters. Material properties were obtained from standard sources with the thermal conductivity of the mylar and ice being input as functions of temperature.

The starting point for each temperature history (time = zero) assumed the heater off, ice thickness established, and full operation in icing conditions.

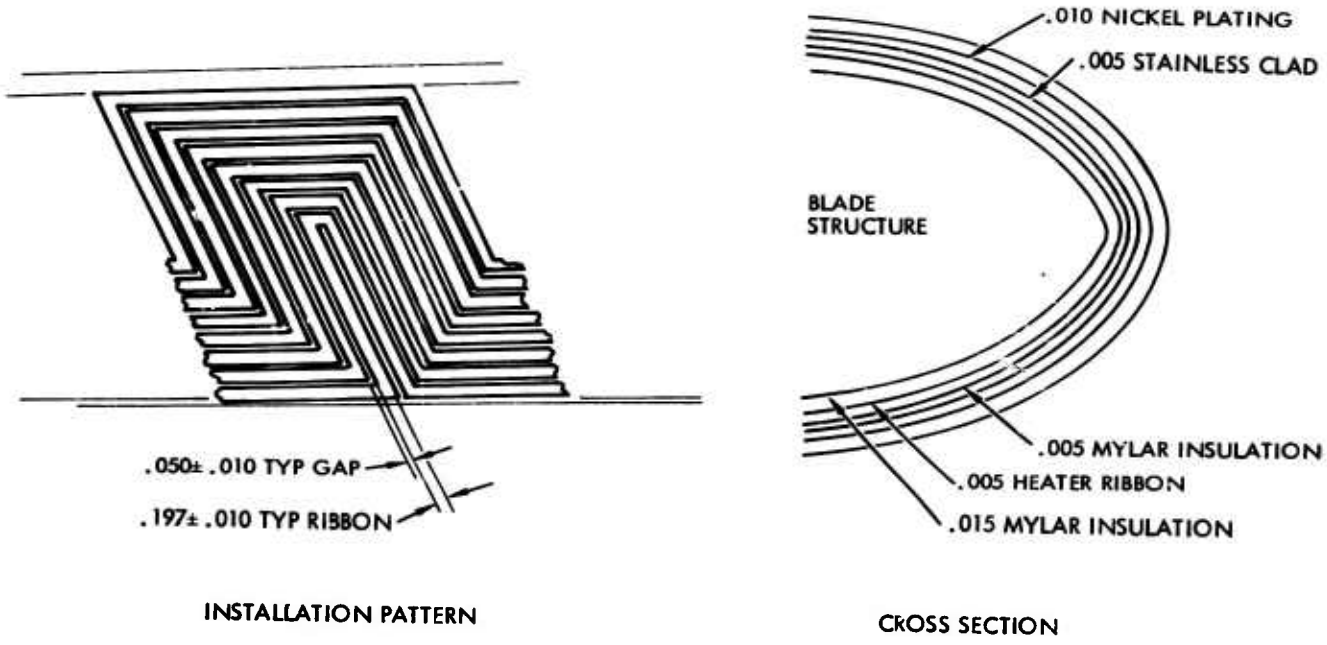

Figure 169. Recommended Blade Heater Design.

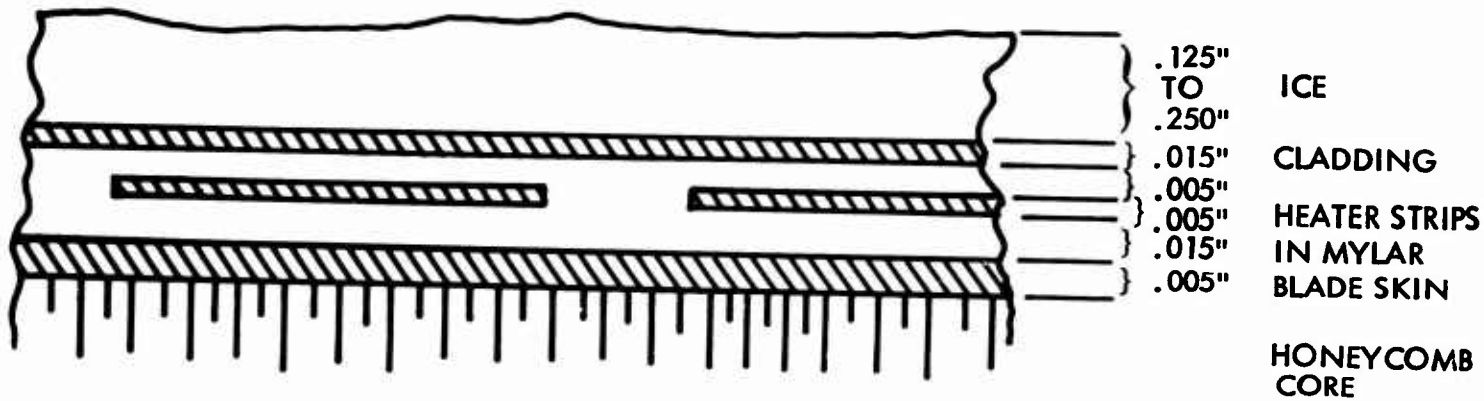

Figure 170. System Schematic.

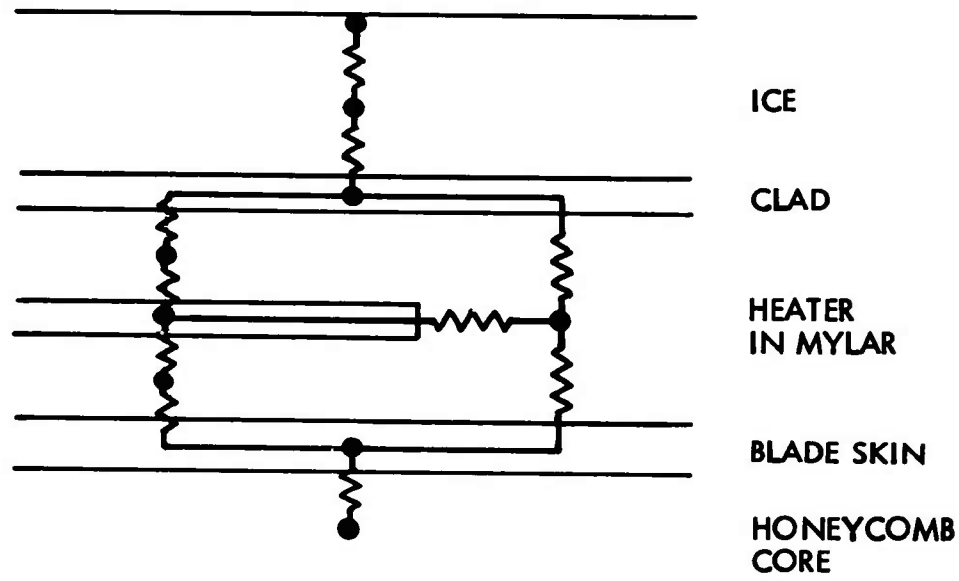

Figure 171. One-Dimensional Thermal Analyzer Model.

Equilibrium starting temperatures for the range of blade relative velocity and for an ambient temperature range of 0°F to 20°F are shown in Figure 172. The equilibrium temperature on the unheated surface is determined by a heat flow balance at the external surface between aerodynamic heating (convection due to relative air velocity) and water catch cooling (the sum of evaporative and sensible cooling). Since the equilibrium temperature is above 32°F for at least some portions of the blade (near the tip) at ambient temperatures above 10°F, no ice will form on those areas.

One-dimensional analyses have been conducted for the root and mid-span rotor stations to determine the effects of dielectric insulation thickness, power density, and ice thickness on the time required for the clad temperature to rise sufficiently to permit ice shedding. Due to the higher equilibrium temperature (on the unheated surface) at the tip, these initial parametric studies were not performed for that blade station. Results of an analysis at the tip are discussed subsequently in this section.

Figures 173 and 174 show the transient thermal response at the root and mid-span locations, respectively, for a 0.015-inch-thick cladding with two insulation thicknesses, three power densities, and 0.125 inch of accumulated ice at an ambient temperature of 0°F. For power densities of 20 and 30 w/in.^{2} the heater element ON time is 7 seconds, while for the 15 w/in.^{2} power density the ON time is 10 seconds. The figures show, as expected, that the higher the power density the quicker the clad reaches 32°F. At the starting time when heat is initially applied (see Figures 173 and 174), equilibrium temperature at mid-span is higher than at the root (due to aerodynamic heating effects); therefore, for the same power densities, the mid-span will heat up more quickly. The effect of increasing the dielectric thickness can be seen as causing an initial temperature lag of about 0.5 second. However, as the heat ON time progresses the time lag decreases, until at the end of the cycle, the clad temperature, regardless of dielectric thickness, is the same. Figure 175 compares directly with Figure 173 and shows the effect of increased ice thickness. Because of the insulative properties of the ice (shielding the cladding from the free stream), for the same power densities, the clad will heat up more quickly with the thicker buildup. Again, the insulative effect of increasing the dielectric thickness is shown as a 0.5 second lag in early warmup. The thermal lag characteristics are highly evident during the cool down power OFF period shown in Figure 173 for the 30 w/in.^{2} case. This lag is similar although not as pronounced for the other power settings.

The effect of varying the dielectric thickness on the heater strip element temperature is shown in Figure 176 for the three blade stations with a power density of 20 w/in.^{2} and an ON time of 7 seconds. This shows that the thicker dielectric, which acts as an insulator, will result in a heater element temperature 30°F higher than the thinner dielectric. These temperatures, less than 90°F, are not critical.

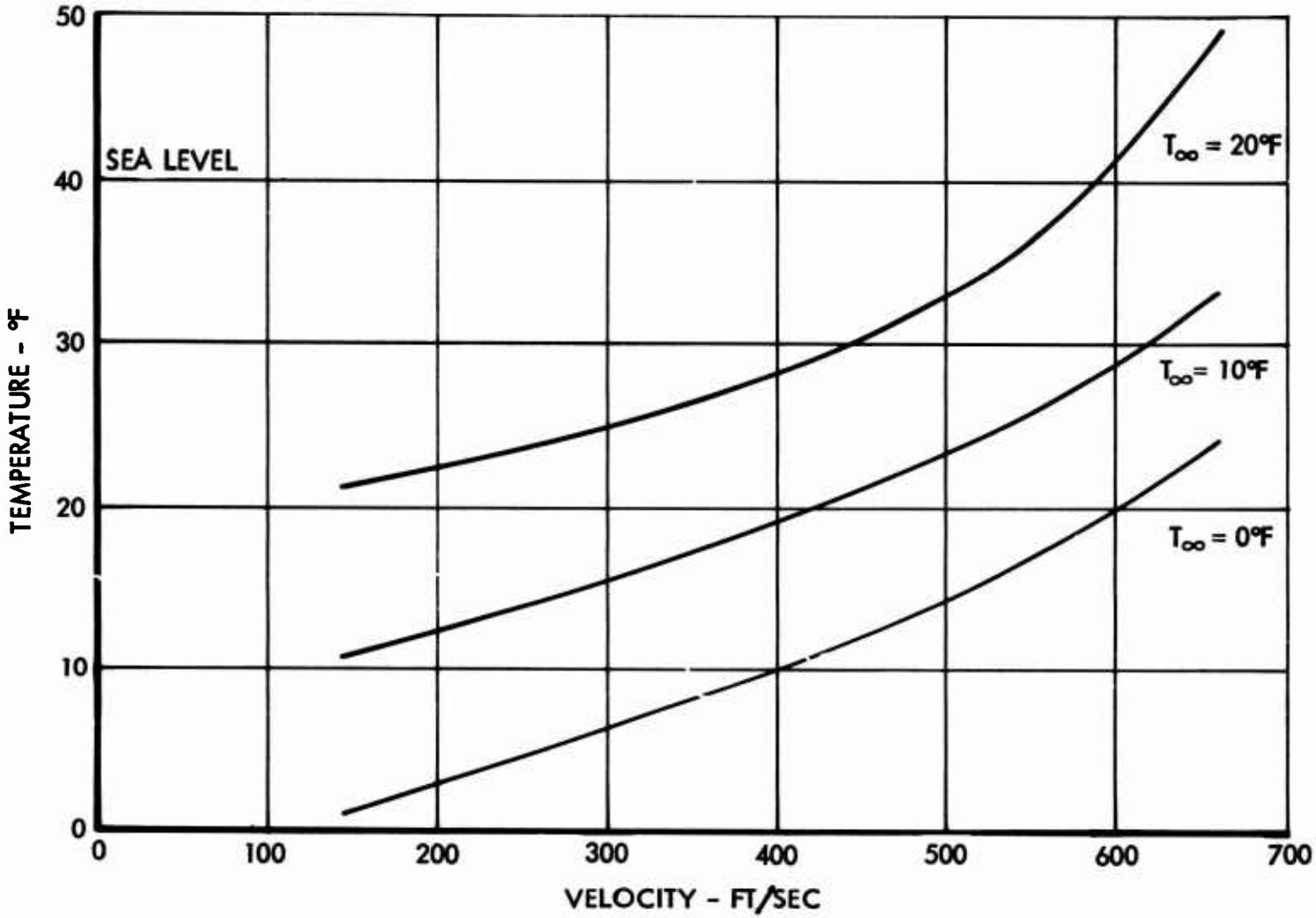

Figure 172. Rotor Blade Equilibrium Temperatures.

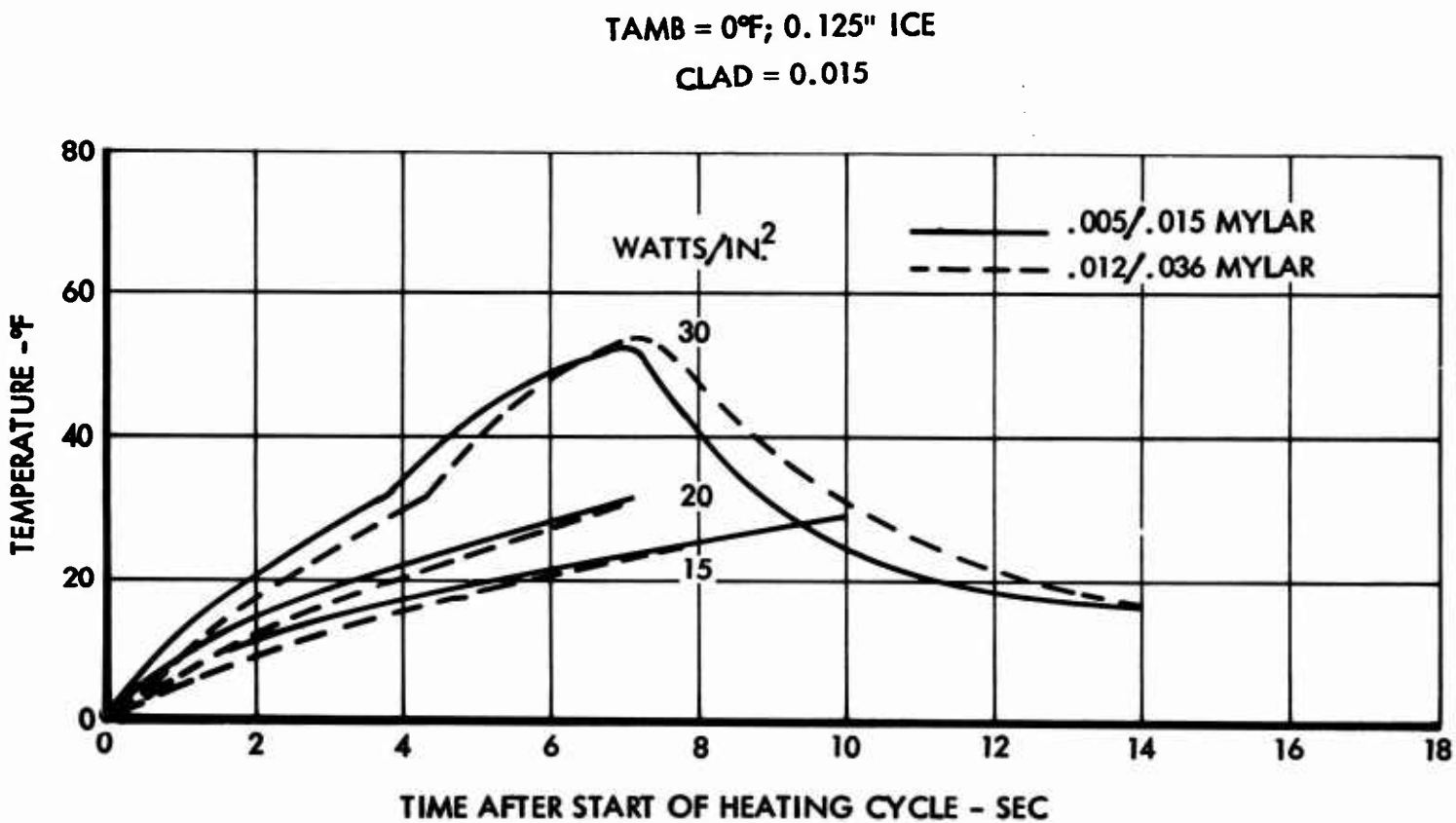

Figure 173. Cladding Temperature History - Root.

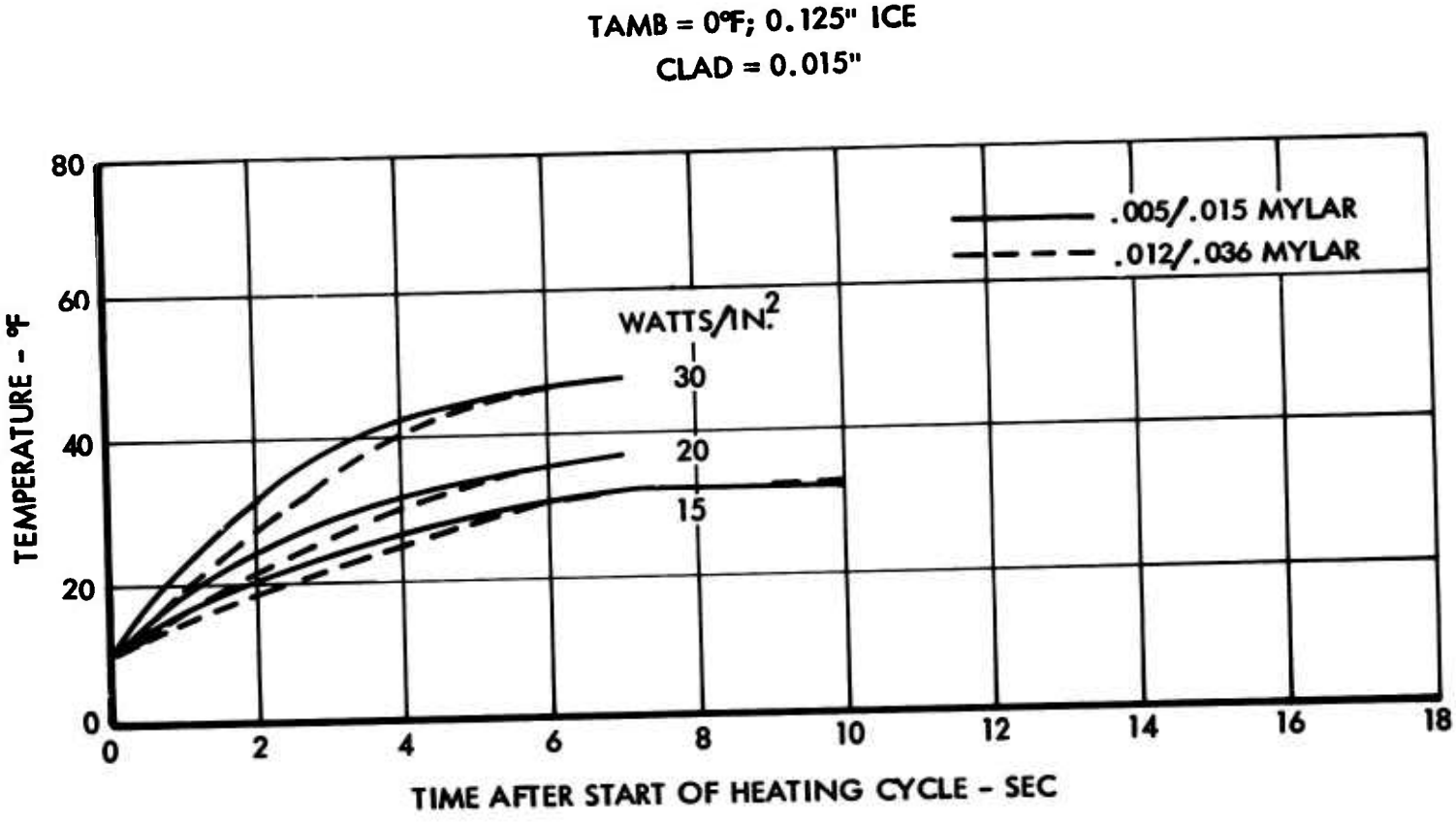

Figure 174. Cladding Temperature History - Mid-Span.

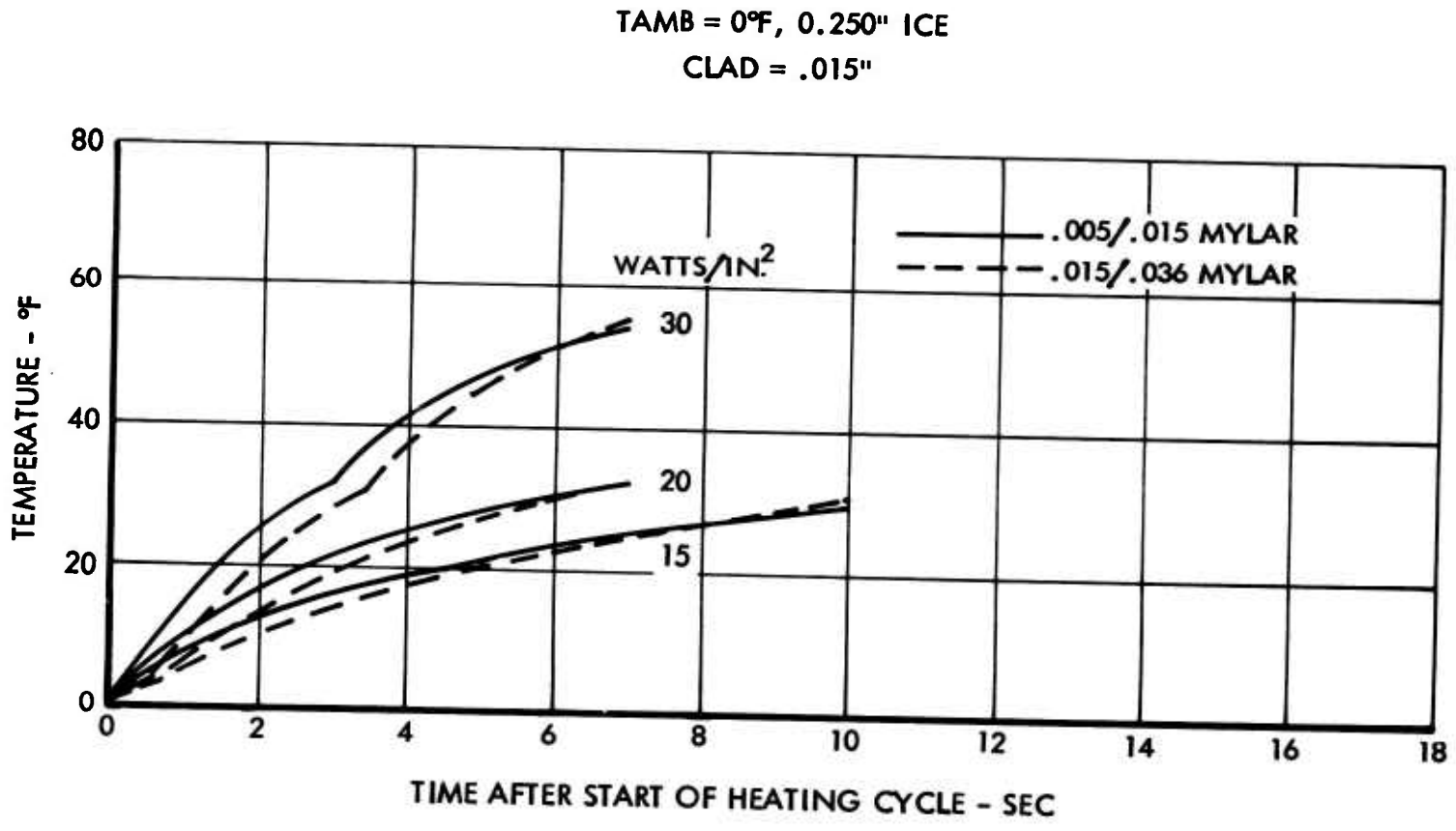

Figure 175. Cladding Temperature History - Root.

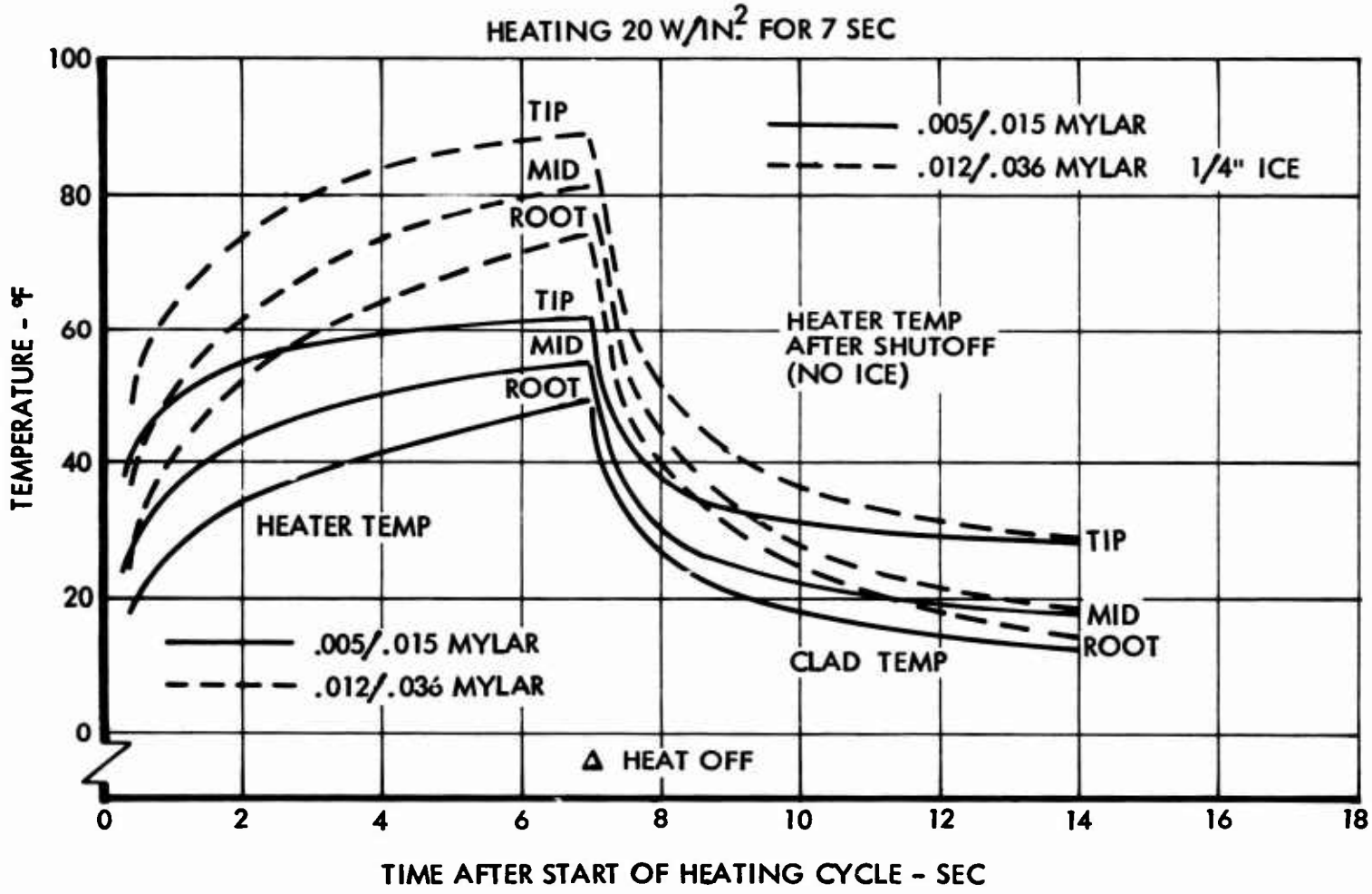

Figure 176. Heater Element Temperature History.

Figures 177, 178, and 179 show the temperature histories at the root, mid-span, and tip stations respectively, for various power densities. These figures show the spanwise power density distribution which can be used to achieve uniform heating and ice shed. These cases all were run at 0°F using a mylar thickness between the heater and clad of 0.005 inch and between the heater and blade of 0.015 inch. The clad is 0.015 inch stainless steel/nickel plated. At a selected cycle ON time, the power densities can be interpolated to determine an optimum power density distribution along the blade. For a 7-second ON time, it can be seen from Figures 177, 178, and 179 that at the root, mid-span, and tip sections the required power densities are approximately 21, 16, and 10 w/in.^{2}, respectively. This distribution is shown as Figure 180.

A series of computer runs were also performed for the same sets of conditions using a more detailed two-dimensional network. The two-dimensional network accounts for gradients in the cladding caused by spacing of the heater strips. For this model, shedding occurred when all cladding nodes were at or above 32°F. Melting of the ice at the ice-cladding interface was included by accounting for the rate of travel of the constant temperature melting interface into the ice as a function of heat available from the cladding. The rate of advance of melting ice is calculated from a heat balance at the melt surface of:

- total heat conducted from cladding through water to melt surface
- portion of total heat used to melt ice
- remainder of total heat conducted to center of ice node.

For a given set of parameters the results were the same with only two salient features distinguishing the models. These were

- At the start of ice melt the two-dimensional model showed a maximum temperature difference of 3°F between the clad nodes above the center of the heater and above the center of the dielectric spacer. Ice shedding occurred, generally, within 0.5 second of start of melting.
- The ice shed times using the two-dimensional model were about 0.5 second slower than those obtained from the one-dimensional model.

From the above results it was determined that results from the one-dimensional model are a good representation of the physical phenomenon. Thus, a one-dimensional representation could be used in the future to simplify the analysis and obtain satisfactory results.

The results of the analysis show:

- There is a considerable advantage in using a thin mylar thickness (0.005 vs. 0.012 inch) for high power intensity heating over short

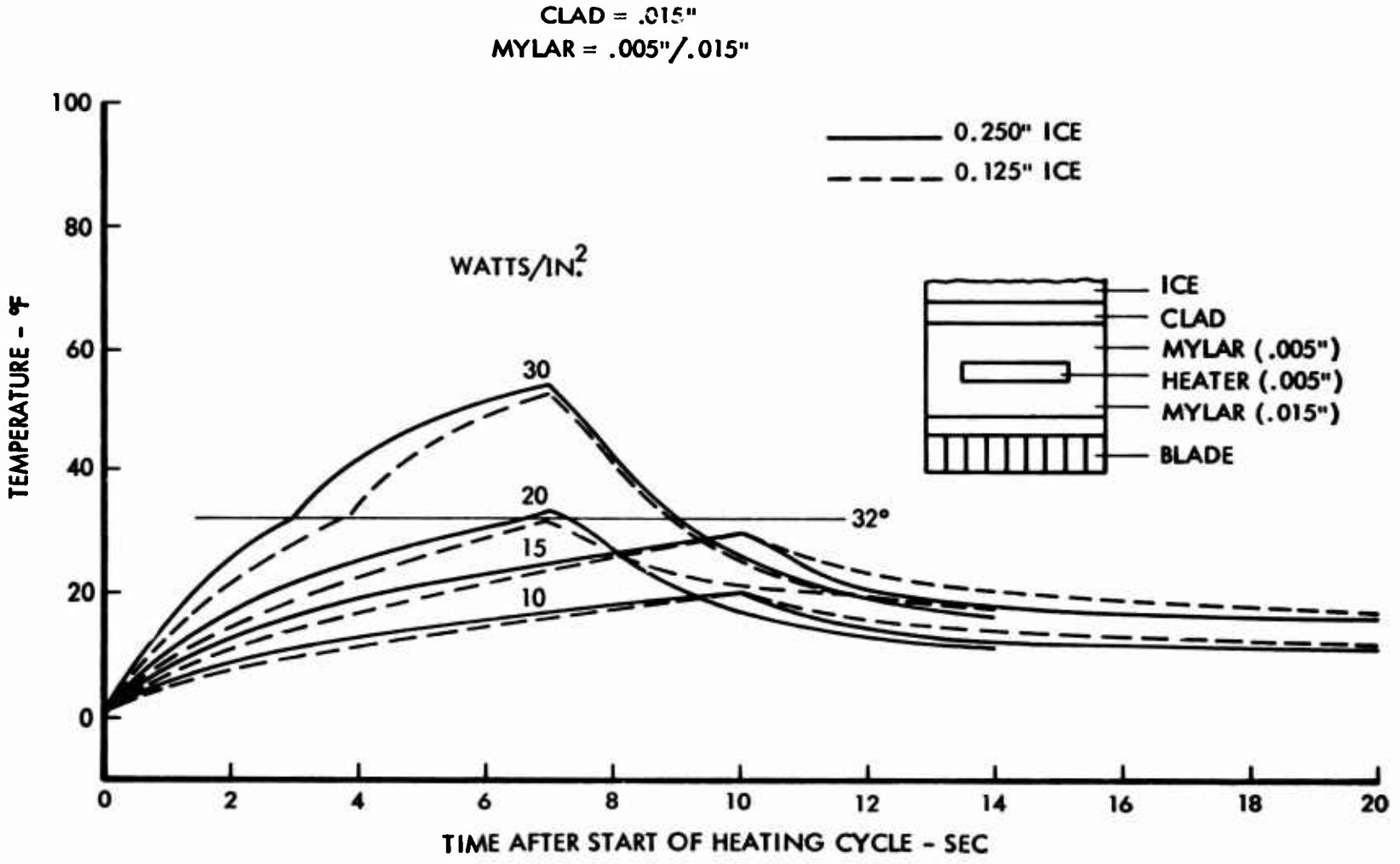

Figure 177. Transient Temperature Response - Rotor Blade Root.

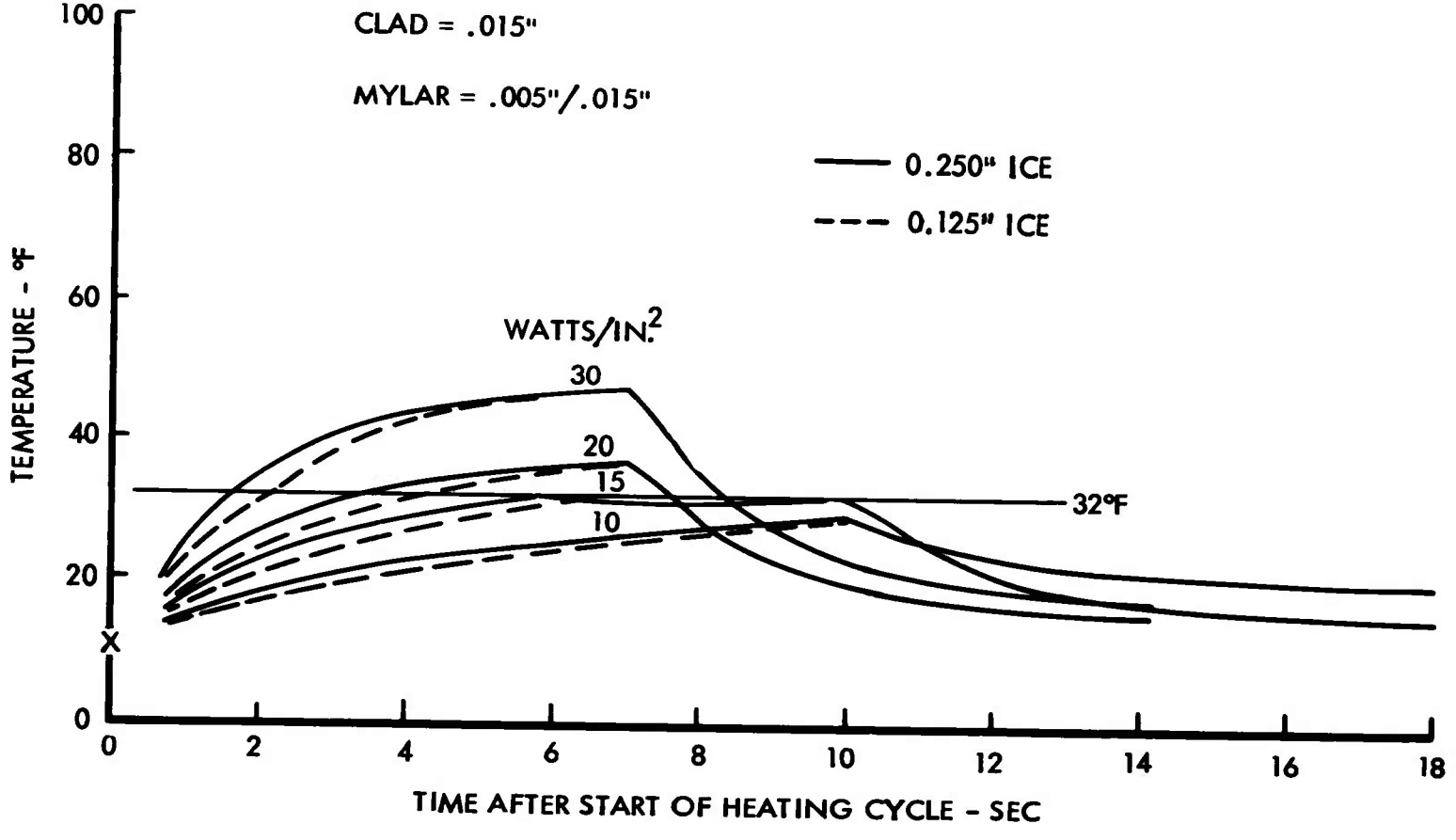

Figure 178. Transient Temperature Response - Rotor Blade Mid-Span.

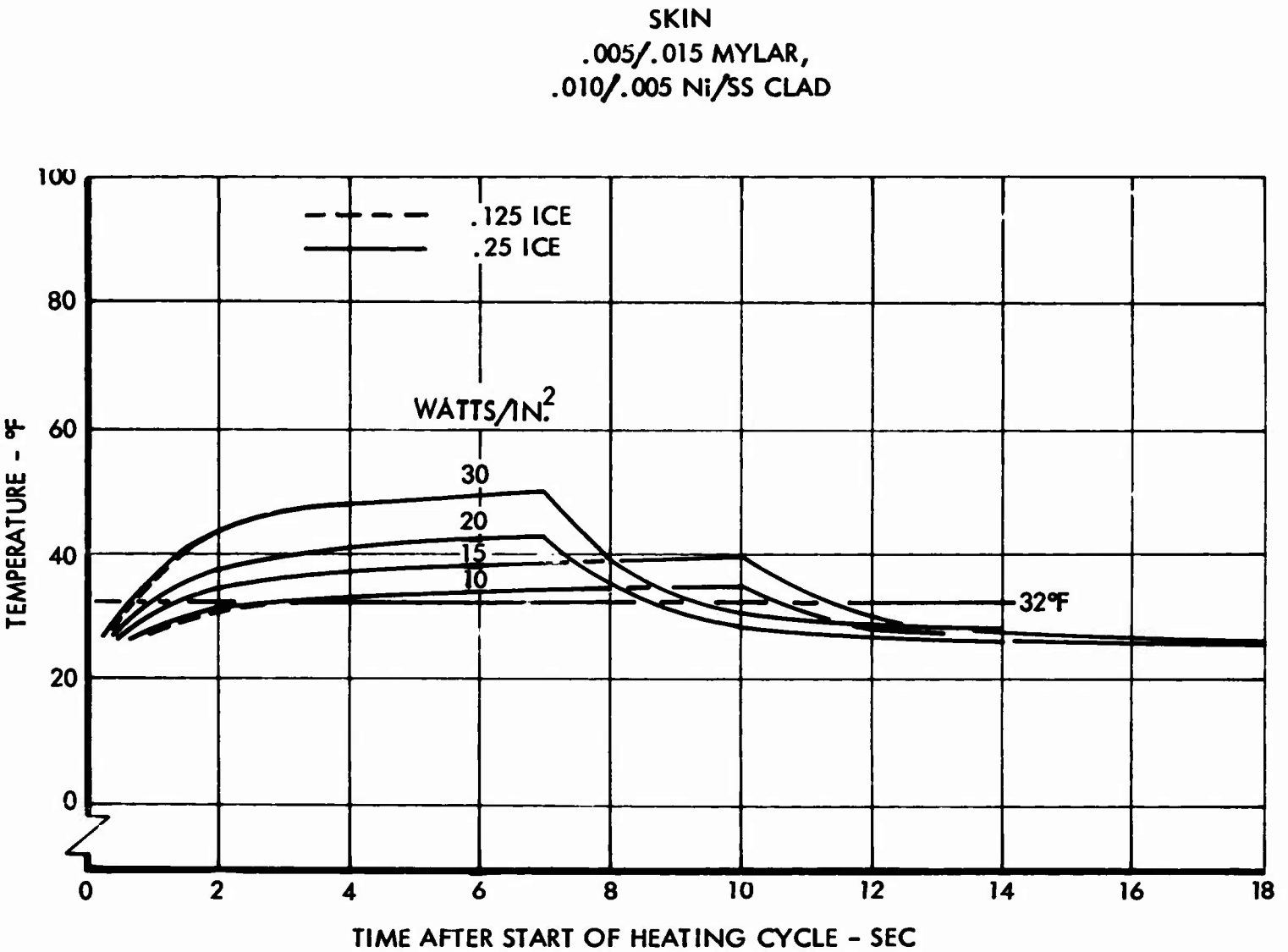

Figure 179. Transient Temperature Response - Rotor Blade Tip.

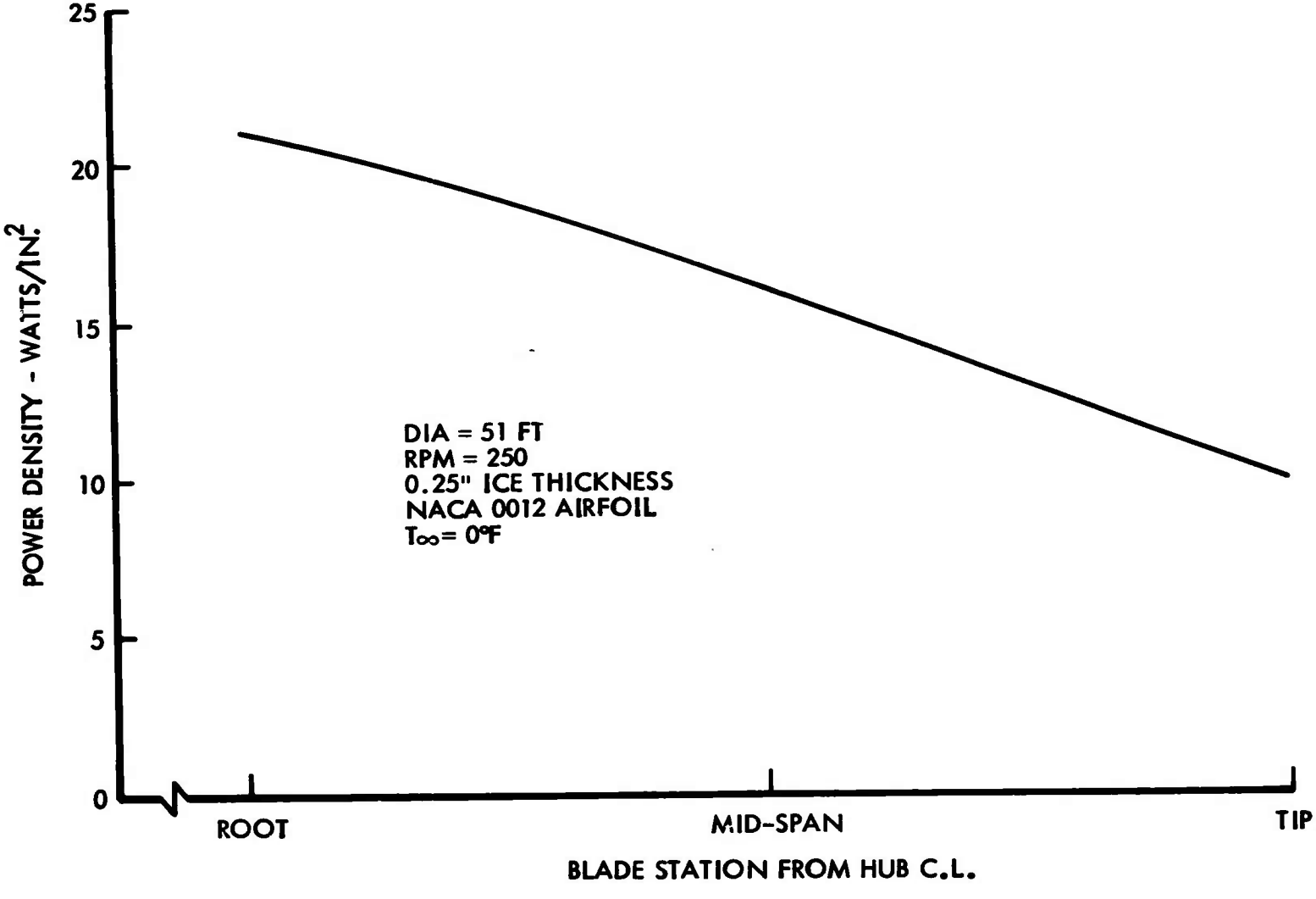

Figure 180. Rotor Blade Spanwise Power Density Distribution.

periods of time (i.e., 40 w/in.^{2} for 3-4 seconds). However, for lower power intensities over longer periods (i.e., 20 w/in.^{2} for 7-10 seconds), there is no appreciable difference in cladding temperature.

- The initial ice thickness is not a dominant factor in determining the heating cycle time, in that the effect of a 0.125 inch thickness increment is a 0.5 second lag in reaching the required ice shed temperature.

- Considerable power savings can be achieved by tapering the power intensity rather than supplying a constant power intensity along the rotor blade span.

The ultimate system control concept for a production vehicle must be determined by a flight test program. Two concepts are recommended for evaluation: a fully automatic system with heater ON time modulated by ambient temperature and OFF time modulated by icing severity; or a semiautomatic system wherein the pilot inputs ambient temperature and his estimate of icing severity. While the fully automatic system would be preferable from a pilot work-load standpoint, it will be complex and may not have the required reliability (unless there is a substantial improvement in ice detector/severity instruments). Significant simplification and more viable operation can be achieved if the pilot is included in the servo loop. The pilot is fully adaptive to the icing environment, and he is able to make decisions that would otherwise require very sophisticated equipment and circuitry. However, the system stands as an advanced system since it does recognize the importance of power conservation and it utilizes advanced state of the art control technology.

The design of the advanced deicing control system is influenced primarily by the need to provide an adaptive type system that offers the highest reliability and most technology advancement. A secondary and more pragmatic objective is that 24 heater sections (for a four-bladed main rotor) be sequentially heated in accord with some program with a minimum of slip rings. This is the basic design objective, and it is not possible to accomplish one without the other. That is, it is essential to reach into advanced technology to control so many heater sections through some minimum number of slip rings.

Figure 167 shows a facsimile of a four-bladed main rotor where each blade is divided into six segments, A through F. Each discrete heater mat takes its identification from the blade number (1 through 4 in a clockwise direction) and one sequence, in which each blade can be deiced, is also shown in Figure 167. Two factors control this format or program: one is the need to keep a balanced three-phase load presented to the generator, and the other is to maintain a minimum out-of-balance moment at any one time. Since there are 24 main rotor heater mats, an eight-period cycle is necessary in

which only three, out of a desired four, mats are heated in any one period. The blade heater mat being omitted in each time period is shown in parentheses.

Based on such a deicing program or sequence, it is required that three heater sections be simultaneously connected to the generator as a balanced three-phase load. Because of this, it is possible to use the sensing of this current balance to determine the presence of any fault on individual heater sections.

A first dictate in approaching the actual design configuration of the deicing control logic is that all power relays that control the twenty-four heater sections be mounted in the rotor head; this is the only way that the number of power slip rings can be minimized. Because of this, a second requirement is that solid-state power devices be used so that the necessary degree of reliability and flexibility of control can be achieved.

Figure 168 is a simplified block diagram of the deicing control for the main and tail rotors. This shows clearly that the only items on the vehicle side of the rotor are the power transformer, the main contactor, the pilot's panel/power logic, and the timer control for the tail rotor which operates independently of, but in parallel with, the main rotor deicing system.

Figure 181 is a more detailed block diagram of the main rotor deicing system, and this will be used to describe the operation and function. The pilot's control panel, which is the heart of the semiautomatic system, is simple, but it contains the basic manual control of the system: an ON/OFF toggle control switch for selection of deicing, a three-position condition switch for selection of the type of icing encounter, a three-scale temperature selector switch (set to the outside air temperature (OAT) on the appropriate scale), and an ice warning light.

Besides the ice warning light, there are two other lights: one is a test light which comes on when a ground test is being performed, and the other is the failure warning light which comes on if for any reason the main contactor is tripped while the system is in operation. If there is any short circuit on one of the heater elements, or an open circuit, or a failure of the electronic commutator (timer and programmer), the main contactor will be tripped and the failure light will come on.

In the functional operation, once the system has been turned on, the condition selector switch will be turned to A, B, or C; A denotes severe icing, B normal icing, and C light icing. Initially the pilot will select NORMAL and turn the temperature selector switch (on the B scale) to the outside air temperature denoted by the OAT instrument. These actions do two things: they set the tap on the power transformer to a mid (of three) positions, so that, say, 140 volts line-to-neutral is furnished to the system; they also determine the length of the ON time of the power to each group of

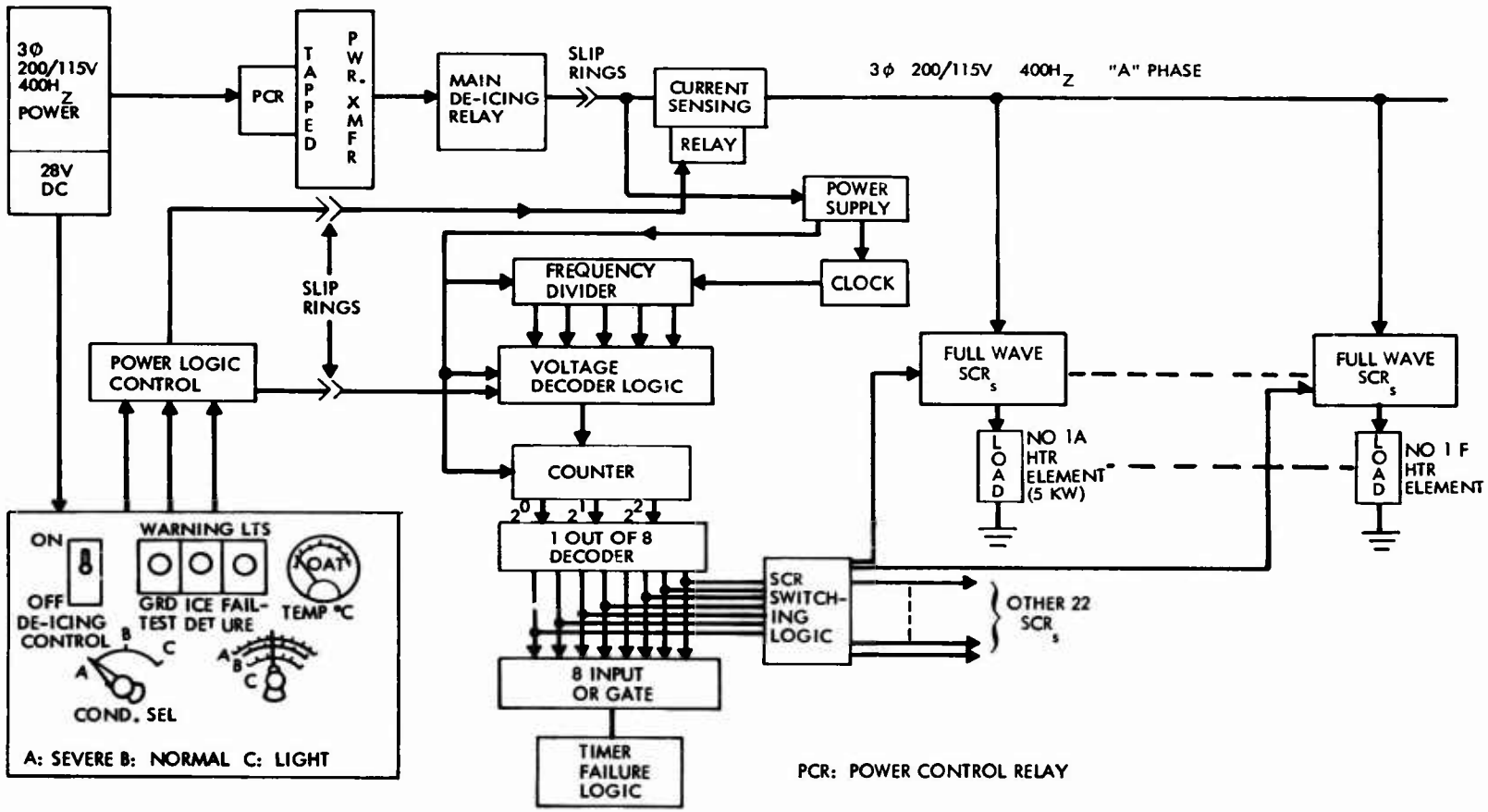

Figure 181. Deicing Control: Block Diagram Schematic.

heater sections. If in this condition the total OFF time between heating one group of elements and coming back to the same group is so long that undesirable ice buildup occurs during that interval, then the pilot turns the condition selector switch to the SEVERE condition and then sets the OAT on the A scale. Under this condition the high tap, say, 180 volts, is selected on the transformer and the ON time is reduced in proportion by the temperature selector switch. In the eight-period cycle design, each heater group has one ON period and seven OFF periods (plus cycle dead time). Thus, if when selected to condition A the ON time is 5 seconds, the OFF time will be 35 seconds plus dead time. In light icing conditions, the opposite prevails; the ON times are lengthened and the OFF times are lengthened (but the watt density is reduced accordingly).

One of the more important elements in the deicing system is the switching system which, under the command of the switching logic, controls the heating sequence of the heater elements. In the past, this has been accomplished by a programmer, or multi-point rotary switch, that steps from one position to the next in response to a timer control. Usually, to protect the contacts on the stepping switch, a power contactor is inserted forward of the selector switch to break and make the current to the heater element. This allows the programmer to step from one position to the next under zero current conditions.

In a modern control system, it is more appropriate to use a solid-state switching system, to achieve the necessary degree of reliability and to permit the use of low-level switching logic control. The basic element in this is the silicon-controlled rectifier (SCR), which is a solid-state device that is especially suited to ac switching. Once the device is turned on, it is difficult to turn off, if a steady voltage potential is held across the anode-cathode. In ac, however, the potential is alternating, and so the switch will automatically turn off when the ac wave goes through zero. However, since the device is self-latching, i.e., it will stay on once gated with a pulse of current, it cannot turn off in less than one-half cycle of the ac wave, without very special commutation circuits. For the deicing control, there is no disadvantage in this half-cycle characteristic since on the 400-Hz supply frequency this amounts to only 1.25 milliseconds delay in switch off.

For a rotary-wing blade deicing load of 17 kw, the load current per controller (or switch) is approximately 64 amps. Normally, an effort would be made to use a triac for this type of operation on ac, since it is a bidirectional device, compared to the SCR, which is a unidirectional device. Unfortunately, as the current is over 40 amps and the frequency is 400 Hz, the state of the art does not allow the use of a triac. Therefore, it is necessary to use two SCR's connected (electrically speaking) back-to-back so as to allow current flow in both directions. In this way, full-wave (both half-cycle) switching is achieved, but the switching logic, or computation of the SCR's, is slightly more complex than the control of a triac.

When using one full-wave solid-state switching device (two SCR's) per heating element, it is necessary to control them only through some switching logic that would cause them to act like an electronic commutator, i.e., a solid state-switching complex that will perform the same function as the programmer or stepping switch. To do this, the key element in Figure 181 is the counter-decoder combination. This combination ensures that a pulse of voltage (or current) appears consecutively at each of the eight output lines of the decoder. The rate or spacing of these individual output voltages is in turn dependent upon the frequency of a gating pulse that comes into the counter itself.

As each output voltage pulse comes from the decoder, the gates of three (full-wave) SCR switches are energized, causing them to conduct current to three separate single-phase elements; namely, 1A, 2A and 3A (Figure 167). After a controlled elapsed period of time, that particular gate signal (from the decoder) ceases and reappears on the next line to cause (in the program proposed in Figure 167) heater elements 1B, 3B and 4A to be connected across the three-phase supply. The cycle then continues until all eight sets of three-phase elements have been consecutively energized. At the end of this cycle, another time delay can be interposed, or the sequence can go on immediately to the next cycle.

The rate at which the programmer (electronic commutator) steps from one group of three heaters to the next is a function of the frequency divider network, which, in turn, is a function of the voltage decoder logic. Because of the requirement to minimize the number of slip rings, it is necessary to convey over one wire, and one slip ring, the timer control information from the OAT sensor. The purpose of this latter function is to vary the ON time of each group of heater elements as an inverse function of the outside air temperature (OAT). Thus the lower the OAT, the higher (or longer) the ON time.

For the semiautomatic system, it is planned that the OAT switch has, say, six temperature selections on each scale - e.g., 0, 5, 10, 15, 20, and 25°F - and that each of the positions will output a discrete level of voltage to the voltage decoder. At the decoder, these six different levels of voltage will be detected, and the particular value associated with each selector switch position will be detected so as to switch one of the six frequencies (coming into the voltage decoder) into the counter. The counter will, therefore, see square-wave voltage pulses that will have a repetition rate determined by the level of voltage coming into the voltage decoder. As each pulse comes into the counter, the output binary address (into the one-out-of-eight decoder) will change to switch each of the eight output lines in a consecutive and unambiguous fashion from one line to another. The eight-line output of the decoder is then fed into the SCR switching logic, which will respond to the signal output of the decoder to control the consecutive groups of blade heating elements.

Protection elements of the system are the only other components in the control system, and these must guard against electrical and mechanical failures. The electrical problems are those associated with short circuits or open circuits in the heater circuits that could result in out-of-balance moments on the rotor system. To detect heater element failures, a current balance control is connected in the three-phase input lines to the rotor deicing system, and this will provide a signal when an out-of-balance current reaches a prescribed limit. Another electrical type of problem is a possible failure of the electronic commutator which would result in the overheating of a particular group of heater elements. To recognize this contingency, an eight-input OR gate looks at the output of the decoder, and if any one signal remains on a single line for a period beyond a prescribed limit of time, the timer failure logic will cause tripping of the main deicing relay. The current balance signal also operates into the main deicing relay control circuit. This particular relay could be an electromechanical rather than solid-state type.

Finally, on the ground, precaution must be taken against overheating during ground operation or test check-outs. For this type of operation, logic is taken from a throttle switch to automatically select the lowest voltage tap on the transformer; at the same time, the shortest ON time is selected for the heater time control (the OAT selector) so a number of complete deicing cycles can be completed to check whether there is any tripping of the main deicing relay.

The physical layout of the components will be dictated primarily by the physical constraints of the particular rotary-wing vehicle. However, as already stated, it is necessary, in order to minimize the number of slip rings, for the power switching elements (the SCR's, the switching logic, logic power supply, protection elements, etc.) to be mounted in the hub of the rotor.

A candidate configuration might consider the mounting of the 24 SCR pairs on two round disc heat sinks, so that 12 SCR pairs and their associated circuitry would be mounted one above the other in the hub enclosure. The steady-state heat dissipation, excluding the low-level logic circuitry, would be approximately 300 watts per disc. A typical SCR for the load under consideration could be a General Electric C45B type that has a 55A RMS rating at 200 volts and a peak forward voltage rating of 500 volts. Thermally speaking, these SCR's could be underrated because of the duty cycle incident upon the six heaters per blade configurations shown in Figure 167.

The physical design of the slip rings and the brush assembly blocks will be similarly dictated by the mechanical design and space constraints around the rotor shaft assembly. The slip rings themselves may be of the face or disc type or the more conventional axial type. In the case of the brush assembly housings, these should be duplicated, and each half will carry a minimum of two brushes per slip ring. On the rotating portion, electrical connections should be taken from the slip rings to the SCR's, and then to the blade heater elements via bolted type electrical connections.

In the mechanical layout, aside from the power connections to and from the SCR's, modular design concepts should be applied to enable elements such as the SCR discs to be easily removed for repair, etc. For the low-current (logic) circuitry, consideration should be given to the unique application of printed circuitry as an integral part of the aluminum disc heat sinks. For vibration resistance, and reliability reasons, a plastic compound filler may be used to fill the voids and spaces between the components, but this must be easily chippable - so as to allow individual replacement of any failed component. An alternative modular concept, which would not necessarily pre-empt the use of any submodular assemblies, would be to consider the whole switching and controller assembly as one modular element which could be removed from the hub by the removal of, say, four bolts and the disconnection of one power supply connector and the electrical connections to the rotor blade elements.

Critical component space constraints will be in the main rotor head; here it is estimated that the switching, control, and miscellaneous circuitry could be accommodated in a cylindrical assembly approximately 11 inches in diameter x 7 inches high.

It is evident that in the past many electrothermal deicing systems have been selected on the basis of the impact or concern of the deicing system requirement on the capacity of the electric system, or vice versa. As a result, there was always a degree of compromise in the design of the deicing system. This is not to say that the systems selected on such criteria were necessarily underdesigned or inadequate, but merely that the deicing system was never optimized as an entity. It has often been said that the effectiveness of any deicing system falls between the consideration of two limits of power: too little power (or energy) - giving rise to excessive ice buildup (during the off periods); and too much power - resulting in runback and refreezing of the ice aft of the surface being deiced. The fears engendered by each of these extremes (or limits) have been the motivation for the development of smart deicing control systems. Such systems are designed to recognize all the pertinent deicing parameters and set up an ideal deicing control schedule, wherein the energy-on/off-time is controlled as a function of the prevailing icing conditions.

Essentially the significant parameters in seeking an optimum system are outside air temperature (OAT) and liquid water content (LWC). Droplet size has its discrete impact on the water catch; but within a considered range of, say, 15 to 25 microns, the design consideration is of lesser importance. Deicing control logic could use this data to determine the supply capacity and the energy-on time. The energy parameter itself, however, is dependent upon the product of the heating intensity ($w/in.^2$) and on-time. Thus, a given quantum of energy can be supplied at say 40 $w/in.^2$ for, say, four seconds or 20 $w/in.^2$ for 8 seconds. This, in fact, is where the choice is variable and is influenced by the capacity of the electric power system.

In a typical helicopter, the limited generator capacity will establish an upper limit of what power is reasonably available for deicing, and it might actually be the governing factor in the $w/in.^2$ selection. The choice of a low wattage value, however, means that not only is the on-time per heater element increased, giving rise to a certain heat transfer leakage back into the skin structure, but the off-time is increased in proportion to the number of heater sections to be energized. Also a design factor implicit in the choice of power intensity is that this lower wattage establishes a lower $\Delta^\circ C/sec$ rise at the inner-ice surface, and so the on-time must be increased proportionally. Because of this, deicing control systems should use the OAT as the most important logic input, since the skin surface temperature must be raised above $0^\circ C$ regardless of the ambient temperature conditions. It has also been suggested that LWC be considered as a system modulating parameter since "cleaner" deicing will occur if there is a certain minimum ice buildup between cycles.

There is a question as to whether the generator system capacity should be designed to meet the worst-case conditions (of the highest LWC values or lowest OAT), or whether the incidence of deicing at the extreme conditions should be taken as a statistical risk. In the past, conservatism has been allowed to prevail at the risk of decreasing the viability of the deicing system and increasing its weight. A compromise to the problem is available by considering the direct impact of electrical overloads on the total service life of a generator's insulation system. While there is not too much statistical data available upon insulation service life versus generator loads, the relationship of insulation temperature and life can be defined. In fact, generator manufacturers make their service life predictions based upon computer models of the insulation temperatures as a function of the load duty profiles - as supplied by the airframe contractor. The oversimplified statement is that the insulation system's life becomes a function of the RMS value of temperature-history of the generator, rather than some short period of operation when the insulation temperature might rise to some high value (due to overload).

The latter statement is the key to the compromise approach: the deicing power requirement should be established by the norm of deicing conditions only, and this should be the value shown on the load analysis sheets, etc. However, the generator system could be capable of inputting more power when required, under the more remote conditions of severe deicing, and this power can come from the intrinsic overload capacity of the generator.

The foregoing discussion addresses the electrothermal aspects of the generator design, but one must also consider the electromagnetic constraints. Here it is necessary to look again at the design constraints on the generator and the specifications that govern its performance. In this regard, the machine design follows documents such as MIL-G-6099, and the power characteristics are defined by documents such as MIL-STD-704 and MIL-G-21480. It is typical (because of these documents) that any generator system

must be capable of operating under many abnormal conditions of faults and overloads, so the generator designer must build adequate magnetic capacity into the machine to meet them. For example, 200 percent load conditions must be met within almost normal voltage limits, and the generator must be able to furnish adequate backup capacity to clear faults (circuit breakers, etc.) while carrying normal loads. Conditions such as these establish the intrinsic magnetic capacity of the machine and make it possible for it to meet short-time deicing overloads. Where, in fact, a generator is direct driven (thus with variable speed), the magnetic capability - or magnetic-motive capability - is dependent upon the ratio of the 100 percent speed condition to the base speed. Thus, under normal helicopter cruise conditions, the iron in the generator is significantly underutilized and to this extent it is overdesigned.

Machines driven by constant-speed drives do not, of course, have this additional magnetic capacity; but extra iron is available in the design of aircraft generators, and this does mitigate the concern for any magnetic overloading under the few abnormal conditions of severe icing. It is pertinent also that the deicing load seldom approaches the full load capacity of the generator, so a 40 percent increase in the deicing load does not necessarily mean a 40 percent overload on the generator.

Another interdependent aspect of overloading an aircraft generator (under severe deicing conditions) is that the cooling system, or more appropriately, its capacity, is also related to the cold conditions, and its effectiveness is usually improved under these atmospheric conditions. This is particularly true of ram-air-cooled generators, where the lower outside air temperature results in a lower total operating temperature in the machine. Also, when the water content is high, as it would be under severe icing conditions, the cooling effectiveness of the generator is further improved by the presence of water.

In the case of indirectly cooled generators, such as the oil cooled machines; an external oil-to-air heat exchanger is usually used to keep the oil within acceptable limits. Here again, however, the effectiveness of the cooler (heat exchanger) is improved by the cold ambients, and this results in a lower inlet oil temperature to the generator. Oil-to-fuel heat exchangers do not offer quite the same advantages, because the bulk fuel temperature is somewhat independent of outside atmospheric temperatures. Again, however, the heat exchanger is usually worst-point designed - either to a condition of minimum fuel flow or to the highest bulk temperature (or both) - so these are variants in the cooling equation.

The foregoing discussion emphasizes the fact that the key to an optimum deicing system is one which has the viability to meet a wide range of deicing conditions. Also, it has been pointed out that the choice of an optimum system should not be unduly constrained by considerations of the

generator nameplate capacity; rather, the approach should be to take advantage of those intrinsic overload capabilities that are provided by specification in the generator design. The airframe contractor specifications often define an insulation service life for a generator system of, say, more than 25,000 hours, and this is usually based upon an empirically established temperature profile that is determined by the load variations anticipated for that particular generator installation. On the basis that icing incidents average 5 percent and severe icing conditions are less than 1/2 percent, it is considered that generator overloads experienced during deicing will be marginal and undetectable in terms of guaranteed service life of the insulation system. The same rationale applies to the magnetics of the generator design, inasmuch as magnetic loadings, and their indirect thermal aspects, will have marginal, if measurable, impact on the electrical and thermal performance of the machine/regulator system.

Thus, it is recommended that future deicing system designs take advantage of the overload capability of the generator system and not be designed to conventional capacity requirements.

SECTION 8 CONCLUSIONS AND RECOMMENDATIONS

The conclusions and recommendations which follow have been divided into the broad categories of needs of helicopters for ice-protection capabilities and limitations of existing ice-protection systems, research and development recommendations, recommended icing severity standards, and miscellaneous.

8.1 NEEDS OF ARMY ROTARY-WING AIRCRAFT FOR ICE PROTECTION

1. Safe flight in moderate icing conditions requires ice-protection systems for critical vehicle components.

2. Critical components requiring anti-icing protection are the engine and its induction system, the windshield, and the pitot-static system. The following design icing criteria are recommended: for fully evaporative engine induction system anti-icing - Figure 2 of MIL-E-38453, down to 0°F (Figures 77 and 78 of this report); for running-wet engine induction system anti-icing - Figure 3 of MIL-E-38453 down to 0°F (Figures 79 and 80 of this report); for windshield anti-icing - MIL-T-5842; for flight probes - MIL-P-26292.

3. Critical components requiring deicing are the main and tail rotors. It is recommended that Figure 2 of MIL-E-38453 down to 0°F (Figures 79 and 80 of this report) be used as the governing document for main and tail rotor ice protection.

4. For components conducive to ice accretion, droplet impingement limits are to be based on a maximum droplet size diameter of 40 microns.

5. Engine bleed air thermal anti-icing systems are to be preferred for engine air induction systems, although electrically heated thermal anti-icing can be satisfactory if adequate design attention is paid to eliminating cold spots.

6. Electrical heat is recommended for windshield and pitot-tube anti-icing, and electrothermal cyclic deicing is recommended for rotor blade ice protection.

7. Full ice-protection equipment is estimated to require 1 to 1-1/2 percent of vehicle empty weight and will impose an engine fuel consumption penalty of approximately 1/4 percent when operating.

8. Engine and induction system protection are required to prevent loss in engine power, flameout, and engine damage. Windshield ice protection is required to assure landing and in-flight

visibility, and pitot-tube ice protection is required to assure correct airspeed indication.

9. Main and tail rotor ice protection is required primarily to prevent structural damage from uncontrolled self-shedding from the blades and to minimize vibrations. On small helicopters, rotor ice protection is also required to minimize the drag in-increase caused by the ice buildup on the blades

10. Deicing systems are to be designed such as to take advantage of the overload capacity of air-cooled generators and not be designed to conventional capacity requirements.

8.2 CAPABILITIES AND LIMITATIONS OF EXISTING ICE-PROTECTION SYSTEMS

1. A comprehensive bibliography covering all facts of icing technology has been informally prepared; it consists of approximately 1500 entries.

2. The current system state of the art will provide satisfactory ice protection for all components except the rotor blade. (Detail design execution is, however, not always satisfactory.)

3. Improvements for rotor blade deicing technology are urgently required in the areas of heater element reliability, reduced power requirements, and lower control and power distribution system weights.

8.3 RESEARCH AND DEVELOPMENT RECOMMENDATIONS

1. A solid-state switching and power distribution system to be installed in the rotor head must be developed to achieve the required weight and reliability goal. The required technology is fundamentally available; the principal development task is to properly package the components.

2. It is recommended that a thinner heating element be developed using a mylar dielectric. This will permit reduced power requirements or, if the same dielectric thickness is used as for today's design, a more rugged unit. The heater blanket must be metal clad for both thermal and reliability considerations, and it is mandatory that the blanket fabrication methods assure a 100 percent void-free bond between the cladding, dielectric, and heating element.

3. It is recommended that a system controller be developed for flight test which can modulate element ON time with ambient temperature and element OFF time with liquid water content. The need for this capability in a production vehicle must be evaluated during the flight test period.

4. The electro-impulse deicing system, which used the principle of skin deflection by electrical induction for ice removal, offers substantial promise of providing an improvement in ice protection technology in terms of reduced power requirements and more effective deicing over a wide range of meteorological conditions (no runback). However, insufficient information is available to validate the claims and, for system design, an Icing Research Tunnel Test Program is recommended to obtain the required data. Upon completion of the test program, a brief design study should be performed to quantitatively compare the benefits of this system with more conventional systems and to determine the feasibility of installation in a rotor system.

8.4 ICING SEVERITY STANDARDS

1. Conventional standard pilot definitions of icing severity encompass the terms trace, light, moderate, and severe (sometimes called heavy). By definition, trace icing is of such a low intensity that ice protection equipment is unnecessary, light icing requires occasional use of deicing equipment, moderate icing requires the use of ice protection equipment, and severe icing is so heavy that continued flight even with full ice-protection equipment is not safe. The upper limit of moderate icing is taken to be the design meteorological conditions.

2. It is recommended that Army rotary-wing aircraft ice-protection systems be designed to meet the meteorological conditions described in the Federal Air Regulation, Part 25, except that the minimum ambient temperature for design be $0^{\circ}F$, rather than $-22^{\circ}F$.

3. Trace icing severity has a liquid water content less than 0.25 gm/m^3, light icing is less than 0.50 gm/m^3, moderate icing is 0.5-1.0 gm/m^3, and severe icing is greater than approximately 1.0 gm/m^3.

4. No experimental evidence is available to determine if an in-flight icing severity measuring system is required for flight safety purposes. Icing severity (liquid water content) varies rapidly in clouds, and it is thus not possible to forecast the icing rate, even knowing a current rate. Thermal ice-protection systems have an inherent "overload" capability, and icing conditions more severe than "moderate" would be of short duration. While fixed-wing experience has indicated that an in-flight icing severity measuring system is not required, further flight experience with rotary-wing vehicles will be required before a final conclusion can be made.

5. No ice detection (or icing severity) meter has yet demonstrated adequate reliability to be considered suitable for monitoring flight safety. Other means (e.g., ice accretion on windshield

wiper blades) have been found to be completely reliable methods of ice detection on fixed wing aircraft.

8.5 MISCELLANEOUS RECOMMENDATIONS

1. It is recommended that the Army modify the Specification AV-E-8593B covering ice, snow and hail ingestion requirements for turboshaft engines to provide for a more stringent specification of ingestion level, and to define the methods of demonstration more completely.

2. It is recommended that a handbook of rotary-wing ice-protection system design be published to ensure more adequate design practice by industry.

LITERATURE CITED

1. Harris, Cyril M., and Crede, Charles E., SHOCK AND VIBRATION HANDBOOK, Vol. 3, McGraw-Hill, 1961.

2. Stallabrass, J. R., et al., ON THE ADHESION OF ICE TO VARIOUS MATERIALS, Journal of the Canadian Aeronautics and Space Institute, pages 199-204, September, 1963

3. Beranek, Leo L., NOISE AND VIBRATION CONTROL, McGraw-Hill, New York, 1971.

4. Stallabrass, J. R., ICING FLIGHT TRIALS OF A BELL HTL-4 HELICOPTER, National Aeronautical Establishment (Canada) Laboratory Report LR-197, July, 1957.

5. Stallabrass, J. R., ICING FLIGHT TRIALS OF A SIKORSKY HO4S-2 HELICOPTER, National Aeronautical Establishment (Canada) Laboratory Report LR-219, April, 1958.

6. Gibbard, G. A., ICING AND DE-ICING FLIGHT TESTS OF A KAMAN HU2K-1 HELICOPTER, National Research Council of Canada Aeronautical Report LR-308, May 1961.

7. Dowden, Donald J., et al, CATEGORY II ICING TEST OF THE HH-53C HELICOPTER, Air Force Flight Test Center (Edwards AFB, Calif.) Report FTC-TR-71-26, June 1971.

8. Lockheed California Company Monthly Test Progress Report Number 34, Contract No. DAA11-66-C-3667 (H), Reporting Period May 1969, pages 207-292.

9. Atkinson, F. S., BEA Helicopters Ltd. Report BEAH/ENG/TD/R/113, A REPORT ON ICING TRAILS WITH THE S61N JAN/APRIL 1971, Dated Feb. 1972.

10. Kowa, Myron M., ENVIRONMENTAL DEVELOPMENT OF U. S. ARMY OH-58A LIGHT OBSERVATION HELICOPTER, American Helicopter Society Preprint No. SW-70-52, November, 1970.

11. Stephenson, Carl D., et al., DESIGN, MANUFACTURE AND TESTING OF THE CH-54 A/B ENGINE AIR PARTICLE SEPARATOR ANTI-ICE SYSTEM, Proceedings of the Tenth Annual National Conference on Environmental Effects on Aircraft and Propulsion Systems, pp. 22-1 to 22-39, May 18, 1971.

12. Nihei, T. A., CHSS-2 ICE PROTECTION SYSTEM TRIALS, Canadian Forces Aerospace Engineering Test Establishment Report 69/119, November 13, 1970.

13. Jones, R. F., ICE FORMATION ON AIRCRAFT, World Meteorological Organization Technical Note No. 39, Geneva, Switzerland, 1961.

14. WEATHER FORECASTERS' GUIDE ON AIRCRAFT ICING, USAF Air Weather Service Manual AWSM 105-39, Jan. 1969.

15. Omond, R. T., ON THE FORMATION OF SNOW CRYSTALS FROM FOG, Journal Scottish Meteorological Society (Edinburgh) 7, 190, 1886.

16. Kline, D. B., and Walker, J. A., METEOROLOGICAL ANALYSIS OF ICING CONDITIONS ENCOUNTERED IN LOW-ALTITUDE STRATIFORM CLOUDS, NACA TN 2306, March 1951.

17 Jones, R. F., ANALYSIS OF REPORTS OF ICE ACCRETION ON AIRCRAFT, MRP 1017, London, 23 November 1956, (AD-139538).

18. Mason, D., AIRCRAFT AND ICING RESEARCH - I AND II, Weather, Vol. 8, No. 8, August 1953, pp. 243-246; Weather, Vol. 8, No. 9, September 1953, pp. 261-267.

19. Thompson, J. K., 1954 ICING PRESENTATION FOR MAJOR COMMANDS, WADC Tech. Note WCT 55-26, WADC April 1955 (AD-69347).

20. Ashley, H., AIRCRAFT ICING OVER NORTHWEST EUROPE, AWSTR 105-46, July 1945, (ATI-65127).

21. Lewis, J. P., INVESTIGATION OF AERODYNAMIC AND ICING CHARACTERISTICS OF A FLUSH ALTERNATE-INLET INDUCTION-SYSTEM AIR SCOOP, NACA Res. Memo E53E07, NACA, July 24, 1953.

22. Simpson, G. C., ICE ACCRETION ON AIRCRAFT, NOTES FOR PILOTS, Prof. Notes No. 82, Great Britain Met. Office, 1942.

23. Kline, D. B., INVESTIGATION OF METEOROLOGICAL CONDITIONS ASSOCIATED WITH AIRCRAFT ICING IN LAYER-TYPE CLOUDS FOR 1947-48 WINTER, NACA Tech. Note 1793, NACA, January 1949.

24. Lewis, W., and Hoecker, W. H., Jr., OBSERVATIONS OF ICING CONDITIONS ENCOUNTERED IN FLIGHT DURING 1948, NACA Tech. Note 1904, NACA, June 1949.

25. Perkins, P. J., PRELIMINARY SURVEY OF ICING CONDITIONS MEASURED DURING ROUTINE TRANSCONTINENTAL AIRLINE OPERATION, NACA Res. Memo E52J06, NACA, December 16, 1952.

26. Perkins, P. J., and Kline, D. B., ANALYSIS OF METEOROLOGICAL DATA OBTAINED DURING FLIGHT IN A SUPERCOOLED STRATIFORM CLOUD OF HIGH LIQUID-WATER CONTENT, NACA Res. Memo E51D18, NACA, July 11, 1951.

27. Reed, R. J., ARCTIC WEATHER ANALYSIS AND FORECASTING, Dept. of Met. Occasional Report No. 11, Univ. of Washington, AF Contract No. 19 (604)-3063, Seattle, January 1959.

28. Cummings, S. C., AIRCRAFT ACCIDENTS IN WHICH ICING WAS A FACTOR - 1 JANUARY 1946 TO 31 DECEMBER 1958, unpublished report, USAF Directorate of Flight Safety Research, May 1959; L/C J. Creeden, unpublished data 1959-1965, USAF Directorate of Aerospace Safety (AWS liasion office).

29. Perkins, P. J., Lewis, W., and Mulholland, D. R., STATISTICAL STUDY OF AIRCRAFT ICING PROBABILITIES AT THE 700-AND 500-MILLIBAR LEVELS OVER OCEAN AREAS IN THE NORTHERN HEMISPHERE, NACA Tech. Note 3984, NACA, May 1957.

30. Katz, L. G., CLIMATOLOGICAL PROBABILITY OF AIRCRAFT ICING, Air Weather Service Technical Report 194, Scott Air Force Base, Illinois, January 1967.

31. Heath, E. D., and Cantrell, L. M., AIRCRAFT ICING CLIMATOLOGY FOR THE NORTHERN HEMISPHERE, Air Weather Service USAF Technical Report 220, Washington, D.C., June 1972.

32. Jailer, Robert W., POTENTIAL AIRCRAFT ICING PROBABILITIES IN THE NORTHERN HEMISPHERE, American Power Jet Company, WADC Technical Report 56-659, Wright Air Development Center, Ohio, November 1956, (AD 110676).

33. Ingram, David M., and Gullion, J. L., ESTIMATED FREQUENCIES OF POTENTIAL ICING CONDITIONS AT SPECIFIED ALTITUDES, MATS Technical Report 182, Air Weather Service, Washington, D.C., September 1964.

34. Guttman, Nathaniel B., STUDY OF WORLDWIDE OCCURRENCE OF FOG, THUNDERSTORMS, SUPERCOOLED LOW CLOUDS AND FREEZING TEMPERATURES, National Oceanic and Atmospheric Administration National Climatic Center for, Commander, Naval Weather Service Command, December 1971.

35. Briggs, J., and Crawford, R. G., PROBABILITY OF ICING BETWEEN 0 AND 5000 FEET, Meteorological Office, Investigations Division Memorandum No. 105, Bracknell, Berkshire, England, 1972.

36. Crutcher, H. L., and Davis, O. M., U. S. NAVY MARINE CLIMATIC ATLAS OF THE WORLD, Volume VIII, Commander, Naval Weather Service Command, NAVAIR 50-1C-52, March 1969.

37. Crutcher, H. L., and Meserve, J. M., SELECTED LEVEL HEIGHTS, TEMPERATURES AND DEW POINTS FOR THE NORTHERN HEMISPHERE, NAVAIR 50-1C-52, Naval Weather Service Command, Washington, D.C., January 1970.

38. Taljaard, J., Van Loon, H., Crutcher, H., and Jenne, R., CLIMATE OF THE UPPER AIR PART 1 - SOUTHERN HEMISPHERE VOLUME 1, NAVAIR 50-1C-55, National Center for Atmospheric Research, National Weather Records Center, and Department of Defense, 1969.

39. Ratner, Benjamin, TEMPERATURE FREQUENCIES IN THE UPPER AIR, U. S. Weather Bureau, Washington, D.C., January 1946.

40. Solomon, Irving, ESTIMATED FREQUENCIES OF SPECIFIED CLOUD AMOUNTS WITHIN SPECIFIED RANGES OF ALTITUDE, Climatic Center Technical Report 167, Air Weather Service, U. S. Air Force, April 1963.

41. Perkins, P. J., STATISTICAL SURVEY OF ICING DATA MEASURED ON SCHEDULED AIRLINE FLIGHTS OVER THE UNITED STATES AND CANADA FROM NOVEMBER 1951 TO JUNE 1952, NASA RM E55F 28a, Lewis Flight Propulsion Laboratory, Cleveland, Ohio, September 1955.

42. Perkins, P. J., Lewis, William and Mulholland, D. R., STATISTICAL STUDY OF AIRCRAFT ICING PROBABILITIES AT THE 100 AND 500 - MILLIBAR LEVELS OVER OCEAN AREAS IN THE NORTHERN HEMISPHERE, NACA Technical Note 3984, Lewis Flight Propulsion Laboratory, Cleveland, Ohio, May 1957.

43. Perkins, P. J., ICING FREQUENCIES EXPERIENCED DURING CLIMB AND DESCENT BY FIGHTER-INTERCEPTOR AIRCRAFT, NACA Technical Note 4314, Lewis Flight Propulsion Laboratory, Cleveland, Ohio, July 1958.

44. Perkins, P. J., SUMMARY OF STATISTICAL ICING CLOUD DATA MEASURED OVER UNITED STATES AND NORTH ATLANTIC, PACIFIC, AND ARCTIC OCEANS DURING ROUTINE AIRCRAFT OPERATIONS, NASA Memorandum 1-19-59E, Lewis Research Center, Cleveland, Ohio, January 1959.

45. Rohan, P. K., and Ohoonghusa, F., AIRCRAFT ICING OVER THE EASTERN NORTH ATLANTIC, Department of Industry and Commerce Meteorological Service Technical Note 21, Dublin, 1956.

46. Crossley, A. F., ICE ACCRETION AND TURBULENCE ON NORTH ATLANTIC AIR ROUTES, Quart. J. Royal Meteorological Soc., Vol. 87, No. 371, January 1961, pp. 55-64.

47. Samuels, L. T., METEOROLOGICAL CONDITIONS DURING THE FORMATION OF ICE ON AIRCRAFT, NACA Technical Note 439, Washington, 1932.

48. Conrad, Victor, PRELIMINARY REPORT ON STATISTICAL INVESTIGATION OF THE MOUNT WASHINGTON SERIES OF ICING OBSERVATIONS, Harvard-Mount Washington Icing Research Report 1946-7, U. S. Air Force Air Materiel Command, Wright-Patterson Air Force Base, Dayton, Ohio, pp. 114-189, June 1948.

49. Climatology of the United States, Decennial Census of the United States Climate, Summary of Hourly Observations, 1951-1960.

50. Zaitsev, V. A., LIQUID WATER CONTENT AND DISTRIBUTION OF DROPS IN CUMULUS CLOUDS, National Research Council of Canada, Technical Translation TT-395, Ottawa, 1953.

51. Lewis, W., METEOROLOGICAL ASPECTS OF AIRCRAFT ICING, Compendium of Meteorology, Editor, Malone, T. F., American Meteorological Society, Boston, pp. 1197-1206, 1951.

52. Minervin, V. E., Mazin, I. P., and Burkorskaya, S. N., SOME NEW DATA ON THE WATER CONTENT OF CLOUDS, Moscow Cent. Aerol. Obs. Trudy Vyp 1963.

53. Pettit, K. G., PROCEEDINGS TORONTO METEOROLOGICAL CONFERENCE, Royal Meteorological Society, London, p. 269, 1953.

54. Diem, M., MEASUREMENTS OF CLOUD PARAMETERS II, Meteorologische Rundshau, p. 261-273 1948.

55. Lewis, William, REVIEW OF ICING CRITERIA, Federal Aviation Administration Aircraft Ice Protection Symposium, April 28-30 1969.

56. Lewis, W., and Bergrun, N., A PROBABILITY ANALYSIS OF THE METEOROLOGICAL FACTORS CONDUCIVE TO AIRCRAFT ICING IN THE UNITED STATES, NACA TN 2738, July 1952.

57. Trunov, O. K., ICING OF AIRCRAFT AND MEANS OF PREVENTING IT, AD-668521 or N68-27134.

58. Savin, V. S., et. al., AIRCRAFT ANTI-ICING SYSTEMS: PRINCIPLES OF DESIGN AND TEST METHODS, U. S. Army Foreign License and Technology Center FSTC-HT-411-69

59. Hacker, P. T., and Dorsch, R. G., A SUMMARY OF METEOROLOGICAL CONDITIONS ASSOCIATED WITH AIRCRAFT ICING AND A PROPOSED METHOD OF SELECTING DESIGN CRITERIONS FOR ICE-PROTECTION EQUIPMENT, NACA TN 2569, 1951.

60. ARMY AVIATION - GENERAL PROVISIONS, AR 95-1 (Army Regulations), September 12, 1969.

61. Thompson, J. K., ALL WEATHER FLIGHT CONCERN OF THE PILOT AND WEATHER FORECASTER, Aeronautical Engineering Review, July 1956.

62. HH43-B Flight Manual, T.O. 1H-43(H) B-1, February 1, 1972.

63. ICING RATE INDICATOR SYSTEM, Rosemount Engineering Company, Minneapolis, REC Rept. #26919B, February 1969.

64. Petach, A. M., A SUMMARY OF AIRCRAFT ICING CRITERIA, Proceedings of the Third National Conference on Environmental Effects, 1963.

65. Anon, STATUS OF ICE PROTECTION SYSTEM DEVELOPMENT ON CHSS-2, Canadian Forces Amen 'A' to L11500 ED-108 (DAE 2-5), July 6, 1972.

66. Bowden, D. T., Gensemer, A. E., and Skeen, C. A., ENGINEERING SUMMARY OF AIRFRAME ICING TECHNICAL DATA, FAA Technical Report ADS-4, Dec. 1963.

67. Langmuir, I. and Blodgett, K., A MATHEMATICAL INVESTIGATION OF WATER DROPLET TRAJECTORIES, AFFTR 5418, Feb. 19, 1946.

68. Sherman, P., Klein, J. S., and Tribus, M., DETERMINATION OF DROP TRAJECTORIES BY MEANS OF AN EXTENSION OF STOKES' LAW, Engineering Research Institute, University of Michigan, April 1952.

69. Weiner, F. R., FURTHER REMARKS ON THE USE OF THE K_o CORRELATION IN ICING PRELIMINARY DESIGN, Third Annual Conference on Environmental Effects on Aircraft Propulsion Systems, U. S. Naval Air Turbine Test Station, Trenton, New Jersey, Sept. 1963.

70. Messinger, B. L., EQUILIBRIUM TEMPERATURE OF AN UNHEATED ICING SURFACE AS A FUNCTION OF AIR SPEED, Journal of the Aeronautical Sciences, January 1953.

71. SAE Aerospace Applied Thermodynamics Manual, Society of Automotive Engineers, Inc., 1969.

72. Eckert, E. R. G., and Livingood, J. N. B., METHOD FOR CALCULATION OF LAMINAR HEAT TRANSFER IN AIR FLOW AROUND CYLINDERS OF ARBITRARY CROSS SECTION (INCLUDING LARGE TEMPERATURE DIFFERENCES IN TRANSPIRATION COOLING), NACA Report 1118, 1953.

73. Stage, W. A., ICING TUNNEL EVALUATION OF THE TKS FLUID ICE PROTECTION SYSTEM FOR AN AIRFOIL, Lockheed-California Company Report LR 22987 (LFT-T-46), November 20, 1969.

74. Stallabrass, J. R., CANADIAN RESEARCH IN THE FIELD OF HELICOPTER ICING, J. of the Helicopter Association of Great Britain, Vol. 12, #4, August 1958.

75. Stallabrass, J. R., THERMAL ASPECTS OF DE-ICER DESIGN, International Helicopter Icing Conference, Ottawa, Canada, May 23, 1972.

76. European Scientific Notes ESN-27-2, February 28, 1973, Office of Naval Research, London, U.S. Navy.

77. Meyer, H. J., McDonnell-Douglas Corporation and McNabb, D. W., Michigan Dynamic Division AMBAC Industries, Inc., ICE PREVENTION AND REMOVAL, Environmental Control IRAD Section of Douglas Aircraft Company, IRAD Line Item Description No. D91-70-909.

78. T.K.S. FLUID DE-ICING SYSTEM PRESENTATION, Michigan Dynamics Division of AMBAC Industries, Inc., Detroit, Michigan Dynamic Filter Systems (#J1258-D5), June 12, 1969.

79. Girrard, G. A., ICING FLIGHT TESTS OF A FLUID ROTOR BLADE ICE PROTECTION SYSTEM ON A BELL HU-1 HELICOPTER, National Research Council of Canada, Ottawa, Canada, Aeronautical Report LR-317, October 1961.

80. Van Wyckhouse, J. F., DEVELOPMENT AND ICING FLIGHT TESTS OF A CHEMICAL ICE PROTECTION SYSTEM FOR THE MAIN AND TAIL ROTORS OF THE HU-1 HELICOPTER, Bell Helicopter Company, Fort Worth, Texas, Report No. 518-099-002, June 5, 1961.

81. Van Wyckhouse, J. F., CHEMICAL ICE PROTECTION FOR HELICOPTER ROTORS AND A COMPARISON WITH THE ELECTRO-THERMAL SYSTEM, from Proceedings of the American Helicopter Society 18th Annual National Forum, Washington, D.C., May 1962.

82. Savin, V. S., et al., AIRCRAFT ANTI-ICING SYSTEM: PRINCIPLES OF DESIGN AND TEST METHODS, Army Foreign Science and Technology Center, Charlottesville, Virginia, January 26, 1961.

83. Wilson, E. G., SYCAMORE MK 14-XE 308 ICING TEST IN THE N.R.C. SPRAY RIG OF THE EXPERIMENTAL FLUID ANTI-ICING SYSTEM, Aeroplane and Armament Experimental Establishment, Ministry of Aviation, London, W.C.2., England 8th Part of Report No. AAEE 1874/6, 1964.

84. Stallabrass, J. R., CANADIAN RESEARCH IN THE FIELD OF HELICOPTER ICING, Journal of the Helicopter Association of Great Britain, Vol. 12, No. 4, August 1958.

85. Stallabrass, J. R., THERMAL ASPECTS OF DE-ICE DESIGN, paper presented at the First International Helicopter Icing Conference, Ottawa, Canada, May 22, 1972.

86. Gunn, F. E., CH-124 FOD SHIELD ICING TESTS, Canadian Forces Aero-Space Engineering Test Establishment Report 70/89, June 7, 1971.

87. Werner, J. B., ANALYSIS OF TRANSIENT TEMPERATURE DISTRIBUTION ON SURFACES OF ELECTRO THERMAL DE-ICER BOOTS, Lockheed Aircraft Corp. Report LR 9541, January 20, 1955.

88. Mastroly, F. R., OPERATIONAL CHARACTERISTICS OF THE P3V ICE PROTECTION SYSTEM, Lockheed Aircraft Corp. California Division Report LR 14248, March 18, 1960.

89. Stallabrass, J. R., and Gibbard, G. A., A COMPARISON BETWEEN THE SPANWISE AND CHORDWISE SHEDDING METHODS OF HELICOPTER ROTOR BLADE DE-ICING, National Research Council of Canada Aeronautical Report LR 270, January 1960.

90. Joyce, D., FLIGHT TEST REPORT OF AN EVALUATION OF THE 107 II ICE PROTECTION SYSTEM, Boeing/Vertol Report 107-T-299 Addendum 1, March 26, 1963.

91. ICING TUNNEL TESTS OF TWO MODELS OF THE ELECTRA AIRFOIL ICING PROTECTION SYSTEMS, Lockheed IRT-14, August 5, 1958.

92. EFFECT OF ICE AND FROST FORMATIONS ON DRAG OF NACA 65 -212 AIRFOIL FOR VARIOUS MODELS OF THERMAL ICE PROTECTION, NACA TN 2962, June 1953.

93. ICING THERMAL TESTS OF EMPENNAGE ICE PROTECTION MODELS INCORPORATING ELECTRO THERMAL DE-ICING, Lockheed LR 14398, March 28, 1960.